Stem Cells International

Current Status and Perspectives of Human Mesenchymal Stem Cell Therapy 2020

Lead Guest Editor: Jane Ru Choi
Guest Editors: Kar Wey Yong and Hui Yin Nam

Current Status and Perspectives of Human Mesenchymal Stem Cell Therapy 2020

Stem Cells International

Current Status and Perspectives of Human Mesenchymal Stem Cell Therapy 2020

Lead Guest Editor: Jane Ru Choi
Guest Editors: Kar Wey Yong and Hui Yin Nam

Contents

Hindawi
Stem Cells International
Volume 2022, Article ID 9801358, 3 pages
https://doi.org/10.1155/2022/9801358

Editorial

Current Status and Perspectives of Human Mesenchymal Stem Cell Therapy 2020

Jane Ru Choi[1], **Kar Wey Yong**[2] **and Hui Yin Nam**[3]

[1]*University of British Columbia, Centre for Blood Research, Life Sciences Centre, 2350 Health Sciences Mall, Vancouver, BC, Canada V6T 1Z3*
[2]*Department of Surgery, Faculty of Medicine & Dentistry, University of Alberta, Edmonton, AB, Canada T6G 2R3*
[3]*Tissue Engineering Group, Department of Orthopaedic Surgery (NOCERAL), Faculty of Medicine, University of Malaya, Lembah Pantai, 50603 Kuala Lumpur, Malaysia*

Correspondence should be addressed to Jane Ru Choi; janeruchoi@gmail.com and Kar Wey Yong; karwey@ualberta.ca

Received 6 December 2021; Accepted 6 December 2021; Published 11 February 2022

Mesenchymal stem cell (MSC) therapy shows a great promise for the treatment of injuries and diseases in regenerative medicine [1, 2]. MSCs have the ability to self-renew and differentiate into multiple lineages, making them an ideal candidate for cell therapy [3, 4]. They exist in adult tissues of different sources such as fat, bone marrow, umbilical cord and menstrual blood [5]. In addition to multilineage potential, these cells have the capability of secreting anti-inflammatory molecules and bioactive factors [6]. Therefore, they are commonly used in clinical settings to treat illnesses including autoimmune, inflammatory, degenerative, musculoskeletal and respiratory diseases [7, 8]. While numerous studies reported the clinical applications of MSCs, multiple challenges are yet to be addressed to achieve successful clinical translations. This special issue underlines the most recent advances in therapeutic applications of MSCs. It also discusses many emerging approaches in enhancing the therapeutic effects of MSCs especially in bioprocessing, assessment of efficacy and safety, and clinical delivery strategies.

A total of 16 articles introduced the therapeutic applications of MSCs for diverse types of diseases, including cancers, respiratory, neurological and ocular diseases. A number of comprehensive review articles highlighted the current status and perspectives of MSC therapy in neurological, ocular, and respiratory diseases along with major challenges of translating the research findings into clinical practice. D. Han et al. reviewed the effects of MSC-mediated mitochondrial transfer on inflammatory processes, cell metabolism, survival, proliferation, and differentiation. They also summarized therapeutic potential of MSC-mediated mitochondrial transfer in neurological diseases such as stroke and spinal cord injury. B. Xie et al. performed meta-analysis on randomized controlled clinical trials of cerebral palsy (CP) to evaluate the efficacy and safety of transplantation of human MSCs in children with CP. The therapy increased gross motor function measure scores and comprehensive function assessment up to 12 months with minimal adverse effects. J. S. Nurković et al. reviewed phenotypic characteristics of limbal epithelial stem cells and corneal stromal stem cells and their therapeutic potential in corneal regeneration. Understanding the phenotypic and functional characteristics of corneal stem cells could improve medical and surgical managements of ocular surface disorders. L. Sun et al. reviewed the recent advances of MSCs in allergic rhinitis therapy. Discussing the roles and mechanisms of MSC immunomodulatory effects allows readers to better understand the potential of MSCs in allergic rhinitis therapy.

D. Rady et al. reviewed the major challenges in clinical applications of human MSCs, including donor-related factors, cell source, discrepancies in cell isolation and culture procedures, risk of tumorigenicity, variability in methods of cell delivery, and alteration of MSC properties in response to various drugs and growth factors. By overcoming these challenges, MSC-based therapies could be successfully translated into clinical practices for many unmet medical conditions. M. N. F. B. Hassan et al. systematically reviewed the bioprocessing

strategies for large-scale expansion of MSCs. Specifically, the large-scale expansion of 7 different sources of MSCs using 4 different bioprocessing strategies, including bioreactor, spinner flask, roller bottle, and multilayered flask, were comprehensively discussed. It was suggested that the optimization of key parameters, including cell seeding density, oxygen partial pressure and medium formulation is crucial to ensure the development of a sustainable and reproducible platform for utilizing MSCs in clinical settings. These bioprocessing approaches show tremendous potential for large-scale expansion of MSCs without compromising cell quality.

A number of research articles in this issue have revealed the potential therapeutic applications of MSCs for several diseases, including breast cancer, skin cancer, allergic airway inflammation, and Alzheimer's disease. Y. Jiao et al. reported the roles of NLRP1 and CASP4 genes in pyroptosis of breast cancer cell line MCF7 induced by bioactive factors secreted by human umbilical cord-derived MSCs (UCMSCs). It was found that NLRP1 interacts with the adapter protein ASC to form an inflammasome complex, which involves in MCF7 cell pyroptosis. Additionally, neither NLPR1 knockdown nor CASP4 knockdown inhibited the hUCMSC-induced pyroptosis in MCF7, indicating that when one pathway was inhibited, the pyroptosis occurred via another pathway. These findings suggest that elucidating the precise mechanism of hUCMSC-induced pyroptosis in MCF7 could aid in the identification of potential therapeutic agents for breast cancer. D. Miloradovic et al. studied the effects of bone marrow-derived MSCs on anti-melanoma immunity. It was reported that these MSCs play a different role at different stages of melanoma growth. The MSCs showed tumor-suppressive effects at the initial stage of melanoma while opposite effects were shown at the later stage. Therefore, the optimal MSC administration timing is critical for efficient modulation of cancer progression. S. Kim et al. demonstrated the use of extracellular vesicles harvested from adipose-derived stem cells (ASC-derived EVs) to suppress allergic airway inflammation in the mouse models of allergic airway inflammation. It was found that ASC-derived EVs ameliorated allergic airway inflammation through differential expressed genes in the lung such as PON1, Bex2, Igfbp6, Fpr1, and Scgb1c1. In order to study the role of MSC therapy in Alzheimer's disease (AD), H. Lim et al. investigated the inhibition of hyperphosphorylation of tau using human UCMSCs. The authors reported that administration of these cells mitigated the hyperphosphorylation of tau in the AD mouse models through galectin-3 secretion, ameliorating the spatial learning and memory impairments.

Other research articles have improved the knowledge-based of MSCs in several aspects, including characteristics of MSCs isolated from breast cancer patients, efficacy and safety of MSCs in healthy volunteers, proangiogenic activity of MSC secretome, influences of antihypertensive medications on MSCs, development of inducible human MSCs, and effects of mechanical strain on tenogenic differentiation of MSCs. P. Thitilertdecha et al. reported the in-depth characteristics of human ASCs in fresh stromal vascular fraction isolated from breast cancer patients. It was shown that fat tissues collected from the patients contain ASCs with a highly homogenous phenotype similar to the classical bone marrow-derived MSC, which is essential for future investigation of its therapeutic approaches. S. Chin et al. assessed the efficacy and safety of intravenous infusion of allogenic human UCMSCs (CLV-100) in healthy volunteers. Six months after the infusion, subjects infused with a high dose of CLV-100 had higher levels of anti-inflammatory markers (IL1-RA and IL-10) and a lower level of pro-inflammatory marker TNF-α compared to those infused with a low dose of CLV-100. Additionally, all subjects did not have any adverse reactions, suggesting that CLV-100 infusion is safe and beneficial for tissue repair and healing. C. M. Chinnici et al. reported that proangiogenic activity of human fetal dermal cell secretome is mainly contributed by EVs. Depletion of EVs from the secretome was found to impair its ability to induce angiogenesis. Additionally, it was shown that more microRNAs with a validated role in angiogenesis were highly expressed in fetal dermal cell-derived EVs compared to adult dermal cell-derived EVs, suggesting that fetal dermal cell-derived EVs are more effective than their adult counterpart in inducing angiogenesis. N. Satani et al. showed that antihypertensive medications such as losartan, captopril, and atenolol with doses prescribed for stroke patients altered immunomodulatory effects of human MSCs. These findings suggest that the effects of antihypertensive drug on MSCs should be taken into consideration for stroke patients receiving MSC therapy. Chen et al. developed inducible human MSC lines to be employed for studies of specific gene activation or inhibition. They found that human MSC-CRISPRi and human MSC-CRISPRa could be useful in studying genes and genetic pathways regulating lineage-specific differentiation of human MSCs. Nam et al. reported that 8% tensile strain at 1 Hz increased expression levels of tenogenic markers and α-subunit of the epithelium sodium channel (ENaC) in human MSCs. Expression levels of tenogenic markers in MSCs were decreased when ENaC function was inhibited, suggesting that ENaC plays a key role in mechanical strain-mediated tenogenic differentiation of MSCs.

In short, this special issue has given outstanding insights into the therapeutic effects of MSC on numerous diseases and highlighted the remaining obstacles and potential approaches to translate the research findings into clinical applications. With many opportunities and remaining challenges, we envision that there will be more studies focusing on resolving the challenges to improve the effectiveness of MSC therapy in the near future.

Conflicts of Interest

The authors declare no conflict of interest.

Jane Ru Choi
Kar Wey Yong
Hui Yin Nam

References

[1] W. K. Z. W. Safwani, J. R. Choi, K. W. Yong, I. Ting, N. A. M. Adenan, and B. Pingguan-Murphy, "Hypoxia enhances the viability, growth and chondrogenic potential of cryopreserved

human adipose-derived stem cells," *Cryobiology*, vol. 75, pp. 91–99, 2017.

[2] W. Jiang and J. Xu, "Immune modulation by mesenchymal stem cells," *Cell Proliferation*, vol. 53, no. 1, article e12712, 2020.

[3] K. W. Yong, J. R. Choi, A. S. Dolbashid, and W. K. Z. Wan Safwani, "Biosafety and bioefficacy assessment of human mesenchymal stem cells: what do we know so far?," *Regenerative Medicine*, vol. 13, no. 2, pp. 219–232, 2018.

[4] Y. Guo, Y. Yu, S. Hu, Y. Chen, and Z. Shen, "The therapeutic potential of mesenchymal stem cells for cardiovascular diseases," *Cell Death & Disease*, vol. 11, no. 5, pp. 1–10, 2020.

[5] Z.-G. Wang, Z.-Y. He, S. Liang, Q. Yang, P. Cheng, and A.-M. Chen, "Comprehensive proteomic analysis of exosomes derived from human bone marrow, adipose tissue, and umbilical cord mesenchymal stem cells," *Stem Cell Research & Therapy*, vol. 11, no. 1, pp. 1–11, 2020.

[6] J. Phelps, A. Sanati-Nezhad, M. Ungrin, N. Duncan, and A. Sen, "Bioprocessing of Mesenchymal Stem Cells and Their Derivatives: Toward Cell-Free Therapeutics," *Stem Cells International*, vol. 2018, Article ID 9415367, 2018.

[7] K. W. Yong, W. K. Z. W. Safwani, F. Xu et al., "Assessment of tumourigenic potential in long-term cryopreserved human adipose-derived stem cells," *Journal of Tissue Engineering and Regenerative Medicine*, vol. 11, no. 8, pp. 2217–2226, 2017.

[8] M. N. Islam, S. R. Das, M. T. Emin et al., "Mitochondrial transfer from bone-marrow-derived stromal cells to pulmonary alveoli protects against acute lung injury," *Nature Medicine*, vol. 18, no. 5, pp. 759–765, 2012.

Hindawi
Stem Cells International
Volume 2020, Article ID 8877003, 13 pages
https://doi.org/10.1155/2020/8877003

Research Article

High Dose of Intravenous Allogeneic Umbilical Cord-Derived Mesenchymal Stem Cells (CLV-100) Infusion Displays Better Immunomodulatory Effect among Healthy Volunteers: A Phase 1 Clinical Study

Sze-Piaw Chin,[1,2] **Mohd-Yusoff Mohd-Shahrizal**,[2] **Mohd-Zuhar Liyana**,[2] **Kong Yong Then**,[2] **and Soon Keng Cheong**[2,3]

[1]*NSCMH Medical Centre, Seremban, Negeri Sembilan, Malaysia*
[2]*Cytopeutics, Cyberjaya, Malaysia*
[3]*Universiti Tunku Abdul Rahman, Bandar Sungai Long, Selangor, Malaysia*

Correspondence should be addressed to Sze-Piaw Chin; chin.sze.piaw@gmail.com

Received 24 April 2020; Revised 18 June 2020; Accepted 11 July 2020; Published 28 September 2020

Academic Editor: Kar Wey Yong

Background. Mesenchymal stem cells (MSCs) express growth factors and other cytokines that stimulate repair and control the immune response. MSCs are also immunoprivileged with low risk of rejection. Umbilical cord-derived MSCs (UCMSCs) are particularly attractive as an off-the-shelf allogeneic treatment in emergency medical conditions. We aim to determine the safety and efficacy of intravenous allogeneic infusion of UCMSCs (CLV-100) by Cytopeutics® (Selangor, Malaysia) in healthy volunteers, and to determine the effective dose at which an immunomodulatory effect is observed. *Methodology*. Umbilical cord samples were collected after delivery of full-term, healthy babies with written consent from both parents. All 3 generations (newborn, parents, and grandparents) were screened for genetic mutations, infections, cancers, and other inherited diseases. Samples were transferred to a certified Good Manufacturing Practice laboratory for processing. Subjects were infused with either low dose (LD, 65 million cells) or high dose (HD, 130 million cells) of CLV-100 and followed up for 6 months. We measured cytokines using ELISA including anti-inflammatory cytokines interleukin 1 receptor antagonist (IL-1RA), interleukin 10 (IL-10), pro-/anti-inflammatory cytokine interleukin 6 (IL-6), and the proinflammatory cytokine tumor necrosis factor-alpha (TNF-α). *Results*. 11 healthy subjects (LD, $n = 5$; HD, $n = 6$; mean age of 55 ± 13 years) were recruited. All subjects tolerated the CLV-100 infusion well with no adverse reaction throughout the study especially in vital parameters and routine blood tests. At 6 months, the HD group had significantly higher levels of anti-inflammatory markers IL1-RA (705 ± 160 vs. 306 ± 36 pg/mL; $p = 0.02$) and IL-10 (321 ± 27 vs. 251 ± 28 pg/mL; $p = 0.02$); and lower levels of proinflammatory marker TNF-α (74 ± 23 vs. 115 ± 15 pg/mL; $p = 0.04$) compared to LD group. *Conclusion*. Allogeneic UCMSCs CLV-100 infusion is safe and well-tolerated in low and high doses. Anti-inflammatory effect is observed with a high-dose infusion.

1. Introduction

Mesenchymal stem cells (MSCs) are multipotent fibroblast-like cells that reside in various tissues of the human body. MSCs have the capacity to regenerate and replicate as well as to differentiate into various specialized cells and tissues in the body, including chondrocytes, adipocytes, osteocytes, and neuron-like cells [1–3]. The self-renewal and multilineage potentials of MSCs in providing new cells for tissue repair by replacing the damaged cells suggest its therapeutic potentials in tissue regeneration [2, 4–8].

Several studies have reported that the mechanism of MSCs in repairing tissue damage is associated to their immunomodulatory properties rather than its capacity for differentiation [9, 10]. One of MSCs' vital biological function, the immunomodulation, provides MSCs with the ability to

Table 1: Key inclusion and exclusion criteria for the enrolled subjects.

Key inclusion criteria
(i) Men and women aged 40 years and older
(ii) Subjects with normoglycemia
(iii) Subjects with normotension
(iv) Subjects with normal fasting lipid profile
(v) Subject must understand patient information sheet and signed informed consent form
Key exclusion criteria
(i) Subject who has enrolled in another investigational drug trial or innovative therapeutics product-related trial or has completed the aforesaid within 3 months
(ii) Subject with history of current or past use (within 1 year) of alcohol, smoking, or drug abuse
(iii) Pregnant or nursing women
(iv) Subject with known documented drug allergies
(v) Subject who is required of the following medicines on a regular basis: anti-histamine, steroid, antibiotic, anti-inflammatory, immunosuppressant, and pain killer medications
(vi) Subject who is currently on any hormone replacement or hormone suppressive therapy for any indication
(vii) Subject with any acute or chronic infections or communicable diseases including hepatitis B, hepatitis C, or HIV
(viii) Subject with any active or past history of neoplasia and primary hematological disease
(ix) Subject with any renal impairment indicated by serum creatinine $\geq 120\ \mu$mol or creatinine clearance <60 mL/min
(x) Subject with any cardiovascular disease including documented coronary disease of more than 50% stenosis, angina, myocardial infarction, heart failure, stroke, transient ischemic attack, and/or peripheral artery disease
(xi) Subject with any diabetes mellitus
(xii) Subject with any liver impairment indicated by serum aspartate transaminase and alanine transaminase greater than 1.5 times upper limit normal
(xiii) Subject with any chronic pulmonary or airways disease
(xiv) Subject with any current or past history of mental illness or cognitive impairment.

migrate and adhere to any injury or inflammation sites found in the body and thereby interact with various immune cells such as T cells, B cells, natural killer cells, dendritic cells, neutrophils, and macrophages before evoking effective immune responses to ameliorate the intense inflammatory reaction of the injured site via direct cell-cell contact mechanism and/or the release of soluble inducible factors [11–13].

MSCs can be isolated from various tissues including bone marrow, peripheral blood, adipose tissue, cord blood, and umbilical cord. Recent studies have shown that MSCs derived from human umbilical cord (UCMSCs) possess several advantages compared to MSCs isolated from other tissues, including high-proliferation and self-renewal capacity and multilineage differentiation capability. Umbilical cord is considered as a medical waste, and the collection of UC-MSCs is noninvasive which eliminates any ethical concern from its collection. [14, 15]. In addition, UCMSCs possess low immunogenicity allowing them to be utilized in allogeneic transplantation without any rejection and thereby providing a new approach for the treatment of autoimmune diseases [16].

Consequently, UCMSCs have been developed as an "off-the-shelf" cell therapy for a variety of diseases especially in autoimmune diseases. Clinical studies in graft-versus-host disease (aGVHD) have demonstrated that UCMSCs dramatically improved the patients' conditions with no adverse effects and no evidence of cancer recurrence throughout the trial period ([17, 18]). Moreover, UCMSCs treatment in active systemic lupus erythematosus (SLE) resulted in amelioration of the disease activity, serologic changes, and stabilization of proinflammatory cytokines in the patients [19].

The production of UCMSCs cells products from manufacturing methods must be tested for its safety prior to be used as therapeutic agents in cell therapy ([20]). Therefore, this Phase 1 clinical study was conducted to establish a new UCMSCs cell line (CLV-100) by assessing the safety and efficacy of intravenous allogeneic infusion of our manufactured UCMSCs (CLV-100) among healthy volunteers. This study also sought to compare the immunomodulatory effect of different dosage of CLV-100 between high-dose and low-dose infusion in healthy volunteers based on several clinical assessments and measurements of changes in systemic biomarkers. The findings of this study will act as a guideline and benchmark for future CLV-100 clinical research.

2. Materials and Methods

2.1. Study Design. This is an open-label nonrandomized Phase 1 study assessing the safety and efficacy of CLV-100 infusion among 11 healthy subjects recruited at NSCMH Medical Centre in Seremban, Malaysia. The subjects were divided into 2 groups; low-dose group received 65 million cells (equivalent to about 1 million cells per kg body weight) (LD, $n = 5$), while high dose group received 130 million cells (equivalent to about 2 million cells per kg body weight) (HD, $n = 6$) of allogeneic infusion of CLV-100. This study was approved by the Medical Research and Ethics Committee (MREC) Ministry of Health Malaysia (NMRR-13-1152-17400) and monitored by independent Data Safety and Monitoring Board (DSMB). All subjects provided written informed consent before participating in the study. The inclusion and exclusion criteria were listed in Table 1.

2.2. Establishing UCMSCs Culture. Umbilical cord samples were collected after delivery of full-term, healthy babies with

Table 2: Clinical characteristics in recruited subjects during baseline assessment.

Parameter	Normal range	Total ($n = 11$)	Low dose ($n = 5$)	High dose ($n = 6$)	p value[a]
Age	—	55 ± 13	52 ± 14	57 ± 13	0.36
Body weight	—	59.6 ± 9.1	55.2 ± 9.4	63.3 ± 7.6	0.15
Male	—	4	2	2	0.82
Female	—	7	3	4	0.82
Routine blood tests					
WBC ($\times 10^9$/L)	4.0-11.0	**6.7 ± 0.9**	**6.0 ± 0.5**	**7.3 ± 0.9**	**0.03***
Hemoglobin (g/dL)	11.5-16.5	13.4 ± 1.4	13.0 ± 1.6	13.8 ± 1.2	0.20
HCT (%)	35-47	41.2 ± 3.7	40.4 ± 3.8	41.9 ± 3.8	0.41
MCV (fl)	76-96	86.1 ± 4.0	86.4 ± 5.5	86.0 ± 2.8	0.52
Platelet ($\times 10^9$/L)	150-400	292 ± 55	292 ± 76	292.7 ± 38	0.72
Creatinine (μmol/L)	44-97	69.2 ± 21.3	65.8 ± 27.3	72.0 ± 17.2	0.36
ESR (mm/hr)	0-20	17.5 ± 17.5	14.4 ± 12.2	20.0 ± 21.9	0.86
AST (IU/L)	0-40	22.2 ± 6.5	19.6 ± 2.6	24.3 ± 8.1	0.27
ALT (IU/L)	0-53	20.7 ± 13.6	16.2 ± 4.4	24.5 ± 17.8	0.52
Albumin (g/L)	30-50	43.6 ± 3.5	44.5 ± 4.4	42.8 ± 2.8	0.58
Globulin (g/L)	20-50	30.9 ± 2.1	30.3 ± 2.6	31.3 ± 1.6	0.46
A/G ratio	1.2-2.5	1.4 ± 0.2	1.5 ± 0.2	1.4 ± 0.2	0.40
Total cholesterol (mmol/L)	<5.2	5.5 ± 0.9	5.4 ± 0.4	5.5 ± 1.3	0.71
HbA1c (%)	3.0-6.0	5.5 ± 0.4	5.7 ± 0.3	5.2 ± 0.4	0.07
FBS (mmol/L)	3.9-5.6	4.7 ± 0.4	4.7 ± 0.3	4.7 ± 0.5	0.93
Insulin (mU/L)	3.0-25.0	6.1 ± 5.6	7.6 ± 8.4	4.9 ± 1.6	1.00
IGF-1(ng/mL)	87-238	166.4 ± 57.5	161 ± 66.2	169.6 ± 59.6	0.88
DHEAS (μmol/L)	1.0-11.7	3.0 ± 2.3	1.5 ± 1.5	3.8 ± 2.3	0.10
Estradiol (pg/mL)	50-100	66.5 ± 79.1	78.9 ± 107.2	54.0 ± 60.7	0.83
Progesterone (ng/mL)	0.57-6.11	2.3 ± 5.1	0.29 ± 0.1	4.4 ± 7.3	0.82
Testosterone (ng/mL)	2.41-8.27	3.8 ± 2.0	-[b]	3.8 ± 2.0	-[b]
hs-CRP (mg/L)	<4.7	1.1 ± 1.5	0.6 ± 0.5	1.6 ± 1.9	0.58
IgE (IU/mL)	<158.0	38.4 ± 42.5	23.3 ± 19.2	49.7 ± 54.5	0.48
Total PSA (ng/mL)	0.0-4.0	1.8 ± 0.7	1.2 ± 0.6	2.3 ± 0.1	0.12
CA125 (U/mL)	<35.0	9.7 ± 4.8	12.8 ± 6.4	7.4 ± 1.6	0.08
CA15.3 (U/mL)	<28.0	8.2 ± 4.5	8.3 ± 4.2	8.2 ± 5.4	0.72
CEA (ng/mL)	<5.0	0.9 ± 0.5	0.8 ± 0.3	1.0 ± 0.6	1.00
CA19.9 (U/mL)	<37.0	19.4 ± 9.1	22.1 ± 7.7	17.1 ± 10.3	0.36
AFP (ng/mL)	<15.0	**3.1 ± 2.1**	**1.7 ± 0.4**	**4.2 ± 2.3**	**0.04***
Vital signs					
SBP (mmHg)	<129	121 ± 12	116 ± 8	125 ± 14	0.14
DBP (mmHg)	<80	75 ± 5	76 ± 6	75 ± 5	0.71
Heart rate (beats/min)	60-100	72 ± 9	73 ± 14	70 ± 5	0.27
Lung function tests					
FEV1 (L)	2.5-4.5	2.5 ± 0.5	2.6 ± 0.6	2.4 ± 0.4	0.36
FVC (L)	2.5-4.5	2.8 ± 0.6	2.9 ± 0.9	2.8 ± 0.3	0.86
FEV1/FVC (%)	>75	89 ± 7	92 ± 6	86 ± 7	0.20
Biomarkers					
IL-6 (pg/mL)	—	16 ± 5	18 ± 6	15 ± 3	0.36

Table 2: Continued.

Parameter	Normal range	Total ($n = 11$)	Low dose ($n = 5$)	High dose ($n = 6$)	p value[a]
IL-10 (pg/mL)	—	269 ± 64	289 ± 42	258 ± 74	0.30
PGE2 (pg/mL)	—	2947 ± 1417	3795 ± 2017	2523 ± 969	0.44
IL1-RA (pg/mL)	—	440 ± 117	447 ± 117	436 ± 128	0.80
TNF-α (pg/mL)	—	96 ± 29	118 ± 10	85 ± 30	0.12
TGF-β (ng/mL)	—	37 ± 5	35 ± 6	37 ± 4	0.80
VEGF (pg/mL)	—	528 ± 383	475 ± 281	556 ± 448	1.00
HGF (pg/mL)	—	855 ± 344	678 ± 254	944 ± 368	0.20

[a]The Mann–Whitney test. [b]Data too low to be computed. *Significant value at $p < 0.05$. Abbreviation: WBC: white blood cells; MCV: mean corpuscular volume; HCT: hematocrit; A/G: albumin/globulin; ESR: erythrocyte sedimentation rate; AST: aspartate aminotransferase; ALT: alanine transaminase; HbA1c: hemoglobin A1c; FBS: fasting blood sugar; IGF-1: insulin growth factor-1; DHEAS: dehydropiandrosterone sulphate; SBP: systolic blood pressure; DBP: diastolic blood pressure; FEV1: forced expiratory volume in one second; FVC: forced vital capacity; hs-CRP: high-sensitivity C-reactive protein; IgE: immunoglobulin E; IL-6: interleukin 6; IL-10: interleukin 10; PGE2: prostaglandin E2; IL1-RA: interleukin 1 receptor antagonist; TNF-α: tumor necrosis factor-alpha.

written consent from both parents. All 3 generations (newborn, parents, and grandparents) were screened for genetic mutations, infections, cancers, and other inherited diseases before the samples were transferred to the laboratory for processing. All cell processing was done in a certified Good Manufacturing Practice (GMP) laboratory in accordance with Malaysia Guidelines for Stem Cell Research and Therapy as published previously [4, 5]. Isolation and culturing have been established and reported previously [21]. The high-quality umbilical cord was digested, and MSCs were isolated based on adherence to flask's surface. The cells then were expanded in proprietary growth medium kept in 37°C, 5% CO_2, and 95% air incubator. After three days, nonadherent cells were discarded and replaced with new growth medium until it reached confluence. Then, the MSCs were cultured in new flasks until the required cell number was achieved. The first few early passages of the cells were cryopreserved and served as a seed for future use. For this study, cells were thawed and expanded from the seed up until Passage 6. Throughout the process, UCMSCs were tested for quality control purposes including immunophenotyping, differentiation assays, as well as to confirm the absence of bacterial, fungal, and mycoplasma contamination.

2.3. Infusion of UCMSCs, Monitoring, and Follow-Up. On the day of CLV-100 infusion, the eligible subjects registered to a medical centre as outpatients. The subjects underwent a routine physical examination, and their vital signs were measured to ensure they were fit and suitable for CLV-100 infusion. Once the subjects were confirmed fit for CLV-100 infusion, a cannula was placed in the subjects' vein. Before CLV-100 infusion, 200 mL of normal saline was infused into subjects for 0.5-1 hours. While waiting for normal saline infusion, 65 million CLV-100 for LD group and 130 million cells for HD group were thawed, washed, and resuspended in 200 mL of normal saline before being infused intravenously to the subjects for 1 hour. Upon completion, 50 mL of normal saline solution was infused to keep the vein open. All standard precautions for intravenous procedure were observed according to routine and standard practice at the medical centre. The subjects were monitored for vital sign and adverse event (AE) (if any) every 15 minutes during infusion and later on an hourly basis for a minimum of 6 hours in the medical centre. We followed the Good Clinical Practice (GCP) guidelines of the International Council for Harmonization (ICH) in defining our AE. The classifications of AE in this study include any untoward medical occurrence in the study subject administered with CLV-100 which may or may not related to the Investigational Product (IP). The monitored AE included but not limited to fever, headache, injection site swelling, or pain. The subjects were discharged if there were no other complications observed after the monitoring period.

Subjects were required to do the 4 times of follow-up (2, 30, 90, and 180 days) postinfusion. During all follow-up, 20 mL blood was withdrawn from the subjects for blood analysis. Subjects were required to immediately inform the medical centre if there is any AE or severe adverse event (SAE).

2.4. Outcome Measures. Baseline data were collected from each subject prior to CLV-100 infusion and information regarding subject particulars; demographic data and medical history were properly recorded. Several clinical assessments were performed at baseline (before CLV-100 infusion) and during postinfusion follow-ups at 2, 30, 90, and 180 days, including routine blood tests, hypersensitivity tests (specifically white cell count, subfraction, and immunoglobulin E), vital signs, lung function tests specifically in the ratio of forced expiratory volume in 1 second to forced vital capacity (FEV1/FVC) via spirometry, renal function tests, liver function tests, full blood count, level of the proinflammatory and the anti-inflammatory markers such as high-sensitivity C-reactive protein (hs-CRP), and albumin globulin ratio (A/G), respectively, as well as cytokines, to examine any changes in the results in each of the subjects.

The primary endpoint of this study was to evaluate the presence or absence of allergic reaction to the infusion, sepsis, organ failure (clinically apparent or subclinical), hospitalization, cancers, and death, as well as any changes in clinical,

Table 3: Baseline and follow-up clinical assessments among subjects in the LD group.

Parameters	Baseline day 0	Follow-up period				p value[a]
		Day 2	Day 30	Day 90	Day 180	
Routine blood tests						
WBC ($\times 10^9$/L)	6.0 ± 0.5	5.4 ± 0.5	5.6 ± 1.3	5.4 ± 1.0	5.8 ± 1.1	0.51
Hemoglobin (g/dL)	13.0 ± 1.6	12.9 ± 1.5	13.0 ± 1.5	13.0 ± 1.6	13.2 ± 1.1	0.74
Creatinine (umol/L)	65.8 ± 27.3	62.6 ± 15.9	66.4 ± 24.0	64.6 ± 14.9	62.6 ± 13.9	0.97
HCT (%)	40.4 ± 3.8	40.0 ± 4.1	40.2 ± 4.1	40.6 ± 4.3	41.4 ± 2.9	0.59
MCV (fl)	86.4 ± 5.5	86.0 ± 4.3	86.2 ± 4.5	85.6 ± 5.4	85.8 ± 4.9	0.72
Platelet ($\times 10^9$/L)	292 ± 77	282 ± 74	282 ± 106	275 ± 3	298 ± 99	0.96
ESR (mm/hr)	14.4 ± 12.2	16.6 ± 11.4	21.6 ± 20.4	15.6 ± 9.5	12.6 ± 6.6	0.69
AST (IU/L)	19.6 ± 2.6	21.6 ± 3.3	20.2 ± 2.2	22.6 ± 4.6	21.4 ± 3.2	0.34
ALT (IU/L)	16.2 ± 4.4	16.2 ± 5.9	16 ± 3.9	17.2 ± 4.7	17.4 ± 1.3	0.92
Albumin (g/L)	44.5 ± 4.4	42.2 ± 3.2	42.2 ± 3.8	43.2 ± 3.5	41.6 ± 2.1	0.07
Globulin (g/L)	30.3 ± 2.6	31.2 ± 2.3	31.2 ± 3.5	31.2 ± 4.2	30.8 ± 2.9	0.96
A/G ratio	1.5 ± 0.2	1.3 ± 0.2	1.4 ± 0.2	1.4 ± 0.2	1.4 ± 0.2	0.06
Total cholesterol (mmol/L)	5.4 ± 0.4	5.2 ± 0.3	5.1 ± 0.5	5.4 ± 0.6	5.3 ± 0.6	0.59
HbA1c (%)	5.7 ± 0.3	—	5.7 ± 0.4	5.7 ± 0.3	5.6 ± 0.3	0.78
FBS (mmol/L)	4.7 ± 0.3	—	4.8 ± 0.3	4.7 ± 0.4	4.6 ± 0.3	0.64
Insulin (mU/L)	7.6 ± 8.4	—	4.4 ± 2.6	2.9 ± 2.0	3.8 ± 0.3	0.68
IGF-1 (ng/mL)	161 ± 66.2	—	123.4 ± 27.4	127.9 ± 44.0	133.2 ± 58.1	0.62
DHEAS (μmol/L)	1.5 ± 1.5	—	1.1 ± 1.1	1.4 ± 1.1	1.2 ± 0.7	0.46
Estradiol (pg/mL)	78.9 ± 107.2	—	85.9 ± 123.3	51.7 ± 40.2	62.4 ± 71.9	0.90
Progesterone (ng/mL)	0.29 ± 0.1	—	7.3 ± 12.3	0.2 ± 0.0	5.7 ± 9.7	0.52
Testosterone (ng/mL)	-[b]	—	-[b]	-[b]	-[b]	-[b]
hs-CRP (mg/L)	**0.6 ± 0.5**	**3.5 ± 3.2**	**2.1 ± 3.3**	**1.1 ± 1.1**	**1.5 ± 1.8**	**0.03**[*]
IgE (IU/mL)	23.3 ± 19.2	23.3 ± 18.4	24.6 ± 19.6	20.9 ± 16.6	22.1 ± 12.0	0.14
Total PSA (ng/mL)	1.2 ± 0.6	—	1.3 ± 1.0	1.2 ± 0.8	1.2 ± 0.9	0.90
CA125 (U/mL)	12.8 ± 6.4	—	11.6 ± 4.5	12.4 ± 5.5	11.3 ± 3.4	0.90
CA15.3 (U/mL)	8.3 ± 4.2	—	9.5 ± 5.4	8.6 ± 4.0	8.6 ± 3.0	0.82
CEA (ng/mL)	0.8 ± 0.3	—	1.1 ± 0.5	0.8 ± 0.3	0.9 ± 0.3	0.23
CA19.9 (U/mL)	22.1 ± 7.7	—	19.4 ± 11.3	19.5 ± 10.2	18.3 ± 9.4	0.52
AFP (ng/mL)	1.7 ± 0.4	—	1.3 ± 0.1	2.2 ± 0.9	1.5 ± 0.3	0.14
Vital signs						
SBP (mmHg)	116 ± 8	119 ± 19	121 ± 18	120 ± 11	117 ± 16	0.89
DBP (mmHg)	76 ± 6	73 ± 8	75 ± 8	78 ± 6	75 ± 6	0.21
Heart rate (beats/min)	73 ± 14	66 ± 10	72 ± 12	71 ± 11	68 ± 13	0.40
Lung function tests						
FEV1 (L)	2.6 ± 0.6	—	—	2.5 ± 0.5	2.3 ± 0.5	0.13
FVC (L)	2.9 ± 0.9	—	—	2.9 ± 0.5	2.7 ± 0.7	0.82
FEV1/FVC (%)	92 ± 6	—	—	87 ± 6	89 ± 9	0.25
Biomarkers						
IL-6 (pg/mL)	18 ± 6	19 ± 14	10 ± 4	—	12 ± 4	0.56
IL-10 (pg/mL)	289 ± 42	271 ± 37	231 ± 13	—	251 ± 28	0.21
PGE2 (pg/mL)	3795 ± 2017	3198 ± 1076	2431 ± 923	—	3206 ± 1533	0.76
IL1-RA (pg/mL)	447 ± 117	415 ± 126	434 ± 225	—	306 ± 36	0.22

Table 3: Continued.

Parameters	Baseline day 0	Follow-up period				p value[a]
		Day 2	Day 30	Day 90	Day 180	
TNF-α (pg/mL)	118 ± 10	115 ± 15	93 ± 16	—	78 ± 3	0.06
TGF-β (ng/mL)	35 ± 6	33 ± 11	28 ± 6	—	35 ± 6	0.54
VEGF (pg/mL)	475 ± 281	648 ± 273	723 ± 258	—	773 ± 258	0.27
HGF (pg/mL)	678 ± 254	859 ± 169	1268 ± 307	—	1037 ± 170	0.13

[a]The Friedman test. [b]Data too low to be computed. *Significant value at $p < 0.05$.

functional parameters and blood tests during the 6 months follow-up period.

2.5. Detection of Cytokines and Growth Factors with ELISA. Serum of every subject during day 0, day 2, day 7, day 30, and day 180 postinfusion was collected and kept frozen at -80°C to allow batch analysis at the end of the study. The anti-inflammatory cytokines including interleukin-10 (IL-10), interleukin-1-receptor antagonist (IL-1RA), and prostaglandin E2 (PGE2); proinflammatory cytokines such as interleukin-6 (IL-6) and tumor necrosis factor-alpha (TNF-α); as well as growth factors including transforming growth factor-beta (TGF-β), vascular endothelial growth factor (VEGF), and hepatocyte growth factor (HGF) were detected and measured with enzyme-linked immunosorbent assay (ELISA) kits (R&D System, USA) in duplicates according to manufacturer's instructions.

2.6. Statistical Analysis. Data analysis was performed by IBM SPSS Statistic v23.0 software (SPSS, Inc., Armonk, NY, USA). Missing data on the primary efficacy variable had their data imputed by the method of Last Observation Carried Forward (LOCF), and the data were presented as means ± SD. The safety of intravenous infusion of CLV-100 towards the subjects was assessed via descriptive statistic analysis. Differences in side effects and blood test between the group of low dose and high dose were calculated using Fisher's exact test (for categorical data) and Mann–Whitney test (for numerical data). As for the efficacy analysis, Mc Nemar test (for categorical data) and Wilcoxon signed rank test (for numerical data) were used to assess the difference (if any) between pre- and post-CLV-100 infusion. It was considered statistically significant when the value of $p < 0.05$.

3. Results

3.1. Baseline Assessments. Throughout the study period, 11 healthy volunteers (male: 4, female: 7) were screened and recruited between May 2017 and January 2018 into the study. As shown in Table 2, the mean age of the subjects during baseline was 55 ± 13 years old. About 1.1 ± 0.2 million cells per kg and 2.1 ± 0.3 million cells per kg were infused into LD subjects and HD subjects, respectively. There were no significant differences were observed in all clinical routine parameters between the two groups except HD subjects have higher but normal white blood cells (WBC) count (7.3 ± 0.9 vs. $6.0 \pm 0.5 \times 10^9$/L; $p = 0.03$) and alpha-fetoprotein (AFP) level (4.2 ± 2.3 vs. 1.7 ± 0.4 ng/mL; $p = 0.04$) compared to LD subjects. We have further looked into individual WBC and AFP parameters. All subjects (either LD or HD) were within the normal range ($4.0 - 11.0 \times 10^9$/L for WBC and less than 10 ng/mL for AFP). Further on that, from 30 to 180 days (to the end of the study) postinfusion follow-up, no statistical significant differences were observed in WBC and AFP parameters.

3.2. Tolerability, Hypersensitivity and Adverse Reactions. Similar clinical assessments were examined throughout the 6-months follow-up among all recruited subjects in both groups to assess the safety of allogeneic CLV-100 infusion as shown in Table 3 and Table 4. All subjects tolerated the CLV-100 infusion well. There were no significant different changes in vital signs variables before, during, and after the CLV-100 in both groups. There was a small but significant increase in hemoglobin (13.8 ± 1.2 vs. 14.4 ± 1.3 g/dL; $p = 0.04$) and MCV (86.0 ± 2.8 vs. 88.2 ± 3.9 fl; $p = 0.02$) at 6 months in HD group.

Specifically, the immunoglobulin E (IgE), which is normally raised in hypersensitivity reactions, remained low within the normal range for both LD (23.3 ± 19.2 vs. 22.1 ± 12.0 IU/mL; $p = 0.14$) and HD (49.7 ± 54.5 vs. 50.2 ± 53.3; $p = 0.79$) groups throughout the study although the values are not significant. Similarly, there was no increase or decrease in total white cell count or its subfractions after infusion. For the lung function test, no significant difference was observed in both FEV1 (2.4 ± 0.4 vs. 2.3 ± 0.2 L; $p = 0.79$) and FEV1/FVC (86 ± 7 vs. 83 ± 6%; $p = 0.95$) levels throughout the follow-up period in HD group. In addition, there were no reported AE or SAE among all subjects throughout the 6 months follow-up period.

3.3. Immunomodulatory Effect of CLV-100 by Measurement of Cytokines. The immunomodulatory effect of CLV-100 infusion in the healthy volunteers of both dosage groups was measured based on the changes in systemic biomarkers detected in the subjects' collected sera. The cytokines levels of the subjects in LD and HD groups were compared between baselines and postinfusion.

In the HD group, the serum level of anti-inflammatory IL-1RA was significantly elevated from day 0 to day 2 (436 ± 128 vs. 610 ± 176 pg/mL; $p = 0.03$), day 30 (436 ± 128 vs. 615 ± 148 pg/mL; $p = 0.03$), and day 180 (436 ± 128 vs. 705 ± 160 pg/mL; $p = 0.03$) postinfusion as depicted in Figure 1. The remaining cytokines (IL-10, IL-6, PGE2, and TNF-α) did not

Table 4: Baseline and follow-up clinical assessments among subjects in the HD group.

Parameters	Baseline day 0	Follow-up period				p value[a]
		Day 2	Day 30	Day 90	Day 180	
Routine blood tests						
WBC ($\times 10^9$/L)	7.3 ± 0.9	6.4 ± 0.7	6.6 ± 0.9	6.6 ± 1.3	6.8 ± 0.7	0.69
Hemoglobin (g/dL)	**13.8 ± 1.2**	**13.6 ± 1.4**	**13.5 ± 1.1**	**14.1 ± 1.1**	**14.4 ± 1.3**	**0.04***
HCT (%)	41.9 ± 3.8	42.0 ± 4.2	42.0 ± 2.9	43.0 ± 3.3	43.7 ± 3.9	0.12
MCV (fl)	**86.0 ± 2.8**	**87.5 ± 3.0**	**87.5 ± 3.7**	**88.3 ± 3.3**	**88.2 ± 3.9**	**0.02***
Platelet ($\times 10^9$/L)	293 ± 39	286 ± 36	297 ± 30	299 ± 26	298 ± 34	0.20
Creatinine (μmol/L)	72.0 ± 17.2	68.8 ± 21.6	70.5 ± 20.2	67.8 ± 13.9	74.7 ± 14.1	0.50
ESR (mm/hr)	20.0 ± 21.9	21.0 ± 16.4	19.5 ± 17.4	17.2 ± 16.0	18.8 ± 19.2	0.13
AST (IU/L)	24.3 ± 8.1	23.3 ± 6.3	23.0 ± 6.4	25.3 ± 4.3	24.2 ± 5.3	0.81
ALT (IU/L)	24.5 ± 17.8	23.3 ± 12.8	21.0 ± 10.3	24.3 ± 13.6	23.2 ± 10.6	0.77
Albumin (g/L)	42.8 ± 2.8	43.2 ± 3.9	43.5 ± 2.9	43.5 ± 2.4	44.2 ± 2.9	0.23
Globulin (g/L)	**31.3 ± 1.6**	**29.5 ± 1.6**	**28.5 ± 1.2**	**28.3 ± 1.6**	**27.8 ± 1.6**	**0.01***
A/G ratio	**1.4 ± 0.2**	**1.5 ± 0.1**	**1.5 ± 0.1**	**1.6 ± 0.1**	**1.6 ± 0.1**	**0.01***
Total cholesterol (mmol/L)	5.5 ± 1.3	5.3 ± 1.0	5.3 ± 0.9	5.4 ± 0.7	6.1 ± 1.3	0.09
HbA1c (%)	5.2 ± 0.4	—	5.5 ± 0.3	5.5 ± 0.4	5.6 ± 0.4	0.08
FBS (mmol/L)	4.7 ± 0.5	—	4.4 ± 0.5	4.4 ± 0.3	4.6 ± 0.3	0.20
Insulin (ng/mL)	4.9 ± 1.6	—	5.2 ± 1.8	5.7 ± 3.6	4.3 ± 2.6	0.14
IGF-1(ng/mL)	169.6 ± 59.6	—	156.4 ± 69.1	155.6 ± 83.3	148.8 ± 44.9	0.78
DHEAS (μmol/L)	3.8 ± 2.3	—	3.2 ± 2.5	3.7 ± 2.6	3.4 ± 2.3	0.12
Estradiol (pg/mL)	54.0 ± 60.7	—	38.6 ± 35.4	66.7 ± 55.0	111.0 ± 87.1	0.15
Progesterone (ng/mL)	4.4 ± 7.3	—	0.9 ± 1.3	0.3 ± 0.1	7.1 ± 12.0	0.86
Testosterone (ng/mL)	3.8 ± 2.0	—	3.8 ± 1.1	5.5 ± 0.5	4.1 ± 1.9	0.62
hs-CRP (mg/L)	**1.6 ± 1.9**	**5.3 ± 4.5**	**1.6 ± 1.6**	**2.7 ± 2.1**	**1.8 ± 2.3**	**0.04***
IgE (IU/mL)	49.7 ± 54.5	46.8 ± 48.4	48.6 ± 52.5	46.1 ± 49.2	50.2 ± 53.3	0.79
Total PSA (ng/mL)	2.3 ± 0.1	—	1.4 ± 0.8	1.4 ± 0.9	1.5 ± 1.0	0.24
CA125 (U/mL)	7.4 ± 1.6	—	7.6 ± 2.8	7.3 ± 1.4	6.5 ± 1.9	0.96
CA15.3 (U/mL)	8.2 ± 5.4	—	8.1 ± 6.1	8.9 ± 7.2	9.6 ± 6.1	0.31
CEA (ng/mL)	1.0 ± 0.6	—	0.9 ± 0.4	0.9 ± 0.5	1.1 ± 0.9	0.21
CA19.9 (U/mL)	17.1 ± 10.3	—	17.0 ± 9.0	15.0 ± 9.1	13.6 ± 11.0	0.06
AFP (ng/mL)	4.2 ± 2.3	—	4.2 ± 2.7	3.8 ± 2.2	4.3 ± 3.1	0.88
Vital signs						
SBP (mmHg)	125 ± 14	120 ± 12	118 ± 17	131 ± 14	125 ± 11	0.16
DBP (mmHg)	75 ± 5	77 ± 5	74 ± 9	76 ± 9	77 ± 5	0.21
Heart rate (beats/min)	70 ± 5	70 ± 3	67 ± 5	71 ± 10	66 ± 2	0.39
Lung function tests						
FEV1 (L)	2.4 ± 0.4	2.3 ± 0.1	—	2.3 ± 0.2	2.3 ± 0.2	0.79
FVC (L)	**2.8 ± 0.3**	**2.7 ± 0.3**	**—**	**2.8 ± 0.3**	**2.8 ± 0.3**	**0.03***
FEV1/FVC (%)	86 ± 7	84 ± 7	—	82 ± 4	83 ± 6	0.95
Biomarkers						
IL-6 (pg/mL)	14 ± 4	13 ± 4	22 ± 7	—	23 ± 5	0.06
IL-10 (pg/mL)	258 ± 74	215 ± 39	307 ± 49	—	321 ± 27	0.13
PGE2 (pg/mL)	2523 ± 969	4987 ± 4059	3208 ± 853	—	3378 ± 691	0.19
IL1-RA (pg/mL)	**436 ± 128**	**610 ± 176**	**615 ± 148**	**—**	**705 ± 160**	**0.03***

Table 4: Continued.

Parameters	Baseline day 0	Follow-up period				p value[a]
		Day 2	Day 30	Day 90	Day 180	
TNF-α (pg/mL)	84 ± 30	74 ± 23	71 ± 15	—	67 ± 19	0.67
TGF-β (pg/mL)	37 ± 4	38 ± 5	34 ± 9	—	37 ± 8	0.42
VEGF (pg/mL)	556 ± 448	510 ± 134	599 ± 335	—	515 ± 297	0.58
HGF (pg/mL)	944 ± 368	1152 ± 436	1174 ± 539	—	1124 ± 628	0.58

[a]The Friedman test. *Significant value at $p < 0.05$.

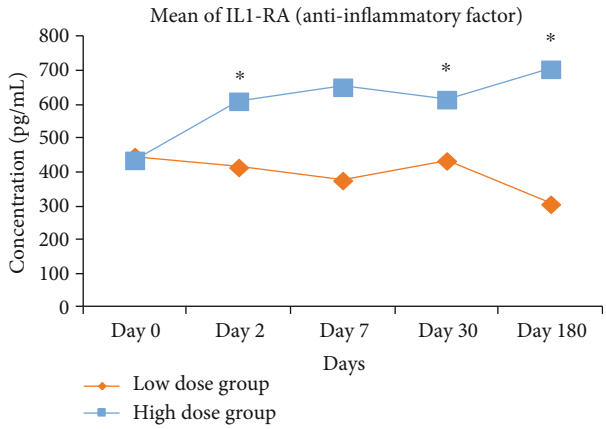

Figure 1: Serum level of IL1-RA measured in every follow-up visits for all subjects in the LD and HD group. The anti-inflammatory IL-1RA was significantly elevated in HD subjects from day 2 to day 180 relative to baseline. Statistical significance of biomarkers between each follow-up visits was assessed by using the Wilcoxon signed-rank test. *Significant value at $p < 0.05$ when compared with baseline.

show any statistical significant mean changes from baseline throughout the monitoring period. In the LD group, the serum levels of IL-10, IL-1RA, IL-6, PGE2, and TNF-α did not show any significant changes within group for each of the follow-up visits as compared to baseline.

The serum cytokines levels at different time points were also compared between LD and HD group (Figure 2). The serum levels of anti-inflammatory factors IL1-RA (705 ± 160 vs. 306 ± 36 pg/mL; $p = 0.02$) and IL-10 (321 ± 27 vs. 251 ± 28 pg/mL; $p = 0.02$) were significantly greater at day 180 post-infusion in HD group than in LD group. In addition, the serum level of proinflammatory factor TNF-α was significantly lower at day 2 (74 ± 23 vs. 115 ± 15 pg/mL; $p = 0.04$) after infusion in the HD group compared to the LD group. Meanwhile, the serum level of IL-6, which has both pro- and anti-inflammatory properties, was significantly higher in HD group at day 30 (22 ± 7 vs. 10 ± 4 pg/mL; $p = 0.05$) postinfusion in relative to LD group, and similar trend was observed as the follow-up continues at day 180 (23 ± 5 vs. 12 ± 4 pg/mL; $p = 0.02$). Finally, there was no significant difference of PGE2 level observed between both groups.

3.4. Albumin Globulin Ratio as a Marker of Anti-Inflammatory State. In the HD group, albumin/globulin (A/G) ratio (1.4 ± 0.2 vs. 1.6 ± 0.1; $p = 0.01$) was significantly elevated, with a corresponding significant drop of globulin (31.3 ± 1.6 vs. 27.8 ± 1.6 g/L; $p = 0.01$) level was observed over 6 months period. When comparing between both groups, the HD subjects have higher A/G ratio compared to the LD subjects at 6 months (1.6 ± 0.1 vs. 1.4 ± 0.2; $p = 0.04$) post-CLV-100 infusion as shown in Figure 3(a).

3.5. Hs-CRP as a Marker of Inflammation, Repair, and Healing. In LD group, high-sensitivity C-reactive protein (hs-CRP) reading was significantly elevated at 2 days postinfusion (0.6 ± 0.5 vs. 3.5 ± 3.2 mg/L; $p = 0.04$) but dropped continuously over 6 months follow-up (1.5 ± 1.8 mg/L; $p = 0.09$). A similar trend was detected among HD subjects where the hs-CRP value significantly raised at 2 days postinfusion (1.6 ± 1.9 vs. 5.3 ± 4.5 mg/L; $p = 0.03$) and subdued tremendously at 6 months (1.8 ± 2.3 mg/L; $p = 0.04$). The hs-CRP serum level in both groups was depicted in Figure 3(b).

3.6. Change in Serum Growth Factors. When the growth factors level of the subjects in LD and HD groups collected sera were measured via systemic biomarkers, all growth factors, which are VEGF (Figure 3(c)), TGF-β (Figure 3(d)), and HGF (Figure 3(e)), did not show any statistical significant mean changes from baseline throughout the monitoring period as well between both groups.

4. Discussion

The main objective of this clinical study was to determine the safety of allogeneic intravenous CLV-100 infusion among healthy volunteers with different doses. Based on the results, there was no complication that occurred during the infusion with no significant AE in both dosage groups during 6 months follow-up, thus demonstrating that UCMSCs infusion was safe among healthy subjects. These outcomes are consistent with other UCMSCs treatment based studies where the group reported that the administration of UCMSCs with the best medical care was safe with reduced ejection fraction among patients with stable heart failure [22]. In addition, UCMSCs infusion posed no SAE among type 2 diabetes mellitus (T2DM) patients with mild improvement in hemoglobin A1c (HbA1c) and fasting blood sugar (FBS) [23].

Apart from assessing the safety of CLV-100 infusion, the outcome of the routine blood tests, lung function tests, and vital parameters in this Phase 1 study demonstrated MSCs' tolerability in allogeneic treatment as it did not trigger or

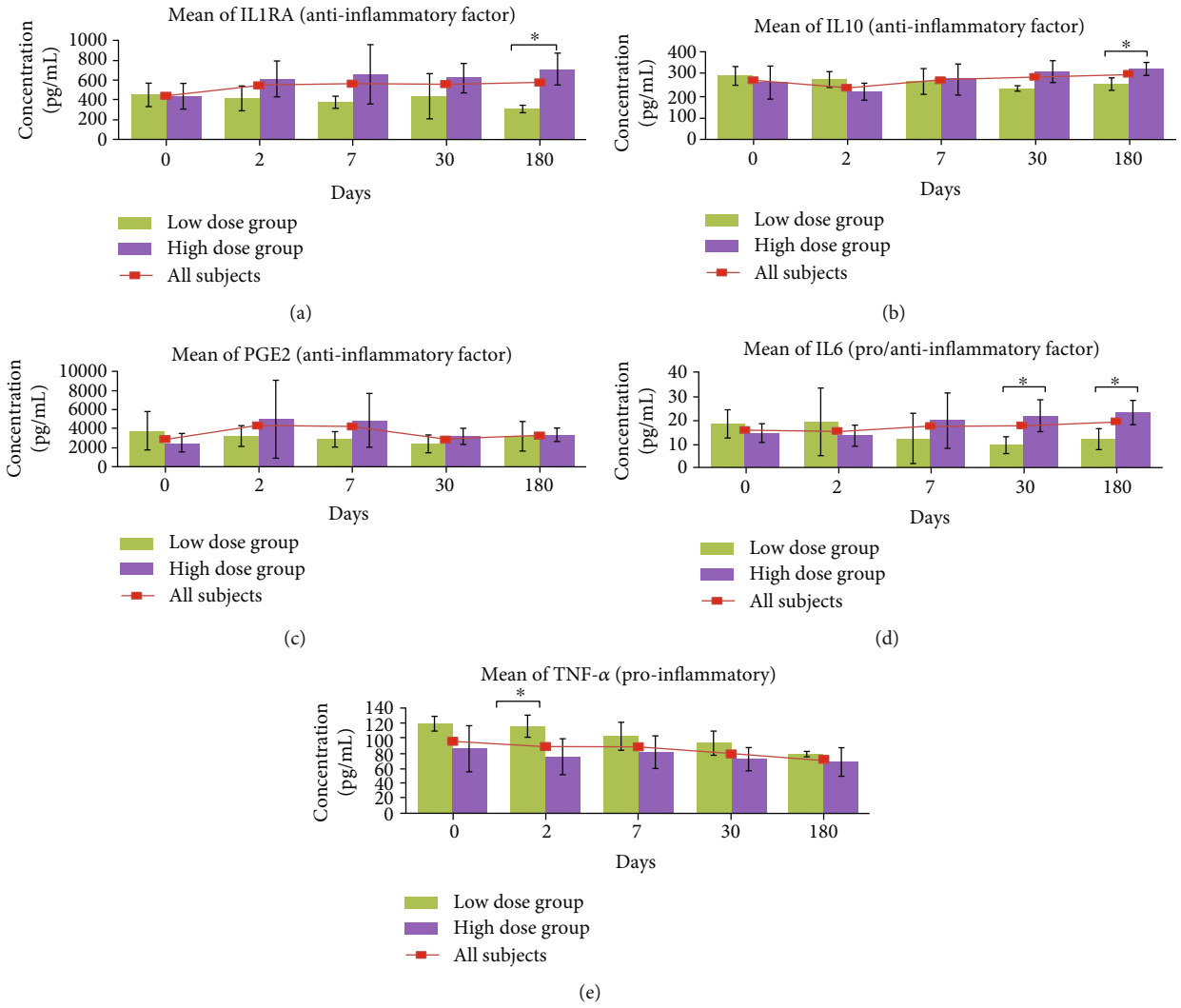

Figure 2: Evaluation of serum levels of cytokines, IL-1RA, IL-10, PGE2, IL-6, and TNF-α, for subjects between LD and HD group. Only serum levels of cytokines IL-1RA, IL-10, IL-6, and TNF-α were found to have significant changes between both groups. Statistical significance of biomarkers between LD and HD groups were assessed by using the Mann–Whitney test. *Significant value at $p < 0.05$.

increase hypersensitivity reactions in both LD and HD groups, which were maintained within the normal range throughout the follow-up period. It has been reported that MSCs administered in patients with moderate-to-severe atopic dermatitis (AD) could reduce allergic symptoms and inflammatory parameters via reduction of serum immunoglobulin E (IgE) levels and eosinophil count without the occurrence of serious AE [24]. We did not demonstrate the decrease in IgE and total white cell count. This is because our study involved healthy volunteers, and it also reaffirms that while MSCs are immunomodulatory, they are not immunosuppressive.

In terms of safety and tolerability, our lung function tests upon CLV-100 administration in both LD and HD groups were consistent with the previous study where MSCs infusion via endobronchial valve (EV) placement was well-tolerated and appear to decrease systemic inflammation in patients with compromised lung function due to severe chronic obstructive pulmonary disease (COPD) without any occurrence of acute administration-related toxicity, SAE, or death reported [25]. These results also proved where lung function test results, gas exchange variables, and blood work obtained after MSCs infusion have no significant alterations with those values obtained before MSCs infusion among patients with bronchiolitis obliterans syndrome [26].

We also found that high-dose CLV-100 infusion provided a significant increase in both hemoglobin level and MCV level that falls within the normal range. Another study indicated that MSCs maintained a better quality of hemoglobin as well as the oxygen-carrying capacity [27] as more hemoglobin helps in controlling the level of nitric oxide, thus expanding the blood vessels for more blood flow. Hemoglobin is also important for immunity where free hemoglobin serves as an alarm molecule that signals bleeding and tissue damage, which drives macrophage production towards a protective, antioxidative macrophage type, that halts lesion progression at later stages of disease [28]. In recent studies, patients with anaemia condition or with inflammatory diseases such as rheumatoid arthritis (RA) frequently have a significant reduction in

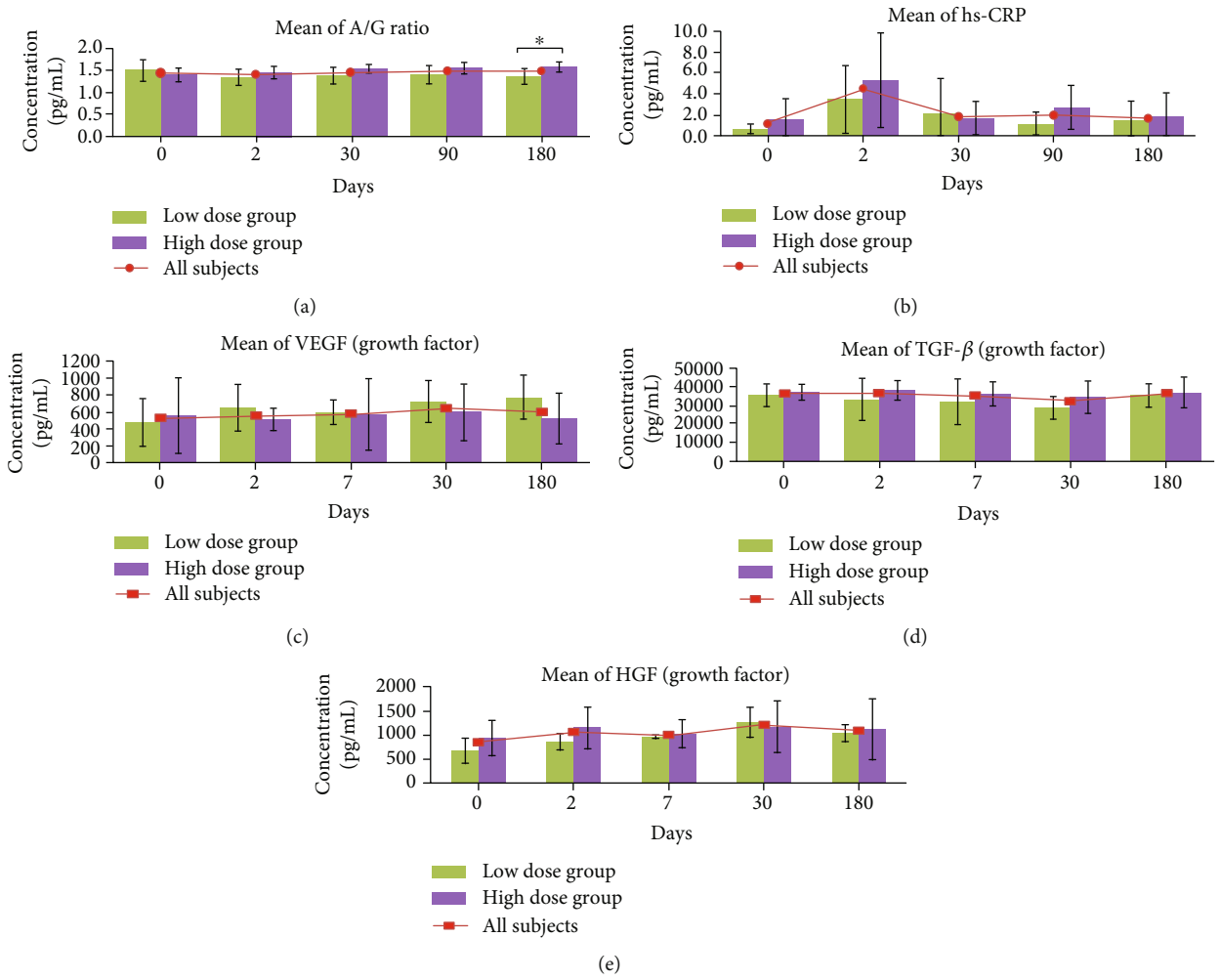

Figure 3: Evaluation of serum levels of A/G ratio, hs-CRP as well as VEGF, TGF-β, and HGF for subjects between LD and HD group. Only serum levels of A/G were found to have significant changes between both groups. Statistical significance of the biomarkers between LD and HD groups were assessed by using the Mann–Whitney test. *Significant value at $p < 0.05$.

hemoglobin and MCV level as compared to healthy or nonanaemic individuals [29, 30]; thus, these indirectly show the importance of MSCs and hemoglobin level towards immunity.

C-reactive protein (CRP) is a nonspecific proinflammatory marker that is commonly produced by the human body under stress condition as a systemic response towards acute infections, inflammatory conditions, and trauma. It plays a role in the recruitment of monocytes, granulocytes, and cytokines to the area of injury and infection to control the damage and initiate repair. As the injury is contained and healing begins, the hs-CRP starts to fall. Persistent hs-CRP, on the other hand, would have indicated or resulted in impaired healing and scarring and may be a risk factor for cardiovascular disease (CVD) [31]. Our results exhibited significant differences in hs-CRP level at different time points in both dosage groups where it was elevated initially followed by gradual declining trend within 6 months.

A similar finding was observed in another study where the hs-CRP and other proinflammatory cytokines including TNF-α and IL-6 raised at 7 days post-MSCs transplantation before receding within 1 month follow-up ([32]). Besides, they reported that the level of IL-10, an anti-inflammatory marker, also peaked at 7 days post-MSCs transplantation which then helped to reduce tissue inflammation after an injury caused by the previously mentioned proinflammatory cytokines [33]. Based on our results, the hs-CRP level was only peaked at 2 days post-MSCs infusion, which later followed by the raised level of IL-10, which peaked on the same day to ease down the inflammation rate even it was not statistically significant. This outcome was also supported by Jiao and colleagues where the levels of CRP and IL-10 were positively correlated among patients with traumatic fracture of lower limb [34].

In addition, the biomarkers assessment results showed a significant steady increase of cytokine IL-1RA level from baseline up until 6 months of posttreatment in the HD group. IL-1RA is a naturally occurring antagonist to the proinflammatory cytokine IL-1 especially IL-1β [35]. It has been reported that elevation in IL-1β activity triggered the increasing level of hs-CRP synthesized in the liver, making hs-CRP to become a surrogate biomarker for IL-1β [36–38]. Hence, due to its anti-inflammatory property, the increasing level of IL-1RA in this study could be

interpreted as a result of the immunoregulatory properties of MSCs to counter-regulate hs-CRP level which also found to be increased in this study. The result is supported by the previous study where hs-CRP and IL-1RA levels were observed to be positively correlated with depressive symptoms in patients with type 2 diabetes (T2D) [39].

Our study clearly demonstrated a difference in immunomodulatory effect between the high dose and low dose. The HD group showed a significantly greater reduction of proinflammatory cytokine TNF-α at day 2 of posttreatment as well as an increased level of anti-inflammatory cytokines, which are IL-6, IL1-RA, and IL-10 within 6 months follow-up in relation to those in LD group. Hence, CLV-100 dosage of 130 million cells or two million MSCs per kilogram of body weight represents the optimal dose level in overcoming inflammatory conditions by displaying the best improvement in all parameters tested, absence of side-effects, and SAE. Our findings were consistent with another study which also concluded UCMSCs dosage of 100 million cells as the optimal dose level in treating frailty disease [40].

Moreover, the data collected in this study suggested that the expression level of IL-6 can be considered as an anti-inflammatory cytokine, because its expression's pattern in HD group is parallel with other anti-inflammatory cytokines, IL-10 and IL-1RA. Although IL-6 possesses proinflammatory properties and often correlates with disease severity, it is also paradoxically linked to anti-inflammatory molecules via complex auto-inhibitory feedback mechanisms where IL-6 plays a protective role in ischemic events by reducing the level of proinflammatory cytokine with the assistance of anti-inflammatory compounds IL-10 in healthy individuals [41].

Lastly, this is the first study that reported the significant changes of A/G ratio and globulin between visits with readings still fall within a normal range in subjects receiving a higher dosage of UCMSCs infusion. Total serum protein test is a common procedure to be included for a health check-up to measure the amount of protein in the body where albumins, globulin, and A/G ratio are the main components to be tested. In this study, a significant reduction of globulin was observed throughout the study. Globulin plays an important role in immunity, and it is known that increases in serum globulins are associated with several immune-mediated diseases (such as rheumatoid diseases, chronic liver disease, nephrotic syndrome, diabetes mellitus, and cancer) as well as related to chronic inflammation [42–44]. Moreover, decrease in globulin level in this study reflects the significant rising level of A/G ratio, a combination of two independent prognostic factors: albumin and globulin. Other researchers examined the relationship between the changes of A/G ratio value with the incidence of chronic diseases in healthy populations, and their findings indicate that healthy subjects with low A/G ratio (<1.1) were found to be at risk for not only liver cancer or hematologic malignancies but all the other common cancers [44]. Besides that, higher A/G ratio due to lower level of globulin may indicate better nutrition, lower inflammation, lower autoimmune disease, and infection and may have a positive effect to the overall survival of patients with solid tumours [42].

5. Conclusion

In conclusion, intravenous allogeneic infusion of CLV-100 was safe, well-tolerated, and free from any concerning AE toward all subjects in both LD and HD groups. Despite the small numbers of subjects, we had demonstrated an initial transient proinflammatory effect followed by a significant and prolonged anti-inflammatory effect. This immunomodulatory effect at high dose was accompanied by beneficial increases in hemoglobin and A/G ratio and with no adverse changes in vital parameters and tests of hypersensitivity. Therefore, high doses of allogenic MSCs could help exert beneficial effects of repair and healing.

Data Availability

The datasets used and/or analyzed during the study are available from the first author upon request.

Conflicts of Interest

All authors have declared that they have no competing interests.

Acknowledgments

The study was sponsored and provided by Cytopeutics Unconditional Research Grant. We would like to thank all staffs from Stem Cell Unit NSCMH Medical Centre for their contribution to the study. Specials thanks to Dato' Dr Rajbans Singh from Pantai Hospital Kuala Lumpur, Ms Manimagelai from NSCMH Medical Centre for their full support and dedication. This study is approved by Malaysia Medical Research and Ethics Committee (NMRR-13-1152-17400 (ISR)). The abstract of this manuscript has been published previously in the 25th International Society Cell & Gene Therapy 2019 Melbourne Annual Meeting with the following DOI: 10.1016/j.jcyt.2019.03.519.

References

[1] P. F. Choong, P. L. Mok, S. K. Cheong, C. F. Leong, and K. Y. Then, "Generating neuron-like cells from BM-derived mesenchymal stromal cells in vitro," *Cytotherapy*, vol. 9, no. 2, pp. 170–183, 2007.

[2] A. D. Ho, W. Wagner, and U. Mahlknecht, "Stem cells and ageing," *EMBO reports*, vol. 6, no. S1, 2005.

[3] Y. Jiang, B. N. Jahagirdar, R. L. Reinhardt et al., "Pluripotency of mesenchymal stem cells derived from adult marrow," *Nature*, vol. 418, no. 6893, pp. 41–49, 2002.

[4] S. P. Chin, A. C. Poey, C. Y. Wong et al., "Intramyocardial and intracoronary autologous bone marrow-derived mesenchymal stromal cell treatment in chronic severe dilated cardiomyopathy," *Cytotherapy*, vol. 13, no. 7, pp. 814–821, 2011.

[5] S. P. Chin, A. C. Poey, C. Y. Wong et al., "Cryopreserved mesenchymal stromal cell treatment is safe and feasible for severe dilated ischemic cardiomyopathy," *Cytotherapy*, vol. 12, no. 1, pp. 31–37, 2010.

[6] J. M. Karp and G. S. Leng Teo, "Mesenchymal stem cell homing: the devil is in the details," *Cell Stem Cell*, vol. 4, no. 3, pp. 206–216, 2009.

[7] L. A. Ortiz, F. Gambelli, C. McBride et al., "Mesenchymal stem cell engraftment in lung is enhanced in response to bleomycin exposure and ameliorates its fibrotic effects," *Proceedings of the National Academy of Sciences of the United States of America*, vol. 100, no. 14, pp. 8407–8411, 2003.

[8] B. R. Troen, "The biology of aging," *Mount Sinai Journal of Medicine*, vol. 70, no. 1, pp. 3–22, 2003.

[9] G. Camussi, M. C. Deregibus, and C. Tetta, "Paracrine/endocrine mechanism of stem cells on kidney repair: role of microvesicle-mediated transfer of genetic information," *Current Opinion in Nephrology and Hypertension*, vol. 19, no. 1, pp. 7–12, 2010.

[10] F. Tögel, K. Weiss, Y. Yang, Z. Hu, P. Zhang, and C. Westenfelder, "Vasculotropic, paracrine actions of infused mesenchymal stem cells are important to the recovery from acute kidney injury," *American Journal of Physiology. Renal Physiology*, vol. 292, no. 5, pp. F1626–F1635, 2007.

[11] A. J. Nauta and W. E. Fibbe, "Immunomodulatory properties of mesenchymal stromal cells," *Blood*, vol. 110, no. 10, pp. 3499–3506, 2007.

[12] S. Shawki, T. Gaafar, H. Erfan, E. El Khateeb, A. El Sheikhah, and R. El Hawary, "Immunomodulatory effects of umbilical cord-derived mesenchymal stem cells," *Microbiology and Immunology*, vol. 59, no. 6, pp. 348–356, 2015.

[13] B. Yang, B. Bai, C. X. Liu et al., "Effect of umbilical cord mesenchymal stem cells on treatment of severe acute pancreatitis in rats," *Cytotherapy*, vol. 15, no. 2, pp. 154–162, 2013.

[14] J. F. Li, H. L. Yin, A. Shuboy et al., "Differentiation of hUC-MSC into dopaminergic-like cells after transduction with hepatocyte growth factor," *Molecular and Cellular Biochemistry*, vol. 381, no. 1-2, pp. 183–190, 2013.

[15] L. L. Lu, Y. J. Liu, S. G. Yang et al., "Isolation and characterization of human umbilical cord mesenchymal stem cells with hematopoiesis-supportive function and other potentials," *Haematologica*, vol. 91, no. 8, pp. 1017–1026, 2006.

[16] M. Meng, Y. Liu, W. Wang et al., "Umbilical cord mesenchymal stem cell transplantation in the treatment of multiple sclerosis," *American Journal of Translational Research*, vol. 10, no. 1, pp. 212–223, 2018.

[17] D. Wang, L. Niu, X. Feng et al., "Long-term safety of umbilical cord mesenchymal stem cells transplantation for systemic lupus erythematosus: a 6-year follow-up study," *Clinical and Experimental Medicine*, vol. 17, no. 3, pp. 333–340, 2017.

[18] K. H. Wu, C. K. Chan, C. Tsai et al., "Effective treatment of severe steroid-resistant acute graft-versus-host disease with umbilical cord-derived mesenchymal stem cells," *Transplantation*, vol. 91, no. 12, pp. 1412–1416, 2011.

[19] L. Sun, D. Wang, J. Liang et al., "Umbilical cord mesenchymal stem cell transplantation in severe and refractory systemic lupus erythematosus," *Arthritis and Rheumatism*, vol. 62, no. 8, pp. 2467–2475, 2010.

[20] Y. Wang, Z. B. Han, Y. P. Song, and Z. C. Han, "Safety of mesenchymal stem cells for clinical application," *Stem Cells International*, vol. 2012, Article ID 652034, 4 pages, 2012.

[21] S. P. Chin, K. Y. Then, C. Y. Wong, G. C. Ooi, and S. K. Cheong, "Allogenic wharton's jelly mesenchymal stromal cells intravenous infusion increase serum insulin-like growth factor-1 and dehydroepi-androsterone in healthy volunteers," *Cytotherapy*, vol. 15, no. 4, p. S18, 2013.

[22] J. Bartolucci, F. J. Verdugo, P. L. González et al., "Safety and efficacy of the intravenous infusion of umbilical cord mesenchymal stem cells in patients with heart failure: a phase 1/2 randomized controlled trial (RIMECARD trial [randomized clinical trial of intravenous infusion umbilical cord mesenchymal stem cells on cardiopathy])," *Circulation Research*, vol. 121, no. 10, pp. 1192–1204, 2017.

[23] J. Hu, Y. Wang, H. Gong et al., "Long term effect and safety of Wharton's jelly-derived mesenchymal stem cells on type 2 diabetes," *Experimental and Therapeutic Medicine*, vol. 12, no. 3, pp. 1857–1866, 2016.

[24] H. S. Kim, J. H. Lee, K. H. Roh, H. J. Jun, K. S. Kang, and T. Y. Kim, "Clinical trial of human umbilical cord blood-derived stem cells for the treatment of moderate-to-severe atopic dermatitis: phase I/IIa studies," *Stem Cells*, vol. 35, no. 1, pp. 248–255, 2017.

[25] H. G. de Oliveira, F. F. Cruz, M. A. Antunes et al., "Combined bone marrow-derived mesenchymal stromal cell therapy and one-way endobronchial valve placement in patients with pulmonary emphysema: a phase I clinical trial," *Stem Cells Translational Medicine*, vol. 6, no. 3, pp. 962–969, 2017.

[26] C. A. Keller, T. A. Gonwa, D. O. Hodge, D. J. Hei, J. M. Centanni, and A. C. Zubair, "Feasibility, safety, and tolerance of mesenchymal stem cell therapy for obstructive chronic lung allograft dysfunction," *Stem Cells Translational Medicine*, vol. 7, no. 2, pp. 161–167, 2018.

[27] Y. Chen, J. Zhang, S. Gu et al., "Mesenchymal stromal cells can be applied to red blood cells storage as a kind of cellular additive," *Bioscience Reports*, vol. 37, no. 5, 2017.

[28] D. J. Schaer and P. W. Buehler, "Cell-free hemoglobin and its scavenger proteins: new disease models leading the way to targeted therapies," *Cold Spring Harbor Perspectives in Medicine*, vol. 3, no. 6, 2013.

[29] E. T. Ali, A. S. Jabbar, and A. N. Mohammed, "A comparative study of interleukin 6, inflammatory markers, ferritin, and hematological profile in rheumatoid arthritis patients with anemia of chronic disease and Iron deficiency anemia," *Anemia*, vol. 2019, Article ID 3457347, 7 pages, 2019.

[30] D. R. Arul and D. P. P. Kumar, "Study of hematological profile in rheumatoid arthritis patients," *IOSR Journal of Dental and Medical Sciences*, vol. 15, no. 9, pp. 96–100, 2016.

[31] D. Kong, H. Wang, Y. Liu, H. Li, H. Wang, and P. Zhu, "Correlation between the expression of inflammatory cytokines IL-6, TNF-α and hs-CRP and unfavorable fetal outcomes in patients with pregnancy-induced hypertension," *Experimental and Therapeutic Medicine*, vol. 16, no. 3, pp. 1982–1986, 2018.

[32] S. S. Wang, S. W. Hu, Q. H. Zhang, A. X. Xia, Z. X. Jiang, and X. M. Chen, "Mesenchymal stem cells stabilize atherosclerotic vulnerable plaque by anti-inflammatory properties," *PLoS One*, vol. 10, no. 8, article e0136026, 2015.

[33] A. Kabłak, T. P. Ziembicka, E. Stępień et al., "Relationship between carotid intima-media thickness, cytokines, atherosclerosis extent and a two-year cardiovascular risk in patients with arteriosclerosis," *Kardiologia Polska*, vol. 69, no. 10, pp. 1024–1031, 2011.

[34] J. Jiao, J. W. Wang, F. Xiao, and Y. C. Huang, "The association between the levels of CRP, IL-10, PLA2, Fbg and prognosis in traumatic fracture of lower limb," *Experimental and Therapeutic Medicine*, vol. 12, no. 5, pp. 3209–3212, 2016.

[35] J. Saltevo, M. Vanhala, H. Kautiainen, E. Kumpusalo, and M. Laakso, "Association of C-reactive protein, interleukin-1 receptor antagonist and adiponectin with the metabolic syndrome," *Mediators of Inflammation*, vol. 2007, 8 pages, 2007.

[36] T. Ahonen, J. Saltevo, M. Laakso, H. Kautiainen, E. Kumpusalo, and M. Vanhala, "Gender differences relating to metabolic syndrome and proinflammation in Finnish subjects with elevated blood pressure," *Mediators of Inflammation*, vol. 2009, Article ID 959281, 6 pages, 2009.

[37] B. Galve-de Rochemonteix, K. Wiktorowicz, I. Kushner, and J. M. Dayer, "C-reactive protein increases production of IL-1α, IL-1β, and TNF-α, and expression of mRNA by human alveolar macrophages," *Journal of Leukocyte Biology*, vol. 53, no. 4, pp. 439–445, 1993.

[38] S. Seppä, S. Tenhola, and R. Voutilainen, "Serum IL-1 receptor antagonist concentrations associate with unfavorable metabolic features in 12-year-old children," *Journal of the Endocrine Society*, vol. 2, no. 8, pp. 870–881, 2018.

[39] C. Herder, A. Schmitt, F. Budden et al., "Association between pro- and anti-inflammatory cytokines and depressive symptoms in patients with diabetes–potential differences by diabetes type and depression scores," *Translational Psychiatry*, vol. 7, no. 11, 2018.

[40] S. Golpanian, D. L. DiFede, A. Khan et al., "Allogeneic human mesenchymal stem cell infusions for aging frailty," *The Journals of Gerontology. Series A, Biological Sciences and Medical Sciences*, vol. 72, no. 11, pp. 1505–1512, 2017.

[41] J. M. Luna, Y. P. Moon, K. M. Liu et al., "High-sensitivity C-reactive protein and interleukin-6-dominant inflammation and ischemic stroke risk: the northern Manhattan study," *Stroke*, vol. 45, no. 4, pp. 979–987, 2014.

[42] J. He, H. Pan, W. Liang et al., "Prognostic effect of albumin-to-globulin ratio in patients with solid tumors: a systematic review and meta-analysis," *Journal of Cancer*, vol. 8, no. 19, pp. 4002–4010, 2017.

[43] T. Koyama, N. Kuriyama, E. Ozaki et al., "Serum albumin to globulin ratio is related to cognitive decline via reflection of homeostasis: a nested case-control study," *BMC Neurology*, vol. 16, no. 1, p. 253, 2016.

[44] B. Suh, S. Park, D. W. Shin et al., "Low albumin-to-globulin ratio associated with cancer incidence and mortality in generally healthy adults," *Annals of Oncology*, vol. 25, no. 11, pp. 2260–2266, 2014.

Hindawi
Stem Cells International
Volume 2020, Article ID 8857344, 11 pages
https://doi.org/10.1155/2020/8857344

Research Article

Generation of Inducible CRISPRi and CRISPRa Human Stromal/Stem Cell Lines for Controlled Target Gene Transcription during Lineage Differentiation

Li Chen,[1,2] **Kaikai Shi**,[1] **Weimin Qiu**,[1] **Lars Aagaard**,[3] **and Moustapha Kassem**[1,4]

[1]*Department of Endocrinology and Metabolism, Molecular Endocrinology Laboratory (KMEB), Odense University Hospital, University of Southern Denmark, Denmark*
[2]*Department of Pathology and Physiopathology, Guilin Medical University, Guilin, 541004 Guangxi, China*
[3]*Department of Biomedicine, Aarhus University, Aarhus C, Denmark*
[4]*Department of Cellular and Molecular Medicine, Danish Stem Cell Center (DanStem), University of Copenhagen, 2200 Copenhagen, Denmark*

Correspondence should be addressed to Li Chen; lchen@health.sdu.dk and Moustapha Kassem; mkassem@health.sdu.dk

Received 21 April 2020; Revised 20 July 2020; Accepted 4 August 2020; Published 19 August 2020

Academic Editor: Hui Yin Nam

Background. Human bone marrow stromal/stem cells (hMSCs, also known as the skeletal stem cells or mesenchymal stem cells) are being employed to study lineage fate determination to osteoblasts, adipocytes, and chondrocytes. However, mechanistic studies employing hMSC have been hampered by the difficulty of deriving genetically modified cell lines due to the low and unstable transfection efficiency. *Methods*. We infected hMSC with a CRISPR/Cas9 lentivirus system, with specific inducible dCas9-coupled transcription activator or repressor: dCas9-KRAB or dCas9-VP64, respectively, and established two hMSC lines (hMSC-CRISPRi and hMSC-CRISPRa) that can inhibit or activate gene expression, respectively. The two cell lines showed similar cell morphology, cell growth kinetics, and similar lineage differentiation potentials as the parental hMSC line. The expression of KRAB-dCas9 or VP64-dCas9 was controlled by the presence or absence of doxycycline (Dox) in the cell culturing medium. To demonstrate the functionality of the dCas9-effector hMSC system, we tested controlled expression of alkaline phosphatase (ALP) gene through transfection with the same single ALP sgRNA. *Results*. In the presence of Dox, the expression of ALP showed 60-90% inhibition in hMSC-CRISPRi while ALP showed more than 20-fold increased expression in hMSC-CRISPRa. As expected, the ALP was functionally active and the cells showed evidence for inhibition or enhancement of in vitro osteoblast differentiation, respectively. *Conclusion*. hMSC-CRISPRi and hMSC-CRISPRa are useful resources to study genes and genetic pathways regulating lineage-specific differentiation of hMSC.

1. Background

Human bone marrow stromal/stem cells (hMSCs, also known as human skeletal or mesenchymal stem cells) are clonal cells present within the bone marrow stroma and are capable of differentiation into various mesoderm-type lineage cells, e.g., osteoblasts, adipocytes and chondrocytes [1]. hMSC has been extensively employed to study the molecular mechanisms of lineage commitment and differentiation and to identify novel factors regulating differentiation processes [2]. We have previously employed global methods of proteomics and transcriptomics to identify specific factors and signaling pathways controlling hMSC differentiation [3–6]. However, follow-up studies focusing on specific factors or a signaling pathway have been hampered by the difficulty in achieving stable hMSC lines that either are deficient or overexpress the target genes of interest at a specific time point of differentiation stages. Moreover, conventional viral mediated gene overexpression in hMSC is technically expensive and time-consuming.

Type II CRISPR-Cas9 system (Clustered Regularly Interspaced Palindromic Repeats–CRISPR-associated 9) is a novel

and powerful technology to manipulate gene expression. It is developed from the bacterial immune system for cleaving foreign DNA [7] and is composed of Cas9 endonuclease and a target-identifying CRISPR RNA (single guide RNA, sgRNA). The sgRNA targets a 18-25 base pair sequence of target gene and thus guides Cas9 to specific DNA sites where it creates a blunt-ended double-stranded break (DSB) within the sequence by its endonuclease activity [8, 9]. This DSB induces the generation of mutations that may cause a frameshift in gene coding sequence [10, 11]. Alternatively, it can supply a repair template with homology to the cut site and facilitates targeted integration of mutation or insertion [12].

Besides the direct gene code editing, the CRISPR-Cas9 system can be employed for studying genetic and epigenetic regulation. The Cas9-sgRNA complex can act as a scaffold to recruit different transcription effectors to specific DNA sequences, allowing gene transcription regulation with either transcriptional activation (CRISPRa) or repression (CRISPRi). This function requires disruption of Cas9 nuclease activity by introducing mutations into two nuclease domains (the RuvC and HNH domains) of Cas9 resulting in a deactivated-Cas9 (dCas9) [13–15]. Artificial transcription factors (effector) fused with dCas9 to form the dCas9-effector and then paired with specific sgRNA can be used to target different genes. Different effector proteins, such as transcription activators or repressors fused to dCas9, can differently activate (CRISPRa) or interfere (CRISPRi) in gene expression. In addition, the CRISPR-dCas9 system can be coupled with inducible systems allowing dynamic control of gene transcription [16].

In the present study, we examined the possibility of developing universal hMSC lines to be employed for studies of specific gene activation or inhibition. We employed a system where dCas9 is fused with two different transcription effectors for either activation or inhibition of gene transcription. One effector is the VP64 activator, an engineered tetramer of the herpes simplex VP16 transcriptional activator domain, which can activate silent genes or upregulate active genes in mammalian cells [16–19]. The second effector is a transcriptional repressor KRAB (Krüppel-associated box) domain of Kox1, an efficient repressor of gene transcription [20]. By infecting hMSC with dCas9-VP64 or dCas9-KRAB lentiviral vectors, respectively, we selected and obtained two hMSC lines to be employed for an easy and quick approach for the activation or inhibition of targeted genes by transfecting targeted sgRNA, and we also showed that the regulation of gene expression is inducible by addition or removal of doxycycline (Dox) in cell culture medium.

2. Methods

2.1. Cell Culture. As a model for primary hMSC, we employed the telomerized hMSC line (hMSC-TERT) which was developed in our lab [21]. The hMSC-TERT was created from primary hMSC derived from the bone marrow sample obtained from a young healthy donor, through stable overexpression of human telomerase reverse transcriptase gene (hTERT). The hMSC-TERT cells express all known markers of hMSC and "stemness" characteristics in vitro and in vivo [21, 22]. For the rest of the manuscript, we will refer to the cell line as hMSC. HEK293T is a human cell line, derived from the HEK 293 cell line and expressing a mutant version of the SV40 large T antigen, and was employed to produce recombinant viruses. Cells were cultured in Minimum Essential Medium (MEM) with 10% fetal bovine serum (FBS) and penicillin-streptomycin (P/S) (1%). All cell culture reagents were purchased from Life Technologies (Taastrup, Denmark). All the remaining chemicals were purchased from Sigma-Aldrich (Copenhagen, Denmark). Cells were incubated in 5% CO_2, at 37°C with a humidity of 95%.

2.2. Lentiviral Vector Production. In order to create inducible CRISPRa cell line, we employed Tet-regulable dCas9-VP64 lentiviral expression vector (pHAGE TRE dCas9-VP64-HA, Addgene, plasmid #50916) [23]; and for inducible CRISPRi cell line, Tet-regulable dCas9-KRAB lentiviral expression vector was utilized (dCas9-TRE-KRAB-HA, Addgene, plasmid #50917) [23]. We also employed two plasmids that express lentivirus envelope proteins for lentiviral packaging and production (psPAX2 and pCMV-VSV-G, Addgene, #12259 and #8454).

HEK293T packaging cells were cultured in MEM with 10% FBS with 1% P/S until 50-60% confluence. The culture medium was changed to fresh prewarmed growth medium (without P/S) 2 hours prior to transfection. We prepared transfection DNA mixture containing dCas9-effector fusion vector, psPAX2, and pCMV-VSV-G (ratio 4 : 3 : 1) in Optimum Medium (Thermo Fisher Scientific, Roskilde, Denmark) and polyethyenimine (PEI) (1 μg/μl in 1x PBS, pH 4.5) at a ratio of 4 : 1 of PEI : DNA. The mixture was incubated for 5-10 min at room temperature and added gradually to the cells. The cells were incubated for 6-8 hours in 3.5% CO_2 in a 37°C cell incubator. The medium was then replaced with fresh growth medium (3% FBS, with 25 mM HEPES) and incubated for 10 hours and mixed with sodium butyrate (10 mM). The cells continue in culture for 48 hours posttransfection.

Cell culture media were pooled from HEK293-transfected cells and stored at 4°C as the 1st medium. Fresh growth medium was added (with the addition of 25 mM HEPES), and the cells were incubated overnight (60-72 hours posttransfection). The 2nd medium was collected and pooled with the 1st medium. One μg DNase I and 1 μl of 1 M $MgCl_2$ per ml of viral supernatant were added, and the mixture was incubated at room temperature for 30 min to digest any carry-over plasmid DNA; this was followed by incubation at 4°C for 2-4 hours. The supernatants were filtered through a 0.45 μm low protein binding filter and utilized in virus purification step. We employed the virus particle purification steps as described in [24]. Briefly, viral particles were obtained by ultracentrifugation; i.e., the collected medium supernatants were centrifuged at 80,000 g for 2 hours at 4°C using a 20% sucrose cushion. The supernatant was discarded without disturbing the pellets. Fresh collected medium supernatants were added, and a second centrifugation step was performed. Finally, the viral pellet collected from 100 ml conditioned medium, was suspended in 200 μl of 1x HBSS buffer.

2.3. Lentiviral Transduction. hMSC line was transduced with lentiviral particles according Addgene's protocol (https://www.addgene.org/protocols/generating-stable-cell-lines/). Briefly, hMSCs were seeded and cultured until 70% confluence and infected using a range of multiplicities of infection (MOIs) (5.0 to 10.0) of the lentivirus in MEM supplemented with 8 μg/ml polybrene. The cells were incubated for 48 hours, and the supernatant media was discarded to remove excess virus particles. For selection, 400 μg/ml G418 (Geneticin) was used for positive section of the infected hMSC and this treatment continued for 5-7 days until all control cells (un-transduced) died. The cells were then trypsinized, and selection was continued for 2-3 weeks using culture in medium containing G418 for in order to obtain stable and pure transduced cell populations.

2.4. Alkaline Phosphatase (ALP) gRNA Design, Synthesis, and Transfection. Human ALP gRNA for transcription regulation was designed in an online CRISPR design tool (http://crispr.mit.edu) based on ALP promoter sequence, from -200 bp to +0 bp. The selected ALP gRNA oligo (TCGTGGCACGACCGGGCCCGC**GGG**) and the universal tracrRNA oligo (Alt-R® CRISPR-Cas9 tracrRNA) were synthesized at Integrated DNA Technologies (Leuven, Belgium). The gRNA-tracrRNA guide complex was mixed as a final duplex of 10 μM in nuclease-free duplex buffer (Integrated DNA Technologies) and denatured by heating at 95°C for 5 min and then allowed to form the heteroduplexes by slowly cooling to 23°C. hMSC-CRISPRi or hMSC-CRISPRa was transfected with ALP crRNA-tracrRNA guide complex employing DharmaFECT™ Transfection Reagent (Dharmacon Inc./VWR International A/S, Søborg, Denmark) according to the manufacturer's instructions (http://dharmacon.gelifesciences.com/uploadedFiles/Resources/basic-dharmafect-protocol.pdf).

2.5. Lipofectamine 2000 Cell Transfection and Electroporation Transfection. To compare the efficiency of gRNAs, siRNA and plasmid inhibition or overexpression in hMSCs utilizing Lipofectamine® 2000 or electroporation were performed to compare with the sgRNA transfection in hMSC-CRISPRi or hMSC-CRISPRa. Alkaline phosphatase (ALP) Silencer® Select validated siRNA was purchased from Ambion (App.-Bio) (#4390821); pcDNA3-Alkaline phosphatase (ALP) plasmid was purchased from PPL (Public Protein/Plasmid Library, Jiangsu, China, #BC009647). siRNA transfection was performed by Lipofectamine® 2000 (Thermo Fisher Scientific, Roskilde, Denmark) as the manufacturer's instructions suggested for siRNA transfection in cells (https://assets.thermofisher.com/TFS-assets/LSG/manuals/Lipofectamine_2000_Reag_protocol.pdf). The plasmid transfection in hMSCs was performed by electroporation by Nucleofector™ 2b Device (Lonza, BioNordika Denmark A/S). Briefly, hMSCs were harvested and suspended with Human MSC Nucleofector Solution (Lonza, #VAPE-1001) at the concentration of 5×10^5 cells/100 μl, mixed with 2 μg plasmid DNA, and transferred into the electroporation chamber, using program U-23. This was immediately followed by the addition of 500 μl of the prewarmed culture medium containing serum and supplements; cells were then transferred into the prepared 6-well plates and, after 2 hours, were changed to fresh cell culturing medium.

2.6. Osteoblastic Differentiation. hMSCs were cultured to reach 80-90% confluence and then incubated in osteoblastic induction medium (OIM) containing 10% FBS, 1% Pen–Strep, 10 mM β-glycerophosphate, 50 μg/ml 2-phosphate ascorbate, 10 nM dexamethasone, and 10 nM 1,25-dihydroxyvitamin D3. OIM medium was replaced every 3 days.

2.7. Adipogenic Differentiation. hMSCs were cultured to reach 95-100% confluence prior to adding adipogenic induction medium (AIM) containing MEM medium supplemented with 10% FBS, 10% horse serum, 1% Pen–Strep, 100 nM dexamethasone, 0.45 mM isobutyl methyl xanthine, 3 μg/ml insulin, and 1 μM rosiglitazone (Cayman, #BRL49653). The AIM medium was replaced every 2 days.

2.8. Chondrogenic Differentiation. For chondrogenesis in hMSCs, 250,000 MSCs were centrifuged at 500 g, 7 min in 15 ml tubes to form pellets at high-density culture. Chondrogenesis was induced for 18 days with MEM medium supplemented with 50 μg/ml L-ascorbic acid-2-phosphate (Sigma-Aldrich.), 1% ITS+1 (BD Bioscience), 10^{-7} M dexamethasone (Sigma-Aldrich), and 10 ng/ml TGFb3 (R&D Systems, Wiesbaden, Germany). The aggregated cells were cultured in tubes with 0.5-1 ml medium/pellet at 37°C in a humidified atmosphere containing 95% air and 5% CO_2. The medium was replaced every other day for 18 days [25].

2.9. Alkaline Phosphatase (ALP) Activity Assay. Cell viability was determined on day 7 of osteoblastic differentiation by Cell Titer-Blue cell viability assay according to the manufacturer's instructions (Promega, Nacka, Sweden). Staining intensity was measured at 579/584 by a FLUO star Omega plate reader (BMG Laboratories, Germany). ALP activity was determined by incubating the cells with 1 mg/ml of p-nitro phenyl phosphate in 50 mM $NaHCO_3$ and 1 mM $MgCl_2$ buffer (pH 9.6) at 37°C for 20 min. The activity was stopped by the addition of 3 M NaOH. The reaction absorbance was measured at 405 nm by a FLUO star Omega plate reader, and ALP activity was corrected for variation in cell number.

2.10. Alkaline Phosphatase Staining. Alkaline phosphatase (ALP) staining was performed at day 7 postinduction. The cells were rinsed with PBS and fixed in acetone/citrate (1.5 : 1, vol : vol) buffer (pH 4.2) for 5 min at room temperature. The cells were incubated for 1 hour at room temperature with ALP staining substrate solution containing 0.2 mg/ml naphthol AS-TR phosphate dissolved in distilled water (1 : 5) and 0.417 mg/ml Fast Red dissolved in 0.1 M Tris buffer.

2.11. Oil Red O Staining. Mature adipocyte formation was visualized on day 12 of adipocytic differentiation by staining lipid droplets with Oil Red O. Cells were washed with phosphate-buffered saline (PBS), fixed with 4% paraformaldehyde for 10 min, and then incubated with fresh-made and filtered (0.45 μM) Oil Red O in 60% isopropanol solution

for 1 hour at room temperature. Images were acquired using an inverted Zeiss microscope.

2.12. Alcian Blue Staining. To evaluate the synthesis of cartilage-specific proteoglycans, sulfated glycosaminoglycans (GAGs) were stained with Alcian blue. Cell pellets from day 18 chondrogenic differentiation were fixed and embedded by paraffin; samples were deparaffinized and hydrated to distilled water, stained in 1% Alcian blue 8-GX (Sigma-Aldrich) in 3% acetic acid in pH 2.5, and then rinsed in distilled water as previously described [26]. The accumulation of GAGs was assessed using microscopic examination.

2.13. Protein Sample Preparation and Western Blot Analysis. For Western blot analysis, we used whole cell lysates. The cells were washed in PBS and lysed in RIPA buffer (Thermo Fisher Scientific) supplemented with a protease inhibitor (Roche, Switzerland). Samples were centrifuged for 10 min at 13,000 rpm (4°C). Protein concentration was determined with a BCA kit (Thermo Fisher Scientific), and equal amounts of proteins were loaded on a polyacrylamide gel (Thermo Fisher Scientific). Blotted nitrocellulose membranes were incubated overnight with HA-tag primary antibody (Santa Cruz Biotechnology). The blots were developed after 1-hour incubation with secondary anti-rabbit horseradish peroxidase-conjugated antibody (Santa Cruz Biotechnology) using an ECL Western blotting kit (Thermo Fisher Scientific) and Kodak films.

2.14. Quantitative Real-Time PCR (qRT-PCR). RNA from cells was isolated at day 2 of osteoblastic differentiation by TRIzol® according to the manufacturer's instructions (Thermo Fisher Scientific). The first strand complementary DNA was synthesized from 1 μg total RNA by Revert aid cDNA kit (Sigma-Aldrich). RT-qPCR was performed by ABI StepOne™ Real time PCR machine with SYBR green (Thermo Fisher Scientific). The data was normalized to geometric means of reference genes and analyzed by a comparative CT method where Δ-CT is the difference between the CT values of the target and geometric mean of reference genes. PCR Primers for human ALP gene are as follows: ACGT GGCTAAGAATGTCATC (forward) and ACGTGGCTA AGAATGTCATC (reverse); and primers for GAPDH are as follows: GGCGATGCTGGCGCTGAGTAC (forward) and TGGTTCACACCCATGACGA (reverse).

2.15. Statistical Analysis. Data were collected from at least 3 independent experiments with each experiment comprising duplicates or triplicates. A one-way analysis of variance (AVOVA) test with the nonparametric Kruskal-Wallis test was used to assess statistical differences in the groups by GraphPad Prism 7.0. Data was expressed as the mean and standard deviation (SD), and $P < 0.05$ was considered as significant.

3. Results

3.1. Generation of Inducible CRISPRi or CRISPRa hMSC. As shown in Figure 1(a), hMSCs were transduced with lentivirus expressing dCas9-KRAB (CRISPRi) or dCas9-VP64 (CRISPRa), which express the CRISPR-dCas9 fused with gene transcription repressor (KRAB) or activator (VP64), respectively, and the expression is driven from a doxycycline- (Dox-) inducible promoter (TRE promoter) [23]. After lentiviral transduction, cells were selected with G418 for 21-28 days in order to obtain stable expression cells (Figure 1(a)). In the absence of Dox, no expression of dCas9-KRAB or dCas-VP64 was detectable in inducible CRISPRi hMSC or CRISPRa hMSC, but when increasing concentrations of Dox adding into the culture medium, there were rapid and dose-dependent increases in their expression reaching a peak at a concentration of 1000 ng/ml (Figure 1(b)). To further prove the dynamic control of dCas9 expression in both cell lines, Dox was removed from culture medium after two-day incubation which led to the disappearance of dCas9 protein expression in both hMSC-CRISPRi and hMSC-CRISPRa within 1-2 days (Figures 1(c) and 1(d)).

3.2. Characterization of Inducible CRISPRi and CRISPRa hMSCs. In the presence of Dox, lentivirus-transduced hMSC-CRISPRi and hMSC-CRISPRa retained spindle-shaped fibroblast-like morphology of the parental hMSC line (Figure 2(a)). We observed no difference in cell proliferation rate between the cell lines in the presence or absence of Dox in 12 days culturing, as evidenced by determination of cell number and cell viability (Figure 2(b)). Following osteoblast (OB) differentiation induction, hMSC-CRISPRi and hMSC-CRISPRa maintained osteoblast differentiation capacity as evidenced by positive staining for ALP and induction of ALP activity (Figure 2(c)). Similarly, both cell lines differentiated readily to adipocytes or chondrocytes as compared to the parental cell line (Figures 2(d) and 2(e)).

3.3. Dynamic Inducible Control of ALP Transcription in hMSC-CRISPRi or hMSC-CRISPRa. To test for regulating gene expression of specific genes in hMSC-CRISPRi or hMSC-CRISPRa, we chose alkaline phosphatase (ALP) gene as a candidate for its known role in osteoblast (OB) differentiation of hMSC [27]. One ALP gRNA was designed, and heteroduplexes were produced and transfected into hMSC-CRISPRi or hMSC-CRISPRa, respectively. After delivery in hMSC-CRISPRi, the expression level of ALP showed no change in the absence of Dox; in the presence of increasing concentrations of Dox, the gene expression of ALP exhibited dose-dependent inhibition; this was also confirmed by ALP staining (Figure 3(a)). Conversely, the expression levels of ALP gene and ALP staining were significantly increased in hMSC-CRISPRa in the presence of Dox in a dose-dependent fashion (Figure 3(b)).

3.4. Regulation of Osteoblast Differentiation of hMSC by Changes in ALP Gene Expression. To further validate the functional relevance of gene regulation in hMSC-CRISPRi or hMSC-CRISPRa, we compared the osteoblast differentiation capacity in hMSC-CRISPRi or hMSC-CRISPRa following transfection with ALP gRNA or negative gRNA (control (Ctrl)). We observed that in the absence of Dox, there were no differences at ALP activities in control gRNA and ALP gRNA-transfected hMSC-CRISPRi or hMSC-

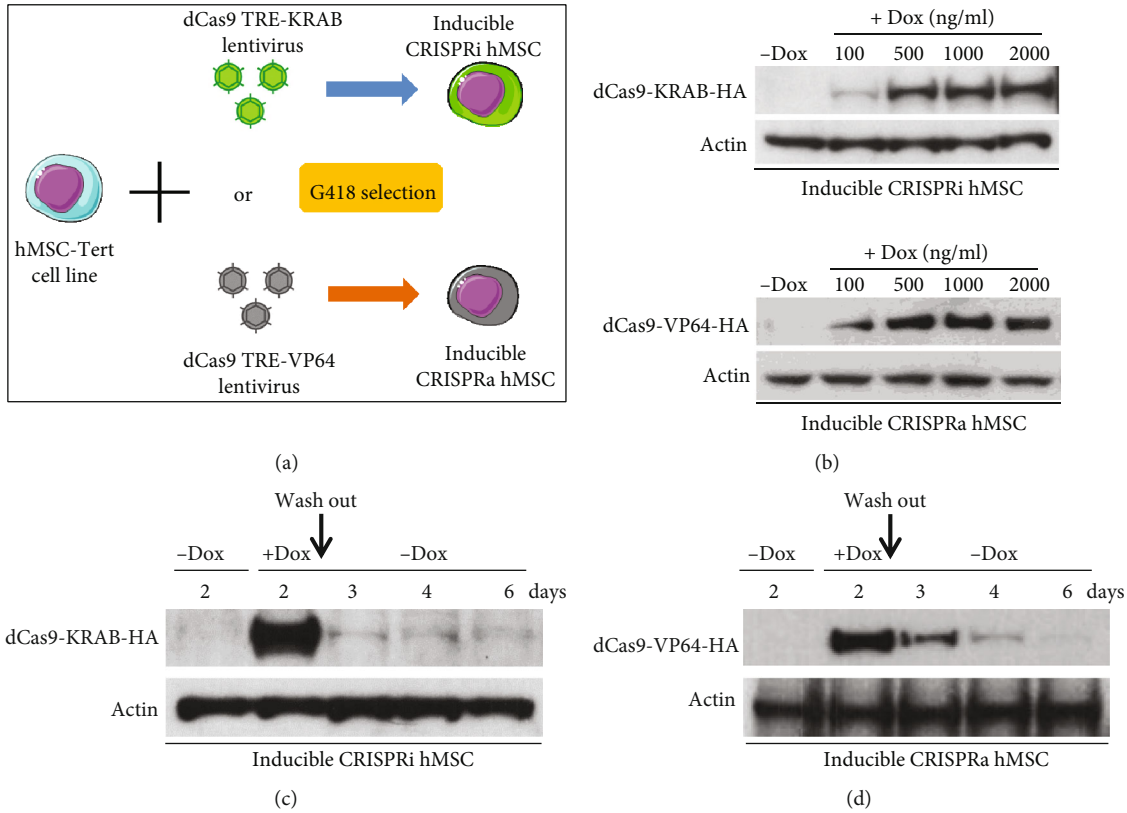

Figure 1: Generation of inducible CRISPRi and CRISPRa hMSCs. (a) Illustration and flow chart for generating inducible CRISPRi using dCAs9 TRE-KRAB and CRISPRa using dCas9 TRE-VP64. (b) Western blot analysis of expression of dCas9-KRAB-HA and dCas9-VP64-HA in the presence of increasing concentrations of doxycycline (Dox) in CRISPRi-hMSC and CRISPRa-hMSC, separately. The effect of the absence or presence of Dox on protein expression of dCas9-KRAB-HA (c) or dCas9-VP64-HA (d). CRISPRi-hMSC and CRISPRa-hMSC were cultured in cell culturing medium with or without Dox (0 or 1000 ng/ml) for 2 days, then washed twice by PBS and changed the cell culturing medium to the medium without Dox, with continuous culturing of the cells till day 6. Cell proteins were harvested on days 2, 3, 4, and 6 and subjected to Western blots to test the expression of dCas9-KRAB and dCas9-VP64 by HA antibody.

CRISPRa (Figures 3(c) and 3(d)), while in presence of Dox, the activity of ALP was significantly repressed in hMSC-CRISPRi or increased in hMSC-CRISPRa, and this was associated with decreased (Figures 3(c)) or increased (Figure 3(d)) ALP staining.

3.5. High Efficiency of Gene Inhibition or Activation in Inducible CRISPRi and CRISPRa hMSCs. To determine the efficiency of specific gene inhibition or activation by gRNA in hMSC-CRISPRi and hMSC-CRISPRa, we compared the gene inhibition with traditional siRNA transfection by Lipofectamine 2000 and the gene overexpression with traditional plasmid transfection by electroporation that we had tested before as the most efficient transient transfections in hMSCs. As shown in Figure 4, both specific siRNA and gRNA transfections in CRISPRi hMSC have significant gene inhibition on day 2 (>90%) or day 7 (>75-85%) after cell transfection (Figures 4(a) and 4(b)). On the other hand, the gene activation by gRNA in CRISPRa hMSC was shown to be much stronger than traditional plasmid overexpression (31-fold vs 2.5-fold on day 2 after transfection) (Figure 4(c)), and the gene activation by gRNA in CRISPRa hMSCs also lasted much longer: 7 days posttransfection, cells demonstrated 10 times overexpression while the plasmid-transfected overexpression effects disappeared (Figure 4(d)).

4. Discussion

Human bone marrow stromal/stem cells (hMSC) are multipotent cells with the ability to differentiate into osteogenic, chondrogenic, and adipogenic lineages. The cells have been utilized in molecular studies aimed at understanding the molecular mechanisms controlling lineage fate determination through targeting specific genes or genetic pathways [3, 5, 28]. Manipulating gene expression in hMSC by plasmid transfection is the most common approach. However, this approach requires specific expensive electroporation instruments or employing relatively toxic chemical formulations, and it usually exhibits low efficiency (usually <25% in our laboratory). Conversely, viral gene delivery is the most efficient way to attain stable gene expression in hMSC; however, this method requires specific laboratory setup, with time-consuming and technical difficulties.

In the present study, we employed CRISPR-dCas9 technology and created two universal hMSC lines to be utilized in specific gene transcriptional inhibition or transcriptional

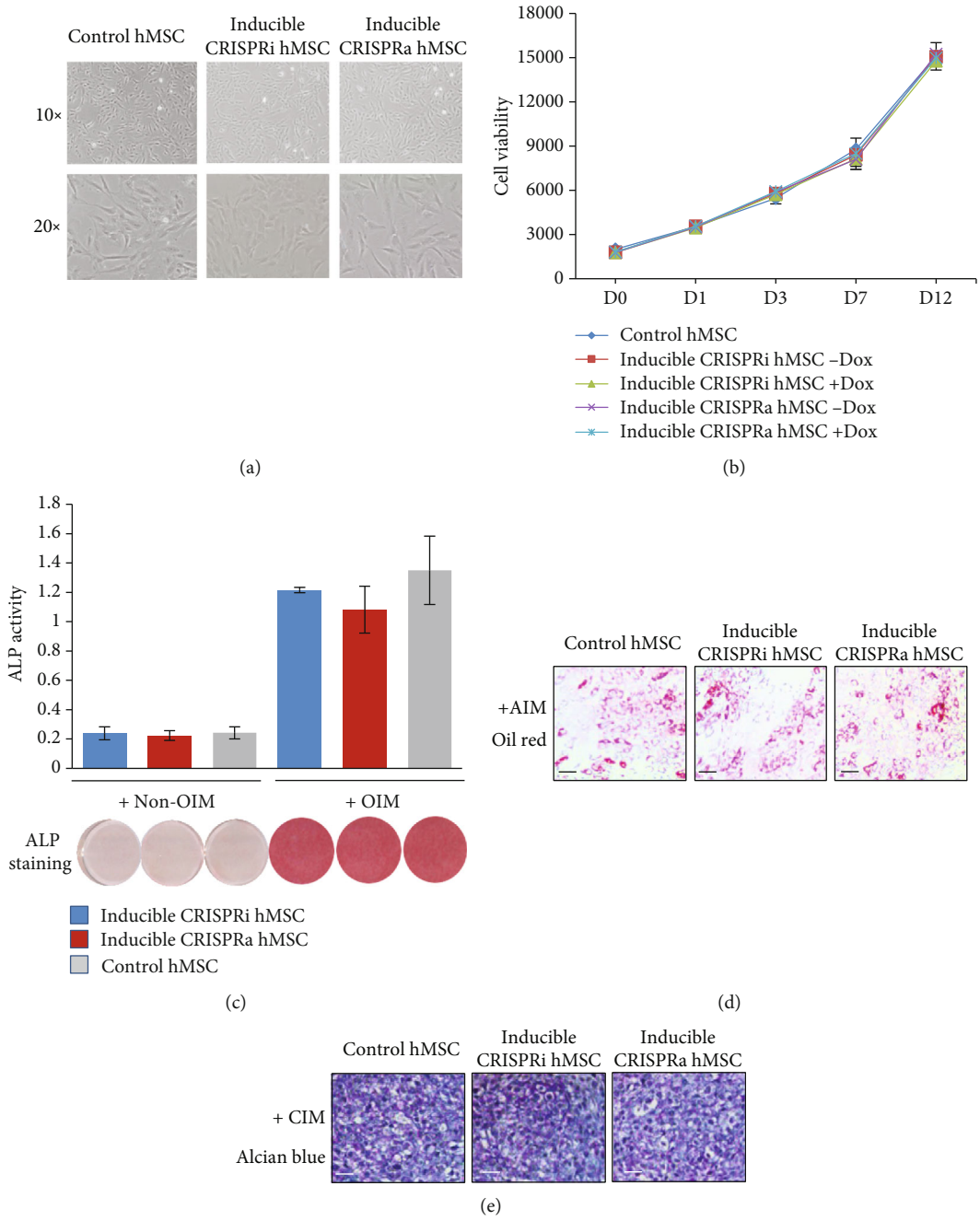

Figure 2: Characterization of inducible CRISPRi and CRISPRa human skeletal stem cells (hMSC). (a) The morphology of control hMSC, inducible hMSC-CRISPRi, or hMSC-CRISPRa. (b) Short-term growth curve of control hMSC, hMSC-CRISPRi, or hMSC-CRISPRa. The cells were seeded in a 96-well plate and cultured in the absence or presence of doxycycline; cell viability assay was performed at different time points during 12 days in culture (D0–D12, D = day). (c–e) Control hMSC, hMSC-CRISPRi, and hMSC-CRISPRa were induced to osteogenic, adipogenic, and chondrogenic differentiation. The cells were cultured for 7 days in osteoblast induction medium (OIM) (c), 12 days in adipocyte induction medium (AIM) (d), or 18 days in chondrogenic induction medium (CIM) (e) as described in Methods. Alkaline phosphatase (ALP) activity and ALP staining (c), Oil Red O staining (d), or Alcian blue staining (e) were performed to visualize different hMSC lineage-differentiated phenotype. Data are expressed as the means ± SD. Scale bar: 100 μm.

activation. We demonstrate that this technology did not affect the growth rate or the functional characteristics of the cells. Moreover, we demonstrated that regulation of gene expression can be achieved by the presence Dox in culture medium that acts as a "switch" to regulate gene expression. To regulate gene expression, a simple transfection by one sgRNA for targeting gene was enough to obtain either inhibition of target gene in hMSC-CRISPRi cells or overexpression in hMSC-CRISPRa cells (summary as shown in Figure 5).

We employed one transcriptional repressor, KRAB domain of Kox1, an efficient repressor of gene transcription [20], to construct with dCas9 and make the hMSC-

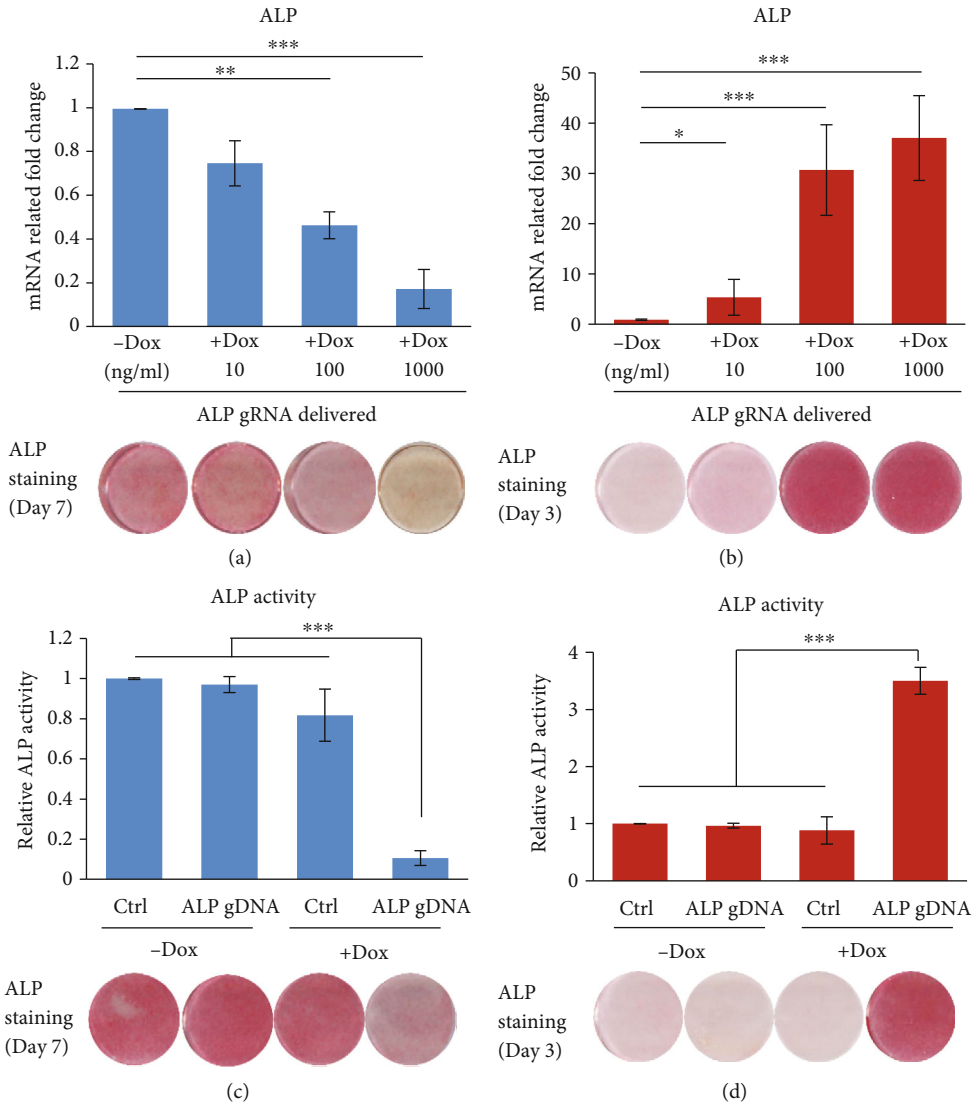

Figure 3: Dynamic regulation of ALP expression during osteoblast differentiation in inducible CRISPRi or CRISPRa hMSC. Inducible CRISPRi (a) or CRISPRa (b) hMSC were transfected with ALP gRNA oligo by DharmaFECT™ Transfection Reagent and cultured with increasing concentrations of Dox. ALP expression was measured by RT-qPCR at day 2. Inducible CRISPRi (c) or CRISPRa (d) hMSC was transfected with ALP gRNA oligo or negative control (Ctrl) and induced to OB differentiation in the absence or presence of Dox (1000 ng/ml). ALP activity and staining (bottom photomicrographs) were performed on day 7 in hMSC-CRISPRi or day 3 in hMSC-CRISPRa to show the most evident change for inhibition or activation. Data are expressed as the means ± SD. $^{*}P < 0.05$, $^{**}P < 0.01$, and $^{***}P < 0.001$.

CRISPRi cells, and we obtained 60-99% inhibition efficiency using only one sgRNA. To further enhance the inhibition efficiency, previous studies have suggested a number of other approaches, including screening of several sgRNAs to identify the most efficient sgRNA [20]; the pooling of several designed sgRNAs of the targeting gene [16, 29]; or combining several fusion transcriptional repressors with dCas9 in the system, such as KRAB, the CS (chromoshadow) domain of HP1a, the WPRW domain of Hes1, and four concatenated copies of the mSin3 domain (SID4X) [14, 16]. We observed that transfection of sgRNAs in CRISPRi cell system resulted in similar levels of gene expression inhibition compared to siRNA-mediated gene inhibition. This is expected as both are small RNA molecules with high transfection efficiency (usually >95% transfection efficiency got in hMSCs for small RNA transfection in our laboratory). However, sgRNA-CRISPRi has the important advantage of the ability to control gene expression by Dox, allowing gene manipulation at different time points at developmental stages of differentiating hMSC.

We observed high efficiency for gene regulation by CRISPR-dCas9 in CRISPRa our activation system. By simply transfecting one small molecular sgRNA of the targeting gene, we routinely obtained 5 to 20-fold overexpression for the targeting genes in hMSCs. This method is much easier than the traditional approaches for gene overexpression, e.g., transfection or infection of gene open reading frame (ORF) cloning plasmid or viral vectors, respectively. We have utilized the VP64 activator in the CRISPRa cell system. Other activator fusion proteins have the employed activation of

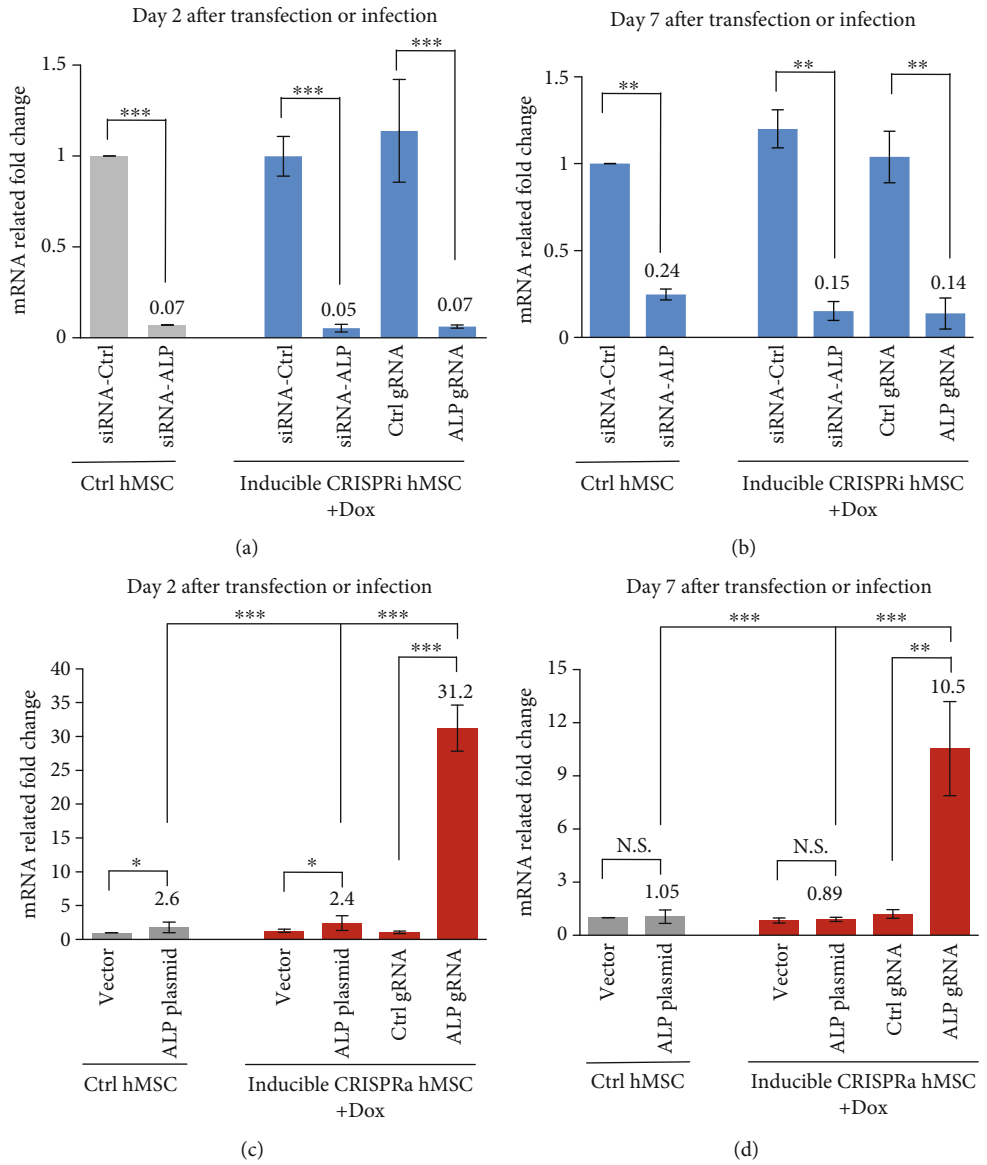

Figure 4: Comparison of the efficiency of gene inhibition or gene activation in control hMSC, inducible CRISPRi hMSC, and CRISPRa hMSC. (a, b) Control (Ctrl) hMSC and inducible CRISPRi were transfected with siRNA-Ctrl, siRNA-ALP, Ctrl gRNA, or ALP gRNA oligo and for 2 or 7 days as described in Methods. ALP expression was measured by RT-qPCR at day 2 (a) or day 7 (b). (c, d) Control (Ctrl) hMSC and inducible CRISPRa were transfected with pcDNA3 vector plasmid, pcDNA3-ALP plasmid by electroporation, or Ctrl gRNA and ALP gRNA oligo by DharmaFECT™ Transfection Reagent as described in Methods. ALP expression was measured by RT-qPCR at day 2 (c) and day 7 (d). Data are expressed as the means ± SD. $^{*}P < 0.05$, $^{**}P < 0.01$, and $^{***}P < 0.001$.

gene expression such as P65 activator, heat shock factor 1 (HSF1), and the viral replication and transcription activator (RTA) [30]. Among these, VP64 infection was proven to demonstrate more efficiency than other reported activities [11]. In addition, several approaches have been described to further enhance gene activation in CRISPRa system, e.g., fusing multirepeats of one transcriptional activator with dCas9 [20, 31]; combining several different transcriptional activators together with dCas9 [32]; or using multiple sgRNAs designed across the targeting gene promoter [19].

One of the most striking advantages for CRISPRi and CRISPRa is the possibility for simultaneous multigene targeting [19, 20, 29]. Through single transfection with several sgRNAs targeting different genes, the method can inhibit or enhance multiple genes allowing examination of the combined effects of multigene inhibition or activation. Moreover, VP64-CRSIPRa and KRAB-CRISPRi hMSC lines can also be employed in screening a large number of effectors by sgRNAs libraries. Combing both CRISPRi and CRISPRa together to study one or several targeting genes by loss-or-gain effects can further help confirming the specific effects of targeting factors and limit the bias of function study.

CRISPR/Cas9 technology is a powerful tool for creating gene knock-ins and knock-outs; however, concerns need to be addressed consequentially to mutations engendered at gene sites other than the intended target site (off-target).

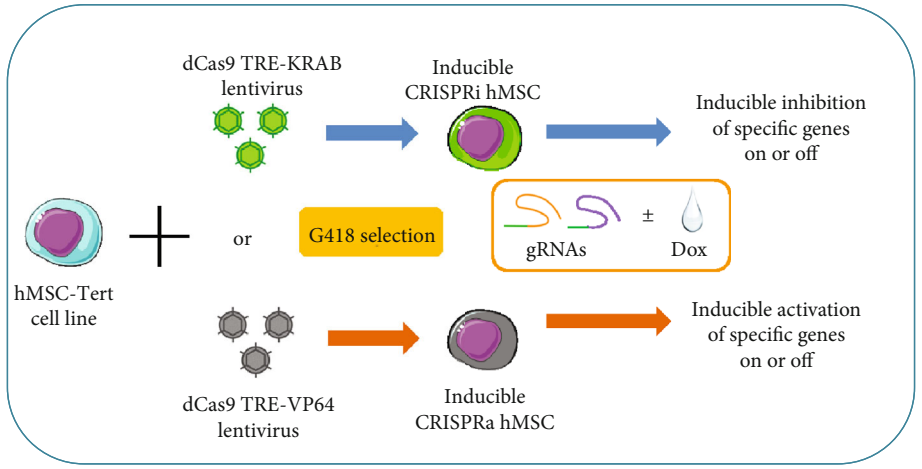

Figure 5: The technical flow chart of inducible inhibition or activation-specific genes in CRISPRi or CRISPRa human stromal/stem cells (hMSCs). Human bone marrow stromal/stem cell line (hMSC-TERT) stable transfected with dCas9 TRE-KRAB or dCas9TRE-VP64 to establish the inducible CRISPRi or CRISPRa cell lines. In these cells, with simply transfecting the small molecular guide RNAs (gRNAs) that target different specific genes, it can easily inhibit or activate specific gene expressions with or without doxycycline (Dox) in cell culturing mediums or differentiation induction medium.

The selection and design of the sgRNA for specific target genes are the key to control the specificity of targeting in our system. We suggest initially selecting several highest scored sgRNAs for the target gene that are designed by different programs. Alternatively, commercially proved sgRNAs (Thermo Fisher Scientific, Merck/Sigma, Takara et al.) are now available. Pooling of several sgRNAs for one target gene might improve the inhibition or activation efficiency of the target gene; however, limiting the number of sgRNAs can benefit the reduction of off-target effects. If one sgRNA has a high enough efficiency, we suggest using one sgRNA targeting for one gene. Several different sgRNAs for one gene can be used in different parallel experiments to obtain consistent results and limit misleading the effects of off-targeted events. Moreover, besides checking the specific target gene, testing the several highest potential off-target genes by the gRNAs can also help to confirm the targeting specificity in the CRISPR cells.

5. Conclusion

The availability of inducible hMSC-CRISPRi and hMSC-CRISPRa cell lines makes it possible to investigate the role of specific genes and genetic pathways at a specific developmental stage of hMSC differentiation and map the genetic regulatory networks underlying lineage differentiation of hMSC. These tools can help to enhance our understanding of hMSC biology and are also relevant to regenerative medicine applications for tissue regeneration.

Abbreviations

hMSCs:	Human bone marrow stromal/stem cells
Dox:	Doxycycline
ALP:	Alkaline phosphatase
Type II CRISPR-Cas9 system:	Clustered Regularly Interspaced Palindromic Repeats–CRISPR-associated 9
sgRNA:	Single guide RNA
DSB:	Double-stranded break
KRAB:	Krüppel-associated box
hMSC-TERT:	Telomerized hMSC line
hTERT:	Human telomerase reverse transcriptase gene
MEM:	Minimum Essential Medium
FBS:	Fetal bovine serum
P/S:	Penicillin-streptomycin
dCas9-TRE-KRAB:	Tet-regulable dCas9-KRAB lentiviral expression vector
pHAGE TRE dCas9-VP64:	Tet-regulable dCas9-VP64 lentiviral expression vector
PEI:	Polyethyenimine
G418:	Geneticin
OIM:	Osteoblastic induction medium
AIM:	Adipogenic induction medium
PBS:	Phosphate-buffered saline
qRT-PCR:	Quantitative real-time PCR
OB:	Osteoblast
Ctrl:	Control
CS:	Chromoshadow
ORF:	Open reading frame.

Data Availability

The data used to support the findings of this study are included within the article. The materials used to support the findings of this study are available from the corresponding author upon request.

Additional Points

Highlight. (i) Using the principle of CRISPR technology, we established two human stromal/stem cell lines: CRISPRi and CRIPSRa. (ii) These two cells overcome the difficulty of plasmid transfection in hMSCs and make gene transcription inhibition and overexpression easily by only transfecting a small guide RNA (gRNA). (iii) The inhibition and activation of specific genes have been proved to be highly efficient in both cell lines. (iv) The transcription regulation in both cell lines can be controlled by Dox induction at different times during differentiation.

Ethical Approval

Consent to generate human cell lines was given by the Danish Ethical committee. Informed patient consent for the generation and subsequent use of the cell lines was given.

Conflicts of Interest

All the authors certify that they have no competing financial or non-financial interests.

Authors' Contributions

LC and KS generated the CRISPR cell lines, performed cell culture and differentiation experiments, and analyzed data. MK and LA assist some technical virus infection and concentration. LC, KS, LA, and MK prepared the manuscript. All authors read and approved the final manuscript. Li Chen and Kaikai Shi contribute equally in the work.

Acknowledgments

The project got partial support from a scholarship from Odense University Hospital PhD-pulje and the University of Southern Denmark (2014). We thank Dr. Linda Harkness for critical reading of this manuscript.

References

[1] W. Zaher, L. Harkness, A. Jafari, and M. Kassem, "An update of human mesenchymal stem cell biology and their clinical uses," *Archives of Toxicology*, vol. 88, no. 5, pp. 1069–1082, 2014.

[2] B. M. Abdallah, A. Jafari, W. Zaher, W. Qiu, and M. Kassem, "Skeletal (stromal) stem cells: an update on intracellular signaling pathways controlling osteoblast differentiation," *Bone*, vol. 70, pp. 28–36, 2015.

[3] L. Chen, K. HolmstrØm, W. Qiu et al., "MicroRNA-34a inhibits osteoblast differentiation and in vivo bone formation of human stromal stem cells," *Stem Cells*, vol. 32, no. 4, pp. 902–912, 2014.

[4] B. M. Abdallah, F. Figeac, K. H. Larsen et al., "CRMP4 inhibits bone formation by negatively regulating BMP and RhoA signaling," *Journal of Bone and Mineral Research*, vol. 32, no. 5, pp. 913–926, 2017.

[5] A. Jafari, D. Qanie, T. L. Andersen et al., "Legumain regulates differentiation fate of human bone marrow stromal cells and is altered in postmenopausal osteoporosis," *Stem Cell Reports*, vol. 8, no. 2, pp. 373–386, 2017.

[6] L. P. Kristensen, L. Chen, M. O. Nielsen et al., "Temporal profiling and pulsed SILAC labeling identify novel secreted proteins during ex vivo osteoblast differentiation of human stromal stem cells," *Molecular & Cellular Proteomics*, vol. 11, no. 10, pp. 989–1007, 2012.

[7] F. J. M. Mojica, C.). Díez-Villaseñor, J. García-Martínez, and E. Soria, "Intervening sequences of regularly spaced prokaryotic repeats derive from foreign genetic elements," *Journal of Molecular Evolution*, vol. 60, no. 2, pp. 174–182, 2005.

[8] M. Jinek, K. Chylinski, I. Fonfara, M. Hauer, J. A. Doudna, and E. Charpentier, "A programmable dual-RNA-guided DNA endonuclease in adaptive bacterial immunity," *Science*, vol. 337, no. 6096, pp. 816–821, 2012.

[9] G. Gasiunas, R. Barrangou, P. Horvath, and V. Siksnys, "Cas9-crRNA ribonucleoprotein complex mediates specific DNA cleavage for adaptive immunity in bacteria," *Proceedings of the National Academy of Sciences of the United States of America*, vol. 109, no. 39, pp. E2579–E2586, 2012.

[10] L. Cong, F. A. Ran, D. Cox et al., "Multiplex genome engineering using CRISPR/Cas systems," *Science*, vol. 339, no. 6121, pp. 819–823, 2013.

[11] P. Mali, L. Yang, K. M. Esvelt et al., "RNA-guided human genome engineering via Cas9," *Science*, vol. 339, no. 6121, pp. 823–826, 2013.

[12] H. Wang, H. Yang, C. S. Shivalila et al., "One-step generation of mice carrying mutations in multiple genes by CRISPR/-Cas-mediated genome engineering," *Cell*, vol. 153, no. 4, pp. 910–918, 2013.

[13] L. S. Qi, M. H. Larson, L. A. Gilbert et al., "Repurposing CRISPR as an RNA-guided platform for sequence-specific control of gene expression," *Cell*, vol. 152, no. 5, pp. 1173–1183, 2013.

[14] S. Konermann, M. D. Brigham, A. E. Trevino et al., "Optical control of mammalian endogenous transcription and epigenetic states," *Nature*, vol. 500, no. 7463, pp. 472–476, 2013.

[15] P. Mali, J. Aach, P. B. Stranges et al., "CAS9 transcriptional activators for target specificity screening and paired nickases for cooperative genome engineering," *Nature Biotechnology*, vol. 31, no. 9, pp. 833–838, 2013.

[16] L. A. Gilbert, M. H. Larson, L. Morsut et al., "CRISPR-mediated modular RNA-guided regulation of transcription in eukaryotes," *Cell*, vol. 154, no. 2, pp. 442–451, 2013.

[17] W. Y. Hwang, Y. Fu, D. Reyon et al., "Efficient genome editing in zebrafish using a CRISPR-Cas system," *Nature Biotechnology*, vol. 31, no. 3, pp. 227–229, 2013.

[18] P. Perez-Pinera, D. D. Kocak, C. M. Vockley et al., "RNA-guided gene activation by CRISPR-Cas9-based transcription factors," *Nature Methods*, vol. 10, no. 10, pp. 973–976, 2013.

[19] A. W. Cheng, H. Wang, H. Yang et al., "Multiplexed activation of endogenous genes by CRISPR-on, an RNA-guided transcriptional activator system," *Cell Research*, vol. 23, no. 10, pp. 1163–1171, 2013.

[20] L. A. Gilbert, M. A. Horlbeck, B. Adamson et al., "Genome-scale CRISPR-mediated control of gene repression and activation," *Cell*, vol. 159, no. 3, pp. 647–661, 2014.

[21] J. L. Simonsen, C. Rosada, N. Serakinci et al., "Telomerase expression extends the proliferative life-span and maintains

the osteogenic potential of human bone marrow stromal cells," *Nature Biotechnology*, vol. 20, no. 6, pp. 592–596, 2002.

[22] B. M. Abdallah, M. Haack-Sørensen, J. S. Burns et al., "Maintenance of differentiation potential of human bone marrow mesenchymal stem cells immortalized by human telomerase reverse transcriptase gene despite of extensive proliferation," *Biochemical and Biophysical Research Communications*, vol. 326, no. 3, pp. 527–538, 2005.

[23] N. A. Kearns, R. M. J. Genga, M. S. Enuameh, M. Garber, S. A. Wolfe, and R. Maehr, "Cas9 effector-mediated regulation of transcription and differentiation in human pluripotent stem cells," *Development*, vol. 141, no. 1, pp. 219–223, 2013.

[24] G. Tiscornia, O. Singer, and I. M. Verma, "Production and purification of lentiviral vectors," *Nature Protocols*, vol. 1, no. 1, pp. 241–245, 2006.

[25] B. Schmitt, J. Ringe, T. Häupl et al., "BMP2 initiates chondrogenic lineage development of adult human mesenchymal stem cells in high-density culture," *Differentiation*, vol. 71, no. 9-10, pp. 567–577, 2003.

[26] L. Chen, D. Qanie, A. Jafari et al., "Delta-like 1/fetal antigen-1 (Dlk1/FA1) is a novel regulator of chondrogenic cell differentiation via inhibition of the Akt kinase-dependent pathway," *The Journal of Biological Chemistry*, vol. 286, no. 37, pp. 32140–32149, 2011.

[27] K. N. Fedde, L. Blair, J. Silverstein et al., "Alkaline phosphatase knock-out mice recapitulate the metabolic and skeletal defects of infantile hypophosphatasia," *Journal of Bone and Mineral Research*, vol. 14, no. 12, pp. 2015–2026, 1999.

[28] W. Qiu, T. E. Andersen, J. Bollerslev, S. Mandrup, B. M. Abdallah, and M. Kassem, "Patients with high bone mass phenotype exhibit enhanced osteoblast differentiation and inhibition of adipogenesis of human mesenchymal stem cells," *Journal of Bone and Mineral Research*, vol. 22, no. 11, pp. 1720–1731, 2007.

[29] S. Konermann, M. D. Brigham, A. E. Trevino et al., "Genome-scale transcriptional activation by an engineered CRISPR-Cas9 complex," *Nature*, vol. 517, no. 7536, pp. 583–588, 2015.

[30] M. F. La Russa and L. S. Qi, "The new state of the art: Cas9 for gene activation and repression," *Molecular and Cellular Biology*, vol. 35, no. 22, pp. 3800–3809, 2015.

[31] M. E. Tanenbaum, L. A. Gilbert, L. S. Qi, J. S. Weissman, and R. D. Vale, "A protein-tagging system for signal amplification in gene expression and fluorescence imaging," *Cell*, vol. 159, no. 3, pp. 635–646, 2014.

[32] A. Chavez, J. Scheiman, S. Vora et al., "Highly efficient Cas9-mediated transcriptional programming," *Nature Methods*, vol. 12, no. 4, pp. 326–328, 2015.

Hindawi
Stem Cells International
Volume 2020, Article ID 5385960, 13 pages
https://doi.org/10.1155/2020/5385960

Research Article

Mechanical Strain-Mediated Tenogenic Differentiation of Mesenchymal Stromal Cells Is Regulated through Epithelial Sodium Channels

Hui Yin Nam,[1] **Malliga Raman Murali**,[1] **Raja Elina Ahmad**,[2] **Belinda Pingguan-Murphy**,[3] **Hanumantha Rao Balaji Raghavendran**,[1] **and Tunku Kamarul**[1]

[1]*Tissue Engineering Group, Department of Orthopaedic Surgery (NOCERAL), Faculty of Medicine, University of Malaya, 50603 Kuala Lumpur, Malaysia*
[2]*Department of Physiology, Faculty of Medicine, University of Malaya, 50603 Kuala Lumpur, Malaysia*
[3]*Department of Biomedical Engineering, Faculty of Engineering, University of Malaya, 50603 Kuala Lumpur, Malaysia*

Correspondence should be addressed to Hui Yin Nam; huiyin26@yahoo.com and Tunku Kamarul; tkzrea@um.edu.my

Received 25 March 2020; Revised 18 June 2020; Accepted 11 July 2020; Published 18 August 2020

Academic Editor: Alessandra Pisciotta

It has been suggested that mechanical strain may elicit cell differentiation in adult somatic cells through activation of epithelial sodium channels (ENaC). However, such phenomenon has not been previously demonstrated in mesenchymal stromal cells (MSCs). The present study was thus conducted to investigate the role of ENaC in human bone marrow-derived MSCs (hMSCs) tenogenic differentiation during uniaxial tensile loading. Passaged-2 hMSCs were seeded onto silicone chambers coated with collagen I and subjected to stretching at 1 Hz frequency and 8% strain for 6, 24, 48, and 72 hours. Analyses at these time points included cell morphology and alignment observation, immunocytochemistry and immunofluorescence staining (collagen I, collagen III, fibronectin, and N-cadherin), and gene expression (ENaC subunits, and tenogenic markers). Unstrained cells at similar time points served as the control group. To demonstrate the involvement of ENaC in the differentiation process, an ENaC blocker (benzamil) was used and the results were compared to the noninhibited hMSCs. ENaC subunits' (α, β, γ, and δ) expression was observed in hMSCs, although only α subunit was significantly increased during stretching. An increase in tenogenic genes' (*collagen1*, *collagen3*, *decorin*, *tenascin-c*, *scleraxis*, and *tenomodulin*) and proteins' (collagen I, collagen III, fibronectin, and N-cadherin) expression suggests that hMSCs underwent tenogenic differentiation when subjected to uniaxial loading. Inhibition of ENaC function resulted in decreased expression of these markers, thereby suggesting that ENaC plays a vital role in tenogenic differentiation of hMSCs during mechanical loading.

1. Introduction

Ion channels have been regarded as an important mediator for a multitude of physiological processes including muscle contraction, synaptic transmission, immune regulation, and many others [1, 2]. It is therefore not surprising that these structures are also involved in specific cellular responses including cell cycle regulation, cytoskeletal reorganization, and apoptosis [3, 4]. Whilst many of the common ion channels have been extensively investigated, the role of the less common ones has been underrated. This has led to the lack of understanding of the mechanism regulating specific cellular function involving these channels such as the signalling process in response to mechanical stimuli. Amongst the less commonly studied ion channels is the epithelial sodium channels (ENaC), which has been reported to have a main role in facilitating movements of fluids across the cells mainly in the lungs, kidneys, and skin [5, 6].

Several studies have reported that ion channels residing in the plasma membrane of chondrocytes and osteoblasts are involved in the transduction of mechanical signals [7–9]. The existence of ENaC in load-bearing cells suggests that ENaC has a mechanoactive role in cellular signalling. Such signalling processes are deemed important for cellular

differentiation to occur. Although the differentiation process of adult somatic cells is thought to be mediated by ENaC, its mechanoactive role in multipotent cells, such as those of mesenchyme origin, has not been previously described. Furthermore, whilst it has been shown that ENaC activation occurs via mechanical stretching, the mechanism resulting in the sequelae of events has never been fully understood.

It is suggested that ENaC functions as transmembrane adhesion molecules that is linked directly to the cytoskeletal microtubules as well as the extracellular matrix (ECM) components such as collagen type IV [10]. As proposed by Shakibaei and Mobasheri [11], ECM macromolecules (collagen type II), β1-integrins, ENaC, and voltage activated calcium channel (VACC) act as putative mechanosensitive receptors that regulate subcellular signal transduction pathways through the perception of physical contact and stresses from the ECM. It is also suggested that the ability of cells to respond to mechanical stimuli is controlled by a series of mechanosensitive receptors or structures that sense and convert mechanical signals into biochemical signalling events. This eventually leads to the control of cellular functions, which include but not limited to cell proliferation, differentiation, and apoptosis. This process, known as mechanotransduction, is deemed to be mediated by sodium currents and thus can be controlled through sodium channels [12]. ENaC activity can be inhibited by potent pharmacological blockers such as benzamil, which disrupts the mechanical transduction process and signalling pathways that would result in cellular activity [13, 14]. Thus, the use of such inhibitor provides an opportunity to study the functional role of ENaC in transducing mechanical stimuli into cell responses.

Mesenchymal stromal cells (MSCs), being undifferentiated and having multipotent differentiation ability, have a tremendous potential for various biomedical and therapeutic applications in the field of regenerative medicine [15, 16]. The application of *in vitro* differentiation of MSCs into tissue progenitors prior to transplantation circumvents the development of ectopic tissue or tumour formation *in vivo* and, in many studies, demonstrates superior tissue repair outcomes [17]. Current strategies to direct tenogenic differentiation of MSCs generally involve physical manipulations as well as treatment with various biochemical factors; these include mechanical stimulation, the use of scaffolds, administration of growth and differentiation factors, gene transfection, and coculture with specific tissues or cells [18–20]. The use of mechanical loading provides a viable alternative [21–23] to enhance cellular differentiation as it simulates the natural stimuli the cells would be exposed to *in vivo* such as the loading that occurs during load-bearing activities of daily living [24]. Indeed, the application of mechanical stimuli with or without scaffolds or growth factors may be an effective strategy to enhance the expression of tendon-specific markers and induce stability of the tenogenic phenotype. However, the mechanisms regulating tenogenic differentiation of MSC induced by mechanical loading remain elusive. Several studies have suggested that ENaC may play an important role in this. This knowledge is important, as the control of ENaC function may lead to better regulation of the tenogenic differentiation process and, indirectly, of tendon regeneration. To establish this, we conducted a study to investigate the mechanoactive role of ENaC in regulating tenogenic differentiation of MSCs, using benzamil to inhibit ENaC function. We hypothesise that ENaC regulates tenogenic differentiation of MSCs and that the restriction of sodium supply induced by ENaC inhibition during cyclical tensile loading will affect the mechanical strain-induced tenogenic differentiation of MSCs and the resultant ECM production by the cells.

2. Materials and Methods

2.1. Harvesting Bone Marrow Specimens from Human. Experiments using human bone marrow-derived mesenchymal stromal cells (hMSCs) were conducted following the approval from the Medical Ethics Committee in University Malaya Medical Centre (reference number: 369.19). Two assigned orthopaedic surgeons were tasked with the job of harvesting bone marrow specimens from patients undergoing knee replacement procedures using a large aspirator. This was done after obtaining written informed consents from 10 patients ($N = 10$; mean age = 65.1 ± 3.07 years). Samples were obtained from either the femur or tibia of these patients.

2.2. Culture of hMSCs. An equal volume of pH 7.2 phosphate-buffered saline (PBS) (Invitrogen-Gibco, Grand Island, NY, USA) was added into bone marrow specimens and slowly layered on top of the 3 mL of the density of 1.077 g/mL Ficoll-Paque PREMIUM (Amersham Biosciences, Uppsala, Sweden). Centrifugation at 2,200 rpm for 25 min was then performed. The mononuclear cells (see Figure 1(a)) were extracted and washed with low-glucose Dulbecco's modified Eagle's medium (DMEM) (Invitrogen-Gibco, USA) and underwent centrifugation at 1,600 rpm for 10 min. The supernatant was then discarded, and the cell pellet (see Figure 1(b)) formed at the bottom was resuspended using 1 mL of fetal bovine serum (FBS) (Invitrogen-Gibco, USA). Cell count and viability test were performed. The mixture of mononuclear cells was then cultured in cell culture medium, which consisted of DMEM, 10% FBS, 1% GlutaMAX-1, and 1% penicillin-streptomycin (Invitrogen-Gibco, USA). Cultures were maintained at 37°C in a humidified atmosphere containing 5% CO_2. Suspended cells were discarded after 5 days of culture, and adherent cells were left to grow on the flask surface. Culture medium was changed every 3 days until the cultures became 75% to 80% confluent. In order to obtain a sufficient number of hMSCs, the cells were serially passaged and expanded up to passage-2 (see Figures 1(c)–1(e)) before being used for experiment use. The hMSCs used in our study were well-characterized by flow cytometric analysis and induction of multilineage differentiation assay, according to the previous protocols used in our laboratory [25, 26].

2.3. Benzamil Treatment on hMSCs. A stock solution 10 mM of benzamil (Sigma, USA) was prepared in 100% methanol. To optimize the concentration of benzamil to be used in this study, benzamil at various concentrations (1 μM, 10 μM, 25 μM, 50 μM, and 100 μM) was diluted with culture

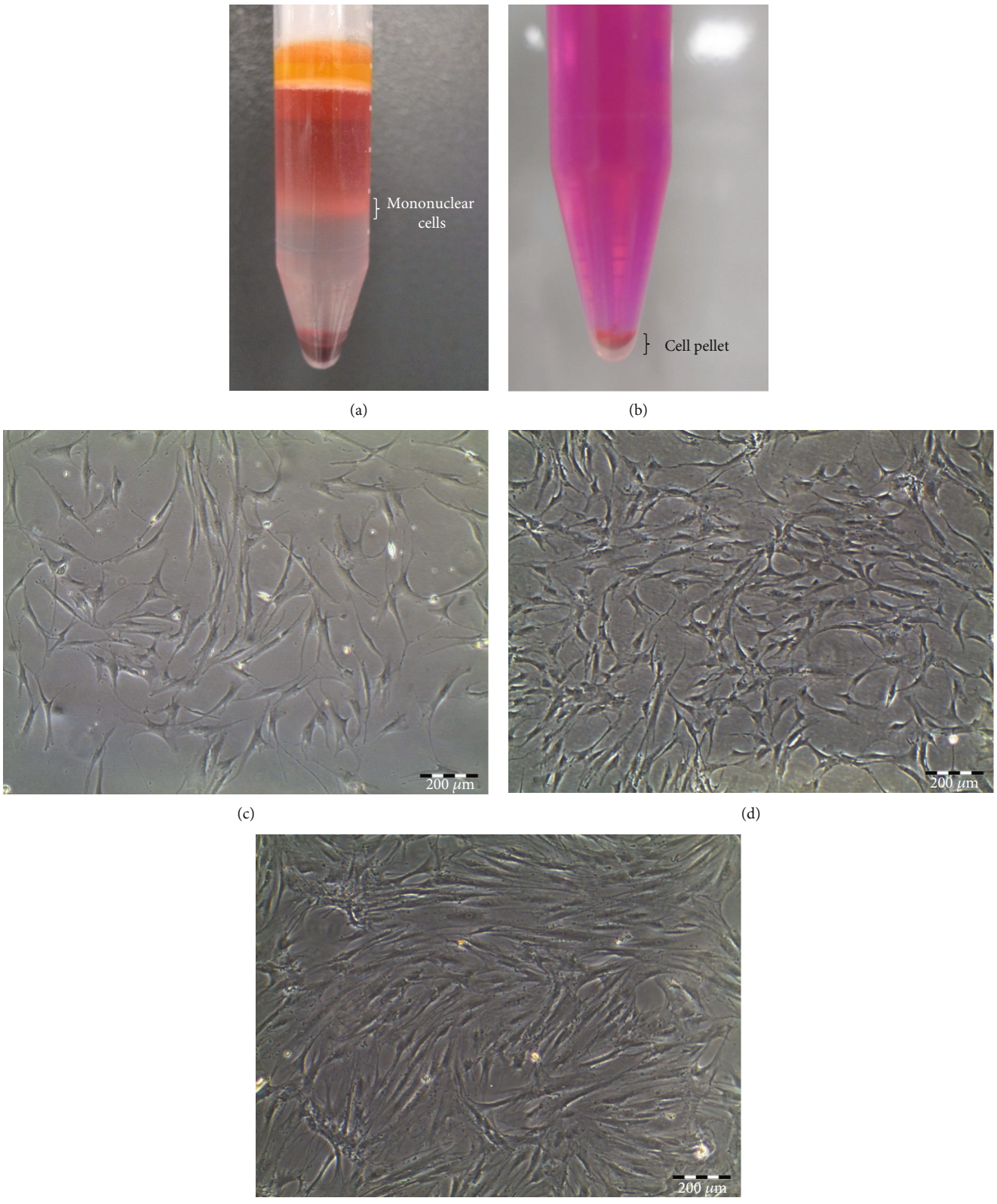

(a) (b)

(c) (d)

(e)

Figure 1: Photomicrographs of human bone marrow-derived MSCs. (a) Mononuclear cells were extracted after density centrifugation. (b) The cell pellet which contains hMSCs was formed and cultured. (c) The primary cultures of the passaged-0 cells contained fibroblastic cells at day 9. (d) Passaged-1 hMSC morphology at day 12. (e) Passaged-2 hMSC morphology at day 14.

medium immediately before the treatment on hMSCs was performed. The cell morphology was observed, and images captured after 72 h were being treated with benzamil.

2.4. Cell Seeding and Application of Mechanical Stretching. hMSCs from the second passage in culture were harvested and counted, and an overall viability of more than 90% was observed using a trypan blue (Invitrogen-Gibco, USA) exclusion test. A total of 10^5 hMSCs were plated on each collagen type I-coated (Sigma, USA) silicone chamber (STREX, Japan). After 48 h of culture, the concentration of FBS was reduced to 1% for 24 h in order to align most cells into the G_0 phase of the cell cycle and changed to growth medium with or without 10 μM benzamil, before assembling into a uniaxial strain device. A commercial instrument (Model ST-140, STREX Co., Ltd., Osaka, Japan) was used to conduct experiments to determine the effects of cyclic uniaxial strained on hMSCs. Uniaxial strain was applied in order to imitate the physiological stretching conditions for tendons and ligaments *in vivo*. Uniaxial cyclic stretching at a frequency of 1 Hz and a magnitude of 8% was applied. This setting was used based on our previous findings which demonstrated an enhanced collagen synthesis or tenogenesis gene expression [23]. Cells in the control group also were cultured on a silicone chamber and maintained in the same incubator but without stretching. The cells were harvested after 6, 24, 48, and 72 h of cyclic loading for downstream experiments, including microscopy of cells, immunostaining (72 h), and gene expression assay.

2.5. Collagen Immunohistochemistry. Collagen staining was performed according to the manufacturer's recommendation (Dako, Denmark). The methanol-fixed unstrained and strained cells were applied using hydrogen peroxidase to reduce nonspecific background for 5 min. Primary antibodies, i.e., rabbit anti-collagen type I or rat anti-collagen type III (Merck, USA), were diluted at 1 : 100 and were applied to each specimen and incubated for 30 min. Subsequently, the specimens were incubated with streptavidin-peroxidase secondary antibody (Dako, Denmark) for 30 min. For signal detection, 3,3′-diaminobenzidine tetrahydrochloride chromogen substrate was applied for 5 min and examined under light microscopy (Nikon Eclipse TE2000-S; Nikon Corporation, Japan).

2.6. N-Cadherin and Fibronectin Immunofluorescence Staining. hMSCs were fixed with 3.7% paraformaldehyde in PBS, followed by permeabilization with -20°C acetone, and incubated with 1% bovine serum albumin to block nonspecific binding of antibodies. For N-cadherin and fibronectin staining, the specimens were incubated with respective primary antibodies (Abcam, UK) diluted at 1 : 300 for 1 h and with appropriate FITC secondary antibodies (Abcam, UK) diluted at 1 : 600 for 1 h. Nuclei were stained by Hoechst (Molecular Probes, USA) in blue. The fluorescently stained samples were imaged by using a laser scanning confocal microscopy system (Leica TCL SL, Germany).

2.7. RNA Isolation and Multiplex Gene Expression Assay. To determine the correlation between the effects of hMSCs by mechanical stimulation and ENaC blocking activity, we used multiplex gene expression assay. Total RNA was extracted from unstrained and strained hMSCs using the RNeasy mini kit (Qiagen, Canada). RNA concentration and purity were assessed using a NanoDrop Spectrophotometer (ND-1000, NanoDrop Technologies, Wilmington, DE), and RNA integrity was assessed with a BioAnalyzer (Model 2100, Agilent Technologies). Only samples with high quality were selected for microsphere-based multiplex branched DNA downstream analysis. The mRNA expression of tenogenic lineages and ENaC subunits (see Table 1) was quantified by the QuantiGene 2.0 Plex assay (2.0 plex set 12082, Panomics/Affymetrix Inc., Fremont, CA, USA). The housekeeping gene was *PGK1* (phosphoglycerate kinase 1), which has been observed in our previous pilot study [26].

2.8. Statistical Analysis. The assays were carried out with a minimum number of technical triplicates ($n = 3$) per experimental run, using six independent samples from different donors ($N = 6$) for each group of the experiment. Data were presented as the mean ± standard deviation (SD). Statistical significance was analysed using one-way analysis of variance (ANOVA). A probability value (p value) of less than 0.5 was deemed to be statistically significant.

3. Results

3.1. Baseline Expression of ENaC Subunits in hMSCs. Semiquantitative PCR was performed to identify the presence of α, β, γ, and δ subunits of ENaC, and it was found that all four subunits are expressed in hMSCs (see Figure 2(a)). On using different strain magnitudes, it was observed that 8% strained cells expressed higher α subunit expressions as compared to 4% and 12% strain (see Figure 2(b)). Upon subjecting the cells to stretching at 1 Hz + 8%, the expression of α subunit increased significantly over time. However, there were no changes in the genes expression of the β, γ, and δ subunits (see Figure 2(c)).

3.2. Morphology of ENaC-Inhibited hMSCs after Mechanical Stimulation. Unstrained hMSCs were treated with different concentrations of benzamil (1, 10, 25, 50, and 100 μM) to identify the optimal concentration of benzamil that can be used in the study without causing morphological changes or cell detachment (see Figure 3(a)). Cells treated at the concentration of 1 μM and 10 μM showed normal fibroblastic appearance of MSCs with a similar cell number to that of the untreated cells. Cells treated with concentration above 10 μM showed apparent changes in the fibroblastic morphology and reduced cell number. Changes at higher concentrations may have been due to cell death and/or cell detachment (see Figure 3(a)). Based on these observations, 10 μM concentration of benzamil was thus selected for our experiments. The unstrained cells grew in random arrangements on silicone chambers, whilst the strained cells appeared elongated and aligned perpendicular to direction of stretch (see Figure 3(b)). There were no obvious morphological differences observed in ENaC-inhibited hMSCs or non-ENaC-inhibited hMSCs.

Table 1: The genes of interest determined in this study.

Related marker	Gene name	Abbreviation
ENaC subunit	Sodium channel, nonvoltage-gated 1, alpha	*SCNN1A*
	Sodium channel, nonvoltage-gated 1, beta (Liddle syndrome)	*SCNN1B*
	Sodium channel, nonvoltage-gated 1, delta	*SCNN1D*
	Sodium channel, nonvoltage-gated 1, gamma	*SCNN1G*
ECM component	Collagen type I, α1	*COL1*
	Collagen type III, α1	*COL3*
	Decorin	*DCN*
Tendon lineage	Tenascin C	*TNC*
	Scleraxis homolog A	*SCX*
	Tenomodulin	*TNMD*
Housekeeping gene	Phosphoglycerate kinase 1	*PGK1*

3.3. Changes in ECM Production during Stretching. Figure 4 shows the expression of collagen I, collagen III, fibronectin, and N-cadherin following immunostaining of the cells in both unstrained and strained cells treated with or without benzamil. Expression of collagen and especially collagen III was found to be slightly decreased in both unstrained and strained cells treated with benzamil as compared to cells without benzamil treatment. The expression of fibronectin and N-cadherin was increased in strained cells compared to unstrained cells; however, their expressions were reduced when treated with benzamil.

3.4. Influence of ENaC Inhibition on Tenogenic Differentiation. Our previous study shows that mechanical stimulation can trigger tenogenic differentiation of hMSCs [26]. From 6 hours to 72 hours, the expression of tenogenic markers appeared to be upregulated, with the exception of scleraxis, which was present at a higher level at 24 hours but decreased at later time points (see Figure 5(a)). The correlation between α-ENaC and hMSC tenogenic differentiation through mechanical stretching is analysed and presented in Table 2. Regression analysis showed that there was a strong positive correlation between α-ENaC expressions with tenogenic markers (with time), except for *SCX*. We then evaluated the effect of ENaC inhibition on mechanical strain-mediated tenogenic differentiation of hMSCs.

Blocking ENaC in cells subjected to mechanical loading resulted in a significant decrease in the expression of tenogenic markers (see Figure 5(b)). Although the expression of ECM components such as *DCN*, *COL1*, and *COL3* appeared to be increased during the earlier time points, these effects were diminished over time. The expressions of tenogenic markers were consistent with the immunostaining results of collagen (see Figure 4). α-ENaC gene (*SCNN1A*) was downregulated following ENaC inhibition. A drop in specific tenogenic gene expression including *TNC*, *SCX*, and *TNMD* was also observed. These observations support our hypothesis that ENaC (or more specifically α-ENaC) plays a vital role in the tenogenic differentiation processes following mechanical loading.

4. Discussion

ENaC, as an ion channel, has been shown to be a potent mechanotransducer in various cell types [27–29], and the mechanoactive role of ENaC particularly on the terminally differentiated cells appears to be well-established [7, 30, 31]. However, to the best of our knowledge, there have not been previous studies demonstrating the role of ENaC in regulating the mechanical strain-mediated tenogenic differentiation of hMSCs. This study is potentially the first to provide evidence of the involvement of ENaC on the mechanotransduction process that underpins the progression of hMSC differentiation in response to mechanical strain.

Previous studies have indicated the existence of four subunits (α, β, γ, and δ) of ENaC in human tissue or cells [32, 33]. Although all subunits were expressed in hMSCs, only α-ENaC appears to be related to the effects of stretching in hMSCs. From previous studies, β- and γ-ENaC have been shown to play an important role in mechanotransduction only in neurons innervating the aortic arch and vascular smooth muscle; and therefore, the lack of expression of these subunits in hMSCs is not unexpected [34]. Nevertheless, chondrocytes being cells of mesenchyme origin appears to response to mechanical signals through the propagation of signalling cascades initiated by the influx of sodium through mechanosensitive α-ENaC channels [11]. Hence, our finding of α-ENaC changes in hMSCs being responsive to stretching correlates well to the observations made in previous studies [35, 36].

We found that during mechanical stimulation, the expression of the functional subunit of α-ENaC increases in tandem with the increase in the expression of tenogenic differentiation markers. This apparent change in ENaC subunit stoichiometry during differentiation may suggest a specific role for the α-subunit of ENaC in the initiation and propagation of tenogenesis in hMSCs. Nevertheless, this does not indicate the lack of importance of the other subunits in this process. It merely suggests that α-ENaC is highly expressed during cell stretching; and based on previous studies, extracellular loops of other ENaC subunits may function as the sensors of mechanical loading that transmit the signal to the channel gating region, thereby enabling α-ENaC to function effectively [37, 38]. This complex interaction of the carboxyl terminal region of the α-ENaC to the actin cytoskeleton is thus necessary to propagate ENaC function, i.e., activating and proliferating the tenogenic differentiation process [38]. It is also worth noting that the subunits of ENaC may be enhanced by actin-disrupting agents or by addition of short actin filaments *in vitro* [37].

Another point worth mentioning is the fact that other studies suggest that certain ENaC subunits appear irrelevant for cellular function [39, 40]. Although it is reported that all subunits of ENaC contribute to the formation of functional channels [41], the existence of homomeric channels of α-

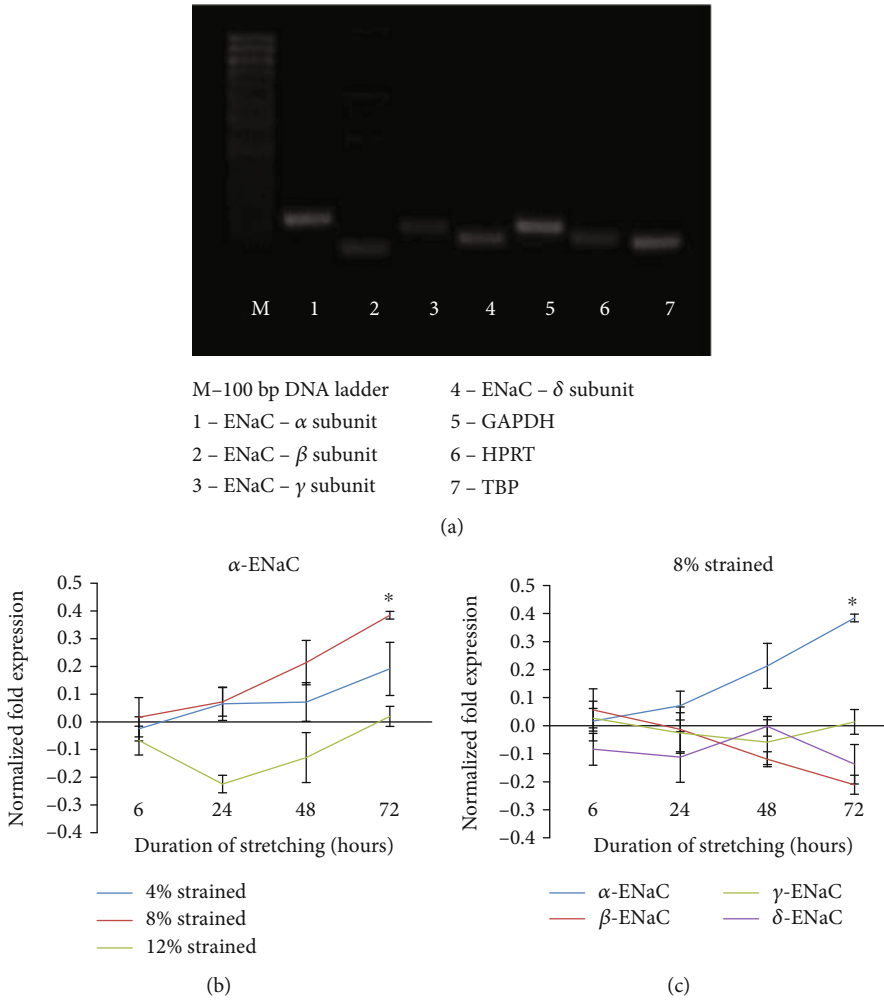

Figure 2: The expression of the α-, β-, γ-, and δ-ENaC mRNA in unstrained and strained hMSCs. (a) Analysis of RT-PCR products from hMSCs indicating the presence of the ENaC subunits. (b) mRNA expression of hMSCs shows α-ENaC expressed highest in 8% strained compared with 4% and 12% strained. (c) Expression of ENaC subunits at 8% strained at 1 Hz. Fold changes of expression were counted by normalizing to the relative expression amount of corresponding control groups (unstrained groups). Statistical significance ($p < 0.05$) was represented by $*$ which compared to unstrained. Error bars represent the SD of the mean of six biological replicates.

ENaC alone with distinct properties was also found in some studies [33, 42]. In fact, similar studies appear to show a single upscaling of this subunit to produce a small amount of amiloride-sensitive currents suggesting the functionality of homomeric α-ENaC [43]. In a study expressing recombinant α-ENaC in stretch-activated cation channel, null cells of human primary osteoblast demonstrated increased nonselective cation channel activity, with an increase in channels permeable to calcium ions [44].

We can therefore conclude that although the other subunits may not have a direct role in tenogenic expressions observed, its presence is necessary for the tenogenic process to be initiated and propagated. Using the ENaC inhibitor benzamil, we were able to demonstrate this apparent observation, albeit benzamil is not a specific blocker of a specific ENaC subunit. Thus, the use of benzamil itself is insufficient to prove that α-ENaC is completely involved in the tenogenic process occurring during mechanical stretching. Furthermore, sodium channel blockers had demonstrated the inhibitory effect on collagen accumulation in extracellular matrix [45]. This may explain the observed decrease in collagen in our experiments on treatment with benzamil. With ENaC blocking and reduced Na^+ influx, the expression of tenogenic markers was also reduced dramatically.

In the present study, the use of benzamil, a specific inhibitor to ENaC but not of its subunits, was chosen instead of amiloride. This was so since it has been suggested, albeit with some sense of lack of conviction, that benzamil is more effective in limiting the adverse effect of ENaC blockage on cell viability [46]. The blocking effect of benzamil appears to result from the benzene ring at the guanidino end of the molecule (see Figure 6(a)) [47], which is deemed to be molecule specific. Furthermore, amiloride has been shown to interfere with several cellular pathway processes, including inhibiting the Na^+/H^+ exchanger mechanisms [48]. Benzamil on the other hand is more stable and has a very high affinity for the Na^+ channel without affecting other major channels including K^+ channels [49, 50]. It has been suggested that

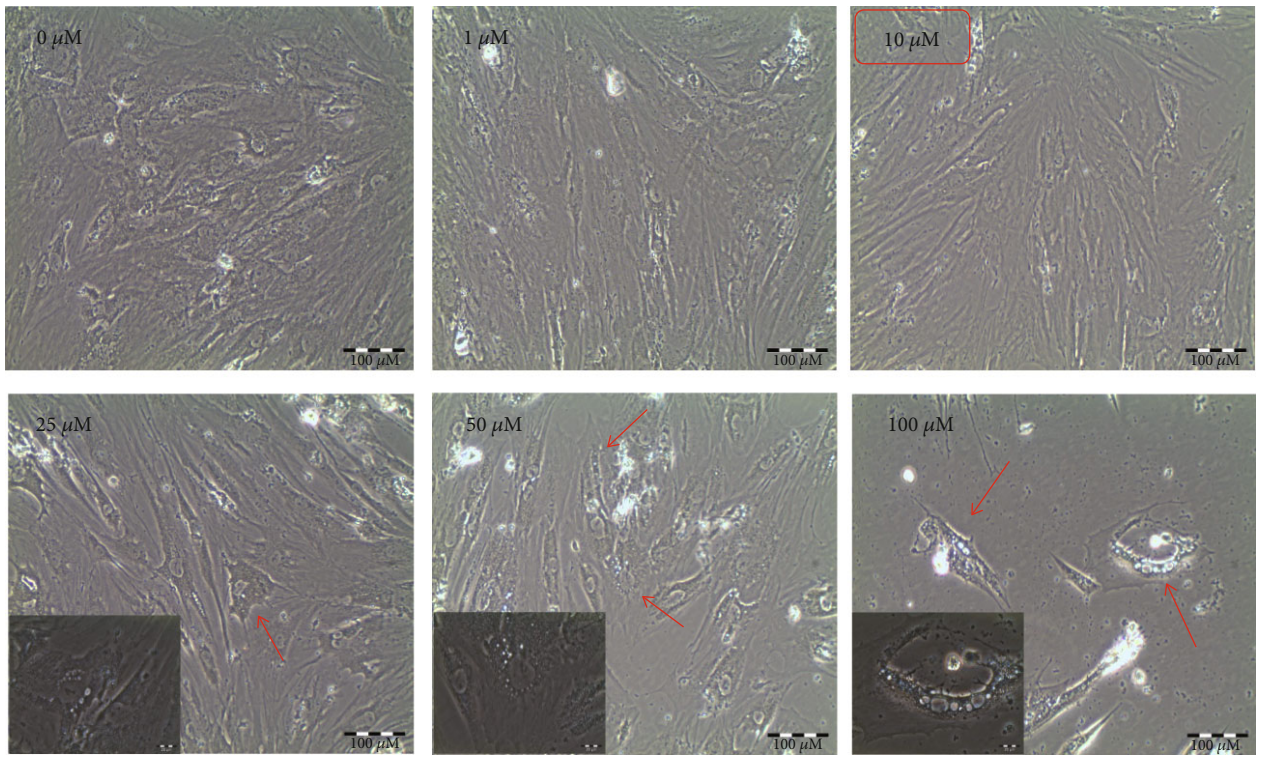

(a)

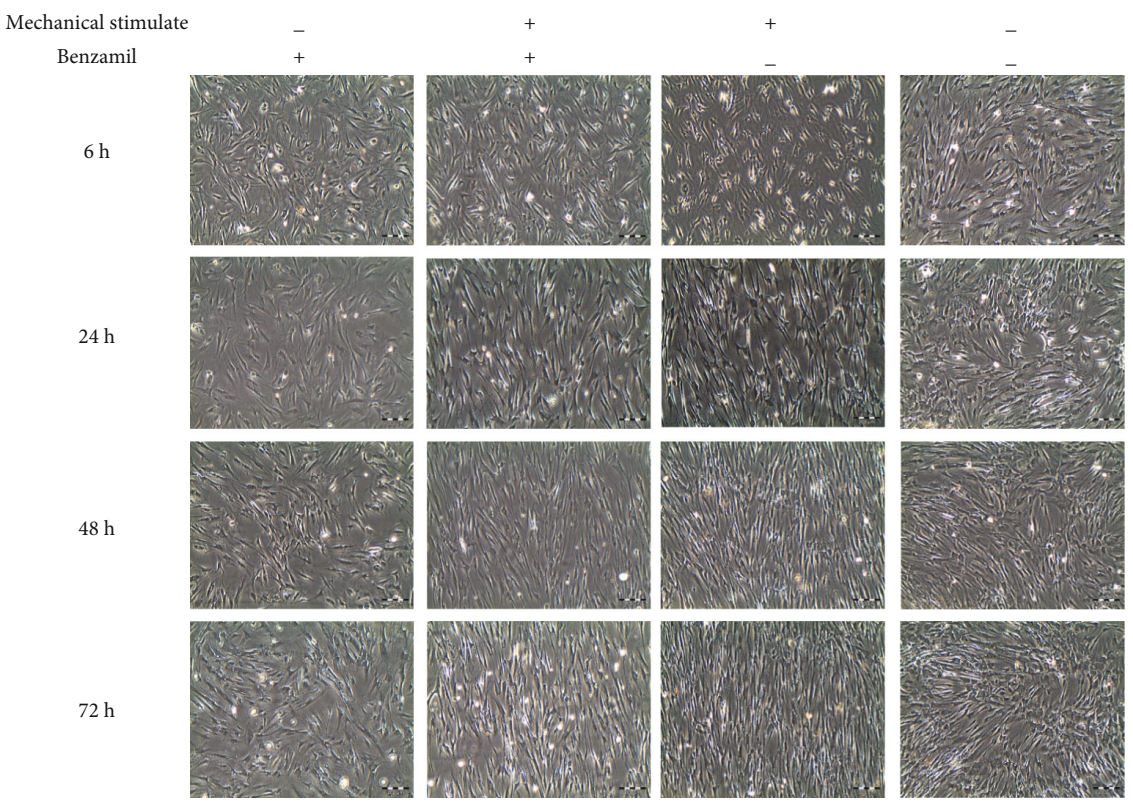

(b)

Figure 3: Morphology of hMSCs after treatment with benzamil. (a) Morphological changes of hMSC cell culture after 72-hour incubation with benzamil. Increasing concentration of benzamil resulted in the appearance of small vesicles (probably apoptotic bodies, see arrow). (b) Morphology of the unstrained and strained cells at 1 Hz, 8%, at different durations of exposure to mechanical stretching, with or without administration of 10 μM benzamil, respectively.

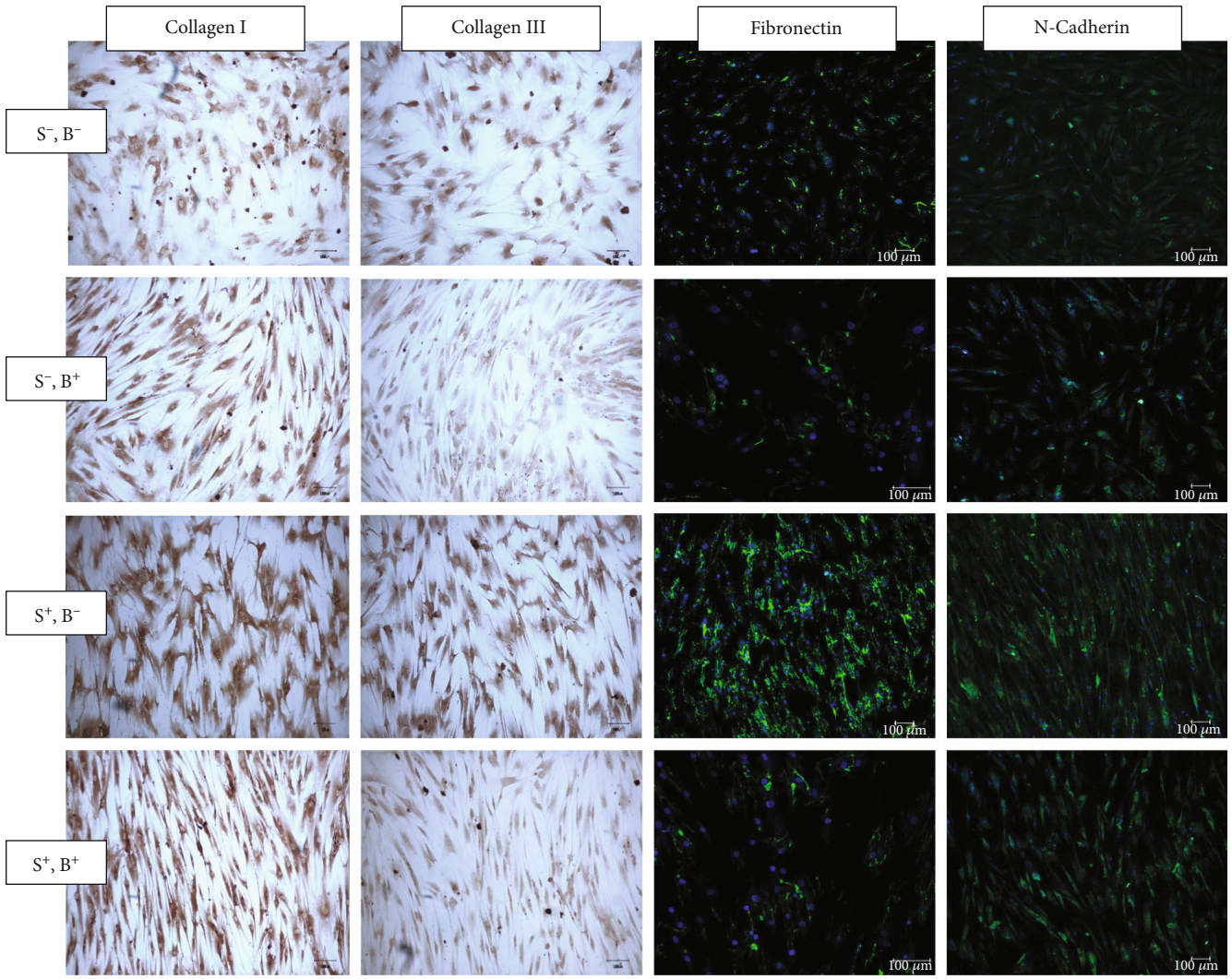

Figure 4: Immunostaining and immunofluorescence images of unstained and strained hMSCs cultured with or without benzamil. The cells were stained with immunostaining antibody collagen I and collagen III. Immunofluorescence was assessed on antibody fibronectin and N-cadherin. Each cell was stained with Hoechst (blue) to reveal the nucleus, and the images were merged with the corresponding fibronectin or N-cadherin (green). S^-: no mechanical stimulation; S^+: cyclic stretching applied; B^-: no benzamil; B^+: with ENaC inhibitor, benzamil.

the ionic channel block using benzamil at 1 μmol L^{-1} results in a complete halt of cellular function and can only be partially reversed. Hence, in minimal amounts, the effect of ENaC blocking can be better appreciated without the need to change the volume of the culture media.

There are several studies using inhibition of certain gene expression with siRNA (small interfering RNA) approach. Whilst the use siRNAs is an option for gene knockdown experiment, it has several issues which need to be taken into consideration such as nonspecific and incomplete silencing. In addition, it has been reported that the transfection ability of the primary cells is limited as compared to cancer cells, and the RNases will be actively engaged in degrading and eliminating the transfected siRNA. This will result in transient inhibition of the siRNA effect as the molecule is active only for a short time [51]. Besides, the transcripts with high turnover are sometimes difficult to silence. Thus, the use of this technique may not be the best choice in this present study.

It has been demonstrated that there are three possibilities as to how ENaC channels can be activated or blocked [52, 53]: (1) by controlling the bilayer tension or curvature directly activating the channel; (2) by controlling the release of another molecule from a cell that in turn activates the channel, for example, in the case of the present study where benzamil works by preventing sodium from moving intracellularly and competitively inhibiting sodium influx; and (3) by activating a tethering mechanism in which the ion channel binds either to the cytoskeleton or to the extracellular matrix. It has also been suggested that ENaC may perform other functions in MSCs, just like those of degenerins [54]. In our study, it was mostly the unstrained hMSCs that express low levels of ENaC. A rise in intracellular sodium activates C-Jun NH2-terminal kinase/stress-activated protein kinase (JNK), a member of the mitogen-activated protein kinase (MAPK) family, and the stress-activated protein kinase (SEK1) [55]. SEK1 can phosphorylate and activate JNK,

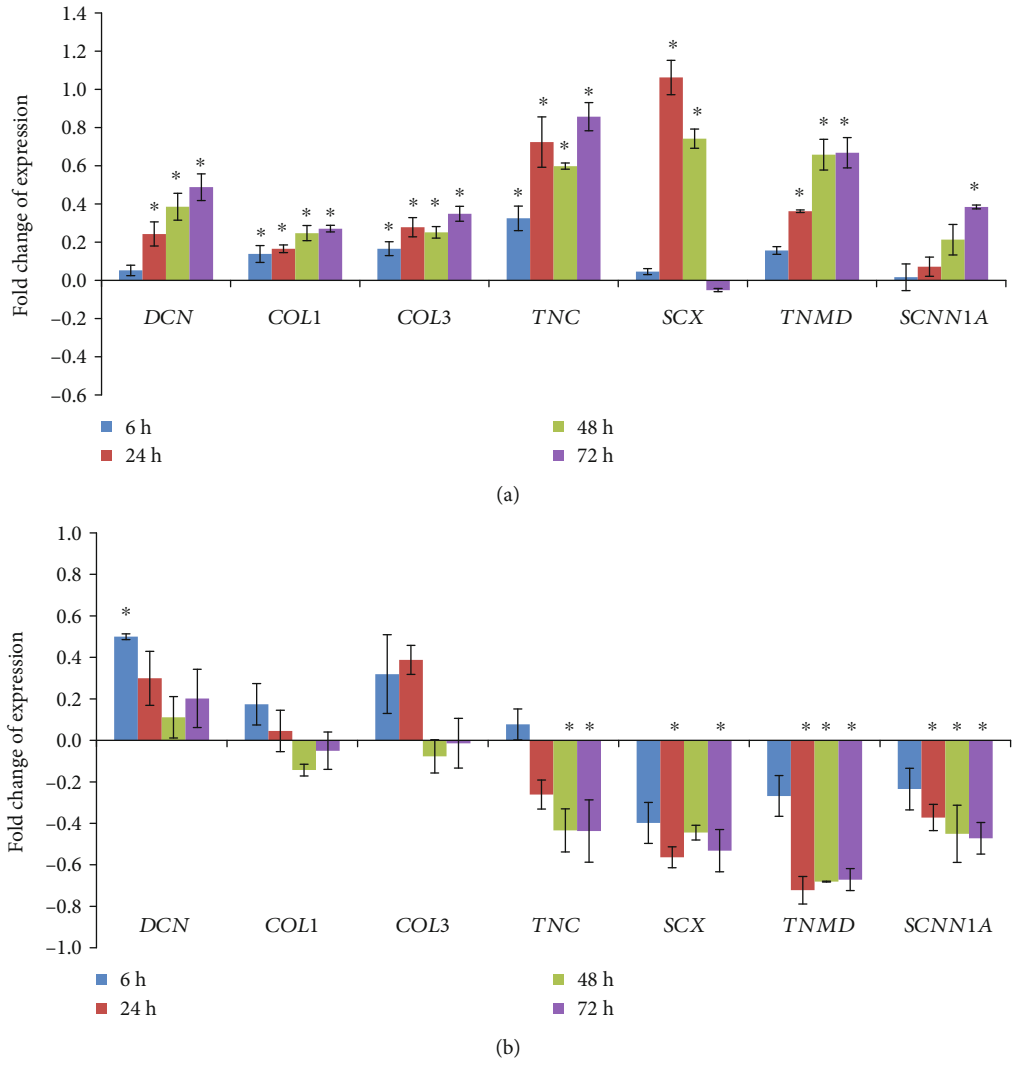

Figure 5: mRNA expression of tenogenic lineage genes and α-ENaC gene subjected to cyclic tensile loading. (a) Tenogenic differentiation of hMSCs is triggered by mechanical stimulation (1 Hz and 8% strain). The expression level of each gene was normalized with the level of housekeeping gene. Fold changes of expression were counted by normalizing to the relative expression amount of corresponding control groups (unstrained groups). Statistical significance ($p < 0.05$) was represented by $*$ compared to unstrained. (b) Tenogenic lineage genes' (*DCN*, *COL1*, *COL3*, *TNC*, *SCX*, and *TNMD*) expression was influenced after adding benzamil to the strained cells. The value of fold change was presented as the ratio of the strained group treated with benzamil to the strained group without benzamil. Statistical significance ($p < 0.05$) was represented by $*$ compared to the strained group without treatment. Error bars represent the SD of the mean of six biological replicates.

Table 2: Regression analysis of the relationship of α-ENaC with different cell lineage genes after mechanical strain.

Gene	Positive or negative correlation (R^2)
COL1	+0.8762
COL3	+0.8761
DCN	+0.9557
TNC	+0.7843
SCX	-0.0253
TNMD	+0.8318

which in turn phosphorylates C-Jun leading to an increased transcriptional activity. Thus, alterations in intracellular sodium concentration could trigger a cascade of transduction signals ultimately interfering with tenocyte-specific transcription factors. In contrast, if the ENaC of the cells is inhibited, there is no balance between extracellular and intracellular sodium concentration thus activating the signalling pathways and influencing tenogenesis expression. This process is illustrated in Figure 6.

Although the current study is robust in its design and provides us with a valuable insight into the role of α-ENaC in hMSC differentiation, there were limitations which were unavoidable but are worth highlighting. To directly investigate elevated ENaC activity, the strained and unstrained

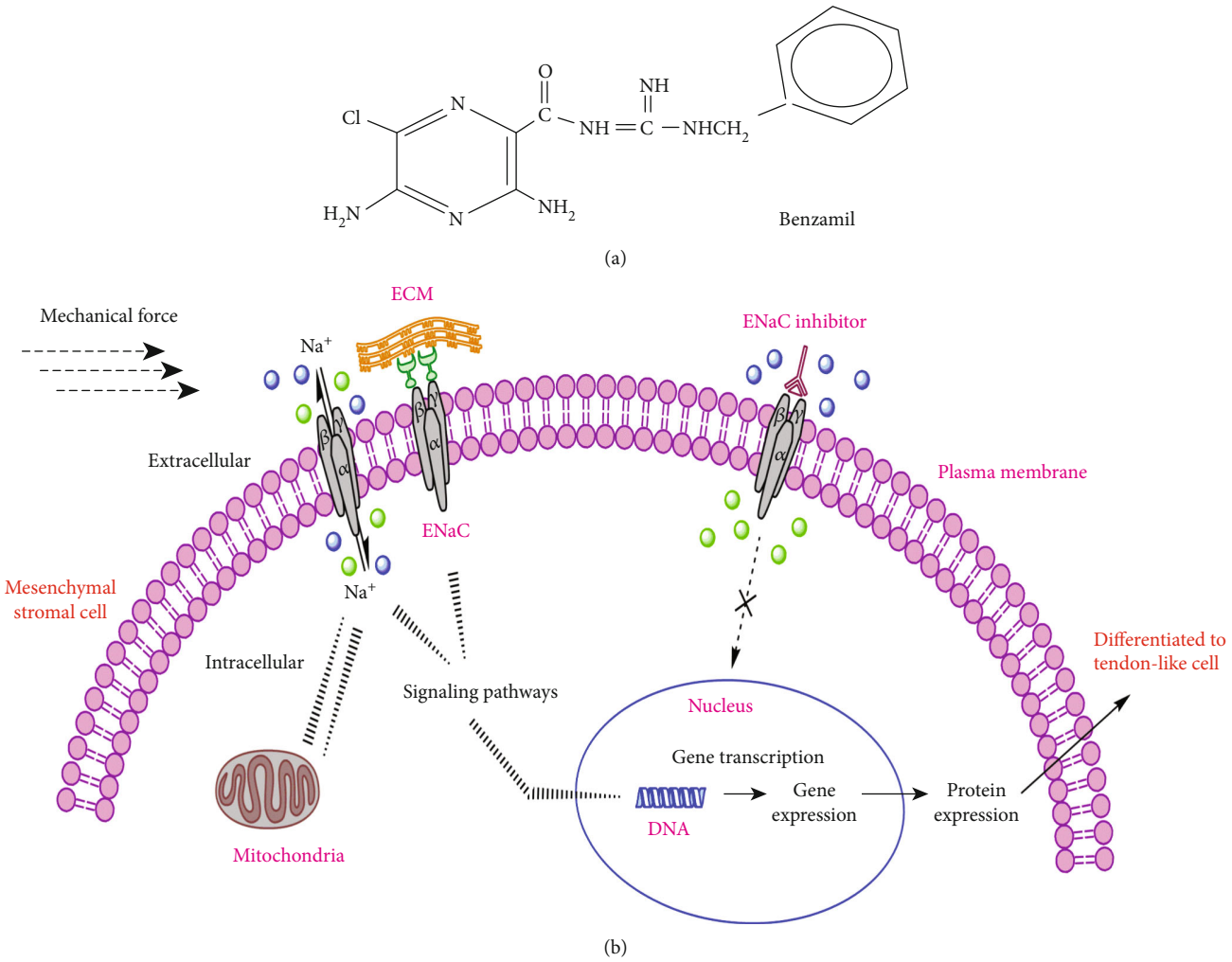

Figure 6: Proposed mechanism for the regulation of hMSCs tenogenic differentiation signaling pathways by ion channel ENaC. (b) ENaC leads to upregulation of the tenogenic gene markers, which in turn activates the tenogenic differentiation signaling pathway. Benzamil (a) which is the ENaC inhibitor, inhibits this pathway, and thus influences the cell differentiation.

hMSCs (either block by benzamil or not) should be subjected to whole-cell patch clamp recordings to analyse the benzamil-sensitive currents. We hope that by implementing this technique in the future, we will able to demonstrate that the ENaC/degenerin family of proteins is capable of mediating both transepithelial sodium transport and is directly responsible for the process of mechanotransduction. Secondly, the present study also did not study the involvement of other ionic fluxes, which, as many would concur, is a dynamic process of interrelated ionic interaction that may contribute to the tenogenic differentiation process.

The findings in this study nevertheless elucidate the roles of biomechanical stimulation and ion channel on hMSC differentiation towards a tendon fibroblast phenotype. As stated earlier, experimental control over progenitor cell lineage specification can be achieved by modulating properties of the cellular microenvironment. Understanding the microenvironments in which the MSCs reside and differentiate *in vivo* and trying to recapitulate these *in vitro* to further control stem cell differentiation has become an increasingly important area of stem cell research. Besides mechanical stimulation, other strategies including the use of soluble factors, ECM proteins, and biomaterials may also play an important role in hMSC differentiation. Several studies have shown that scaffolds (e.g., bioactive nanofibers and rope-like silk scaffolds) and growth factors (e.g., GDF5 and GDF7) can activate multiple signalling cascades, including MAPK, ERK, and Rho/ROCK, ultimately leading to the MSC tenogenic differentiation [56, 57]. Therefore, the application of growth factors and scaffolds in combination with mechanical stimuli may synergistically enhance tenogenic differentiation of hMSCs through amplification of the signalling pathways. However, the interactions between biochemical and mechanical cues in directing hMSC differentiation towards tenogenic lineage are still not fully understood and remain to be explored. Therefore, the focus of future studies could be directed in investigating the mechanisms underlying the synergistic effect of the biochemical and mechanical signals in influencing cell fate. With a better understanding of this process, incorporation of growth factors and/or

scaffold in combination with mechanotransduction may constitute a novel approach to achieve successful tendon tissue engineering via effective regulation of cellular differentiation.

5. Conclusions

The present study demonstrated that (1) although α, β, γ, and δ subunits of ENaC were expressed in hMSCs, only the expression of the functional α subunit is higher during stretching at 1 Hz and 8% strain, thus suggesting that α-ENaC is the main mechanosensitive ion channel that influences tenogenic differentiation of hMSCs, (2) uniaxial strains at 8% is required to elicit significant tenogenic expressions, and (3) there is a positive correlation between the α-ENaC expression and tenogenic marker expressions which is altered in the presence of ENaC blocker benzamil, thus strengthening our hypothesis that ENaC (and more specifically the α-ENaC subunit) may be implicated in regulating the tenogenic differentiation process of hMSCs during cell stretching.

Data Availability

The data used to support the findings of this study are included within the article.

Conflicts of Interest

The authors declare that there is no conflict of interest regarding the publication of this paper.

Acknowledgments

This work was supported by the Fundamental Research Grant Scheme (FRGS) (Grant number FP029-2010B) and University of Malaya Research Grant (UMRG) (Grant number RP005F-13HTM). The authors thank all volunteers and patients for their donation of bone marrow. We express our gratitude to Prof. Dr. Azlina Amir Abbas and Prof. Dr. Azhar Mahmood Merican from the Department of Orthopaedic Surgery, University of Malaya, for their assistance to provide necessary samples for this study. We also thank the University of Malaya for a PhD thesis scholarship for the first author.

References

[1] T. Bose, A. Cieślar-Pobuda, and E. Wiechec, "Role of ion channels in regulating Ca^{2+} homeostasis during the interplay between immune and cancer cells," *Cell Death & Disease*, vol. 6, no. 2, article e1648, 2015.

[2] R. Gessmann, N. Kourtis, K. Petratos, and N. Tavernarakis, "Molecular modeling of mechanosensory ion channel structural and functional features," *PLoS One*, vol. 5, no. 9, article e12814, 2010.

[3] L. He, M. Ahmad, and N. Perrimon, "Mechanosensitive channels and their functions in stem cell differentiation," *Experimental Cell Research*, vol. 374, no. 2, pp. 259–265, 2019.

[4] H. Y. Nam, H. R. Balaji Raghavendran, B. Pingguan-Murphy, A. A. Abbas, A. M. Merican, and T. Kamarul, "Fate of tenogenic differentiation potential of human bone marrow stromal cells by uniaxial stretching affected by stretch-activated calcium channel agonist gadolinium," *PLoS One*, vol. 12, no. 6, article e0178117, 2017.

[5] I. Hanukoglu and A. Hanukoglu, "Epithelial sodium channel (ENaC) family: phylogeny, structure-function, tissue distribution, and associated inherited diseases," *Gene*, vol. 579, no. 2, pp. 95–132, 2016.

[6] Y. Marunaka, N. Niisato, A. Taruno et al., "Regulation of epithelial sodium transport via epithelial Na^+ channel," *Journal of Biomedicine & Biotechnology*, vol. 2011, Article ID 978196, 8 pages, 2011.

[7] A. Mobasheri, R. Barrett-Jolley, M. Shakibaei, C. M. Canessa, and P. Martín-Vasallo, "Enigmatic roles of the epithelial sodium channel (ENaC) in articular chondrocytes and osteoblasts: mechanotransduction, sodium transport or extracellular sodium sensing?," in *Mechanosensitivity in Cells and Tissues*, A. Kamkin and I. Kiseleva, Eds., Academia, Moscow, 2005.

[8] C. Parisi, V. V. Chandaria, and N. C. Nowlan, "Blocking mechanosensitive ion channels eliminates the effects of applied mechanical loading on chick joint morphogenesis," *Philosophical transactions of the Royal Society of London. Series B, Biological Sciences*, vol. 373, no. 1759, article 20170317, 2018.

[9] K. Takahashi, Y. Matsuda, and K. Naruse, "Mechanosensitive ion channels," *AIMS Biophysics*, vol. 3, no. 1, pp. 63–74, 2016.

[10] K. A. Jansen, D. M. Donato, H. E. Balcioglu, T. Schmidt, E. H. Danen, and G. H. Koenderink, "A guide to mechanobiology: where biology and physics meet," *Biochimica et Biophysica Acta*, vol. 1853, no. 11, pp. 3043–3052, 2015.

[11] M. Shakibaei and A. Mobasheri, "Beta1-integrins co-localize with Na, K-ATPase, epithelial sodium channels (ENaC) and voltage activated calcium channels (VACC) in mechanoreceptor complexes of mouse limb-bud chondrocytes," *Histology and Histopathology*, vol. 18, no. 2, pp. 343–351, 2003.

[12] S. S. Ranade, R. Syeda, and A. Patapoutian, "Mechanically activated ion channels," *Neuron*, vol. 87, no. 6, pp. 1162–1179, 2015.

[13] T. Fujii, J. Youssefzadeh, M. Novel, and J. Neman, "Introduction to the ventricular system and choroid plexus," in *The choroid plexus and cerebrospinal fluid*, J. Neman and T. C. Chen, Eds., pp. 1–13, Academic Press, San Diego, 2016.

[14] C. A. West, W. Han, N. Li, and S. M. Masilamani, "Renal epithelial sodium channel is critical for blood pressure maintenance and sodium balance in the normal late pregnant rat," *Experimental Physiology*, vol. 99, no. 5, pp. 816–823, 2014.

[15] R. E. B. Fitzsimmons, M. S. Mazurek, A. Soos, and C. A. Simmons, "Mesenchymal stromal/stem cells in regenerative medicine and tissue engineering," *Stem Cells International*, vol. 2018, Article ID 8031718, 16 pages, 2018.

[16] S. Kariminekoo, A. Movassaghpour, A. Rahimzadeh, M. Talebi, K. Shamsasenjan, and A. Akbarzadeh, "Implications of mesenchymal stem cells in regenerative medicine," *Artificial Cells, Nanomedicine, and Biotechnology*, vol. 44, no. 3, pp. 749–757, 2016.

[17] M. T. Harris, D. L. Butler, G. P. Boivin, J. B. Florer, E. J. Schantz, and R. J. Wenstrup, "Mesenchymal stem cells used for rabbit tendon repair can form ectopic bone and express alkaline phosphatase activity in constructs," *Journal of Orthopaedic Research*, vol. 22, no. 5, pp. 998–1003, 2004.

[18] J. L. Chen, W. Zhang, Z. Y. Liu, B. C. Heng, H. W. Ouyang, and X. S. Dai, "Physical regulation of stem cells differentiation into teno-lineage: current strategies and future direction," *Cell and Tissue Research*, vol. 360, no. 2, pp. 195–207, 2015.

[19] M. Leung, S. Jana, C. T. Tsao, and M. Zhang, "Tenogenic differentiation of human bone marrow stem cells via a combinatory effect of aligned chitosan-poly-caprolactone nanofibers and TGF-β3," *Journal of Materials Chemistry B*, vol. 1, no. 47, pp. 6516–6524, 2013.

[20] C. Perucca Orfei, M. Viganò, J. R. Pearson et al., "In vitro induction of tendon-specific markers in tendon cells, adipose- and bone marrow-derived stem cells is dependent on TGFβ3, BMP-12 and ascorbic acid stimulation," *International Journal of Molecular Sciences*, vol. 20, no. 1, p. 149, 2019.

[21] J. R. Choi, K. W. Yong, and J. Y. Choi, "Effects of mechanical loading on human mesenchymal stem cells for cartilage tissue engineering," *Journal of Cellular Physiology*, vol. 233, no. 3, pp. 1913–1928, 2018.

[22] K. H. Vining and D. J. Mooney, "Mechanical forces direct stem cell behaviour in development and regeneration," *Nature Reviews. Molecular Cell Biology*, vol. 18, no. 12, pp. 728–742, 2017.

[23] H. Y. Nam, B. Pingguan-Murphy, A. A. Abbas, A. M. Merican, and T. Kamarul, "The proliferation and tenogenic differentiation potential of bone marrow-derived mesenchymal stromal cell are influenced by specific uniaxial cyclic tensile loading conditions," *Biomechanics and Modeling in Mechanobiology*, vol. 14, no. 3, pp. 649–663, 2015.

[24] T. Mammoto and D. E. Ingber, "Mechanical control of tissue and organ development," *Development*, vol. 137, no. 9, pp. 1407–1420, 2010.

[25] H. Y. Nam, P. Karunanithi, W. C. P. Loo et al., "The effects of staged intra-articular injection of cultured autologous mesenchymal stromal cells on the repair of damaged cartilage: a pilot study in caprine model," *Arthritis Research & Therapy*, vol. 15, no. 5, article R129, 2013.

[26] H. Y. Nam, B. Pingguan-Murphy, A. A. Abbas, A. M. Merican, and T. Kamarul, "Uniaxial cyclic tensile stretching at 8% strain exclusively promotes tenogenic differentiation of human bone marrow-derived mesenchymal stromal cells," *Stem Cells International*, vol. 2019, Article ID 9723025, 16 pages, 2019.

[27] M. Fronius, R. Bogdan, M. Althaus, R. E. Morty, and W. G. Clauss, "Epithelial Na+ channels derived from human lung are activated by shear force," *Respiratory Physiology & Neurobiology*, vol. 170, no. 1, pp. 113–119, 2010.

[28] E. C. Kim, D. S. Ahn, S. I. Yeon, M. Lim, and Y. H. Lee, "Epithelial Na+ channel proteins are mechanotransducers of myogenic constriction in rat posterior cerebral arteries," *Experimental Physiology*, vol. 97, no. 4, pp. 544–555, 2012.

[29] R. Raouf, F. Rugiero, H. Kiesewetter et al., "Sodium channels and mammalian sensory mechanotransduction," *Molecular Pain*, vol. 8, p. 1744-8069-8-21, 2012.

[30] S. Matalon, R. Bartoszewski, and J. F. Collawn, "Role of epithelial sodium channels in the regulation of lung fluid homeostasis," *American Journal of Physiology. Lung Cellular and Molecular Physiology*, vol. 309, no. 11, pp. L1229–L1238, 2015.

[31] A. Tarjus, C. González-Rivas, I. Amador-Martínez et al., "The absence of endothelial sodium channel α (αENaC) reduces renal ischemia/reperfusion injury," *International Journal of Molecular Sciences*, vol. 20, no. 13, article 3132, 2019.

[32] N. Bangel-Ruland, K. Sobczak, T. Christmann et al., "Characterization of the epithelial sodium channel delta-subunit in human nasal epithelium," *American Journal of Respiratory Cell and Molecular Biology*, vol. 42, no. 4, pp. 498–505, 2010.

[33] B. Krueger, U. Schlötzer-Schrehardt, S. Haerteis et al., "Four subunits ($\alpha\beta\gamma\delta$) of the epithelial sodium channel (ENaC) are expressed in the human eye in various locations," *Investigative Ophthalmology & Visual Science*, vol. 53, no. 2, pp. 596–604, 2012.

[34] H. A. Drummond, D. Gebremedhi, and D. R. Harder, "Degenerin/epithelial $^{Na+Channel}$ proteins," *Hypertension*, vol. 44, no. 5, pp. 643–648, 2004.

[35] S. B. Mustafa, J. Isaac, S. R. Seidner, P. S. Dixon, B. M. Henson, and R. J. DiGeronimo, "Mechanical stretch induces lung α-epithelial Na(+) channel expression," *Experimental Lung Research*, vol. 40, no. 8, pp. 380–391, 2014.

[36] S. Shi, M. D. Carattino, R. P. Hughey, and T. R. Kleyman, "ENaC regulation by proteases and shear stress," *Current Molecular Pharmacology*, vol. 6, no. 1, pp. 28–34, 2013.

[37] S. Chifflet and J. A. Hernández, "The plasma membrane potential and the organization of the actin cytoskeleton of epithelial cells," *International Journal of Cell Biology*, vol. 2012, Article ID 121424, 13 pages, 2012.

[38] C. Mazzochi, J. K. Bubien, P. R. Smith, and D. J. Benos, "The carboxyl terminus of the alpha-subunit of the amiloride-sensitive epithelial sodium channel binds to F-actin," *The Journal of Biological Chemistry*, vol. 281, no. 10, pp. 6528–6538, 2006.

[39] J. Loffing and L. Schild, "Functional domains of the epithelial sodium channel," *Journal of the American Society of Nephrology: JASN*, vol. 16, no. 11, pp. 3175–3181, 2005.

[40] P. M. Snyder, C. Cheng, L. S. Prince, J. C. Rogers, and M. J. Welsh, "Electrophysiological and biochemical evidence that DEG/ENaC cation channels are composed of nine subunits," *The Journal of Biological Chemistry*, vol. 273, no. 2, pp. 681–684, 1998.

[41] L. Schild, E. Schneeberger, I. Gautschi, and D. Firsov, "Identification of amino acid residues in the alpha, beta, and gamma subunits of the epithelial sodium channel (ENaC) involved in amiloride block and ion permeation," *The Journal of General Physiology*, vol. 109, no. 1, pp. 15–26, 1997.

[42] A. Staruschenko, E. Adams, R. E. Booth, and J. D. Stockand, "Epithelial Na^+ channel subunit stoichiometry," *Biophysical Journal*, vol. 88, no. 6, pp. 3966–3975, 2005.

[43] C. M. Canessa, L. Schild, G. Buell et al., "Amiloride-sensitive epithelial Na^+ channel is made of three homologous subunits," *Nature*, vol. 367, no. 6462, pp. 463–467, 1994.

[44] L. Lu, L. Wu, H. Jia et al., "The epithelial sodium channel is involved in dexamethasone-induced osteoblast differentiation and mineralization," *Cell Biology and Toxicology*, vol. 28, no. 5, pp. 279–289, 2012.

[45] V. Ivanov, S. Ivanova, T. Kalinovsky, A. Niedzwiecki, and M. Rath, "Inhibition of collagen synthesis by select calcium and sodium channel blockers can be mitigated by ascorbic acid and ascorbyl palmitate," *American Journal of Cardiovascular Disease*, vol. 6, no. 2, pp. 26–35, 2010.

[46] D. Wesch, M. Althaus, P. Miranda et al., "Differential N termini in epithelial Na^+ channel δ-subunit isoforms modulate channel trafficking to the membrane," *American Journal of Physiology Cell Physiology*, vol. 302, no. 6, pp. 868–879, 2012.

[47] T. Cox, "Amiloride analog stimulation of short-circuit current in larval frog skin epithelium," *The Journal of Experimental Biology*, vol. 200, no. 23, pp. 3055–3065, 1997.

[48] P. G. Vallés, V. Bocanegra, A. Gil Lorenzo, and V. V. Costantino, "Physiological functions and regulation of the Na^+/H^+ exchanger [NHE1] in renal tubule epithelial cells," *Kidney & Blood Pressure Research*, vol. 40, no. 5, pp. 452–466, 2015.

[49] D. J. Benos, S. Cunningham, R. R. Baker, K. B. Beason, Y. Oh, and P. R. Smith, "Molecular characteristics of amiloride-sensitive sodium channels," *Reviews of Physiology, Biochemistry And Pharmacology*, vol. 120, pp. 31–113, 1992.

[50] L. Simchowitz, T. R. Kleyman, and E. J. Cragoe, "An overview of the structure - activity relations in the amiloride series," in *Amiloride and its analogs - unique cation transport inhibitors*, E. J. Cragoe, T. Kleyman, and L. Simchowitz, Eds., pp. 9–24, Wiley-VCH, New York, 1992.

[51] C. Gardmo, P. Kotokorpi, H. Helander, and A. Mode, "Transfection of adult primary rat hepatocytes in culture," *Biochemical Pharmacology*, vol. 69, no. 12, pp. 1805–1813, 2005.

[52] D. J. Benos, "Sensing tension: recognizing enac as a stretch sensor," *Hypertension*, vol. 44, no. 5, pp. 616-617, 2004.

[53] O. P. Hamill and B. Martinac, "Molecular basis of mechanotransduction in living cells," *Physiological Reviews*, vol. 81, no. 2, pp. 685–740, 2001.

[54] N. Golestaneh, C. Klein, F. Valamanesh, G. Suarez, M. K. Agarwal, and M. Mirshahi, "Mineralocorticoid receptor-mediated signaling regulates the ion gated sodium channel in vascular endothelial cells and requires an intact cytoskeleton," *Biochemical and Biophysical Research Communications*, vol. 280, no. 5, pp. 1300–1306, 2001.

[55] D. W. Kuroki, A. Minden, I. Sánchez, and E. V. Wattenberg, "Regulation of a c-Jun amino-terminal kinase/stress-activated protein kinase cascade by a sodium-dependent signal transduction pathway," *The Journal of Biological Chemistry*, vol. 272, no. 38, pp. 23905–23911, 1997.

[56] E. Maharam, M. Yaport, N. L. Villanueva et al., "Rho/Rock signal transduction pathway is required for MSC tenogenic differentiation," *Bone Research*, vol. 3, no. 1, 2015.

[57] Y. J. Zhang, X. Chen, G. Li et al., "Concise review: stem cell fate guided by bioactive molecules for tendon regeneration," *Stem Cells Translational Medicine*, vol. 7, no. 5, pp. 404–414, 2018.

Hindawi
Stem Cells International
Volume 2020, Article ID 8889379, 18 pages
https://doi.org/10.1155/2020/8889379

Research Article

Small Extracellular Vesicles from Human Fetal Dermal Cells and Their MicroRNA Cargo: KEGG Signaling Pathways Associated with Angiogenesis and Wound Healing

Cinzia Maria Chinnici,[1,2] **Giandomenico Amico**,[1,2] **Alessia Gallo**,[2] **Gioacchin Iannolo**,[2] **Nicola Cuscino**,[2] **Serena Vella**,[3] **Claudia Carcione**,[1] **David Nascari**,[1,4] **and Pier Giulio Conaldi**[2]

[1]*Fondazione Ri.MED, Palermo, Italy*
[2]*Department of Research, IRCCS-ISMETT, Palermo, Italy*
[3]*Innovation and Development Department, Anemocyte Srl, Gerenzano, Italy*
[4]*McGowan Institute for Regenerative Medicine, University of Pittsburgh, Pittsburgh PA, USA*

Correspondence should be addressed to Cinzia Maria Chinnici; cchinnici@fondazionerimed.com

Received 21 April 2020; Revised 8 July 2020; Accepted 21 July 2020; Published 13 August 2020

Academic Editor: Kar Wey Yong

The use of cell secreted factors in clinical settings could be an alternative to conventional cell therapy, with the advantage of limiting concerns generally associated with traditional cell transplantation, such as tumorigenicity, immunoreactivity, and carrying of infections. Based on our published data, we predict a potential role for extracellular vesicles (EVs) in contributing to the proangiogenic activity of human fetal dermal cell secretome. Depletion of nanosized EVs from secretome significantly impaired its ability to induce formation of mesh-like structures *in vitro*. The isolated EVs were characterized for size and concentration by nanoparticle tracking analysis, and for protein markers ($Rab5^+$, $Alix^+$, $CD63^+$, and $calnexin^-$). The microRNA profile of EVs revealed 87 microRNAs significantly upregulated (≥15-fold increase) in fetal compared to adult dermal cell-derived EVs. Interestingly, these upregulated microRNAs included microRNAs with a validated role in angiogenesis according to literature. Moreover, the DIANA-TarBase v7.0 analysis confirmed enrichment in the KEGG signaling pathways associated with angiogenesis and wound healing, with the identification of putative target genes including thrombospondin 1. To validate the *in silico* data, EVs were also characterized for total protein contents. When tested in *in vitro* angiogenesis, fetal dermal cell-derived EVs were more effective than their adult counterpart in inducing formation of complete mesh-like structures. Furthermore, treatment of fibroblasts with fetal dermal-derived EVs determined a 4-fold increase of thrombospondin 1 protein amounts compared with the untreated fibroblasts. Finally, visualization of CSFE-labeled EVs in the cytosol of target cells suggested a successful uptake of these particles at 4-8 hours of incubation. We conclude that EVs are important contributors of the proangiogenic effect of fetal dermal cell secretome. Hence, EVs could also serve as vehicle for a successful delivery of microRNAs or other molecules of therapeutic interest to target cells.

1. Introduction

The list of clinical conditions related to insufficient angiogenesis is wide, ranging from cardiovascular diseases to impaired wound healing [1]. Therefore, there is a great interest in developing clinical strategies ensuring vasculature formation, such as delivery of different cell populations, or administration of proangiogenic growth factors. Among the cell-based therapies, the use of mesenchymal stromal cells (MSCs), which are closely related to pericytes and produce diverse proangiogenic factors, is a promising approach with the potential to stimulate vasculature tissue development [2].

MSC-based therapy applied to regenerative medicine counts hundreds of registered clinical trials with excellent

records of safety and efficacy (http://www.clinicaltrials.gov and http://www.clinicaltrialsregister.eu). Despite earlier works ascribing the therapeutic effects of MSCs to their ability to engraft and differentiate to form new permanent tissues, the current consensus view is that MSCs are short-lived after delivery and exert therapeutic benefits through secretion of bioactive factors [3]. In support of MSC paracrine activity, animal studies have shown that administration of MSC-derived soluble factors recapitulates the effects of cell-based therapy [4]. Consequently, the attention has been brought to the vast array of molecules produced by MSCs [5, 6]. The mixture of growth factors, cytokines, chemokines, and extracellular vesicles (EVs) released by cells is known as secretome and can be collected as cell culture conditioned medium (CM).

Human fetal skin cell therapy has been used to replace older skin cell therapy to treat patients with skin ulcers [7, 8], as well as burns [9, 10], thus resulting in a safe and more efficacious procedure. At that time, the authors suggested the differential gene expression profiling observed in fetal versus adult skin cells as responsible for the efficacy of fetal skin cell therapy [8]. Moreover, since no trace of fetal skin cells was found in recipient biopsies, a paracrine mechanism of healing was suggested [10]. Although an extensive characterization of cell phenotype and secreted factors was missing, those studies open up new research perspectives on the use of cell secretome for regenerative medicine applications.

In a previous study [11], we isolated human fetal dermal cells, which we named multipotent fetal dermal cells based on *in vitro* characteristics, such as the MSC-like immunophenotype, the multilineage differentiation potential, and the low immunogenicity. We also confirmed the practical advantages of culturing fetal skin cells in comparison to adult skin cells described by others [7, 9, 10], including faster isolation technique and higher proliferative capacity of fetal cells. More recently [12], we used liquid chromatography and tandem mass spectrometry (LC-MS/MS) to show a set of proteins related to angiogenesis and wound healing, which were significantly upregulated in fetal dermal cell secretome compared to adult dermal cell secretome. Proteome finding was corroborated by the remarkable *in vitro* proangiogenic capacity of fetal dermal cell secretome compared to its adult counterpart.

In the present study, we investigated whether the presence of EVs could contribute to the biological functions of fetal dermal cell secretome. EVs are released by several cell types and are essential for cell-to-cell communication [13]. These particles are internalized by target cells [14] and once in the cytosol, discharge their material such as proteins, mRNAs, and microRNAs (miRNAs). Administration of MSC-derived EVs has been shown to have beneficial effects in various animal models of organ injury by regulating angiogenesis, cell proliferation, cell migration, and collagen synthesis [15, 16]. Nevertheless, EV-based therapy for skin repair consists only of one registered clinical trial aims at studying the effects of plasma-derived exosomes on cutaneous wound healing (http://www.clinicaltrials.gov, NCT02565264).

Herein, EVs were isolated from secretome of fetal and adult dermal cells and characterized for size and concentration by nanoparticle tracking analysis (NTA). Then, we tested the capacity of EV-depleted secretome in inducing *in vitro* angiogenesis and migration of target cells such as human umbilical vein endothelial cells (HUVECs) and fibroblasts. The miRNA expression profile of fetal dermal cell- vs. adult dermal cell-derived EVs was also analyzed, and a bioinformatics approach was used to identify the Kyoto Encyclopedia of Genes and Genomes (KEGG) signaling pathways most likely affected by these miRNAs. The predicted angiogenic/wound healing-related effects of fetal dermal cell-derived EVs were further validated in *in vitro* cell-based assays of angiogenesis and cell migration by preconditioning of target cells with different concentrations of EV preparations. Finally, we investigated whether carboxyfluorescein succinimidyl ester- (CSFE-) labeled EVs from fetal dermal cells might be taken up by target cells.

2. Materials and Methods

2.1. Cell Procurement. Fetal skin biopsies were taken from 20- to 22-gestational-week human fetuses obtained from therapeutic abortions, according to a protocol approved by ISMETT's Institutional Research Review Board (IRRB/00/2015) and Ethics Committee. Signed informed consent form was obtained from each donor. Fetal dermal cells were isolated and characterized as previously described [11]. Adult skin biopsies (45–55-year-old donors) were provided by Istituto Humanitas (Rozzano, Milan). Fetal and adult dermal cells were isolated under the same conditions. Normal dermal fibroblasts and HUVECs were purchased from Thermo Fisher Scientific (Waltham, MA, USA) and used as target cells in *in vitro* cell-based assays.

2.2. Cell Cultures, CM Collection, Isolation, and Storage of EVs. Fetal dermal cells and adult dermal cells, previously cryopreserved in Dulbecco's modified Eagle's medium (DMEM) (Sigma-Aldrich, St. Louis, MO, USA) supplemented with 10% dimethyl sulfoxide (DMSO) (CryoSure, WAK-Chemie Medical GmbH, Steinbach, Germany) and 30% fetal bovine serum (FBS), were grown in 75 cm^2 tissue flasks (SARSTEDT, Numbrecht, Germany) as previously described [11]. For CM collection, serum-free alpha-minimum essential medium (MEM) (Gibco, Thermo Fisher Scientific) was added to 80% confluent cells and collected 24 hours later. EVs were isolated by differential ultracentrifugation of CM according to a protocol [17] and as previously described [18]. In brief, CM was centrifuged at $1800 \times g$ for 10 minutes to remove cell debris, centrifuged again at $17000 \times g$ for 15 minutes, and then at $160000 \times g$ for 1 hour in the ultracentrifuge (Optima MAX-XP, Beckman Coulter Inc., Irving, TX, USA). All centrifugation steps were done at 4°C. The pellet was resuspended in phosphate-buffered saline (PBS) without Ca^{2+}/Mg^{2+} (Sigma-Aldrich) or subjected to total protein extraction or total RNA extraction.

2.3. Characterization of EVs by Nanoparticle Tracking Analysis. Pellet particles resuspended in PBS (three fetal

and three adult samples) were analyzed for size and concentration by nanoparticle tracking analysis (NTA) [19] using the NanoSight (NS300, Malvern Instruments, Westborough, MA, USA). Briefly, samples were diluted in PBS, 300 μl of sample was loaded into the chamber, and five videos for each sample were recorded. Data analysis was performed with the NTA software and data were presented as the mean ± standard deviation (SD) of the five videos.

2.4. Extraction of Total RNA from EVs, Reverse Transcription (RT), qPCR, and TaqMan Low-Density Arrays (TLDA) for miRNA Profiling. Total RNA was extracted from EVs of fetal and adult dermal cells using the miRNeasy Mini Kit (Qiagen, Hilden, Germany), according to manufacturer's instructions. The purity of isolated RNA was determined by $OD_{260/280}$ using a NanoDrop (ND-1000, Thermo Fisher Scientific). Reverse transcription (RT) and preamplification were done using the High-Capacity cDNA Reverse Transcription Kit (Applied Biosystems, Thermo Fisher Scientific) according to manufacturer's instructions. The kit includes the Megaplex PreAmp Primers Human Pool A v2.1 and the Megaplex PreAmp Primers Human Pool B v3.0 (both primers from Applied Biosystems, Thermo Fisher Scientific). miRNA profiling of three fetal vs. three adult EV preparations was done with TaqMan Array Human MicroRNA A+B Cards (Life Technologies, Carlsbad, CA, USA), which analyzes 754 human miRNAs. PCR was done with the Applied Biosystems 7900 HT Real-Time PCR system. The expression level of each miRNA was determined by equation $2^{-\Delta\Delta CT}$. Student's t-test was used to calculate the p value, and the threshold was set at ≤0.05. Data were considered significant at a fold change > 15. Furthermore, significantly upregulated miRNAs in fetal vs. adult samples were screened out with the online prediction software program DIANA-miRPath v.3 [20]. We selected DIANA-TarBase v7.0 for analysis and set the p value ≤ 0.05 to analyze miRNAs and their target genes. KEGG enrichment analysis was used to identify signaling pathways most enriched by our miRNAs. In order to identify single genes targeted by multiple miRNAs, KEGG analysis was performed with the "genes intersection" option.

2.5. Quantification of EV Total Protein Contents. Total protein extraction from EVs was done with radioimmunoprecipitation assay (RIPA) buffer (Thermo Fisher Scientific) supplemented with halt protease and phosphatase inhibitors cocktail (Thermo Fisher Scientific). Tissue extracts were centrifuged at 12000 × g for 15 minutes at 4°C. Total protein contents were quantified with the bicinchoninic acid (BCA) assay (Thermo Fisher Scientific) by using the Tecan Spark 10 M microplate reader (BioExpress, VWR, Radnor, PA, USA). Both freshly isolated and frozen EV preparations were used in functional assays.

2.6. Western Blot Analysis. For biochemical characterization of EVs, 30 μg/lane of total protein extracts was separated by sodium dodecyl sulfate- (SDS-) polyacrylamide gel electrophoresis and transferred to nitrocellulose membranes (Bio-Rad Laboratories, Richmond, CA, USA). The membranes were blocked with 5% nonfat milk in T-TBS (50 mmol/l Tris pH 7.5, 0.9% NaCl, and 0.1% Tween-20) (all from Sigma-Aldrich) overnight at 4°C and incubated 1 hour at room temperature with the following primary antibodies: mouse monoclonal antibody raised against recombinant human Rab5 (F-9, sc-373725, Santa Cruz Biotechnology, Santa Cruz, CA, USA; 1 : 500 dilution), mouse monoclonal antibody against Alix (3A9, 2171, Cell Signaling Technology, Danvers, MA, USA; 1 : 1000 dilution), and mouse monoclonal antibody against CD63 (MX-49.129.5, sc-5275, Santa Cruz Biotechnology; 1 : 200 dilution). As a negative marker of EVs, a rabbit monoclonal antibody against calnexin (C5C9, 2679, Cell Signaling; 1 : 1000 dilution) was used. For this latter, total protein extracts from cells were also included in the analysis.

For validation of the *in silico* analysis, fibroblasts were treated with 10 μg/ml of fetal-derived EVs for 24, 48, and 72 hours. 30 μg/lane of fibroblast total protein extracts was separated by SDS polyacrylamide gel electrophoresis and transferred to nitrocellulose membranes (Bio-Rad Laboratories). The membranes were incubated 1 hour at room temperature with a rabbit monoclonal antibody against recombinant human thrombospondin 1 (THBS1) (ab267388, Abcam, Cambridge, UK; 1 : 1000 dilution). Beta-actin was used as an internal loading control (sc-81178, Santa Cruz Biotechnology; 1 : 1000 dilution). After three washings with T-TBS, the membranes were incubated for 1 hour at room temperature with horseradish peroxidase-conjugated secondary antibodies (Santa Cruz Biotechnology; 1 : 10000 dilution). After washing, the signal was detected with an enhanced chemiluminescence reagent (ECL; Amersham, Arlington Heights, IL, USA). Densitometric analysis of Western blot analysis was done with the Image Lab software, version 6.0.1 (Bio-Rad Laboratories).

2.7. EV/CM-Induced In Vitro Angiogenesis. Serum-starved HUVECs were resuspended in serum-free culture medium supplemented with different concentrations of EVs (100, 50, 10, or 5 μg/ml) from fetal and adult dermal cells. Approximately 10000 cells/well were plated in triplicate onto Matrigel from the *in vitro* angiogenesis assay kit (Millipore, Billerica, MA, USA) in flat bottom 96-well plastic plates (Costar Corning Inc., Costar, NY, USA). HUVECs plated in fetal dermal cell CM or in serum-free culture medium were used as positive and negative control, respectively. Plates were incubated at 37°C in a humidified atmosphere with 5% CO_2. Formation of mesh-like structures was monitored for 24 hours with an inverted microscope (Olympus CKX41, Tokyo, Japan) coupled with a camera (Olympus U-TV0.5XC-3) for image acquisition. Numerical values (score from 0 to 5) were assigned to each pattern according to manufacturer's specifications (Millipore) and as previously described [12]. Formation of mesh-like structures was quantified by calculating the number of junctions, nodes, total mesh area, and total segments length, with ImageJ software of the Angiogenesis Analyzer plugin (https://imagej.nih.gov/ij/).

2.8. In Vitro EV/CM-Induced Cell Migration. Cell migration was monitored by using the Cellular Invasion/Migration (CIM) Plate 16 with the XCELLigence Real-Time Cell

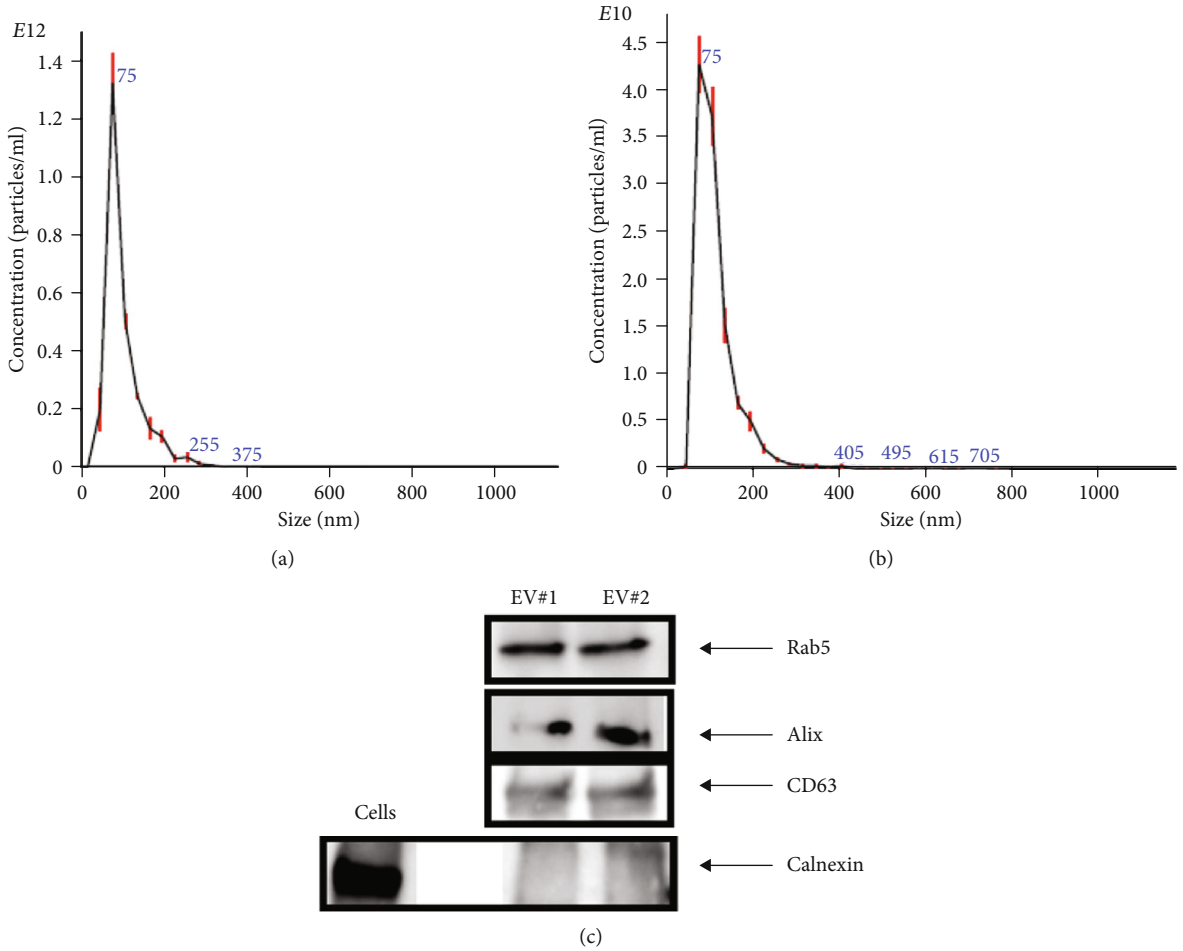

Figure 1: Physical characterization of EVs by NTA and protein expression. (a) Representative histogram of EVs isolated from secretome of fetal dermal cells showing a peak corresponding to a mode value of 77.5 ± 0.8 nm size and a concentration of 2.59×10^{12} particles/ml. (b) Representative histogram of EVs isolated from secretome of adult dermal cells showing a peak corresponding to a mode value of 87.2 ± 2.8 nm size and a concentration of 1.12×10^{11} particles/ml. The results shown are representative of three independent experiments. (c) Representative Western blot analysis of two fetal dermal-derived EV samples showing expression of EV markers Rab5, Alix, and CD63 in total protein extracts of pellet particles. Negative control, calnexin in cell protein extracts, and pellet particles are also shown. NTA: nanoparticle tracking analysis; EVs: extracellular vesicles; cells: total protein extracts of human fetal dermal cells; EV#1: sample 1; EV#2: sample 2.

Analyzer (RTCA) dual purpose (DP) instrument (Acea Biosciences Inc., San Diego, CA, USA), which detects the real-time migration of cells [21]. Briefly, serum-starved fibroblasts were resuspended in culture medium supplemented with 100, 50, 10, or 5 μg/ml EVs from fetal and adult dermal cells or in culture medium without EVs, and added to the upper chamber (30000 cells/chamber) of the CIM plate. Culture medium 0.5% FBS was used as chemoattractant and loaded to the lower chamber. The CIM plates were assembled into the RTCA-DP instrument and placed in the incubator at 37°C in a humidified atmosphere with 5% CO_2. Cell migration was recorded every 15 minutes for 7 hours. Each time point was calculated from duplicate values, and cell migration was expressed as cell index (CI) at a 7-hour time point. Analysis was performed with the RTCA Software 1.2 of the xCELLigence system.

2.9. Quantitative Analysis of EV-Depleted CM by Luminex Technology. EV-depleted CM from fetal dermal cells was subjected to quantitative evaluation by Luminex xMAP technology (Luminex 200; Luminex Corp., Austin, TX, USA), enabling the simultaneous detection of analytes. The analyzed soluble factors included human growth factors such as VEGF-A and HGF, and chemokines with a documented role in angiogenesis and wound healing, such SDF-1 alpha, MCP-1, IL-8, and GRO-alpha. These factors were included in a customized panel (ProcartaPlex, Thermo Fisher Scientific). Briefly, undiluted or 1 : 10 diluted CM was loaded into the multiplex and processed according to manufacturer's instructions. Concentration of soluble factors was calculated by using software provided by the manufacturer, and the results normalized to the total number of attached cells. The concentration of soluble factors was expressed as pg/ml

Table 1: EV-derived miRNAs found highly expressed in fetal samples (Ct values ≤ 26), which were also upregulated compared to adult samples (see also Supplemental Material S1).

miRNA name	Role in angiogenesis/tissue regeneration	References	Fold increase in fetal vs. adult samples	*p* value
hsa-let-7b-5p	It targets VEGF gene; validated role in angiogenesis	Hua et al., 2006 [36]; Landskroner-Eiger et al., 2013 [34]	26.2091	0.0074
hsa-let-7g-5p	Validated role in angiogenesis	Landskroner-Eiger et al., 2013 [34]	175.3585	0.021
hsa-miR-10a-5p	Validated role in angiogenesis; angiogenesis influencer	Landskroner-Eiger et al., 2013 [34]	242.9505	0.03
hsa-miR-10b-3p			17.9198	0.0346
hsa-miR-15b-5p	Angiogenesis regulator; delivered in regenerative medicine for cardiac repair	Curtin et al., 2018 [29]; Wang & Olson, 2009 [39]	2624.268	0.0003
hsa-miR-16-5p	Angiogenesis regulator; it targets VEGF gene; regulator of angiogenesis; induces tube formation of HUVECs	Hua et al., 2006 [36]; Poliseno et al., 2006 [78]; Suarez & Sessa, 2009 [38]; Wang & Olson, 2009 [39]	149.6445	0.0183
hsa-miR-17-5p	Angiogenesis regulator; it targets VEGF gene	Caporali & Emanueli, 2011 [33]; Hua et al., 2006 [36], Wang & Olson, 2009 [39]	133.7475	0.0032
hsa-miR-19a-3p	Validated role in angiogenesis	Landskroner-Eiger et al., 2013 [34]; Wang & Olson, 2009 [39]	51.8807	0.0114
hsa-miR-19b-3p	Angiogenesis regulator	Caporali & Emanueli, 2011 [33]; Wang & Olson, 2009 [39]	109.3557	0.0044
hsa-miR-20a-5p	It targets VEGF gene; validated role in angiogenesis	Hua et al., 2006 [36]; Landskroner-Eiger et al., 2013 [34]; Wang & Olson, 2009 [39]	56.7629	0.0004
hsa-miR-21-5p	Angiogenesis regulator; wound healing regulator	Wang & Olson, 2009 [39]; Wang et al., 2012 [32]	157.6826	0.0046
hsa-miR-24-3p	Highly expressed by endothelial cells	Suarez & Sessa, 2009 [38]; Zhou et al., 2011 [40]	25.4984	0.0059
hsa-miR-26a-5p	Proregenerative (it promotes osteogenesis-angiogenesis in mouse)	Li et al., 2013 [47]	132.6638	0.0122
hsa-miR-26b-5p	Tissue repair; remodeling in wound healing	Banerjee & Sen, 2013 [31]; Sen et al., 2015 [30]	95.4933	0.0183
hsa-miR-27b-3p	It targets VEGF gene; validated role in angiogenesis	Hua et al., 2006 [36]; Landskroner-Eiger et al., 2013 [34]; Wang & Olson, 2009 [39]; Zhou et al., 2011 [40]	950.021	0.0096
hsa-miR-28-3p			49.9995	0.0082
hsa-miR-29b-3p	Regulator of tissue regeneration; proregenerative (delivered for ECM remodeling in fibrosis treatment)	Monaghan et al., 2014 [42]; van Rooij et al., 2008 [43]	61.9175	0.0105
hsa-miR-30a-3p	It targets VEGF gene; endothelial cell modulator	Bridge et al., 2012 [35]; Hua et al., 2006 [36]	185.51	0.0099
hsa-miR-30b-5p	Angiogenesis regulator; endothelial cell modulators; it targets VEGF gene	Bridge et al., 2012 [35]; Hua et al., 2006 [36]	32.3336	0.0004
hsa-miR-30c-5p	Endothelial cell modulator	Bridge et al., 2012 [35]	30.1373	0.0002
hsa-miR-30e-3p	Endothelial cell modulator	Bridge et al., 2012 [35]	41.2049	0.0041
hsa-miR-31-5p	Angiogenesis regulator; wound healing	Li et al., 2015 [79]; Wang et al., 2012 [32]	60.803	0.0027
hsa-miR-31-3p	Angiogenesis regulator; wound healing	Li et al., 2015 [79]; Wang et al., 2012 [32]	229.5474	0.0097
hsa-miR-34a-5p	It targets VEGF gene		2254.5936	0

Table 1: Continued.

miRNA name	Role in angiogenesis/tissue regeneration	References	Fold increase in fetal vs. adult samples	p value
hsa-miR-92a-3p	Validated role in angiogenesis	Curtin et al., 2018 [29]; Landskroner-Eiger et al., 2013 [34]; Wang & Olson, 2009 [39]	32.781	0.0001
hsa-miR-93-3p			149.3753	0.0065
hsa-miR-99b-3p	Angiogenesis promoter	Kane et al., 2012 [37]	37.2967	0.0134
hsa-miR-99b-5p	Angiogenesis promoter	Kane et al., 2012 [37]	41.1216	0.0031
hsa-miR-103a-3p			809.2304	0.008
hsa-miR-106a-5p	It targets VEGF gene; regulator of angiogenesis	Hua et al., 2006 [36]	67.8178	0.0047
hsa-miR-106b-5p	It targets VEGF gene; regulator of angiogenesis	Hua et al., 2006 [36]; Landskroner-Eiger et al., 2013 [34]	56.2099	0.0084
hsa-miR-125a-5p	Tube formation of HUVECs; it targets VEGF gene	Hua et al., 2006 [36]; Poliseno et al., 2006 [78]	128.8981	0.0061
hsa-miR-125b-5p	Angiogenesis regulator; tube formation of HUVECs	Poliseno et al., 2006 [78]; Zhou et al., 2015 [80]	18.6552	0.0041
hsa-miR-127-3p			19.2386	0.0001
hsa-miR-132-3p	Validated role in angiogenesis during chronic wound healing; proregenerative (it promotes angiogenesis in myocardial infarction)	Landskroner-Eiger et al., 2013 [34]; Li et al., 2017 [81]; Ma et al., 2018 [44]	3664.7066	0.0034
hsa-miR-136-3p			164.0836	0.0268
hsa-miR-138-5p			52.6792	0.0162
hsa-miR-145-5p	Angiogenesis regulator	Fan et al., 2012 [82]	42.2841	0.0067
hsa-miR-146a-3p	Wound healing (inflammatory phase)	Banerjee & Sen, 2013 [31]	172.0832	0.0135
hsa-miR-146b-3p	Wound healing (inflammatory phase); angiogenesis promoter	Ahn et al., 2013 [83]; Banerjee & Sen, 2013 [31]	203.771	0.0161
hsa-miR-149-5p	Scarless wound healing	Lang et al., 2017 [84]	37.5122	0.0102
hsa-miR-151a-5p			126.8167	0.005
hsa-miR-151a-3p			17.732	0.0246
hsa-miR-152-3p			20.0452	0.0097
hsa-miR-155-5p	Wound healing (inflammatory phase); amyotrophic lateral sclerosis; anti-inflammatory action; angiogenesis regulator	Banerjee & Sen, 2015 [31]; Curtin et al., 2018 [29]; Suarez & Sessa, 2009 [38]	32.5772	0.04
hsa-miR-181a-5p	Angiogenesis promoter	Kane et al., 2012 [37]	112.4827	0.0011
hsa-miR-186-5p			78.0074	0.0165
hsa-miR-191-5p	It may regulate the angiogenic actions of VEGF	Landskroner-Eiger et al., 2013 [34]	66.0569	0.0121
hsa-miR-193a-5p	It targets VEGF gene	Hua et al., 2006 [36]	108.2673	0.0061
hsa-miR-193b-3p	Proregenerative (chondrogenesis)	Meng et al., 2018 [45]	16.6788	0.0057
hsa-miR-197-3p			47.9232	0.01
hsa-miR-199a-3p	It targets VEGF gene; proregenerative (cardiac regeneration)	Hua et al., 2006 [36]; Lesizza et al., 2017 [46]	79.9505	0.0112
hsa-miR-214-3p			34.8695	0.0131
hsa-miR-214-5p	It targets VEGF gene	Hua et al., 2006 [36]	493.6614	0.0151
hsa-miR-218-5p	Validated role in angiogenesis	Landskroner-Eiger et al., 2013 [34]	32.9227	0.0092
hsa-miR-221-3p	Validated role in angiogenesis	Landskroner-Eiger et al., 2013 [34]	27.5391	0.0003
hsa-miR-222-3p	Angiogenesis in wound healing; validated role in angiogenesis	Banerjee & Sen, 2015 [31]; Landskroner-Eiger et al., 2013 [34]	38.7974	0.0103
hsa-miR-224-5p			21.5539	0.0039

Table 1: Continued.

miRNA name	Role in angiogenesis/tissue regeneration	References	Fold increase in fetal vs. adult samples	p value
hsa-miR-320a	It targets VEGF gene; validated role in angiogenesis	Hua et al., 2006 [36]; Landskroner-Eiger et al., 2013 [34]	56.2268	0.0086
hsa-miR-323a-3p			686.8069	0.0163
hsa-miR-324-3p			137.7004	0.0144
hsa-miR-331-3p	It targets VEGF gene	Hua et al., 2006 [36]	43.6136	0.0043
hsa-miR-342-3p			169.8914	0.0114
hsa-miR-345-5p			200.3964	0.0134
hsa-miR-365a-3p			526.7213	0.0115
hsa-miR-370-3p			99.3169	0.0081
hsa-miR-374a-5p			44.7501	0.0225
hsa-miR-376a-3p			216.5826	0.0246
hsa-miR-376c-3p			216.5826	0.0246
hsa-miR-382-5p			6102.4887	0.0009
hsa-miR-409-3p			173.9373	0.0097
hsa-miR-411-5p			99.6678	0.0353
hsa-miR-424-3p			482.6326	0.0137
hsa-miR-432-5p			125.5471	0.0385
hsa-miR-433-3p			778.7489	0.0057
hsa-miR-455-5p			611.2326	0.0122
hsa-miR-484			85.625	0.0066
hsa-miR-487b-3p			131.5413	0.0028
hsa-miR-493-3p			1303.6278	0.0053
hsa-miR-532-3p			42.572	0.0015
hsa-miR-532-5p	Angiogenesis	Slater et al., 2018 [85]	1363.2918	0.0072
hsa-miR-539-5p			350.9595	0.0063
hsa-miR-574-3p			59.5134	0.0121
hsa-miR-625-3p			77.7476	0.002
hsa-miR-708-5p			59.2604	0.0013
hsa-miR-766-3p			1533.4818	0.016
hsa-miR-886-5p			75.0277	0.0048
hsa-miR-1290			24.3418	0.0021

Plotted values (mean ± SD) represent fetal samples ($n = 3$) compared to adult samples ($n = 3$).

/1.5×10^6 cells/24 hours. Data from EV-depleted CM were compared with those from whole CM.

2.10. EV Labeling and Cellular Uptake Assay. EVs from fetal dermal cells were labeled with CSFE (Thermo Fisher Scientific) according to manufacturer's instructions with minor modifications. Briefly, 1 : 1000 diluted CSFE was added to 10 μg of EV preparation and incubated at 37°C for 15 minutes. 1 ml of 1% bovine serum albumin (BSA) (Sigma-Aldrich) was added to stop the labeling, and the mixture was ultracentrifuged at $100000 \times g$ for 70 minutes at 4°C. The supernatant was discharged, the pellet resuspended in serum-free DMEM, and EV labeling was verified by flow cytometry with a FACS Canto II (Becton Dickinson, BD, Franklin Lake, NJ, USA) in a log range by using 50 nm diameter reference beads as size standard (MicroBeads, Miltenyi, Bergisch Gladbach, Germany), as previously described [22]. Fibroblasts and HUVECs previously grown to 60% confluence in 4-well glass chamber slides were incubated with DMEM containing CSFE-labeled EVs at a ratio 1 μg EVs per 10000 adherent cells. At the end of incubation time (2, 4, and 8 hours), cells were washed twice with PBS and fixed with 4% paraformaldehyde/PBS for 10 minutes at room temperature. Nuclei were stained with DAPI (Sigma-Aldrich) and then mounted with Permafluor and a coverslip (Thermo Fisher Scientific). Cellular uptake of EVs was visualized under a Leica confocal station (Leica SP5 confocal system) mounted on a Leica DM6000 inverted microscope (Leica Microsystems Inc., Buffalo Grove, IL, USA).

2.11. Statistical Analysis. For NTA and miRNAs analysis, three fetal-derived and three adult-derived EV samples were analyzed. For *in vitro* angiogenesis, four different samples corresponding to treatment with fetal-derived EVs and three

Table 2: KEGG signaling pathways and their association with angiogenesis and wound healing.

KEGG signaling pathway	Role in angiogenesis/wound healing	References	$\log_{10}$ (p value)
Adherens junction	Wound closure	Fenteany et al., 2000 [47]	$5.10E-07$
HIPPO	Organ regeneration	Juan & Hong, 2016 [48]; Lee et al., 2014 [49]; Zhao et al., 2011 [51]; Wang et al., 2017 [50]	$3.73E-06$
p53	Promotes VEGF expression and angiogenesis	Farhang Ghahremani et al., 2013 [52]	$9.63E-06$
TGF-beta	Skin wound healing	Finnson et al., 2013 [53]; Ramirez et al., 2014 [54]	$2.39E-05$
ECM-receptor interaction	Wound repair	Olczyk et al., 2014 [55]	$4.53E-05$
Focal adhesion	Cell migration; angiogenesis	Zhao & Guan, 2011 [56]	0.000175201
mTOR	Interconnected to PI3K-Akt pathway to accelerate epithelial wound healing; angiogenesis	Castilho et al., 2013 [56]; Karar & Maity, 2011 [59]	0.000176029
HIF-1	Accelerating wound healing by enhancing angiogenesis	Hong et al., 2014 [60]	0.000538735
ErbB	Mediates proliferation and migration of keratinocytes in wound healing (ErbB1)	Pastore et al., 2008 [61]	0.001490837
FoxO	Upstream in the activation of both TGF-beta and PI3K-Akt signaling pathways		0.002880647
Wnt	Participates to each stage of the healing process	Whyte et al., 2012 [62]	0.00326995
Notch	Angiogenesis and endothelial cell formation; essential in organ regeneration; vasculature repair after brain trauma and wound healing	Carlson et al., 2007 [63]; Raya et al., 2003 [66]; Ran et al., 2015 [65]; Chigurupati et al., 2007 [64]	0.004876559
Neurotrophin	Novel regulator of angiogenesis	Kraemer & Hempstead, 2003 [67]	0.009582793
MAPK	Skin reepithelialization	Deng et al., 2006 [68]	0.008652606
Insulin	Upstream to PI3k/Akt and mTOR	Karar & Maity, 2011 [59]	0.014139516

DIANA tool analysis of the 87 miRNAs considered significantly upregulated in fetal vs. adult dermal cell-derived EVs.

different samples corresponding to the remaining treatments (adult-derived EVs, fetal-derived CM, and the corresponding EV-depleted CM) were analyzed. For cell migration assay, three different samples of each condition were analyzed (fetal-derived EVs, adult-derived EVs, fetal CM, and the corresponding EV-depleted CM). For quantitative analysis by Luminex of whole CM vs. EV-depleted CM, ten fetal CM samples were analyzed. Data were analyzed with *R* [23] and expressed as the mean ± SD. Data from two different groups were compared with Student's *t*-test. Differences between the groups were considered significant at a p value of ≤ 0.05.

Angiogenesis data were analyzed with GraphPad Prism 8.4.2 and expressed as the mean ± SD. Data from each condition were compared to treatment with fetal-derived EVs with the one-way ANOVA.

3. Results

3.1. Characterization of EVs by Nanoparticle Tracking Analysis and Protein Marker Expression. The NTA of pellet preparations obtained by differential ultracentrifugation of CM from fetal and adult dermal cells indicated a "mode" diameter size (representing the size of the most abundant particles in a sample preparation) consistent with that of "small EVs" (<200 nm [24]). The mode sizes of a representative fetal sample (77.5 ± 0.8 nm) and that of a representative adult sample (87.2 ± 2.8 nm) are shown in Figure 1(a) and Figure 1(b), respectively. The concentration of EVs from both fetal and adult cells was in a range of 10^{11}-10^{12} particles/ml. Moreover, characterization by Western blot analysis revealed that pellet particles expressed Rab5, Alix, and CD63 proteins, and while were negative for calnexin protein, this latter found in total protein extracts from human fetal dermal cells (Figure 1(c)).

3.2. Differential Expression of EV miRNAs and Their Association with Signaling Pathways Related to Angiogenesis and Wound Healing. We found 87 highly expressed miRNAs (Ct values ≤ 26) in fetal dermal cell-derived EVs. These highly expressed miRNAs were also considered significantly upregulated in fetal compared to adult dermal cell-derived EVs (Table 1; Supplemental Material S1). In addition, 21 miRNAs had a validated role in angiogenesis according to literature (Table 1; Supplemental Material S1).

KEGG analysis with DIANA-TarBase of these 87 miRNAs evidenced 85 signaling pathways, 15 of which related to angiogenesis/wound healing (Table 2; Supplemental Material S2), (Figure 2). By setting 29 as a threshold (genes intersection) [20], we selected 4 signaling pathways associated with angiogenesis and wound healing from the obtained list (Figure 3; Supplemental Material S3). In particular, we found 46 out of 87 miRNAs enriched in ECM-receptor interaction signaling pathway, with two putative target genes, THBS1 and fibronectin (FN1) (Supplemental Material S3); 69 miRNAs enriched in the p53 signaling pathway with the target genes THBS1, cyclin D1 (CCND1), cyclin D2 (CCND2),

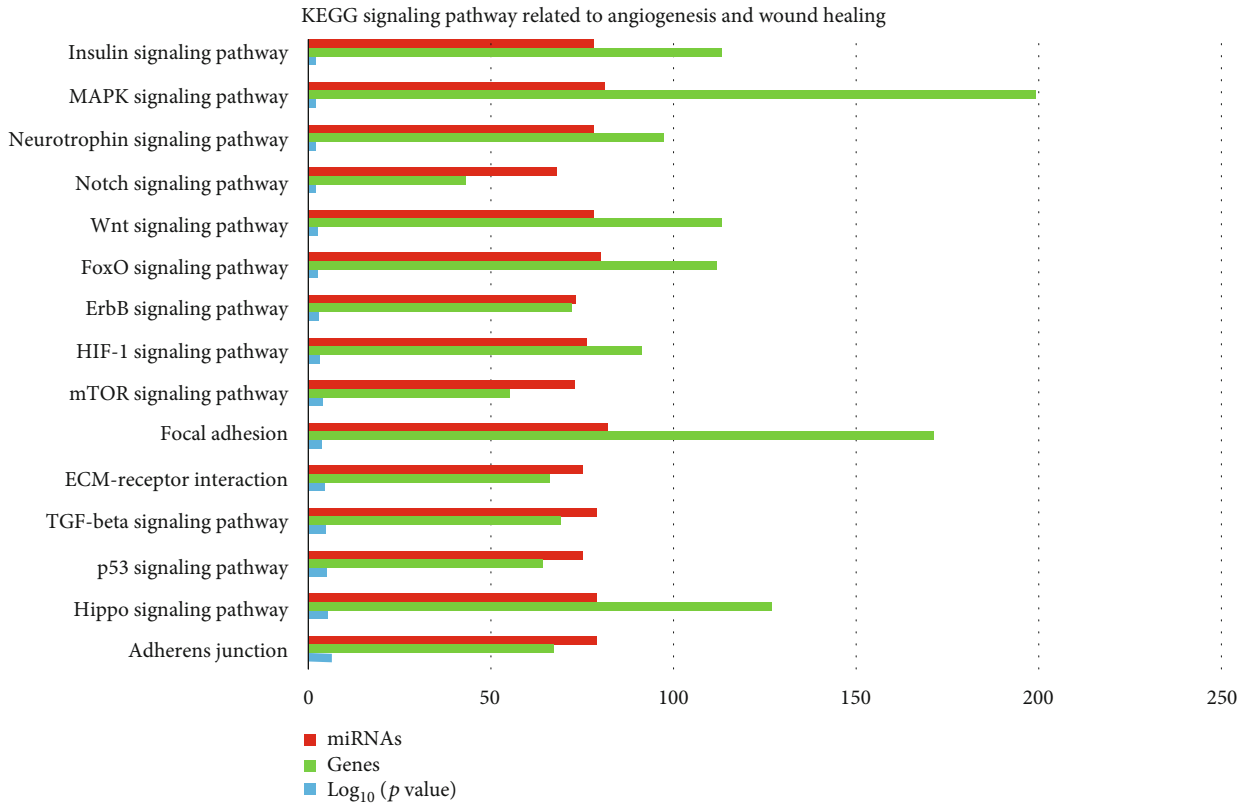

Figure 2: KEGG signaling pathways related to angiogenesis and wound healing obtained by screening out the 87 miRNAs considered significantly upregulated in fetal cell- vs. adult cell-derived EVs with the DIANA-miRPath v.3 software. The figure shows $\log_{10}$ (p value) (blue bars) associated with the number of miRNAs (red bars) targeting specific genes (green bars) within each pathway.

cyclin-dependent kinase inhibitor 1 (CDKN1A), cell division protein kinase 6 (CDK6), TNF receptor superfamily member 10b (TNFRSF10B), and mouse double minute 2 homolog (MDM2) (S3); 73 miRNAs enriched in the PIK3/Akt signaling pathway with putative target genes THBS1, FN1, CCND2, CCND1, CDKN1A, CDK6, MDM2, insulin-like growth factor 1 receptor (IGF1R), and MCL1 (S3); 64 miRNAs enriched in the FoxO signaling pathway with the target genes CCND2, CCND1, MDM2, and IGF1R (S3).

3.3. Validation of the In Silico Analysis by Western Blot. The amount of THBS1 protein in fibroblasts treated for 72 hours with 10 μg/ml of fetal-derived EVs was higher than the amount of THBS1 protein in both untreated fibroblasts (Figure 4(a)) and the earlier time points of treatment (24 and 48 hours, data not shown). The amount of THBS1 protein in fibroblasts following a 72-hour treatment with fetal-derived EVs was approximately 4-fold higher than the amount of THBS1 protein in untreated fibroblasts at the same time point (Figure 4(b)).

3.4. EV/CM-Induced Mesh-Like Organization of HUVECs In Vitro. HUVECs cultured in culture medium supplemented with 100, 50, or 10 μg/ml of fetal dermal cell-derived EVs achieved the "complete mesh-like structures" pattern (maximum score 5) 8 hours after plating on Matrigel (Figure 5(a) obtained with 10 μg/ml EVs), while only achieved the "sprouting of new capillary tubes" pattern (score 3) when cultured in the presence of 10 μg/ml of adult dermal cell-derived EVs (Figure 5(b); Supplemental Material S4). The score 5 was achieved faster (approximately 3 hours) when cells were cultured in serum-free CM than in EVs of fetal dermal cells (Figure 5(c)). Interestingly, culturing HUVECs in EV-depleted CM only determined the achievement of score 3 (Figure 5(d)). Negative control HUVECs cultured in the absence of EVs maintained the "individual cells" pattern (score 0) for all the duration of the experiment (Figure 5(e)) (Table 3). Lower doses of fetal dermal cell-derived EVs ($\leq$5 μg/ml) were ineffective in inducing formation of mesh-like structures (data not shown). The results were confirmed by angiogenesis parameters quantified on images ($n = 4$ for treatment with fetal-derived EVs; $n = 3$ for the other treatments). In the case of HUVECs cultured in the presence of 10 μg/ml of adult dermal cell-derived EVs, histograms were lower to those of HUVECs cultured in the presence of fetal cell-derived EVs, but differences were not statistically significant, probably due to the high SD values. Data were expressed as total mesh area (Figure 6(a)), number of junctions (Figure 6(b)), number of nodes (Figure 6(c)), number of segments (Figure 6(d)), and total length of segments (Figure 6(e)) ($^{*}p$ value ≤ 0.05; $^{**}p$ value ≤ 0.001).

3.5. EV/CM-Induced Migration of Fibroblasts In Vitro. Fibroblasts in the presence of 100, 50, or 10 μg/ml of fetal dermal cell-derived EVs (green, red, and dark blue curves,

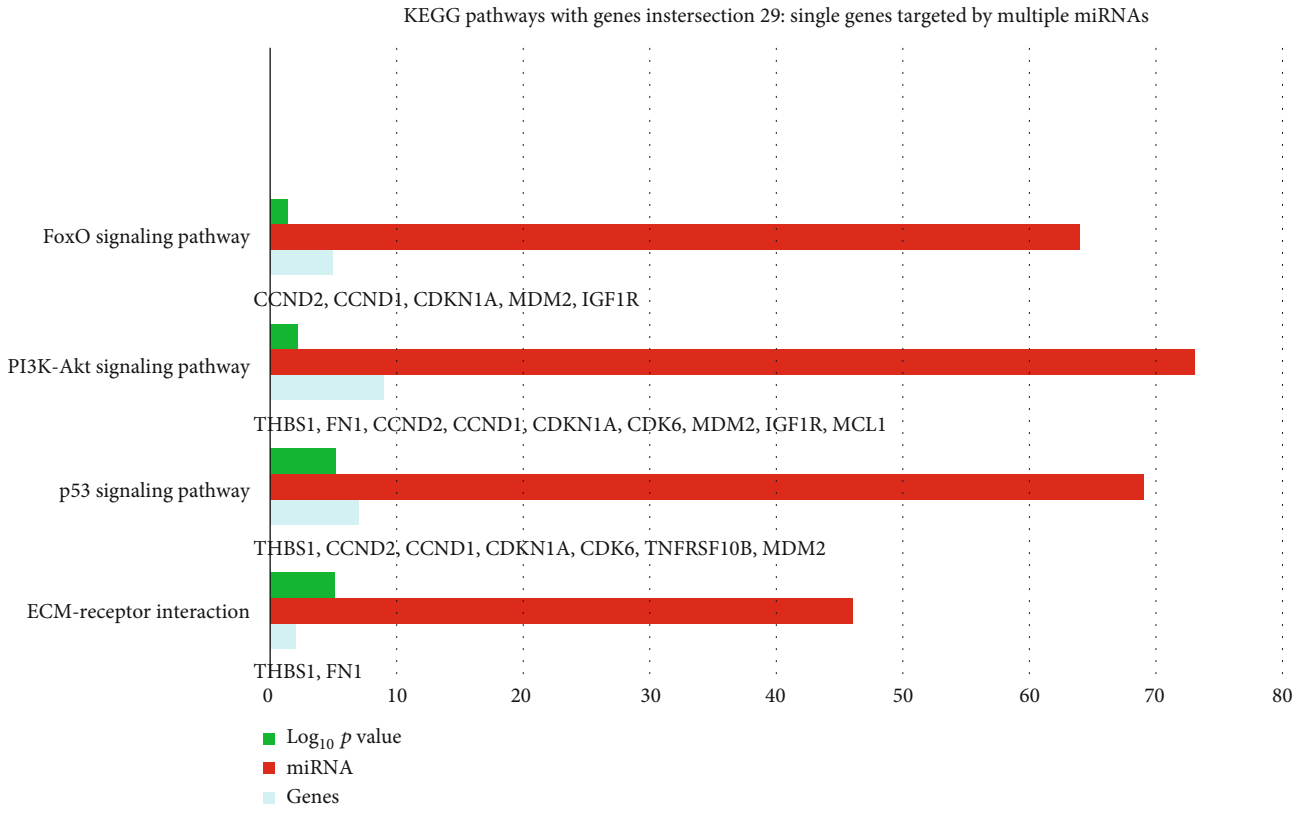

Figure 3: KEGG signaling pathways related to angiogenesis and wound healing obtained with genes intersection 29 to show putative genes targeted by multiple miRNAs within each pathway. DIANA tool was performed with the 87 miRNAs considered significantly upregulated in fetal dermal cell-derived EVs compared to adult dermal cell-derived EVs.

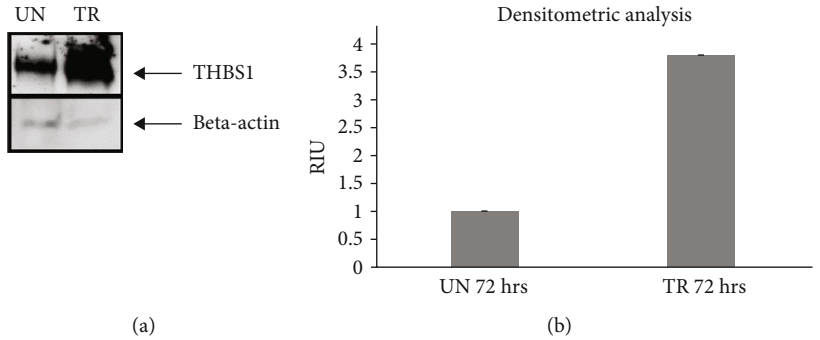

Figure 4: Validation of the *in silico* data. (a) Representative Western blot of THBS1 protein in total protein extracts of fibroblasts, untreated or treated with 10 μg/ml of fetal-derived EVs for 72 hours. Beta-actin was used as internal loading control. (b) Densitometric analysis of the 72-hour time point. UN: untreated; TR: treated; THBS1: thrombospondin 1; EV: extracellular vesicle; RIU: relative intensity unit.

respectively) migrated toward the lower chamber (containing culture medium 0.5% FBS as chemoattractant) with similar CI values. A lower concentration of EVs (5 μg/ml) (light blue curve) resulted in the absence of migration, and CI values similar to those of negative control fibroblasts seeded in the absence of EVs (pink curve) (Figure 7). The CI values of cell migration induced by 10 μg/ml of adult-derived EVs were similar to those induced by EVs of fetal origin (dark blue and orange curves, respectively) (data not shown).

3.6. Amount of Growth Factors and Chemokines in EV-Depleted CM. The levels of growth factors and chemokines in EV-depleted CM were similar to the levels in whole fetal dermal cell CM. The growth factor detected with the highest amount was VEGF-A, while the chemokine detected with the highest amount was SDF-1-alpha (Table 4).

3.7. Cellular Uptake of EVs. Labeling of fetal dermal cell-derived EVs with CSFE was successfully verified by flow cytometry. We clearly identified a discrete population of fluorescent particles in the range of small EVs compared to control, unlabeled EVs (Figure 8(a)). The fluorescent signal of CSFE-labeled EVs was visualized into the cytosol starting from 4 hours of incubation (Figure 8(b)), while at later time

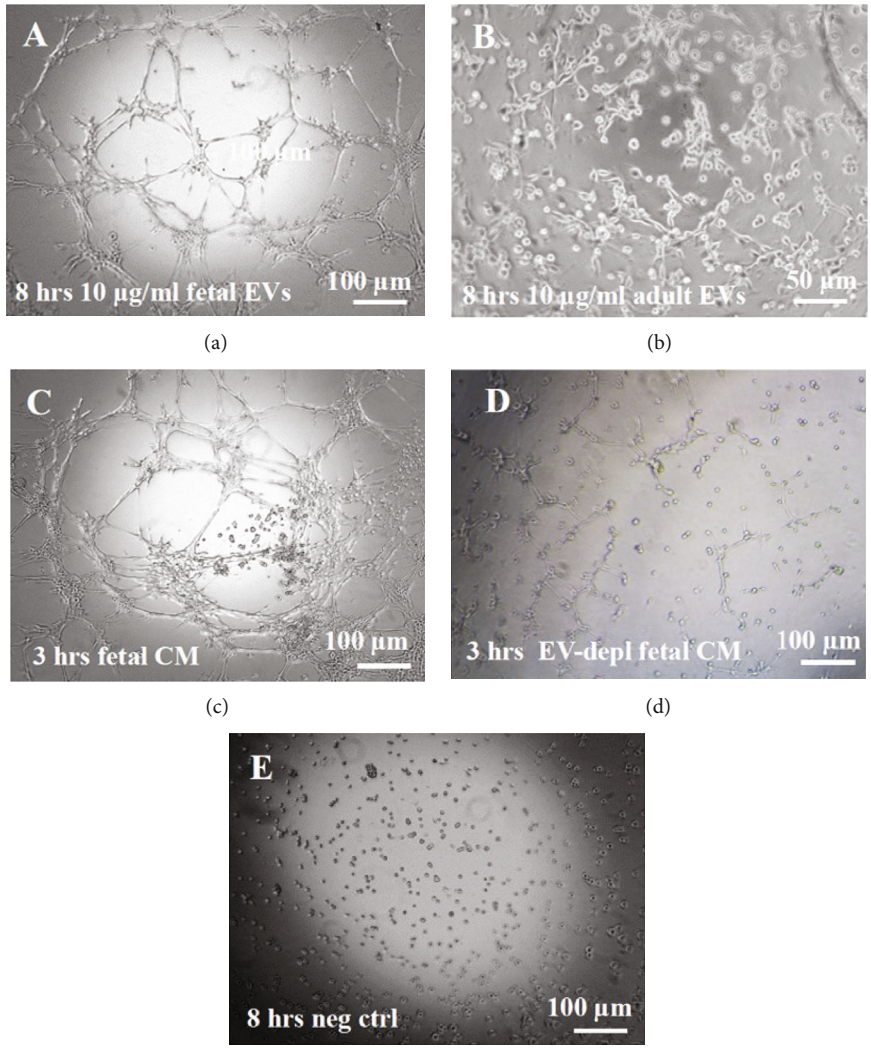

Figure 5: Effect of EVs on formation of mesh-like structures of HUVECs *in vitro*. (a) HUVECs in culture medium supplemented with 10 μg/ml of fetal dermal cell-derived EVs 8 hours after plating on Matrigel. (b) HUVECs in culture medium supplemented with 10 μg/ml of adult dermal cell-derived EVs 8 hours after plating. (c) HUVECs in fetal dermal cell-derived CM 3 hours after plating. (d) HUVECs in EV-depleted CM of fetal dermal cells 3 hours after plating. Negative control HUVECs in serum-free culture medium 8 hours after plating. Scale bars: 100 μm (a, c, d, e) and 50 μm (b). EV: extracellular vesicles; CM: conditioned medium; depl: depleted; neg. ctrl: negative control. The results shown are representative of four independent experiments.

Table 3: Numerical value assigned to each pattern associated with the degree of *in vitro* angiogenesis. A representative sample for each condition is shown, corresponding to Figure 5.

Sample	Pattern	Score
Fetal EVs	Complete mesh-like structures	5
Adult EVs	Sprouting of new capillary tubes	3
Fetal CM	Complete mesh-like structures	5
EV-depleted fetal CM	Sprouting of new capillary tubes	3
Negative control	Individual cells, well separated	0

EV: extracellular vesicles; CM: conditioned medium.

points (8 hours of incubation; Figure 8(c)), the signal was mainly detected in the perinuclear region of target cells. No differences were found when using targeted HUVECs or fibroblasts (data not shown).

4. Discussion

As a continuation of the previous study [12] and in search for the molecules contributing to functional activity of secretome, we herein focused on isolation and characterization of EVs from secretome of human fetal dermal cells. We used equal numbers of cultured cells and collected equal volumes of secretome at the same time, in the attempt to standardize the EV source. We followed the updated guidelines of the International Society for Extracellular Vesicles (ISEV), which

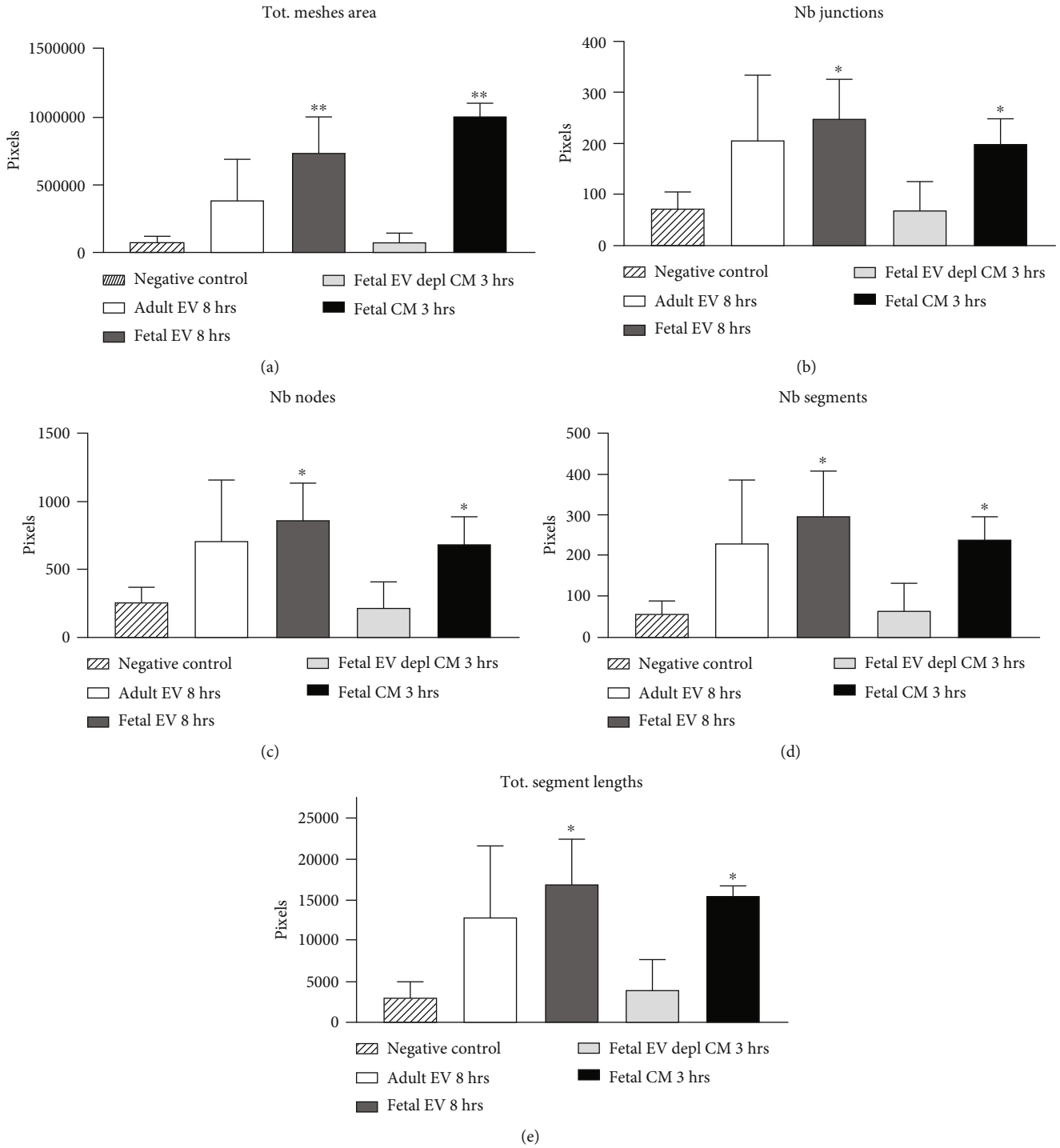

Figure 6: Angiogenic parameters quantified with the Angiogenesis Analyzer of ImageJ on images indicating (a) total mesh area, (b) number of junctions, (c) number of nodes, (d) number of segments, and (e) total segment length. 10 μg/ml of EVs was always used. The images corresponded to the 3-hour time point for treatments with CM and to the 8-hour time point for treatment with EVs and for negative controls. Plotted values (mean ± SD) represent samples ($n = 3$ for each condition, except $n = 4$ for treatment with fetal dermal cell-derived EVs). $^{*}p \leq 0.05$; $^{**}p \leq 0.001$. Differences not denoted with an asterisk are not significant. Tot: total; EV: extracellular vesicle; depl: depleted; CM: conditioned medium; Nb: number.

recommend to use the generic term "EVs" for particles naturally secreted by cells, whose characterization is mainly based on physical parameters, such as size and concentrations [24]. The NTA of pellet particles obtained by ultracentrifugation of secretome of both fetal and adult dermal cells revealed a size diameter of approximately 70 nm, thus suggesting that we may have isolated "small EVs." In fact, the general characterization suggested by the ISEV discriminates EV subtypes

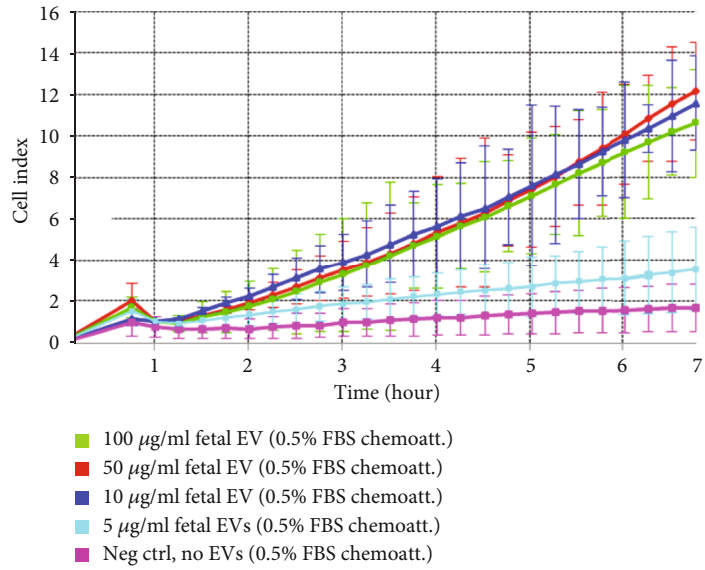

Figure 7: Effect of EVs on migration of fibroblasts *in vitro*. RTCA curves showing fibroblasts seeded in the presence of 100, 50, 10, and 5 μg/ml of fetal dermal cell-derived EVs. Culture medium containing a small amount of FBS (0.5%) was used as chemoattractant. RTCA curve of negative control fibroblasts seeded without EVs is also shown. RTCA: real-time cell analyzer; EVs: extracellular vesicles; chemoatt: chemoattractant; FBS: fetal bovine serum; neg ctrl: negative control. The results shown are representative of six independent experiments.

Table 4: Customized ProcartaPlex human growth factor and chemokine panel. Amount of soluble factors in EV-depleted vs. whole CM of fetal dermal cells.

Soluble factor	Role in MSC-mediated wound healing	EV-depleted CM (pg/ml/10^6 cells/24 h)	Whole CM (pg/ml/10^6 cells/24 h)
VEGF-A	Angiogenesis [86]	**6049 ± 1603**	**5899 ± 618**
HGF	Epithelialization, neovascularization [87]	**1031 ± 246**	**1448 ± 121**
SDF-1 alpha (CXCL-12)	Angiogenesis [88]; cell migration [89]	**6016 ± 1860**	**5983 ± 231**
MCP-1 (CCL-2)	Angiogenesis [1]; recruitment of neutrophils [90]; remodeling [91]	**1771 ± 795**	**1233 ± 54**
IL-8	Recruitment of neutrophils, epidermal cell migration, angiogenesis [91]	**1546 ± 293**	**788 ± 697**
GRO-alpha (CXCL-1)	Recruitment of neutrophils [91]; angiogenesis [1]	**907 ± 328**	**973 ± 100**

Plotted values (mean ± SD) represent EV-depleted CM ($n = 10$) compared to whole CM ($n = 10$). Differences not denoted with an asterisk are not significant. EV: extracellular vesicle; CM: conditioned medium.

in small EVs (<200 nm size) and larger EVs [24]. Furthermore, the isolated EVs were positive for Rab5 and Alix, and CD63 while were negative for calnexin [24]. Since there is no a perfect quantification method, we followed the most common, which is based on total protein amounts in our dose-response studies [24].

Depletion of EVs by differential ultracentrifugation almost abrogated the *in vitro* proangiogenic effect of fetal dermal cell secretome. Since depletion of EVs only slightly reduced the efficiency of cell migration, we suggest that perhaps the amount of chemokines such as SDF-1 alpha and MCP-1 in EV-depleted secretome may be sufficient to ensure a migratory response. On the contrary, a VEGF-A concentration of approximately 5000 pg/ml in EV-depleted secretome could not be sufficient to ensure formation of mesh-like structures normally requiring higher doses of VEGF-A (e.g., 20000 pg/ml or more) [25]. Nevertheless, the multitude of factors contained in secretome is extremely difficult to establish which factor might be responsible for one activity or another.

According to the current version of the database Exocarta [26, 27], 9769 proteins, 1116 lipids, 3408 mRNAs, and 2838 miRNAs have been identified in EV/exosomes from several cell types and organisms. Research studies have often hypothesized that the transfer of miRNAs in particular will account for the understood EV-mediated effects [14]. miRNA-based therapy entered in clinical studies mainly for cancer treatments, while it is still in early stages for

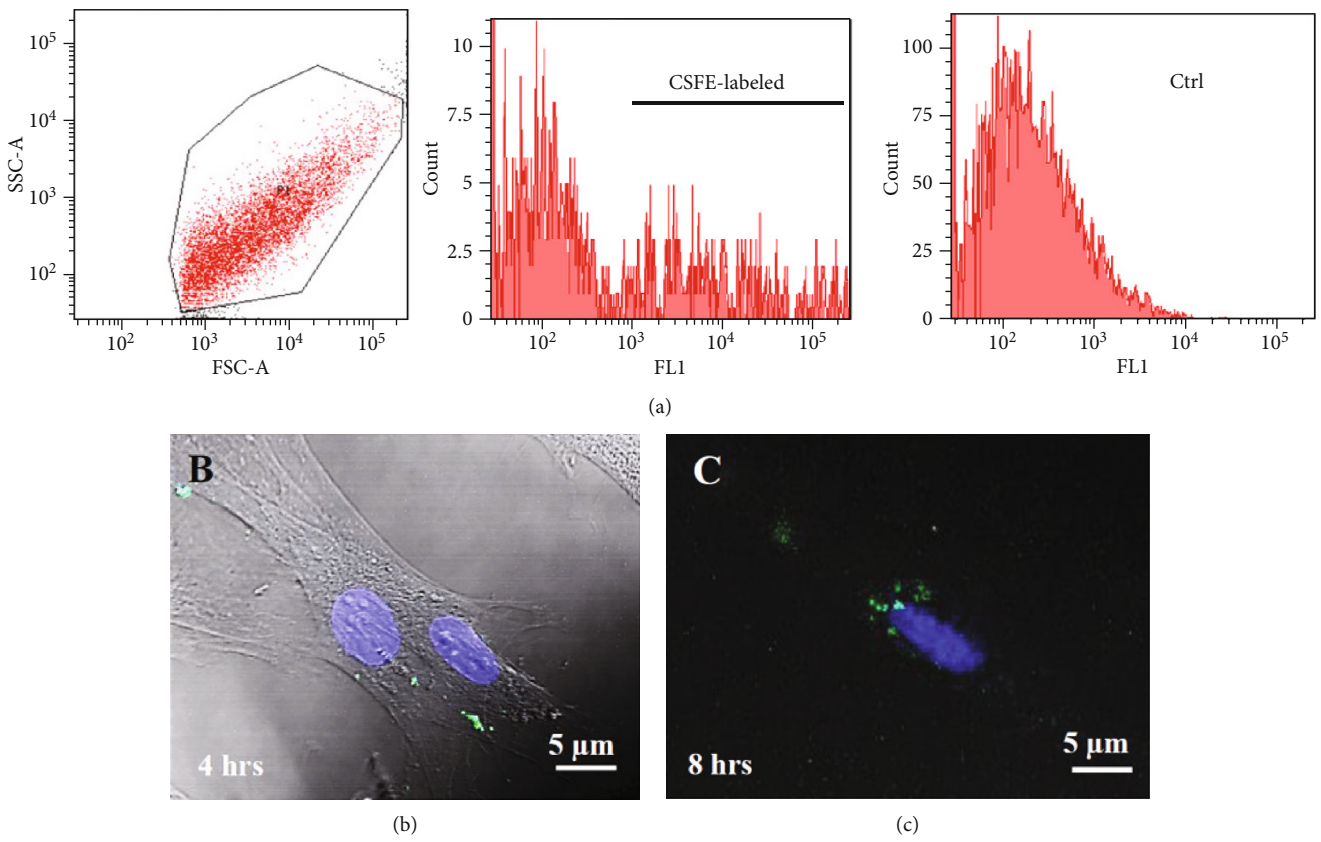

Figure 8: Internalization of CSFE-labeled EVs by targeted fibroblasts. (a) EVs analyzed by flow cytometry in a linear range for physical parameters FSC vs. SSC (forward scatter vs. side scatter) using Miltenyi beads as size marker. CSFE-labeled EVs and negative control, unlabeled EVs are also shown. Confocal images showing uptake of CSFE-labeled EVs by fibroblast target cells at 4- and 8-hour incubation times. (b) Bright field image merged with green (CSFE) and blue (DAPI) showing cytoplasmic localization of fluorescent signal at 4 hours of incubation. (c) Dual-channel confocal fluorescence showing cytoplasmic localization of fluorescent signal at 8 hours of incubation. The results shown are representative of three independent experiments. CSFE: carboxyfluorescein succinimidyl ester; EVs: extracellular vesicles; FL1: fluorescence 1. Scale bar: 5 μm.

applications of regenerative medicine [28, 29]. However, emerging reports are available indicating the vast potential of miRNAs for the repair of several tissues including bone/-cartilage muscle, cardiovascular tissue, neurological tissue, skin, and even in angiogenesis [29, 30]. With respect to organ repair and angiogenesis, the involvement of miRNAs in different phases of wound healing has been documented [31, 32], and several proangiogenic miRNAs have been identified and validated [33, 34] .

By analyzing the miRNA expression profile of dermal cell-derived EVs, we identified 87 miRNAs significantly upregulated in fetal- vs. adult-derived EVs, which included miRNAs validated in angiogenesis such as let-7b-5p, let-7g-5p, miRNA-10a, -15b, -16-5p, members of the cluster 17-92 (-17-5p, -19a-3p, -19b-3p, -20a-5p, -92a-3p), -21-5p, members of the cluster 23-27 (-24-3p, -27b-3p), -31-3p, -31-5p, -132-3p, -199a-3p, -218-5p, -221-3p, -222-3p, and -320a [29, 34–40] (Table 1). Since the depletion of EVs from fetal dermal cell secretome impaired the *in vitro* tube formation, we suggest that the proangiogenic effect of fetal dermal cell secretome reported in our previous study [12] could largely depend on an EV-mediated transfer of these miRNAs. Interestingly, significantly upregulated miRNAs in fetal- vs. adult cell-derived EVs also included proregenerative miRNAs such as -26a [41], -29b [42, 43], -132 [44], -193b-3p [45], and -199a-3p [46], which have been delivered in animal models to improve angiogenesis, bone and cartilage regeneration, cardiac regeneration, and for fibrosis treatment (Table 1).

According to KEGG analysis, 85 signaling pathways were detected as targets for the 87 miRNAs upregulated in fetal- vs. adult-derived EVs. Each of the pathways was targeted by multiple miRNAs, and 15 of the 85 pathways were associated with angiogenesis and wound healing. These 15 pathways included adherent junction [47], HIPPO [48–51], p53 [52], TGF-beta [53, 54], ECM-receptor interaction [55], focal adhesion [56], mTOR (interconnected to PI3K-Akt) [57–59], HIF-1 [60], ErbB [61], FoxO (upstream in the activation of TGF-beta and PI3k-Akt), Wnt [62], Notch [63–66], neurotrophin [67], MAPK [68], and insulin (upstream to mTOR) signaling pathways. Of particular interest was the HIPPO signaling, whose role in regulating regeneration of organs such as the intestine, liver, heart, nervous system, and skin is well documented. By setting genes intersection option (29), 10 putative target genes (THBS1, FN1, CCND1,

CCND2, CDKN1A, CDK6, TNFRSF10B, MDM2, IGF1R, and MCL1) associated with 4 of the 15 signaling pathways (ECM-receptor interaction, PI3K/Akt, p53, and FoxO) were obtained and predicted as targets for our miRNAs. Among the putative target genes, we focused on THBS1 to validate the *in silico* analysis. THBS1 is a multifunctional extracellular matrix glycoprotein produced by several cell types, facilitating tissue repair in different healing models [69–71]. Western blot analysis showed a significant increase of THBS1 protein amounts (approximately 4-fold) in fibroblasts treated for 72 hours with fetal dermal-derived EVs against untreated fibroblasts.

Both freshly isolated and frozen EVs were tested in cell-based assays of angiogenesis and cell migration, thus showing no differences in their performances. This observation was in agreement with a previous report showing that the storage in the absence of cryoprotectant at -20°C did not affect the biochemical activity of EVs [72]. While EVs from both cell types stimulated cell migration with a similar efficacy, fetal dermal cell-derived EVs were far more effective than adult dermal cell-derived EVs in inducing formation of mesh-like structures. Even if this result was not statistically significant, the slide in Supplemental Material S4 clearly shows this difference. Overall, we observed a delay in EV-induced cellular responses compared to secretome/CM-induced cellular responses. Since the delay was independent from the used EV concentrations (e.g., either 100 or 10 μg/ml), we suggest that the delay could be due to the dynamic of EV internalization by target cells.

In view of the promising prospective of miRNA-based therapeutics, the research is dedicated in solving some challenges in order to make it more translationally valuable. These challenges include the off-target effects of miRNA or their low internalization by target cells making their delivery difficult [73]. Typically, miRNAs for therapeutics have been delivered by direct injection, viral vectors, or coupled to scaffolds [74]. A number of studies indicate that EVs may exert their effect via horizontal transfer of their cargo [14]. Therefore, EVs could serve as a vehicle to successfully deliver miRNAs of interest to several therapeutic applications [75]. Confocal microscope observations of a punctuated green fluorescent pattern inside target cells suggest successful internalization of CSFE-labeled EVs. The signal was visualized in the cytosol of both HUVECs and fibroblasts at not earlier than 4 hours of incubation, and in the perinuclear region at later time points (from 8 hours of incubation). To conclude, the proangiogenic features of secretome of human fetal dermal cells appear largely related to the presence of small EVs. Although there is much to be learned in the field of EV research, the unique properties of these particles clearly represent a new therapeutic opportunity for tissue regeneration [15, 76], since it could offer a number of advantages over traditional cell transplantation as a cell-free product. As with conventional drugs, EVs can be standardized and tested in terms of dose and biological activity. Furthermore, EVs can be produced in clinical grade, freeze, and easily delivered. Finally, EV-based therapy could overcome the challenge of a successful delivery of miRNA molecules *in vivo* [77].

Data Availability

The data concerning the NTA of EVs, the heat map graph, the figures and graphs of in vitro angiogenesis, the curves of cell migration, the flow cytometry graphs of CSFE-labeled EVs, and the uptake of EVs used to support the findings of this study are included within the article. The miRNA data used to support the findings of this study are included as a table within the articles, but also in supplementary information file S1 The KEGG data used to support the findings of this study are included within the article (as graphs), and also in supplementary information files S2 and S3.

Conflicts of Interest

The authors declare no conflicts of interest.

Acknowledgments

We wish to thank the Gynecology Unit of Ospedale Civico (Palermo, Italy) for providing the fetal skin biopsies. We thank Prof. Marcello Monti and Dr. Stefania Motta of Istituto Humanitas (Rozzano, Italy) for providing the adult skin biopsies. We also thank Dr. Vitale Miceli of IRCCS-ISMETT (Palermo, Italy) for providing additional EVs for biochemical characterization. This work was supported by the Italian Ministry of Education, University and Research (MIUR) (NOP for Research and Competitiveness 2007–2013, IRMI (CTN01_00177_888744)).

Supplementary Materials

S1 (excel file): list of significantly upregulated miRNAs in fetal vs. adult EVs; a list of all analyzed miRNAs is also included. S2 (excel file): complete list of the KEGG signaling pathways; list of the KEGG signaling pathways associated with angiogenesis and wound healing. S3 (excel file): complete list of the KEGG signaling pathways obtained with genes intersection 29, including putative target genes. S4 (power point slide): pictures of HUVECs treated with fetal-derived EVs ($n = 4$) and adult-derived EVs ($n = 3$). Each picture represents an independent experiment. *(Supplementary Materials)*

References

[1] J. Folkman, "Angiogenesis in cancer, vascular, rheumatoid and other disease," *Nature Medicine*, vol. 1, no. 1, pp. 27–30, 1995.

[2] G. P. Lasala, J. A. Silva, and J. J. Minguell, "Therapeutic angiogenesis in patients with severe limb ischemia by transplantation of a combination stem cell product," *The Journal of Thoracic and Cardiovascular Surgery*, vol. 144, no. 2, pp. 377–382, 2012.

[3] E. Eggenhofer, V. Benseler, A. Kroemer et al., "Mesenchymal stem cells are short-lived and do not migrate beyond the lungs after intravenous infusion," *Frontiers in Immunology*, vol. 3, p. 297, 2012.

[4] M. E. Fung and B. Thébaud, "Stem cell-based therapy for neonatal lung disease: it is in the juice," *Pediatric Research*, vol. 75, no. 1, pp. 2–7, 2014.

[5] J. A. Pawitan, "Prospect of stem cell conditioned medium in regenerative medicine," *BioMed Research International*, vol. 2014, Article ID 965849, 14 pages, 2014.

[6] C. Tran and M. S. Damaser, "Stem cells as drug delivery methods: application of stem cell secretome for regeneration," *Advanced Drug Delivery Reviews*, vol. 82-83, pp. 1–11, 2015.

[7] N. Hirt-Burri, A.-A. Ramelet, W. Raffoul et al., "Biologicals and fetal cell therapy for wound and scar management," *ISRN Dermatology*, vol. 2011, Article ID 549870, 16 pages, 2011.

[8] A. A. Ramelet, N. Hirt-Burri, W. Raffoul et al., "Chronic wound healing by fetal cell therapy may be explained by differential gene profiling observed in fetal versus old skin cells," *Experimental Gerontology*, vol. 44, no. 3, pp. 208–218, 2009.

[9] A. S. De Buys Roessingh, J. Hohlfeld, C. Scaletta et al., "Development, characterization, and use of a fetal skin cell bank for tissue engineering in wound healing," *Cell Transplantation*, vol. 15, no. 8–9, pp. 823–834, 2006.

[10] J. Hohlfeld, A. De Buys Roessingh, N. Hirt-Burri et al., "Tissue engineered fetal skin constructs for paediatric burns," *The Lancet*, vol. 366, no. 9488, pp. 840–842, 2005.

[11] C. M. Chinnici, G. Amico, M. Monti et al., "Isolation and characterization of multipotent cells from human fetal dermis," *Cell Transplantation*, vol. 23, no. 10, pp. 1169–1185, 2014.

[12] M. Gaetani, C. M. Chinnici, A. P. Carreca, C. Di Pasquale, G. Amico, and P. G. Conaldi, "Unbiased and quantitative proteomics reveals highly increased angiogenesis induction by the secretome of mesenchymal stromal cells isolated from fetal rather than adult skin," *Journal of Tissue Engineering and Regenerative Medicine*, vol. 12, no. 2, pp. e949–e961, 2018.

[13] G. Raposo and W. Stoorvogel, "Extracellular vesicles: exosomes, microvesicles, and friends," *The Journal of Cell Biology*, vol. 200, no. 4, pp. 373–383, 2013.

[14] L. A. Mulcahy, R. C. Pink, and D. R. F. Carter, "Routes and mechanisms of extracellular vesicle uptake," *Journal of Extracellular Vesicles*, vol. 3, no. 1, p. 3, 2014.

[15] H. Jing, X. He, and J. Zheng, "Exosomes and regenerative medicine: state of the art and perspectives," *Translational Research*, vol. 196, pp. 1–16, 2018.

[16] T. Katsuda and T. Ochiya, "Molecular signatures of mesenchymal stem cell-derived extracellular vesicle-mediated tissue repair," *Stem Cell Research & Therapy*, vol. 6, no. 1, p. 212, 2015.

[17] F. Marqués-García and M. Isidoro-García, "Protocols for exosome isolation and RNA profiling," *Methods in Molecular Biology*, vol. 1434, pp. 153–167, 2016.

[18] C. M. Chinnici, G. Pietrosi, G. Iannolo et al., "Mesenchymal stromal cells isolated from human fetal liver release soluble factors with a potential role in liver tissue repair," *Differentiation*, vol. 105, pp. 14–26, 2019.

[19] R. A. Dragovic, C. Gardiner, A. S. Brooks et al., "Sizing and phenotyping of cellular vesicles using nanoparticle tracking analysis," *Nanomedicine: Nanotechnology, Biology and Medicine*, vol. 7, no. 6, pp. 780–788, 2011.

[20] I. S. Vlachos, N. Kostoulas, T. Vergoulis et al., "DIANA miRPath v.2.0: investigating the combinatorial effect of microRNAs in pathways," *Nucleic Acids Research*, vol. 40, no. W1, pp. W498–W504, 2012.

[21] R. Limame, A. Wouters, B. Pauwels et al., "Comparative analysis of dynamic cell viability, migration and invasion assessments by novel real-time technology and classic endpoint assays," *PLoS One*, vol. 7, no. 10, article e46536, 2012.

[22] G. Iannolo, M. R. Sciuto, G. M. Raffa, M. Pilato, and P. G. Conaldi, "MiR34 inhibition induces human heart progenitor proliferation," *Cell Death & Disease*, vol. 9, no. 3, p. 368, 2018.

[23] R. B. Dessau and C. B. Pipper, ""R"- project for statistical computing," *Ugeskrift for Laeger*, vol. 170, no. 5, pp. 328–330, 2008.

[24] C. Théry, K. W. Witwer, E. Aikawa et al., "Minimal information for studies of extracellular vesicles 2018 (MISEV2018): a position statement of the International Society for Extracellular Vesicles and Update of the MISEV2014 Guidelines," *Journal of Extracellular Vesicles*, vol. 7, no. 1, 2018.

[25] A. Taktak-BenAmar, M. Morjen, H. Ben Mabrouk et al., "Expression, purification and functionality of bioactive recombinant human vascular endothelial growth factor VEGF165 in E. coli," *AMB Express*, vol. 7, no. 1, p. 33, 2017.

[26] S. Mathivanan, C. J. Fahner, G. E. Reid, and R. J. Simpson, "ExoCarta 2012: database of exosomal proteins, RNA and lipids," *Nucleic Acids Research*, vol. 40, no. D1, pp. D1241–D1244, 2011.

[27] http://www.exocarta.org..

[28] A. Christopher, R. Kaur, G. Kaur, A. Kaur, V. Gupta, and P. Bansal, "MicroRNA therapeutics: discovering novel targets and developing specific therapy," *Perspectives in Clinical Research*, vol. 7, no. 2, pp. 68–74, 2016.

[29] C. M. Curtin, I. M. Castaño, and F. J. O'Brien, "Scaffold-based microRNA therapies in regenerative medicine and cancer," *Advanced Healthcare Materials*, vol. 7, no. 1, 2018.

[30] C. K. Sen and S. Ghatak, "MiRNA control of tissue repair and regeneration," *The American Journal of Pathology*, vol. 185, no. 10, pp. 2629–2640, 2015.

[31] J. Banerjee and C. K. Sen, "MicroRNAs in skin and wound healing," *Methods in Molecular Biology*, vol. 936, no. 10, pp. 343–356, 2013.

[32] T. Wang, Y. Feng, H. Sun et al., "MiR-21 regulates skin wound healing by targeting multiple aspects of the healing process," *The American Journal of Pathology*, vol. 181, no. 6, pp. 1911–1920, 2012.

[33] A. Caporali and C. Emanueli, "MicroRNA regulation in angiogenesis," *Vascular Pharmacology*, vol. 55, no. 4, pp. 79–86, 2011.

[34] S. Landskroner-Eiger, I. Moneke, and W. C. Sessa, "MiRNAs as modulators of angiogenesis," *Cold Spring Harbor Perspectives in Medicine*, vol. 3, no. 2, 2013.

[35] G. Bridge, R. Monteiro, S. Henderson et al., "The microRNA-30 family targets DLL4 to modulate endothelial cell behavior during angiogenesis," *Blood*, vol. 120, no. 25, pp. 5063–5072, 2012.

[36] Z. Hua, Q. Lv, W. Ye et al., "MiRNA-directed regulation of VEGF and other angiogenic factors under hypoxia," *PLoS One*, vol. 1, no. 1, p. e116, 2006.

[37] N. M. Kane, L. Howard, B. Descamps et al., "Role of microRNAs 99b, 181a, and 181b in the differentiation of human embryonic stem cells to vascular endothelial cells," *Stem Cells*, vol. 30, no. 4, pp. 643–654, 2012.

[38] Y. Suárez and W. C. Sessa, "MicroRNAs as novel regulators of angiogenesis," *Circulation Research*, vol. 104, no. 4, pp. 442–454, 2009.

[39] S. Wang and E. N. Olson, "AngiomiRs—key regulators of angiogenesis," *Current Opinion in Genetics & Development*, vol. 19, no. 3, pp. 205–211, 2009.

[40] Q. Zhou, R. Gallagher, R. Ufret-Vincenty, X. Li, E. N. Olson, and S. Wang, "Regulation of angiogenesis and choroidal

neovascularization by members of microRNA-23~27~24 clusters," *Proceedings of the National Academy of Sciences of the United States of America*, vol. 108, no. 20, pp. 8287–8292, 2011.

[41] Y. Li, L. Fan, S. Liu et al., "The promotion of bone regeneration through positive regulation of angiogenic-osteogenic coupling using microRNA-26a," *Biomaterials*, vol. 34, no. 21, pp. 5048–5058, 2013.

[42] M. Monaghan, S. Browne, K. Schenke-Layland, and A. Pandit, "A collagen-based scaffold delivering exogenous microRNA-29B to modulate extracellular matrix remodeling," *Molecular Therapy*, vol. 22, no. 4, pp. 786–796, 2014.

[43] E. Van Rooij, L. B. Sutherland, J. E. Thatcher et al., "Dysregulation of microRNAs after myocardial infarction reveals a role of MiR-29 in cardiac fibrosis," *Proceedings of the National Academy of Sciences of the United States of America*, vol. 105, no. 35, pp. 13027–13032, 2008.

[44] T. Ma, Y. Chen, Y. Chen et al., "MicroRNA-132, delivered by mesenchymal stem cell-derived exosomes, promote angiogenesis in myocardial infarction," *Stem Cells International*, vol. 2018, Article ID 3290372, 11 pages, 2018.

[45] F. Meng, Z. Li, Z. Zhang et al., "MicroRNA-193b-3p regulates chondrogenesis and chondrocyte metabolism by targeting HDAC3," *Theranostics*, vol. 8, no. 10, pp. 2862–2883, 2018.

[46] P. Lesizza, G. Prosdocimo, V. Martinelli, G. Sinagra, S. Zacchigna, and M. Giacca, "Single-dose intracardiac injection of pro-regenerative microRNAs improves cardiac function after myocardial infarction," *Circulation Research*, vol. 120, no. 8, pp. 1298–1304, 2017.

[47] G. Fenteany, P. A. Janmey, and T. P. Stossel, "Signaling pathways and cell mechanics involved in wound closure by epithelial cell sheets," *Current Biology*, vol. 10, no. 14, pp. 831–838, 2000.

[48] W. C. Juan and W. Hong, "Targeting the Hippo signaling pathway for tissue regeneration and cancer therapy," *Genes*, vol. 7, no. 9, p. 55, 2016.

[49] M. J. Lee, M. R. Byun, M. Furutani-Seiki, J. H. Hong, and H. S. Jung, "YAP and TAZ regulate skin wound healing," *The Journal of Investigative Dermatology*, vol. 134, no. 2, pp. 518–525, 2014.

[50] Y. Wang, A. Yu, and F. X. Yu, "The Hippo pathway in tissue homeostasis and regeneration," *Protein & Cell*, vol. 8, no. 5, pp. 349–359, 2017.

[51] B. Zhao, K. Tumaneng, and K. L. Guan, "The Hippo pathway in organ size control, tissue regeneration and stem cell self-renewal," *Nature Cell Biology*, vol. 13, no. 8, pp. 877–883, 2011.

[52] M. Farhang Ghahremani, S. Goossens, D. Nittner et al., "P53 promotes VEGF expression and angiogenesis in the absence of an intact P21-Rb pathway," *Cell Death and Differentiation*, vol. 20, no. 7, pp. 888–897, 2013.

[53] K. W. Finnson, P. R. Arany, and A. Philip, "Transforming growth factor beta signaling in cutaneous wound healing: lessons learned from animal studies," *Advances in Wound Care*, vol. 2, no. 5, pp. 225–237, 2013.

[54] H. Ramirez, S. B. Patel, and I. Pastar, "The role of TGFβ signaling in wound epithelialization," *Advances in Wound Care*, vol. 3, no. 7, pp. 482–491, 2014.

[55] P. Olczyk, Ł. Mencner, and K. Komosinska-Vassev, "The role of the extracellular matrix components in cutaneous wound healing," *BioMed Research International*, vol. 2014, Article ID 747584, 8 pages, 2014.

[56] X. Zhao and J. L. Guan, "Focal adhesion kinase and its signaling pathways in cell migration and angiogenesis," *Advanced Drug Delivery Reviews*, vol. 63, no. 8, pp. 610–615, 2011.

[57] R. Castilho, C. Squarize, and J. Gutkind, "Exploiting PI3K/MTOR signaling to accelerate epithelial wound healing," *Oral Diseases*, vol. 19, no. 6, pp. 551–558, 2013.

[58] J. Chen, R. Crawford, C. Chen, and Y. Xiao, "The key regulatory roles of the PI3K/Akt signaling pathway in the functionalities of mesenchymal stem cells and applications in tissue regeneration," *Tissue Engineering. Part B, Reviews*, vol. 19, no. 6, pp. 516–528, 2013.

[59] J. Karar and A. Maity, "PI3K/AKT/MTOR pathway in angiogenesis," *Frontiers in Molecular Neuroscience*, vol. 4, 2011.

[60] W. X. Hong, M. S. Hu, M. Esquivel et al., "The role of hypoxia-inducible factor in wound healing," *Advances in Wound Care*, vol. 3, no. 5, pp. 390–399, 2014.

[61] S. Pastore, F. Mascia, V. Mariani, and G. Girolomoni, "The epidermal growth factor receptor system in skin repair and inflammation," *Journal of Investigative Dermatology*, vol. 128, no. 6, pp. 1365–1374, 2008.

[62] J. L. Whyte, A. A. Smith, and J. A. Helms, "Wnt signaling and injury repair," *Cold Spring Harbor Perspectives in Biology*, vol. 4, no. 8, article a008078, 2012.

[63] M. E. Carlson, M. S. O'Connor, M. Hsu, and I. M. Conboy, "Notch signaling pathway and tissue engineering," *Frontiers in Bioscience*, vol. 12, no. 12, pp. 5143–5156, 2007.

[64] S. Chigurupati, T. V. Arumugam, T. G. Son et al., "Involvement of Notch signaling in wound healing," *PLoS One*, vol. 2, no. 11, p. e1167, 2007.

[65] Q. S. Ran, Y. H. Yu, X. H. Fu, and Y. C. Wen, "Activation of the Notch signaling pathway promotes neurovascular repair after traumatic brain injury," *Neural Regeneration Research*, vol. 10, no. 8, pp. 1258–1264, 2015.

[66] A. Raya, C. M. Koth, D. Büscher et al., "Activation of Notch signaling pathway precedes heart regeneration in zebrafish," *Proceedings of the National Academy of Sciences of the United States of America*, vol. 100, Supplement 1, pp. 11889–11895, 2003.

[67] R. Kraemer and B. L. Hempstead, "Neurotrophins: novel mediators of angiogenesis," *Frontiers in Bioscience*, vol. 8, no. 6, pp. s1181–s1186, 2003.

[68] M. Deng, W.-L. Chen, A. Takatori et al., "A role for the mitogen-activated protein kinase kinase kinase 1 in epithelial wound healing," *Molecular Biology of the Cell*, vol. 17, no. 8, pp. 3446–3455, 2006.

[69] L. A. DiPietro, N. N. Nissen, R. L. Gamelli, A. E. Koch, J. M. Pyle, and P. J. Polverini, "Thrombospondin 1 synthesis and function in wound repair," *The American Journal of Pathology*, vol. 148, no. 6, pp. 1851–1860, 1996.

[70] A. Agah, T. R. Kyriakides, J. Lawler, and P. Bornstein, "The lack of thrombospondin-1 (TSP1) dictates the course of wound healing in double-TSP1/TSP2-null mice," *The American Journal of Pathology*, vol. 161, no. 3, pp. 831–839, 2002.

[71] K. Uno, M. Kuroki, H. Hayashi, H. Uchida, M. Kuroki, and K. Oshima, "Impairment of thrombospondin-1 expression during epithelial wound healing in corneas of vitamin A-deficient mice," *Histology and Histopathology*, vol. 20, no. 2, pp. 493–499, 2005.

[72] A. V. Vlassov, S. Magdaleno, R. Setterquist, and R. Conrad, "Exosomes: current knowledge of their composition, biological

functions, and diagnostic and therapeutic potentials," *Biochimica et Biophysica Acta*, vol. 1820, no. 7, pp. 940–948, 2012.

[73] D. Ben-Shushan, E. Markovsky, H. Gibori, G. Tiram, A. Scomparin, and R. Satchi-Fainaro, "Overcoming obstacles in microRNA delivery towards improved cancer therapy," *Drug Delivery and Translational Research*, vol. 4, no. 1, pp. 38–49, 2014.

[74] B. Peng, Y. Chen, and K. W. Leong, "MicroRNA delivery for regenerative medicine," *Advanced Drug Delivery Reviews*, vol. 88, pp. 108–122, 2015.

[75] G. Hu, K. M. Drescher, and X. M. Chen, "Exosomal miRNAs: biological properties and therapeutic potential," *Frontiers in Genetics*, vol. 3, p. 56, 2012.

[76] A. G. E. Ibrahim, K. Cheng, and E. Marbán, "Exosomes as critical agents of cardiac regeneration triggered by cell therapy," *Stem Cell Reports*, vol. 2, no. 5, pp. 606–619, 2014.

[77] H. Xin, Y. Li, B. Buller et al., "Exosome-mediated transfer of MiR-133b from multipotent mesenchymal stromal cells to neural cells contributes to neurite outgrowth," *Stem Cells*, vol. 30, no. 7, pp. 1556–1564, 2012.

[78] L. Poliseno, A. Tuccoli, L. Mariani et al., "MicroRNAs modulate the angiogenic properties of HUVECs," *Blood*, vol. 108, no. 9, pp. 3068–3071, 2006.

[79] D. Li, X. Li, A. Wang et al., "MicroRNA-31 promotes skin wound healing by enhancing keratinocyte proliferation and migration," *The Journal of Investigative Dermatology*, vol. 135, no. 6, pp. 1676–1685, 2015.

[80] S. Zhou, P. Zhang, P. Liang, and X. Huang, "The expression of miR-125b regulates angiogenesis during the recovery of heat-denatured HUVECs," *Burns*, vol. 41, no. 4, pp. 803–811, 2015.

[81] X. Li, D. Li, J. D. Wikstrom et al., "MicroRNA-132 promotes fibroblast migration via regulating RAS P21 protein activator 1 in skin wound healing," *Scientific Reports*, vol. 7, no. 1, p. 7797, 2017.

[82] L. Fan, Q. Wu, X. Xing, Y. Wei, and Z. Shao, "MicroRNA-145 targets vascular endothelial growth factor and inhibits invasion and metastasis of osteosarcoma cells," *Acta Biochimica et Biophysica Sinica*, vol. 44, no. 5, pp. 407–414, 2012.

[83] J. Ahn, H. Lee, C. H. Jung, and T. Jeon, "MicroRNA-146b promotes adipogenesis by suppressing the SIRT1-FOXO1 cascade," *EMBO Molecular Medicine*, vol. 5, no. 10, pp. 1602–1612, 2013.

[84] H. Lang, F. Zhao, T. Zhang et al., "MicroRNA-149 contributes to scarless wound healing by attenuating inflammatory response," *Molecular Medicine Reports*, vol. 16, no. 2, pp. 2156–2162, 2017.

[85] S. C. Slater, E. Jover, A. Martello et al., "MicroRNA-532-5p regulates pericyte function by targeting the transcription regulator BACH1 and angiopoietin-1," *Molecular Therapy*, vol. 26, no. 12, pp. 2823–2837, 2018.

[86] P. Bao, A. Kodra, M. Tomic-Canic, M. S. Golinko, H. P. Ehrlich, and H. Brem, "The role of vascular endothelial growth factor in wound healing," *Journal of Surgical Research*, vol. 153, no. 2, pp. 347–358, 2009.

[87] J. F. Li, H. F. Duan, C. T. Wu et al., "HGF accelerates wound healing by promoting the dedifferentiation of epidermal cells through -integrin/ILK pathway," *BioMed Research International*, vol. 2013, Article ID 470418, 9 pages, 2013.

[88] R. Guo, L. Chai, L. Chen et al., "Stromal cell-derived factor 1 (SDF-1) accelerated skin wound healing by promoting the migration and proliferation of epidermal stem cells," *In Vitro Cellular & Developmental Biology - Animal*, vol. 51, no. 6, pp. 578–585, 2015.

[89] R. Salcedo, K. Wasserman, H. A. Young et al., "Vascular endothelial growth factor and basic fibroblast growth factor induce expression of CXCR4 on human endothelial cells," *The American Journal of Pathology*, vol. 154, no. 4, pp. 1125–1135, 1999.

[90] T. Yamamoto, B. Eckes, C. Mauch, K. Hartmann, and T. Krieg, "Monocyte chemoattractant protein-1 enhances gene expression and synthesis of matrix metalloproteinase-1 in human fibroblasts by an autocrine IL-1α loop," *Journal of Immunology*, vol. 164, no. 12, pp. 6174–6179, 2000.

[91] E. Engelhardt, A. Toksoy, M. Goebeler, S. Debus, E. B. Bröcker, and R. Gillitzer, "Chemokines IL-8, GROα, MCP-1, IP-10, and Mig are sequentially and differentially expressed during phase-specific infiltration of leukocyte subsets in human wound healing," *The American Journal of Pathology*, vol. 153, no. 6, pp. 1849–1860, 1998.

Hindawi
Stem Cells International
Volume 2020, Article ID 8837654, 45 pages
https://doi.org/10.1155/2020/8837654

Review Article

Mesenchymal Stem/Progenitor Cells: The Prospect of Human Clinical Translation

Dina Rady,[1,2] **Marwa M. S. Abbass**,[1,2] **Aiah A. El-Rashidy**,[2,3] **Sara El Moshy**,[1,2] **Israa Ahmed Radwan**,[1,2] **Christof E. Dörfer**,[4] **and Karim M. Fawzy El-Sayed**[2,4,5]

[1]*Oral Biology Department, Faculty of Dentistry, Cairo University, Cairo, Egypt*
[2]*Stem Cells and Tissue Engineering Research Group, Faculty of Dentistry, Cairo University, Cairo, Egypt*
[3]*Biomaterials Department, Faculty of Dentistry, Cairo University, Cairo, Egypt*
[4]*Clinic for Conservative Dentistry and Periodontology, School of Dental Medicine, Christian Albrechts University, Kiel, Germany*
[5]*Oral Medicine and Periodontology Department, Faculty of Dentistry, Cairo University, Cairo, Egypt*

Correspondence should be addressed to Karim M. Fawzy El-Sayed; karim.fawzy@gmail.com

Received 27 April 2020; Revised 19 June 2020; Accepted 20 July 2020; Published 11 August 2020

Academic Editor: Kar Wey Yong

Mesenchymal stem/progenitor cells (MSCs) are key players in regenerative medicine, relying principally on their differentiation/regeneration potential, immunomodulatory properties, paracrine effects, and potent homing ability with minimal if any ethical concerns. Even though multiple preclinical and clinical studies have demonstrated remarkable properties for MSCs, the clinical applicability of MSC-based therapies is still questionable. Several challenges exist that critically hinder a successful clinical translation of MSC-based therapies, including but not limited to heterogeneity of their populations, variability in their quality and quantity, donor-related factors, discrepancies in protocols for isolation, in vitro expansion and premodification, and variability in methods of cell delivery, dosing, and cell homing. Alterations of MSC viability, proliferation, properties, and/or function are also affected by various drugs and chemicals. Moreover, significant safety concerns exist due to possible teratogenic/neoplastic potential and transmission of infectious diseases. Through the current review, we aim to highlight the major challenges facing MSCs' human clinical translation and shed light on the undergoing strategies to overcome them.

1. Introduction

Tissue engineering combines stem/progenitor cells with proper signaling molecules to be seeded on biocompatible scaffolds in the presence of physical stimuli to function in place of or to support regeneration of specific tissues or organs [1–3]. Mesenchymal stem/progenitor cells (MSCs) are key players in regenerative medicine, owing to their remarkable differentiation and regeneration potentials in addition to their immunomodulatory properties, paracrine effect [4, 5], and potent homing ability with no ethical concerns [6–8]. MSCs are multipotent cells, hallmarked by their ability to differentiate into a variety of cell types upon stimulation. They should at least express clusters of differentiation (CD) CD105, CD90, and CD73 and lack the expression of CD11b, CD79a, CD19, and human leukocyte antigen-DR isotype (HLA-DR) [9]. Interestingly, MSCs uniquely display low immunogenicity, lack the expression of the major histocompatibility complex- (MHC-) II, express low levels of MHC-I, and are not inductive to lymphocytes, which reduces their chances of eliciting an immune response upon transplantation [10]. MSCs have been successfully isolated from most tissues of the body, including bone marrow, dental tissues, adipose tissues, skin, liver, lung, umbilical cord, cord blood, and placenta [11–18]. Even though clinical studies have demonstrated remarkable properties for MSCs [19, 20], reproducible, cost-efficient, standardized, and mass production of these cells and minimization of their populations' heterogeneity are important issues that are yet to be addressed, to allow for a human clinical translational therapy

[21]. Through the current review, we aim to highlight the major obstacles facing MSCs' human clinical translation and how they can be overcome.

2. Donor-Related Factors

MSCs' quality, quantity, and characteristics rely upon a variety of donor-related factors [22], including body mass index [23, 24], age [25, 26], gender [27], and systemic and autoimmune diseases [28–30]. The variability of MSC markers' expression in correlation with their tissue source is presented in Table 1.

2.1. Donor's Obesity and MSCs. Obesity could impact MSCs' characteristics and regenerative potential. Comparing adipose stem/progenitor cells (ASCs) isolated from obese and nonobese patients, a significant decrease in cellular proliferation [23, 31] and colony formation [23] of ASCs obtained from obese patients was evident. Moreover, ASCs from obese patients showed altered expression of cell surface markers, with significantly decreased expression of CD54, CD66, CD90 [23], and CD29 [31] and an increased expression of CD106 and HLA II [31], in addition to significantly lower osteogenic [23, 32] and adipogenic differentiation potentials [23], as compared to ASCs obtained from nonobese patients. This was attributed to the different microenvironment associated with obesity, including adipose tissues' hypoxia, which results in increased expression of proinflammatory cytokines. Obesity-associated adipose tissue inflammation could influence ASC multilineage differentiation [23, 33]. Moreover, obesity can alter ASC stemness and expression of stem/progenitor cell-related genes (Oct4, Sal4, Sox15, KLF4, and BMI1), aside from influencing their senescence and secretome profiles [18, 24]. Additionally, obesity could diminish ASCs' immunomodulatory properties [28]. ASCs derived from obese patients were further associated with upregulation in the expression of the inflammatory cytokines interleukin- (IL-) 1β, IL-6, tumor necrosis factor-alpha (TNF-α), and monocyte chemoattractant protein-1 (MCP-1) as compared to ASCs acquired from nonobese patients [28]. These alterations were hypothesized to be mediated through activation of protein kinase C delta expression [24].

The therapeutic potential of ASCs acquired from obese and nonobese patients was explored in mice with an experimental autoimmune encephalomyelitis multiple sclerosis model. ASCs from obese patients showed an increased expression of proinflammatory cytokines as well as stimulated the proliferation and differentiation of T-cells, resulting in a failed improvement in the multiple sclerosis-associated central nervous system inflammation disease model, indicating that obesity can negatively impact the anti-inflammatory and immune-modulatory ability of ASCs [34]. ASCs from obese patients further demonstrated significantly reduced bone formation in vivo upon implantation in critical-size calvarial defects in mice, as compared to ASCs from nonobese individuals [32].

2.2. Donor's Age and MSCs. MSCs' number and regenerative potential are further proposed to be largely influenced by the donor's age. Rats demonstrated an age-related decrease in bone marrow mesenchymal stem/progenitor cell (BMSC) yield [26, 35] and proliferation rate as well as a significant reduction in their osteogenic capacity in vitro [26] and in vivo following subcutaneous implantation [36]. Likewise, human BMSCs and ASCs displayed an age-related increase in cellular senescence (apoptosis) and expression of p53 gene [25] in addition to a decrease in the cellular proliferation rate [25, 37] and osteogenic [25, 37–40] and chondrogenic differentiation in vitro [37, 41], with an increase in adipogenic potential, reflected clinically by an increased adipose deposition in the bone marrow [40]. Comparing human MSCs acquired from young and old donors, an age-related decrease in cellular proliferation and increased apoptosis, attributed to p53/p21 and p53/BAX pathway activation, respectively, was observed. In addition, an increase in cells positive for senescence-associated β-galactosidase and a decrease in osteogenic differentiation, alkaline phosphatase (ALP), Runt-related transcription factor-2 (RUNX-2), Osterix, bone sialoprotein, and osteocalcin expressions was observed. This was attributed to an upregulation of p53 gene expression, which negatively correlates with osteoblastogenesis [25].

Interestingly, nonadherent, less differentiated rodents' BMSCs in suspension cultures appeared to be more resistant to the effect of aging in vitro [42]. Nonadherent cells showed elevated expression of pluripotency markers Nanog, Oct4, and Sox2. Further, the generation of colonies by nonadherent MSCs collected from old rats was not reduced as compared to young rats [42].

In addition to epigenetic changes leading to cellular senescence, aging of MSCs is believed to be further caused by DNA damage, telomere shortening, and accumulation of oxidative stress. All these events could in isolation or combined lead to changes in MSC cellular functions including proliferation and differentiation [43–46]. Reactive oxygen species (ROS) accumulates intracellularly in MSCs with age. Increasing levels of ROS subsequently cause oxidation of cellular components, senescence, and DNA damage, negatively influencing the differentiation ability of MSCs [47, 48]. Aging is further associated with dysregulation in micro-RNAs (miRNAs), the noncoding RNA regulating gene expression [43]. In this context, aging processes were observed to be accompanied by a decline in miR-27a associated with osteogenic differentiation [49] as well as an upregulation in miR-335 [50], miR-199b-5p [51], miR-31a-5p [52], and miR-29c-3p [53] associated with increased senescence, decreased proliferation, and osteogenic differentiation [50–53].

Senescent MSCs display changes in expression of genes associated with proliferation, signaling, function, and maintenance of MSCs, with an age-related loss in MSC response to biological signals. In addition to age-related change in DNA methylation, a reduction in expression of the transcription factors ALX1, PITX2, HOXB6, HOXB7, and IRF6 and increased expression of TBX18 and FOXP2 involved in cellular senescence, disruption in mitochondrial function, and reduction in differentiation ability of MSCs have been reported [51]. As continuous shortening of the telomeres results in reduced proliferation and differentiation, BMSCs

Table 1: Variability of MSC markers' expression with respect to source basis.

Mesenchymal stem cells	MSC source	Markers		Differentiation potential	Advantages	Disadvantages
		Positive	Negative			
BMSCs	Bone marrow aspirate [166]	CD29, CD44, CD73, CD90, CD105 CD166, Sca-1, and CD106 [548–551]	CD14, CD34, CD45, CD19, CD11b, CD31, and HLA-DR [548–551]	Adipocyte, astrocyte, cardiomyocytes, chondrocyte, hepatocyte, mesangial cells, myocytes, neuron, osteoblast, and stromal cell [552]	(i) Superior osteogenic and chondrogenic potential [142]. (ii) Multiple studies confirmed safety and efficacy of this type of cells [552].	(i) Bone marrow harvesting is invasive [143]. (ii) Fewer number of mesenchymal progenitors cells and lower proliferation rate as compared to MSCs from other sources [144, 145].
ADSCs	Adipose tissue obtained from liposuction [553]	CD29, CD44, CD13, CD166, CD73, CD90, CD105, CD34, CD49e, and CD10 [551, 554, 555]	CD31, CD45, CD14, CD11b, CD34, CD19, CD56, CD146, and HLA-DR [551, 554, 555]	Adipocytes, chondrocyte, myocytes,osteoblast, stromal cell [552]	(i) Less invasive isolation procedure [147]. (ii) Yield more progenitor cells [148, 149]. (iii) Have a higher proliferation rate as compared to BMSCs [145, 150].	(i) Adipogenic differentiation tendency [153, 154]. (ii) Low proangiogenic factors and cytokine secretion as compared to BMSCs [155, 156].
Dental stem cells	(i) Dental pulp stem cells isolated from dental pulp tissues of permanent teeth (ii) Pulp tissues of human shed deciduous teeth (SHED) (iii) Periodontal ligament stem cells isolated from periodontal tissues (iv) Dental follicle stem cells usually isolated from dental follicle surrounding third molar (v) Alveolar bone-derived stem cells, stem cells isolated from apical papilla at the apices of immature permanent teeth (vi) Tooth germ progenitor cells isolated from late bell stage third molar's tooth	CD105, CD73, and CD90 [164].	CD45, CD34, CD14, CD11b, CD79a, CD19, and HLA-DR [164]	Osteoblasts, chondroblasts, adipocytes, neuron, and angiogenic potential [161, 164]	(i) Relatively easier to isolate during routine dental treatments without teeth scarification [161] (ii) Possess higher proliferation rates, as compared to either BMSCs or ASCs [162, 163].	(i) Some types are inaccessible to isolate (ii) Difficult to isolate in sufficient amount (iii) Not readily feasible throughout the patient's life [165].

Table 1: Continued.

Mesenchymal stem cells		MSC source	Markers		Differentiation potential	Advantages	Disadvantages
			Positive	Negative			
		germs (vi) Gingival stem cells, isolated from gingival tissues [18].					
Perinatal tissues	Placenta MSCs	Human placenta [556, 557]	CD29, CD44, CD9, CD105, and CD166 [558]	CD34 and HLA-DR [558]	Hepatocytes, osteoblasts, adipocytes, insulin-producing cells, cardiomyocytes, and myoblasts [559, 560]	(i) Perinatal stem cells are acquired in a noninvasive manner. (ii) Perinatal stem cells are easily acquired from a material that was for long considered as medical waste (iii) They possess high proliferative rates (iv) Perinatal stem cells exhibit longer culture times, higher expansion, and delayed senescence and display high differentiation potential; additionally, placenta and umbilical cord provide a large number of progenitors as compared to MSCs from other sources [61, 166–170].	(i) Placental stem cell safety, contamination, tumorigenic transformation, and cellular changes following cell culture still merit further studying. (ii) Standardization of laboratory isolation protocols is still required [179].
	Umbilical cord MSCs	MSCs can be acquired from Wharton's jelly or umbilical cord blood [561].	CD29, CD44, CD73, CD90, CD105, CD106, CD117, CD133, and CD166 [562]	CD31, CD34, CD86, and HLA-DR [562]	Osteoblast, adipocytes, chondrocytes, hepatocytes, insulin-producing cells, cardiomyocytes, and neurons [563]		(i) Isolation and culture of stem cells from the umbilical cord are difficult (ii) Private banking is expensive and lacks strict regulations (iii) Lifelong storage is still unstudied [171].
	Umbilical cord blood MSCs	Cord blood is isolated prior to or immediately after delivery. It contains MSCs [561]	CD29, CD44, CD73, CD90, CD105, and CD166 [564, 565]	CD14, CD31, CD34, CD45, CD106, and HLA-DR [564, 565]	Osteoblast, adipocytes, chondrocytes, and myoblasts [566]		(i) Slow engraftment as compared to bone marrow [173]. (ii) Limited volume [176, 177] (iii) Low stem cell yield [178] (iv) Private banking is expensive and lacks strict regulations [172, 173]. (v) Lifelong storage is still unstudied [174, 175].

transduced with telomerase gene maintained proliferation and differentiation potentials in vitro [54].

The effect of aging on MSCs can also be ascribed to age-associated inflammation, as levels of inflammatory cytokines especially TNF-α tend to increase with age [55]. TNF-α at high concentrations exhibited a capacity to induce MSC apoptosis in a dose-dependent manner. Additionally, its amalgamation with IFN-γ considerably hastens this procedure, by switching the signaling of an IFN-γ-activated nonapoptotic form of TNF receptor superfamily member 6 (Fas) to a caspase-3- and caspase-8-associated proapoptotic cascade, accompanied by a reduction in intracellular NF-κB levels, apoptotic pathway activation, and culmination of cell death [56]. Excessive inflammation therefore appears to drive cellular senescence.

Conversely, other studies concurred that the aging process had an insignificant effect on ASC senescence and regenerative capacity [57, 58]. Intradonor comparison of ASCs collected from different donors and cryopreserved for 7 to 12 years with ASCs isolated from the same donor at a later time-point revealed a non-age-related decrease in the number of progenitor cells or proliferation rate. Additionally, cells from different timelines were capable of adipogenic, osteogenic, and chondrogenic differentiation, further denoting that the regenerative capacity of ASCs could be preserved with age [57]. Interestingly, human dental pulp MSCs collected from different age groups further displayed remarkable proliferative and differentiation abilities into bone, endothelial, glial, and neuronal cells during early passages in vitro and a potent regenerative capacity upon loading on scaffolds and implantation in rats' calvarial defects in vivo [59]. However, periodontal ligament-derived MSCs showed an age-related decrease in cell proliferation and adipogenic and osteogenic differentiation [60].

Thus, ASCs [57, 58] and dental pulp MSCs [59] could offer a convenient alternative to BMSCs for regenerative purposes in aging patients. Still, MSCs' banking from a younger age population and allogenic MSC transplantation could represent beneficial alternatives to overcome age-associated depletion in the number and regenerative capacity of MSCs [58, 61].

2.3. Donor's Gender and MSCs. The effect of gender on MSC regenerative abilities is still disputable. Female rats demonstrated a lower number of bone marrow progenitor cells and significantly decreased osteogenic and adipogenic potentials as compared to male rats [35]. On the contrary, BMSCs isolated from female rhesus monkeys demonstrated a higher neurogenic potential as compared to those isolated from male rhesus monkeys [27].

2.4. Donor's Systemic Diseases and MSCs. MSCs from patients with systemic diseases, including type II diabetes mellitus [28, 62], rheumatoid arthritis [29], and osteoarthritis [30], and from cows suffering from endometritis [63] have demonstrated altered cellular functions.

ASCs acquired from obese donors with type II diabetes mellitus showed a significant upregulation of their expression of the immune modulators IL-1β, IL-6, TNF-α, and MCP-1 as well as inflammatory regulators, including NLRP1, NLRP3, and caspase-1. They further demonstrated less ability to suppress T- and B-cell proliferation and were associated with diminished activation of the immunomodulatory M2 macrophage phenotype, indicating that obesity and type II diabetes are associated with a reduction in the immunosuppressive effect of ASCs [28]. Concomitantly, culturing ASCs isolated from both diabetic and nondiabetic patients at high glucose concentrations significantly decreased cellular proliferation, colony-forming abilities, and osteogenic and chondrogenic differentiation as well as additionally increased senescence, apoptosis, and adipogenic differentiation, with a more pronounced effect observed on diabetic ASCs [64]. Type II diabetes-associated alteration in MSCs was attributed to diabetic hyperglycemia, chronic systemic inflammation, increase in proinflammatory cytokines [65, 66], and accumulation of advanced glycation end products (AGEs) [66]. Accumulation of AGEs results in ROS production and increased oxidative stresses [65, 67].

Bone marrow MSCs isolated from patients with rheumatoid arthritis displayed a decreased proliferative and migration activity and a reduced ability to inhibit T-helper 17 cell polarization, responsible for maintaining chronic inflammation [29]. Similarly, those isolated from patients with osteoarthritis showed reduced proliferative, chondrogenic, and adipogenic potentials [30].

A significant improvement in cardiac functions with a significant decrease in myocardial apoptosis was detected in a coronary artery disease rat model following transplantation of MSCs isolated from patients suffering from coronary artery disease as compared to those isolated from patients suffering from coronary artery disease and diabetes [62]. Endometrial MSCs isolated from cows with endometritis showed a decrease in colony formation and adipogenic differentiation. Additionally, healthy cows' endometrial MSCs exposed to inflammatory mediator prostaglandin E2 in vitro displayed alteration in expression of 1127 genes related to cellular biological processes [63].

2.5. Inflammation and MSCs. MSCs have well-documented immunomodulatory properties. Yet, MSCs derived from chronic inflammatory environment could display different altered immunological characteristics [68]. TNF-α impact on MSCs depends upon dosage and exposure duration. Short-term TNF-α treatment has displayed a dose-dependent effect on murine MSCs in vitro. Lower doses increased osteogenic differentiation while higher doses negatively impacted MSCs and reduced osteogenic differentiation via the NF-κB signaling pathway. On contrary, long-term treatment inhibited osteogenesis at both dosage regimens [69].

MSCs isolated from human calcified aortic aneurysm with chronic inflammation displayed strong osteogenic differentiation and mineralization in addition to pathologic vasculogenesis. Short-term culturing of MSCs isolated from a healthy aorta for 24 hours with TNF-α or IL-1β enhanced their osteogenic differentiation in vitro [70]. Similarly, MSCs injected into a mouse model of collagen-induced arthritis exhibiting chronic inflammatory environment were associated with dysregulation in their immunomodulatory

function. Additionally, MSC pretreatment with TNF-α inhibited their ability to suppress T-cell proliferation in vitro, demonstrating the ability of TNF-α to inhibit MSC immunomodulation [71].

Periodontal ligament stem/progenitor cells derived from inflamed tissues displayed altered characteristics, with higher proliferation and migration tendency as compared to MSCs derived from healthy periodontal ligaments. They further displayed reduced immunomodulatory properties in addition to downregulation in osteogenesis-related genes (osteocalcin, RUNX-2, and ALP), while adipogenic differentiation was maintained [72, 73]. Coculturing of periodontal ligament stem/progenitor cells derived from inflamed tissues with peripheral blood mononuclear cells showed reduced ability to inhibit T-cell proliferation, T-helper 17 differentiation, and IL-17 secretion [74]. Treatment of human periodontal ligament stem/progenitor cells during osteogenic differentiation with high doses of TNF-α was found to be associated with downregulation in ALP, bone sialoprotein, osteocalcin, and RUNX-2 expression. The indicated inhibition of osteogenic potential denotes the negative effect of inflammatory cytokines in high concentration on osteogenic differentiation. On the other hand, BMSCs were more resistant to the inhibitory effect of TNF-α [75].

MSCs isolated from healthy buccal mucosa showed a higher proliferation rate and higher ability to suppress T-cell proliferation as compared to MSCs isolated from oral lichen planus lesions. MSCs harvested from lichen planus lesions further showed higher adipogenic tendency [76].

Stem/progenitor cells from healthy pulps showed a higher initial proliferation rate, as well as stronger adipogenic, chondrogenic, and osteogenic potentials, than stem/progenitor cells from inflamed dental pulp tissues. They also displayed higher expression of cell surface markers CD73, CD90, and CD166 in addition to HLA-G, involved in immunomodulation as well as stronger suppression of T-cell proliferation as compared to dental MSCs derived from inflamed pulp [77]. Further, T-lymphocytes cultured with MSCs derived from inflamed dental pulps secreted a higher amount of IL-2, TNF-α, and TNF-β [78].

Similarly, umbilical cord-MSCs treated with either interferon gamma (IFN-γ), TNF-α, IL-1β, IL-2, or IL-6 for 3 or 7 days presented altered phenotype and function. INF-γ, TNF-α, and IL-1β upregulated the expression of CD54, while TNF-α upregulated CD106 expression. TNF-α and IL-1β reduced the proliferation rate, while IL-6 stimulated cell migration. All inflammatory cytokines were reported to inhibit the adipogenic capacity, while chondrogenic and osteogenic differentiation capacity was enhanced by TNF-α and IL-1β coculture. Additionally, indoleamine 2,3 dioxygenase (IDO) was inhibited by TNF-α [79].

2.6. MSC Preactivation with Inflammatory Mediators. MSC preactivation (licensing or preconditioning) involves pretreatment of MSCs with inflammatory mediators including IFN-γ, IL-1β, and TNF-α to enhance their immunosuppressive properties and therefore increase immune-tolerance, following allogenic stem/progenitor cell transplantation [80–82].

BMSCs preconditioned with IFN-γ for 48 hours showed upregulated HLA-DR and IDO expression. Activation of MSCs was associated with upregulation of HLA class II and programmed death-ligand 1, which induces inhibition of T-helper cells. Activated MSCs also inhibited HLA-mismatched T-helper cell proliferation and demonstrated the ability to take up and process antigens [83]. Equine BMSCs exposed to inflammatory stimulation via preconditioning with TNF-α, IFN-γ, or inflamed synovial fluid revealed downregulated expression of migration-related genes with upregulation in adhesion-related molecules and MHC-I gene expression. TNF-α and IFN-γ were associated with dose-dependently increased expression of immunoregulatory molecules responsible for T-cell suppression, including cyclooxygenase 2, inducible nitric oxide synthase, IDO, and IL-6, in addition to upregulation of MHC-II expression [84]. Similarly, activation of ASCs with IFN-γ enhanced their ability to inhibit T-cell proliferation.

However, pretreatment with TNF-α, IL-1β, IL-17, tissue growth factor-β, or stromal cell-derived factor-1α did not show similar effect [85]. Treatment of MSCs from healthy buccal mucosa with IFN-γ was associated with the initial increase in proliferation followed by reduction in the rate of proliferation, following 12 days of IFN-γ treatment. Furthermore, IFN-γ treatment promoted MSC-mediated T-cell proliferation inhibition via IDO activity [76]. Likewise, IDO expression was upregulated upon stimulation of human periodontal ligament stem/progenitor cells by IFN-γ in vitro [86]. MSCs preactivated with IFN-γ prior to cryopreservation effectively blocked T-cell proliferation and secretion of T-helper cells promoting cytokines [87].

Preconditioning of human MSCs with IL-17 [88], IL-1α, or IL-1β [89] was also associated with a positive outcome. IL-17 effectively enhanced MSC immunomodulatory functions without increasing MHC-I or MHC-II [88]. Preconditioning of human BMSCs with IL-1α or IL-1β for 24 hours demonstrated an increase in the secretion of granulocyte colony-stimulating factor, which was not observed upon preconditioning with TNF-α or IFN-γ [89].

Thus, it can be concluded that the surrounding environment can modulate characteristics and immune-related functions of MSCs as it can either promote anti-inflammatory or proinflammatory reaction of MSCs, implicating them in the pathogenesis of multiple disorders and reducing their regenerative applications. The severity of inflammation, nature, dose, and duration of the proinflammatory cytokines govern and direct MSC reaction. Further, the differentiation capacity of MSCs under inflammatory challenge is highly influenced by the original tissue source and microenvironment of donor tissue [90–96].

3. Cell Source

Heterogeneity of cell sources is a further challenge for clinical applications of MSCs. Cell source heterogeneity is related to the donor (whether autograft or allograft) and the organ/tissue selected for MSC isolation [21].

3.1. Autogenic versus Allogenic Cell Sources. MSCs can be either acquired from the same recipient (autogenic graft) or another donor within the same species (allogenic graft) [97]. Autogenous grafting is a safe disease-free approach in MSCs' therapy [98]. However, many variables could affect autogenous cell grafting, including donors' age [25, 26], sex [27], body mass index [23, 24], and systemic autoimmune and inflammatory diseases [28–30] (discussed above), making it difficult to obtain a sufficient number of healthy MSCs without ex vivo expansion [99, 100]. The process of isolation of autogenous MSCs can further be costly and time-consuming, limiting its use in acute conditions.

Several studies endorse the utilization of allogenic MSCs instead of autogenic ones for regenerative purposes [101–103]. The low immunogenicity of MSCs encouraged the use of allogenic MSCs as they are less likely to elicit an immune reaction. MSCs are characterized by low expression of MHC-I and lack of expression of MHC-II as well as B- and T-cell stimulating antigens CD40, CD80, CD86, B7-1, and B7-2 [104–106]. Loading-induced cartilage defects in rabbits' femoral condyles with either allogenic or autogenic BMSCs were associated with an effective repair of these defects [107]. Furthermore, autogenous or allogenic ovine BMSCs loaded on scaffolds, following osteogenic differentiation and implanted in an ovine critical-size segmental defect model, showed positive results in bone regeneration, with no significant differences observed between them [108]. Similarly, positive results were attained upon allogenic MSC intra-articular injection in horses [109]. Transplantation of allogenic MSCs further showed promising results in neurogenic regeneration in a canine spinal cord injury model [110] and regeneration in a muscular dystrophy hamster model [111]. Randomized clinical trials demonstrated a potent regenerative potential of allogenic MSC administration on cardiac [101, 102, 112], hepatic [103], and cartilage [113] tissues with no adverse effects. Patients suffering from left ventricular dysfunction were randomly assigned to receive either autogenic or allogenic MSCs via transendocardial injection. Both treatments yielded equally positive outcomes with no reported undesirable side effects [101, 102]. Additionally, upon administrating bone marrow, umbilical cord, or cord blood allogenic MSCs to patients with chronic hepatic failure via intravenous infusion, clinical improvements were observed in all groups with no adverse effects [103]. Promising results were also observed in cartilage regeneration in patients with osteoarthritis [113].

In this context, commercialized allograft can provide a reproducible, readily available product with reduced cost and production time, compatible with quality standards, and good manufacturing practice (GMP), making it an efficient alternative to autogenous stem/progenitor cell therapy [99, 102]. Remestemcel-L (Prochymal) was one of the first commercial cryopreserved allogenic BMSCs used successfully for the management of graft versus host disease to be approved in Canada [114, 115]. In Japan, TEMCELL, allogenic BMSCs, was also approved for management of graft versus host disease [116]. Darvadstrocel (Alofisel), a cryopreserved allogenic ASC and the first allogenic stem cell therapy to be approved in Europe, was further used for the treatment of perianal fistulas caused by Crohn's disease [117].

However, results reported in literature regarding the impact of cryopreservation on BMSC banking are controversial. A systematic review that analyzed forty-one in vitro studies concluded that cryopreservation does not affect BMSCs' morphology and surface markers, differentiation, or proliferation potential. However, varied results exist regarding its effect on colony-forming ability, viability, attachment, migration, genomic stability, and paracrine functions. This was primarily attributed to the vast variations in the cryopreservation process and lack of standardized assays [118].

Further, it was suggested that MSCs could be immune evasive in vivo rather than being truly immune privileged as previously thought and can trigger an adverse immune response [119, 120]. Some studies demonstrated the presence of antibodies against allogenic MSCs with subsequent rejection of administered allogenic MSCs in animal models [80, 119, 121–123]. Inflammatory prestimulation of MSCs in particular could induce a negative effect, as preconditioning of MSCs was commonly associated with increased MHC expression [83, 84], stimulating an elevated antibody production, leading to subsequent adverse reactions and heightening of the immune clearance, especially following repeated allogenic stem cell transplantation. In the same context, equine BMSCs primed with proinflammatory cytokine displayed higher expression of MHC-I and MHC-II. Following intra-articular injection in the osteoarthritis equine model, allogenic primed MSCs mediated antibody production and primary humoral responses in horses with equine leukocyte antigen expression, partially compatible and incompatible with donor MSCs. Repeated MSC injection was associated with secondary humoral immune response. Although demonstrating less antibody production, these antibodies easily targeted primed MSCs because of their higher MHC expression and showed high cytotoxicity toward allogenic MSCs as compared to unprimed MSCs [124]. Thus, transplanted allogenic MSCs should be subjected to extensive characterization, and their immunogenicity should be thoroughly assessed prior to implantation.

MSC secretome was further suggested as a novel cell-free therapeutic product that recapitulates various cytokines, growth factors, extracellular matrix (ECM) proteins, and vesicles secreted by MSCs [18, 125–129]. MSC secretome might represent a clinical alternative to treat patients instantly, while overcoming the limitations and risks associated with cell-based therapy [130, 131]. Although MSC conditioned medium (CM) and extracellular vesicles have demonstrated regenerative potential in treating diseases and injuries of the nervous system, heart, lung, liver, periodontium, and soft and hard tissues [18, 132–140], several issues must be addressed before its successful clinical application, including the elimination of any xenogenic constitutions and the determination of the exact dosage, frequency of administration, protein composition, and mechanism of action [18, 131, 141].

3.2. Donor Tissue Source. As previously mentioned, MSCs have been isolated from multiple sources. Tissue of origin can highly impact MSCs' characteristics and differentiation ability [11]. BMSCs have superior osteogenic and chondrogenic potentials [142]. Yet, bone marrow harvesting is a rather invasive procedure [143], the percentage of mesenchymal progenitors in bone marrow is relatively low [144], and BMSCs have lower proliferation rate as compared to MSCs from other sources [145].

ASCs were originally described as a more convenient alternative to BMSCs [146] with less invasive isolation procedure [147], higher yield of progenitor cells [148, 149], and greater proliferation rate [145, 150]. The density and properties of ASCs depend on the location of the adipose tissues from which they were isolated [23, 151, 152]. ASCs isolated from visceral adipose tissue showed reduced proliferation and adipogenic and osteogenic differentiation as compared to ASCs isolated from subcutaneous tissues of the same donor [23]. Further, rats' cervical brown fat showed significantly higher MSCs' yield as compared to other locations [152]. Unfortunately, ASCs have a strong adipogenic differentiation tendency [153, 154], in addition to decreased proangiogenic factors and cytokine secretion as compared to BMSCs [155, 156].

Dental tissues further represent a potent source of MSCs, isolated via minimally invasive procedures [157, 158]. Dental MSCs include dental pulp stem/progenitor cells isolated from dental pulp tissues of permanent teeth, stem/progenitor cells extracted from pulp tissues of human exfoliated deciduous teeth (SHED), periodontal ligament stem/progenitor cells isolated from periodontal tissues, dental follicle stem/-progenitor cells isolated from dental follicle surrounding the third molar, alveolar bone-derived stem/progenitor cells, stem/progenitor cells isolated from apical papilla at the apices of immature permanent teeth, tooth germ progenitor cells isolated from late bell stage third molar's tooth germs, and gingival stem/progenitor cells isolated from gingival tissues [18].

Dental stem/progenitor cells especially gingival and alveolar bone proper MSCs [157, 159, 160] can be isolated during routine dental treatments [161] and possess higher proliferation rates, as compared to either BMSCs or ASCs [162, 163]. Additionally, they have high osteogenic, chondrogenic, adipogenic, neurogenic, and angiogenic potentials [161, 164]. Even though dental stem/progenitor cells provide an appealing source for tissue regeneration, some types as gingival stem/progenitor cells may be inaccessible while others as SHED, dental follicle stem/progenitor cells, stem/progenitor cells from apical papilla, and dental pulp stem/progenitor cells may be difficult to isolate in sufficient amounts [165].

Perinatal MSCs isolated from the placenta, umbilical cord, and umbilical cord blood were further suggested to offer a noninvasive alternative source to adult MSCs. They are easily acquired, possess higher proliferative rates, and exhibit longer culture times, higher expansion, delayed senescence, and high differentiation potentials. Additionally, the placenta and umbilical cord provide a large number of progenitors as compared to MSCs from other sources [61, 166–170]. Yet, the isolation and culture of MSCs from the umbilical cord are difficult [171], while private banking of the umbilical cord and umbilical cord blood is expensive [171, 172] and lacks strict regulations [171, 173]. Moreover, the effect of lifelong storage of umbilical tissue or umbilical cord blood is still unstudied [171, 174, 175]. The major problem associated with the application of umbilical cord blood remains to be the limited amount of cells extracted from each donor as cord blood volume is limited [176], where a single umbilical cord blood unit contains 50 to 200 ml of blood [177]. Umbilical cord blood yields a much lower amount of MSCs as compared to BMSCs [178]. It also has slow engraftment as compared to BMSCs [173]. Placental MSCs further carry a safety hazard regarding possibility of contamination during placenta collection and possible tumorigenic transformation [179].

4. MSCs' Isolation Procedures

MSC isolation from different tissues is one of the most critical steps prior to their ex vivo preparation, greatly impacting their quality and quantity [61]. For clinical applications, great attention should be given to the selection of the proper method of isolation [180]. Challenges facing MSC isolation are related to different factors, including the presence of various isolation protocols, the diverse MSC sources, and the fact that MSCs are usually present in very minute concentrations in their respective tissue sources [61, 150]. Although MSCs possess unique properties and have a great potential for clinical application, up to date, no exclusive set of markers exists for their identification and isolation [181]. Hence, there is currently a mandatory demand to increase the minimal criteria proposed by the International Society for Cellular Therapy in 2006 for MSC identification [9], to encompass the inclusion of paracrine factors or immunomodulatory properties of MSCs [182] as important predictors for their success during clinical application [183]. Furthermore, discovering unique markers for MSC isolation with high purity is a prerequisite for developing reliable and reproducible protocols for clinical application [184, 185].

Currently, the different categories of available techniques for MSC isolation from heterogeneous cell populations depend on their unique cellular properties, including surface charge and adhesion, cell size, density, morphology, and physiology in addition to surface markers [186]. There are various categories of cell isolation techniques, namely, enzymatic, mechanical, explant culture, and density-gradient centrifugation methods [61] (Table 2).

The enzymatic method, one of the commonly used approaches, digests the tissue especially their ECM using one, two, or in some protocols three proteolytic enzymes. The differences between the several protocols described for this method include variations in the concentrations of the used enzymes, number of washing steps, centrifugation parameters, and filtration procedures [187, 188]. The efficiency and viability of the cells acquired through the enzymatic method depend on the concentration and type of the used enzyme [189–191]. Digestion periods over five minutes can affect MSCs' surface antigens [192] and cytoskeletal

component, disrupt intramembranous particles, and change cell surface topography [193], which negatively affects the quality of the isolation process. Combining the enzymatic method with mechanical dissociation revealed a 70% increase in the cell yield as compared to the enzymatic method alone [194]. To overcome the problems associated with the enzymatic method, mechanical methods were introduced, using different forces such as shear, radiation, centrifugation, and pressure. Although great efforts were put into standardizing the mechanical methods, these nonenzymatic methods are still variable according to the used protocol [188].

The explant culture represents the earliest technique for cell isolation and in vitro cultivation. The tissue is cut into small fragments about few millimeters in size to facilitate nutrient delivery to the cells, avoiding excessive cutting, which may cause mechanical destruction to the cells. Following dry adhesion to the plastic culture dishes, cells start to migrate out of tissue fragments and adhere to the culture substrate surface. Subsequently, tissue fragments can be removed [11, 77, 90, 91, 158, 195–197]. The explant method demonstrates a more homogenous cell population, higher cell viability, and increased cell proliferation rates and avoids enzymatic damage as compared to the enzymatic method [198–200], which could be attributed to the gradual transition of cells from in vivo to in vitro condition [180, 201]. Comparison between ASCs isolated by either enzymatic or explant methods reveled a simultaneous expression of surface markers CD73, CD90, and CD105, as well as the absence of CD14, CD31, CD34, and CD45, making ASCs isolated by both techniques phenotypically and functionally equivalent [202]. However, the explant method depends primarily on the manual skills of the operator, which makes this method difficult to be standardized, in addition to the risk of contamination, which could affect the MSC clinical application [61].

The density-gradient centrifugation method depends on the physical and chemical parameters of the isolated cells like size, density, and hydrophobic properties. In this method, the cells move and accumulate in a position that matches the density of the medium or at the interphase in case of using two solutions with different densities [181]. Lack of high resolution in separating MSCs from other cells remains the most important limitation of this method as there is no absolute difference in size between cells [203]. Consequently, this method is mainly used as a primary step for MSC enrichment and is followed by the explant method or other higher resolution techniques such as fluorescence-activated cell sorting (FACS) and magnetic-activated cell sorting (MACS) [204, 205].

Cell isolation techniques based on antibody binding are widely advocated for the purification of MSCs with high resolution. Among the most commonly used antibody-mediated cell isolation techniques are FACS and MACS. Both FACS and MACS basically share the same idea. In the case of FACS, antibodies are linked to a fluorescent dye, while in MACS they are linked to magnetic beads and only the antibody bounded cells are separated [206, 207]. The greatest challenge for these methods of isolation remains however to be the lack of an exclusive marker of identifying MSCs [181]. Further limitations include the probability for cell contamination during sorting procedures, physical stresses exerted on the cells [208], and the dependence on adherent cell purification, where the use of enzymes for cell detachment can cause proteolytic damage to cell surface proteins [61]. Some of those concerns were postulated to be overcome with the development of the CliniMACS Cell Isolation System, a device that is currently clinically approved and takes advantage of conjugating colloidal suspension of superparamagnetic microbeads to a monoclonal anti-human antibody that is capable of binding to its antigen in bone marrow, umbilical cord blood products, and peripheral blood in a sterile GMP system [209].

Recently, the emergence of different isolation methods changed the typical pattern of adherent MSCs and provided another source of MSCs known as "nonadherent cell population" (NACP) [210, 211]. These NACP were obtained during medium exchange of marrow MSC culture, where the floating cells were centrifuged and replated in separate flasks. Surprisingly, these cells revealed the same proliferation and differentiation potentials as the originally attached MSCs in vitro [210]. Likewise, NACP isolated from fat resources demonstrated similar proliferation and differentiation potentials as MSCs [212]. These findings demonstrated that NACP could be a simple method to enrich MSCs' number for clinical application.

Choosing the proper MSC isolation method depends mainly on certain features that should be compared between the different available techniques, including cell purity, cell recovery rate, cell yield, and cell viability [186, 213]. Moreover, the selected technique should be minimally invasive, rapid, and with high-resolution quality [214]. Therefore, for successful clinical translation of MSCs, a well-established method for cell isolation is a mandatory step to ensure the quality of these cells.

5. Cell Culture Procedures

The first challenge following MSC isolation is that their number in the primary culture without a subsequent lengthy ex vivo expansion would usually be insufficient for an immediate clinical application. Therefore, cell expansion is essential to generate a clinically appropriate number of MSCs, keeping in mind that the efficacy and safety of clinically applied MSCs are dependent on such bioprocessing procedures [215]. Thus, optimizing culture conditions to generate MSCs that retain proliferation, differentiation, and regenerative properties is one of the greatest challenges that face MSC translation to clinical application. Currently, several cell culture variables, such as the number of passages, cell seeding density, culture surface substrate, medium formulation, and the physiochemical environment in addition to different subculture protocols, are being studied [216].

5.1. Cell Expansion. MSC expansion could be affected by the age of MSC donors, where MSCs from young donors can

Table 2: Overview of main cell isolation/purification techniques used for MSC separation.

Isolation method	Isolation principle	Isolation technique
Enzymatic [11, 188]	Digestion of the tissue extracellular components by proteolytic enzymes	(1) Use of proteolytic enzymes such as collagenase and trypsin to digest the extracellular matrix. (2) After the extracellular matrix has dissolved, the released cells are seeded into culture dishes in growth medium.
Explant culture [11, 195]	Cell surface charge and adhesion to plastic surfaces	(1) The tissue is rinsed to remove blood cells. (2) The tissue is cut into smaller pieces of no more than a few millimeters in length. (3) The pieces are placed in culture dishes or flasks with growth medium. (4) Cells start to migrate out of tissue and adhere to the culture surface, and after several days, the tissue pieces can be removed.
Density-gradient centrifugation methods [567]	Cell size and/or density	(1) The sample is positioned on one or more layers having distinct densities, which are intermediate between those of the cells that are to be isolated and all other cells in the sample. (2) After that, centrifugation of the sample at the appropriate speed fractionates it into distinct phases between the different density layers.
Fluorescence-activated cell sorting (FACS) [181, 568]	Fluorescently labeled antibodies bind to surface or intracellular molecules	(1) Cells are labeled with a mixture of fluorescently conjugated antibodies. (2) The labeled cells pass aligned one by one through a nozzle which vibrates to produce droplets containing individual cells at a defined distance from the nozzle. (3) As the cells pass through the light source, a computer registers their individual light scatter and multiple fluorescent properties to detect cells that meet the preestablished criteria for selection. (4) A mild electrical charge is used to charge the drop where wanted cells are present. When the charged droplets pass between the two electrically charged metal plates, it deflects into a different collection tube.
Magnetic-activated cell sorting (MACS) [181, 567]	Magnetically labeled antibodies bind to surface molecules	(1) Cells are labeled with antibodies conjugated to biodegradable iron-based nanobeads. (2) The labeled cells pass through a strong magnetic field. (3) Cells conjugated with magnetic particles stay on the column, while nonconjugated cells pass though.

undergo a higher number of population doublings in comparison to older MSCs before reaching replicative senescence [217] (discussed above). Due to this phenomenon, during the first two to three weeks of early passages, MSCs grow at a constant rate, while with the increasing number of passages, an increase in the cell doubling time until the growth stops due to senescence is observed [218]. This "replicative senescence" is caused by progressive shortening of telomere upon cell passaging in vitro due to the absence of telomerase activity [54, 219]. Despite the fact that 70–80% confluence is the recommended cellular density before passage, the decision is operator-dependent [61]. It was found that upon prolonging the MSC expansion for 43-77 days, cells demonstrated senescence features, including abnormality in morphology, arrested proliferation, decreased expression of cell surface markers, loss of differentiation capacity [220], and decrease in their capacity for migration [221]. Furthermore, prolonged cultivation of MSCs may cause chromosomal changes, which could predispose for malignant transformation [222]. It has been reported that upon comparing human umbilical cord-MSCs at passages 3, 6, and 15, the cells showed similar morphology, biomarker expression, and cytokine secretion. At passage 15, despite the fact that the cells were still potent regarding adipogenic differentiation and cytokine secretion such as IL-6 and VEGF, they revealed inferior cell proliferation ability and less osteogenic and chondrogenic differentiation potentials. Moreover, human umbilical cord-MSCs at passage 15 revealed impaired hematologic supporting effect in vitro and declined therapeutic potential on a GVHD in vivo [223].

To overcome cellular senescence, MSCs could be genetically modified by a retroviral vector containing the gene for the catalytic subunit of human telomerase reverse transcriptase (TERT). Transduced cells (MSCs-TERT) demonstrated telomerase activity, with the ability to undergo more than 260 population doublings, in contrast to nontransduced control cells, which underwent senescence-associated proliferation arrest after 26 population doublings [54]. Upon subcutaneous implantation in immunodeficient mice, MSCs-TERT formed more bone as compared to their controls. However, in a further study, MSCs-TERT showed loss of contact inhibition and anchorage independence and lead to tumor formation in all mice [224]. Therefore, although considering intermittent activation of the TERT gene may

be an interesting approach, it may be linked to dangers related to tumorigenicity.

On the other hand, telomerase activation was found to influence the MSC regulatory path, where ectopic expression of the TERT gene in human postnatal BMSCs sustained their osteogenic potential and upon xenogenic transplantation formed more bone tissue with a normal structure as compared to the control human postnatal BMSCs [225]. This enhancement was attributed to the high expression of early preosteogenic stem cell marker STRO-1, which revealed that telomerase expression assists in maintaining the osteogenic potential of MSCs during their expansion.

Moreover, the differentiation potential of an immortal adipose stromal cell line (ATSC) transduced with a retroviral vector expressing TERT was assessed in vitro [226]. ATSC-TERT cells significantly accumulated calcium one week after being cultured in osteogenic induction medium, while control ATSC cells began to accumulate it after three to four weeks. Additionally, the expression of osteoblastic markers (osteoblast-specific factor 2, chondroitin sulfate proteoglycan 4, and TNF receptor superfamily) was increased in ATSC-TERT cells as compared to control ATSC. The insulin-like growth factor (IGF) signaling pathway especially, IGF-induced AKT phosphorylation, and ALP activity were postulated to be involved in the mechanisms through which the TERT gene enhances osteoblastic differentiation [227].

Another important factor to consider during MSC expansion is the prior usage of proteolytic enzymes for cell detachment during the expansion process. Proteomic results revealed differential expression of 36 proteins in trypsin-treated cells and an upregulation of the expression of proteins related to apoptosis, with downregulation of proteins related to cell growth, cell adhesion, regulation of metabolism, and mitochondria electron transport [228]. Three-dimensional (3D) culture systems may be the solution to overcome all the limitations associated with MSC expansion, as it could allow their propagation without the use of proteolytic enzymes [229]. Consequently, great attention should be given to 3D culture systems to standardize their effect on MSCs.

5.2. Cell Seeding Density. Cell seeding density impacts cell proliferation, differentiation, and ECM formation [230–232]. BMSCs seeded at lower density (100 cells/cm^2) possessed a faster proliferation rate than those seeded at higher density (5000 cells/cm^2) [233]. Moreover, high cell seeding density of (10^6 cells/cm^2) caused a minimal increase in the cell number in comparison to lower seeding density on 3D scaffolds [234]. The low growth rate of MSCs seeded at high densities could be attributed to contact inhibition, while a higher growth rate associated with low seeding density could be attributed to the presence of the small and agranular cells (recycling stem cells) in the log phase. Those cells are postulated to give rise to large numbers of cells during the log phase of exponential growth [235]. The log and exponential phases last for longer duration in cells seeded at low density, and therefore, more population doublings occur [236]. Unfortunately, there is a limitation of low initial seeding density as it has been reported that BMSCs platted at 10-100 cells/cm^2 did not expand effectively and the cells were senesced after four to five passages [237]. Although low seeding densities revealed higher proliferation rates, it is unrealistic for large-scale clinical MSC production as the needed number of culture flasks exceeds the manageable limit of practical handling and cost-effectiveness [238].

The cell seeding density affects the stemness gene expression and senescence of MSCs, where lower density seeding (200 cells/cm^2) of ASCs caused upregulation of stemness genes Oct4, Nanog, SRY-box 2, KLF4, c-Myc, and lin-28 homolog A, especially Nanog and c-Myc in comparison to high-density seeding (5000 cells/cm^2) [239]. Moreover, it was reported that the optimal cell growth of BMSCs could be achieved at a plating density of 200 cells/cm^2, with no differences observable in their differentiation potential at different densities (20, 200, and 2000 cells/cm^2) up to 5 passages [236]. It was further demonstrated that high cellular seeding density (5×10^6 cells/ml) of BMSCs on collagen microspheres favored chondrogenic differentiation [240]. Comparing dental pulp MSCs cultured under sparse (5×10^3 cells/cm^2) and dense (1×10^5 cells/cm^2) seeding conditions for four days revealed observable enhancement in mineralized nodule formation in densely plated dental pulp MSCs [241]. In addition, densely plated dental pulp MSCs demonstrated more pronounced mineralized tissue formation in comparison to sparsely plated dental pulp MSCs when implanted into mouse bone cavities [241].

These findings suggest that cell seeding density could favor the differentiation of MSCs toward specific cell lineages. Determining the optimum cell seeding density designed for maximum cell expansion is therefore of great significance for clinical application, as it could shorten the cell culture time and consequently decrease the risk of culture contamination and alteration in the MSC characteristics [242].

5.3. Culture Media. Choosing a well-formulated culture medium for expansion and therapeutic application of MSCs is very crucial [243]. A typical culture medium is composed of amino acids, vitamins, glucose, inorganic salts, and serum [244]. Culture media can affect MSCs' secretion profile. Studies deduced that cytokine and growth factor secretion is donor-specific [125] and that cellular passaging does not significantly influence MSCs' secretome properties [18, 245], while other investigations demonstrated that the cell culture medium might affect the MSC secretory potential to varying degrees [246, 247].

Among the commonly used basal medium formulations for culturing of human MSCs are Dulbecco's modified Eagle's medium (DMEM) and alpha minimal essential medium (α-MEM). Although DMEM was widely used for MSC expansion [248–252], later it was demonstrated that α-MEM could show better performance in isolation, expansion [253], and osteogenic induction of MSCs [233] as primary dental pulp MSCs [241]. MSC differentiation into various cell types could be achieved by adding certain substrates to the culture media. Osteogenic differentiation could be mediated by β-glycerophosphate and ascorbate phosphate; adipogenic differentiation could be induced by

isobutyl-methylxanthine and indomethacin, while chondrogenic medium usually contains transforming growth factor-β (TGFβ1) and ascorbic acid [254, 255]. Neural differentiation was achieved in media supplemented with both epidermal growth factor (EGF) and fibroblast growth factor- (FGF-) 2 [256, 257], while hepatic differentiation occurred in media supplemented with hepatocyte growth factor (HGF), bFGF, and oncostatin [255].

Basal media do not contain proteins or growth-promoting agents and therefore require supplementation with fetal bovine serum (FBS), typically 10% to 20% [61]. FBS is the most excessively used serum in cellular culture procedures, as it provides important elements such as nutrients, hormones, growth factors, and carrier proteins. These carrier proteins encompass hormones, vitamins, attachment and spreading factors, lipids, metals, protease inhibitors, and buffering agents, whose cumulative function is to back up cellular growth [258]. A number of successful clinical trials were conducted utilizing MSCs expanded in FBS-containing media [259, 260].

Yet, the usage of animal-derived serum is not the best choice for clinical applications, due to the risk of the possible transmission of nonhuman infectious pathogens such as viruses, prions, mycoplasma, and endotoxins [261–270]. Furthermore, the high content of xenogenic antigens in FBS could elicit an immune response in recipients following MSC transplantation [268, 269, 271, 272]. Moreover, lack of uniformity in the composition of serum between different companies and the high degree of lot-to-lot variation in terms of growth factor concentrations [263, 273] contribute to the heterogeneity of the results following MSC transplantation [273, 274]. Thus, before utilization, regular testing could be needed in order to ensure the quality of each batch, an additional obstacle that hinders the fabrication of an MSC-based standardized product [216].

The presence of serum in media may interfere with the purification and expansion of cell culture products since it could contain growth-inhibiting factors as fetuin (γ globulin) and growth-promoting factors that occasionally could inhibit cell growth depending on their concentration and the stimulus-response decisions made by the stem/progenitor cells [275]. These growth factors include but not limited to platelet-derived growth factor (PDGF), IGF, and EGF [276] in addition to TGFβ, which regulates the actions of many other signaling molecules. TGFβ was documented to inhibit the growth of mouse keratinocytes [277], while EGF was reported to inhibit human epidermoid carcinoma cells [278]. The diversity of these factors might lead to clinical complication and data misinterpretation [244] (effects of different growth factors are discussed later in MSCs and Growth Factors).

In order to consider MSCs as an advanced therapy medicinal product, serum-free media have been proposed to attain large-scale quality and relatively low-cost production of clinical-grade MSCs [279, 280]. These medium formulations incorporated defined quantities of binding proteins (i.e., albumin and transferrin), additional nutrients (i.e., lipids, vitamins, and amino acids), physiochemical reagent (i.e., buffer), hormones (i.e., insulin), growth factors (i.e., EGF, PDGF, and FGF), and attachment factors [281, 282], which are all usually provided by the serum. The optimization of defined serum-free medium for a specific cell type is very difficult and influenced by multiple variables regarding cell characteristics, FDA-approved serum-free/-xeno-free culture media as an example for such substitutes [283–286].

An ideal FBS alternative for clinical GMP production should possess a well-defined composition, a reduced degree of contaminants, no risk of xenogenic compound transmission, low production costs, easy availability, and no ethical issues [250]. Using autologous or allogenic serum, plasma, or platelet lysates was further proposed for cultivating and expanding human MSCs [280, 287], although it may be difficult to attain sufficient amounts from these substrates. Moreover, their beneficial effect may decrease with age, becoming nonapplicable in elderly patients [61]. Furthermore, autologous or allogenic serum may not contain sufficient growth factors to support the growth of MSCs [258].

Human platelet lysate (hPL), prepared by lysis of the platelet membrane, was found to meet most of these requirements and was suggested as a natural reservoir of growth factors and cytokines such as basic FGF, EGF, HGF, IGF-1, PDGF, TGFβ1, and vascular endothelial growth factor (VEGF) [259, 288], which conjointly have a positive influence on MSC proliferation and differentiation [289]. Despite this growth factor-enriched milieu, it has been reported that MSCs cultured with hPL did not express differentiation markers and differentiation only occurred upon induction [290], in contrast to media supplemented with serum, where unplanned differentiation might occur [279]. hPL can be easily obtained from autologous peripheral blood in large quantities and with minimal donor site morbidity [291]. hPL has been successfully utilized for MSC expansion in numerous in vitro studies [170, 292–300] overcoming most of the challenges associated with FBS. The composition variability, which is donor-related, may be reduced by pooling harvests of fresh blood from different donors [297, 301]. Despite its rare occurrence, the possible transmission of human diseases caused by viruses, as HIV-1 and HIV-2 or hepatitis C, can be hindered through sterilization processes employing short-wave ultraviolet light [302]. Several studies have been published evaluating the use of hPL or other xeno-free supplements for MSC ex vivo expansion, following GMP protocols [303–306]. The substitution of FBS by hPL has been reported to increase cell proliferation without affecting MSC immunophenotype, immunomodulatory potential, differentiation potential, and relative telomere length [306]. Similar results were attained when comparing two serum-free (xeno-free) media (α-MEM and DMEM) supplemented with 10% of hPL with DMEM supplemented with 20% FBS and 10 ng/ml bFGF. The highest proliferation rate was detected in α-MEM supplemented with 10% hPL [307]. It has been reported that hPL and predefined serum-free media increased the proliferation of BMSCs and ASCs [249, 285, 296]. Human umbilical cord-MSCs expanded in serum-free media propagated more slowly and were different in growth rate, telomerase, and gene expression profile from human umbilical cord-MSCs

expanded in serum-containing media, yet they remained their multipotency and their therapeutic potentials [308]. On the other hand, umbilical cord-MSC expanded in hPL revealed enhanced proangiogenic and bone formation features, upon implantation combined with collagen microbeads in an immune-competent mouse model [309].

The high proliferation rate attained by hPL can reduce the MSC manufacturing time and accelerate the production of MSCs in therapeutic application. The effect of hPL on the immunomodulatory attributes of MSCs remains controversial and needs to be further evaluated, as some researchers claimed that hPL-expanded MSCs exhibited diminished immunosuppressive properties [292, 310], while others reported that hPL maintain these immunosuppressive properties [250, 311]. These discrepancies could be attributed to the differences in the hPL production assay.

In order to identify the effect of culture "micromilieu" on the critical stemness properties that could influence MSC clinical performance, dental pulp MSCs and alveolar BMSCs were cultured in two commercially available serum/xeno-free GMP culture systems (StemPro (Life Technologies); StemMacs (Miltenyi Biotek)), in comparison to conventional FBS supplemented media. Prolonged expansion of both MSC types especially in the serum/-xeno-free-expanded BMSCs resulted in downregulation of CD146, CD105, Stro-1, SSEA-1, and SSEA-4, as well as in an increase of SA-gal-positive cells, cell size, and granularity and a decrease in telomere length. Moreover, expansion under serum/xeno-free systems caused an upregulation of osteogenic markers and elimination of chondrogenic and adipogenic markers while only minor changes were detected with serum-based media. Dental pulp MSCs in serum-based and StemPro revealed a diminishing mineralization potential with passaging, while with StemMacs, the opposite occurred [312].

The development of a completely defined media that lack any biological products from animals is the ultimate goal in cell-based therapy. Although serum-free media containing growth factors are postulated to maintain the main phenotypic and functional characteristics of MSCs, they are currently still inferior to FBS-containing media. hPL, which to date meets the GMP guidelines, could provide hope in this perspective.

5.4. Two-Dimensional (2D) Culture Systems. Conventionally, MSCs are propagated as a monolayer in two-dimensional (2D) plastic culture plates. 2D culture techniques have been developed for establishing primary cultures, cell lines, and different analytical assays [313]. In addition, 2D cultures are used for MSC differentiation into many specialized cells [314, 315].

However, the 2D culture system possesses several limitations. The first limitation of the 2D culture system is the need for cell expansion to increase the cell numbers for clinical applications. Expansion in 2D cultures is highly inefficient and yields heterogeneous populations of MSCs [316]. Moreover, 2D culture systems cause changes in cell shape [317], flattening of cells with alteration of the internal cytoskeleton and the shape of the nucleus [318], which could subsequently affect the gene expression [319, 320] and change the cell fate as well as the differentiation potential [254, 321, 322]. Within the 2D culture system, MSCs tend to undergo nonspecific differentiation where MSCs may partially differentiate or dedifferentiate with loss of functionality [316]. Besides, 2D culture conditions fail to mimic the living physiology or the in vivo MSC niche [323]. The 3D microenvironment is responsible for determining MSC fate in vivo, where it allows interactions between MSCs, ECM, and gradients of oxygen, nutrients, and byproducts [324]. In order to overcome all of these limitations, 3D culture systems have been developed to mimic the ECM composition and stiffness in vitro to control MSCs' fate [318, 324–326].

5.5. Three-Dimensional (3D) Culture Systems. In order to imitate the in vivo MSCs' niches, maintain the MSCs in their undifferentiated stem/progenitor cellular status, induce their differentiation into particular tissue for regenerative purposes, or expand them for industrial usage; various 3D culture systems have been proposed and developed. 3D culture systems vary from simple cellular aggregates (spheroids) to complex systems using dynamic bioreactors with incorporated biomaterials (Figure 1).

The spheroids allow cell-cell and cell-ECM interactions without any additional substrates [327]. These spheroids could be prepared by different techniques, including hanging drop, rotating culture, or low-adhesion culture plates in suspension culture and microwells. Human amnion mesenchymal stem cells (hAMSCs) were cultured in 2 ml of culture medium (5×10^5 cells/ml) in a suspended state in a 6-well ultralow attachment plate to allow spheroid formation. The viability, multipotency, and the secretory ability for angiogenic and immunosuppressive factors were upregulated in hAMSC spheroids kept in the 3D culture system as compared to those maintained in 2D cultures. Moreover, an improved paracrine effect was recorded in vitro in the form of an increased capillary maturation as well as greater inhibition of peripheral blood mononuclear cell proliferation in the presence of 3D conditioned media as compared to both 2D conditioned media and 2D exosomes [328].

Static culture plates (culture dishes, T-shaped flasks) that are ordinarily used in 2D cultures can be modified to be dynamic to allow spheroid formation. A scaffold-free 3D culture sphere was attained upon seeding periosteum-derived progenitor cells on nonadhesive culture dishes and cultivating them at a rotation rate of 60 rpm using an orbital shaker. The resultant spheres maintained their viability and proliferation ability. Expression levels of stemness genes and proteins were upregulated in cells grown on 3D culture as compared to 2D culture systems [329]. Being heterogeneous in nature, spheroids are employed in studying cell differentiation and cancer biology [327, 330]. Upon short-term culturing, spheroids improved the medicinal properties of MSCs [331], while in long-term spheroids, culturing MSCs underwent differentiation [332].

An upregulated expression of chondrogenic genes (ACAN, COL2B, COL10, SOX9, and 18S) was recorded upon in vitro 3D culturing of equine MSCs for 4 weeks in alginate, fibrin 0.3% alginate (FA), and pellet culture systems

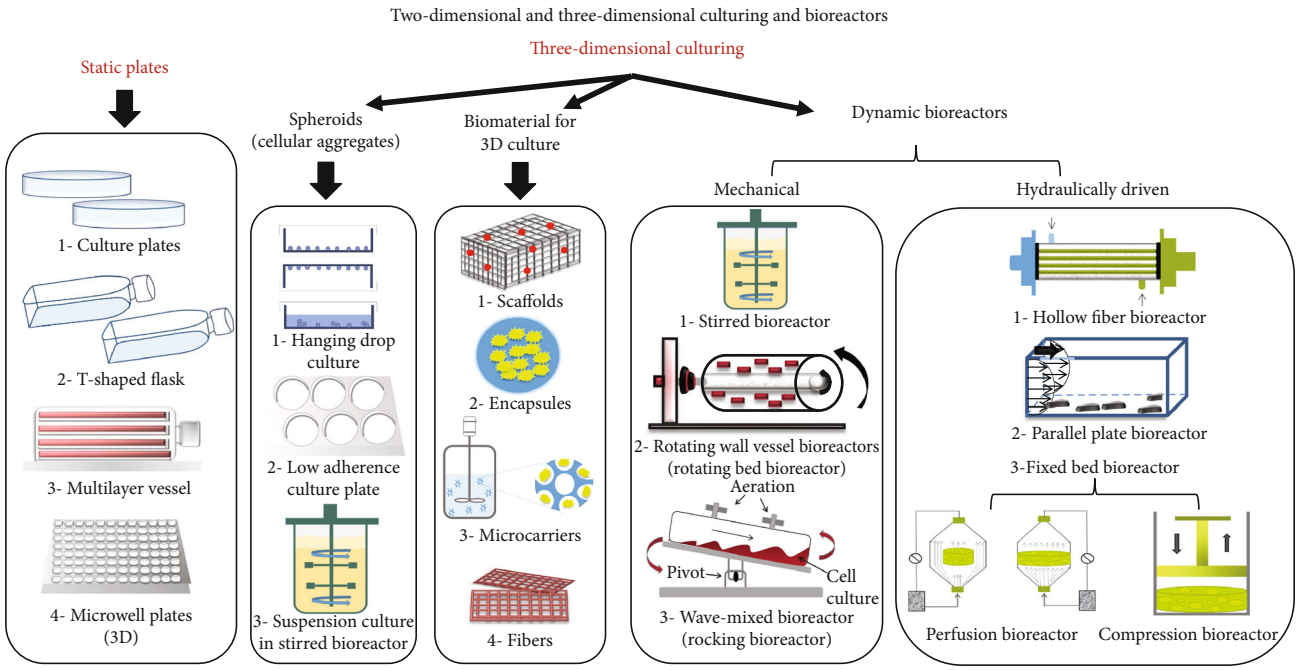

Figure 1: Two-dimensional and three-dimensional culturing plates and bioreactors.

(2.5×10^5 cells and 5×10^5 cells) [333]. Furthermore, the immunomodulatory characteristics of MSCs cultured in 3D culture systems constructed using collagen, chitosan, and PLGA substrates were shown to be enhanced and affected by the 3D geometry not the type of the substrate. MSCs under 3D culture demonstrated a higher growth rate and stemness and maintained their phenotype and an enhanced immunosuppression effect [334].

Yet, the wide-range growth of MSCs using these methods is challenging due to the incapability of controlling their size, leading to cell death and suppression of cell propagation as a result of a high degree of confluence and nutrient deprivation [331]. Moreover, transport and removal of nutrients and waste metabolites, respectively, from the scaffold upon 3D expansion represent a crucial obstacle. The latter process occurs in the 2D culture systems simply by diffusion [335]. While static bioreactors are limited by the demand for batch medium changes, dynamic bioreactors can be highly governable, permitting better homogenous media and cell spatial distribution, despite the increase of the scaffold. Thus, dynamic bioreactors can be utilized in tissue-engineering applications to alleviate problems related to traditional static culture conditions [336].

Incorporation of natural and synthetic biomaterials in the culture could supply diverse biological signals and allow different degrees of mechanical strength [337]. Biomaterials are utilized in the 3D culturing for fabrication of microcarriers, capsules, fibers, and scaffolds. Scaffold constructs provide the ECM 3D organization and multicellular complexity [338, 339]. Yet, natural biomaterials are more difficult to control in vitro as they often transduce uncontrollable biological signals to the cells. Moreover, the batch-to-batch variability and the potential xenogenic origin might limit their usage [340].

Dynamic bioreactor culture systems, in which the culture variables such as pH, temperature, oxygen, and carbon dioxide concentration are properly controlled and monitored, are essential for in vitro cultivation and maturation of tissue-engineering grafts [341]. These closed systems maintain a homogeneous physicochemical environment required for culturing cells and reduce the handling steps, hence reducing contamination potential in accordance with GMP and quality standards [342]. The generated hydrodynamic stress on the cells could be alleviated through utilizing biomaterials in the form of microcapsules or microcarriers [316]. Microcarriers are small beads (100–300 μm diameter) that provide a surface for the cells to attach and grow while microcapsules are semipermeable membranes within which the cells are immobilized. Microcapsules allow the diffusion of nutrients, oxygen, and growth factors essential for cellular growth [316]. The selection of an appropriate biomaterial for the fabrication of either microcapsules or microcarriers as well as harvesting cells from them is among the challenges in the 3D cultures.

A rotary cell culture system (RCCS) combined with 3D culture was suggested to provide an effective means for enhanced MSCs' proliferation in vitro and to maintain a differentiation potential required for tissue engineering. The microarray analysis of BMSCs cultured in the RCCS-3D system revealed an enhanced proliferation and colony formation, as well as maintained the differentiation potential when compared with conventional static 2D and static 3D culture conditions [343].

Dynamic bioreactors (fully reviewed in articles [341, 344, 345]) could be classified into mechanically driven bioreactors that include stirred tank bioreactors, rocking bioreactors, and rotating wall vessel bioreactor, as well as hydraulically driven

bioreactors, which include parallel plate bioreactors, hollow fiber bioreactors, and fixed-bed bioreactors that can be modified to perfusion and compression bioreactors widely used in bone tissue engineering (reviewed in articles [341, 346]).

Spinner flasks and stirred tank bioreactors are the most frequently used stirred systems. In these systems, impellers are used to promote mixing, resulting in a homogeneous culture system with operation versatility (batch, fed-batch, and perfusion). A large number of cells could be produced in just one vessel, thereby avoiding vessel-to-vessel variability and minimizing costs related to labor and consumables [280]. MSCs aggregated using static microwell plates prior to being inoculated in the bioreactor environment preformed controlled size aggregates possessing the ability to form large, irregular super aggregates after a few days of suspension culture. On the contrary, single MSCs inoculated directly into suspension bioreactors formed a more uniform population of smaller aggregates after a definite culture period of eight days. Both techniques showed initial deposition of ECM within the aggregates [347].

A rocking (wave) bioreactor consists of a disposable plastic bag placed on a platform whose agitated fluid motion induces the formation of waves that subsequently provide good nutrient distribution and excellent oxygen transfer with moderate shear stress. It also presents a minimum risk of contamination (closed system), scalability (up to 500 l), and flexibility [344]. No difference in differentiation and immunomodulatory capacity as well as no genetic aberrations was displayed upon culturing MSCs in flasks, Scinus bioreactor (rocking bioreactor), and spinner flasks. MSCs cultured within the Scinus bioreactor system showed equality to flask-expanded cells with respect to their immunomodulatory properties [348].

A hollow fiber bioreactor is advantageous in culturing MSCs due to its relatively homogeneous culture environment and low shear stress. The cells are inoculated within the fiber, while the culture medium flows and wastes diffuse through the pores of the fibers to the space between the cylinder and the fibers [344]. The secretory products (exosomes) of MSCs cultured using hollow fiber and their therapeutic efficacy in a murine model of cisplatin-induced acute kidney injury (AKI) in vivo and in vitro have been investigated. In vivo, both 2D- and 3D-exosomes significantly alleviated cisplatin-induced murine AKI evidenced by improved renal function, attenuated pathological changes of renal tubules, reduced inflammatory factors, and repressed T-cell and macrophage infiltration; however, the 3D-exosomes were superior to the 2D-exosomes. Furthermore, 3D-exosomes were efficiently captured by tubular epithelial cells, thereby improving their viability and inducing an upregulated anti-inflammatory effect in vitro [349].

The rotating wall vessel (RWV) and a rotating bed bioreactor (RBB) consist of a cylindrical vessel rotating horizontally around its axis. This environment eliminates most of the disruptive shear forces associated with a conventional bioreactor, randomizing the gravitational forces acting on the cell surface and allowing the combined culture of several cell/scaffold constructs [341, 350]. Collision of scaffolds with the bioreactor wall is a major disadvantage of the RWV system and may damage the scaffolds and disrupt the seeded cells. This can be alleviated by using the RBB concept, where constructs are attached directly on the axis. Another crucial disadvantage of this rotating system is that the mineralization is confined to the outer part of the scaffold upon use in bone tissue engineering and that the internal nutrient transport is deficient [346]. Thus, rotating wall vessels are limited to the small-sized constructs of flat bones or as bone patches for restorative applications of the skeletal system [351].

In bone tissue engineering using MSCs, shear stress caused by mixing or perfusion of the medium is crucial for osteogenesis, as it exposes the cells to mechanical stimulation. In vivo, mechanical stimulation increases the production of prostaglandins, ALP, and collagen type I, creating a milieu required for osteoblastic proliferation and mineralization [352]. Moreover, mechanical stimulation encourages the cells to produce ECM in a shorter time period in vitro and in a more homogeneous manner than in static culture [353].

A fixed-bed bioreactor consists of a column (bed) holding an immobilized scaffold, where the cells are incorporated. As the cells remain immobilized on the carrier surface, this system has an advantage of presenting a low shear stress environment. Although this bioreactor allows 3D cell growth and better imitation to in vivo conditions, spatial cell concentration gradients may occur [354]. Modifying the fixed-bed bioreactor has been performed to overcome the poor perfusion of media through the center of the scaffold. Bioreactors that use a pump system to perfuse media directly through a scaffold are known as perfusion bioreactors [355]. Flow perfusion bioreactors have been shown to provide more homogeneous cell distribution throughout the scaffolds and provide a uniform mixing of the media, enabling better control of the environment and better physical stimulation of the cells particularly in the bone tissue [335, 356]. The major challenges in these systems are the design of the perfusion chamber and optimization of the flow rate, which depends on the composition, porosity, and geometry of the scaffold [335]. Despite the fact that the increase in the flow rate leads to an increase in the deposition of the mineralized matrix, it seems that the optimal flow rate values have an enhanced positive effect on osteoblastic differentiation, ECM deposition, and distribution range from 0.2 to 1 ml/min [335]. Yet, perfusion bioreactor is suggested to be the ideal ex vivo culturing system for growing large bone grafts [357].

Compression bioreactors that provide mechanical loading, combined with flow perfusion, can also promote survival and functional cellular differentiation within the scaffold. Short-term mechanical stimulation enhanced the expression of several osteogenic genes, including RUNX-2, osteopontin, integrin-β1, TGFβR1, SMAD5, annexin-V, and PDGFα [351]. The compression bioreactors provide a promising tool for bone fracture tissue engineering [341].

Overall from the previous section, it could be deduced that although the 3D culturing maintained or even improved the therapeutic potential of the MSCs, the complexity and the diversity of these systems in terms of selecting the appropriate biomaterial to be used and bioreactor design make them additional challenges in cell-based therapy.

5.6. Mimicking the Biological Interactions in the Human Body. Mimicking the in vivo microenvironment to attain efficient proliferation and secretion of soluble paracrine factors and extracellular vesicles could be further achieved by hypoxia (2% O_2) that enhances stemness in MSCs, without affecting their multipotent differentiation potential [358]. Hypoxic preconditioning (2% O_2) of adipose-derived MSCs upregulated the proliferative ability of MSCs by enhancing the expression of normal cellular prion protein and inhibited oxidative stress-induced apoptosis via inactivation of cleaved caspase-3 in vitro. Similar results were attained upon treating a murine hindlimb ischemia model with hypoxic adipose-derived MSCs. Enhanced functional recovery of the ischemic tissue, including limb salvage, neovascularization, and the ratio of blood flow perfusion, was reported [359]. Moreover, BMSC hypoxic pretreatment enhanced significantly cell survival and promoted angiogenesis in the lower limb of ischemic diabetic rats through increasing autophagy and significantly decreasing apoptosis [360]. Additionally, hypoxic conditions increased the release of MSC exosomes that effectively enhanced the regeneration of cardiac tissues in a myocardial infarction mouse model [361].

Coculturing of MSCs with other cells could provide a promising aspect in regenerative medicine, through providing the signaling molecules, including growth factors and cytokines involved in the cross-talk between cells. In a recent study using hybrid human umbilical vein endothelial cell/rat MSC cocultures, the role of each cell type on the genes and proteins regulating angiogenesis, including VEGF, PDGF, and TGFβ, was investigated. It has been reported that MSCs inhibited the expression of angiogenic factors in endothelial cells early in cocultures due to juxtacrine signaling-mediated suppression of cell proliferation, while later on, a shift occurred, where the restrained action of MSCs reverts to a stimulatory one by paracrine signaling. The ratio 3 : 1 endothelial cells/MSCs induced the strongest upregulation of the angiogenesis pathway [362]. Additionally, provision of inflammatory milieu responsible for certain diseases was demonstrated to induce the cells to secrete regenerative factors. Intravenous infusion of human MSCs improved the cardiac function and decreased scarring in a mouse model of myocardial infarction. In the presence of a high level of inflammatory cytokines, human MSCs secreted excessive amounts of anti-inflammatory cytokine TNF-α-stimulated gene/protein 6 (TSG-6) that enhanced tissue regeneration [363]. Despite the fact that coculturing and direct cell-cell contact between MSCs and endothelial progenitor cells induced MSC differentiation toward a pericyte-like phenotype [44], it was demonstrated that intravenous administration of MSCs inhibited angiogenesis and endothelial cell proliferation, induced by cell-cell contact through modulation of the VE-Cadherin/β-catenin signaling pathways [364].

6. MSCs and Growth Factors

Growth factors are molecules that cause several biological effects, such as changes in motility, proliferation, morphogenesis, and survival of the cell [15, 365]. Various growth factors affect MSC properties (Table 3).

In mammals, three isotypes of TGFβ are present: TGFβ1, TGFβ2, and TGFβ3 [366]. The three isotypes are well-known inducer of MSC chondrogenesis that lead to proteoglycan and collagen type II deposition when applied as single factors [367, 368]. TGFβ influences the proliferation and chondrogenic differentiation of MSCs [368–372]. TGFβ plays a role through all phases of chondrogenesis, promoting mesenchymal condensation, chondrocyte proliferation, and ECM deposition and inhibiting terminal differentiation [373–375]. Moreover, TGFβ1 has been reported to switch the human MSC fate from adipogenic to osteogenic when added under adipogenic culture differentiation conditions [376]. On the other hand, TGFβ1 decreased the number of osteoprogenitor cells during the in vitro expansion of human BMSCs and downregulated ALP and STRO-1 expression [377]. These results suggest that TGFβ1 effect could depend on the commitment state of the MSCs.

Bone morphogenetic proteins (BMPs) that belong to the TGFβ superfamily play an essential role in regulating MSCs' proliferation and lineage-specific differentiation [378, 379]. BMP2, BMP4, BMP6, BMP7, and BMP9 induce osteoblastic differentiation of MSCs [380, 381]. MSCs exposed to these osteogenic BMPs increased the expression of ALP, osteocalcin as well as osteopontin, connective tissue growth factor, inhibitor of DNA binding, and Cbfa1/RUNX-2 [380–386]. BMP9 is considered as one of the most potent BMPs to induce MSC osteogenic differentiation [387–389]. Even though BMP2, BMP4, BMP6, BMP7, and BMP9 revealed the ability to induce adipogenic differentiation of MSCs [382], BMP2 [390], BMP4 [391], and BMP6 [392] promoted chondrogenesis only when applied in combination with TGFβ. Although BMP3 stimulated MSC proliferation, it did not promote their adipogenic differentiation [393].

VEGF is known as a potent angiogenic factor that has been reported to increase prosurvival factors, phosphorylated-Akt, and Bcl-xL expression besides enhancing MSC proliferation in vitro [394]. Furthermore, VEGF favors MSC osteoblastic differentiation at the expense of adipogenic differentiation through regulating RUNX-2 and PPARγ2 [395]. Additionally, in the presence of VEGF-A, MSCs differentiated into endothelial cells both in vitro and in vivo [396, 397]. Intracellular blockage of VEGF signaling by retroviral transduction of human MSCs to express a decoy soluble VEGF receptor-2 that sequesters endogenous VEGF in vivo resulted in spontaneous chondrogenic differentiation. Implanting transduced MSCs seeded on collagen sponges subcutaneously in nude mice activated TGFβ signaling by blocking of angiogenesis and generation of a hypoxic environment that led to hyaline cartilage formation [398]. VEGF coinjection with BMSCs into a myocardial infarction heart mouse model led to increased cell engraftment and improvement of cardiac function as compared to injection of BMSCs or VEGF alone [394]. The proangiogenic effects of intramyocardial injection of FGF2 (bFGF) as well as intramyocardial and intravenous VEGF in a porcine model of chronic hibernating myocardium were further evaluated. The myocardial blood flow increased significantly only by the intramyocardial injection, which could be attributed to the diffusion of the factors from the point of injection and their ability to

Table 3: Various growth factors and their effects on MSCs.

Growth factor family	Growth factor	Effect on MSC
TGFβ	TGFβ1	Increase proliferation & induce chondrogenic differentiation [369, 370].
	TGFβ2	Induce chondrogenic differentiation [368, 372].
	TGFβ3	Induce chondrogenic differentiation [371, 372].
	BMP2	Promote chondrogenesis [390], induce osteogenic differentiation [380–382], & induced adipogenic differentiation [382].
	BMP3	Stimulate proliferation [393].
	BMP4	Promote chondrogenesis [391], induce osteogenic differentiation [380–382], & induced adipogenic differentiation [382].
	BMP6	Promote chondrogenesis [392], induce osteogenic differentiation [380–382], & induced adipogenic differentiation [382].
	BMP7	Induce osteogenic differentiation [380–382] & induced adipogenic differentiation [382].
	BMP9	Induce osteogenic differentiation [380–382] & induced adipogenic differentiation [382].
VDGF	VDGF	Increase proliferation [394], favor osteogenic differentiation [395], differentiate into endothelial cells [396, 397], & induce chondrogenic differentiation [398].
FGF	FGF2	Increases migration [400], increases proliferation [401, 402], induces neuronal differentiation [403], and stimulates chondrogenic differentiation [404, 405], adipogenic differentiation [406], & osteogenic differentiation [407–409].
	FGF4	Increase proliferation [401, 402].
PDGF	PDGF-AA	Increases migration & osteogenic differentiation [415].
	PDGF-BB	Protect against apoptosis and senescence [416].

initiate the migration of cells [399]. FGF2 increased the migratory activity of MSCs through activation of the Akt/-protein kinase B pathway [400]. These results were confirmed by analyzing the orientation of the cytoskeleton, where actin filaments acquired a parallelized pattern that was strongly correlated with the FGF2 gradient. Remarkably, FGF2 influence was confined not only to attracting MSCs but also in routing them as it has been revealed that low concentrations of FGF2 led to MSC attraction, while higher concentrations resulted in repulsion.

The FGF family includes members that affect MSC proliferation as well as differentiation where FGF2 and FGF4 increased proliferation potentials of BMSCs [401, 402]. FGF2 induced neuronal differentiation of human dental pulp MSCs [403] and stimulated chondrogenic differentiation of human MSCs [404, 405] and adipogenic differentiation of rat MSCs [406]. FGF2 promoted osteogenic differentiation of MSCs by inducing osteocalcin gene expression and enhancing calcium deposition [407, 408]. Additionally, a low dose of FGF2 enhanced the in vitro osteogenic differentiation of MSCs induced by BMP6 as well as bone formation in vivo [409]. However, there are contradictions in the literature about the exact role of FGF on MSCs. FGF2 was reported to inhibit mouse MSC differentiation by upregulation of Twist2 and Spry4 and the suppression of extracellular signal-regulated kinase 1/2 activation [410]. Moreover, FGF1 and FGF2 inhibited adipogenic and osteogenic differentiation of human BMSCs [411, 412]. FGF2 was also reported to inhibit osteogenic differentiation of mouse BMSCs at the early stage, promoted it in the medium phase, and maintained it in the later stage during osteogenic induction [413].

PDGFs are known to enhance cell proliferation and migration. There are four types of PDGFs (AA, BB, CC, and DD) [414]. PDGF-AA was reported to promote MSC migration and osteogenic differentiation [415]. PDGF-BB protected MSCs derived from immune thrombocytopenia patients against apoptosis and senescence, where PDGF-BB decreased p53 and p21 expression, while increasing the surviving markers' expression [416]. The combination of PDGF-BB, FGF-2, and TGFβ1 led to synergistic enhancement of human MSC propagation with retained phenotypic, differentiation, and colony-forming unit potential [417].

Collectively, growth factors offer a promising approach to enhance MSC proliferation, differentiation, survival, and expansion. Choosing the proper growth factor is governed by three major criteria. First is the ability of the growth factor/s to prolong the proliferation in order to generate a sufficient number of MSC differentiation into the desired cell type. Second is the ability to replace the animal serum or xenographic substances. Finally is utilizing the properly localized and controlled method for delivering growth factors in vivo to take the benefit of their sustained release without inducing MSC uncontrolled proliferation and subsequent tumor formation [365]. Although using a single growth factor has advantages in increasing MSC proliferation, differentiation, and migration, combined growth factor treatment could provide more benefits due to possible synergistic effects on MSCs.

7. Risk of Tumorigenicity (Figure 2)

Every medical therapy carries some risk to the patients, and a careful weighing of the probable risks against the provided benefits should be carried out. Although the risk of tumorigenicity is far less with adult cells, with little evidence of tumor formation [418], it should never be neglected.

Stem/progenitor cells and cancer cells share some features suggesting a link between these two populations of cells, including long life spans, relative apoptotic resistance, and an ability to replicate for extended periods of time. Moreover, both share the same growth regulators and cell maintenance control mechanisms [419]. Stem/progenitor cell trafficking pathways seem to be further utilized by cancer cells for metastasis [420]. Stromal cell-derived factor-(SDF-) 1 impinges cancer cell behavior and migration and at the same time plays a role in stem/progenitor cell homing [421–423]. Also, CXCR2 and 4 receptors found on both stem/progenitor and cancer cells can influence both stem/-progenitor cells' homing and cancer cells' invasion/metastases [419]. In addition, cancer and stem/progenitor cells have an inherent ability to evade host immune recognition [424]. Therefore, the malignant transformation of MSCs used in cell-based therapy might take place in the following circumstances: first during in vitro expansion of MSCs and second during genetic manipulation of MSCs.

7.1. In Vitro Malignant Transformation. In vitro expansion and culture of MSCs prior to cell administration may result in changes in their characteristics due to intracellular and extracellular influences. Harmful mutations during cell division as well as failure to correct these alterations may occur, causing tumorigenic transformation [425]. Some studies suggested that the tumorigenicity of MSCs increases proportionally with the length of in vitro culturing duration [426]. MSCs from different animals such as rat [427–429], rabbit [430], and cynomolgus [431] undergo spontaneous transformation during long-term in vitro culture. Moreover, these spontaneously transformed MSCs were found to be highly tumorigenic when inserted into immunodeficient mice [432, 433]. Spontaneous malignant transformation of mouse neural precursor cells was detected following ten in vitro passages, producing tumors in rodent brains [434].

An investigation studied the characteristics of the transformed MSCs (tMSCs) obtained from long-term culturing of rat MSCs. They revealed that tMSCs maintained typical MSC surface markers. Meanwhile, they exhibited a high proliferation rate with very limited senescence, lost contact inhibition property and mesodermal lineage potency, and subsequently acquired the ability for anchorage-independent growth [435]. The authors attributed the results to the increased levels of mutant p53 in the tMSCs that led to a significant upregulated expression of survivin, the main factor for the unlimited proliferation of transformed MSCs, and undetectable expression levels of the key senescence regulator p16 [435]. Moreover, silencing of the key regulator genes for cellular senescence such as p21 [436] and p16 [437], in addition to unscheduled epigenetic alterations, may be further key reasons for the cell to initiate this transformation [428].

Furthermore, long-term culture (exceeding five weeks) of human bone marrow- and liver-derived MSCs was evaluated for transformed cells. Four out of 46 batches had transformed cells that were able to induce sarcoma-like tumors in immunodeficient mice. High-resolution genome-wide DNA array and short tandem repeat profiling excluded the possibility of cell line contamination. Fortunately, the authors identified a gene expression signature using gene and microRNA expression arrays that may help to screen cultures for signs of early malignant transformation events. These genes include CKMT1A that was elevated over 10,000-fold and miR-182 and miR-378 that were upregulated nearly 500- and 100-fold, respectively, in transformed MSCs [438].

In contrast, several articles verified the absence of tumorigenic potential of cultured MSCs originating from different tissues even at advanced in vitro culture times [439–441]. Human MSCs from bone marrow, chorionic villi, and amniotic fluid were found to be nonprone to malignant transformation, following extensive in vitro expansion [442]. Moreover, human umbilical cord-MSCs were not susceptible to spontaneous malignant transformation during long-term in vitro culturing. Human umbilical cord-MSCs exhibited positive expression of human telomerase reverse transcriptase and did not exhibit shortening of the relative telomere length. Nevertheless, malignant transformation could still be prompted by chemical carcinogens as 3-MCA [443].

A systematic review that enrolled seven studies comprising 593 patients, 334 treated with MSCs and 259 as a control group without treatment, reported safe cell infusion with no oncogenesis in the follow-up period of 10 to 60 months [444]. Another systematic review reported no association between MSC implantation and tumor formation. The reported malignancies occurring in patients following implantation was related to ongoing or previous ones with no de novo formation [445]. On the other hand, evidence of tumor formation was noticed four years following fetal neural stem cell transplantation into the brain and the fluid surrounding it of a boy with ataxia-telangiectasia. By genetic typing, it was demonstrated that the tumor cells were of donor origin [446]. Similarly, eight-year postintraspinal olfactory mucosal cell autoimplantation for treating spinal cord injury, a young patient developed a spinal cord tumor mass autograft-derived. Seemingly, autologous treatment strategies could be more hazardous contradicting the expectation to be less immunogenic and more long-lasting than allogenic ones [447].

The in vitro potential tumorigenicity of MSCs could be related to genomic instability, accumulation of DNA damage, and loss of cell cycle regulation during long-term culture. The absence of transformation potential must be demonstrated before clinical use. Therefore, it is beneficial to decide during preclinical development whether the manufacturing process leads to chromosomal abnormalities using various assessment techniques for genetic stability [448].

7.2. MSC Malignant Transformation due to Genetic Modification. Genetic modification is the process of modifying or inserting new genetic materials (transgene) into specific cells to generate a therapeutic effect by correcting an

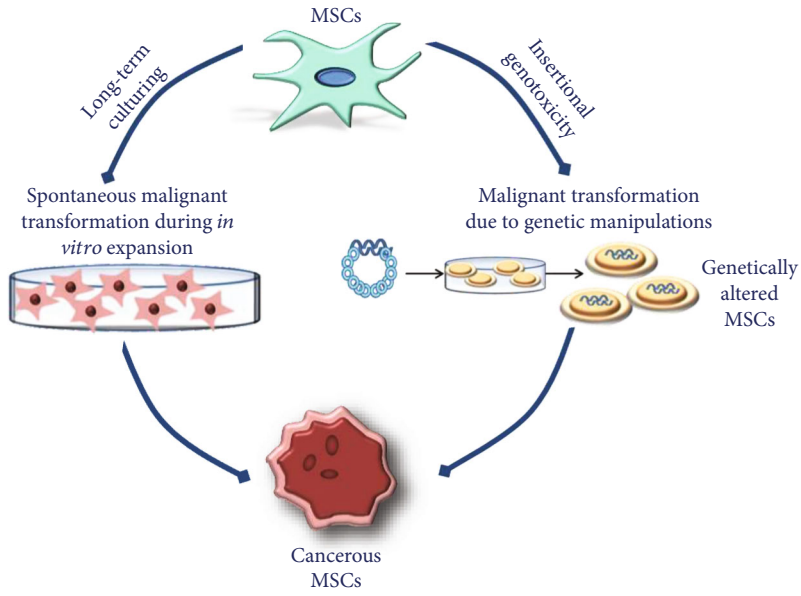

Figure 2: Direct involvement of mesenchymal stem cells in cancer through malignant transformation.

existing abnormality or providing the cells with a new function into a cell [449].

MSCs can be genetically modified by viral and nonviral methods. These techniques have been proven to be a very significant advancement in treating various diseases such as neurological, blood, vascular, and musculoskeletal disorders and cancer (reviewed in [450]). Nonviral vectors comprise physical and chemical methods of gene transfer that can deliver more transgenes than viral methods and possess less stimulating effect on the immune system; however, their main drawback is the low transfection efficiency and transient gene expression [451, 452].

Viral vectors include retrovirus, adenovirus, adeno-associated virus, and lentivirus [453]. Viral vector genomes are modified by deleting some areas of their genomes so that their replication becomes deranged; therefore, they are considered to be safer. Yet, there are some limitations, including their confined transgenic capacity size and their marked immunogenicity that can prompt the inflammatory system causing degeneration of transduced tissue and insertional mutagenesis [454, 455]. "Insertional genotoxicity" is a key factor that should be considered when choosing a vector type and design for cell therapy. Insertions may cause dominant gain-of-function mutations (such as activation of protooncogenes flanking an insertion site) mediated by either enhancer and/or promoter elements in the vector or by aberrant splicing from the vector transcript. This is favored by the genetic structure of the retroviruses and the frequently used transfection agents. Since the experiments that monitored the insertional mutagenesis are often performed in rodents with relatively short life spans, the true mutagenic risk cannot be determined on the basis of vector choice and the total integration load in the transplanted cells alone; therefore, the true risk remains ill-defined. Primate animal models that are able to tolerate a larger number of transplanted MSCs and with longer life spans where transient transfections could be proposed [456] were used.

Yet, it should be clearly noted that any therapy involving genetic manipulations may result in MSC malignant transformation through either tumorigenic transformation of the transgene or disruption of the MSC's genome by the inserted transgenes, causing MSC subsequent transformation [457]. Stricter control and safety measures are required in the production of MSCs for cell-based therapy, taking into consideration that MSCs can further turn malignant as a result of long-term culture and due to genetic manipulation. Governing the cell handling procedures in order to minimize the risk of malignant transformation is ultimately needed. Unfortunately, studying cancer development is a long process and requires a long follow-up of treated patients to verify safety in this context.

8. Cell Delivery

8.1. Delivery Route. Among the challenges that hinder the clinical translation of stem/progenitor cell-based therapies is the uncertainty in the therapeutic efficacy of MSCs. This could be attributed to the paradoxical results obtained from both animal studies and clinical trials, showing controversial effectiveness, partly due to the method of MSC delivery [61, 458].

In general, cells could be introduced locally or systemically into the tissues. The optimal delivery method depends mainly on two factors, namely, whether the targeted disease is local or systemic [61] and the mechanism of action of the used cells [458]. Whether or not MSC optimal performance is achieved when present at the target site of injury/inflammation is hereby an important question. If MSCs should exert their function mainly through secretion of cytokines and growth factors in the circulation, i.e., having paracrine and autocrine effects or through regulating the local immune response [459–461], the presence of MSCs in the target site would not be necessary and systemic effects could be

achieved using a cell reservoir [61]. But if the presence of MSCs at the target site is mandatory, for example, by differentiating into replacement cells [462], or through the local production of angiogenic or antiapoptotic factors [459], then the delivery route must place the cells at the target site or facilitate their migration to the site of interest [61].

Tissue defects are preferably treated with either local injection, for example, intramuscular, intramyocardial, or injection at the injury site of the spinal cord [463], or implantation of cell-loaded scaffolds [464]. Local cell delivery is currently the most promising in tissue-engineering applications, where cell-loaded scaffolds are locally transplanted at the target site. The use of 3D synthetic or natural scaffold biomaterials was shown to protect the cells from the aggressive in vivo environment, protect against substantial cell loss following systemic delivery due to the pulmonary "first-pass" effect, enhance MSC homing [61, 465], and promote functional integration and regeneration of the damaged tissues [466]. The local delivery of MSCs, applied in conjunction with or without biomaterials, has shown vast therapeutic efficacy in musculoskeletal regeneration for repair of osteochondrogenic diseases/disorders, including rheumatoid arthritis, osteoporosis, osteogenesis imperfecta, osteoarthritis, nonunion bone fracture, and craniosynostosis in preclinical and some clinical settings [464, 467]. In addition, direct surgical intramyocardial injection of MSCs and catheter-based transendocardial injection have been investigated in preclinical and clinical studies for the treatment of cardiovascular diseases, showing promising efficacy and safety [468–474], through allowing for higher cell retention rates and providing a targeted delivery route without requiring the availability of chemotactic factors [475]. Although local MSC delivery may be desirable and promising in specific applications, the need for certain procedures and/or surgery could be associated with some risks [476].

Systemic delivery of MSCs is adopted when the target disease is systemic or the need to regenerate several damaged tissues is present. Intravascular injection benefits form wider distribution of cells throughout the body and are being minimally invasive. Systemic delivery is divided based on the vascular route into intravenous (IV) or intra-arterial (IA).

The most commonly investigated method for delivering MSCs is the IV route [458]. Significant entrapment of the IV-delivered cells in the lungs results in a significant reduction in the numbers of cells reaching the organ of interest due to pulmonary "first-pass" effect [477, 478]. MSCs have an estimated diameter of 20–30 μm [477, 479], and experiments with microspheres have demonstrated that most particles of this size are filtered out by the lungs [477]. Yet, the number of entrapped cells in the lungs could be decreased with the administration of a vasodilator [478, 479]. Aside from the effect of cell size, adhesion to the pulmonary vascular endothelium may also contribute to pulmonary cell trapping as was evident from IV delivery of MSCs in a rat model [477]. Thus, lung entrapment may explain the low engraftment of IV-delivered cells in clinical trials [458, 480].

IA delivery of MSCs in animals enhanced the engraftment of injected cells through bypassing the pulmonary entrapment [481–483]. In a rat model of transient ischemic stroke, IA injection of allogenic MSCs into the internal carotid artery showed the ability of the IA-transplanted cells to migrate into the ischemic brain, resulting in improved neurological function and reduction of the infarct volumes [484]. In addition, IA delivery of MSCs reduced the expression of calcineurin (CaN), a serine/threonine phosphatase which mediates neuronal homeostasis, after ischemic stroke in a rat model. CaN hyperactivation following ischemic stroke triggers apoptotic signaling. Thus, significant improvement in functional activity and normalized oxidative parameters were evident in rats receiving IA MSC treatment as compared to the stroke group [485]. Renal IA delivery of MSCs in a porcine renal ischemia-reperfusion model resulted in MSC distribution throughout the kidney, mostly in the renal cortex, particularly inside glomeruli, thus limiting off-target delivery. In addition, MSC viability in the kidney eight hours following IA infusion ranged between 70% and 80%, which could permit more efficient interaction with injured tissue and enhanced regenerative effect [486]. In a clinical trial investigating subjects with subacute spinal cord injury, IA delivery (via the vertebralis artery) of BMSCs resulted in greater functional improvement as compared to the IV route [487]. However, a careful balance between achieving high cellular engraftment without compromising blood flow due to arterial occlusion is mandatory [482].

In the treatment of cardiovascular diseases, intracoronary infusion of stem/progenitor cells is a relatively less complex technique. Still, the possibility of myocardial necrosis resulting from microvascular obstruction by the infused cells greatly questions the safety of this route [474]. A meta-analysis investigated the efficacy of four different routes of MSC delivery in acute myocardial infarction in swine and in clinical trials. The investigated routes of delivery included transendocardial injection, intramyocardial injection, IV infusion, and intracoronary infusion. Results showed the superiority of the transendocardial injection route due to both reduction in infarct size and improvement in left ventricular ejection fraction in preclinical and clinical trials [488].

Other routes of administrations are available for specific therapeutic applications [476]. Notably, the intranasal delivery route is proposed as an efficient and noninvasive route to the brain and for systemic administration to the central nervous system, demonstrating enhanced cellular retention and several improved neurological/psychiatric outcomes [489]. The intranasal delivery route depends on the ability of cells to bypass the cribriform plate through various routes, such as the olfactory bulb or the cerebrospinal fluid [490]. A study demonstrated that MSCs administrated via the intranasal route have the ability to migrate toward the injured cortex in a mouse model of traumatic brain injury. The authors employed superparamagnetic iron oxide tagged with a fluorescein isothiocyanate fluorophore as a noninvasive magnetic resonance imaging probe for MSC labeling and tracking [491]. In a rat model of Parkinson's disease, intranasal delivery of MSCs resulted in the appearance of cells in the olfactory bulb, cortex, hippocampus, striatum, cerebellum, brainstem, and spinal cord [492]. However, more experimental studies on the safety and efficacy of the intranasal delivery route of MSCs are needed; as to date, only few animal studies and no clinical studies are available.

A recently developed "cell spray" method [493] was investigated as a novel delivery method for transplantation of allogenic human ASCs in the porcine myocardial infarction model. This new cell delivery method was reported to be safe, feasible, and effective and resulted in successful transplantation of ASCs forming a graft-like gel film covering the infarct myocardium, significantly improving cardiac function [493].

8.2. Dose. Administration of an optimal cell dose is an important requirement to obtain therapeutic efficacy of MSCs' transplantation [466, 475, 494]. The determination of the pharmacologically optimally effective dose range is a critical issue for clinical translation of stem/progenitor cell-based therapies. Challenges in defining an optimal cell dose for specific therapeutic applications are related to the large variabilities in MSC clinical trials, including different disease categories, study design, target tissue/organs, types of MSCs used, manufacturing protocols, routes of delivery, and dosing employed [495, 496]. Thus, standardization of study design is mandatory to allow for better evaluation and correlation of results among similar clinical trials [496]. The variability in the optimal dosing identified by the various trials is primarily affected by the different routes of delivery employed. IV injection is the most commonly used and investigated method for delivering MSCs to the blood, being the least invasive method. As discussed earlier, due to entrapment of most injected MSCs in the lungs (pulmonary first-pass effect), IV has the highest average MSC dose, compared to cell doses employed with other routes of delivery. IA injection allows MSCs to bypass the pulmonary entrapment; thus, clinical trials employing this route have significantly lower average doses in a narrower range than IV. However, IA is used in a smaller number of trials as it is more invasive than IV. Consequently, local routes of delivery which locate the cells in a target site require lower average cell doses than the wider cell distribution in the body and faster wash-out following IV injection [497].

It is assumed that the number of administered cells should vary proportionally with the observed clinical efficacy. However, the data that had arisen from preclinical studies and clinical trials on the stem/progenitor cell dosage has yielded contradictory results [474, 475]. Recently, multiple dosing of stem/progenitor cells has been demonstrated to be more effective than the administration of a single large dose [498–500]. These studies show that the full benefits of stem/progenitor cell-based therapies could be underestimated or unnoticed if they are measured after a single dose. These results suggest that although the optimal cell dose remains indefinable, multiple dosing of stem/progenitor cells may provide therapeutic superiority in cardiac repair [475, 498]. This could be explained by the fact that a single large dose initially presents a high number of cells but soon gets "washed out," while multiple dosing could offer a more durable cell persistence and paracrine signal for tissue repair, by replacing the cells that die after transplantation. Yet, repeated dosing using invasive delivery routes such as intramyocardial and intracoronary injections is considered unsafe. In such situation, a systemic route of delivery such as IV administration should be proposed [501].

8.3. Homing and Functional Integration. A major concern in systemic delivery of MSCs is that cells may become entrapped within organs that filter the blood (first-pass effect), for example, the liver, lungs, and spleen. To avoid this, several strategies to minimize lung entrapment (as discussed before) and to improve the homing of systemically introduced cells are employed [466]. Although there are numerous reports of stem/progenitor cells homing to injured tissue, the exact mechanism is not yet clear. Among the proposed factors were defective vascular architectures found in tumors [502] or leaky vasculature in injured tissues due to the effect of histamine and other inflammatory mediators [503], resulting in passive entrapment in the interstitial space; other biochemical and biomechanical factors could also be involved.

Homing of MSCs depends primarily on the chemokine receptor, C-X-C chemokine receptor type 4 (CXCR4), and its binding partner SDF-1, also known as C-X-C motif chemokine 12 (CXCL12) [481]. SDF-1 chemokine is released by the injured tissue and interacts with the chemokine receptors (CXCR4 and CXCR7) leading to the migration of MSCs to the injured tissue [481, 504]. Several other cytokines and growth factors, including IL-1 to IL-6, PDGF, VEGF, and BMP, are secreted by platelets, inflammatory cells, and macrophages arriving at the site of injury which could promote migration of MSCs [505]. Additionally, the released inflammatory cytokines TGFβ1, IL-1β, and TNF-α in injured/inflamed tissue enhance migration by upregulation of matrix metalloproteases (MMPs) that cleave gelatin, laminin, and type IV collagen, constituting the basement membrane of blood vessels, promoting transendothelial migration of MSCs [481, 506].

Biomechanical factors could also contribute to MSC homing [507]. Intermittent hydrostatic pressure was shown to promote the migration of MSCs in vitro, which could be attributed to the increased concentration of SDF-1 released from MSCs in culture medium with increased hydrostatic pressure [507]. Mechanogrowth factor (MGF), an isoform of IGF-1, is further generated by cells in response to mechanical stimulation and plays a key role in regulating MSC function, including proliferation and migration [508]. Culturing of rat MSCs with MGF increased cell migration in a concentration-dependent manner by altering the mechanical properties of MSCs and activating the extracellular signal-regulated kinase (ERK) 1/2 signaling pathway in vitro. MGF-induced MSCs' migration increased the phosphorylation level of ERK 1/2, cell traction force, cell stiffness, and cell fluidization as compared with the control (without MGF). The activation of the ERK 1/2 signaling pathway and remodeling of the cytoskeletal structure to regulate rat MSC mechanics suggest the potential biomechanical and biological role of MGF in inducing MSC migration [508].

Migration of BMSCs is also affected by several chemical and mechanical factors [509]. Mechanical factors include hemodynamic forces applied to the walls of the blood vessel, in the forms of cyclic mechanical strain and blood shear stress, through focal adhesion kinase (FAK) and ERK 1/2 signals, SDF-1α/CXCR4, and c-Jun N-terminal kinase (JNK) and p38 mitogen-activated protein kinase (MAPK) pathways.

Also, the elastic modulus (stiffness) of the ECM transmits complex biophysical signals that exert an important role in modulating MSC behavior, including promoting cell migration. The microgravity environment encountered during spaceflight was also shown to affect MSC migration, where simulated microgravity inhibited the migration of BMSCs via reorganizing or decreasing the expression of F-actin, increasing cell stiffness, and reducing SDF-1α [509].

Yet, any endogenous homing mechanism is insufficient, with less than 1% of delivered cells found in target tissues [458, 510]. Improving homing of the exogenous MSCs would greatly improve the functional integration of the cells into the target tissues [510]. Several different strategies for improving exogenous cell homing to the target site have been investigated (reviewed in [458, 510]). In brief, the different strategies can be divided into two main categories: (1) methods that increase the ability of stem/progenitor cells to respond to the chemotactic, homing, and migratory stimuli and (2) methods for modifying the target sites to enhance chemotaxis of stem/progenitor cells [510].

Stem/progenitor cell-based strategies include genetic modifications, priming of cells with growth factors and cytokines, cell preconditioning with hypoxia, treatment with certain chemical compounds that can trigger signaling pathways, and coating of the cell surface with double affinity antibodies or with homing ligands by streptavidin linkers and glycoengineering. Although different strategies have been introduced to increase the ability of stem/progenitor cells to respond to migratory stimuli, ex vivo expansion and manipulation may alter cell properties, such as proliferative capacity, differentiation potential, and genetic stability of cells, negatively affecting their safety at the clinical level. Thus, some prefer to modify the target sites, through designing more attractive environments to enhance stem cell recruitment. Target tissue-based strategies include direct transfection of target tissue with chemokine encoding genes, direct injection of chemokines or injection of ectopic chemokine expressing cells, the use of scaffolds as delivery vehicles, and application of electrical fields [510].

As discussed earlier, MSCs enhance tissue repair mainly through differentiating into replacement cells and/or paracrine effects [511], depending on therapeutic purposes of the transplanted stem/progenitor cells they could be introduced to act locally or systemically. For MSCs to achieve their intended therapeutic effect at the target site, functional engraftment of transplanted stem/progenitor cells is a prerequisite for achieving efficient regeneration via MSC differentiation to replace the damaged host cells. Even if cell therapy is used to provide paracrine factors or exosomes locally to support tissue repair or activate endogenous regeneration, initial engraftment of the transplanted cells to the target organ is necessary [512]. For the cells to integrate/engraft into the target tissue, cells need to adhere to the ECM of the tissues through the SDF-1/CXCR4 axis, failure of such interaction might trigger cell apoptosis in anchorage-dependent cells due to loss of contact with ECM, a process termed anoikis [504].

The limited functional integration of either autologous or allogenic stem/progenitor cell-based therapies remains a major clinical challenge. Following tissue injury, as in the case of myocardial infarction or cerebral stroke, the transplanted cells must replace billons of host dead cells to restore organ function, although the number of cells that actually home to and survive in the target organ is considerably low (as discussed before) [512]. In addition, cell survival into ischemic environment or inflamed tissue is quite low, due to lack of adequate oxygenation and the presence of inflammatory cytokine and ROS production after hypoxia and reoxygenation. Genetic engineering of MSCs with antiapoptotic and prosurvival factors such as the kinase Pim-1 was shown to enhance the repair of damaged myocardium in infarcted hearts [513].

Even in cases of physical engraftment of transplanted MSCs in injured tissues, successful functional integration, such as integration of transplanted cardiomyocytes with the host myocardium to allow a synchronized beating of the heart, is uncommon. Transplantation of more immature cells in a progenitor state might enable better in vivo functional integration [512]; however, transplantation of more immature stem cells caries the risk of tumorigenicity that could impair their therapeutic safety. That risk is lower if they are differentiated before transplantation, but differentiation results in increased immune recognition marker expression, triggering unwanted immune response. Thus, a balance between tumorigenicity and immunogenicity must be achieved [514].

Collectively, for more efficient and predictable outcomes of the transplanted MSCs, several important factors have to be taken in consideration. Choosing the optimal delivery route for each specific application, while carefully evaluating the merits and demerits of each delivery method, is recommended, based on the intended mechanism of action of the transplanted cells and the characteristics of the target organ/-tissue. The recommendations of the optimal cell dose for each therapeutic application and delivery route are still not available, yet multiple dosing is suggested to offer enhanced and more predictable therapeutic effect through providing a prolonged cell persistence and paracrine signal for tissue repair. Adapting novel strategies to enhance the homing of exogenous MSCs are greatly needed to improve the functional integration of the cells into the target tissues, as any endogenous homing mechanism is insufficient for efficient integration of the transplanted cells. In addition, integrated personalized therapeutic approaches aimed at engineering the transplanted cells, to be more resistant to harsh environments and to enhance their survival and integration, might be necessary. Modification of the target site, for example, by rejuvenation of the vasculature and transplanting stem/progenitor cells together with bioactive factors and cytokines with/without biomaterials or mural cells, could aid in creation of a healthy paracrine environment, enhancing the functionality of transplanted cells [512].

9. Application of Biomaterials

As discussed above, the use of biomaterial-based 3D scaffolds for local delivery of MSCs could represent a promising and effective approach for modifying the target tissue and protecting the cells against the harsh environment in the diseased/injured tissues, enhancing cellular retention and functional integration. In addition, biomaterials can serve as carriers for bioactive molecules and growth factors that boost the regenerative capacity of MSCs such as VEGF, bFGF, HGF, IGF-1,

and TGFβ [465]. The optimal combinations of stem/progenitor cells and biomaterials that best suite each tissue and clinical therapeutic situation are still not clear. Significant efforts are being made to optimize compatible biomaterials with each stem/progenitor cell type for specific therapeutic applications [515].

In ischemic heart diseases, the natural architecture, vascularity, and metabolism of normal cardiac tissues are lost. Thus, cardiac tissue engineering, through engineering stem/-progenitor cells on scaffolds, has been the ultimate purpose for cardiac repair [475, 516]. Hydrogels and/or bioactive agents are suggested to act as injectable delivery vehicles for MSCs to enhance the survival, retention, and efficacy of these cells in the injured myocardium. In addition, 3D patch-based systems are being widely investigated for myocardial repair to improve the therapeutic efficacy of stem/progenitor cell transplantation, while avoiding the risk associated with needle injection [465]. In a murine model of myocardial infarction, the application of BMSC-loaded poly(ε-caprolactone) (PCL)/gelatin cardiac patch supported the repair of the infarcted myocardium and enhanced the cardiac function. The MSC-loaded PCL/gelatin patch promoted the regeneration and angiogenesis of the injured myocardium, which may be attributed to the protection of the cells against the harsh hypoxic environment. In addition to the paracrine effect offered by the transplanted MSCs, the cytokines released enhanced the activation of the epicardium and recruited the endogenous c-kit$^+$ cells [517]. A study [518] investigated the proangiogenic potential of cytokine-conjugated collagen patches seeded with human MSCs in a rat model of myocardial infarction. The investigated patches allowed prolonged cytokine release in the target site, together with enhancing cell infiltration and promoting functional neovessel formation, thus preserving cardiac function in the rat model.

There are many challenges facing the preparation of synthetic scaffolds that could mimic the natural cell microenvironment, which has directed the research interest toward utilizing naturally derived ECM itself, obtained through the process of decellularization [519]. Decellularized tissue scaffolds attract great interest in bone tissue engineering due to its natural 3D porous architecture and natural biochemical component arrangement, providing osteoinductive properties [520, 521]. However, the clinical translation of decellularized scaffolds is hindered by the challenge to balance between the optimal decellularization methods, to maintain the structural proteins that should have a positive impact on cell functions, while removing resident cells and genetic material that could cause an immunogenic response [519, 521].

Hence, the use of biomaterials could offer great benefits in enhancing the therapeutic outcomes, through supporting the cell integration and function aside from protecting them from the harsh in vivo environments of the injured/diseased tissues.

10. Effect of Antimicrobials, Local Anesthetics, and Other Drugs on MSC Properties

Different drugs and chemicals administrated, although being needed for specific therapeutic or prophylactic effects, could exert adverse effects or alter the properties of the transplanted MSCs, thus compromising/altering the effectiveness of MSC-based therapies.

10.1. Effect of Antimicrobials. The effect of several antimicrobial drugs, including antibiotics, antifungals, antivirals, antimalarials, natural peptides, and Chinese traditional drug extracts, on the differentiation potential of BMSCs has been reviewed in the literature [522]. Antibiotics or antimicrobials are commonly used to supplement culture media to avoid any bacterial contamination of the cell culture [523]. Isolation and cultivation of ASCs or oral MSCs usually involve the presence of the penicillin-streptomycin mixture [524]. Gentamycin is also commonly used. The use of amphotericin B is also suggested due to its widespread antifungal activity, but due to its cytotoxic effect on human cells, less toxic forms of the amphotericin B are currently available including a complex of amphotericin B with copper (II) ions (AmB-Cu2$^+$) [525]. Unfortunately, antibiotics in a cell culture may change the regenerative potential and other biologic properties in many types of cells; for instance, penicillin-streptomycin mixture and gentamycin negatively affected the growth rate and target mRNA expression level of differentiating embryonic stem cells [526]. A study [527] investigated the effects of a penicillin-streptomycin mixture, amphotericin B, AmB-Cu^{2+}, and their combinations on the proliferation and differentiation of ASCs in vitro. Data showed the effect of the investigated antibiotics on modulating the differentiation process, which is influenced by the duration of exposure and the combination of antibiotics employed [527].

Various antimicrobial drugs, although having a crucial role in the treatment of bone and joint infections and in prevention of postoperative infections, could exert specific effects on BMSC properties, specifically their differentiation potential. Cefazolin, a first-generation cephalosporin commonly used in arthroplasty to prevent infection, showed an irreversible negative effect on human BMSC migration and proliferation, in a time- and dose-dependent manner [528]. Rifampicin is a potent antibiotic commonly used in combination with ciprofloxacin in controlling orthopedic infections. High rifampicin concentrations, particularly higher than 16 mg/ml, exerted inhibitory effects on the in vitro proliferation and osteogenic differentiation of BMSCs [529].

10.2. Effect of Local Anesthetics. Intra-articular administration of amide-type local anesthetics is routinely performed during arthroscopic joint surgery to alleviate pain. In orthopedic cartilage repair operations, the delivery of human MSCs is often required via intra-articular injection, and it is common to introduce local anesthetics prior to, during, and following this procedure [530].

Lidocaine is one of the most commonly used amide-type local anesthetics due to its faster onset of action, superior safety profile, low cost, and wide availability compared to older local anesthetics. In vitro exposure of human ASCs to increasing concentrations of lidocaine resulted in a decreasing number of viable MSCs. Furthermore, reduction in cell proliferation was evident with the increasing exposure time, which suggests that lidocaine has a dose- and time-dependent cytotoxic effect on MSCs. MSCs subjected to

lidocaine at various dilutions (2 mg/ml to 8 mg/ml) and exposure times (0.5 to 4 hours) showed upregulation of genes normally associated with responses to stress and cytoprotective mechanisms, while higher concentration of lidocaine (8 mg/ml and more) resulted in a significant drop in gene expression. Exposure of MSCs to high concentrations of lidocaine for prolonged periods was shown to negatively affect MSC viability, proliferation, and/or functions [531]. A recent study investigated the effect of lidocaine applied during tumescent local anesthesia prior to liposuction. Abdominal subcutaneous fat tissue was infiltrated with lidocaine-containing tumescent local anesthesia on the left and non-lidocaine-containing on the right side of the abdomen and harvested subsequently for cell analysis. Lidocaine showed no adverse effects on the distribution, cell number, and viability of ASCs [532].

Bupivacaine, ropivacaine, and mepivacaine are the members of the pipecoloxylidide group of amide local anesthetics, which differ in their onset of action, analgesic duration, and potency. Their analgesic potency increases in a ratio of 1 : 1.5 : 4 from mepivacaine to ropivacaine to bupivacaine, respectively [533]. Lidocaine, bupivacaine, ropivacaine, and mepivacaine were cytotoxic to rabbit ASCs during in vitro early chondrogenic differentiation, as evident by decreased viability and increased apoptotic rate of ASC monolayer cell culture experiments in a dose- and drug type-dependent manner. 1% lidocaine induced relatively lower cytotoxic effects on ASCs, and 2% mepivacaine and 1% lidocaine appeared to exhibit a less pronounced influence on chondrogenesis-associated mRNA expression [530].

In addition, local anesthetics could alter MSC secretory function, depending on the anesthetic dose and potency, along with the existing inflammatory environment [534]. A systematic review [535] evaluating the effect of various local anesthetics on different types of MSCs concluded that all amide-based local anesthetics exhibited cytotoxic effects on MSCs, and these effects were dependent on the dose, exposure time, and drug type. Cytotoxicity could also be cell type-dependent; however, there is currently insufficient evidence to support this hypothesis. Nevertheless, the study suggested that ropivacaine could offer less cytotoxicity than other types of local anesthetics and might be preferred for use in MSC-based therapy [535].

Future in vivo studies are crucial to better understand the interactions of these agents with MSCs in a more physiological environment, in terms of anesthetics' pharmacokinetics and the in vivo response and recovery of MSCs, to provide enough supporting evidence for future clinical trials [535].

10.3. Effect of Other Drugs. Heparin supplementation during culturing of human BMSCs was found to alter the cell biological properties, even at low doses, which warrants great caution regarding the application of heparin as a culture supplement for in vitro expansion of BMSCs. Also, heparin showed variable effects on gene expression and proliferation of human BMSCs in a donor-dependent manner, and MSCs harvested from patients receiving chronic heparin therapy could show altered properties [536].

MSCs have immunosuppressive properties (discussed above), and the presence of immunosuppressive drugs could offer synergistic effect, augmenting MSCs' immunosuppressive action [537, 538]. In vitro culturing of human BMSCs and ASCs in the presence of clinical doses of six widely used immunosuppressive drugs (cyclosporine A, mycophenolate mofetil, rapamycin, glucocorticoids, prednisone, and dexamethasone) was conducted to investigate their effect on immunosuppressive properties of MSCs. ASCs were less sensitive to the presence of immunosuppressive drugs than BMSCs. Glucocorticoids, especially dexamethasone, exerted the most prominent effects on both types of MSCs and suppressed the expression of the majority of the immunosuppressive factors tested [539].

Duloxetine (a serotonin and norepinephrine reuptake inhibitor) and fluoxetine (a selective serotonin reuptake inhibitor) are commonly used antidepressants for the management of major depressive disorders. Daily nontoxic concentration of both drugs exerted time-dependent effects on ASCs in vitro. In short-term exposure, both drugs influenced the proliferation and stemness properties of noncommitted ASCs, while following after 21 days of daily drug treatments, both cell proliferation and mesenchymal stromal cell marker expression were comparable to cells cultured in basal medium. Treatment with fluoxetine did not lead to morphological alterations during adipogenic or osteogenic differentiation of committed cells. Treatment with duloxetine resulted in slowing down lipid accumulation [540], which contradicts weight gain documented in patients treated for long durations [541] and increased mineral deposition, which could be correlated with the upregulation in gene expression of early and late osteogenic markers in ASCs treated with duloxetine [540].

Nonsteroidal anti-inflammatory drugs showed no interference with BMSC potential to proliferate and differentiate into osteogenic lineage in vitro, while inhibiting their chondrogenic potential [542].

In summary, it is evident that various drugs and chemicals used during MSC in vitro culturing and ex vivo expansion or during MSC transplantation could alter the cell viability, proliferation, properties, and/or function. The exact mechanism or consequences of each drug are still not clear, based on the currently available evidence in literature, and further future standardized in vitro studies, in vivo animal investigations, and clinical trials are greatly needed to carefully evaluate the effects of different drugs and chemicals used/needed during MSC-based therapies.

11. Conclusion

The results of MSCs' clinical applications are mixed and contradictory, preventing the advancement of MSCs into cell-based therapy. Although a considerable number of studies have proved the regenerative capacity of MSCs, significant limitations still exist hindering their usage as a clinically safe and efficient therapeutic approach.

Stem/progenitor cell-based therapy compromises variations related to the donor, their isolation, and expansion, as well as to the wide range of used media and their constituents and finally related to the recipients. All these variabilities suggest the need for developing a biological database, following

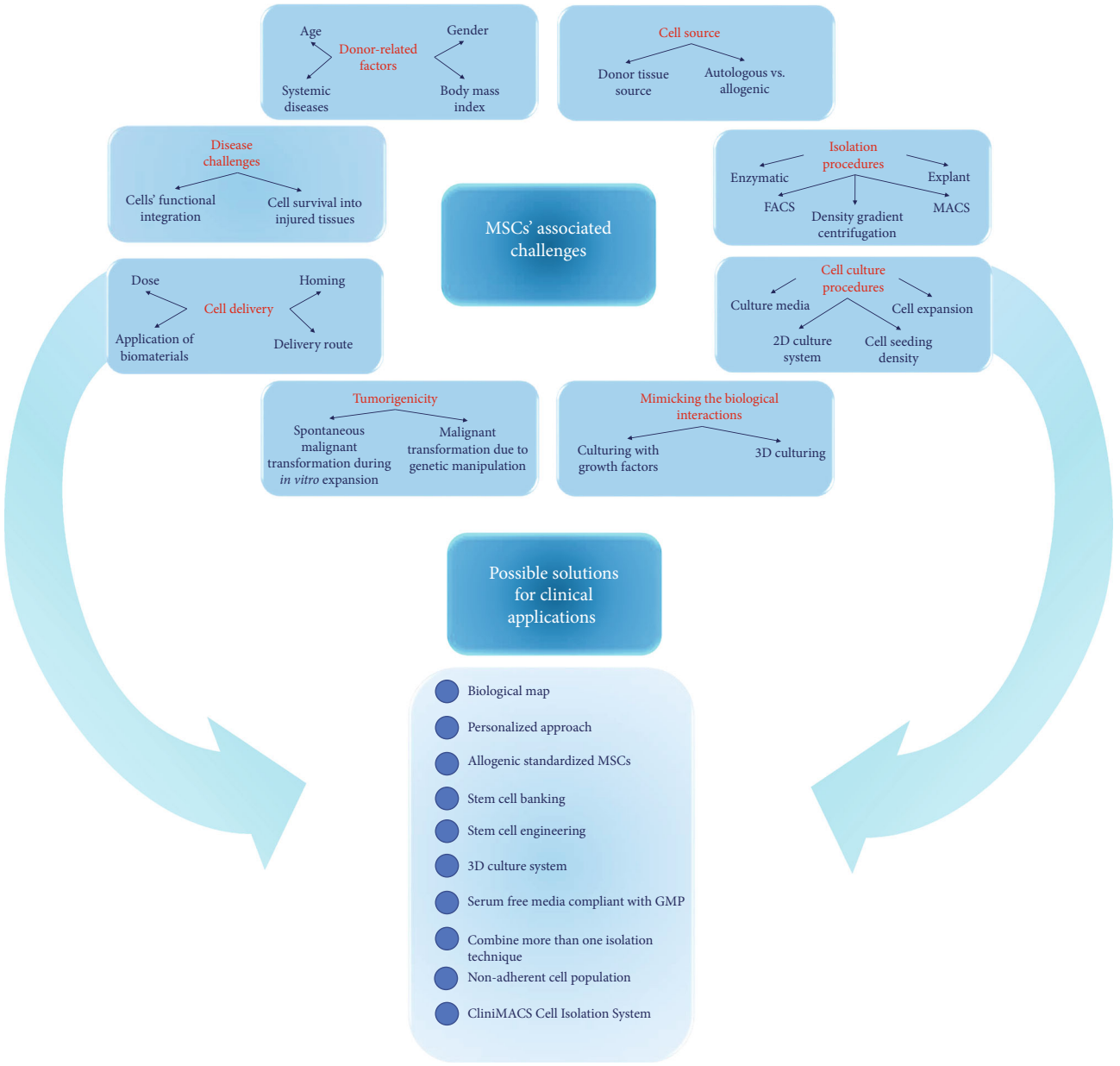

Figure 3: Challenges facing human clinical translation of MSC application and suggested strategies to overcome them.

reviewing the literature for the growth factors and cytokines associated with age, gender, health status, and immune response. Such biological map could enable the therapists to design a personalized protocol for each patient, considering the donor- and the recipient-related variations. Further, limiting and overcoming donor-related variations entail using standardized allogenic MSC transplantation following rigorous characterization and immunophenotyping [58, 61, 100]. Alternative cell sources as ASCs [57, 58], dental pulp MSCs [59], and stem/progenitor cell banking [61] should be considered for therapeutic use in aged patients instead of BMSCs.

Standardizing the materials used and the protocols utilized during fabrication is mandatory to alleviate the discrepancies during MSC fabrication. A chairside characterization facility should exist to examine the autogenous products from the patients (autoserum, for example) in order to overcome the immunogenicity and the time consumption associated with other alternatives. Moreover, the cell dose or cell delivery must be optimized according to the type and state of illness, utilized MSC predefined criteria, and condition of the patient. In addition, various drugs and chemicals used during MSC in vitro culturing and ex vivo expansion or during MSC transplantation could alter the cell viability, proliferation, properties, and/or function; thus, careful investigation of their effect on MSCs is mandatory.

Hence, for long-term therapeutic effectiveness and safety of MSC-based therapies, more research on both the preclinical and clinical levels has to be accomplished, focusing on optimizing the protocol for MSC isolation and in vitro expansion and preengineering to enhance their in vivo survival, differentiation, homing, and

functional integration into the diseased/injured target site. In an attempt to prime the cells to be able to survive the harsh in vivo environment postinjury and to augment MSCs' biological and functional properties, preconditioning/pretreatment with hypoxia, growth factors, and/or drugs and genetic engineering of MSCs are an area of active research [543–547]. In addition, the establishment of personalized treatment approaches for patients adapted to their condition, disease state, and type of MSCs delivered is crucial. All these tactics (Figure 3) would greatly contribute to the successful and efficacious translation of MSC-based therapies into the clinical practice to be able to achieve the long-awaited regenerative and therapeutic role of MSCs.

Conflicts of Interest

All authors declare that they do not have any conflict of interest related to this work.

References

[1] X. Guan, M. Avci-Adali, E. Alarçin et al., "Development of hydrogels for regenerative engineering," *Biotechnology Journal*, vol. 12, no. 5, 2017.

[2] G. Gao and X. Cui, "Three-dimensional bioprinting in tissue engineering and regenerative medicine," *Biotechnology Letters*, vol. 38, no. 2, pp. 203–211, 2016.

[3] F. Berthiaume, T. J. Maguire, and M. L. Yarmush, "Tissue engineering and regenerative medicine: history, progress, and challenges," *Annual Review of Chemical and Biomolecular Engineering*, vol. 2, no. 1, pp. 403–430, 2011.

[4] N. Kim and S.-G. Cho, "Clinical applications of mesenchymal stem cells," *The Korean Journal of Internal Medicine*, vol. 28, no. 4, pp. 387–402, 2013.

[5] F. Gao, S. M. Chiu, D. A. L. Motan et al., "Mesenchymal stem cells and immunomodulation: current status and future prospects," *Cell Death & Disease*, vol. 7, no. 1, article e2062, 2016.

[6] S. Shahrokhi, S. Daneshmandi, and F. Menaa, "Tumor necrosis factor-α/CD40 ligand-engineered mesenchymal stem cells greatly enhanced the antitumor immune response and lifespan in mice," *Human Gene Therapy*, vol. 25, no. 3, pp. 240–253, 2014.

[7] C. H. Ryu, S. A. Park, S. M. Kim et al., "Migration of human umbilical cord blood mesenchymal stem cells mediated by stromal cell-derived factor-1/CXCR4 axis via Akt, ERK, and p38 signal transduction pathways," *Biochemical and Biophysical Research Communications*, vol. 398, no. 1, pp. 105–110, 2010.

[8] I. Ullah, R. B. Subbarao, and G. J. Rho, "Human mesenchymal stem cells - current trends and future prospective," *Bioscience Reports*, vol. 35, no. 2, 2015.

[9] M. Dominici, K. le Blanc, I. Mueller et al., "Minimal criteria for defining multipotent mesenchymal stromal cells. The International Society for Cellular Therapy position statement," *Cytotherapy*, vol. 8, no. 4, pp. 315–317, 2006.

[10] K. Le Blanc, C. Tammik, K. Rosendahl, E. Zetterberg, and O. Ringdén, "HLA expression and immunologic propertiesof differentiated and undifferentiated mesenchymal stem cells," *Experimental Hematology*, vol. 31, no. 10, pp. 890–896, 2003.

[11] D. Mushahary, A. Spittler, C. Kasper, V. Weber, and V. Charwat, "Isolation, cultivation, and characterization of human mesenchymal stem cells," *Cytometry Part A*, vol. 93, no. 1, pp. 19–31, 2018.

[12] K. M. Fawzy El-Sayed, C. Dorfer, F. Fandrich, F. Gieseler, M. H. Moustafa, and H. Ungefroren, "Erratum to: adult mesenchymal stem cells explored in the dental field," in *Mesenchymal Stem Cells - Basics and Clinical Application II*, vol. 130 of Advances in Biochemical Engineering/Biotechnology, pp. 301-302, 2013.

[13] K. M. Fawzy El-Sayed, C. Dorfer, F. Fandrich, F. Gieseler, M. H. Moustafa, and H. Ungefroren, "Adult mesenchymal stem cells explored in the dental field," in *Mesenchymal Stem Cells - Basics and Clinical Application II*, vol. 130 of Advances in Biochemical Engineering/Biotechnology, pp. 89–103, 2012.

[14] K. M. Fawzy El-Sayed and C. E. Dorfer, "Gingival mesenchymal stem/progenitor cells: a unique tissue engineering gem," *Stem Cells International*, vol. 2016, Article ID 7154327, 16 pages, 2016.

[15] K. M. Fawzy El-Sayed and C. E. Dorfer, "Animal models for periodontal tissue engineering: a knowledge-generating process," *Tissue Engineering Part C: Methods*, vol. 23, no. 12, pp. 900–925, 2017.

[16] K. M. Fawzy El-Sayed, K. Jakusz, A. Jochens, C. Dorfer, and F. Schwendicke, "Stem cell transplantation for pulpal regeneration: a systematic review," *Tissue Engineering Part B: Reviews*, vol. 21, no. 5, pp. 451–460, 2015.

[17] G. M. Ahmed, E. A. Abouauf, N. AbuBakr, C. E. Dörfer, and K. F. el-Sayed, "Tissue engineering approaches for enamel, dentin, and pulp regeneration: an update," *Stem Cells International*, vol. 2020, Article ID 5734539, 15 pages, 2020.

[18] S. El Moshy, I. A. Radwan, D. Rady et al., "Dental stem cell-derived secretome/conditioned medium: the future for regenerative therapeutic applications," *Stem Cells International*, vol. 2020, Article ID 7593402, 29 pages, 2020.

[19] V. Volarevic, B. Ljujic, P. Stojkovic, A. Lukic, N. Arsenijevic, and M. Stojkovic, "Human stem cell research and regenerative medicine–present and future," *British Medical Bulletin*, vol. 99, no. 1, pp. 155–168, 2011.

[20] V. Volarevic, S. Erceg, S. S. Bhattacharya, P. Stojkovic, P. Horner, and M. Stojkovic, "Stem cell-based therapy for spinal cord injury," *Cell Transplantation*, vol. 22, no. 8, pp. 1309–1323, 2013.

[21] K.-H. Roh, R. M. Nerem, and K. Roy, "Biomanufacturing of therapeutic cells: state of the art, current challenges, and future perspectives," *Annual Review of Chemical and Biomolecular Engineering*, vol. 7, no. 1, pp. 455–478, 2016.

[22] T. R. J. Heathman, Q. A. Rafiq, A. K. C. Chan et al., "Characterization of human mesenchymal stem cells from multiple donors and the implications for large scale bioprocess development," *Biochemical Engineering Journal*, vol. 108, pp. 14–23, 2016.

[23] L. De Girolamo, D. Stanco, L. Salvatori et al., "Stemness and osteogenic and adipogenic potential are differently impaired in subcutaneous and visceral adipose derived stem cells (ASCs) isolated from obese donors," *International Journal of Immunopathology and Pharmacology*, vol. 26, 1 Supplement, pp. 11–21, 2013.

[24] R. S. Patel, G. Carter, G. el Bassit et al., "Adipose-derived stem cells from lean and obese humans show depot specific differences in their stem cell markers, exosome contents and

senescence: role of protein kinase C delta (PKCδ) in adipose stem cell niche," *Stem Cell Investigation*, vol. 3, p. 2, 2016.

[25] S. Zhou, J. S. Greenberger, M. W. Epperly et al., "Age-related intrinsic changes in human bone-marrow-derived mesenchymal stem cells and their differentiation to osteoblasts," *Aging Cell*, vol. 7, no. 3, pp. 335–343, 2008.

[26] A. Stolzing, E. Jones, D. McGonagle, and A. Scutt, "Age-related changes in human bone marrow-derived mesenchymal stem cells: consequences for cell therapies," *Mechanisms of Ageing and Development*, vol. 129, no. 3, pp. 163–173, 2008.

[27] J. Yuan, J.-x. Yu, and J. Ge, "Sexual dimorphism on the neurogenic potential of rhesus monkeys mesenchymal stem cells," *Biochemical and Biophysical Research Communications*, vol. 396, no. 2, pp. 394–400, 2010.

[28] C. Serena, N. Keiran, V. Ceperuelo-Mallafre et al., "Obesity and type 2 diabetes alters the immune properties of human adipose derived stem cells," *Stem Cells*, vol. 34, no. 10, pp. 2559–2573, 2016.

[29] Y. Sun, W. Deng, L. Geng et al., "Mesenchymal stem cells from patients with rheumatoid arthritis display impaired function in inhibiting Th17 cells," *Journal of Immunology Research*, vol. 2015, Article ID 284215, 13 pages, 2015.

[30] J. M. Murphy, K. Dixon, S. Beck, D. Fabian, A. Feldman, and F. Barry, "Reduced chondrogenic and adipogenic activity of mesenchymal stem cells from patients with advanced osteoarthritis," *Arthritis and Rheumatism*, vol. 46, no. 3, pp. 704–713, 2002.

[31] G. Pachón-Peña, C. Serena, M. Ejarque et al., "Obesity determines the immunophenotypic profile and functional characteristics of human mesenchymal stem cells from adipose tissue," *Stem Cells Translational Medicine*, vol. 5, no. 4, pp. 464–475, 2016.

[32] A. L. Strong, R. S. Hunter, R. B. Jones et al., "Obesity inhibits the osteogenic differentiation of human adipose-derived stem cells," *Journal of Translational Medicine*, vol. 14, no. 1, p. 27, 2016.

[33] J. Ye and J. M. Gimble, "Regulation of stem cell differentiation in adipose tissue by chronic inflammation," *Clinical and Experimental Pharmacology and Physiology*, vol. 38, no. 12, pp. 872–878, 2011.

[34] A. L. Strong, A. C. Bowles, R. M. Wise et al., "Human adipose stromal/stem cells from obese donors show reduced efficacy in halting disease progression in the experimental autoimmune encephalomyelitis model of multiple sclerosis," *Stem Cells*, vol. 34, no. 3, pp. 614–626, 2016.

[35] O. Katsara, L. G. Mahaira, E. G. Iliopoulou et al., "Effects of donor age, gender, and in vitro cellular aging on the phenotypic, functional, and molecular characteristics of mouse bone marrow-derived mesenchymal stem cells," *Stem Cells and Development*, vol. 20, no. 9, pp. 1549–1561, 2011.

[36] S. C. Mendes, J. M. Tibbe, M. Veenhof et al., "Bone tissue-engineered implants using human bone marrow stromal cells: effect of culture conditions and donor age," *Tissue Engineering*, vol. 8, no. 6, pp. 911–920, 2002.

[37] M. S. Choudhery, M. Badowski, A. Muise, J. Pierce, and D. T. Harris, "Donor age negatively impacts adipose tissue-derived mesenchymal stem cell expansion and differentiation," *Journal of Translational Medicine*, vol. 12, no. 1, p. 8, 2014.

[38] M. Liu, H. Lei, P. Dong et al., "Adipose-derived mesenchymal stem cells from the elderly exhibit decreased migration and differentiation abilities with senescent properties," *Cell Transplantation*, vol. 26, no. 9, pp. 1505–1519, 2017.

[39] M. Zhu, E. Kohan, J. Bradley, M. Hedrick, P. Benhaim, and P. Zuk, "The effect of age on osteogenic, adipogenic and proliferative potential of female adipose-derived stem cells," *Journal of Tissue Engineering and Regenerative Medicine*, vol. 3, no. 4, pp. 290–301, 2009.

[40] M. Bethel, B. R. Chitteti, E. F. Srour, and M. A. Kacena, "The changing balance between osteoblastogenesis and adipogenesis in aging and its impact on hematopoiesis," *Current Osteoporosis Reports*, vol. 11, no. 2, pp. 99–106, 2013.

[41] K. A. Payne, D. M. Didiano, and C. R. Chu, "Donor sex and age influence the chondrogenic potential of human femoral bone marrow stem cells," *Osteoarthritis and Cartilage*, vol. 18, no. 5, pp. 705–713, 2010.

[42] A. Stolzing, E. Bauer, and A. Scutt, "Suspension cultures of bone-marrow-derived mesenchymal stem cells: effects of donor age and glucose level," *Stem Cells and Development*, vol. 21, no. 14, pp. 2718–2723, 2012.

[43] D. Cakouros and S. Gronthos, "The changing epigenetic landscape of mesenchymal stem/stromal cells during aging," *Bone*, vol. 137, article 115440, 2020.

[44] S. Fukada, Y. Ma, and A. Uezumi, "Adult stem cell and mesenchymal progenitor theories of aging," *Frontiers in Cell Developmental Biology*, vol. 2, 2014.

[45] A. Behrens, J. M. van Deursen, K. L. Rudolph, and B. Schumacher, "Impact of genomic damage and ageing on stem cell function," *Nature Cell Biology*, vol. 16, no. 3, pp. 201–207, 2014.

[46] S. Neri and R. M. Borzì, "Molecular mechanisms contributing to mesenchymal stromal cell aging," *Biomolecules*, vol. 10, no. 2, p. 340, 2020.

[47] S.-R. Yang, J.-R. Park, and K.-S. Kang, "Reactive oxygen species in mesenchymal stem cell aging: implication to lung diseases," *Oxidative Medicine and Cellular Longevity*, vol. 2015, Article ID 486263, 11 pages, 2015.

[48] J. A. Fafián-Labora, M. Morente-López, and M. C. Arufe, "Effect of aging on behaviour of mesenchymal stem cells," *World Journal of Stem Cells*, vol. 11, no. 6, pp. 337–346, 2019.

[49] L. You, L. Pan, L. Chen, W. Gu, and J. Chen, "miR-27a is essential for the shift from osteogenic differentiation to adipogenic differentiation of mesenchymal stem cells in postmenopausal osteoporosis," *Cellular Physiology Biochemistry*, vol. 39, no. 1, pp. 253–265, 2016.

[50] M. Tomé, J. C. Sepúlveda, M. Delgado et al., "miR-335 correlates with senescence/aging in human mesenchymal stem cells and inhibits their therapeutic actions through inhibition of AP-1 activity," *Stem Cells*, vol. 32, no. 8, pp. 2229–2244, 2014.

[51] M. J. Peffers, J. Collins, Y. Fang et al., "Age-related changes in mesenchymal stem cells identified using a multi-omics approach," *European Cells Materials*, vol. 31, pp. 136–159, 2016.

[52] R. Xu, X. Shen, Y. Si et al., "MicroRNA-31a-5p from aging BMSCs links bone formation and resorption in the aged bone marrow microenvironment," *Aging Cell*, vol. 17, no. 4, article e12794, 2018.

[53] J. Shang, Y. Yao, X. Fan et al., "miR-29c-3p promotes senescence of human mesenchymal stem cells by targeting CNOT6 through p53-p21 and p16-pRB pathways," *Biochimica et Biophysica Acta (BBA) - Molecular Cell Research*, vol. 1863, no. 4, pp. 520–532, 2016.

[54] J. L. Simonsen, C. Rosada, N. Serakinci et al., "Telomerase expression extends the proliferative life-span and maintains the osteogenic potential of human bone marrow stromal cells," *Nature Biotechnology*, vol. 20, no. 6, pp. 592–596, 2002.

[55] D. de Gonzalo-Calvo, K. Neitzert, M. Fernández et al., "Differential inflammatory responses in aging and disease: TNF-α and IL-6 as possible biomarkers," *Free Radical Biology Medicine*, vol. 49, no. 5, pp. 733–737, 2010.

[56] Y. Liu, L. Wang, T. Kikuiri et al., "Mesenchymal stem cell-based tissue regeneration is governed by recipient T lymphocytes via IFN-γ and TNF-α," *Nature Medicine*, vol. 17, no. 12, pp. 1594–1601, 2011.

[57] L. E. Kokai, D. O. Traktuev, L. Zhang et al., "Adipose stem cell function maintained with age: an intra-subject study of long-term cryopreserved cells," *Aesthetic Surgery Journal*, vol. 37, no. 4, pp. 454–463, 2017.

[58] D. Dufrane, "Impact of age on human adipose stem cells for bone tissue engineering," *Cell Transplantation*, vol. 26, no. 9, pp. 1496–1504, 2017.

[59] E. Bressan, L. Ferroni, C. Gardin et al., "Donor age-related biological properties of human dental pulp stem cells change in nanostructured scaffolds," *PLoS One*, vol. 7, no. 11, article e49146, 2012.

[60] J. Zhang, Y. An, L.-N. Gao, Y.-J. Zhang, Y. Jin, and F.-M. Chen, "The effect of aging on the pluripotential capacity and regenerative potential of human periodontal ligament stem cells," *Biomaterials*, vol. 33, no. 29, pp. 6974–6986, 2012.

[61] I. Mastrolia, E. M. Foppiani, A. Murgia et al., "Challenges in clinical development of mesenchymal stromal/stem cells: concise review," *Stem Cells Translational Medicine*, vol. 8, no. 11, pp. 1135–1148, 2019.

[62] Y. Liu, Z. Li, T. Liu et al., "Impaired cardioprotective function of transplantation of mesenchymal stem cells from patients with diabetes mellitus to rats with experimentally induced myocardial infarction," *Cardiovascular Diabetology*, vol. 12, no. 1, p. 40, 2013.

[63] E. Lara, A. Velásquez, J. Cabezas et al., "Endometritis and in vitro PGE2 challenge modify properties of cattle endometrial mesenchymal stem cells and their transcriptomic profile," *Stem Cells International*, vol. 2017, Article ID 4297639, 16 pages, 2017.

[64] C. Cramer, E. Freisinger, R. K. Jones et al., "Persistent high glucose concentrations alter the regenerative potential of mesenchymal stem cells," *Stem Cells and Development*, vol. 19, no. 12, pp. 1875–1884, 2010.

[65] K. Kornicka, J. Houston, and K. Marycz, "Dysfunction of mesenchymal stem cells isolated from metabolic syndrome and type 2 diabetic patients as result of oxidative stress and autophagy may limit their potential therapeutic use," *Stem Cell Reviews Reports*, vol. 14, no. 3, pp. 337–345, 2018.

[66] M. Blair, "Diabetes mellitus review," *Urologic Nursing*, vol. 36, no. 1, pp. 27–36, 2016.

[67] C. Piperi, A. Goumenos, C. Adamopoulos, and A. G. Papavassiliou, "AGE/RAGE signalling regulation by miRNAs: associations with diabetic complications and therapeutic potential," *The International Journal of Biochemistry Cell Biology*, vol. 60, pp. 197–201, 2015.

[68] C. Ciavarella and G. Pasquinelli, "The dual nature of mesenchymal stem cells (MSCs): yin and yang of the inflammatory process," in *Update on Mesenchymal and Induced Pluripotent Stem Cells*, Intech Open, 2019.

[69] H. Huang, N. Zhao, X. Xu et al., "Dose-specific effects of tumor necrosis factor alpha on osteogenic differentiation of mesenchymal stem cells," *Cell Proliferation*, vol. 44, no. 5, pp. 420–427, 2011.

[70] C. Ciavarella, E. Gallitto, F. Ricci, M. Buzzi, A. Stella, and G. Pasquinelli, "The crosstalk between vascular MSCs and inflammatory mediators determines the pro-calcific remodelling of human atherosclerotic aneurysm," *Stem Cell Research & Therapy*, vol. 8, no. 1, p. 99, 2017.

[71] F. Djouad, V. Fritz, F. Apparailly et al., "Reversal of the immunosuppressive properties of mesenchymal stem cells by tumor necrosis factor α in collagen-induced arthritis," *Arthritis & Rheumatism*, vol. 52, no. 5, pp. 1595–1603, 2005.

[72] H. N. Tang, Y. Xia, Y. Yu, R. X. Wu, L. N. Gao, and F. M. Chen, "Stem cells derived from "inflamed" and healthy periodontal ligament tissues and their sheet functionalities: a patient-matched comparison," *Journal of Clinical Periodontology*, vol. 43, no. 1, pp. 72–84, 2016.

[73] K. M. Fawzy El-Sayed, M. Elahmady, Z. Adawi et al., "The periodontal stem/progenitor cell inflammatory-regenerative cross talk: a new perspective," *Journal of Periodontal Research*, vol. 54, no. 2, pp. 81–94, 2018.

[74] D. Liu, J. Xu, O. Liu et al., "Mesenchymal stem cells derived from inflamed periodontal ligaments exhibit impaired immunomodulation," *Journal of Clinical Periodontology*, vol. 39, no. 12, pp. 1174–1182, 2012.

[75] J. Zhang, Z.-G. Li, Y.-M. Si, B. Chen, and J. Meng, "The difference on the osteogenic differentiation between periodontal ligament stem cells and bone marrow mesenchymal stem cells under inflammatory microenviroments," *Differentiation*, vol. 88, no. 4-5, pp. 97–105, 2014.

[76] Z. Zhang, Y. Han, J. Song et al., "Interferon-γ regulates the function of mesenchymal stem cells from oral lichen planus via indoleamine 2, 3-dioxygenase activity," *Journal of Oral Pathology Medicine*, vol. 44, no. 1, pp. 15–27, 2015.

[77] K. M. Fawzy El-Sayed, R. Elsalawy, N. Ibrahim et al., "The dental pulp stem/progenitor cells-mediated inflammatory-regenerative axis," *Tissue Engineering Part B: Reviews*, vol. 25, no. 5, pp. 445–460, 2019.

[78] F. B. Yazid, N. Gnanasegaran, W. Kunasekaran, V. Govindasamy, and S. Musa, "Comparison of immunodulatory properties of dental pulp stem cells derived from healthy and inflamed teeth," *Clinical Oral Investigations*, vol. 18, no. 9, pp. 2103–2112, 2014.

[79] C. Yang, Y. Chen, F. Li et al., "The biological changes of umbilical cord mesenchymal stem cells in inflammatory environment induced by different cytokines," *Molecular Cellular Biochemistry*, vol. 446, no. 1-2, pp. 171–184, 2018.

[80] M. D. Griffin, A. E. Ryan, S. Alagesan, P. Lohan, O. Treacy, and T. Ritter, "Anti-donor immune responses elicited by allogeneic mesenchymal stem cells: what have we learned so far?," *Immunology Cell Biology*, vol. 91, no. 1, pp. 40–51, 2013.

[81] M. J. Crop, C. C. Baan, S. S. Korevaar et al., "Inflammatory conditions affect gene expression and function of human adipose tissue-derived mesenchymal stem cells," *Clinical & Experimental Immunology*, vol. 162, no. 3, pp. 474–486, 2010.

[82] P. Lohan, O. Treacy, M. D. Griffin, T. Ritter, and A. E. Ryan, "Anti-donor immune responses elicited by allogeneic mesenchymal stem cells and their extracellular vesicles: are we still learning?," *Frontiers in Immunology*, vol. 8, p. 1626, 2017.

[83] K. M. Van Megen, E. J. T. van 't Wout, J. Lages Motta, B. Dekker, T. Nikolic, and B. O. Roep, "Activated mesenchymal stromal cells process and present antigens regulating adaptive immunity," *Frontiers in Immunology*, vol. 10, p. 694, 2019.

[84] L. Barrachina, A. R. Remacha, A. Romero et al., "Effect of inflammatory environment on equine bone marrow derived mesenchymal stem cells immunogenicity and immunomodulatory properties," *Veterinary Immunology Immunopathology*, vol. 171, pp. 57–65, 2016.

[85] P. Mancheño-Corvo, R. Menta, B. del Río et al., "T lymphocyte prestimulation impairs in a time-dependent manner the capacity of adipose mesenchymal stem cells to inhibit proliferation: role of interferon γ, poly I: C, and tryptophan metabolism in restoring adipose mesenchymal stem cell inhibitory effect," *Stem Cells Development*, vol. 24, no. 18, pp. 2158–2170, 2015.

[86] O. Andrukhov, J. S.-A. Hong, O. Andrukhova, A. Blufstein, A. Moritz, and X. Rausch-Fan, "Response of human periodontal ligament stem cells to IFN-γ and TLR-agonists," *Scientific Reports*, vol. 7, no. 1, article 12856, 2017.

[87] R. Chinnadurai, I. B. Copland, M. A. Garcia et al., "Cryopreserved mesenchymal stromal cells are susceptible to T-cell mediated apoptosis which is partly rescued by IFNγ licensing," *Stem Cells*, vol. 34, no. 9, pp. 2429–2442, 2016.

[88] K. N. Sivanathan, D. M. Rojas-Canales, C. M. Hope et al., "Interleukin-17A-induced human mesenchymal stem cells are superior modulators of immunological function," *Stem Cells*, vol. 33, no. 9, pp. 2850–2863, 2015.

[89] E. Redondo-Castro, C. Cunningham, J. Miller et al., "Interleukin-1 primes human mesenchymal stem cells towards an anti-inflammatory and pro-trophic phenotype in vitro," *Stem Cell Research & Therapy*, vol. 8, no. 1, p. 79, 2017.

[90] K. Fawzy El-Sayed, C. Graetz, T. Kohnlein, M. Mekhemar, and C. Dorfer, "Effect of total sonicated Aggregatibacter actinomycetemcomitans fragments on gingival stem/progenitor cells," *Medicina Oral Patología Oral y Cirugia Bucal*, vol. 23, no. 5, pp. e569–e578, 2018.

[91] K. M. Fawzy El-Sayed, D. Hein, and C. E. Dorfer, "Retinol/inflammation affect stemness and differentiation potential of gingival stem/progenitor cells via Wnt/β-catenin," *Journal of Periodontal Research*, vol. 54, no. 4, pp. 413–423, 2019.

[92] M. Mekhemar, J. Tölle, C. Dörfer, and K. Fawzy el-Sayed, "TLR3 ligation affects differentiation and stemness properties of gingival mesenchymal stem/progenitor cells," *Journal of Clinical Periodontology*, vol. 47, no. 8, pp. 991–1005, 2020.

[93] M. K. Mekhemar, S. Adam-Klages, D. Kabelitz, C. E. Dorfer, and K. M. Fawzy El-Sayed, "TLR-induced immunomodulatory cytokine expression by human gingival stem/progenitor cells," *Cellular Immunology*, vol. 326, pp. 60–67, 2018.

[94] L. Zhou, C. E. Dorfer, L. Chen, and K. M. Fawzy El-Sayed, "Porphyromonas gingivalislipopolysaccharides affect gingival stem/progenitor cells attributes through NF-κB, but not Wnt/β-catenin, pathway," *Journal of Clinical Periodontology*, vol. 44, no. 11, pp. 1112–1122, 2017.

[95] L. L. Zhou, W. Liu, Y. M. Wu, W. L. Sun, C. E. Dorfer, and K. M. Fawzy El-Sayed, "Oral mesenchymal stem/progenitor cells: the immunomodulatory masters," *Stem Cells International*, vol. 2020, Article ID 1327405, 16 pages, 2020.

[96] M. Al Bahrawy, K. Ghaffar, A. Gamal, K. El-Sayed, and V. Iacono, "Effect of inflammation on gingival mesenchymal stem/progenitor cells' proliferation and migration through microperforated membranes: an in vitro study," *Stem Cells International*, vol. 2020, Article ID 5373418, 10 pages, 2020.

[97] S. Alagesan and M. D. Griffin, "Autologous and allogeneic mesenchymal stem cells in organ transplantation," *Current Opinion in Organ Transplantation*, vol. 19, no. 1, pp. 65–72, 2014.

[98] J. Ji, X. Tong, X. Huang et al., "Sphere-shaped nano-hydroxyapatite/chitosan/gelatin 3D porous scaffolds increase proliferation and osteogenic differentiation of human induced pluripotent stem cells from gingival fibroblasts," *Biomedical Materials*, vol. 10, no. 4, 2015.

[99] J. Zhang, X. Huang, H. Wang et al., "The challenges and promises of allogeneic mesenchymal stem cells for use as a cell-based therapy," *Stem Cell Research & Therapy*, vol. 6, no. 1, 2015.

[100] J. C. Ra, S. K. Kang, I. S. Shin et al., "Stem cell treatment for patients with autoimmune disease by systemic infusion of culture-expanded autologous adipose tissue derived mesenchymal stem cells," *Journal of Translational Medicine*, vol. 9, no. 1, 2011.

[101] J. M. Hare, J. E. Fishman, G. Gerstenblith et al., "Comparison of allogeneic vs autologous bone marrow–derived mesenchymal stem cells delivered by transendocardial injection in patients with ischemic cardiomyopathy: the POSEIDON randomized trial," *JAMA*, vol. 308, no. 22, pp. 2369–2379, 2012.

[102] J. M. Hare, D. L. DiFede, A. C. Rieger et al., "Randomized comparison of allogeneic versus autologous mesenchymal stem cells for nonischemic dilated cardiomyopathy: POSEIDON-DCM trial," *Journal of the American College of Cardiology*, vol. 69, no. 5, pp. 526–537, 2017.

[103] J. Liang, H. Zhang, C. Zhao et al., "Effects of allogeneic mesenchymal stem cell transplantation in the treatment of liver cirrhosis caused by autoimmune diseases," *International Journal of Rheumatic Diseases*, vol. 20, no. 9, pp. 1219–1226, 2017.

[104] P. Lohan, C. M. Coleman, J. M. Murphy, M. D. Griffin, T. Ritter, and A. E. Ryan, "Changes in immunological profile of allogeneic mesenchymal stem cells after differentiation: should we be concerned?," *Stem Cell Research & Therapy*, vol. 5, no. 4, p. 99, 2014.

[105] R. M. Dean and M. R. Bishop, "Graft-versus-host disease: emerging concepts in prevention and therapy," *Current Hematology Reports*, vol. 2, no. 4, pp. 287–294, 2003.

[106] K. Le Blanc, L. Tammik, B. Sundberg, S. E. Haynesworth, and O. Ringdén, "Mesenchymal stem cells inhibit and stimulate mixed lymphocyte cultures and mitogenic responses independently of the major histocompatibility complex," *Scandinavian Journal of Immunology*, vol. 57, no. 1, pp. 11–20, 2003.

[107] L. X. Tay, R. E. Ahmad, H. Dashtdar et al., "Treatment outcomes of alginate-embedded allogenic mesenchymal stem cells versus autologous chondrocytes for the repair of focal articular cartilage defects in a rabbit model," *The American Journal of Sports Medicine*, vol. 40, no. 1, pp. 83–90, 2012.

[108] A. Berner, J. C. Reichert, M. A. Woodruff et al., "Autologous vs. allogenic mesenchymal progenitor cells for the reconstruction of critical sized segmental tibial bone defects in aged sheep," *Acta Biomaterialia*, vol. 9, no. 8, pp. 7874–7884, 2013.

[109] D. D. Carrade, S. D. Owens, L. D. Galuppo et al., "Clinicopathologic findings following intra-articular injection of autologous and allogeneic placentally derived equine mesenchymal stem cells in horses," *Cytotherapy*, vol. 13, no. 4, pp. 419–430, 2011.

[110] D.-I. Jung, J. Ha, B.-T. Kang et al., "A comparison of autologous and allogenic bone marrow-derived mesenchymal stem cell transplantation in canine spinal cord injury," *Journal of the Neurological Sciences*, vol. 285, no. 1-2, pp. 67–77, 2009.

[111] A. Shabbir, D. Zisa, M. Leiker, C. Johnston, H. Lin, and T. Lee, "Muscular dystrophy therapy by nonautologous mesenchymal stem cells: muscle regeneration without immunosuppression and inflammation," *Transplantation*, vol. 87, no. 9, pp. 1275–1282, 2009.

[112] T. Chakravarty, R. R. Makkar, D. D. Ascheim et al., "ALLogeneic heart STem cells to achieve myocardial regeneration (ALLSTAR) trial: rationale and design," *Cell Transplantation*, vol. 26, no. 2, pp. 205–214, 2017.

[113] Y. B. Park, C. W. Ha, C. H. Lee, Y. C. Yoon, and Y. G. Park, "Cartilage regeneration in osteoarthritic patients by a composite of allogeneic umbilical cord blood-derived mesenchymal stem cells and hyaluronate hydrogel: results from a clinical trial for safety and proof-of-concept with 7 years of extended follow-up," *Stem Cells Translational Medicine*, vol. 6, no. 2, pp. 613–621, 2017.

[114] P. Kebriaei, L. Isola, E. Bahceci et al., "Adult human mesenchymal stem cells added to corticosteroid therapy for the treatment of acute graft-versus-host disease," *Biology of Blood Marrow Transplantation*, vol. 15, no. 7, pp. 804–811, 2009.

[115] A. Daly, "Remestemcel-L, the first cellular therapy product for the treatment of graft-versus-host disease," *Drugs Today*, vol. 48, no. 12, pp. 773–783, 2012.

[116] T. Goto and M. Murata, "Mesenchymal stem cell therapy in hematopoietic stem cell transplantation," *The Japanese Journal of Clinical Hematology*, vol. 59, no. 2, pp. 195–204, 2018.

[117] S. Chaplin, "Darvadstrocel for the treatment of complex perianal fistulas," *Prescriber*, vol. 30, no. 11, pp. 32-33, 2019.

[118] S. Bahsoun, K. Coopman, and E. C. Akam, "The impact of cryopreservation on bone marrow-derived mesenchymal stem cells: a systematic review," *Journal of Translational Medicine*, vol. 17, no. 1, p. 397, 2019.

[119] A.-J. Joswig, A. Mitchell, K. J. Cummings et al., "Repeated intra-articular injection of allogeneic mesenchymal stem cells causes an adverse response compared to autologous cells in the equine model," *Stem Cell Research & Therapy*, vol. 8, no. 1, p. 42, 2017.

[120] J. A. Ankrum, J. F. Ong, and J. M. Karp, "Mesenchymal stem cells: immune evasive, not immune privileged," *Nature Biotechnology*, vol. 32, no. 3, pp. 252–260, 2014.

[121] S. Schu, M. Nosov, L. O'Flynn et al., "Immunogenicity of allogeneic mesenchymal stem cells," *Journal of Cellular and Molecular Medicine*, vol. 16, no. 9, pp. 2094–2103, 2012.

[122] M. Seifert, M. Stolk, D. Polenz, and H.-D. Volk, "Detrimental effects of rat mesenchymal stromal cell pre-treatment in a model of acute kidney rejection," *Frontiers in Immunology*, vol. 3, 2012.

[123] I. A. Isakova, C. Lanclos, J. Bruhn et al., "Allo-reactivity of mesenchymal stem cells in rhesus macaques is dose and haplotype dependent and limits durable cell engraftment in vivo," *PloS one*, vol. 9, no. 1, article e87238, 2014.

[124] L. Barrachina, A. Cequier, A. Romero et al., "Allo-antibody production after intraarticular administration of mesenchymal stem cells (MSCs) in an equine osteoarthritis model: effect of repeated administration, MSC inflammatory stimulation, and equine leukocyte antigen (ELA) compatibility," *Stem Cell Research & Therapy*, vol. 11, no. 1, p. 52, 2020.

[125] N. Kalinina, D. Kharlampieva, M. Loguinova et al., "Characterization of secretomes provides evidence for adipose-derived mesenchymal stromal cells subtypes," *Stem Cell Research and Therapy*, vol. 6, no. 1, 2015.

[126] K. D. Salazar, S. M. Lankford, and A. R. Brody, "Mesenchymal stem cells produce Wnt isoforms and TGF-β1that mediate proliferation and procollagen expression by lung fibroblasts," *American Journal of Physiology-Lung Cellular and Molecular Physiology*, vol. 297, no. 5, pp. L1002–L1011, 2009.

[127] T. P. Lozito and R. S. Tuan, "Mesenchymal stem cells inhibit both endogenous and exogenous MMPs via secreted TIMPs," *Journal of Cellular Physiology*, vol. 226, no. 2, pp. 385–396, 2011.

[128] E. R. Andreeva and D. K. Matveeva, "Multipotent mesenchymal stromal cells and extracellular matrix: regulation under hypoxia," *Human Physiology*, vol. 44, no. 6, pp. 696–705, 2018.

[129] S. H. Bhang, S. Lee, J. Y. Shin, T. J. Lee, H. K. Jang, and B. S. Kim, "Efficacious and clinically relevant conditioned medium of human adipose- derived stem cells for therapeutic angiogenesis," *Molecular Therapy*, vol. 22, no. 4, pp. 862–872, 2014.

[130] T. N. A. Gunawardena, M. T. Rahman, B. J. J. Abdullah, and N. H. Abu Kasim, "Conditioned media derived from mesenchymal stem cell cultures: the next generation for regenerative medicine," *Journal of Tissue Engineering and Regenerative Medicine*, vol. 13, no. 4, pp. 569–586, 2019.

[131] G. D. Sagaradze, P. P. Nimiritsky, Z. A. Akopyan, P. I. Makarevich, and A. Y. Efimenko, ""Cell-free therapeutics" from components secreted by mesenchymal stromal cells as a novel class of biopharmaceuticals," in *Biopharmaceuticals*, InTech, London, UK, 2018.

[132] J. A. Pawitan, "Prospect of stem cell conditioned medium in regenerative medicine," *BioMed Research International*, vol. 2014, Article ID 965849, 14 pages, 2014.

[133] B.-R. Zhou, Y. Xu, S. L. Guo et al., "The effect of conditioned media of adipose-derived stem cells on wound healing after ablative fractional carbon dioxide laser resurfacing," *BioMed Research International*, vol. 2013, Article ID 519126, 9 pages, 2013.

[134] A. G. Kay, G. Long, G. Tyler et al., "Mesenchymal stem cell-conditioned medium reduces disease severity and immune responses in inflammatory arthritis," *Scientific Reports*, vol. 7, no. 1, p. 18019, 2017.

[135] S. Dahbour, F. Jamali, D. Alhattab et al., "Mesenchymal stem cells and conditioned media in the treatment of multiple sclerosis patients: clinical, ophthalmological and radiological assessments of safety and efficacy," *CNS Neuroscience & Therapeutics*, vol. 23, no. 11, pp. 866–874, 2017.

[136] Y. Fujita, T. Kadota, J. Araya, T. Ochiya, and K. Kuwano, "Clinical application of mesenchymal stem cell-derived extracellular vesicle-based therapeutics for inflammatory lung diseases," *Journal of Clinical Medicine*, vol. 7, no. 10, p. 355, 2018.

[137] M. Gimona, K. Pachler, S. Laner-Plamberger, K. Schallmoser, and E. Rohde, "Manufacturing of human extracellular vesicle-based therapeutics for clinical use," *International Journal of Molecular Sciences*, vol. 18, no. 6, p. 1190, 2017.

[138] G. Qiu, G. Zheng, M. Ge et al., "Mesenchymal stem cell-derived extracellular vesicles affect disease outcomes via

transfer of microRNAs," *Stem Cell Research & Therapy*, vol. 9, no. 1, p. 320, 2018.

[139] D. G. Phinney and M. F. Pittenger, "Concise review: MSC-derived exosomes for cell-free therapy," *Stem Cells*, vol. 35, no. 4, pp. 851–858, 2017.

[140] I. A. Radwan, D. Rady, M. M. S. Abbass et al., "Induced pluripotent stem cells in dental and nondental tissue regeneration: a review of an unexploited potential," *Stem Cells International*, vol. 2020, Article ID 1941629, 24 pages, 2020.

[141] C. Kichenbrand, E. Velot, P. Menu, and V. Moby, "Dental pulp stem cell-derived conditioned medium: an attractive alternative for regenerative therapy," *Tissue Engineering Part B: Reviews*, vol. 25, no. 1, pp. 78–88, 2019.

[142] H. Lin, J. Sohn, H. Shen, M. T. Langhans, and R. S. Tuan, "Bone marrow mesenchymal stem cells: aging and tissue engineering applications to enhance bone healing," *Biomaterials*, vol. 203, pp. 96–110, 2019.

[143] O. L. Abbas, O. Özatik, Z. B. Gönen et al., "Comparative analysis of mesenchymal stem cells from bone marrow, adipose tissue, and dental pulp as sources of cell therapy for zone of stasis burns," *Journal of Investigative Surgery*, vol. 32, no. 6, pp. 477–490, 2018.

[144] M. F. Pittenger, A. M. Mackay, S. C. Beck et al., "Multilineage potential of adult human mesenchymal stem cells," *Science*, vol. 284, no. 5411, pp. 143–147, 1999.

[145] L. Peng, Z. Jia, X. Yin et al., "Comparative analysis of mesenchymal stem cells from bone marrow, cartilage, and adipose tissue," *Stem Cells and Development*, vol. 17, no. 4, pp. 761–774, 2008.

[146] P. Bourin, B. A. Bunnell, L. Casteilla et al., "Stromal cells from the adipose tissue-derived stromal vascular fraction and culture expanded adipose tissue-derived stromal/stem cells: a joint statement of the International Federation for Adipose Therapeutics and Science (IFATS) and the International Society for Cellular Therapy (ISCT)," *Cytotherapy*, vol. 15, no. 6, pp. 641–648, 2013.

[147] J. W. Kuhbier, B. Weyand, C. Radtke, P. M. Vogt, C. Kasper, and K. Reimers, "Isolation, characterization, differentiation, and application of adipose-derived stem cells," *Advances in Biochemical Engineering/Biotechnology*, vol. 123, pp. 55–105, 2010.

[148] J. K. Fraser, I. Wulur, Z. Alfonso, and M. H. Hedrick, "Fat tissue: an underappreciated source of stem cells for biotechnology," *Trends in Biotechnology*, vol. 24, no. 4, pp. 150–154, 2006.

[149] R. A. Sabol, A. C. Bowles, A. Côté, R. Wise, N. Pashos, and B. A. Bunnell, "Therapeutic potential of adipose stem cells," *Advances in Experimental Medicine and Biology*, 2018.

[150] S. Kern, H. Eichler, J. Stoeve, H. Klüter, and K. Bieback, "Comparative analysis of mesenchymal stem cells from bone marrow, umbilical cord blood, or adipose tissue," *Stem Cells*, vol. 24, no. 5, pp. 1294–1301, 2006.

[151] B. Prunet-Marcassus, B. Cousin, D. Caton, M. André, L. Pénicaud, and L. Casteilla, "From heterogeneity to plasticity in adipose tissues: site-specific differences," *Experimental Cell Research*, vol. 312, no. 6, pp. 727–736, 2006.

[152] A. Kurzyk, T. Dębski, W. Święszkowski, and Z. Pojda, "Comparison of adipose stem cells sources from various locations of rat body for their application for seeding on polymer scaffolds," *Journal of Biomaterials Science Polymer Edition*, vol. 30, no. 5, pp. 376–397, 2019.

[153] L. Xu, Y. Liu, Y. Sun et al., "Tissue source determines the differentiation potentials of mesenchymal stem cells: a comparative study of human mesenchymal stem cells from bone marrow and adipose tissue," *Stem Cell Research & Therapy*, vol. 8, no. 1, p. 275, 2017.

[154] E. M. Fennema, L. A. H. Tchang, H. Yuan et al., "Ectopic bone formation by aggregated mesenchymal stem cells from bone marrow and adipose tissue: a comparative study," *Journal of Tissue Engineering and Regenerative Medicine*, vol. 12, no. 1, pp. e150–e158, 2018.

[155] W. J. Du, Y. Chi, Z. X. Yang et al., "Heterogeneity of proangiogenic features in mesenchymal stem cells derived from bone marrow, adipose tissue, umbilical cord, and placenta," *Stem Cell Research & Therapy*, vol. 7, no. 1, p. 163, 2016.

[156] J. S. Elman, M. Li, F. Wang, J. M. Gimble, and B. Parekkadan, "A comparison of adipose and bone marrow-derived mesenchymal stromal cell secreted factors in the treatment of systemic inflammation," *Journal of Inflammation*, vol. 11, no. 1, p. 1, 2014.

[157] K. M. Fawzy El-Sayed, S. Paris, C. Graetz et al., "Isolation and characterisation of human gingival margin-derived STRO-1/MACS$^+$ and MACS$^-$ cell populations," *International Journal of Oral Science*, vol. 7, no. 2, pp. 80–88, 2015.

[158] K. M. Fawzy El-Sayed, S. Paris, S. T. Becker et al., "Periodontal regeneration employing gingival margin-derived stem/-progenitor cells: an animal study," *Journal of Clinical Periodontology*, vol. 39, no. 9, pp. 861–870, 2012.

[159] K. M. Fawzy El-Sayed, S. Paris, S. Becker et al., "Isolation and characterization of multipotent postnatal stem/progenitor cells from human alveolar bone proper," *Journal of Cranio-Maxillofacial Surgery*, vol. 40, no. 8, pp. 735–742, 2012.

[160] K. M. Fawzy El-Sayed, C. Dorfer, H. Ungefroren, N. Kassem, J. Wiltfang, and S. Paris, "Effect of Emdogain enamel matrix derivative and BMP-2 on the gene expression and mineralized nodule formation of alveolar bone proper-derived stem/-progenitor cells," *Journal of Cranio-Maxillofacial Surgery*, vol. 42, no. 5, pp. 568–576, 2014.

[161] H. Egusa, W. Sonoyama, M. Nishimura, I. Atsuta, and K. Akiyama, "Stem cells in dentistry - part I: stem cell sources," *Journal of Prosthodontic Research*, vol. 56, no. 3, pp. 151–165, 2012.

[162] X. Wang, X.-J. Sha, G.-H. Li et al., "Comparative characterization of stem cells from human exfoliated deciduous teeth and dental pulp stem cells," *Archives of Oral Biology*, vol. 57, no. 9, pp. 1231–1240, 2012.

[163] M. F. Abdullah, S. F. Abdullah, N. S. Omar et al., "Proliferation rate of stem cells derived from human dental pulp and identification of differentially expressed genes," *Cell Biology International*, vol. 38, no. 5, pp. 582–590, 2014.

[164] G. T. J. Huang, S. Gronthos, and S. Shi, "Mesenchymal stem cells derived from dental tissues vs. those from other sources: their biology and role in regenerative medicine," *Journal of Dental Research*, vol. 88, no. 9, pp. 792–806, 2009.

[165] M. Rouabhia, "Advantages and limitations of oral stem cell use for oral tissue replacement," *Journal of Oral Biosciences*, vol. 2, no. 1, pp. 9–17, 2015.

[166] R. Hass, C. Kasper, S. Böhm, and R. Jacobs, "Different populations and sources of human mesenchymal stem cells (MSC): a comparison of adult and neonatal tissue-derived MSC," *Cell Communication and Signaling*, vol. 9, no. 1, 2011.

[167] H. J. Jin, Y. K. Bae, M. Kim et al., "Comparative analysis of human mesenchymal stem cells from bone marrow, adipose tissue, and umbilical cord blood as sources of cell therapy," *International Journal of Molecular Sciences*, vol. 14, no. 9, pp. 17986–18001, 2013.

[168] M. S. Choudhery, M. Badowski, A. Muise, and D. T. Harris, "Utility of cryopreserved umbilical cord tissue for regenerative medicine," *Current Stem Cell Research & Therapy*, vol. 8, no. 5, pp. 370–380, 2013.

[169] X. Zhang, M. Hirai, S. Cantero et al., "Isolation and characterization of mesenchymal stem cells from human umbilical cord blood: reevaluation of critical factors for successful isolation and high ability to proliferate and differentiate to chondrocytes as compared to mesenchymal stem cells from bone marrow and adipose tissue," *Journal of Cellular Biochemistry*, vol. 112, no. 4, pp. 1206–1218, 2011.

[170] M. A. Avanzini, M. E. Bernardo, A. M. Cometa et al., "Generation of mesenchymal stromal cells in the presence of platelet lysate: a phenotypic and functional comparison of umbilical cord blood- and bone marrow-derived progenitors," *Haematologica*, vol. 94, no. 12, pp. 1649–1660, 2009.

[171] M. Ziaei, J. Zhang, D. V. Patel, and C. N. J. McGhee, "Umbilical cord stem cells in the treatment of corneal disease," *Survey of Ophthalmology*, vol. 62, no. 6, pp. 803–815, 2017.

[172] A. J. Kaimal, C. C. Smith, R. K. Laros Jr., A. B. Caughey, and Y. W. Cheng, "Cost-effectiveness of private umbilical cord blood banking," *Obstetrics and Gynecology*, vol. 114, no. 4, pp. 848–855, 2009.

[173] K. J. Moise Jr., "Umbilical cord stem cells," *Obstetrics & Gynecology*, vol. 106, no. 6, pp. 1393–1407, 2005.

[174] K. K. Ballen, "Advances in umbilical cord blood transplantation," *Current Stem Cell Research & Therapy*, vol. 1, no. 3, pp. 317–324, 2006.

[175] R. Waller-Wise, "Umbilical cord blood: information for childbirth educators," *The Journal of Perinatal Education*, vol. 20, no. 1, pp. 54–60, 2011.

[176] B. Percer, "Umbilical cord blood banking: helping parents make informed choices," *Nursing for Women's Health*, vol. 13, no. 3, pp. 216–223, 2009.

[177] L. Gonzalez-Ryan, K. Van Syckle, K. D. Coyne, and N. Glover, "Umbilical cord blood banking: procedural and ethical concerns for this new birth option," *Pediatric Nursing*, vol. 26, no. 1, pp. 105–110, 2000.

[178] S. A. Wexler, C. Donaldson, P. Denning-Kendall, C. Rice, B. Bradley, and J. M. Hows, "Adult bone marrow is a rich source of human mesenchymal 'stem' cells but umbilical cord and mobilized adult blood are not," *British Journal of Haematology*, vol. 121, no. 2, pp. 368–374, 2003.

[179] A. Fierabracci, L. Lazzari, M. Muraca, and O. Parolini, "How far are we from the clinical use of placental-derived mesenchymal stem cells?," *Expert Opinion on Biological Therapy*, vol. 15, no. 5, pp. 613–617, 2015.

[180] F. Hendijani, "Explant culture: an advantageous method for isolation of mesenchymal stem cells from human tissues," *Cell Proliferation*, vol. 50, no. 2, article e12334, 2017.

[181] A. Nicodemou and L. Danisovic, "Mesenchymal stromal/-stem cell separation methods: concise review," *Cell and Tissue Banking*, vol. 18, no. 4, pp. 443–460, 2017.

[182] A. I. Caplan and D. Correa, "PDGF in bone formation and regeneration: New insights into a novel mechanism involving MSCs," *Journal of Orthopaedic Research*, vol. 29, no. 12, pp. 1795–1803, 2011.

[183] R. M. Samsonraj, B. Rai, P. Sathiyanathan et al., "Establishing criteria for human mesenchymal stem cell potency," *Stem Cells*, vol. 33, no. 6, pp. 1878–1891, 2015.

[184] H. Rozemuller, H.-J. Prins, B. Naaijkens, J. Staal, H.-J. Bühring, and A. C. Martens, "Prospective isolation of mesenchymal stem cells from multiple mammalian species using cross-reacting anti-human monoclonal antibodies," *Stem Cells and Development*, vol. 19, no. 12, pp. 1911–1921, 2010.

[185] S. Kuci, Z. Kuci, H. Kreyenberg et al., "CD271 antigen defines a subset of multipotent stromal cells with immunosuppressive and lymphohematopoietic engraftment-promoting properties," *Haematologica*, vol. 95, no. 4, pp. 651–659, 2010.

[186] M. J. Tomlinson, S. Tomlinson, X. B. Yang, and J. Kirkham, "Cell separation: terminology and practical considerations," *Journal of Tissue Engineering*, vol. 4, no. 1, 2012.

[187] M. Aguena, R. Dalto Fanganiello, L. A. L. Tissiani et al., "Optimization of parameters for a more efficient use of adipose-derived stem cells in regenerative medicine therapies," *Stem Cells International*, vol. 2012, Article ID 303610, 7 pages, 2012.

[188] E. Oberbauer, C. Steffenhagen, C. Wurzer, C. Gabriel, H. Redl, and S. Wolbank, "Enzymatic and non-enzymatic isolation systems for adipose tissue-derived cells: current state of the art," *Cell Regeneration*, vol. 4, no. 1, pp. 4–7, 2015.

[189] H.-S. Wang, S.-C. Hung, S.-T. Peng et al., "Mesenchymal stem cells in the Wharton's jelly of the human umbilical cord," *Stem Cells*, vol. 22, no. 7, pp. 1330–1337, 2004.

[190] A. Can and S. Karahuseyinoglu, "Concise review: human umbilical cord stroma with regard to the source of fetus-derived stem cells," *Stem Cells*, vol. 25, no. 11, pp. 2886–2895, 2007.

[191] K. E. Mitchell, M. L. Weiss, B. M. Mitchell et al., "Matrix cells from Wharton's jelly form neurons and glia," *Stem Cells*, vol. 21, no. 1, pp. 50–60, 2003.

[192] O. Fakhri and R. S. H. Tan, "The effect of trypsin on cell surface antigens," *Cellular Immunology*, vol. 15, no. 2, pp. 452–456, 1975.

[193] L. T. Furcht and G. Wendelschafer-Crabb, "Trypsin-induced coordinate alterations in cell shape, cytoskeleton, and intrinsic membrane structure of contact-inhibited cells," *Experimental Cell Research*, vol. 114, no. 1, pp. 1–14, 1978.

[194] C. K. Tong, S. Vellasamy, B. Chong Tan et al., "Generation of mesenchymal stem cell from human umbilical cord tissue using a combination enzymatic and mechanical disassociation method," *Cell Biology International*, vol. 35, no. 3, pp. 221–226, 2011.

[195] R. I. Freshney, *Culture of Animal Cells: A Manual of Basic Technique and Specialized Applicationsle*, Wiley-Blackwell, 6th edition, 2010.

[196] K. M. Fawzy El-Sayed, J. Boeckler, and C. E. Dorfer, "TLR expression profile of human alveolar bone proper-derived stem/progenitor cells and osteoblasts," *Journal of Cranio-Maxillofacial Surgery*, vol. 45, no. 12, pp. 2054–2060, 2017.

[197] K. M. Fawzy El-Sayed, M. K. Mekhemar, B. E. Beck-Broichsitter et al., "Periodontal regeneration employing gingival margin-derived stem/progenitor cells in conjunction with IL-1ra-hydrogel synthetic extracellular matrix," *Journal of Cranio-Maxillofacial Surgery*, vol. 42, no. 5, pp. 448–457, 2015.

[198] J. H. Yoon, E. Y. Roh, S. Shin et al., "Comparison of explant-derived and enzymatic digestion-derived MSCs and the growth factors from Wharton's jelly," *BioMed Research International*, vol. 2013, Article ID 428726, 8 pages, 2013.

[199] P. Salehinejad, N. B. Alitheen, A. M. Ali et al., "Comparison of different methods for the isolation of mesenchymal stem cells from human umbilical cord Wharton's jelly," *In Vitro Cellular and Developmental Biology-Animal*, vol. 48, no. 2, pp. 75–83, 2012.

[200] P. Hilkens, P. Gervois, Y. Fanton et al., "Effect of isolation methodology on stem cell properties and multilineage differentiation potential of human dental pulp stem cells," *Cell and Tissue Research*, vol. 353, no. 1, pp. 65–78, 2013.

[201] R. O. Hynes, "The extracellular matrix: not just pretty fibrils," *Science*, vol. 326, no. 5957, pp. 1216–1219, 2009.

[202] N. Priya, S. Sarcar, A. S. Majumdar, and S. Sundarraj, "Explant culture: a simple, reproducible, efficient and economic technique for isolation of mesenchymal stromal cells from human adipose tissue and lipoaspirate," *Journal of Tissue Engineering and Regenerative Medicine*, vol. 8, no. 9, pp. 706–716, 2014.

[203] B. Zhu and S. K. Murthy, "Stem cell separation technologies," *Current Opinion in Chemical Engineering*, vol. 2, no. 1, pp. 3–7, 2013.

[204] R. J. Cuthbert, P. V. Giannoudis, X. N. Wang et al., "Examining the feasibility of clinical grade CD271+ enrichment of mesenchymal stromal cells for bone regeneration," *PLoS One*, vol. 10, no. 3, article e0117855, 2015.

[205] D. Gothard, J. Greenhough, E. Ralph, and R. O. C. Oreffo, "Prospective isolation of human bone marrow stromal cell subsets: a comparative study between Stro-1-, CD146- and CD105-enriched populations," *Journal of Tissue Engineering*, vol. 5, Article ID 204173141455176, 2014.

[206] W. A. Bonner, H. R. Hulett, R. G. Sweet, and L. A. Herzenberg, "Fluorescence activated cell sorting," *Review of Scientific Instruments*, vol. 43, no. 3, pp. 404–409, 1972.

[207] S. Miltenyi, W. Müller, W. Weichel, and A. Radbruch, "High gradient magnetic cell separation with MACS," *Cytometry*, vol. 11, no. 2, pp. 231–238, 1990.

[208] T. W. E. Chippendale, A. Haj, K. Coopman, Q. Rafiq, and C. J. Hewitt, "Isolation of mesenchymal stem cells from bone marrow aspirate," in *Comprehensive Biotechnolgy. 5*, Medical Biotechnology and Healthcare, 2nd edition, 2011.

[209] S. T. Avecilla, C. Goss, S. Bleau, J. A. Tonon, and R. C. Meagher, "How do i perform hematopoietic progenitor cell selection?," *Transfusion*, vol. 56, no. 5, pp. 1008–1012, 2016.

[210] C. Wan, Q. He, M. McCaigue, D. Marsh, and G. Li, "Non-adherent cell population of human marrow culture is a complementary source of mesenchymal stem cells (MSCs)," *Journal of Orthopaedic Research*, vol. 24, no. 1, pp. 21–28, 2006.

[211] N. Di Maggio, A. Mehrkens, A. Papadimitropoulos et al., "Fibroblast growth factor-2 maintains a niche-dependent population of self-renewing highly potent non-adherent mesenchymal progenitors through FGFR2c," *Stem Cells*, vol. 30, no. 7, pp. 1455–1464, 2012.

[212] A. Mehrkens, N. di Maggio, S. Gueven et al., "Non-adherent mesenchymal progenitors from adipose tissue stromal vascular fraction," *Tissue Engineering-Part A*, vol. 20, no. 5-6, pp. 1081–1088, 2014.

[213] A. Orfao and A. Ruiz-Argüelles, "General concepts about cell sorting techniques," *Clinical Biochemistry*, vol. 29, no. 1, pp. 5–9, 1996.

[214] T. G. Fernandes, C. A. V. Rodrigues, M. M. Diogo, and J. M. S. Cabral, "Stem cell bioprocessing for regenerative medicine," *Journal of Chemical Technology & Biotechnology*, vol. 89, no. 1, pp. 34–47, 2014.

[215] E. M. Horwitz, R. T. Maziarz, and P. Kebriaei, "MSCs in hematopoietic cell transplantation," *Biology of Blood and Marrow Transplantation*, vol. 17, no. 1, pp. S21–S29, 2011.

[216] S. Jung, K. M. Panchalingam, L. Rosenberg, and L. A. Behie, "Ex vivo expansion of human mesenchymal stem cells in defined serum-free media," *Stem Cells International*, vol. 2012, Article ID 123030, 21 pages, 2012.

[217] K. Stenderup, J. Justesen, C. Clausen, and M. Kassem, "Aging is associated with decreased maximal life span and accelerated senescence of bone marrow stromal cells', " *Bone*, vol. 33, no. 6, pp. 919–926, 2003.

[218] M. Kassem, "Stem cells: potential therapy for age-related diseases," *Annals of the New York Academy of Sciences*, vol. 1067, no. 1, pp. 436–442, 2006.

[219] S. Zimmermann, M. Voss, S. Kaiser, U. Kapp, C. F. Waller, and U. M. Martens, "Lack of telomerase activity in human mesenchymal stem cells," *Leukemia*, vol. 17, no. 6, pp. 1146–1149, 2003.

[220] W. Wagner, S. Bork, P. Horn et al., "Aging and replicative senescence have related effects on human stem and progenitor cells," *PLoS One*, vol. 4, no. 6, article e5846, 2009.

[221] J. M. Karp and G. S. Leng Teo, "Mesenchymal stem cell homing: the devil is in the details," *Cell Stem Cell*, vol. 4, no. 3, pp. 206–216, 2009.

[222] U. Ben-David, Y. Mayshar, and N. Benvenisty, "Large-scale analysis reveals acquisition of lineage-specific chromosomal aberrations in human adult stem cells," *Cell Stem Cell*, vol. 9, no. 2, pp. 97–102, 2011.

[223] Q. Zhao, L. Zhang, Y. Wei et al., "Systematic comparison of hUC-MSCs at various passages reveals the variations of signatures and therapeutic effect on acute graft-versus-host disease," *Stem Cell Research & Therapy*, vol. 10, no. 1, p. 354, 2019.

[224] N. Serakinci, P. Guldberg, J. S. Burns et al., "Adult human mesenchymal stem cell as a target for neoplastic transformation," *Oncogene*, vol. 23, no. 29, pp. 5095–5098, 2004.

[225] S. Shi, S. Gronthos, S. Chen et al., "Bone formation by human postnatal bone marrow stromal stem cells is enhanced by telomerase expression," *Nature Biotechnology*, vol. 20, no. 6, pp. 587–591, 2002.

[226] S. K. Kang, L. Putnam, J. Dufour, J. Ylostalo, J. S. Jung, and B. A. Bunnell, "Expression of telomerase extends the lifespan and enhances osteogenic differentiation of adipose tissue-derived stromal cells," *Stem Cells*, vol. 22, no. 7, pp. 1356–1372, 2004.

[227] H. Saeed, W. Qiu, C. Li, A. Flyvbjerg, B. M. Abdallah, and M. Kassem, "Telomerase activity promotes osteoblast differentiation by modulating IGF-signaling pathway," *Biogerontology*, vol. 16, no. 6, pp. 733–745, 2015.

[228] H. L. Huang, H. W. Hsing, T. C. Lai et al., "Trypsin-induced proteome alteration during cell subculture in mammalian cells," *Journal of Biomedical Science*, vol. 17, no. 1, p. 36, 2010.

[229] F. A. Saleh, J. E. Frith, J. A. Lee, and P. G. Genever, "Three-dimensional in vitro culture techniques for mesenchymal

stem cells," *Methods in Molecular Biology*, vol. 916, pp. 31–45, 2012.

[230] A. J. Almarza and K. A. Athanasiou, "Effects of initial cell seeding density for the tissue engineering of the temporomandibular joint disc," *Annals of Biomedical Engineering*, vol. 33, no. 7, pp. 943–950, 2005.

[231] M. Bitar, R. A. Brown, V. Salih, A. G. Kidane, J. C. Knowles, and S. N. Nazhat, "Effect of cell density on osteoblastic differentiation and matrix degradation of biomimetic dense collagen scaffolds," *Biomacromolecules*, vol. 9, no. 1, pp. 129–135, 2008.

[232] L. Wang, K. Seshareddy, M. L. Weiss, and M. S. Detamore, "Effect of initial seeding density on human umbilical cord mesenchymal stromal cells for fibrocartilage tissue engineering," *Tissue Engineering-Part A*, vol. 15, no. 5, pp. 1009–1017, 2009.

[233] S. K. Both, A. J. C. Muijsenberg, C. A. Blitterswijk, J. Boer, and J. D. Bruijn, "A rapid and efficient method for expansion of human mesenchymal stem cells," *Tissue Engineering*, vol. 13, no. 1, pp. 3–9, 2007.

[234] A. Lode, A. Bernhardt, and M. Gelinsky, "Cultivation of human bone marrow stromal cells on three-dimensional scaffolds of mineralized collagen: influence of seeding density on colonization, proliferation and osteogenic differentiation," *Journal of Tissue Engineering and Regenerative Medicine*, vol. 2, no. 7, pp. 400–407, 2008.

[235] D. C. Colter, R. Class, C. M. DiGirolamo, and D. J. Prockop, "Rapid expansion of recycling stem cells in cultures of plastic-adherent cells from human bone marrow," *Proceedings of the National Academy of Sciences*, vol. 97, no. 7, pp. 3213–3218, 2000.

[236] B. Neuhuber, S. A. Swanger, L. Howard, A. Mackay, and I. Fischer, "Effects of plating density and culture time on bone marrow stromal cell characteristics," *Experimental Hematology*, vol. 36, no. 9, pp. 1176–1185, 2008.

[237] K. Mareschi, D. Rustichelli, R. Calabrese et al., "Multipotent mesenchymal stromal stem cell expansion by plating whole bone marrow at a low cellular density: a more advantageous method for clinical use," *Stem Cells International*, vol. 2012, Article ID 920581, 10 pages, 2012.

[238] C. Ikebe and K. Suzuki, "Mesenchymal stem cells for regenerative therapy: optimization of cell preparation protocols," *BioMed Research International*, vol. 2014, Article ID 951512, 11 pages, 2014.

[239] D. S. Kim, M. W. Lee, T. H. Lee, K. W. Sung, H. H. Koo, and K. H. Yoo, "Cell culture density affects the stemness gene expression of adipose tissue-derived mesenchymal stem cells," *Biomedical Reports*, vol. 6, no. 3, pp. 300–306, 2017.

[240] T. Y. Hui, K. M. C. Cheung, W. L. Cheung, D. Chan, and B. P. Chan, "In vitro chondrogenic differentiation of human mesenchymal stem cells in collagen microspheres: influence of cell seeding density and collagen concentration," *Biomaterials*, vol. 29, no. 22, pp. 3201–3212, 2008.

[241] S. Noda, N. Kawashima, M. Yamamoto et al., "Effect of cell culture density on dental pulp-derived mesenchymal stem cells with reference to osteogenic differentiation," *Scientific Reports*, vol. 9, no. 1, p. 5430, 2019.

[242] E. Fossett and W. S. Khan, "Optimising human mesenchymal stem cell numbers for clinical application: a literature review," *Stem Cells International*, vol. 2012, Article ID 465259, 5 pages, 2012.

[243] W. Gregory Hamilton and R. G. Ham, "Clonal growth of Chinese hamster cell lines in protein-free media," *In Vitro*, vol. 13, no. 9, pp. 537–547, 1977.

[244] M. Arora, "Cell culture media: a review," *Materials and Methods*, vol. 3, 2013.

[245] S. C. Serra, J. C. Costa, R. C. Assunção-Silva et al., "Influence of passage number on the impact of the secretome of adipose tissue stem cells on neural survival, neurodifferentiation and axonal growth," *Biochimie*, vol. 155, pp. 119–128, 2018.

[246] M. S. Lee, C. Youn, J. H. Kim et al., "Enhanced cell growth of adipocyte-derived mesenchymal stem cells using chemically-defined serum-free media," *International Journal of Molecular Sciences*, vol. 18, no. 8, p. 1779, 2017.

[247] Q. Zhang, X. Sun, J. Ding et al., "Autoserum: an optimal supplement for bone marrow mesenchymal stem cells of liver-injured rats," *Stem Cells International*, vol. 2015, Article ID 459580, 10 pages, 2015.

[248] A. A. Inamdar and A. C. Inamdar, "Culture conditions for growth of clinical grade human tissue derived mesenchymal stem cells: comparative study between commercial serum-free media and human product supplemented media," *Journal of Regenerative Medicine and Tissue Engineering*, vol. 2, no. 1, p. 10, 2013.

[249] A. Oikonomopoulos, W. K. van Deen, A.-R. Manansala et al., "Optimization of human mesenchymal stem cell manufacturing: the effects of animal/xeno-free media," *Scientific Reports*, vol. 5, no. 1, 2015.

[250] M. Cimino, R. M. Gonçalves, C. C. Barrias, and M. C. L. Martins, "Xeno-free strategies for safe human mesenchymal stem/stromal cell expansion: supplements and coatings," *Stem Cells International*, vol. 2017, Article ID 6597815, 13 pages, 2017.

[251] E. Fernandez-Rebollo, B. Mentrup, R. Ebert et al., "Human platelet lysate versus fetal calf serum: these supplements do not select for different mesenchymal stromal cells," *Scientific Reports*, vol. 7, no. 1, p. 5132, 2017.

[252] S. Kandoi, B. Patra, P. Vidyasekar et al., "Evaluation of platelet lysate as a substitute for FBS in explant and enzymatic isolation methods of human umbilical cord MSCs," *Scientific Reports*, vol. 8, no. 1, p. 12439, 2018.

[253] P. A. Sotiropoulou, S. A. Perez, M. Salagianni, C. N. Baxevanis, and M. Papamichail, "Characterization of the optimal culture conditions for clinical scale production of human mesenchymal stem cells," *Stem Cells*, vol. 24, no. 2, pp. 462–471, 2006.

[254] N. Beeravolu, I. Khan, C. McKee et al., "Isolation and comparative analysis of potential stem/progenitor cells from different regions of human umbilical cord," *Stem Cell Research*, vol. 16, no. 3, pp. 696–711, 2016.

[255] K. D. Lee, T. K. C. Kuo, J. Whang-Peng et al., "In vitro hepatic differentiation of human mesenchymal stem cells," *Hepatology*, vol. 40, no. 6, pp. 1275–1284, 2004.

[256] A. Hermann, R. Gastl, S. Liebau et al., "Efficient generation of neural stem cell-like cells from adult human bone marrow stromal cells," *Journal of Cell Science*, vol. 117, no. 19, pp. 4411–4422, 2004.

[257] K. L. Mung, Y. P. Tsui, E. W. Y. Tai, Y. S. Chan, D. K. Y. Shum, and G. K. H. Shea, "Rapid and efficient generation of neural progenitors from adult bone marrow stromal cells by hypoxic preconditioning," *Stem Cell Research & Therapy*, vol. 7, no. 1, p. 146, 2016.

[258] L. R. Devireddy, M. Myers, R. Screven, Z. Liu, and L. Boxer, "A serum-free medium formulation efficiently supports isolation and propagation of canine adipose-derived mesenchymal stem/stromal cells," *PLoS One*, vol. 14, no. 2, p. e0210250, 2019.

[259] K. Bieback, "Platelet lysate as replacement for fetal bovine serum in mesenchymal stromal cell cultures," *Transfusion Medicine and Hemotherapy*, vol. 40, no. 5, pp. 326–335, 2013.

[260] S. Riis, V. Zachar, S. Boucher, M. C. Vemuri, C. P. Pennisi, and T. Fink, "Critical steps in the isolation and expansion of adipose-derived stem cells for translational therapy," *Expert Reviews in Molecular Medicine*, vol. 17, article e11, 2015.

[261] S. J. Wessman and R. L. Levings, "Benefits and risks due to animal serum used in cell culture production," *Developments in Biological Standardization*, vol. 99, pp. 3–8, 1999.

[262] M. S. Even, C. B. Sandusky, and N. D. Barnard, "Serum-free hybridoma culture: ethical, scientific and safety considerations," *Trends in Biotechnology*, vol. 24, no. 3, pp. 105–108, 2006.

[263] J. van der Valk, D. Brunner, K. de Smet et al., "Optimization of chemically defined cell culture media - replacing fetal bovine serum in mammalian *in vitro* methods," *Toxicology in Vitro*, vol. 24, no. 4, pp. 1053–1063, 2010.

[264] A. Heiskanen, T. Satomaa, S. Tiitinen et al., "N-Glycolylneuraminic acid xenoantigen contamination of human embryonic and mesenchymal stem cells is substantially reversible," *Stem Cells*, vol. 25, no. 1, pp. 197–202, 2007.

[265] A. Ivan and L. L. Indrei, "Emergence of transmissible disorders, a continuous process–a new type of viral meningoencephalitis," *Revista medico-chirurgicala a Societatii de Medici si Naturalisti din Iasi*, vol. 104, no. 2, pp. 51–55, 2000.

[266] A. Mackensen, R. Dräger, M. Schlesier, R. Mertelsmann, and A. Lindemann, "Presence of IgE antibodies to bovine serum albumin in a patient developing anaphylaxis after vaccination with human peptide-pulsed dendritic cells," *Cancer Immunology Immunotherapy*, vol. 49, no. 3, pp. 152–156, 2000.

[267] T. A. Selvaggi, R. E. Walker, and T. A. Fleisher, "Development of antibodies to fetal calf serum with arthus-like reactions in human immunodeficiency virus-infected patients given syngeneic lymphocyte infusions," *Blood*, vol. 89, no. 3, pp. 776–779, 1997.

[268] J. L. Spees, C. A. Gregory, H. Singh et al., "Internalized antigens must be removed to prepare hypoimmunogenic mesenchymal stem cells for cell and gene therapy," *Molecular Therapy*, vol. 9, no. 5, pp. 747–756, 2004.

[269] M. Sundin, O. Ringdén, B. Sundberg, S. Nava, C. Götherström, and K. Le Blanc, "No alloantibodies against mesenchymal stromal cells, but presence of anti-fetal calf serum antibodies, after transplantation in allogeneic hematopoietic stem cell recipients," *Haematologica*, vol. 92, no. 9, pp. 1208–1215, 2007.

[270] L. Tuschong, S. L. Soenen, R. M. Blaese, F. Candotti, and L. M. Muul, "Immune response to fetal calf serum by two adenosine deaminase-deficient patients after T cell gene therapy," *Human Gene Therapy*, vol. 13, no. 13, pp. 1605–1610, 2002.

[271] C. A. Gregory, E. Reyes, M. J. Whitney, and J. L. Spees, "Enhanced engraftment of mesenchymal stem cells in a cutaneous wound model by culture in allogenic species-specific serum and administration in fibrin constructs," *Stem Cells*, vol. 24, no. 10, pp. 2232–2243, 2006.

[272] N. Haque, N. H. A. Kasim, and M. T. Rahman, "Optimization of pre-transplantation conditions to enhance the efficacy of mesenchymal stem cells," *International Journal of Biological Sciences*, vol. 11, no. 3, pp. 324–334, 2015.

[273] D. T. B. Shih and T. Burnouf, "Preparation, quality criteria, and properties of human blood platelet lysate supplements for *ex vivo* stem cell expansion," *New Biotechnology*, vol. 32, no. 1, pp. 199–211, 2015.

[274] M. Johnson, "Fetal bovine serum," *Materials and Methods*, vol. 2, 2012.

[275] K. C. Clause, L. J. Liu, and K. Tobita, "Directed stem cell differentiation: the role of physical forces," *Cell Communication & Adhesion*, vol. 17, no. 2, pp. 48–54, 2010.

[276] C. Tekkatte, G. P. Gunasingh, K. M. Cherian, and K. Sankaranarayanan, ""Humanized" stem cell culture techniques: the animal serum controversy," *Stem Cells International*, vol. 2011, Article ID 504723, 14 pages, 2011.

[277] F. Bertolero, M. E. Kaighn, R. F. Camalier, and U. Saffiotti, "Effects of serum and serum-derived factors on growth and differentiation of mouse keratinocytes," *In Vitro Cellular & Developmental Biology*, vol. 22, no. 7, pp. 423–428, 1986.

[278] X. Zheng, H. Baker, W. S. Hancock, F. Fawaz, M. McCaman, and E. Pungor Jr., "Proteomic analysis for the assessment of different lots of fetal bovine serum as a raw material for cell culture. Part IV. Application of proteomics to the manufacture of biological drugs," *Biotechnology Progress*, vol. 22, no. 5, pp. 1294–1300, 2006.

[279] S. Gottipamula, M. S. Muttigi, U. Kolkundkar, and R. N. Seetharam, "Serum-free media for the production of human mesenchymal stromal cells: a review," *Cell Proliferation*, vol. 46, no. 6, pp. 608–627, 2013.

[280] K. M. Panchalingam, S. Jung, L. Rosenberg, and L. A. Behie, "Bioprocessing strategies for the large-scale production of human mesenchymal stem cells: a review," *Stem Cell Research & Therapy*, vol. 6, no. 1, 2015.

[281] L. A. Solchaga, K. Penick, V. M. Goldberg, A. I. Caplan, and J. F. Welter, "Fibroblast growth factor-2 enhances proliferation and delays loss of chondrogenic potential in human adult bone-marrow-derived mesenchymal stem cells," *Tissue Engineering-Part A*, vol. 16, no. 3, pp. 1009–1019, 2010.

[282] K. Tamama, H. Kawasaki, and A. Wells, "Epidermal growth factor (EGF) treatment on multipotential stromal cells (MSCs). Possible enhancement of therapeutic potential of MSC," *BioMed Research International*, vol. 2010, Article ID 795385, 10 pages, 2010.

[283] H. Agata, N. Watanabe, Y. Ishii et al., "Feasibility and efficacy of bone tissue engineering using human bone marrow stromal cells cultivated in serum-free conditions," *Biochemical and Biophysical Research Communications*, vol. 382, no. 2, pp. 353–358, 2009.

[284] L. G. Chase, S. Yang, V. Zachar et al., "Development and characterization of a clinically compliant xeno-free culture medium in good manufacturing practice for human multipotent mesenchymal stem cells," *Stem Cells Translational Medicine*, vol. 1, no. 10, pp. 750–758, 2012.

[285] B. Lindroos, S. Boucher, L. Chase et al., "Serum-free, xeno-free culture media maintain the proliferation rate and

multipotentiality of adipose stem cells *in vitro*," *Cytotherapy*, vol. 11, no. 7, pp. 958–972, 2009.

[286] J. Zhang, J. Guan, X. Qi et al., "Dimethyloxaloylglycine promotes the angiogenic activity of mesenchymal stem cells derived from iPSCs via activation of the PI3K/Akt pathway for bone regeneration," *International Journal of Biological Sciences*, vol. 12, no. 6, pp. 639–652, 2016.

[287] K. Tateishi, et al.W. Ando, C. Higuchi et al., "Comparison of human serum with fetal bovine serum for expansion and differentiation of human synovial MSC: potential feasibility for clinical applications," *Cell Transplantation*, vol. 17, no. 5, pp. 549–557, 2008.

[288] T. Burnouf, D. Strunk, M. B. C. Koh, and K. Schallmoser, "Human platelet lysate: replacing fetal bovine serum as a gold standard for human cell propagation?," *Biomaterials*, vol. 76, pp. 371–387, 2016.

[289] J. Y. Lee, H. Nam, Y. J. Park et al., "The effects of platelet-rich plasma derived from human umbilical cord blood on the osteogenic differentiation of human dental stem cells," *In Vitro Cellular and Developmental Biology-Animal*, vol. 47, no. 2, pp. 157–164, 2011.

[290] N. Azouna, F. Jenhani, Z. Regaya et al., "Phenotypical and functional characteristics of mesenchymal stem cells from bone marrow: comparison of culture using different media supplemented with human platelet lysate or fetal bovine serum," *Stem Cell Research and Therapy*, vol. 3, no. 1, p. 6, 2012.

[291] S. Watatani, H. Terashi, K. Saigo et al., "Autologous platelet-rich plasma (PRP) is more useful than fetal calf serum (FCS) in adipose-derived stem cells (ADSCS) culture for bone regeneration," *International Journal of Oral and Maxillofacial Surgery*, vol. 34, p. 123, 2005.

[292] H. Abdelrazik, G. M. Spaggiari, L. Chiossone, and L. Moretta, "Mesenchymal stem cells expanded in human platelet lysate display a decreased inhibitory capacity on T- and NK-cell proliferation and function," *European Journal of Immunology*, vol. 41, no. 11, pp. 3281–3290, 2011.

[293] R. Crespo-Diaz, A. Behfar, G. W. Butler et al., "Platelet lysate consisting of a natural repair proteome supports human mesenchymal stem cell proliferation and chromosomal stability," *Cell Transplantation*, vol. 20, no. 6, pp. 797–812, 2011.

[294] N. Fekete, M. Gadelorge, D. Fürst et al., "Platelet lysate from whole blood-derived pooled platelet concentrates and apheresis-derived platelet concentrates for the isolation and expansion of human bone marrow mesenchymal stromal cells: production process, content and identification of active components," *Cytotherapy*, vol. 14, no. 5, pp. 540–554, 2012.

[295] A. Flemming, K. Schallmoser, D. Strunk, M. Stolk, H. D. Volk, and M. Seifert, "Immunomodulative efficacy of bone marrow-derived mesenchymal stem cells cultured in human platelet lysate," *Journal of Clinical Immunology*, vol. 31, no. 6, pp. 1143–1156, 2011.

[296] R. Gruber, F. Karreth, B. Kandler et al., "Platelet-released supernatants increase migration and proliferation, and decrease osteogenic differentiation of bone marrow-derived mesenchymal progenitor cells underin vitroconditions," *Platelets*, vol. 15, no. 1, pp. 29–35, 2009.

[297] H. Hemeda, B. Giebel, and W. Wagner, "Evaluation of human platelet lysate versus fetal bovine serum for culture of mesenchymal stromal cells," *Cytotherapy*, vol. 16, no. 2, pp. 170–180, 2014.

[298] M. Lohmann, G. Walenda, H. Hemeda et al., "Donor age of human platelet lysate affects proliferation and differentiation of mesenchymal stem cells," *PLoS ONE*, vol. 7, no. 5, article e37839, 2012.

[299] K. Schallmoser and D. Strunk, "Preparation of pooled human platelet lysate (pHPL) as an efficient supplement for animal serum-free human stem cell cultures," *Journal of Visualized Experiments*, vol. 32, article e1523, 2009.

[300] G. Walenda, H. Hemeda, R. K. Schneider, R. Merkel, B. Hoffmann, and W. Wagner, "Human platelet lysate gel provides a novel three dimensional-matrix for enhanced culture expansion of mesenchymal stromal cells," *Tissue Engineering-Part C: Methods*, vol. 18, no. 12, pp. 924–934, 2012.

[301] K. Schallmoser, C. Bartmann, E. Rohde et al., "Human platelet lysate can replace fetal bovine serum for clinical-scale expansion of functional mesenchymal stromal cells," *Transfusion*, vol. 47, no. 8, pp. 1436–1446, 2007.

[302] S. Viau, L. Chabrand, S. Eap et al., "Pathogen reduction through additive-free short-wave UV light irradiation retains the optimal efficacy of human platelet lysate for the expansion of human bone marrow mesenchymal stem cells," *PLoS One*, vol. 12, no. 8, article e181406, 2017.

[303] M. C. Corotchi, M. Popa, A. Remes, L. Sima, I. Gussi, and M. Lupu Plesu, "Isolation method and xeno-free culture conditions influence multipotent differentiation capacity of human Wharton's jelly-derived mesenchymal stem cells," *Stem Cell Research and Therapy*, vol. 4, no. 4, p. 81, 2013.

[304] J. M. Díez, E. Bauman, R. Gajardo, and J. I. Jorquera, "Culture of human mesenchymal stem cells using a candidate pharmaceutical grade xeno-free cell culture supplement derived from industrial human plasma pools," *Stem Cell Research and Therapy*, vol. 6, no. 1, 2015.

[305] A. Blázquez-Prunera, J. M. Díez, R. Gajardo, and S. Grancha, "Human mesenchymal stem cells maintain their phenotype, multipotentiality, and genetic stability when cultured using a defined xeno-free human plasma fraction," *Stem Cell Research and Therapy*, vol. 8, no. 1, p. 103, 2017.

[306] V. Becherucci, L. Piccini, S. Casamassima et al., "Human platelet lysate in mesenchymal stromal cell expansion according to a GMP grade protocol: a cell factory experience," *Stem Cell Research and Therapy*, vol. 9, no. 1, p. 124, 2018.

[307] J. Czapla, S. Matuszczak, K. Kulik et al., "The effect of culture media on large-scale expansion and characteristic of adipose tissue-derived mesenchymal stromal cells," *Stem Cell Research and Therapy*, vol. 10, no. 1, p. 235, 2019.

[308] Y. Wang, H. Wu, Z. Yang et al., "Human mesenchymal stem cells possess different biological characteristics but do not change their therapeutic potential when cultured in serum free medium," *Stem Cell Research and Therapy*, vol. 5, no. 6, p. 132, 2014.

[309] I. Silva-Cote, M. Cruz-Barrera, M. Cañas-Arboleda et al., "Strategy for the generation of engineered bone constructs based on umbilical cord mesenchymal stromal cells expanded with human platelet lysate," *Stem Cells International*, vol. 2019, 17 pages, 2019.

[310] J. Plumas, L. Chaperot, M. J. Richard, J. P. Molens, J. C. Bensa, and M. C. Favrot, "Mesenchymal stem cells induce apoptosis of activated T cells," *Leukemia*, vol. 19, no. 9, pp. 1597–1604, 2005.

[311] C. Menard, L. Pacelli, G. Bassi et al., "Clinical-grade mesenchymal stromal cells produced under various good manufacturing

practice processes differ in their immunomodulatory properties: standardization of immune quality controls," *Stem Cells and Development*, vol. 22, no. 12, pp. 1789–1801, 2013.

[312] A. Bakopoulou, D. Apatzidou, E. Aggelidou et al., "Isolation and prolonged expansion of oral mesenchymal stem cells under clinical-grade, GMP-compliant conditions differentially affects "stemness" properties," *Stem Cell Research and Therapy*, vol. 8, no. 1, p. 247, 2017.

[313] A. Skardal, T. Shupe, and A. Atala, "Organoid-on-a-chip and body-on-a-chip systems for drug screening and disease modeling," *Drug Discovery Today*, vol. 21, no. 9, pp. 1399–1411, 2016.

[314] S. G. Almalki and D. K. Agrawal, "Key transcription factors in the differentiation of mesenchymal stem cells," *Differentiation*, vol. 92, no. 1-2, pp. 41–51, 2016.

[315] H. Yamamoto, G. Quinn, A. Asari et al., "Differentiation of embryonic stem cells into hepatocytes: biological functions and therapeutic application," *Hepatology*, vol. 37, no. 5, pp. 983–993, 2003.

[316] C. McKee and G. R. Chaudhry, "Advances and challenges in stem cell culture," *Colloids and Surfaces B: Biointerfaces*, vol. 159, pp. 62–77, 2017.

[317] F. Guilak, D. M. Cohen, B. T. Estes, J. M. Gimble, W. Liedtke, and C. S. Chen, "Control of stem cell fate by physical interactions with the extracellular matrix," *Cell Stem Cell*, vol. 5, no. 1, pp. 17–26, 2009.

[318] E. Knight and S. Przyborski, "Advances in 3D cell culture technologies enabling tissue-like structures to be createdin vitro," *Journal of Anatomy*, vol. 227, no. 6, pp. 746–756, 2015.

[319] C. H. Thomas, J. H. Collier, C. S. Sfeir, and K. E. Healy, "Engineering gene expression and protein synthesis by modulation of nuclear shape," *Proceedings of the National Academy of Sciences of the United States of America*, vol. 99, no. 4, pp. 1972–1977, 2002.

[320] L. Vergani, M. Grattarola, and C. Nicolini, "Modifications of chromatin structure and gene expression following induced alterations of cellular shape," *International Journal of Biochemistry and Cell Biology*, vol. 36, no. 8, pp. 1447–1461, 2004.

[321] J. J. Bara, R. G. Richards, M. Alini, and M. J. Stoddart, "Concise review: bone marrow-derived mesenchymal stem cells change phenotype following in vitro culture: implications for basic research and the clinic," *Stem Cells*, vol. 32, no. 7, pp. 1713–1723, 2014.

[322] S. P. Bruder, N. Jaiswal, and S. E. Haynesworth, "Growth kinetics, self-renewal, and the osteogenic potential of purified human mesenchymal stem cells during extensive subcultivation and following cryopreservation," *Journal of Cellular Biochemistry*, vol. 64, no. 2, pp. 278–294, 1997.

[323] J. W. Haycock, "3D cell culture: a review of current approaches and techniques," *3D Cell Culture*, vol. 695, pp. 1–15, 2011.

[324] J. Lee, M. J. Cuddihy, and N. A. Kotov, "Three-dimensional cell culture matrices: state of the art," *Tissue Engineering Part B: Reviews*, vol. 14, no. 1, pp. 61–86, 2008.

[325] L. Jongpaiboonkit, W. J. King, and W. L. Murphy, "Screening for 3D environments that support human mesenchymal stem cell viability using hydrogel arrays," *Tissue Engineering-Part A*, vol. 15, no. 2, pp. 343–353, 2009.

[326] C. R. Kothapalli and R. D. Kamm, "3D matrix microenvironment for targeted differentiation of embryonic stem cells into neural and glial lineages," *Biomaterials*, vol. 34, no. 25, pp. 5995–6007, 2013.

[327] P. R. Baraniak and T. C. McDevitt, "Scaffold-free culture of mesenchymal stem cell spheroids in suspension preserves multilineage potential," *Cell and Tissue Research*, vol. 347, no. 3, pp. 701–711, 2012.

[328] V. Miceli, M. Pampalone, S. Vella, A. P. Carreca, G. Amico, and P. G. Conaldi, "Comparison of immunosuppressive and angiogenic properties of human amnion- derived mesenchymal stem cells between 2D and 3D culture systems," *Stem Cells International*, vol. 2019, Article ID 7486279, 16 pages, 2019.

[329] H. M. Cha, S. M. Kim, Y. S. Choi, and D. I. Kim, "Scaffold-free three-dimensional culture systems for mass production of periosteum-derived progenitor cells," *Journal of Bioscience and Bioengineering*, vol. 120, no. 2, pp. 218–222, 2015.

[330] A. Abbott, "Biology's new dimension," *Nature*, vol. 424, no. 6951, pp. 870–872, 2003.

[331] T. J. Bartosh, J. H. Ylostalo, A. Mohammadipoor et al., "Aggregation of human mesenchymal stromal cells (MSCs) into 3D spheroids enhances their antiinflammatory properties," *Proceedings of the National Academy of Sciences of the United States of America*, vol. 107, no. 31, pp. 13724–13729, 2010.

[332] S. Alimperti, P. Lei, Y. Wen, J. Tian, A. M. Campbell, and S. T. Andreadis, "Serum-free spheroid suspension culture maintains mesenchymal stem cell proliferation and differentiation potential," *Biotechnology Progress*, vol. 30, no. 4, pp. 974–983, 2014.

[333] A. E. Watts, J. C. Ackerman-Yost, and A. J. Nixon, "A comparison of three-dimensional culture systems to evaluate in vitro chondrogenesis of equine bone marrow-derived mesenchymal stem cells," *Tissue Engineering-Part A*, vol. 19, no. 19-20, pp. 2275–2283, 2013.

[334] J. Li, T. Chen, X. Huang et al., "Substrate-independent immunomodulatory characteristics of mesenchymal stem cells in three-dimensional culture," *PLoS ONE*, vol. 13, no. 11, p. e0206811, 2018.

[335] D. A. Gaspar, V. Gomide, and F. J. Monteiro, "The role of perfusion bioreactors in bone tissue engineering," *Biomatter*, vol. 2, no. 4, pp. 167–175, 2014.

[336] L. E. Freed, F. Guilak, X. E. Guo et al., "Advanced tools for tissue engineering: scaffolds, bioreactors, and signaling," *Tissue Engineering*, vol. 12, no. 12, pp. 3285–3305, 2006.

[337] A. M. Bratt-Leal, R. L. Carpenedo, M. D. Ungrin, P. W. Zandstra, and T. C. McDevitt, "Incorporation of biomaterials in multicellular aggregates modulates pluripotent stem cell differentiation," *Biomaterials*, vol. 32, no. 1, pp. 48–56, 2011.

[338] S. M. Dellatore, A. S. Garcia, and W. M. Miller, "Mimicking stem cell niches to increase stem cell expansion," *Current Opinion in Biotechnology*, vol. 19, no. 5, pp. 534–540, 2008.

[339] R. C. Dutta and A. K. Dutta, "Cell-interactive 3D-scaffold; advances and applications," *Biotechnology Advances*, vol. 27, no. 4, pp. 334–339, 2009.

[340] T. P. Kraehenbuehl, R. Langer, and L. S. Ferreira, "Three-dimensional biomaterials for the study of human pluripotent stem cells," *Nature methods*, vol. 8, no. 9, pp. 731–736, 2011.

[341] I. Marijanovic, M. Antunovic, I. Matic, M. Panek, and A. Ivkovic, *Bioreactor-Based Bone Tissue Engineering*, InTech, 2016.

[342] S. Jung, K. M. Panchalingam, R. D. Wuerth, L. Rosenberg, and L. A. Behie, "Large-scale production of human mesenchymal stem cells for clinical applications," *Biotechnology and Applied Biochemistry*, vol. 59, no. 2, pp. 106–120, 2012.

[343] Y. Tang, Y. Xu, Z. Xiao et al., "The combination of three-dimensional and rotary cell culture system promotes the proliferation and maintains the differentiation potential of rat BMSCs," *Scientific Reports*, vol. 7, no. 1, p. 192, 2017.

[344] A. Mizukami and K. Swiech, "Mesenchymal stromal cells: from discovery to manufacturing and commercialization," *Stem Cells International*, vol. 2018, Article ID 4083921, 13 pages, 2018.

[345] V. Jossen, R. Pörtner, S. C. Kaiser, M. Kraume, D. Eibl, and R. Eibl, *Mass Production of Mesenchymal Stem Cells — Impact of Bioreactor Design and Flow Conditions on Proliferation and Differentiation*, InTech, 2014.

[346] J. Rauh, F. Milan, K. P. Günther, and M. Stiehler, "Bioreactor systems for bone tissue engineering," *Tissue Engineering-Part B: Reviews*, vol. 17, no. 4, pp. 263–280, 2011.

[347] L. M. Allen, J. Matyas, M. Ungrin, D. A. Hart, and A. Sen, "Serum-free culture of human mesenchymal stem cell aggregates in suspension bioreactors for tissue engineering applications," *Stem Cells International*, vol. 2019, 18 pages, 2019.

[348] R. Das, R. Roosloot, M. van Pel et al., "Preparing for cell culture scale-out: establishing parity of bioreactor- and flask-expanded mesenchymal stromal cell cultures," *Journal of Translational Medicine*, vol. 17, no. 1, p. 241, 2019.

[349] J. Cao, B. Wang, T. Tang et al., "Three-dimensional culture of MSCs produces exosomes with improved yield and enhanced therapeutic efficacy for cisplatin-induced acute kidney injury," *Stem Cell Research & Therapy*, vol. 11, no. 1, p. 206, 2020.

[350] C. Granet, N. Laroche, L. Vico, C. Alexandre, and M. H. Lafage-Proust, "Rotating-wall vessels, promising bioreactors for osteoblastic cell culture: comparison with other 3D conditions," *Medical and Biological Engineering and Computing*, vol. 36, no. 4, pp. 513–519, 1998.

[351] M. Sladkova and G. de Peppo, "Bioreactor systems for human bone tissue engineering," *Processes*, vol. 2, no. 2, pp. 494–525, 2014.

[352] S. A. Kuznetsov, N. Cherman, and P. G. Robey, "In vivo bone formation by progeny of human embryonic stem cells," *Stem Cells and Development*, vol. 20, no. 2, pp. 269–287, 2011.

[353] K. H. Vining and D. J. Mooney, "Mechanical forces direct stem cell behaviour in development and regeneration," *Nature Reviews Molecular Cell Biology*, vol. 18, no. 12, pp. 728–742, 2017.

[354] C. A. V. Rodrigues, T. G. Fernandes, M. M. Diogo, C. L. da Silva, and J. M. S. Cabral, "Stem cell cultivation in bioreactors," *Biotechnology Advances*, vol. 29, no. 6, pp. 815–829, 2011.

[355] A. B. Yeatts and J. P. Fisher, "Bone tissue engineering bioreactors: dynamic culture and the influence of shear stress," *Bone*, vol. 48, no. 2, pp. 171–181, 2011.

[356] B. Subia, J. Kundu, and S. C. Kundu, "Biomaterial scaffold fabrication techniques for potential tissue engineering applications," *Tissue Engnineering*, vol. 3, pp. 141–159, 2010.

[357] F. K. Kasper, J. Liao, J. D. Kretlow, V. I. Sikavitsas, and A. G. Mikos, "Flow perfusion culture of mesenchymal stem cells for bone tissue engineering," in *Stem Book*, Harvard Stem Cell Institute, 2008.

[358] W. L. Grayson, F. Zhao, B. Bunnell, and T. Ma, "Hypoxia enhances proliferation and tissue formation of human mesenchymal stem cells," *Biochemical and Biophysical Research Communications*, vol. 358, no. 3, pp. 948–953, 2007.

[359] Y. S. Han, J. H. Lee, Y. M. Yoon, C. W. Yun, H. Noh, and S. H. Lee, "Hypoxia-induced expression of cellular prion protein improves the therapeutic potential of mesenchymal stem cells," *Cell Death and Disease*, vol. 7, no. 10, p. e2395, 2016.

[360] J. Liu, H. Hao, H. Huang et al., "Hypoxia regulates the therapeutic potential of mesenchymal stem cells through enhanced autophagy," *International Journal of Lower Extremity Wounds*, vol. 14, no. 1, pp. 63–72, 2015.

[361] L. P. Zhu, T. Tian, J. Y. Wang et al., "Hypoxia-elicited mesenchymal stem cell-derived exosomes facilitates cardiac repair through miR-125b-mediated prevention of cell death in myocardial infarction," *Theranostics*, vol. 8, no. 22, pp. 6163–6177, 2018.

[362] M. Santoro, T. O. Awosika, K. L. Snodderly, A. C. Hurley-Novatny, M. J. Lerman, and J. P. Fisher, "Endothelial/mesenchymal stem cell crosstalk within bioprinted cocultures," *Tissue Engineering-Part A*, vol. 26, no. 5-6, pp. 339–349, 2020.

[363] H. G. Wisniewski and J. Vilček, "Cytokine-induced gene expression at the crossroads of innate immunity, inflammation and fertility: TSG-6 and PTX3/TSG-14," *Cytokine & Growth Factor Reviews*, vol. 15, no. 2-3, pp. 129–146, 2004.

[364] T. Menge, M. Gerber, K. Wataha et al., "Human mesenchymal stem cells inhibit endothelial proliferation and angiogenesis via cell-cell contact through modulation of the VE-Cadherin/β-catenin signaling pathway," *Stem Cells and Development*, vol. 22, no. 1, pp. 148–157, 2013.

[365] M. Rodrigues, L. G. Griffith, and A. Wells, "Growth factor regulation of proliferation and survival of multipotential stromal cells," *Stem Cell Research and Therapy*, vol. 1, no. 4, p. 32, 2010.

[366] P. M. van der Kraan, E. N. Blaney Davidson, A. Blom, and W. B. van den Berg, "TGF-beta signaling in chondrocyte terminal differentiation and osteoarthritis:," *Osteoarthritis Cartilage*, vol. 17, no. 12, pp. 1539–1545, 2009.

[367] A. M. Mackay, S. C. Beck, J. M. Murphy, F. P. Barry, C. O. Chichester, and M. F. Pittenger, "Chondrogenic differentiation of cultured human mesenchymal stem cells from marrow," *Tissue Engineering*, vol. 4, no. 4, pp. 415–428, 1998.

[368] F. Barry, R. E. Boynton, B. Liu, and J. M. Murphy, "Chondrogenic differentiation of mesenchymal stem cells from bone marrow: differentiation-dependent gene expression of matrix components," *Experimental Cell Research*, vol. 268, no. 2, pp. 189–200, 2001.

[369] R. Tuli, S. Tuli, S. Nandi et al., "Transforming growth factor-β-mediated chondrogenesis of human mesenchymal progenitor cells involves N-cadherin and mitogen-activated protein kinase and Wnt signaling cross-talk," *Journal of Biological Chemistry*, vol. 278, no. 42, pp. 41227–41236, 2003.

[370] T. Ogawa, T. Akazawa, and Y. Tabata, "In vitro proliferation and chondrogenic differentiation of rat bone marrow stem cells cultured with gelatin hydrogel microspheres for TGF-β1 release," *Journal of Biomaterials Science, Polymer Edition*, vol. 21, no. 5, pp. 609–621, 2012.

[371] H. Afizah, Z. Yang, J. H. P. Hui, H. W. Ouyang, and E. H. Lee, "A comparison between the chondrogenic potential of

human bone marrow stem cells (BMSCs) and adipose-derived stem cells (ADSCs) taken from the same donors," *Tissue Engineering*, vol. 13, no. 4, pp. 659–666, 2007.

[372] C. Vinatier, D. Mrugala, C. Jorgensen, J. Guicheux, and D. Noël, "Cartilage engineering: a crucial combination of cells, biomaterials and biofactors," *Trends in Biotechnology*, vol. 27, no. 5, pp. 307–314, 2009.

[373] C. M. Leonard, H. M. Fuld, D. A. Frenz, S. A. Downie, J. Massague, and S. A. Newman, "Role of transforming growth factor-β in chondrogenic pattern formation in the embryonic limb: stimulation of mesenchymal condensation and fibronectin gene expression by exogenenous TGF-β and evidence for endogenous TGF-β-like activity," *Developmental Biology*, vol. 145, no. 1, pp. 99–109, 1991.

[374] W. M. Kulyk, B. J. Rodgers, K. Greer, and R. A. Kosher, "Promotion of embryonic chick limb cartilage differentiation by transforming growth factor-β," *Developmental Biology*, vol. 135, no. 2, pp. 424–430, 1989.

[375] R. T. Ballock, A. Heydemann, L. M. Wakefield, K. C. Flanders, A. B. Roberts, and M. B. Sporn, "TGF-β1 prevents hypertrophy of epiphyseal chondrocytes: regulation of gene expression for cartilage matrix proteins and metalloproteases," *Developmental Biology*, vol. 158, no. 2, pp. 414–429, 1993.

[376] E. J. Van Zoelen, I. Duarte, J. M. Hendriks, and S. P. Van Der Woning, "TGFβ-induced switch from adipogenic to osteogenic differentiation of human mesenchymal stem cells: identification of drug targets for prevention of fat cell differentiation," *Stem Cell Research and Therapy*, vol. 7, no. 1, p. 123, 2016.

[377] S. Walsh, C. Jefferiss, K. Stewart, and J. N. Beresford, "TGFbeta1 limits the expansion of the osteoprogenitor fraction in cultures of human bone marrow stromal cells," *Cell and Tissue Research*, vol. 311, no. 2, pp. 187–198, 2003.

[378] R. N. Wang, J. Green, Z. Wang et al., "Bone morphogenetic protein (BMP) signaling in development and human diseases," *Genes & Diseases*, vol. 1, no. 1, pp. 87–105, 2014.

[379] Z. L. Deng, K. A. Sharff, N. Tang et al., "Regulation of osteogenic differentiation during skeletal development," *Frontiers in Bioscience*, vol. 13, no. 13, pp. 2001–2021, 2008.

[380] H. H. Luu, W. X. Song, X. Luo et al., "Distinct roles of bone morphogenetic proteins in osteogenic differentiation of mesenchymal stem cells," *Journal of Orthopaedic Research*, vol. 25, no. 5, pp. 665–677, 2007.

[381] T. C. He, "Distinct osteogenic activity of BMPs and their orthopaedic applications," *Journal of Musculoskeletal and Neuronal Interactions*, vol. 5, no. 4, pp. 363–366, 2005.

[382] Q. Kang, W. X. Song, Q. Luo et al., "A comprehensive analysis of the dual roles of BMPs in regulating adipogenic and osteogenic differentiation of mesenchymal progenitor cells," *Stem Cells and Development*, vol. 18, no. 4, pp. 545–558, 2009.

[383] Q. Luo, Q. Kang, W. Si et al., "Connective tissue growth factor (CTGF) is regulated by Wnt and bone morphogenetic proteins signaling in osteoblast differentiation of mesenchymal stem cells," *Journal of Biological Chemistry*, vol. 279, no. 53, pp. 55958–55968, 2004.

[384] Y. Peng, Q. Kang, H. Cheng et al., "Transcriptional characterization of bone morphogenetic proteins (BMPs)-mediated osteogenic signaling," *Journal of Cellular Biochemistry*, vol. 90, no. 6, pp. 1149–1165, 2003.

[385] Y. Peng, Q. Kang, Q. Luo et al., "Inhibitor of DNA binding/-differentiation helix-loop-helix proteins mediate bone morphogenetic protein-induced osteoblast differentiation of mesenchymal stem cells," *Journal of Biological Chemistry*, vol. 279, no. 31, pp. 32941–32949, 2004.

[386] K. Gu, L. Zhang, T. Jin, and R. B. Rutherford, "Identification of potential modifiers of Runx 2/Cbfa 1 activity in C2C12 cells in response to bone morphogenetic protein-7," *Cells Tissues Organs*, vol. 176, no. 1-3, pp. 28–40, 2004.

[387] G. Luther, E. R. Wagner, G. Zhu et al., "BMP-9 induced osteogenic differentiation of mesenchymal stem cells: molecular mechanism and therapeutic potential," *Current Gene Therapy*, vol. 11, no. 3, pp. 229–240, 2011.

[388] J. D. Lamplot, J. Qin, G. Nan et al., "BMP9 signaling in stem cell differentiation and osteogenesis," *American Journal of Stem Cells*, vol. 2, no. 1, pp. 1–21, 2013.

[389] Q. Kang, M. H. Sun, H. Cheng et al., "Characterization of the distinct orthotopic bone-forming activity of 14 BMPs using recombinant adenovirus-mediated gene delivery," *Gene Therapy*, vol. 11, no. 17, pp. 1312–1320, 2004.

[390] B. Schmitt, J. Ringe, T. Häupl et al., "BMP2 initiates chondrogenic lineage development of adult human mesenchymal stem cells in high-density culture," *Differentiation*, vol. 71, no. 9-10, pp. 567–577, 2003.

[391] I. Sekiya, B. L. Larson, J. T. Vuoristo, R. L. Reger, and D. J. Prockop, "Comparison of effect of BMP-2, -4, and -6 on in vitro cartilage formation of human adult stem cells from bone marrow stroma," *Cell and Tissue Research*, vol. 320, no. 2, pp. 269–276, 2005.

[392] I. Sekiya, D. C. Colter, and D. J. Prockop, "BMP-6 enhances chondrogenesis in a subpopulation of human marrow stromal cells," *Biochemical and Biophysical Research Communications*, vol. 284, no. 2, pp. 411–418, 2001.

[393] A. Stewart, H. Guan, and K. Yang, "BMP-3 promotes mesenchymal stem cell proliferation through the TGF-beta/activin signaling pathway," *Journal of Cellular Physiology*, vol. 223, no. 3, pp. 658–666, 2010.

[394] J. Pons, Y. Huang, J. Arakawa-Hoyt et al., "VEGF improves survival of mesenchymal stem cells in infarcted hearts," *Biochemical and Biophysical Research Communications*, vol. 376, no. 2, pp. 419–422, 2008.

[395] Y. Liu, et al.A. D. Berendsen, S. Jia et al., "Intracellular VEGF regulates the balance between osteoblast and adipocyte differentiation," *Journal of Clinical Investigation*, vol. 122, no. 9, pp. 3101–3113, 2012.

[396] M. Khaki, A. H. Salmanian, H. Abtahi, A. Ganji, and G. Mosayebi, "Mesenchymal stem cells differentiate to endothelial cells using recombinant vascular endothelial growth factor -A," *Reports of Biochemistry & Molecular Biology*, vol. 6, no. 2, pp. 144–150, 2018.

[397] K. Jin, B. Li, L. Lou et al., "In vivo vascularization of MSC-loaded porous hydroxyapatite constructs coated with VEGF-functionalized collagen/heparin multilayers," *Scientific Reports*, vol. 6, no. 1, 2016.

[398] A. Marsano, C. M. Medeiros da Cunha, S. Ghanaati et al., "Spontaneous in vivo chondrogenesis of bone marrow-derived mesenchymal progenitor cells by blocking vascular endothelial growth factor signaling," *Stem Cells Translational Medicine*, vol. 5, no. 12, pp. 1730–1738, 2016.

[399] G. C. Hughes, S. S. Biswas, B. Yin et al., "Therapeutic angiogenesis in chronically ischemic porcine myocardium:

comparative effects of bFGF and VEGF," *Annals of Thoracic Surgery*, vol. 77, no. 3, pp. 812–818, 2004.

[400] A. Schmidt, D. Ladage, T. Schinköthe et al., "Basic fibroblast growth factor controls migration in human mesenchymal stem cells," *Stem Cells*, vol. 24, no. 7, pp. 1750–1758, 2006.

[401] Y. W. Eom, J. E. Oh, J. I. Lee et al., "The role of growth factors in maintenance of stemness in bone marrow-derived mesenchymal stem cells," *Biochemical and Biophysical Research Communications*, vol. 445, no. 1, pp. 16–22, 2014.

[402] S. C. Choi, S. J. Kim, J. H. Choi, C. Y. Park, W. J. Shim, and D. S. Lim, "Fibroblast growth factor-2 and -4 promote the proliferation of bone marrow mesenchymal stem cells by the activation of the PI3K-Akt and ERK1/2 signaling pathways," *Stem Cells and Development*, vol. 17, no. 4, pp. 725–736, 2008.

[403] T. Osathanon, N. Nowwarote, and P. Pavasant, "Basic fibroblast growth factor inhibits mineralization but induces neuronal differentiation by human dental pulp stem cells through a FGFR and PLCγ signaling pathway," *Journal of Cellular Biochemistry*, vol. 112, no. 7, pp. 1807–1816, 2011.

[404] L. A. Solchaga, K. Penick, J. D. Porter, V. M. Goldberg, A. I. Caplan, and J. F. Welter, "FGF-2 enhances the mitotic and chondrogenic potentials of human adult bone marrow-derived mesenchymal stem cells," *Journal of Cellular Physiology*, vol. 203, no. 2, pp. 398–409, 2005.

[405] L. Varas, L. B. Ohlsson, G. Honeth et al., "α10 integrin expression is up-regulated on fibroblast growth factor-2-treated mesenchymal stem cells with improved chondrogenic differentiation potential," *Stem Cells and Development*, vol. 16, no. 6, pp. 965–978, 2007.

[406] M. Neubauer, C. Fischbach, P. Bauer-Kreisel et al., "Basic fibroblast growth factor enhances PPARγ ligand-induced adipogenesis of mesenchymal stem cells," *FEBS Letters*, vol. 577, no. 1-2, pp. 277–283, 2004.

[407] K. Hanada, J. E. Dennis, and A. I. Caplan, "Stimulatory effects of basic fibroblast growth factor and bone morphogenetic protein-2 on osteogenic differentiation of rat bone marrow-derived mesenchymal stem cells," *Journal of Bone and Mineral Research*, vol. 12, no. 10, pp. 1606–1614, 1997.

[408] A. Scutt and P. Bertram, "Basic fibroblast growth factor in the presence of dexamethasone stimulates colony formation, expansion, and osteoblastic differentiation by rat bone marrow stromal cells," *Calcified Tissue International*, vol. 64, no. 1, pp. 69–77, 1999.

[409] R. Visser, P. M. Arrabal, L. Santos-Ruiz, J. Becerra, and M. Cifuentes, "Basic fibroblast growth factor enhances the osteogenic differentiation induced by bone morphogenetic protein-6 *in vitro* and *in vivo*," *Cytokine*, vol. 58, no. 1, pp. 27–33, 2012.

[410] W. T. Lai, V. Krishnappa, and D. G. Phinney, "Fibroblast growth factor 2 (Fgf 2) inhibits differentiation of mesenchymal stem cells by inducing Twist 2 and Spry 4, blocking extracellular regulated kinase activation, and altering fgf receptor expression levels," *Stem Cells*, vol. 29, no. 7, pp. 1102–1111, 2011.

[411] S. Le Blanc, M. Simann, F. Jakob, N. Schütze, and T. Schilling, "Fibroblast growth factors 1 and 2 inhibit adipogenesis of human bone marrow stromal cells in 3D collagen gels," *Experimental Cell Research*, vol. 338, no. 2, pp. 136–148, 2015.

[412] M. Simann, S. le Blanc, V. Schneider et al., "Canonical FGFs prevent osteogenic lineage commitment and differentiation of human bone marrow stromal cells via ERK1/2 signaling," *Journal of Cellular Biochemistry*, vol. 118, no. 2, pp. 263–275, 2017.

[413] R. Wang, W. Liu, M. Du, C. Yang, X. Li, and P. Yang, "The differential effect of basic fibroblast growth factor and stromal cell-derived factor-1 pretreatment on bone morrow mesenchymal stem cells osteogenic differentiation potency," *Molecular Medicine Reports*, vol. 17, no. 3, pp. 3715–3721, 2018.

[414] J. Andrae, R. Gallini, and C. Betsholtz, "Role of platelet-derived growth factors in physiology and medicine," *Genes & Development*, vol. 22, no. 10, pp. 1276–1312, 2008.

[415] A. Li, X. Xia, J. Yeh et al., "PDGF-AA promotes osteogenic differentiation and migration of mesenchymal stem cell by down-regulating PDGFRα and derepressing BMP-Smad1/5/8 signaling," *PLoS ONE*, vol. 9, no. 12, p. e113785, 2014.

[416] J.-m. Zhang, F.-e. Feng, Q.-m. Wang et al., "Platelet-derived growth factor-BB protects mesenchymal stem cells (MSCs) derived from immune thrombocytopenia patients against apoptosis and senescence and maintains MSC-mediated immunosuppression," *STEM CELLS Translational Medicine*, vol. 5, no. 12, pp. 1631–1643, 2016.

[417] L. G. Chase, U. Lakshmipathy, L. A. Solchaga, M. S. Rao, and M. C. Vemuri, "A novel serum-free medium for the expansion of human mesenchymal stem cells," *Stem Cell Research and Therapy*, vol. 1, no. 1, p. 8, 2010.

[418] J. A. Heslop, T. G. Hammond, I. Santeramo et al., "Concise review: workshop review: understanding and assessing the risks of stem cell-based therapies," *STEM CELLS Translational Medicine*, vol. 4, no. 4, pp. 389–400, 2015.

[419] H. C. Li, C. Stoicov, A. B. Rogers, and J. M. Houghton, "Stem cells and cancer: evidence for bone marrow stem cells in epithelial cancers," *World Journal of Gastroenterology*, vol. 12, no. 3, pp. 363–371, 2006.

[420] Z. Liang, T. Wu, H. Lou et al., "Inhibition of breast cancer metastasis by selective synthetic polypeptide against CXCR4," *Cancer Research*, vol. 64, no. 12, pp. 4302–4308, 2004.

[421] D. Lyden, K. Hattori, S. Dias et al., "Impaired recruitment of bone-marrow-derived endothelial and hematopoietic precursor cells blocks tumor angiogenesis and growth," *Nature Medicine*, vol. 7, no. 11, pp. 1194–1201, 2001.

[422] M. del Carmen Rodríguez, A. Bernad, M. Fau-Aracil, and M. Aracil, "Interleukin-6 deficiency affects bone marrow stromal precursors, resulting in defective hematopoietic support," *Blood*, vol. 103, no. 9, pp. 3349–3354, 2004.

[423] K. Toh, T. Kukita, Z. Wu et al., "Possible involvement of *MIP-1α* in the recruitment of osteoclast progenitors to the distal tibia in rats with adjuvant-induced arthritis," *Laboratory Investigation*, vol. 84, no. 9, pp. 1092–1102, 2004.

[424] T. Reya, S. J. Morrison, M. F. Clarke, and I. L. Weissman, "Stem cells, cancer, and cancer stem cells," *Nature*, vol. 414, no. 6859, pp. 105–111, 2001.

[425] T. E. Werbowetski-Ogilvie, M. Bossé, M. Stewart et al., "Characterization of human embryonic stem cells with features of neoplastic progression," *Nature Biotechnology*, vol. 27, no. 1, pp. 91–97, 2009.

[426] P. S. Knoepfler, "Deconstructing stem cell tumorigenicity: a roadmap to safe regenerative medicine," *Stem Cells*, vol. 27, no. 5, pp. 1050–1056, 2009.

[427] Y. Zheng, C.-J. Hu, R.-H. Zhuo, Y.-S. Lei, N.-N. Han, and L. He, "Inhibition of autophagy alleviates the senescent state

of rat mesenchymal stem cells during long-term culture," *Molecular Medicine Reports*, vol. 10, no. 6, pp. 3003–3008, 2014.

[428] Y. Zheng, L. He, Y. Wan, and J. Song, "H3K9me-enhanced DNA hypermethylation of the p16INK4a gene: an epigenetic signature for spontaneous transformation of rat mesenchymal stem cells," *Stem Cells and Development*, vol. 22, no. 2, pp. 256–267, 2013.

[429] Y. F. Zhou, M. Bosch-Marce, H. Okuyama et al., "Spontaneous transformation of cultured mouse bone marrow–derived stromal cells," *Cancer Research*, vol. 66, no. 22, pp. 10849–10854, 2006.

[430] N. Ahmadbeigi, et al.A. Shafiee, E. Seyedjafari et al., "Early spontaneous immortalization and loss of plasticity of rabbit bone marrow mesenchymal stem cells," *Cell Proliferation*, vol. 44, no. 1, pp. 67–74, 2011.

[431] Z. Ren, J. Wang, W. Zhu et al., "Spontaneous transformation of adult mesenchymal stem cells from cynomolgus macaques in vitro," *Experimental Cell Research*, vol. 317, no. 20, pp. 2950–2957, 2011.

[432] J. Tolar, A. J. Nauta, M. J. Osborn et al., "Sarcoma derived from cultured mesenchymal stem cells," *Stem Cells*, vol. 25, no. 2, pp. 371–379, 2007.

[433] M.-H. Xu, X. Gao, D. Luo, X. D. Zhou, W. Xiong, and G. X. Liu, "EMT and acquisition of stem cell-like properties are involved in spontaneous formation of tumorigenic hybrids between lung cancer and bone marrow-derived mesenchymal stem cells," *PLoS One*, vol. 9, no. 2, article e87893, 2014.

[434] F. A. Siebzehnrubl, I. Jeske, D. Müller et al., "Spontaneous in vitro transformation of adult neural precursors into stem-like cancer cells," *Brain Pathology*, vol. 19, no. 3, pp. 399–408, 2009.

[435] L. He, F. Zhao, Y. Zheng, Y. Wan, and J. Song, "Loss of interactions between p53 and survivin gene in mesenchymal stem cells after spontaneous transformation *in vitro*," *The International Journal of Biochemistry & Cell Biology*, vol. 75, pp. 74–84, 2016.

[436] S. Cialfi, R. Palermo, S. Manca et al., "Loss of Notch1-dependent p21Waf1/Cip1expression influences the Notch1 outcome in tumorigenesis," *Cell Cycle*, vol. 13, no. 13, pp. 2046–2245, 2014.

[437] K. M. LaPak and C. E. Burd, "The molecular balancing act of p16INK4ain cancer and aging," *Molecular Cancer Research*, vol. 12, no. 2, pp. 167–183, 2014.

[438] Q. Pan, S. M. G. Fouraschen, P. E. de Ruiter et al., "Detection of spontaneous tumorigenic transformation during culture expansion of human mesenchymal stromal cells," *Experimental Biology and Medicine*, vol. 239, no. 1, pp. 105–115, 2014.

[439] M. E. Bernardo, N. Zaffaroni, F. Novara et al., "Human bone marrow–derived mesenchymal stem cells do not undergo transformation after long-term in vitro culture and do not exhibit telomere maintenance mechanisms," *Cancer Research*, vol. 67, no. 19, pp. 9142–9149, 2007.

[440] G. Chen, A. Yue, Z. Ruan et al., "Human umbilical cord-derived mesenchymal stem cells do not undergo malignant transformation during long-term culturing in serum-free medium," *PLoS One*, vol. 9, no. 6, article e98565, 2014.

[441] J. P. Martins, J. M. Santos, J. M. Almeida et al., "Towards an advanced therapy medicinal product based on mesenchymal stromal cells isolated from the umbilical cord tissue: quality and safety data," *Stem Cell Research Therapy*, vol. 5, no. 1, p. 9, 2014.

[442] A. Poloni, G. Maurizi, L. Babini et al., "Human mesenchymal stem cells from chorionic villi and amniotic fluid are not susceptible to transformation after extensive in vitro expansion," *Cell Transplantation*, vol. 20, no. 5, pp. 643–654, 2011.

[443] Q. Tang, Q. Chen, X. Lai et al., "Malignant transformation potentials of human umbilical cord mesenchymal stem cells both spontaneously and via 3-methycholanthrene induction," *PLoS One*, vol. 8, no. 12, p. e81844, 2013.

[444] S. A. Fisher, A. Cutler, C. Doree et al., "Mesenchymal stromal cells as treatment or prophylaxis for acute or chronic graft-versus-host disease in haematopoietic stem cell transplant (HSCT) recipients with a haematological condition," *Cochrane Database of Systematic Reviews*, vol. 1, 2019.

[445] M. M. Lalu, L. McIntyre, C. Pugliese et al., "Safety of cell therapy with mesenchymal stromal cells (SafeCell): a systematic review and meta-analysis of clinical trials," *PLoS One*, vol. 7, no. 10, article e47559, 2012.

[446] N. Amariglio, A. Hirshberg, B. W. Scheithauer et al., "Donor-derived brain tumor following neural stem cell transplantation in an ataxia telangiectasia patient," *PLoS Medicine*, vol. 6, no. 2, article e1000029, 2009.

[447] B. J. Dlouhy, O. Awe, R. C. Rao, P. A. Kirby, and P. W. Hitchon, "Autograft-derived spinal cord mass following olfactory mucosal cell transplantation in a spinal cord injury patient: case report," *Journal of Neurosurgery: Spine*, vol. 21, no. 4, pp. 618–622, 2014.

[448] S. Neri, "Genetic stability of mesenchymal stromal cells for regenerative medicine applications: a fundamental biosafety aspect," *International Journal of Molecular Sciences*, vol. 20, no. 10, p. 2406, 2019.

[449] M. I. Phillips and Y. L. Tang, "Genetic modification of stem cells for transplantation," *Advanced Drug Delivery Reviews*, vol. 60, no. 2, pp. 160–172, 2008.

[450] J. Reiser, X.-Y. Zhang, C. S. Hemenway, D. Mondal, L. Pradhan, and V. F. La Russa, "Potential of mesenchymal stem cells in gene therapy approaches for inherited and acquired diseases," *Expert Opinion on Biological Therapy*, vol. 5, no. 12, pp. 1571–1584, 2005.

[451] H. Hirai, E. Satoh, M. Osawa et al., "Use of EBV-based vector/HVJ-liposome complex vector for targeted gene therapy of EBV-associated neoplasms," *Biochemical and Biophysical Research Communication*, vol. 241, no. 1, pp. 112–118, 1997.

[452] E. S. Robertson, T. Ooka, and E. D. Kieff, "Epstein-Barr virus vectors for gene delivery to B lymphocytes," *Proceedings of the National Academy of Sciences*, vol. 93, no. 21, pp. 11334–11340, 1996.

[453] N. Nayerossadat, T. Maedeh, and P. A. Ali, "Viral and nonviral delivery systems for gene delivery," *Advanced Biomedical Research*, vol. 1, 2012.

[454] R. Gardlík, R. Pálffy, J. Hodosy, J. Lukács, J. Turna, and P. Celec, "Vectors and delivery systems in gene therapy," *Medical Science Monitor*, vol. 11, no. 4, pp. RA110–RA121, 2005.

[455] D. P. Katare and V. Aeri, "Progress in gene therapy: a review," *IJTPR*, vol. 1, no. 2, pp. 33–41, 2010.

[456] E. Z. Keung, P. J. Nelson, and C. Conrad, "Concise review: genetically engineered stem cell therapy targeting angiogenesis and tumor stroma in gastrointestinal malignancy," *Stem Cells*, vol. 31, no. 2, pp. 227–235, 2013.

[457] M. Takeuchi, K. Takeuchi, A. Kohara et al., "Chromosomal instability in human mesenchymal stem cells immortalized with human papilloma virus E6, E7, and hTERT genes," *In Vitro Cellular Developmental Biology-Animal*, vol. 43, no. 3-4, pp. 129–138, 2007.

[458] T. J. Kean, P. Lin, A. I. Caplan, and J. E. Dennis, "MSCs: delivery routes and engraftment, cell-targeting strategies, and immune modulation," *Stem Cells International*, vol. 2013, Article ID 732742, 13 pages, 2013.

[459] A. I. Caplan and J. E. Dennis, "Mesenchymal stem cells as trophic mediators," *Journal of cellular biochemistry*, vol. 98, no. 5, pp. 1076–1084, 2006.

[460] R. H. Lee, A. A. Pulin, M. J. Seo et al., "Intravenous hMSCs improve myocardial infarction in mice because cells embolized in lung are activated to secrete the anti-inflammatory protein TSG-6," *Cell Stem Cell*, vol. 5, no. 1, pp. 54–63, 2009.

[461] A. I. Caplan and D. Correa, "The MSC: an injury drugstore," *Cell Stem Cell*, vol. 9, no. 1, pp. 11–15, 2011.

[462] A. I. Caplan, "Osteogenesis imperfecta, rehabilitation medicine, fundamental research and mesenchymal stem cells," *Connective Tissue Research*, vol. 31, no. sup4, pp. s9–s14, 2009.

[463] C. A. Herberts, M. S. G. Kwa, and H. P. H. Hermsen, "Risk factors in the development of stem cell therapy," *Journal of Translational Medicine*, vol. 9, no. 1, 2011.

[464] A. Arthur, A. Zannettino, and S. Gronthos, "The therapeutic applications of multipotential mesenchymal/stromal stem cells in skeletal tissue repair," *Journal of Cellular Physiology*, vol. 218, no. 2, pp. 237–245, 2009.

[465] P. Müller, H. Lemcke, and R. David, "Stem cell therapy in heart diseases-cell types, mechanisms and improvement strategies," *Cellular Physiology and Biochemistry*, vol. 48, no. 6, pp. 2607–2655, 2018.

[466] O. Y. Bang, E. H. Kim, J. M. Cha, and G. J. Moon, "Adult stem cell therapy for stroke: challenges and progress," *Journal of Stroke*, vol. 18, no. 3, pp. 256–266, 2016.

[467] A. F. Steinert, L. Rackwitz, F. Gilbert, U. Nöth, and R. S. Tuan, "Concise review: the clinical application of mesenchymal stem cells for musculoskeletal regeneration: current status and perspectives," *Stem Cells Translational Medicine*, vol. 1, no. 3, pp. 237–247, 2012.

[468] K. H. Schuleri, G. S. Feigenbaum, M. Centola et al., "Autologous mesenchymal stem cells produce reverse remodelling in chronic ischaemic cardiomyopathy," *European Heart Journal*, vol. 30, no. 22, pp. 2722–2732, 2009.

[469] H. Hamamoto, J. H. Gorman III, L. P. Ryan et al., "Allogeneic mesenchymal precursor cell therapy to limit remodeling after myocardial infarction: the effect of cell dosage," *Annals of Thoracic Surgery*, vol. 87, no. 3, pp. 794–801, 2009.

[470] J. M. Hare, J. E. Fishman, G. Gerstenblith et al., "Comparison of allogeneic vs autologous bone marrow-derived mesenchymal stem cells delivered by transendocardial injection in patients with ischemic cardiomyopathy," *JAMA*, vol. 308, no. 22, pp. 2369–2379, 2012.

[471] A. R. Williams, K. E. Hatzistergos, B. Addicott et al., "Enhanced effect of combining human cardiac stem cells and bone marrow mesenchymal stem cells to reduce infarct size and to restore cardiac function after myocardial infarction," *Circulation*, vol. 127, no. 2, pp. 213–223, 2013.

[472] A. W. Heldman, D. L. DiFede, J. E. Fishman et al., "Transendocardial mesenchymal stem cells and mononuclear bone marrow cells for ischemic cardiomyopathy: the TAC-HFT randomized trial," *JAMA*, vol. 311, no. 1, pp. 62–73, 2014.

[473] V. Karantalis, D. L. DiFede, G. Gerstenblith et al., "Autologous mesenchymal stem cells produce concordant improvements in regional function, tissue perfusion, and fibrotic burden when administered to patients undergoing coronary artery bypass grafting," *Circulation Research*, vol. 114, no. 8, pp. 1302–1310, 2014.

[474] S. Golpanian, I. H. Schulman, R. F. Ebert et al., "Concise review: review and perspective of cell dosage and routes of administration from preclinical and clinical studies of stem cell therapy for heart disease," *Stem Cells Translational Medicine*, vol. 5, no. 2, pp. 186–191, 2016.

[475] R. Wu, X. Hu, and J.'. Wang, "Concise review: optimized strategies for stem cell-based therapy in myocardial repair: clinical translatability and potential limitation," *Stem Cells*, vol. 36, no. 4, pp. 482–500, 2018.

[476] H. Caplan, S. D. Olson, A. Kumar et al., "Mesenchymal stromal cell therapeutic delivery: translational challenges to clinical application," *Frontiers in Immunology*, vol. 10, article 1645, 2019.

[477] U. M. Fischer, M. T. Harting, F. Jimenez et al., "Pulmonary passage is a major obstacle for intravenous stem cell delivery: the pulmonary first-pass effect," *Stem Cells and Development*, vol. 18, no. 5, pp. 683–692, 2009.

[478] J. Gao, J. E. Dennis, R. F. Muzic, M. Lundberg, and A. I. Caplan, "The dynamic in vivo distribution of bone marrow-derived mesenchymal stem cells after infusion," *Cells Tissues Organs*, vol. 169, no. 1, pp. 12–20, 2001.

[479] S. Schrepfer, T. Deuse, H. Reichenspurner, M. P. Fischbein, R. C. Robbins, and M. P. Pelletier, "Stem cell transplantation: the lung barrier," *Transplantation Proceedings*, vol. 39, no. 2, pp. 573–576, 2007.

[480] J. Leibacher and R. Henschler, "Biodistribution, migration and homing of systemically applied mesenchymal stem/stromal cells," *Stem Cell Research & Therapy*, vol. 7, no. 1, 2016.

[481] A. Sohni and C. M. Verfaillie, "Mesenchymal stem cells migration homing and tracking," *Stem Cells International*, vol. 2013, Article ID 130763, 8 pages, 2013.

[482] P. Walczak, J. Zhang, A. A. Gilad et al., "Dual-modality monitoring of targeted intraarterial delivery of mesenchymal stem cells after transient ischemia," *Stroke*, vol. 39, no. 5, pp. 1569–1574, 2008.

[483] A. V. Pendharkar, J. Y. Chua, R. H. Andres et al., "Biodistribution of neural stem cells after intravascular therapy for hypoxic-ischemia," *Stroke*, vol. 41, no. 9, pp. 2064–2070, 2010.

[484] A. Toyoshima, T. Yasuhara, M. Kameda et al., "Intra-arterial transplantation of allogeneic mesenchymal stem cells mounts neuroprotective effects in a transient ischemic stroke model in rats: analyses of therapeutic time window and its mechanisms," *PLoS One*, vol. 10, no. 6, article e0127302, 2015.

[485] J. Saraf, D. Sarmah, K. Vats et al., "Intra-arterial stem cell therapy modulates neuronal calcineurin and confers neuroprotection after ischemic stroke," *International Journal of Neuroscience*, vol. 129, no. 10, pp. 1039–1044, 2019.

[486] J. M. Sierra-Parraga, A. Munk, C. Andersen et al., "Mesenchymal stromal cells are retained in the porcine renal cortex independently of their metabolic state after renal intra-arterial infusion," *Stem Cells and Development*, vol. 28, no. 18, pp. 1224–1235, 2019.

[487] E. Sykova, P. Jendelova, L. Urdzikova, P. Lesny, and A. Hejcl, "Bone marrow stem cells and polymer hydrogels–two strategies for spinal cord injury repair," *Cellular and Molecular Neurobiology*, vol. 26, no. 7-8, pp. 1113–1129, 2006.

[488] A. J. Kanelidis, C. Premer, J. Lopez, W. Balkan, and J. M. Hare, "Route of delivery modulates the efficacy of mesenchymal stem cell therapy for myocardial infarction: a meta-analysis of preclinical studies and clinical trials," *Circulation Research*, vol. 120, no. 7, pp. 1139–1150, 2017.

[489] Y. Zhang, Y. Zhao, X. Song et al., "Modulation of stem cells as therapeutics for severe mental disorders and cognitive impairments," *Front Psychiatry*, vol. 11, p. 80, 2020.

[490] B. Rodríguez-Frutos, L. Otero-Ortega, M. Gutiérrez-Fernández, B. Fuentes, J. Ramos-Cejudo, and E. Díez-Tejedor, "Stem cell therapy and administration routes after stroke," *Translational Stroke Research*, vol. 7, no. 5, pp. 378–387, 2016.

[491] R. A. Au-Shahror, C.-C. Au-Wu, Y.-H. Au-Chiang, and K.-Y. Au-Chen, "Tracking superparamagnetic iron oxide-labeled mesenchymal stem cells using MRI after intranasal delivery in a traumatic brain injury murine model," *JoVE*, vol. 153, no. 153, article e60450, 2019.

[492] L. Danielyan, R. Schäfer, A. von Ameln-Mayerhofer et al., "Therapeutic efficacy of intranasally delivered mesenchymal stem cells in a rat model of Parkinson disease," *Rejuvenation Research*, vol. 14, no. 1, pp. 3–16, 2011.

[493] D. Mori, S. Miyagawa, S. Yajima et al., "Cell spray transplantation of adipose-derived mesenchymal stem cell recovers ischemic cardiomyopathy in a porcine model," *Transplantation*, vol. 102, no. 12, pp. 2012–2024, 2018.

[494] F. Menaa, S. Shahrokhi, and V. P. Shastri, "Corrigendum to "impact and challenges of mesenchymal stem cells in medicine: an overview of the current knowledge"," *Stem Cells International*, vol. 2019, Article ID 5493654, 1 pages, 2019.

[495] J. Galipeau and L. Sensébé, "Mesenchymal stromal cells: clinical challenges and therapeutic opportunities," *Cell Stem Cell*, vol. 22, no. 6, pp. 824–833, 2018.

[496] I. Martin, J. Galipeau, C. Kessler, K. Le Blanc, and F. Dazzi, "Challenges for mesenchymal stromal cell therapies," *Science Translational Medicine*, vol. 11, no. 480, p. eaat2189, 2019.

[497] M. Kabat, I. Bobkov, S. Kumar, and M. Grumet, "Trends in mesenchymal stem cell clinical trials 2004-2018: is efficacy optimal in a narrow dose range?," *Stem Cells Translational Medicine*, vol. 9, no. 1, pp. 17–27, 2020.

[498] Y. Tokita, X.-L. Tang, Q. Li et al., "Repeated administrations of cardiac progenitor cells are markedly more effective than a single administration: a new paradigm in cell therapy," *Circulation Research*, vol. 119, no. 5, pp. 635–651, 2016.

[499] Y. Guo, M. Wysoczynski, Y. Nong et al., "Repeated doses of cardiac mesenchymal cells are therapeutically superior to a single dose in mice with old myocardial infarction," *Basic Research in Cardiology*, vol. 112, no. 2, p. 18, 2017.

[500] H. Reich, E. Tseliou, G. de Couto et al., "Repeated transplantation of allogeneic cardiosphere-derived cells boosts therapeutic benefits without immune sensitization in a rat model of myocardial infarction," *The Journal of Heart and Lung Transplantation*, vol. 35, no. 11, pp. 1348–1357, 2016.

[501] J. N. Tang, J. Cores, K. Huang et al., "Concise review: is cardiac cell therapy dead? Embarrassing trial outcomes and new directions for the future," *Stem Cells Translational Medicine*, vol. 7, no. 4, pp. 354–359, 2018.

[502] H. Maeda, J. Wu, T. Sawa, Y. Matsumura, and K. Hori, "Tumor vascular permeability and the EPR effect in macromolecular therapeutics: a review," *Journal of controlled release: official journal of the Controlled Release Society*, vol. 65, no. 1-2, pp. 271–284, 2000.

[503] L. Claesson-Welsh, "Vascular permeability—the essentials," *Upsala Journal of Medical Sciences*, vol. 120, no. 3, pp. 135–143, 2015.

[504] K. W. Yong, J. R. Choi, A. S. Dolbashid, and W. K. Z. Wan Safwani, "Biosafety and bioefficacy assessment of human mesenchymal stem cells: what do we know so far?," *Regenerative Medicine*, vol. 13, no. 2, pp. 219–232, 2018.

[505] X. Wang, Y. Wang, W. Gou, Q. Lu, J. Peng, and S. Lu, "Role of mesenchymal stem cells in bone regeneration and fracture repair: a review," *International Orthopaedics*, vol. 37, no. 12, pp. 2491–2498, 2013.

[506] C. Ries, V. Egea, M. Karow, H. Kolb, M. Jochum, and P. Neth, "MMP-2, MT1-MMP, and TIMP-2 are essential for the invasive capacity of human mesenchymal stem cells: differential regulation by inflammatory cytokines," *Blood*, vol. 109, no. 9, pp. 4055–4063, 2007.

[507] S. Y. Kim, S. H. Park, J. W. Shin et al., "Mechanical stimulation and the presence of neighboring cells greatly affect migration of human mesenchymal stem cells," *Biotechnology Letters*, vol. 35, no. 11, pp. 1817–1822, 2013.

[508] J. Wu, K. Wu, F. Lin et al., "Mechano-growth factor induces migration of rat mesenchymal stem cells by altering its mechanical properties and activating ERK pathway," *Biochemical and Biophysical Research Communications*, vol. 441, no. 1, pp. 202–207, 2013.

[509] X. Fu, G. Liu, A. Halim, Y. Ju, Q. Luo, and A. G. Song, "Mesenchymal stem cell migration and tissue repair," *Cells*, vol. 8, no. 8, p. 784, 2019.

[510] H. Naderi-Meshkin, A. R. Bahrami, H. R. Bidkhori, M. Mirahmadi, and N. Ahmadiankia, "Strategies to improve homing of mesenchymal stem cells for greater efficacy in stem cell therapy," *Cell Biology International*, vol. 39, no. 1, pp. 23–34, 2015.

[511] S. Liu, J. Zhou, X. Zhang et al., "Strategies to optimize adult stem cell therapy for tissue regeneration," *International Journal of Molecular Sciences*, vol. 17, no. 6, p. 982, 2016.

[512] S. Dimmeler, S. Ding, T. A. Rando, and A. Trounson, "Translational strategies and challenges in regenerative medicine," *Nature Medicine*, vol. 20, no. 8, pp. 814–821, 2014.

[513] S. Mohsin, M. Khan, H. Toko et al., "Human cardiac progenitor cells engineered with Pim-I kinase enhance myocardial repair," *Journal of the American College of Cardiology*, vol. 60, no. 14, pp. 1278–1287, 2012.

[514] A. S. Lee, C. Tang, M. S. Rao, I. L. Weissman, and J. C. Wu, "Tumorigenicity as a clinical hurdle for pluripotent stem cell therapies," *Nature Medicine*, vol. 19, no. 8, pp. 998–1004, 2013.

[515] Z. Liu, M. Tang, J. Zhao, R. Chai, and J. Kang, "Looking into the future: toward advanced 3D biomaterials for stem-cell-based regenerative medicine," *Advanced Materials*, vol. 30, no. 17, article e1705388, 2018.

[516] R. Chaudhuri, M. Ramachandran, P. Moharil, M. Harumalani, and A. K. Jaiswal, "Biomaterials and cells for cardiac tissue engineering: current choices," *Materials Science and Engineering: C*, vol. 79, pp. 950–957, 2017.

[517] Q.-l. Wang, H.-j. Wang, Z.-h. Li, Y.-l. Wang, X.-p. Wu, and Y.-z. Tan, "Mesenchymal stem cell-loaded cardiac patch

promotes epicardial activation and repair of the infarcted myocardium," *Journal of Cellular and Molecular Medicine*, vol. 21, no. 9, pp. 1751–1766, 2017.

[518] H. Qu, B. D. Xie, J. Wu et al., "Improved left ventricular aneurysm repair with cell- and cytokine-seeded collagen patches," *Stem Cells International*, vol. 2018, Article ID 4717802, 16 pages, 2018.

[519] A. Gilpin and Y. Yang, "Decellularization strategies for regenerative medicine: from processing techniques to applications," *Biomed Res Int*, vol. 2017, article 9831534, 13 pages, 2017.

[520] E. Nyberg, A. Rindone, A. Dorafshar, and W. L. Grayson, "Comparison of 3D-printed poly-ε-caprolactone scaffolds functionalized with tricalcium phosphate, hydroxyapatite, bio-oss, or decellularized bone matrix," *Tissue Engineering Part A*, vol. 23, no. 11-12, pp. 503–514, 2017.

[521] A. R. Pereira, D. Trivanović, and M. Herrmann, "Approaches to mimic the complexity of the skeletal mesenchymal stem/-stromal cell niche in vitro," *European Cells & Materials*, vol. 37, pp. 88–112, 2019.

[522] H. Li and B. Yue, "Effects of various antimicrobial agents on multi-directional differentiation potential of bone marrow-derived mesenchymal stem cells," *World Journal of Stem Cells*, vol. 11, no. 6, pp. 322–336, 2019.

[523] A. H. Ryu, W. L. Eckalbar, A. Kreimer, N. Yosef, and N. Ahituv, "Use antibiotics in cell culture with caution: genome-wide identification of antibiotic-induced changes in gene expression and regulation," *Scientific Reports*, vol. 7, no. 1, p. 7533, 2017.

[524] B. M. Buehrer and B. Cheatham, "Isolation and characterization of human adipose-derived stem cells for use in tissue engineering," in *Organ Regeneration: Methods and Protocols*, J. Basu and J. W. Ludlow, Eds., pp. 1–11, Humana Press, Totowa, NJ, USA, 2013.

[525] B. Chudzik, G. Czernel, A. Miaskowski, and M. Gagoś, "Amphotericin B-copper(II) complex shows improved therapeutic index *in vitro*," *European Journal of Pharmaceutical Sciences*, vol. 97, pp. 9–21, 2017.

[526] S. Cohen, A. Samadikuchaksaraei, J. M. Polak, and A. E. Bishop, "Antibiotics reduce the growth rate and differentiation of embryonic stem cell cultures," *Tissue Engineering*, vol. 12, no. 7, pp. 2025–2030, 2006.

[527] A. Skubis, J. Gola, B. Sikora et al., "Impact of antibiotics on the proliferation and differentiation of human adipose-derived mesenchymal stem cells," *International Journal of Molecular Sciences*, vol. 18, no. 12, p. 2522, 2017.

[528] H. Pilge, J. Fröbel, S. Lensing-Höhn, C. Zilkens, and R. Krauspe, "Cefazolin irreversibly inhibits proliferation and migration of human mesenchymal stromal cells," *BioMed Research International*, vol. 2016, Article ID 2042687, 6 pages, 2016.

[529] Z. Zhang, X. Wang, F. Luo et al., "Effects of rifampicin on osteogenic differentiation and proliferation of human mesenchymal stem cells in the bone marrow," *Genetics and Molecular Research: GMR*, vol. 13, no. 3, pp. 6398–6410, 2014.

[530] T. Wu, Z. Shi, H. Song, Y. Li, and J.-H. Li, "Cytotoxicity of local anesthetics on rabbit adipose-derived mesenchymal stem cells during early chondrogenic differentiation," *Experimental and Therapeutic Medicine*, vol. 16, no. 4, pp. 2843–2850, 2018.

[531] H. Nie, E. Kubrova, T. Wu et al., "Effect of lidocaine on viability and gene expression of human adipose–derived mesenchymal stem cells: an in vitro study," *PM & R*, vol. 11, no. 11, pp. 1218–1227, 2019.

[532] F. Grambow, R. Rutkowski, F. Podmelle et al., "The impact of lidocaine on adipose-derived stem cells in human adipose tissue harvested by liposuction and used for lipotransfer," *International Journal of Molecular Sciences*, vol. 21, no. 8, p. 2869, 2020.

[533] A. Breu, S. Eckl, W. Zink, R. Kujat, and P. Angele, "Cytotoxicity of local anesthetics on human mesenchymal stem cells in vitro," *Arthroscopy: The Journal of Arthroscopic & Related Surgery*, vol. 29, no. 10, pp. 1676–1684, 2013.

[534] A. Gray, I. Marrero-Berrios, M. Ghodbane et al., "Effect of local anesthetics on human mesenchymal stromal cell secretion," *Nano Life*, vol. 5, no. 2, pp. 1550001–1550014, 2015.

[535] T. Wu, J. Smith, H. Nie et al., "Cytotoxicity of local anesthetics in mesenchymal stem cells," *American Journal of Physical Medicine & Rehabilitation*, vol. 97, no. 1, pp. 50–55, 2018.

[536] L. Ling, E. T. Camilleri, T. Helledie et al., "Effect of heparin on the biological properties and molecular signature of human mesenchymal stem cells," *Gene*, vol. 576, no. 1, pp. 292–303, 2016.

[537] F. Casiraghi, N. Perico, and G. Remuzzi, "Mesenchymal stromal cells to promote solid organ transplantation tolerance," *Current Opinion in Organ Transplantation*, vol. 18, no. 1, pp. 51–58, 2013.

[538] W. Ge, J. Jiang, M. L. Baroja et al., "Infusion of mesenchymal stem cells and rapamycin synergize to attenuate alloimmune responses and promote cardiac allograft tolerance," *American Journal of Transplantation*, vol. 9, no. 8, pp. 1760–1772, 2009.

[539] E. Javorkova, J. Vackova, M. Hajkova et al., "The effect of clinically relevant doses of immunosuppressive drugs on human mesenchymal stem cells," *Biomedicine & Pharmacotherapy*, vol. 97, pp. 402–411, 2018.

[540] L. Ferroni, C. Gardin, G. Bellin, V. Vindigni, C. Pavan, and B. Zavan, "Effects of novel antidepressant drugs on mesenchymal stem cell physiology," *Biomedicine & Pharmacotherapy*, vol. 114, p. 108853, 2019.

[541] F. Uguz, M. Sahingoz, B. Gungor, F. Aksoy, and R. Askin, "Weight gain and associated factors in patients using newer antidepressant drugs," *General Hospital Psychiatry*, vol. 37, no. 1, pp. 46–48, 2015.

[542] I. Pountos, P. V. Giannoudis, E. Jones et al., "NSAIDS inhibit in vitro MSC chondrogenesis but not osteogenesis: implications for mechanism of bone formation inhibition in man," *Journal of Cellular and Molecular Medicine*, vol. 15, no. 3, pp. 525–534, 2011.

[543] S. Golpanian, A. Wolf, K. E. Hatzistergos, and J. M. Hare, "Rebuilding the damaged heart: mesenchymal stem cells, cell-based therapy, and engineered heart tissue," *Physiological Reviews*, vol. 96, no. 3, pp. 1127–1168, 2016.

[544] S. Der Sarkissian, T. Lévesque, and N. Noiseux, "Optimizing stem cells for cardiac repair: current status and new frontiers in regenerative cardiology," *World Journal of Stem Cells*, vol. 9, no. 1, pp. 9–25, 2017.

[545] C. P. Hodgkinson, J. A. Gomez, M. Mirotsou, and V. J. Dzau, "Genetic engineering of mesenchymal stem cells and its application in human disease therapy," *Human Gene Therapy*, vol. 21, no. 11, pp. 1513–1526, 2010.

[546] S. Kulandavelu, W. Balkan, and J. M. Hare, "Next-generation stem cell therapy: genetically modified mesenchymal stem

cells for cardiac repair," *Cardiovascular Drugs and Therapy*, vol. 31, no. 1, pp. 5–7, 2017.

[547] N. de Cássia Noronha, A. Mizukami, C. Caliári-Oliveira et al., "Priming approaches to improve the efficacy of mesenchymal stromal cell-based therapies," *Stem Cell Research & Therapy*, vol. 10, no. 1, p. 131, 2019.

[548] M. Gnecchi and L. G. Melo, "Bone marrow-derived mesenchymal stem cells: isolation, expansion, characterization, viral transduction, and production of conditioned medium," in *Stem Cells in Regenerative Medicine*, J. Audet and W. L. Stanford, Eds., pp. 281–294, Humana Press, Totowa, NJ, USA, 2009.

[549] M. Khatun, A. Sorjamaa, M. Kangasniemi et al., "Niche matters: the comparison between bone marrow stem cells and endometrial stem cells and stromal fibroblasts reveal distinct migration and cytokine profiles in response to inflammatory stimulus," *PLoS One*, vol. 12, no. 4, article e0175986, 2017.

[550] M. L. da Silva, P. C. Chagastelles, and N. B. Nardi, "Mesenchymal stem cells reside in virtually all post-natal organs and tissues," *Journal of Cell Science*, vol. 119, no. 11, pp. 2204–2213, 2006.

[551] P. A. Zuk, M. Zhu, P. Ashjian et al., "Human adipose tissue is a source of multipotent stem cells," *Molecular Biology of the Cell*, vol. 13, no. 12, pp. 4279–4295, 2002.

[552] R. Mafi, S. Hindocha, P. Mafi, M. Griffin, and W. Khan, "Sources of adult mesenchymal stem cells applicable for musculoskeletal applications-a systematic review of the literature," *The Open Orthopaedics Journal*, vol. 5, no. 1, pp. 242–248, 2011.

[553] J.-A. Yang, H.-M. Chung, C.-H. Won, and J.-H. Sung, "Potential application of adipose-derived stem cells and their secretory factors to skin: discussion from both clinical and industrial viewpoints," *Expert Opinion on Biological Therapy*, vol. 10, no. 4, pp. 495–503, 2010.

[554] A. Mildmay-White and W. Khan, "Cell surface markers on adipose-derived stem cells: a systematic review," *Current Stem Cell Research & Therapy*, vol. 12, no. 6, pp. 484–492, 2017.

[555] D. A. De Ugarte, Z. Alfonso, P. A. Zuk et al., "Differential expression of stem cell mobilization-associated molecules on multi-lineage cells from adipose tissue and bone marrow," *Immunology Letters*, vol. 89, no. 2-3, pp. 267–270, 2003.

[556] P. Zhao, H. Ise, M. Hongo, M. Ota, I. Konishi, and T. Nikaido, "Human amniotic mesenchymal cells have some characteristics of cardiomyocytes," *Transplantation*, vol. 79, no. 5, pp. 528–535, 2005.

[557] G. Pasquinelli, P. Tazzari, F. Ricci et al., "Ultrastructural characteristics of human mesenchymal stromal (stem) cells derived from bone marrow and term placenta," *Ultrastructural Pathology*, vol. 31, no. 1, pp. 23–31, 2009.

[558] Y.-C. Huang, Z.-M. Yang, X.-H. Chen et al., "Isolation of mesenchymal stem cells from human placental decidua basalis and resistance to hypoxia and serum deprivation," *Stem Cell Reviews and Reports*, vol. 5, no. 3, pp. 247–255, 2009.

[559] M. S. Oliveira and J. B. Barreto-Filho, "Placental-derived stem cells: culture, differentiation and challenges," *World Journal of Stem Cells*, vol. 7, no. 4, pp. 769–775, 2015.

[560] Y. Fukuchi, H. Nakajima, D. Sugiyama, I. Hirose, T. Kitamura, and K. Tsuji, "Human placenta-derived cells have mesenchymal stem/progenitor cell potential," *Stem Cells*, vol. 22, no. 5, pp. 649–658, 2004.

[561] Z. Li and Z. C. Han, "Introduction of perinatal tissue-derived stem cells," in *Perinatal Stem Cells*, pp. 1–7, Springer, 2019.

[562] G. La Rocca, R. Anzalone, S. Corrao et al., "Isolation and characterization of Oct-4^+/HLA-G^+ mesenchymal stem cells from human umbilical cord matrix: differentiation potential and detection of new markers," *Histochemistry and Cell Biology*, vol. 131, no. 2, pp. 267–282, 2009.

[563] E. Karaöz and Ç. İnci, "Umbilical cord tissue and Wharton's jelly mesenchymal stem cells properties and therapeutic potentials," in *Perinatal Tissue-Derived Stem Cells: Alternative Sources of Fetal Stem Cells*, B. Arjmand, Ed., pp. 41–63, Springer International Publishing, Cham, 2016.

[564] T. T. Sibov, P. Severino, L. C. Marti et al., "Mesenchymal stem cells from umbilical cord blood: parameters for isolation, characterization and adipogenic differentiation," *Cytotechnology*, vol. 64, no. 5, pp. 511–521, 2012.

[565] T. Tondreau, N. Meuleman, A. Delforge et al., "Mesenchymal stem cells derived from CD133-positive cells in mobilized peripheral blood and cord blood: proliferation, Oct 4 expression, and plasticity," *Stem Cells*, vol. 23, no. 8, pp. 1105–1112, 2005.

[566] E. J. Gang, S. H. Hong, J. A. Jeong et al., "In vitro mesengenic potential of human umbilical cord blood-derived mesenchymal stem cells," *Biochemical and Biophysical Research Communications*, vol. 321, no. 1, pp. 102–108, 2004.

[567] M. Almeida, A. C. García-Montero, and A. Orfao, "Cell purification: a new challenge for biobanks," *Pathobiology*, vol. 81, no. 5-6, pp. 261–275, 2015.

[568] S. A. Brooks, U. Schumacher, and D. Davies, *Cell Separations by Flow Cytometry*, Humana Press, 2003.

Hindawi
Stem Cells International
Volume 2020, Article ID 8894168, 28 pages
https://doi.org/10.1155/2020/8894168

Research Article

Medications for Hypertension Change the Secretome Profile from Marrow Stromal Cells and Peripheral Blood Monocytes

Nikunj Satani,[1] **Kaavya Giridhar**,[1] **Chunyan Cai**,[2] **Natalia Wewior**,[1] **Dominique D. Norris**,[1] **Jaroslaw Aronowski**,[1] **and Sean I. Savitz**[1]

[1]*Institute for Stroke and Cerebrovascular Diseases, McGovern Medical School at UTHealth, Houston, Texas, USA*
[2]*Center for Clinical and Translational Sciences, McGovern Medical School at UTHealth, Houston, Texas, USA*

Correspondence should be addressed to Nikunj Satani; nikunj.b.satani@uth.tmc.edu

Received 15 April 2020; Revised 1 June 2020; Accepted 15 July 2020; Published 1 August 2020

Academic Editor: Kar Wey Yong

Marrow stromal cells (MSCs) are in different stages of clinical trials for stroke patients. MSCs are proposed to promote recovery through the release of secretomes that modulate the function of beneficial immune cells. The majority of stroke patients have comorbidities including hypertension, for which they are prescribed antihypertensive medications that might affect the function of MSCs, when they are administered in stroke patients. Here, we studied the effects of common antihypertensive medications on the secretomes of human MSCs and their modulation of human monocytes (Mo) derived from stroke patients. MTT assay was used to assess the proliferation of MSCs after they were exposed to increased levels of antihypertensive medications. MSCs were exposed to the following medications: atenolol, captopril, and losartan. Monocytes were isolated from stroke patients with NIHSS ranging from 11 to 20 and from healthy controls. MSC-Mo cocultures were established, and a secretome profile was analyzed using the Magpix Multiplex cytokine array from Luminex technology. The linear mixed-effect model was used for statistical analysis. All analyses were performed using SAS 9.4, and p values less than 0.05 were considered significant. At clinically relevant levels, there was no change in MSC proliferation after exposure to atenolol, captopril, or losartan. Atenolol increased IL-1RA in stroke-Mo and decreased IL-8 secretion from MSCs indicating an anti-inflammatory effect of atenolol on secretomes of these cells. Captopril increased IL-8 from stroke-Mo and increased IL-6, IL-8, and MCP-1 secretions from MSCs. Captopril also increased IL-6 secretion from cocultures of stroke-Mo and MSCs indicating a strong proinflammatory effect on MSCs and their interaction with Mo. Atenolol increased the secretion of IL-8 and MCP-1 while captopril increased the secretion of IL-6 and MCP-1 from MSCs. Losartan decreased the release of IL-6 from MSCs. Losartan reduced MCP-1 and TNF-α from stroke-Mo and reduced IL-8 from cocultures of stroke-Mo and MSCs. Our results show that antihypertensive medications such as atenolol, captopril, and losartan, at concentrations comparable to doses prescribed for patients hospitalized for acute stroke, modulate the secretome profile of MSCs and their modulatory effects on target immune cells. Our results suggest that stroke trials involving the use of intravenous MSCs should consider the effect of these antihypertensive drugs administered to stroke patients.

1. Introduction

Stroke is one of the major causes of death and disability around the world. Acute stroke is characterized by a sudden increase of inflammation that leads to secondary brain injury. Cell-based therapies [1–5] are under investigation as a treatment for stroke. Among different types of cell-based therapies, human bone marrow-derived mesenchymal stromal cells (MSCs) have been shown in preclinical trials to promote recovery after stroke by releasing various biological factors called the secretome which promote immunomodulation [6, 7]. Patients with an acute ischemic stroke are prescribed medications upon admission to the hospital. Many stroke patients have comorbidities such as hypertension, have elevated blood pressure in the hospital after a stroke, and are prescribed antihypertensive medications such as beta-blockers, ACE inhibitors, and angiotensive II receptor blockers. The effects of these drugs in altering long-term

outcomes after stroke have been well documented; however, the effect of these commonly prescribed drugs on MSCs is unknown. The interactions of medications with MSCs are important since clinical trials are testing the intravenous administration of these cells in stroke patients [8, 9]. Extensive studies have tested MSCs in rodent models of focal ischemic stroke where the timing of administration is 24 hrs after symptom onset. A recent meta-analysis conducted on 141 preclinical trials testing MSCs in a rodent model of ischemic stroke showed that MSCs promote functional recovery regardless of their dose, when administered up to 7 days after stroke [10]. However, clinical trials that would test the IV administration of MSCs in this time frame would involve patients being prescribed antihypertensive medications. After intravenous administration, MSCs interact with various immune cells in the circulation and peripheral organs. Among various peripheral circulating immune cells, monocytes (Mo) play an important immunoregulatory role after stroke and could be a direct target of MSCs [11, 12]. MSCs could help Mo acquire beneficial phenotypes through its secretome and hence aid in poststroke repair processes [13]. Hence, in this study, we aimed to study how antihypertensive medications change the secretomes of MSCs and the interaction of MSCs with such target immune cells as monocytes from the blood of stroke patients.

2. Methods

2.1. Isolation and Culture of Human Mesenchymal Stromal Cells (MSCs). MSCs were isolated from commercially available fresh human bone marrow aspirates (AllCells, Alameda, CA) using density centrifugation and plastic adherence as previously described [14]. An adherent population of MSCs was obtained 3 weeks after the initiation of culture. The cells were screened for typical spindle-like morphology and growth kinetics. These MSCs strongly expressed MSC markers CD73 and CD90 and were negative for hematopoietic markers HLA-DR, CD11b, CD34, CD45, and CD19 as previously described [15]. The cells were further expanded by plating 10^6 passage 2 cells at 200 cells/cm^2 in 2528 cm^2 in Nunc™ Cell Factory™ Systems with complete culture medium (CCM) that consisted of α-minimal essential medium (α-MEM; Life Technologies, Grand Island, NY), 17% fetal bovine serum (FBS; Atlanta Biologicals, Norcross, GA), 100 units/ml penicillin (Life Technologies, Carlsbad, CA), 100 μg/ml streptomycin (Life Technologies, Carlsbad, CA), and 2 mM L-glutamine (Life Technologies). At 70% cell confluency, the medium was discarded, the cultures were washed with phosphate-buffered saline (PBS) (Life Technologies, Carlsbad, CA), and the adherent cells were harvested with 0.25% trypsin (Life Technologies, Carlsbad, CA) for 5 min at 37°C and frozen at 1×10^7 cells/ml for subsequent experiments as passage 3.

2.2. Collection of Human Blood Samples. The Institutional Review Board approved all the studies and protocols involving human subjects. Peripheral blood was collected either from healthy controls or from ischemic stroke patients 24 hours after the presentation of initial symptoms through phlebotomy. Inclusion criteria for stroke patients included any acute ischemic stroke patients with NIHSS between 11 and 20.

2.3. Isolation of Human Peripheral Blood Monocytes. Peripheral Blood Mononuclear Cells (PBMCs) were isolated from peripheral human blood by Ficoll gradient. CD14+ monocytes (Mo) were isolated from PBMCs of healthy humans and stroke patients using an indirect magnetically labelling technique using a magnetic bead-based isolation as previously described [16]. A negative selection technique was used whereby a cocktail of biotin-conjugated monoclonal antibodies labelled nonmonocyte cells such as T cells, NK cells, B cells, dendritic cells, and basophils, and nonlabelled monocytes were collected for further cell culture work.

2.4. Cocultures of MSCs and Mo. Isolated monocytes were plated in a 48-well plate at 50,000 cells per well in a serum-free DMEM media. Subsequently, they were exposed to different doses of atenolol, captopril, and losartan. MSCs or an equal amount of media (control) were added in each well at 50,000 cells per well to set up a contact coculture. Monocytes exposed to drugs alone without MSCs were used as a control. After an additional 24 hours of incubation, media from monocytes exposed to drugs alone or media from contact cocultures were collected from each well and secretomes were measured. A similar method was used to collect secretomes from MSCs cultured alone in the presence of each drug.

2.5. Cell Proliferation Assays. MSCs were exposed to various drug concentrations of all 3 drugs. Atenolol was used from concentration ranging from 4 mM to 4 nM. Captopril was used from concentrations ranging from 5 mM to 5 nM. Losartan was used from concentrations ranging from 2 mM to 2 nM. At 24 and 48 hours of incubation, cell proliferation of MSCs was measured using MTT assay by comparing each concentration with the vehicle control.

2.6. Experimental Groups. MSCs as well as Mo were exposed to either atenolol (40 μM to 4 nM), captopril (50 μM to 5 nM), or losartan (20 μM to 2 nM). The groups were as follows: (a) MSCs alone exposed to each drug, (b) healthy subject Mo alone exposed to each drug, (c) stroke patient Mo alone exposed to each drug, (d) MSC-Mo cocultures (healthy subject Mo) with each drug, and (e) MSC-Mo cocultures (stroke patient Mo) with each drug. The dose range for each drug was selected based on the plasma concentrations these drugs might attain.

2.7. Analysis of Secretome Using ELISA and Multiplex Cytokine Assays. Conditioned media collected from treated MSCs, Mo, and MSC-Mo cocultures were analyzed for the presence of secretomes by using the MagPix magnetic bead-based ELISA assay (Millipore) as previously described [16, 17]. Data were averaged for 3 donors. Briefly, 96-well Magpix plates were used and supernatant media were incubated with magnetic cytokine beads overnight at 4°C. The next day, detection antibodies were added and incubated for 1 hour at room temperature. A Luminex Magpix plate

reader was used to measure the concentrations of multiple cytokines in the supernatant.

2.8. Statistical Analysis. We evaluated the dose effect of atenolol, captopril, and losartan on MSCs and Mo from healthy control or stroke patients through a mixed-effect model. We applied base-2 logarithm transformation on fold change data to normalize the secretome levels of the interested biomarkers. Mixed models were fitted to the normalized data. In a mixed model, for each source of Mo alone, MSC alone, and Mo-MSC cocultures, we considered dose level as the fixed effect. The effects from biological replicates of Mo and MSCs were considered as random effects. Based on the mixed model, we estimated $\log_2$(fold change) on the secretome levels for different dose levels. All analyses were performed using SAS 9.4 (Cary, NC), and a p value less than 0.05 was considered as significant.

3. Results

The following experimental groups were analyzed: (a) MSCs alone, (b) healthy subject Mo alone, (c) stroke patient Mo alone, (d) MSC-Mo cocultures with healthy subject Mo, and (e) MSC-Mo cocultures with stroke patient Mo. Each of the experimental groups was exposed to either atenolol (40 μM to 4 nM), captopril (50 μM to 5 nM), or losartan (20 μM to 2 nM).

3.1. Clinically Prescribed Medications Do Not Alter the Proliferation of MSCs at Physiologically Relevant Doses. When we subjected MSCs in our experiment to various doses of atenolol (ranging from 4 mM to 4 nM), captopril (ranging from 5 mM to 5 nM), and losartan (ranging from 2 mM to 2 nM) for 24 and 48 hours, we found no significant difference in the proliferation of MSCs at physiologically relevant doses of all three drugs as compared to vehicle controls (Fig S1).

3.2. Antihypertensive Medications Alter the Secretome of Monocytes from Healthy Controls and Stroke Patients. We subjected Mo in our experiment to therapeutically relevant doses of atenolol, captopril, and losartan. We measured the secretome levels of IL-1RA, IL-8, IL-10, MCP-1, IFN-gamma, and TNF-alpha.

3.2.1. Atenolol Increased the Secretions of IL-1RA and TNF-α from Stroke Patient-Derived Monocytes. Atenolol reduced the secretions of IL-1RA from Mo derived from healthy controls after 24 hours at physiologically relevant concentrations; however, it increased the secretions of IL-1RA from Mo derived from stroke patients ($p < 0.05$) (Figure 1(a)). Atenolol, at higher doses (more than 400 nM), increased the secretions of TNF-α from stroke-Mo ($p < 0.05$) but did not have any effect on TNF-α release from Mo harvested from healthy controls after 24 hours of exposure. MCP-1 secretions were reduced after 24 hours, but only from healthy control-derived monocytes and not from stroke-Mo (Figures 1(b)–1(d)).

3.2.2. Captopril Increased the Secretions of IL-1RA and IL-8 from Stroke Patient-Derived Monocytes. In Mo from stroke patients, captopril after 24 hours of exposure, similar to what we have seen for atenolol, increased the secretions of IL-1RA at physiologically relevant concentrations ($p < 0.05$). Captopril also increased the secretion of IL-8 from stroke patients as well as healthy control Mo after 24 hours ($p < 0.05$). There was no effect of captopril on IL-1RA when using healthy control Mo (Figures 1(e)–1(h)).

3.2.3. Losartan Did Not Have Any Effect on Secretions of IL-1RA, IL-8, MCP-1, and TNF-α from Stroke Patient-Derived Monocytes. Losartan at doses lower than 200 nM reduced the secretions of MCP-1 and TNF-α from Mo derived from healthy controls at 24 hours ($p < 0.05$); however, it did not have an effect on secretomes from stroke-Mo (Figures 1(i)–1(l)).

3.3. Antihypertensive Medications Alter Secretomes from MSCs. We subjected MSCs in our experiment to physiological doses of atenolol, captopril, and losartan. We measured the levels of IL-4, IL-6, IL-8, IL-10, MCP-1, IFN-gamma, and TNF-alpha. We saw significant changes only in the levels of IL-6, IL-8, and MCP-1 after MSCs were exposed to antihypertensive medications.

3.3.1. Atenolol Decreases the Levels of IL-8 and MCP-1 Released from MSCs. When MSCs were exposed to atenolol, it significantly decreased the levels of IL-8 after 24 hours of exposure. The decrease in IL-8 seen after exposure to atenolol was dose dependent, and 400 nM dose produced a significant reduction in the release of IL-8 ($p < 0.05$) (Figures 2(a)–2(c)). 40 nM and 4 nM doses produced a reduction in IL-8 secretion, but it was not significant. MCP-1 levels decreased significantly after 24 hours of exposure at 40 nM and 4 nM dose ($p < 0.05$) (Figures 2(a)–2(c)).

3.3.2. Captopril Increased the Levels of IL-6, IL-8, and MCP-1 from MSCs. When MSCs were exposed to captopril, it increased the release of IL-6 significantly at all doses ranging from 500 nM to 5 nM at 24 hours after exposure ($p < 0.05$) (Figures 2(d)–2(f)). Both IL-8 and MCP-1 secretions also increased significantly from MSCs after 24 hours of exposure to captopril ($p < 0.05$) (Figures 2(d)–2(f)).

3.3.3. Losartan Increased the Levels of IL-8. Losartan increased the release of IL-8 from MSCs at 24 hours at all doses except 2 nM dose at 24 hours after exposure ($p < 0.05$) (Figures 2(g)–2(i)). On the contrary, it reduced the levels of IL-6 and MCP-1 but only for the lowest dose of 2 nM at 24 hours ($p < 0.05$) (Figures 2(g)–2(i)).

3.4. Antihypertensive Medications Change the Secretome from MSC/Monocyte Cocultures Only when Mo Are Derived from Healthy Controls but Not from Stroke Patients. To determine whether MSCs exposed to antihypertensive medications in the presence of Mo derived from stroke patients, as compared to normal healthy controls, have different effects, we cocultured these MSCs with Mo (from stroke patients and healthy control patients) and measured the secretomes released from them.

3.4.1. Atenolol Reduced the Release of Cytokines from Cocultures of MSCs with Monocytes from Healthy Controls but Had No Effect on Cocultures with Stroke Patient-Derived Monocytes. Atenolol reduced the release of IL-1β, IL-8, MCP-1, TNF-α, IL-1RA, IL-6, Fractalkine, and VEGF from cocultures of MSCs with Mo from healthy controls after 24 hours of exposure ($p < 0.05$). Atenolol had no effect on secretome in cocultures with stroke-Mo (Figure 3).

3.4.2. Captopril Increased the Secretion of IL-6 from Cocultures of MSCs with Stroke Patient-Derived Mo. Captopril reduced secretions of IL-8, MCP-1, TNF-α, and IL-1RA from cocultures of MSCs with healthy control monocytes but had no effect on these secretomes in cocultures with stroke-Mo after 24 hours of exposure. More importantly, captopril increased the secretions of IL-6 from cocultures of MSCs with stroke-Mo at therapeutically relevant doses at 24 hours (5000 nM to 50 nM, $p < 0.05$) (Figure 4). On the contrary, captopril exposure reduced the IL-6 secretions from cocultures of MSCs with healthy control monocytes at 24 hours of exposure (Figure 4).

3.4.3. Losartan Reduced the Release of Cytokines from Cocultures of MSCs with Monocytes from Healthy Controls. Losartan reduced the release of IL-8 from cocultures of MSCs with both stroke-derived and healthy control monocytes after 24 hours of exposure (Figure 5). On the contrary, for all other cytokines measured (IL-1β, MCP-1, TNF-α, IL-1RA, and IL-6), secretions were reduced only from cocultures with healthy monocytes, and not from stroke-Mo at 24 hours (Figure 5).

4. Discussion

The release of biological factors is considered to play an important role underlying how MSCs exert beneficial effects in stroke [18, 19]. The number of passages, storage conditions, and types of solvents of MSCs impact the viability and immunomodulatory effects of MSCs [20–24] [17]. Stroke patients also take concurrent medications for their comorbidities. A recent STEPS 4 consortium recommended the need to study the effect of these concurrent medications on cell-based therapies [25]. Since intravenously administered MSCs have advanced to clinical trials in stroke patients, we posed clinically relevant questions about the effects of antihypertensive medications commonly taken by hospitalized stroke patients because of preexisting hypertension. We sought to evaluate the effects of these medications on Mo and MSCs by specifically studying Mo- and MSC-derived secretomes and the immunomodulatory effects of MSCs on monocytes. A range of drug concentrations was studied to simulate clinically relevant drug ranges in a patient's bloodstream and to assess for dose-dependent effects. In addition, we studied secretome released from each of these cell types. IL-1β and TNF-α are known to play a proinflammatory role after stroke and worsen stroke outcomes [26, 27]. IL-8 and MCP-1 are both chemotactic factors and attract immune cells towards the brain after ischemic stroke [26]. IL-6 is a proinflammatory cytokine and plays a key role in the pathogenesis of stroke because of its ability to play a dual role [26]. Fractalkine is a proinflammatory chemokine, whose downregulation is beneficial in stroke [26]. IL-1RA and VEGF are well-known anti-inflammatory and angiogenic cytokines, respectively. Hence, we selected these cytokines to get a broader picture of immunomodulation after MSCs are exposed to atenolol, captopril, and losartan.

Atenolol is a second-generation beta-1-selective adrenergic antagonist which is indicated for the treatment of hypertension, angina pectoris, and acute myocardial infarction. For hypertension, atenolol is usually given at the dose of 50-100 mg/day [28]. After a 100 mg dose, the peak plasma concentration of atenolol reaches around 600 ng/ml after 3 hours of administration and decreases to 50-70 ng/ml after 24 hours [29]. This translates to around 2.25 μM concentration in plasma at 3 hours to 200 nM concentration at 24 hours. Hence, we studied the following doses for atenolol: 40 μM, 4 μM, 400 nM, 40 nM, and 4 nM, to encompass the entire therapeutic range for atenolol. Atenolol increased IL-1RA release from Mo derived from stroke patients but had no significant effect on healthy control Mo at therapeutic levels. On the contrary, atenolol decreased the IL-1RA secretions from healthy control Mo, indicating that it may have different effects in stroke patients. Atenolol also reduced the secretions of IL-6, IL-8, and MCP-1 from MSCs indicating a beneficial anti-inflammatory effect on them. MCP-1 is a key chemokine that regulates the migration and infiltration of monocytes and macrophages [30]. Our results raise the possibility that atenolol could alter the release of MCP-1 from MSCs in stroke patients enrolled in an MSC trial. Reducing MCP-1 might therefore alter the effect of MSCs to promote migration of monocytes to the brain. Atenolol also reduced the secretions of IL-8 at 400 nM dose. IL-8 is known as a neutrophil chemotactic factor and has two important immunomodulatory functions. IL-8 promotes chemotaxis in target cells, primarily neutrophils, and assists their migration towards the site of injury. IL-8 also stimulates phagocytosis and is a potent promoter of angiogenesis. Reducing IL-8 can lead to negative regulation of phagocytosis and angiogenesis, thereby reducing the clearance of dead cells around the damaged stroke brain, as well as reducing the formation of new blood vessels, thereby potentially altering stroke recovery. When atenolol was exposed to cocultures of MSCs and Mo, curiously, they did not change secretions of any cytokines in cocultures when using monocytes from stroke patients. On the other hand, with cocultures involving healthy control Mo, secretions of all cytokines were reduced. In addition, when we compared the effect of atenolol between stroke patient-derived Mo alone and their cocultures with MSCs, higher doses of atenolol showed an increase in TNF-α secretions from stroke patient-derived Mo alone. However, this effect was abolished in the presence of MSCs, indicating the possibility that MSCs may be able to curb the TNF-α secretions from stroke patient-derived Mo in the presence of atenolol. Overall, atenolol did show some anti-inflammatory tendency towards Mo and MSC alone, but there was no consistent beneficial effect in cocultures unlike aspirin which has been shown to produce beneficial effects on cocultures of MSCs and stroke-derived monocytes [16].

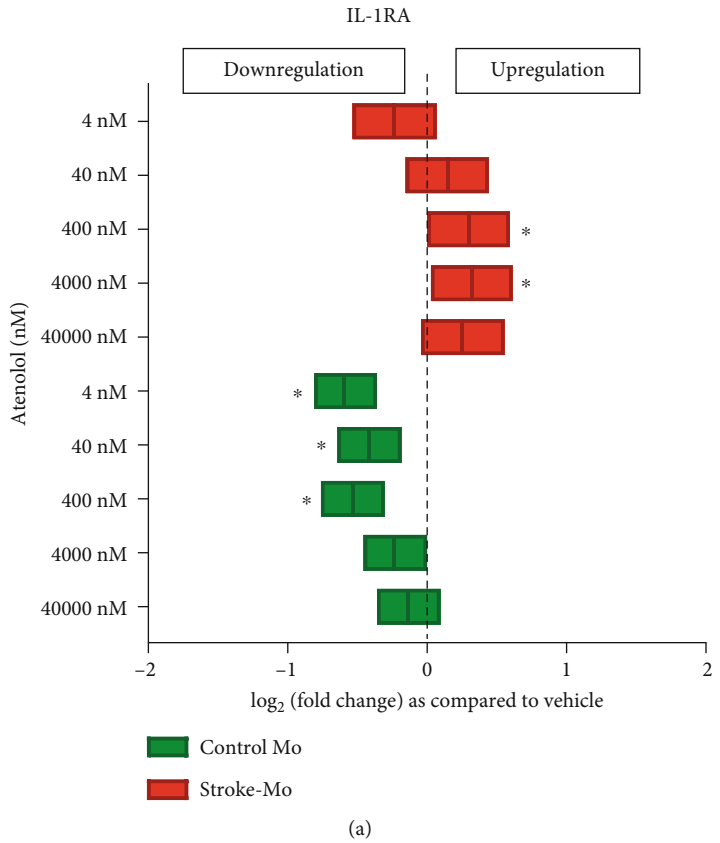

(a)

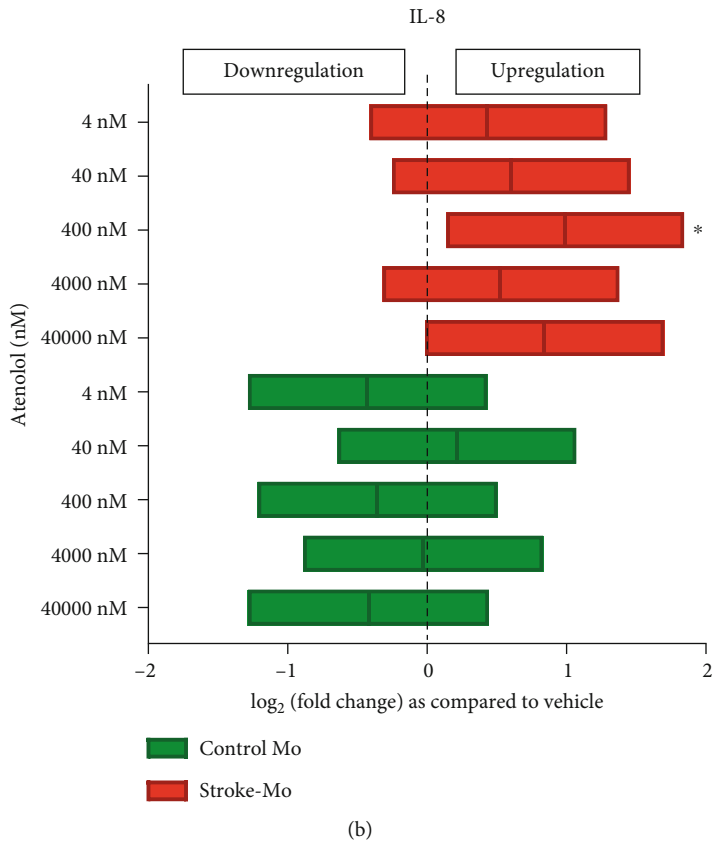

(b)

Figure 1: Continued.

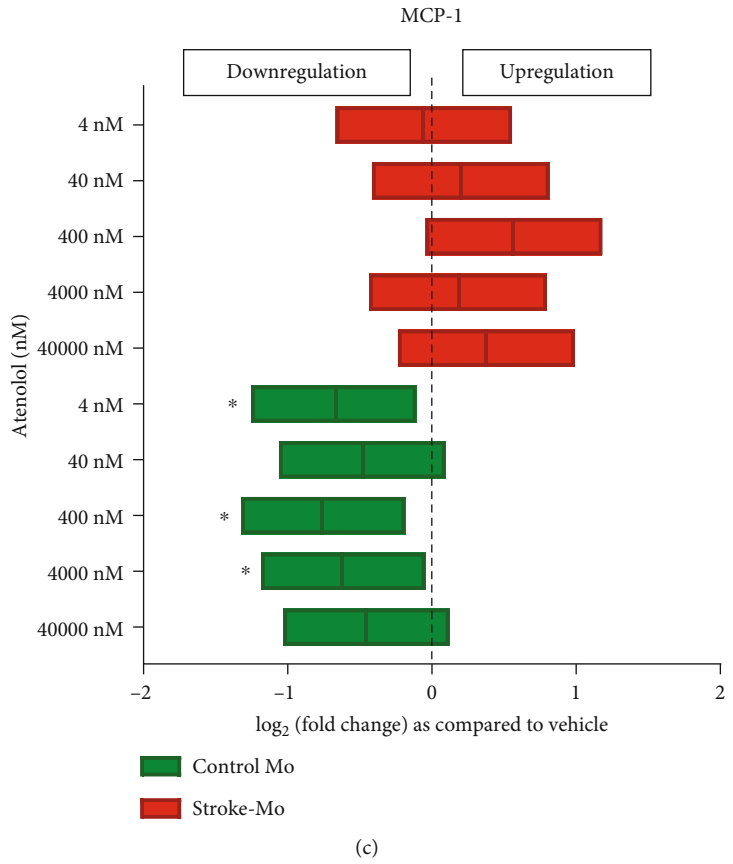

(c)

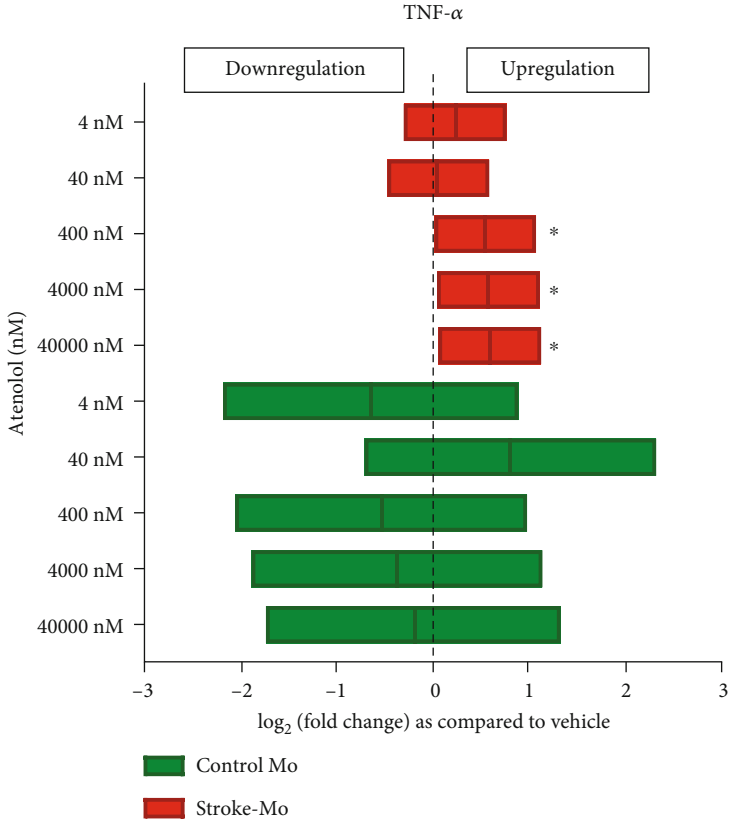

(d)

Figure 1: Continued.

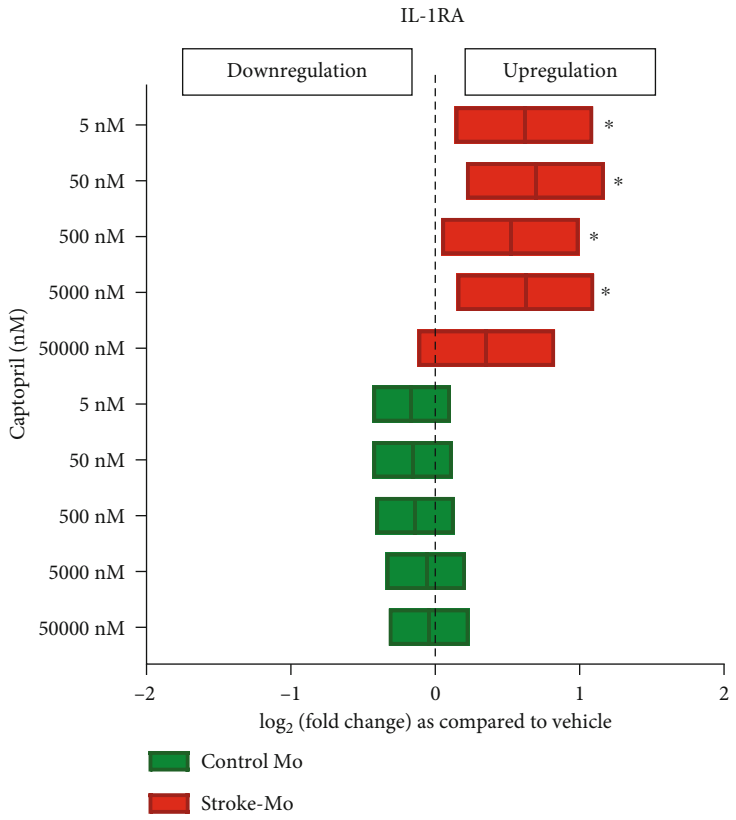

(e)

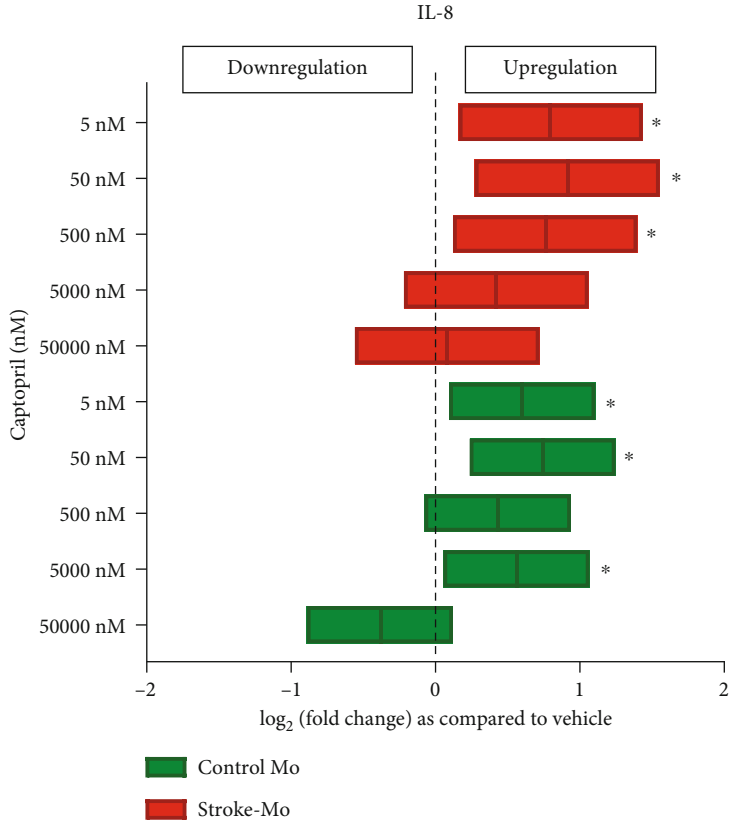

(f)

Figure 1: Continued.

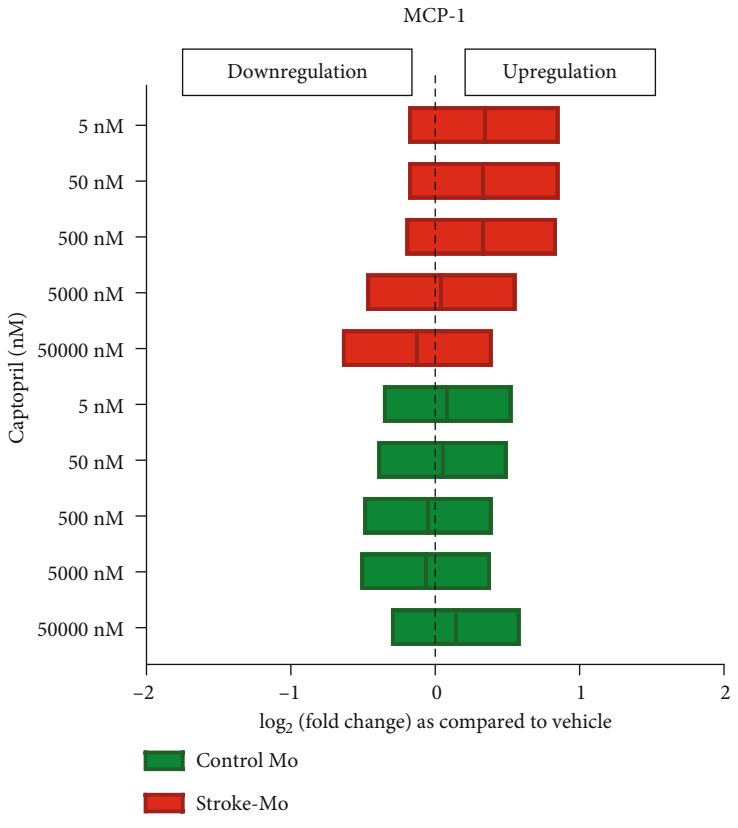

(g)

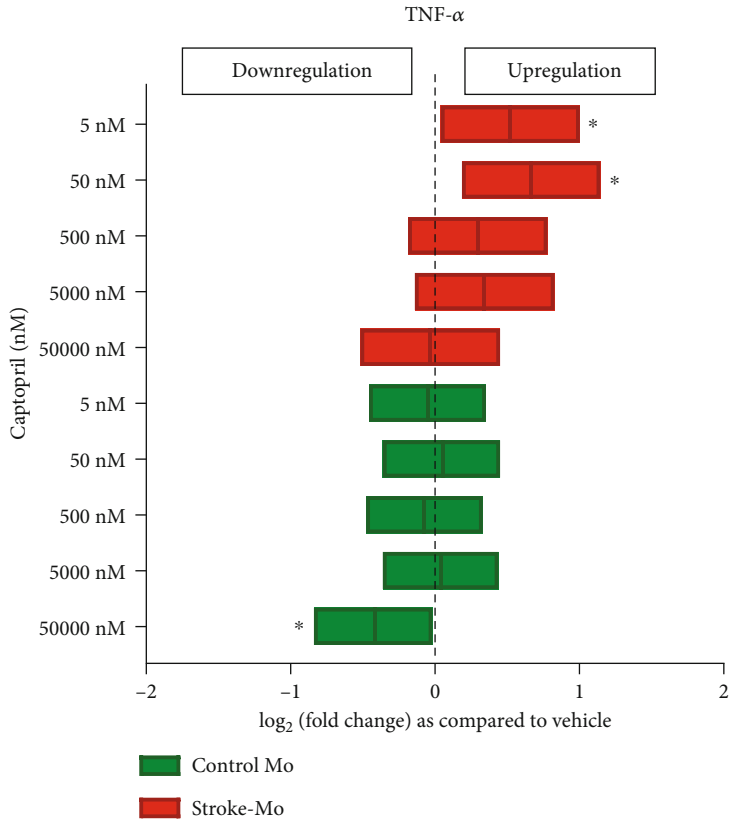

(h)

Figure 1: Continued.

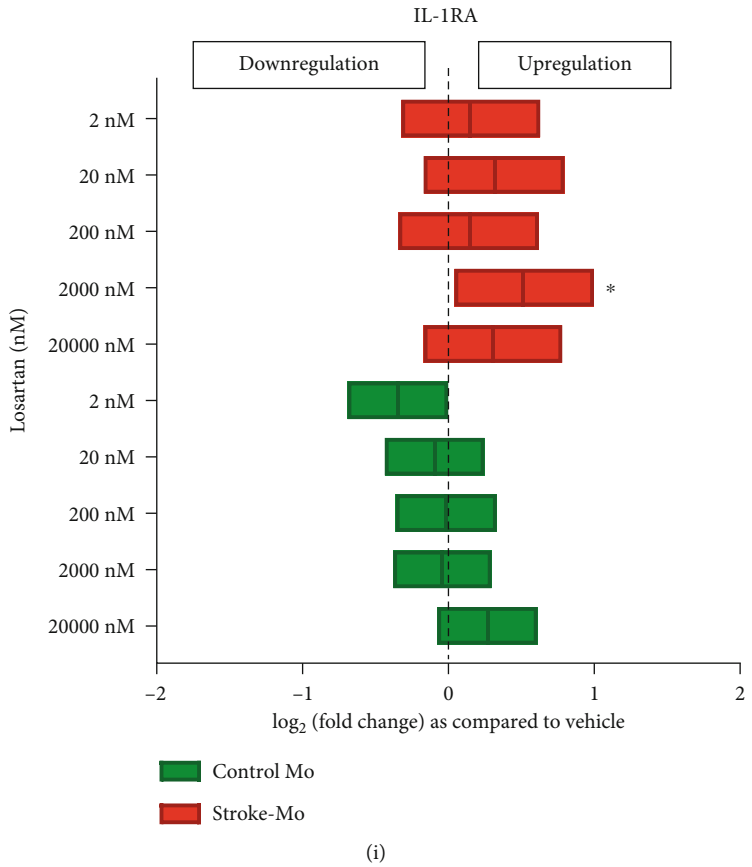

(i)

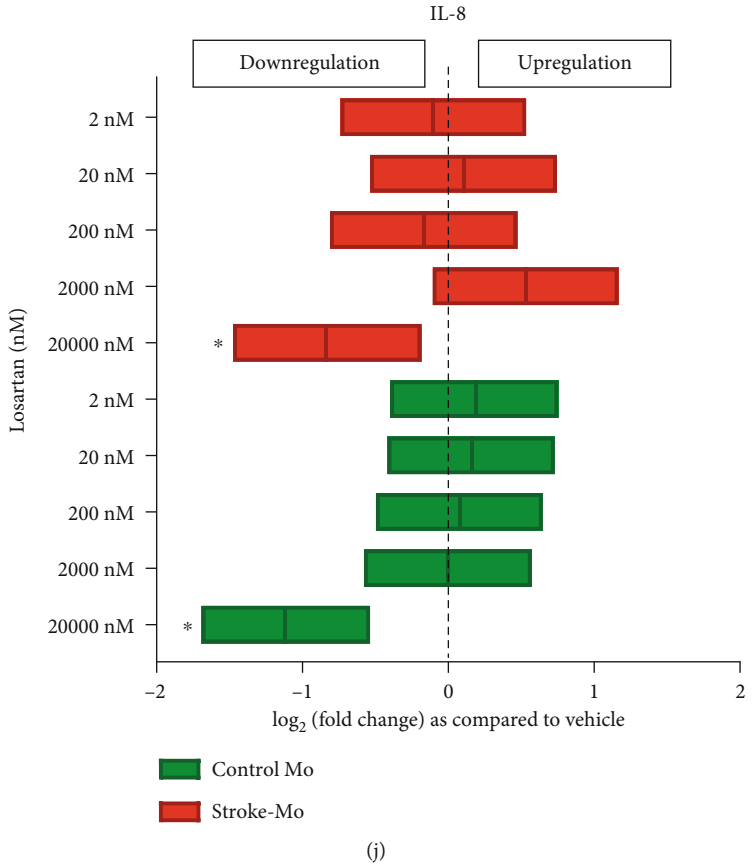

(j)

Figure 1: Continued.

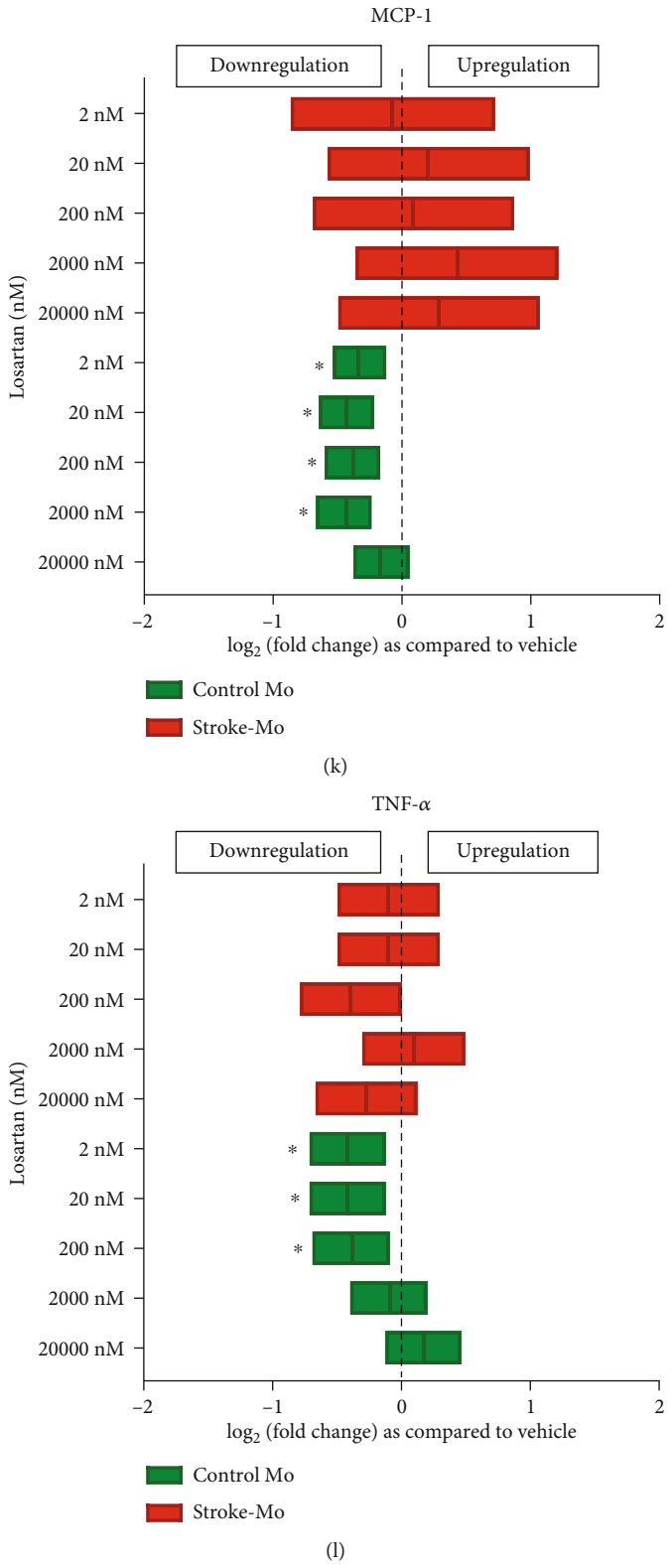

Figure 1: Antihypertensive medications alter the secretome of monocytes from healthy controls and stroke patients after 24 hours of exposure. Atenolol (a–d) increased IL-1RA and TNF-α secretions from stroke patient-derived monocytes but reduced the IL-1RA and MCP-1 secretions from health control monocytes. Captopril (e–h) increased IL-1RA secretions from stroke patient-derived monocytes but increased IL-8 secretions from both healthy control and stroke monocytes. Losartan (i–l) did not alter cytokine secretions from stroke patient-derived monocytes but reduced MCP-1 secretions from healthy control monocytes. Significance is shown by $^{*}p < 0.05$. All fold changes are as compared to vehicle control.

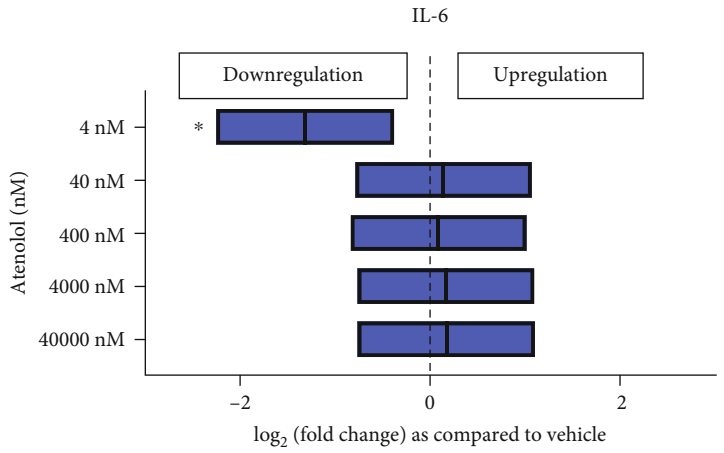

(a)

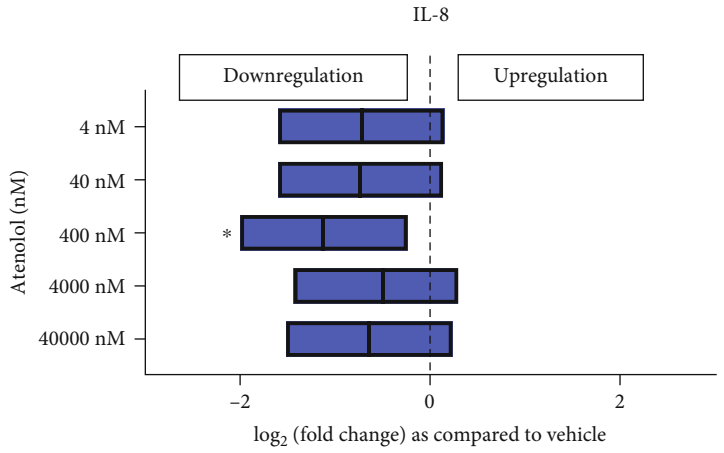

(b)

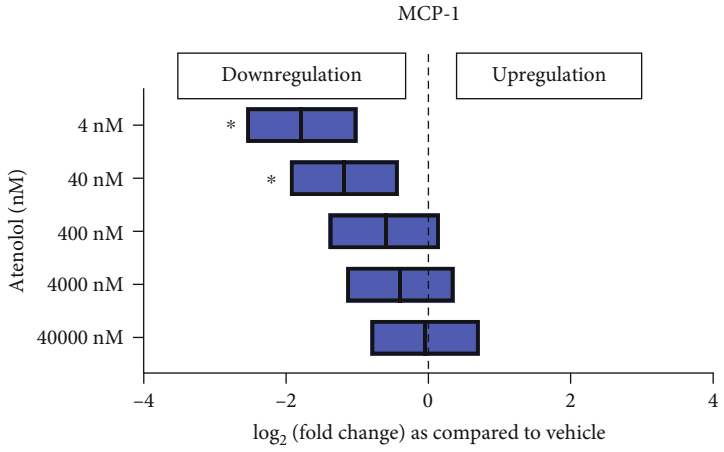

(c)

Figure 2: Continued.

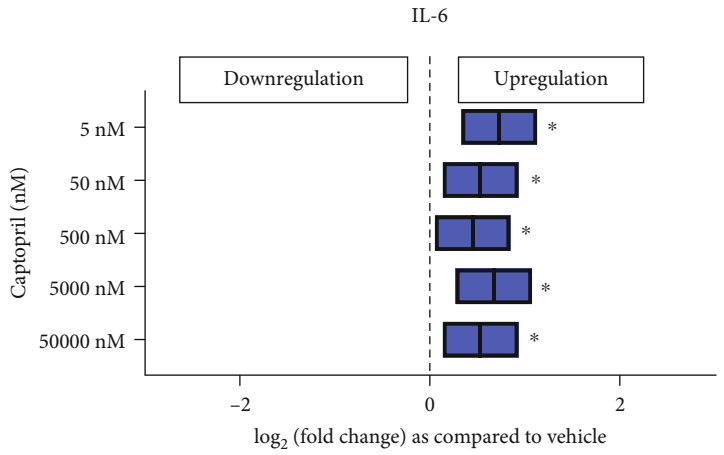

(d)

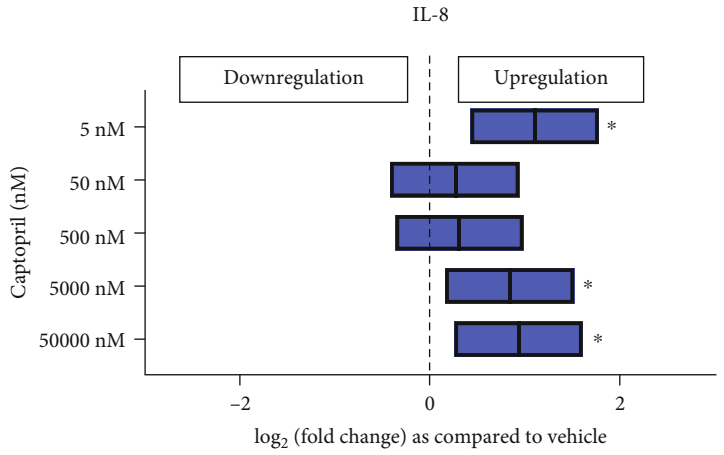

(e)

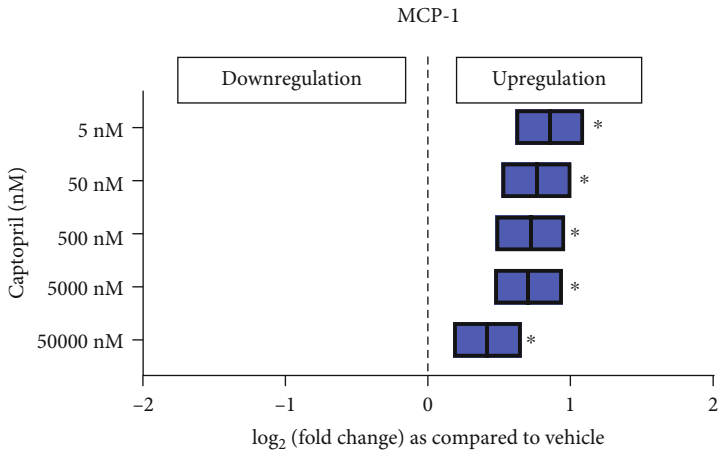

(f)

Figure 2: Continued.

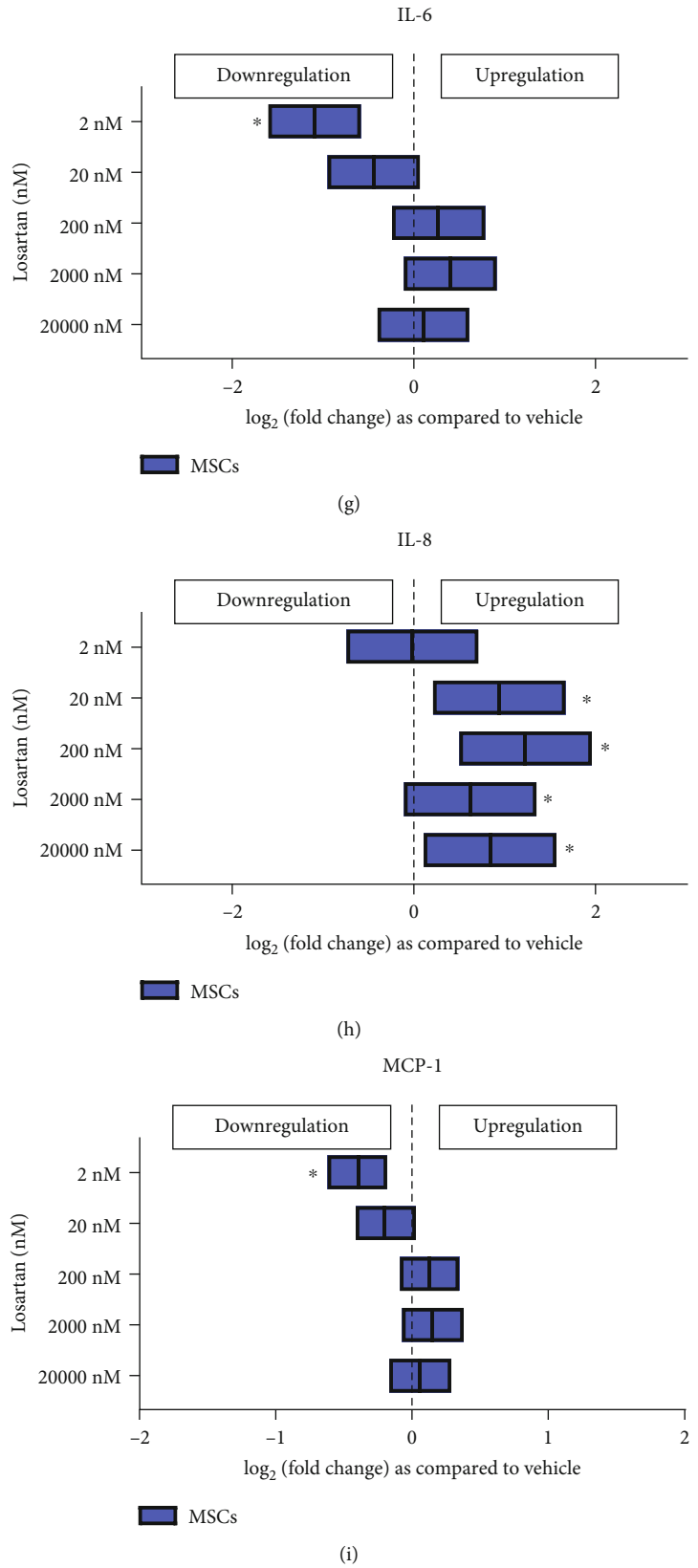

Figure 2: Antihypertensive medications alter the secretome of MSCs after 24 hours of exposure. Atenolol (a–c) reduced IL-6, MCP-1, and IL-8 secretions; captopril (d–f) increased IL-6, IL-8, and MCP-1 secretions; and losartan (g–i) increased IL-8 but reduced IL-6 and MCP-1 secretions. Significance is shown by $^{*}p < 0.05$. All fold changes are as compared to vehicle control.

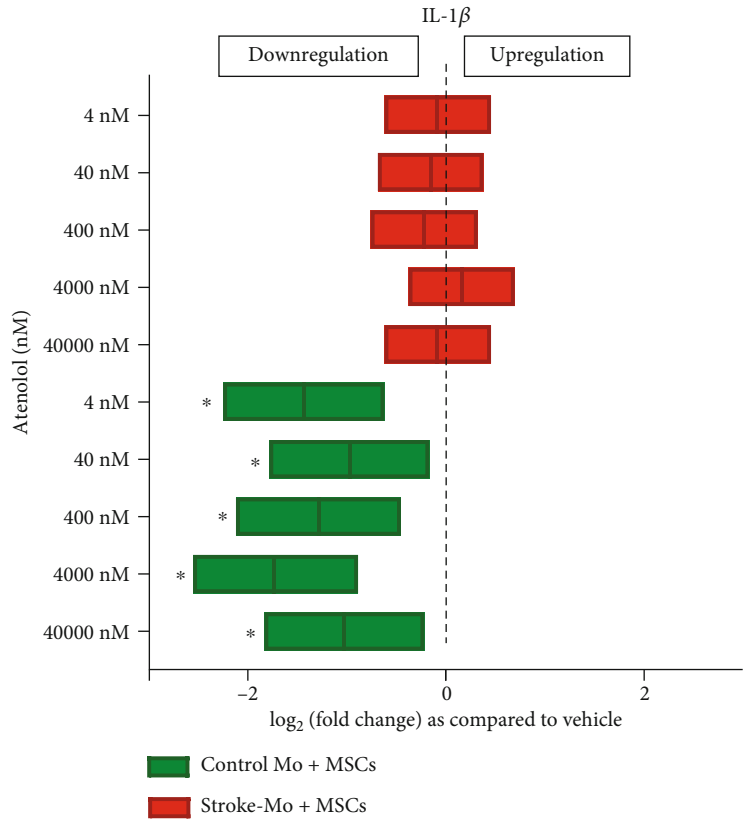

(a)

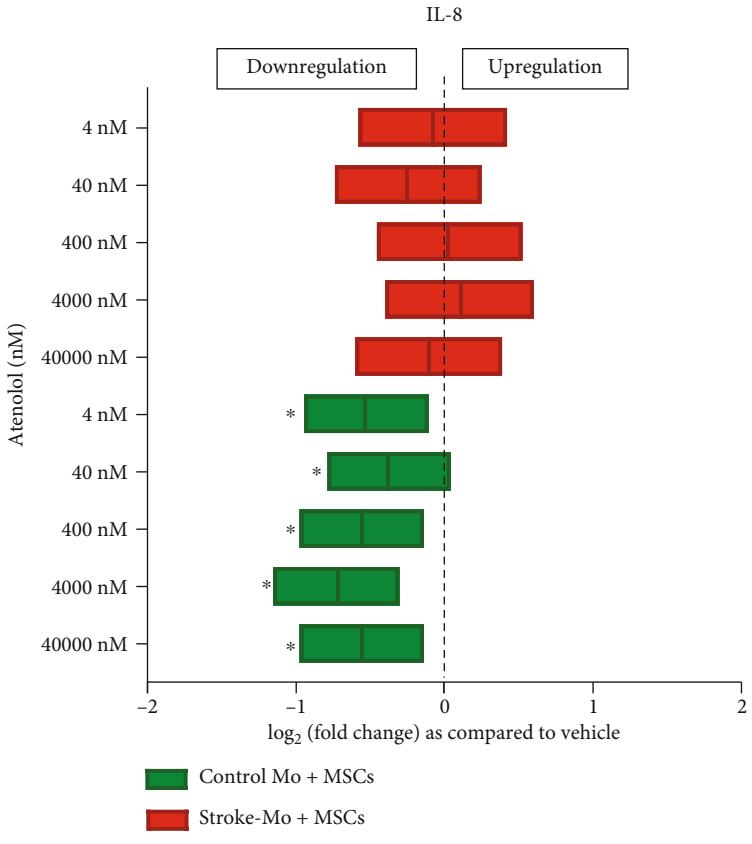

(b)

Figure 3: Continued.

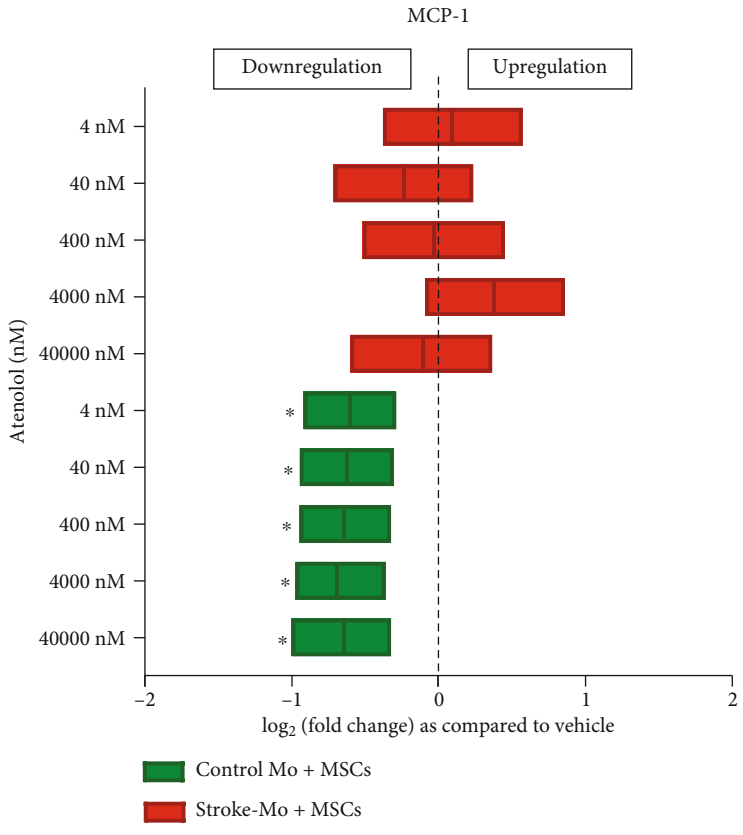

(c)

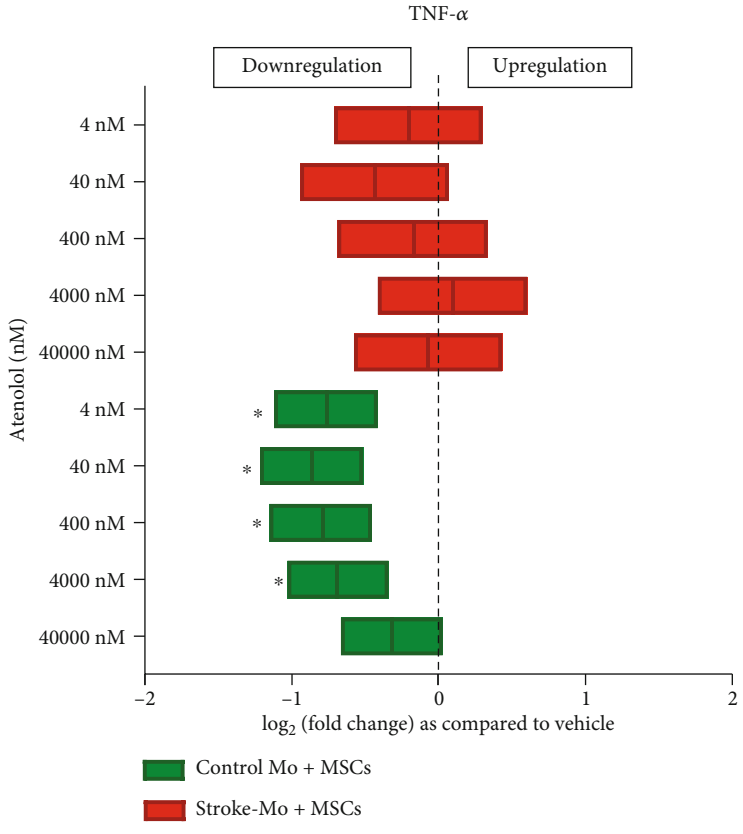

(d)

Figure 3: Continued.

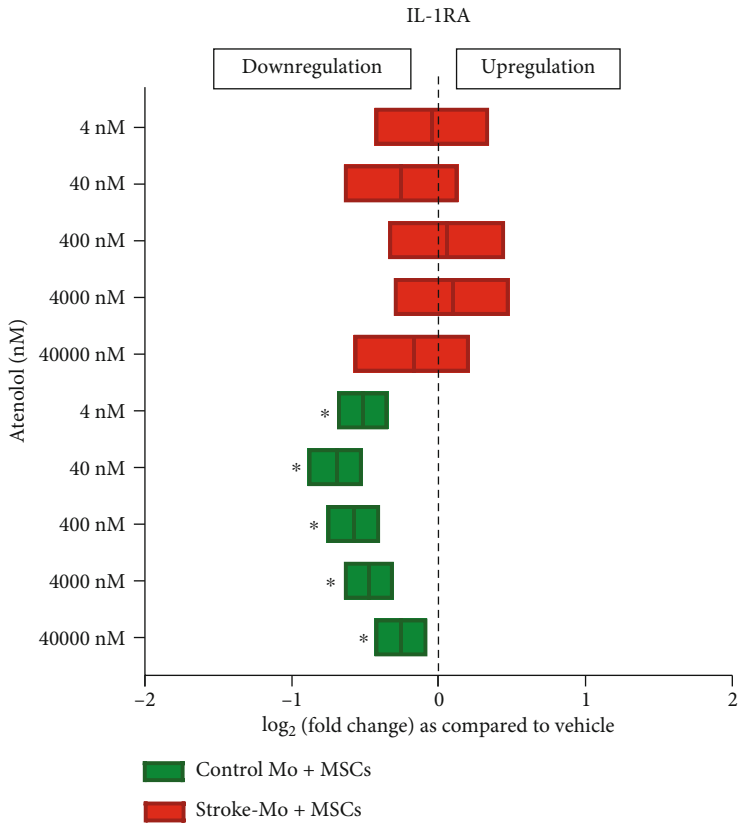

(e)

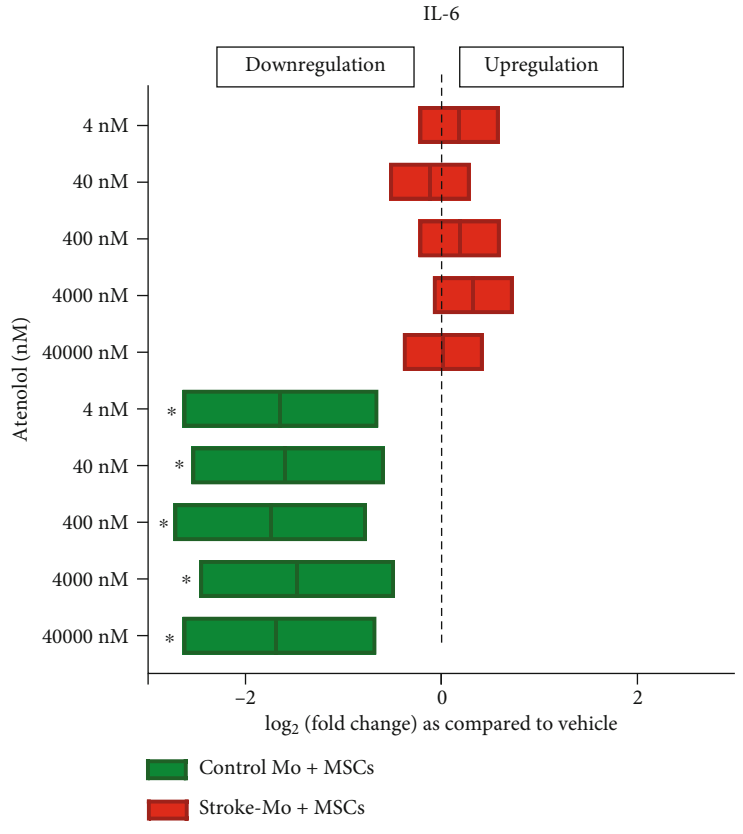

(f)

Figure 3: Continued.

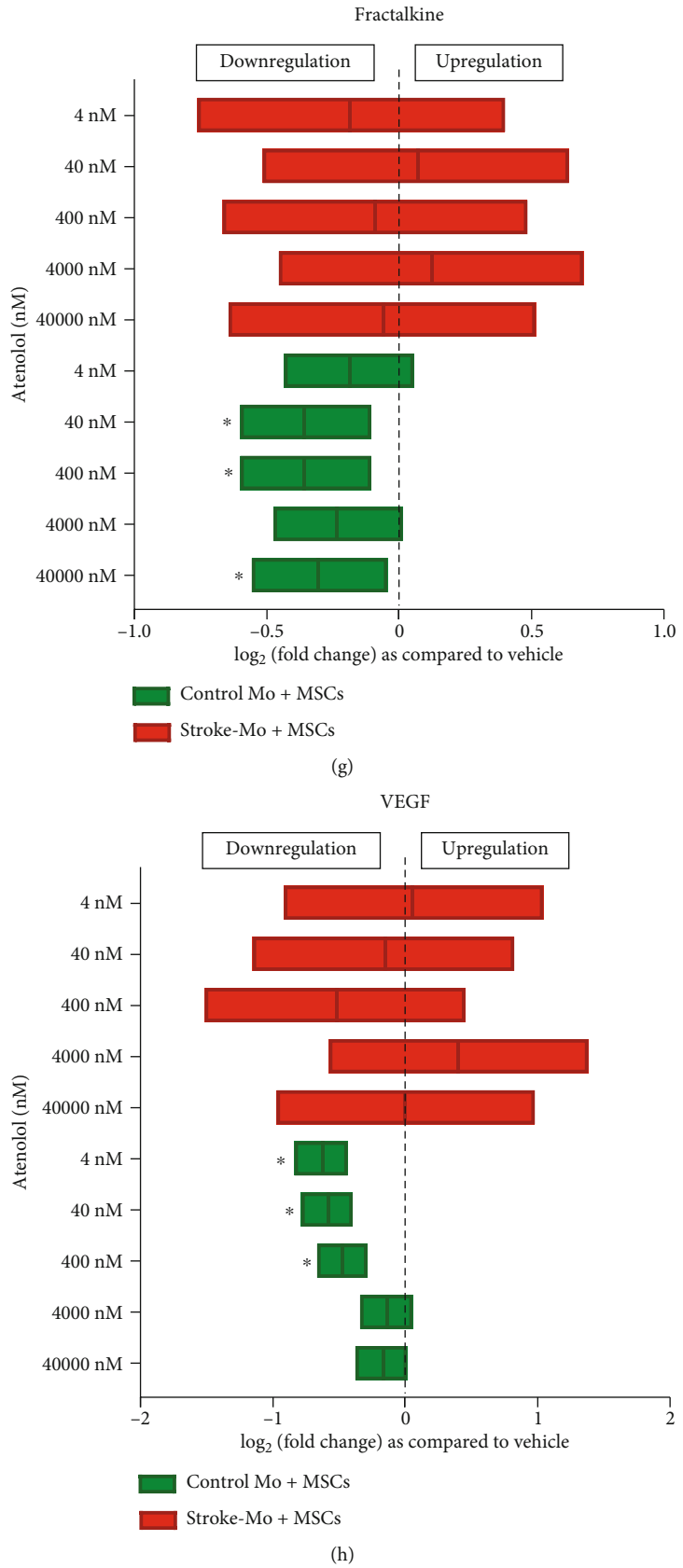

Figure 3: Atenolol reduces the cytokine secretions of IL-1β, IL-8, MCP-1, TNF-α, IL-IRA, IL-6, Fractalkine, and VEGF from cocultures of healthy control monocytes with MSCs after 24 hours of exposure but does not alter any cytokine secretions from cocultures involving stroke patient-derived monocytes. Significance is shown by $^{*}p < 0.05$. All fold changes are as compared to vehicle control.

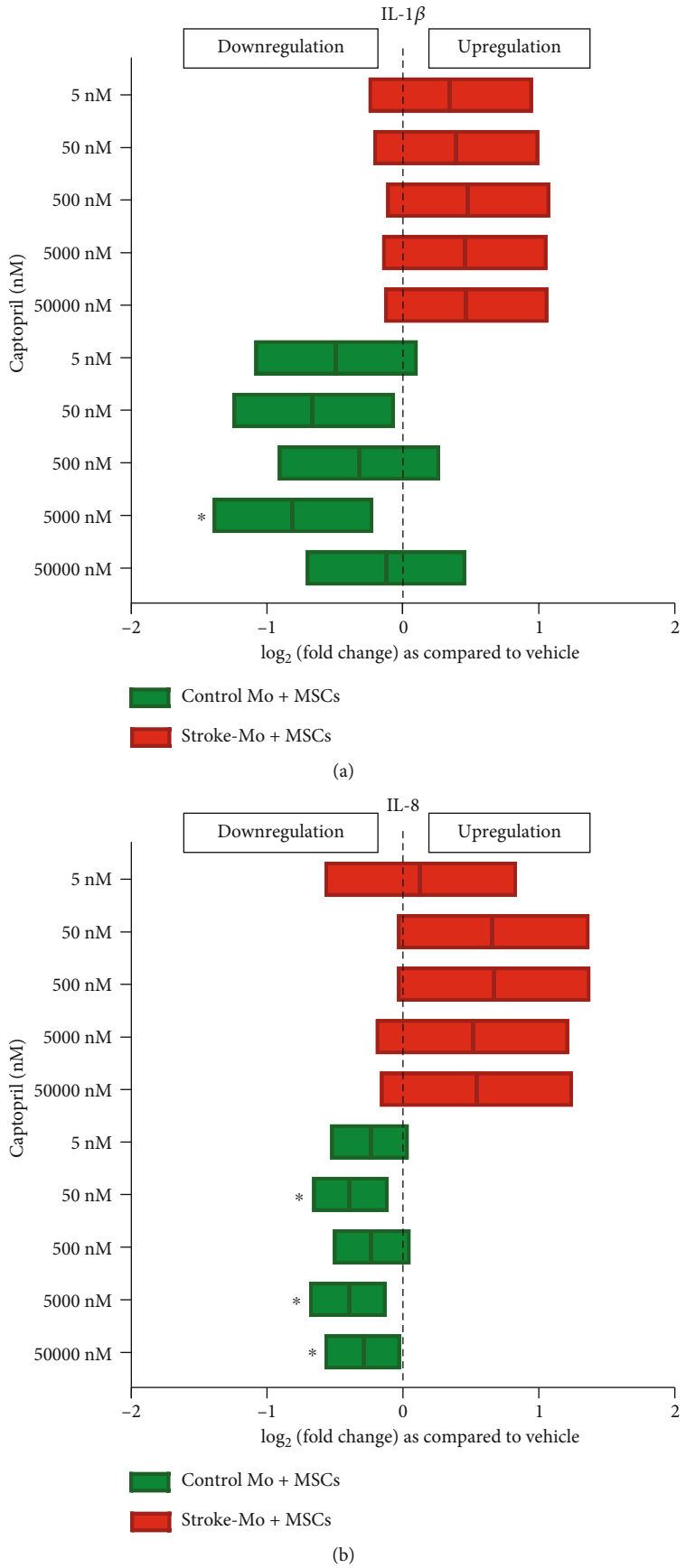

Figure 4: Continued.

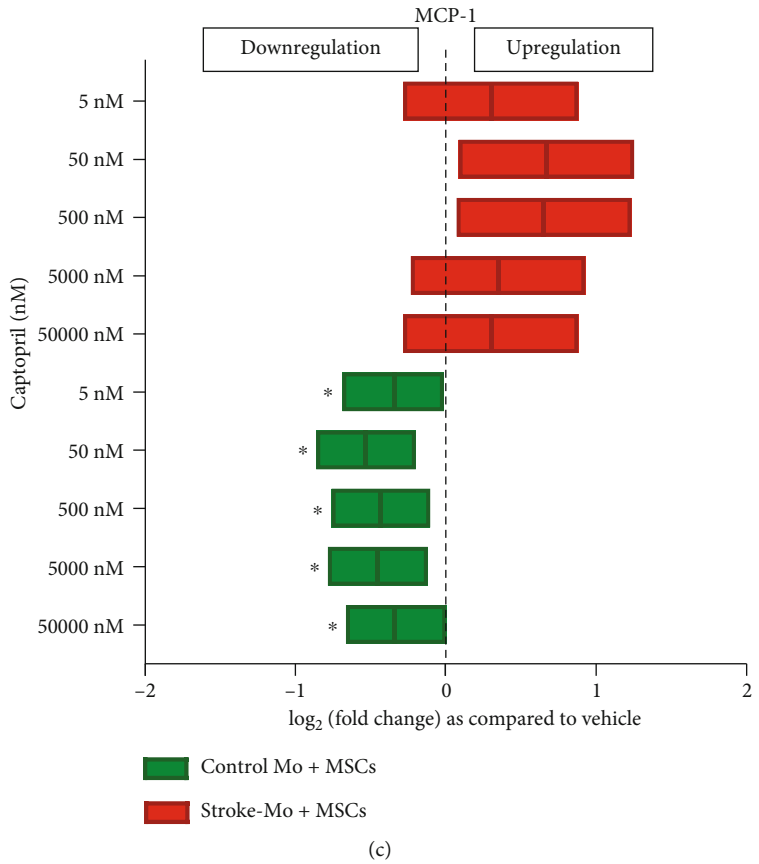

(c)

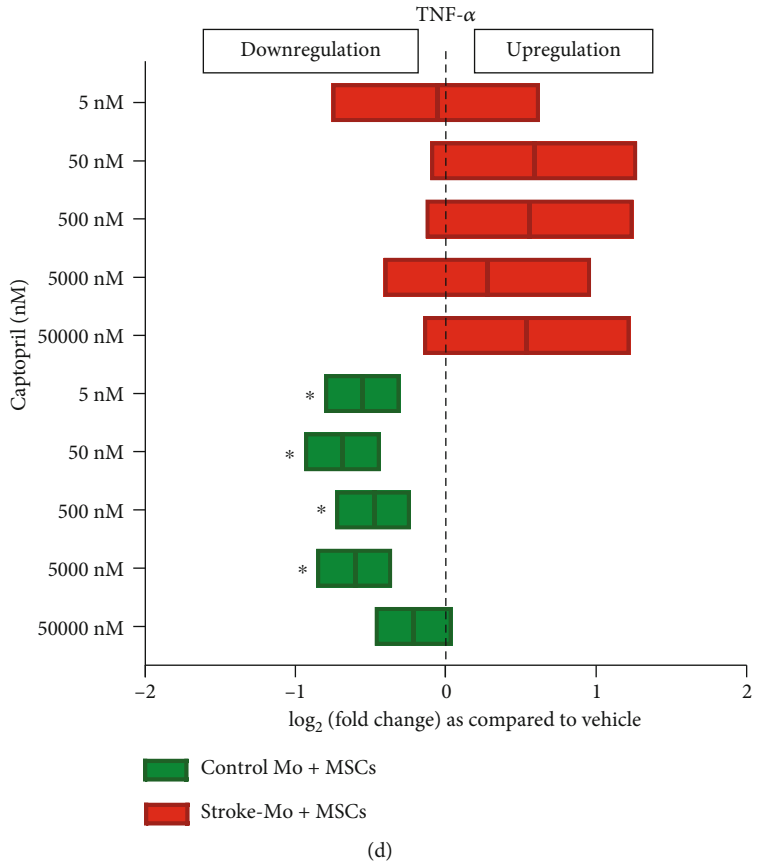

(d)

Figure 4: Continued.

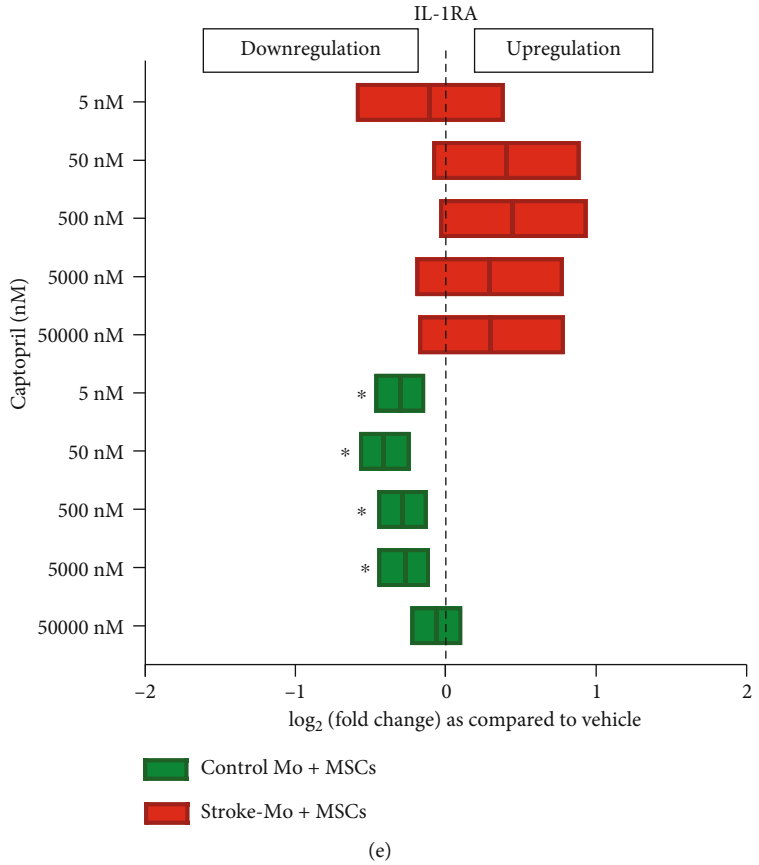

(e)

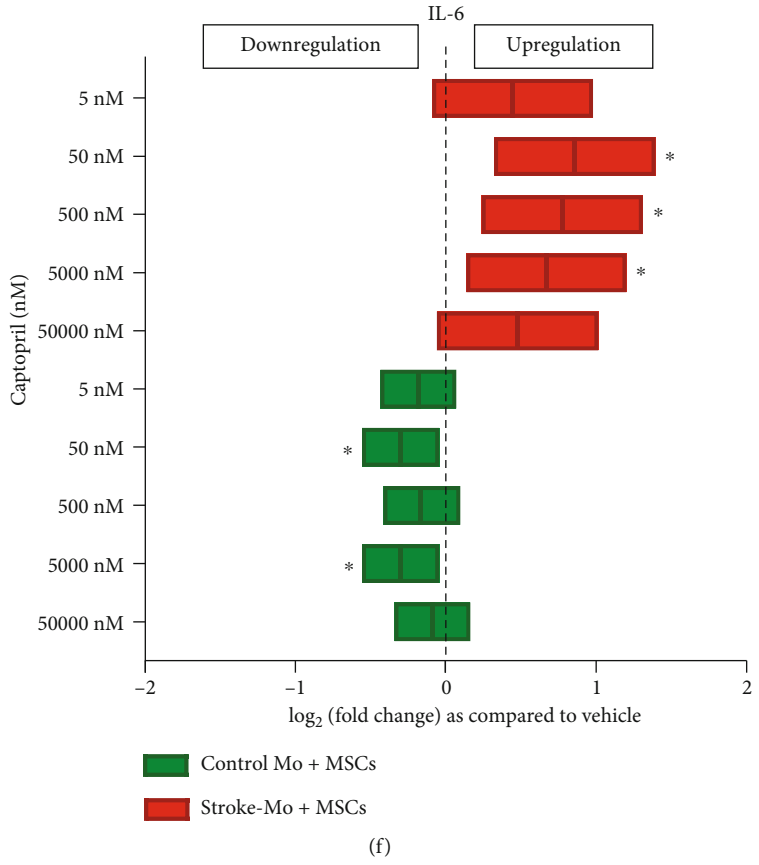

(f)

Figure 4: Continued.

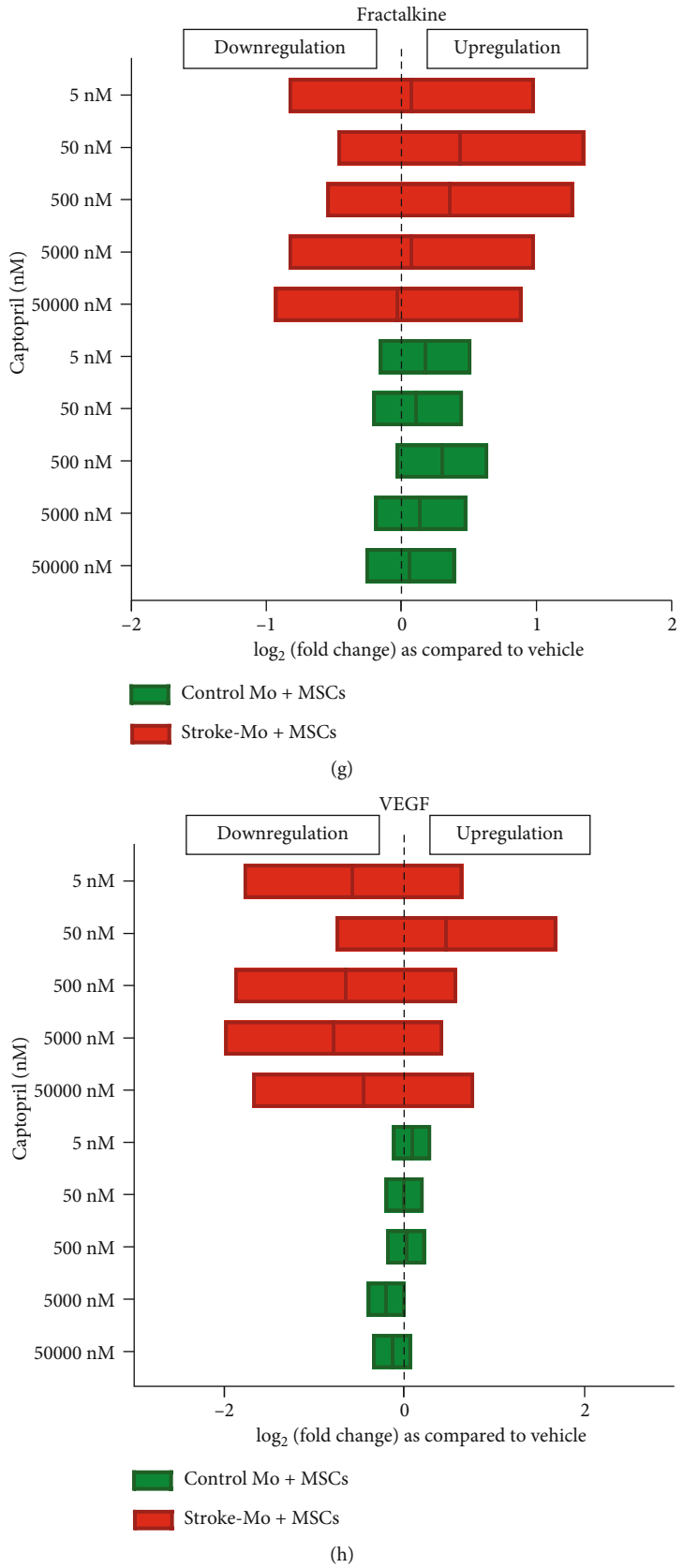

Figure 4: Captopril reduces the cytokine secretions of IL-8, MCP-1, TNF-α, IL-1RA, and IL-6 from cocultures of healthy control monocytes with MSCs after 24 hours but increases only IL-6 secretions from cocultures involving stroke patient-derived monocytes without changing any other cytokine secretions. Significance is shown by $^{*}p < 0.05$. All fold changes are as compared to vehicle control.

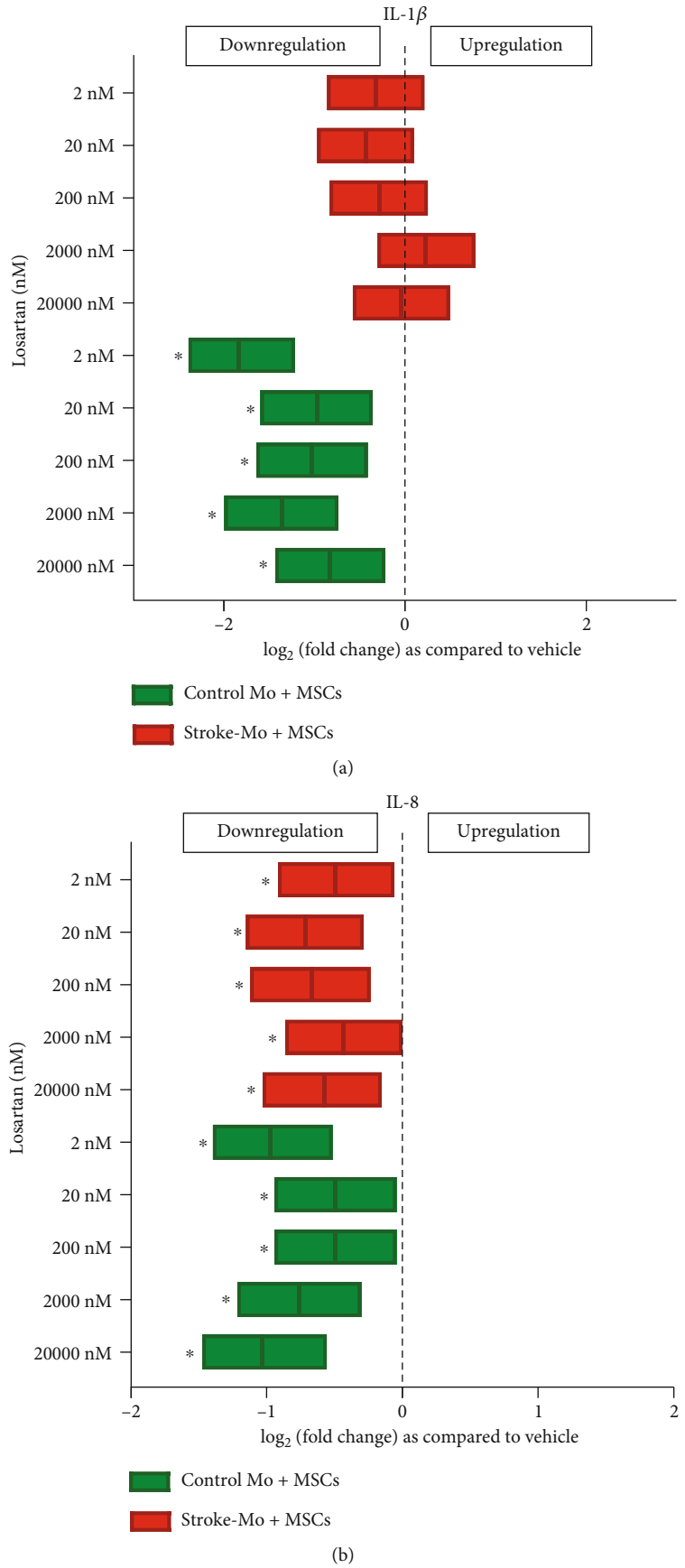

Figure 5: Continued.

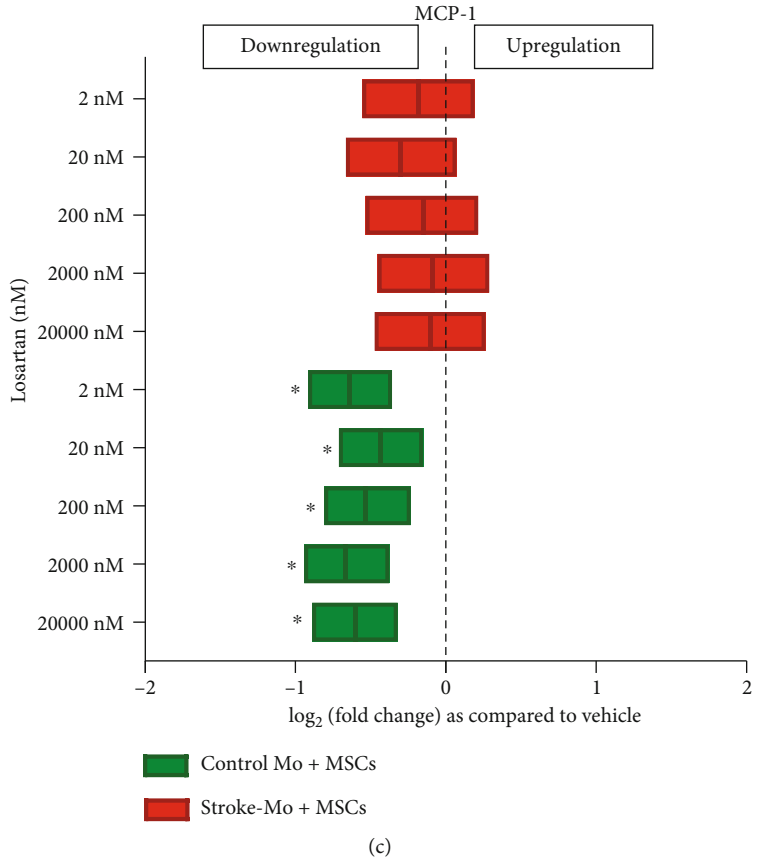

(c)

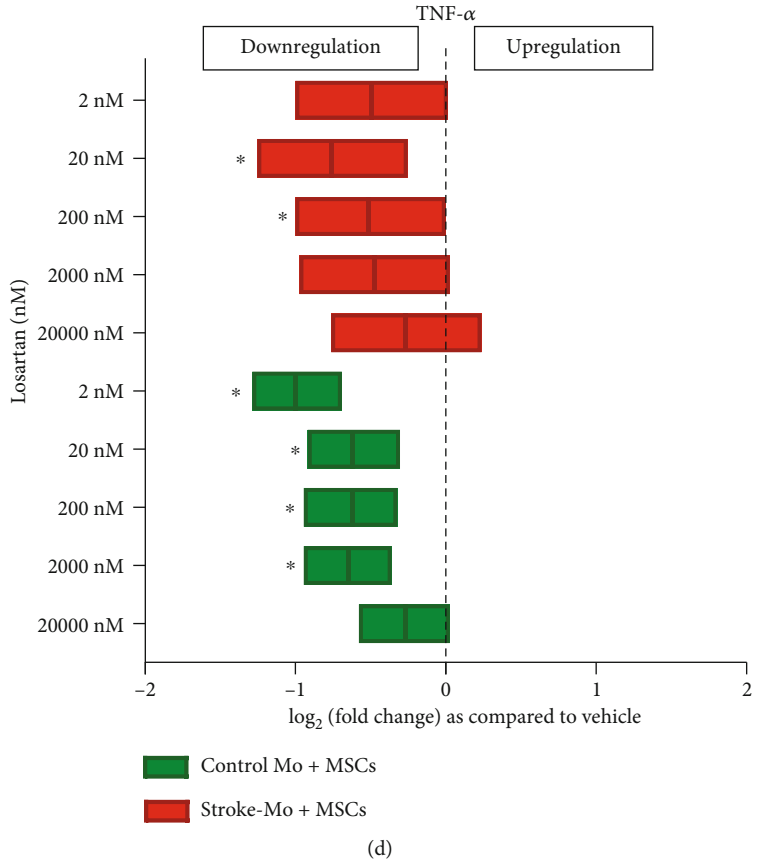

(d)

Figure 5: Continued.

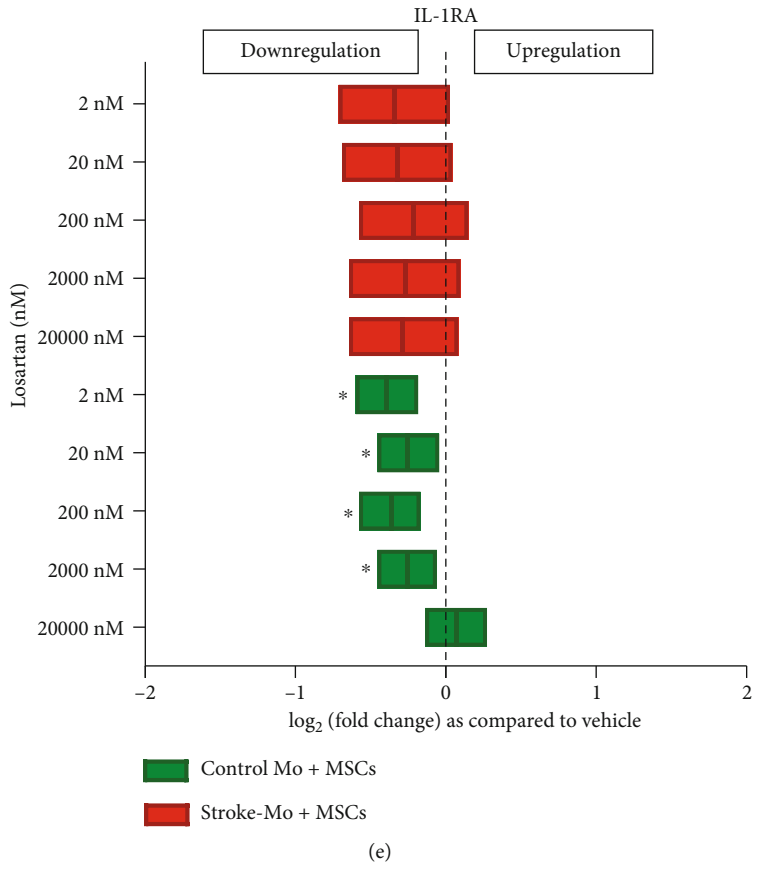

(e)

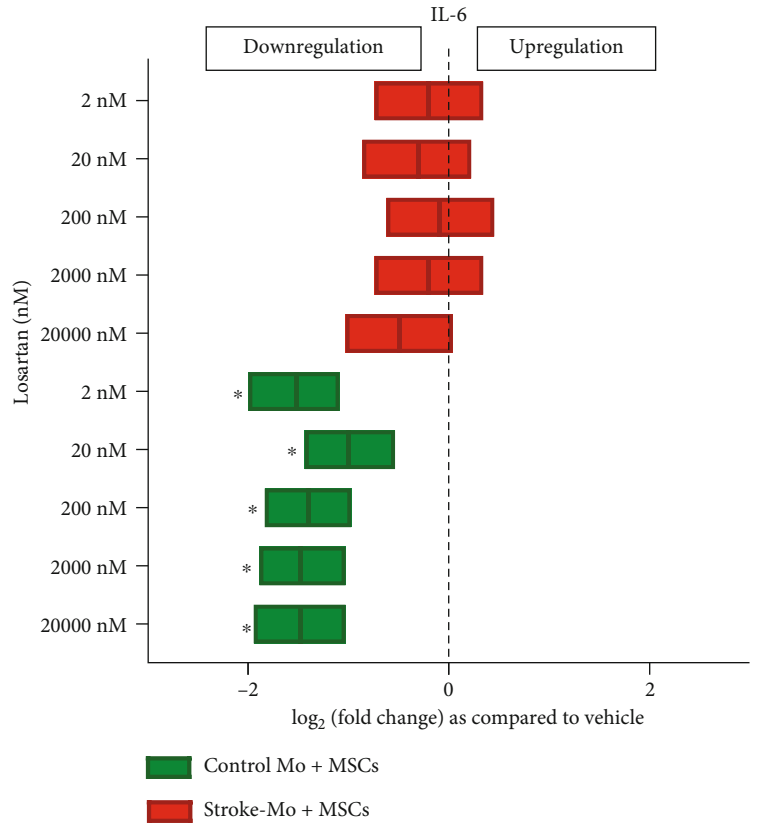

(f)

Figure 5: Continued.

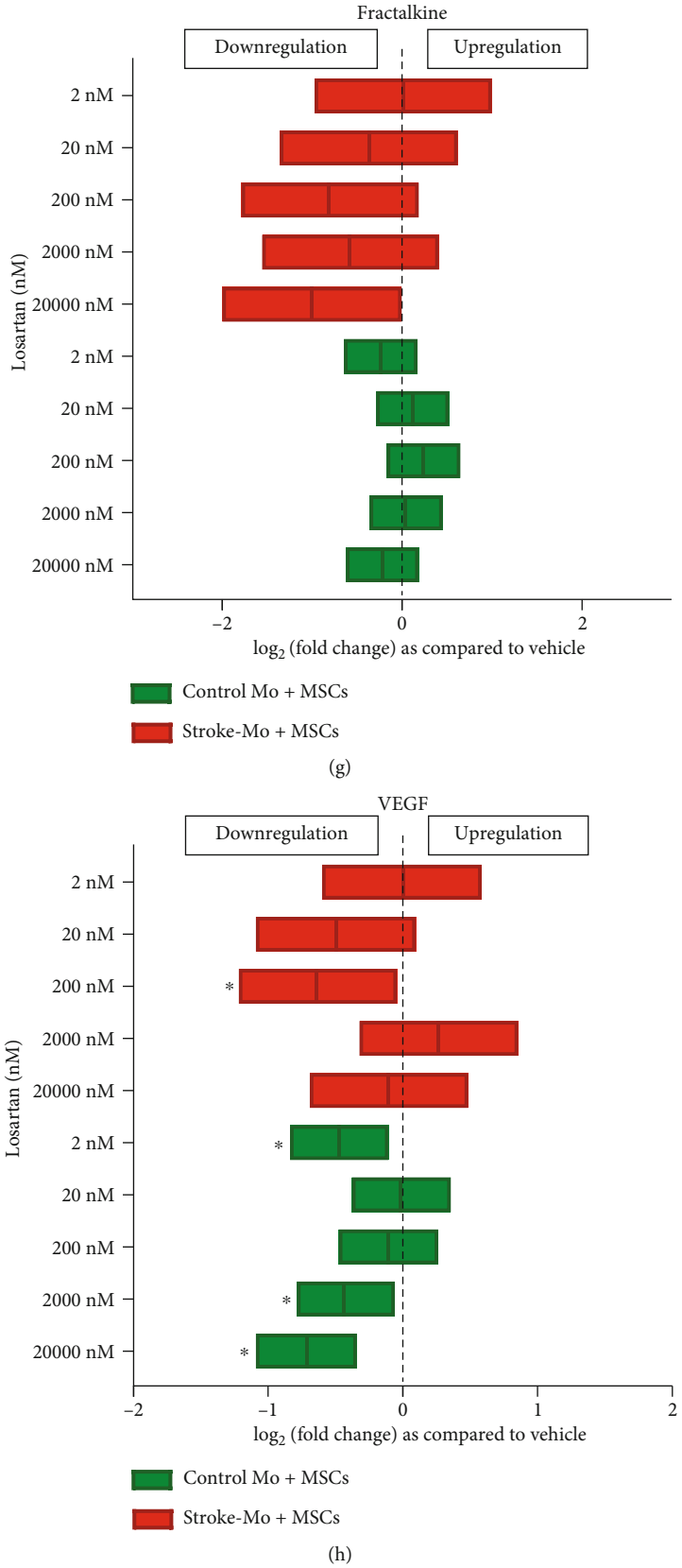

Figure 5: Losartan reduces the cytokine secretions of IL-1β, IL-8, MCP-1, TNF-α, IL-1RA, IL-6, and VEGF from cocultures of healthy control monocytes with MSCs after 24 hours of exposure, while decreasing only IL-8 secretions from cocultures involving stoke patient-derived monocytes without changing any other cytokine secretions. Significance is shown by $^{*}p < 0.05$. All fold changes are as compared to vehicle control.

Captopril is an angiotensin-converting enzyme (ACE) inhibitor and prevents the conversion of angiotensin I to angiotensin II. For hypertension, captopril can be given at doses ranging from 25 mg to 150 mg twice per day (BID) or three times per day (TID) [31]. The plasma concentrations of captopril range from 15 to 250 ng/ml, which translates to a concentration of 1000 nM to 50 nM [32]. To study the entire therapeutic range, we used 50 μM, 5 μM, 500 nM, 50 nM, and 5 nM captopril concentrations. Captopril increased IL-8 secretion from stroke as well as healthy control Mo indicating that they could have proinflammatory effects on monocytes. When MSCs were exposed to captopril, IL-6, IL-8, and MCP-1 secretions increased significantly indicating a strong inflammatory response. Cocultures with stroke-Mo and MSCs showed a significant increase in IL-6 secretion when they were exposed to captopril. There was no change in cytokine secretion for other cytokines with cocultures of stroke-Mo and MSCs, but cocultures with healthy Mo showed a consistent decrease in secretions of IL-1RA, IL-8, MCP-1, and TNF-α. In addition, when we compared the effect of captopril between stroke patient-derived Mo alone and their cocultures with MSCs, captopril showed an increase in IL-8 and TNF-α secretions from stroke patient-derived Mo alone. However, this effect was abolished in the presence of MSCs, indicating the possibility that MSCs may be able to curb the IL-8 and TNF-α secretions from stroke patient-derived Mo in the presence of captopril. Overall, captopril showed a consistent proinflammatory tendency towards both MSCs and stroke-Mo.

Losartan is a selective and competitive angiotensin II receptor blocker. It is approved as one of the first-line drugs for stage 1 hypertension [33]. Losartan is usually given at doses ranging from 25 to 100 mg once a day (OD). The peak serum levels of losartan after a 50 mg dose was between 200 and 250 ng/ml. However, serum levels can range from 50 to 300 ng/ml with 100 ng OD dosage [34]. This translates to a serum concentration range of 200 nM to 1200 nM. In this study, we used 20 μM, 2 μM, 200 nM, 20 nM, and 2 nM concentrations of losartan. Losartan did not change secretions of any measured cytokines from stroke-derived Mo but reduced MCP-1 and TNF-α from healthy control Mo. When MSCs were exposed to losartan, there was a consistent increase in IL-8 secretion. On the contrary, IL-8 secretion was consistently decreased in cocultures of MSCs and Mo for both stroke-Mo and healthy control Mo. Cocultures of MSCs and stroke-Mo failed to show any significant change of other released cytokines, but cocultures involving healthy Mo showed consistently reduced secretions of all cytokines measured in this study. Losartan did not show any differences in secretome when stroke patient-derived Mo alone was compared with cocultures of stroke-Mo and MSCs, indicating that losartan does not change the effects of MSCs on stroke-Mo.

ACE inhibitors or ARBs are commonly given to stroke patients to control blood pressure. MSCs exposed to the ACE inhibitor, captopril (doses ranging from 5000 nM to 5 nM), showed increased secretion of IL-6, IL-8, and MCP-1 at 24 hours after exposure. MSCs exposed to the ARB, losartan, showed a significant reduction in IL-6 secretion at 2 nM dose but showed a significant increase in IL-8 secretion at all doses higher than 20 nM. Our results indicate that blocking ACE enhances proinflammatory signals from MSCs while blocking angiotensin II receptor reduces proinflammatory signals from MSCs. A study by Krikov et al. showed that blocking angiotensin II receptor reduced stroke volume and improved functional outcome significantly, while blocking ACE did not produce any such effect [35]. Our results are consistent with this effect and in fact take it one step further by indicating that MSC treatment could be beneficial in combination with losartan by reducing IL-6 at low doses but not captopril, which increases IL-6 secretions. Our results also show that there is no consistent effect of these drugs on cocultures of MSCs and stroke-derived Mo, even though the secretome was markedly reduced from cocultures with healthy control-derived Mo. The only significant change was with captopril, which increased IL-6 secretion from cocultures involving stroke-Mo but reduced IL-6 from cocultures with healthy Mo. The limitation of this study is that it is difficult to attribute secretome change due to these drugs to either Mo or MSCs in the coculture experiments. However, in a clinical scenario involving MSCs in stroke patients, both Mo and MSCs will be present. Antihypertensive drugs are a variable which will change from patient-to-patient. Hence, our study provides a framework for designing clinical trials involving MSCs in stroke patients on these medications. Our results also strongly indicate that atenolol may have an anti-inflammatory effect on the secretome when administered in stroke patients, while captopril could be proinflammatory for secretomes derived from interactions between MSCs and Mo.

Overall, our results show that antihypertensive medications at clinically relevant doses have significant effects on the secretomes and immunomodulatory signaling of MSCs. Since immunomodulation is a key mechanism of MSCs in promoting stroke recovery in animal studies, our results suggest the possibility that antihypertensive medications may exert drug interactions on MSCs and exposure to these medications may be an important variable that should be considered in clinical trials testing MSCs in stroke patients.

Data Availability

The data used to support the findings of this study are available from the corresponding author upon request.

Conflicts of Interest

As an employee of the institution (UTHealth), Dr. Sean I. Savitz has served in the following roles: as a site investigator in clinical trials sponsored by industry companies—Athersys, Genentech, Pfizer, Dart Neuroscience, and SanBio, for which UTHealth receives payments on the basis of clinical trial contracts; as an investigator on clinical trials supported by the National Institutes of Health (NIH) grants, Department of Defense, Let us Cure CP, the Texas Institute for Rehabilitation and Research Foundation, and the Cord Blood Registry Systems; as a principal investigator on NIH-funded grants in basic science research; and as a principal investigator for

an imaging analysis center for clinical trials sponsored by SanBio. Whereas UTHealth uses Dr. Savitz with expertise in stroke, UTHealth has served as a consultant to Neuralstem, SanBio, Mesoblast, ReNeuron, Lumosa, Celgene, Dart Neuroscience, BlueRock, and Aldagen. All funding goes to the institution.

Acknowledgments

We thank Dr. Adrian Gee and Dr. Scott D. Olson for providing us with human MSCs. This work was supported in part by a grant from Bentson Stroke Center and by N-01, NHLBI (PI: Sean Savitz).

Supplementary Materials

Supplementary Figure S1: supplementary figure showing that the clinically relevant drugs do not alter the cell proliferation of MSCs at physiologically relevant concentrations after 24 and 48 hours of exposure to atenolol, captopril, and losartan. *(Supplementary materials)*

References

[1] D. C. Hess, L. R. Wechsler, W. M. Clark et al., "Safety and efficacy of multipotent adult progenitor cells in acute ischaemic stroke (MASTERS): a randomised, double-blind, placebo-controlled, phase 2 trial," *Lancet Neurology*, vol. 16, no. 5, pp. 360–368, 2017.

[2] F. Moniche, P. H. Rosado-de-Castro, I. Escudero et al., "Increasing dose of autologous bone marrow mononuclear cells transplantation is related to stroke outcome: results from a pooled analysis of two clinical trials," *Stem Cells International*, vol. 2016, Article ID 8657173, 8 pages, 2016.

[3] F. Moniche, I. Escudero, E. Zapata-Arriaza et al., "Intra-arterial bone marrow mononuclear cells (BM-MNCs) transplantation in acute ischemic stroke (IBIS trial): protocol of a phase II, randomized, dose-finding, controlled multicenter trial," *International Journal of Stroke*, vol. 10, no. 7, pp. 1149–1152, 2015.

[4] K. Prasad, A. Sharma, A. Garg et al., "Intravenous autologous bone marrow mononuclear stem cell therapy for ischemic stroke: a multicentric, randomized trial," *Stroke*, vol. 45, no. 12, pp. 3618–3624, 2014.

[5] S. I. Savitz, V. Misra, M. Kasam et al., "Intravenous autologous bone marrow mononuclear cells for ischemic stroke," *Annals of Neurology*, vol. 70, no. 1, pp. 59–69, 2011.

[6] Y. Gu, M. He, X. Zhou et al., "Endogenous IL-6 of mesenchymal stem cell improves behavioral outcome of hypoxic-ischemic brain damage neonatal rats by supressing apoptosis in astrocyte," *Scientific Reports*, vol. 6, no. 1, 2016.

[7] O. Y. Bang, K. S. Jin, M. N. Hwang et al., "The effect of CXCR4 overexpression on mesenchymal stem cell transplantation in ischemic stroke," *Cell Med.*, vol. 4, no. 2, pp. 65–76, 2012.

[8] O. Honmou, K. Houkin, T. Matsunaga et al., "Intravenous administration of auto serum-expanded autologous mesenchymal stem cells in stroke," *Brain*, vol. 134, no. 6, pp. 1790–1807, 2011.

[9] J. S. Lee, J. M. Hong, G. J. Moon et al., "A long-term follow-up study of intravenous autologous mesenchymal stem cell transplantation in patients with ischemic stroke," *Stem Cells*, vol. 28, no. 6, pp. 1099–1106, 2010.

[10] N. Satani, C. Cai, K. Giridhar et al., "World-wide efficacy of bone marrow derived mesenchymal stromal cells in preclinical ischemic stroke models: systematic review and meta-analysis," *Frontiers in Neurology*, vol. 10, p. 405, 2019.

[11] S. M. Melief, S. B. Geutskens, W. E. Fibbe, and H. Roelofs, "Multipotent stromal cells skew monocytes towards an anti-inflammatory interleukin-10-producing phenotype by production of interleukin-6," *Haematologica*, vol. 98, no. 6, pp. 888–895, 2013.

[12] A. J. Cutler, V. Limbani, J. Girdlestone, and C. V. Navarrete, "Umbilical cord-derived mesenchymal stromal cells modulate monocyte function to suppress T cell proliferation," *Journal of immunology (Baltimore, Md: 1950)*, vol. 185, no. 11, pp. 6617–6623, 2010.

[13] S. M. Melief, E. Schrama, M. H. Brugman et al., "Multipotent stromal cells induce human regulatory T cells through a novel pathway involving skewing of monocytes toward anti-inflammatory macrophages," *Stem Cells*, vol. 31, no. 9, pp. 1980–1991, 2013.

[14] S. V. Boregowda, V. Krishnappa, and D. G. Phinney, "Isolation of mouse bone marrow mesenchymal stem cells," *Methods in molecular biology (Clifton, NJ)*, vol. 1416, pp. 205–223, 2016.

[15] D. J. Kota, K. S. Prabhakara, N. Toledano-Furman et al., "Prostaglandin E2 indicates therapeutic efficacy of mesenchymal stem cells in experimental traumatic brain injury," *Stem Cells*, vol. 35, no. 5, pp. 1416–1430, 2017.

[16] N. Satani, K. Giridhar, C. Cai et al., "Aspirin in stroke patients modifies the immunomodulatory interactions of marrow stromal cells and monocytes," *Brain Research*, vol. 1720, article 146298, 2019.

[17] K. Parsha, O. Mir, N. Satani et al., "Mesenchymal stromal cell secretomes are modulated by suspension time, delivery vehicle, passage through catheter, and exposure to adjuvants," *Cytotherapy*, vol. 19, no. 1, pp. 36–46, 2017.

[18] D. Drago, C. Cossetti, N. Iraci et al., "The stem cell secretome and its role in brain repair," *Biochimie*, vol. 95, no. 12, pp. 2271–2285, 2013.

[19] F. G. Teixeira, M. M. Carvalho, N. Sousa, and A. J. Salgado, "Mesenchymal stem cells secretome: a new paradigm for central nervous system regeneration?," *Cellular and Molecular Life Sciences*, vol. 70, no. 20, pp. 3871–3882, 2013.

[20] K. S. Lee, H. W. Kang, H. T. Lee et al., "Sequential sub-passage decreases the differentiation potential of canine adipose-derived mesenchymal stem cells," *Research in Veterinary Science*, vol. 96, no. 2, pp. 267–275, 2014.

[21] H. E. Gruber, S. Somayaji, F. Riley et al., "Human adipose-derived mesenchymal stem cells: serial passaging, doubling time and cell senescence," *Biotechnic & Histochemistry*, vol. 87, no. 4, pp. 303–311, 2011.

[22] B. Yang, K. Parsha, K. Schaar et al., "Cryopreservation of bone marrow mononuclear cells alters their viability and subpopulation composition but not their treatment effects in a rodent stroke model," *Stem cells international*, vol. 2016, Article ID 5876836, 7 pages, 2016.

[23] N. I. Nikolaev, Y. Liu, H. Hussein, and D. J. Williams, "The sensitivity of human mesenchymal stem cells to vibration and cold storage conditions representative of cold transportation," *J R Soc Interface*, vol. 9, no. 75, pp. 2503–2515, 2012.

[24] M. Francois, I. B. Copland, S. Yuan, R. Romieu-Mourez, E. K. Waller, and J. Galipeau, "Cryopreserved mesenchymal stromal cells display impaired immunosuppressive properties as a

result of heat-shock response and impaired interferon-γ licensing," *Cytotherapy*, vol. 14, no. 2, pp. 147–152, 2012.

[25] J. Boltze, M. M. Modo, R. W. Mays et al., "Stem cells as an emerging paradigm in stroke 4: advancing and accelerating preclinical research," *Stroke*, vol. 50, no. 11, pp. 3299–3306, 2019.

[26] R. Jin, L. Liu, S. Zhang, A. Nanda, and G. Li, "Role of inflammation and its mediators in acute ischemic stroke," *Journal of cardiovascular translational research.*, vol. 6, no. 5, pp. 834–851, 2013.

[27] H. Boutin, R. A. LeFeuvre, R. Horai, M. Asano, Y. Iwakura, and N. J. Rothwell, "Role of IL-1alpha and IL-1beta in ischemic brain damage," *The Journal of Neuroscience*, vol. 21, no. 15, pp. 5528–5534, 2001.

[28] B. Rehman, D. P. Sanchez, and S. Shah, *Atenolol*, Stat Pearls, Treasure Island (FL), 2020.

[29] G. Leonetti, L. Terzoli, C. Bianchini, C. Sala, and A. Zanchetti, "Time-course of the anti-hypertensive action of vatenolol: comparison of response to first dose and to maintained oral administration," *European Journal of Clinical Pharmacology*, vol. 18, no. 5, pp. 365–374, 1980.

[30] S. L. Deshmane, S. Kremlev, S. Amini, and B. E. Sawaya, "Monocyte chemoattractant protein-1 (MCP-1): an overview," *Journal of Interferon & Cytokine Research*, vol. 29, no. 6, pp. 313–326, 2009.

[31] F. Marte and M. Cassagnol, *Captopril*, Stat Pearls, Treasure Island (FL), 2020.

[32] T. R. Shaw, F. M. Duncan, B. C. Williams et al., "Plasma free captopril concentrations during short and long term treatment with oral captopril for heart failure," *British Heart Journal*, vol. 54, no. 2, pp. 160–165, 1985.

[33] S. Mulla and W. J. Siddiqui, *Losartan*, Stat Pearls, Treasure Island (FL), 2020.

[34] D. A. Sica, T. W. B. Gehr, and S. Ghosh, "Clinical pharmacokinetics of losartan," *Clinical Pharmacokinetics*, vol. 44, no. 8, pp. 797–814, 2005.

[35] M. Krikov, C. Thone-Reineke, S. Muller, A. Villringer, and T. Unger, "Candesartan but not ramipril pretreatment improves outcome after stroke and stimulates neurotrophin BNDF/TrkB system in rats," *Journal of Hypertension*, vol. 26, no. 3, pp. 544–552, 2008.

Hindawi
Stem Cells International
Volume 2020, Article ID 5701920, 10 pages
https://doi.org/10.1155/2020/5701920

Review Article

Therapeutic Evidence of Human Mesenchymal Stem Cell Transplantation for Cerebral Palsy: A Meta-Analysis of Randomized Controlled Trials

Baocheng Xie, Minyi Chen, Runkai Hu, Weichao Han, and Shaobo Ding

Affiliated Dongguan People's Hospital, Southern Medical University Dongguan, Guangdong, China

Correspondence should be addressed to Shaobo Ding; 943098759@qq.com

Received 13 March 2020; Revised 31 May 2020; Accepted 4 June 2020; Published 20 July 2020

Academic Editor: Kar Wey Yong

Cerebral palsy (CP) is a kind of movement and posture disorder syndrome in early childhood. In recent years, human mesenchymal stem cell (hMSC) transplantation has become a promising therapeutic strategy for CP. However, clinical evidence is still limited and controversial about clinical efficacy of hMSC therapy for CP. Our aim is to evaluate the efficacy and safety of hMSC transplantation for children with CP using a meta-analysis of randomized controlled trials (RCTs). We conducted a systematic literature search including Embase, PubMed, ClinicalTrials.gov, Cochrane Controlled Trials Register databases, Chinese Clinical Trial Registry, and Web of Science from building database to February 2020. We used Cochrane bias risk assessment for the included studies. The result of pooled analysis showed that hMSC therapy significantly increased gross motor function measure (GMFM) scores (standardized mean difference (SMD) = 1.10, 95%CI = 0.66-1.53, $P < 0.00001$, high-quality evidence) and comprehensive function assessment (CFA) (SMD = 1.30, 95%CI = 0.71-1.90, $P < 0.0001$, high-quality evidence) in children with CP, compared with the control group. In the subgroup analysis, the results showed that hMSC therapy significantly increased GMFM scores of 3, 6, and 12 months and CFA of 3, 6, and 12 months. Adverse event (AE) of upper respiratory infection, diarrhea, and constipation was not statistically significant between the two groups. This meta-analysis synthesized the primary outcomes and suggested that hMSC therapy is beneficial, effective, and safe in improving GMFM scores and CFA scores in children with CP. In addition, subgroup analysis showed that hMSC therapy has a lasting positive benefit for CP in 3, 6, and 12 months.

1. Introduction

Cerebral palsy (CP) is a syndrome of posture disorders and movement disorders caused by nonprogressive damage in brain development. Patients with CP are associated with sensory and perceptual impairments, cognition difficulties, and behavioral disorders, as well as secondary musculoskeletal disorders and epilepsy [1, 2]. Movement disorders in CP are often accompanied by sensory, perceptual, cognitive, communication, and behavioral disorders [2]. Although with the development of obstetrics and perinatology, the prevalence of CP is 2 and 3 per 1000 live births, CP is considered the major cause of disabilities and death of childhood. CP in children has become a very important public health issue that severely affected patients' quality of life and caused a burden on the patient's family and national financial resources [3, 4]. At present, the main treatment is to rely on orthopedic surgery, hyperbaric oxygen treatments, and neurotrophic drugs. The clinical efficacy is limited since there is no advantage of treatment for CP. Therefore, clinicians need to seek a novel therapeutic option for CP to improve quality of life and promote physical function of patients.

In recent years, stem cells transplantation was considered as a promising treatment strategy in clinical practices and various clinical trials [5–7]. Therefore, studies on stem cell therapy for cerebral palsy provide a new treatment strategy. Currently, the stem cells mainly used to treat CP are neural progenitor cells, hematopoietic stem cells, bone marrow mesenchymal stem cell (BMSC), and umbilical cord mesenchymal stem cell (UC-MSC) [8–11]. Compared with other types of stem cells, human mesenchymal stem cells (hMSCs) have the potential advantages of easy accessibility,

immunosuppression, and low immunogenicity, so they are attractive and promising in treating various diseases. A trial of UC-MSC transplantation for children with CP showed that UC-MSC transplantation could significantly increase GMFM and CFA scores at 3, 6, 12, and 24 months. The study indicated that UC-MSC transplantation would be effective in improving functions for CP [12]. Another RCT also found that UC-MSC transplantation significantly improved GMFM and CFA scores without statistical significance in the incidence of AE between the two groups [13]. Increasing evidences show that hMSC transplantation has a therapeutic potential in the treatment of CP in some clinical studies. However, there is a lack of evidence-based medical evidence whether hMSC transplantation could treat CP. In this study, we sought to evaluate the efficacy and safety of hMSC transplantation therapy for CP by grading of recommendation assessment, development, and evaluation (GRADE) of RCTs.

2. Materials and Methods

The detailed protocol, which followed the template of Cochrane review for interventions, is registered in the PROSPERO (CRD42020171773). The preferred reporting items for systematic reviews and meta-analysis (PRISMA) were used to complete this study.

2.1. Literature Search. A comprehensive literature search was performed in Embase database, Cochrane Library, PubMed database, Web of Science, Chinese Clinical Trial Registry, and Clinical Trials.gov from building the database until February 2020. The MeSH and keywords search terms included the following: # (a) Cerebral palsy, CP, # (b) Human mesenchymal stem cell, hMSC, umbilical cordderived mesenchymal stem cell, mesenchymal stem cell, MSC, # (c) Randomized controlled trials.

2.2. Data Extraction. Two reviewers (Xie BC and Chen MY) screened the full-text content of RCTs of hMSC therapy in CP and extracted experimenter data in predesigned data extraction form. Controversial opinion was resolved by consensus by the third independent investigator (Han WC). Data extracted were key variables of study design and registration, number of eligible patients, average age of patients, therapeutic strategy, follow-up time, and primary outcome.

2.3. Assessment of Risk of Bias. To address the risk of bias of studies, we used the Cochrane bias risk tool to evaluate RCTs. We evaluated the research methodology one by one according to the items listed as follows: (1) adequacy of random sequence generation, (2) allocation concealment, (3) blinding of study participants, (4) incomplete outcome data reporting, (5) selective outcome depiction, and (6) other potential sources of bias.

2.4. Outcome Measures. (1) The primary efficacy outcomes are as follows: gross motor function measure (GMFM) scores of 3, 6, and 12 months and comprehensive function assessment (CFA) of 3, 6, and 12 months. (2) The primary safety outcomes are as follows: adverse event (AE) of upper respiratory infection, diarrhea, and constipation.

2.5. Quality of Evidence. We use the GRADE methodology to assess the quality of evidence of pooled outcome indicators. We mainly use GRADE pro software to evaluate the outcome indicators with the bias, inconsistency, discontinuity, imprecision, and risk of publication bias and then evaluate the quality of evidence as very low, low, medium, or high.

2.6. Inclusion and Exclusion Criteria. The inclusion criteria of our study included (1) RCTs; (2) eligibility criteria for participants included a diagnosis of CP; (3) hMSC group treated with hMSC therapy and control group treated with normal saline or rehabilitation therapy; and (4) follow-up of at least 3 months. We excluded studies that met the following criteria: (1) nonrandomized trials; (2) republished studies; (3) ongoing RCTs and retraction study; (4) less than 3 months of follow-up; (5) review and meta-analysis; and (6) letters, case reports, cross-sectional studies, cohort studies, purely experimental design scheme researches, and articles without reporting outcomes of primary data articles.

2.7. Data Synthesis and Analysis. The statistical interpretation of data was performed using Review Manager 5.3 software and STATA 13.0 software. Dichotomous data were analyzed using risk ratio (RR) with 95% confidence intervals (CIs). Continuous data were presented as standardized mean difference (SMD) with 95% CI. Heterogeneity among RCTs for each outcome was calculated by means of the χ^2 test and I^2 statistic, where $I^2 < 25\%$ represents slight inconsistency, I^2 between 25% and 50% with a medium heterogeneity. If $I^2 > 50\%$, the study had a severe heterogeneity; we conservatively used random-effects models to estimate the pooled outcomes to reduce the heterogeneity of studies. If not, pooled outcomes were estimated with a fixed effects model with RR and 95% CI. We performed sensitivity analyses to evaluate the robustness of the model and the impact of selected measures of study characteristics for the primary study outcomes. We performed the subgroup analyses to explore potential effects of GMFM scores of 3, 6, and 12 months and CFA of 3, 6, and 12 months.

3. Results

3.1. Data Selection. Our systematic search identified 310 citations published from building the database until February 2020. A total of 58 duplicated studies were excluded in NoteExpress. Then, after reading the titles and abstracts of the literature, we further excluded 207 studies with the following reasons: (a) nonrandomized trials; (b) review and meta-analysis; (c) case report, abstract, poster, letters, case reports, cross-sectional studies, cohort studies, or presentation; and (d) not patients with CP. Next, we excluded 41 studies of articles without reporting outcomes of primary data articles, ongoing study, and the study reporting rationale and design after reading the full text of the literature. Finally, we included 4 studies on hMSC transplantation for CP in this meta-analysis (Figure 1).

3.2. Characteristics of Included Studies. Four studies of 189 participants were included in this analysis. The hMSC group

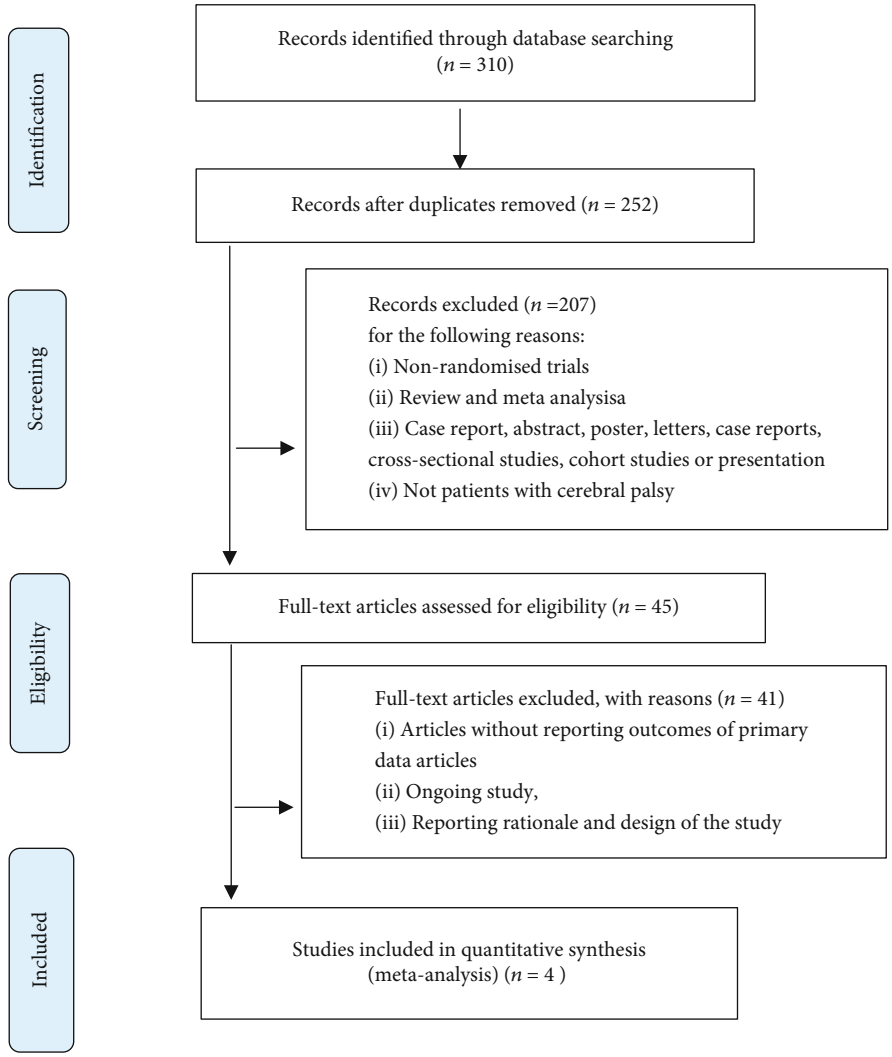

Figure 1: Flow diagram and strategy of this meta-analysis.

was treated with hMSC therapy and the control group was treated with normal saline. The clinical trial registration numbers of the three RCTs were ChiCTR1800016554, CHiCTR-TRC-12002568, and NCT01929434. The stem cell therapy used in the three RCTs was hUC-MSCs; the other stem cell used in the RCT was BMSC. The amount of hMSC transplants in RCTs of Huang et al. [12] and Gu et al. [13] and were 5×10^7 and $(5.00 \pm 0.50) \times 10^7$. The dosage of hMSC transplants in the other two studies was 1×10^6/kg and 1×10^7. The primary efficacy outcomes in RCTs were GMFM scores of 3, 6, and 12 months and CFA of 3, 6, and 12 months. The primary safety outcomes in RCTs were AE of upper respiratory infection, diarrhea, constipation, and fever (Table 1).

3.3. Quality Assessment. The RCTs of Liu et al. [14] and Gu et al. [13] were assigned to two groups according to the randomization table. We evaluated them as "low risk" studies in selection bias. RCTs of Huang et al. and Peng et al. [15] did not report randomized methods and were assessed of "unclear risk" and "high risk" in selection bias. After randomization, the study processes of Liu et al. [14] and Gu et al. [13] were blinded to the patient groups, participant surgeons, coordinators, and the investigators. We evaluated them as "low risk" in selection bias, performance bias, and detection bias. The study of Huang et al. reported that the patients and their families were blinded. But, we did not find out whether the study was reported blind to the investigators and participant surgeons; we evaluated it as "unclear risk" in selection bias, performance bias, and detection bias. The studies of Gu et al. and Liu et al. [14] reported that one patient and two patients in the hMSC group were lost to follow-up. We evaluated them as "unclear risk" in attrition bias. The results of the studies showed low correlation between the impact of patients' lifestyle and privacy, and we considered that reporting bias with the low possibility and evaluated them as "unclear risk" in reporting bias (Figure 2).

3.4. Quality of Evidence. We used the GRADE methodology to assess quality of evidence. We evaluated that hMSC therapy significantly increased GMFM scores and CFA score

Table 1: Characteristics of included articles.

Study	Registered number	Design	Participants	Intervention		Dosage	Outcomes
				hMSC group	Control group		
Gu et al. [13]	ChiCTR1800016554	RCT	40	hMSC therapy	Normal saline	$(5.00 \pm 0.50) \times 10^7$	GMFM, CFA, AE
Huang et al. [12]	NA	RCT	54	hMSC therapy	Normal saline	5×10^7	GMFM, CFA, AE
Liu et al. [14]	CHiCTR-TRC-12002568	RCT	70	hMSC therapy	Rehabilitation therapy	1×10^6/kg	GMFM, FMFM, AE
Peng et al. [15]	NCT01929434	RCT	25	hMSC therapy	Nonintervention therapy	1×10^7	SF, AE

Note: RCT: randomized controlled trial; hMSC: human mesenchymal stem cell; GMFM: gross motor function measure; CFA: comprehensive function assessment; AE: adverse event; FMFM: fine motor function measure; SF: drooling severity and frequency scale.

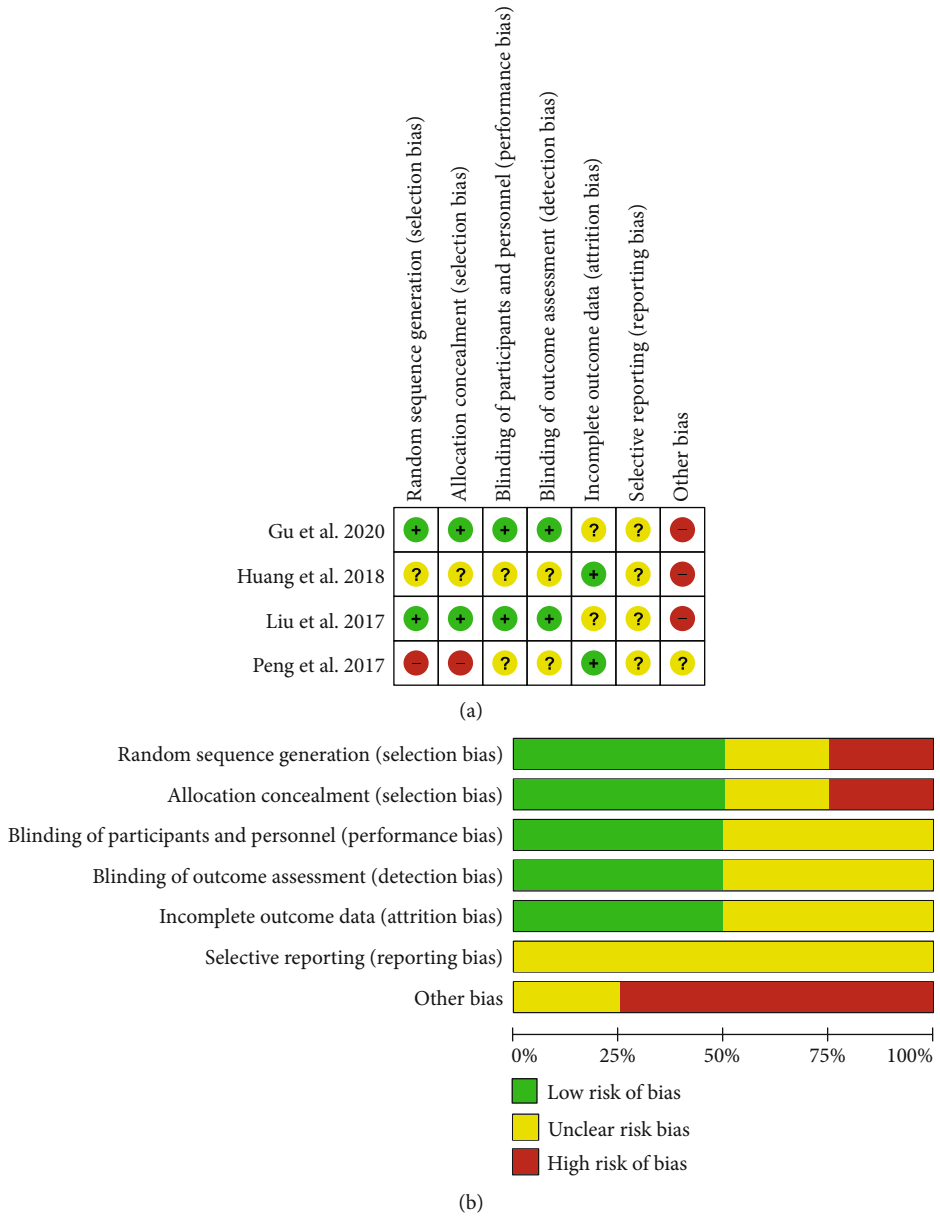

Figure 2: The quality assessment of each study according to the Cochrane collaboration manual. (a) Detailed analysis one by one of the risk of bias summary of included studies. (b) The risk bias graph shows a summary of the quality of each study.

with high-quality evidence. We evaluated that AE of upper respiratory infection, diarrhea, and constipation was not statistically significant with moderate-quality evidence, between the hMSC therapy group and the control group (Table 2).

3.5. GMFM Scores. GMFM scores were reported in 3 studies of 81 patients with hMSC therapy and 82 patients in the control group. We used a random-effects model after heterogeneity analysis ($I^2 = 80 > 50\%$). Pooled analysis showed that hMSC therapy significantly increased GMFM scores (SMD = 1.10, 95%CI = 0.66-1.53, $P < 0.00001$, high-quality evidence) (Figure 3, Table 2), compared with the control group. Subgroup analysis with random-effects model showed that hMSC therapy significantly increased GMFM scores in 3 months (SMD = 0.89, 95%CI = 0.19-1.59, $P = 0.01$), 6 months (SMD = 1.19, 95%CI = 0.28-2.11, $P = 0.01$), and 12 months (SMD = 1.23, 95%CI = 0.25-2.21, $P = 0.01$), compared with the control group in children with CP (Figure 3).

3.6. CFA Scores. CFA scores were reported in 2 RCTs of 46 patients treated with hMSC therapy and 47 patients in the control group. A random-effects model was used to analyze after heterogeneity analysis ($I^2 = 80\%$). Pooled analysis indicated that hMSC therapy significantly improved CFA scores (SMD = 1.30, 95%CI = 0.71-1.90, $P < 0.0001$, high-quality evidence) (Figure 4, Table 2), compared with the control group. Subgroup analysis with random-effects model showed that hMSC therapy significantly increased CFA scores in 3 months (SMD = 1.12, 95%CI = 0.46-1.77, $P = 0.0008$) and 6

Table 2: GRADE summary of human mesenchymal stem cell transplantation for cerebral palsy.

Outcome	Absolute effect estimates (95% CI) Control	hMSC therapy	Relative effect (95% CI)	Participants (studies)	Evidence (GRADE)[†]	Comments
GMFM	—	SMD 1.1 higher (0.66 to 1.53 higher)	—	163 (3)	⊕⊕⊕⊕ High	hMSC therapy has important benefit in increasing GMFM.
CFA	—	SMD 1.3 higher (0.71 to 1.90 higher)	—	96 (3)	⊕⊕⊕⊕ Moderate	hMSC therapy has important benefit in increasing CFA.
Upper respiratory infection	468 per 1000	417 per 1000 (267 to 651) Difference: 51 fewer per 1000 (201 to 183)	RR 0.89 (0.57 to 1.39)	93 (2)	⊕⊕⊕◯ Moderate	hMSC therapy did not increase AE of upper respiratory infection.
Diarrhea	298 per 1000	241 per 1000 (125 to 468) Difference: 57 fewer per 1000 (173 to 170)	RR 0.81 (0.42 to 1.57)	93 (2)	⊕⊕⊕◯ Moderate	hMSC therapy did not increase AE of diarrhea.
Constipation	106 per 1000	65 per 1000 (16 to 260) Difference: 41 fewer per 1000 (90 to 153)	RR 0.61 (0.15 to 2.44)	93 (2)	⊕⊕⊕◯ Moderate	hMSC therapy did not increase AE of constipation.

[†]High: we are confident that the true effect of outcomes lies close to the estimate of the effect. Moderate: we are moderately confident that the assessed effects and the true effect are likely to be close to the assessed effects. CI: confidence interval; RR: risk ratio; AE: adverse event; SMD: standardized mean difference.

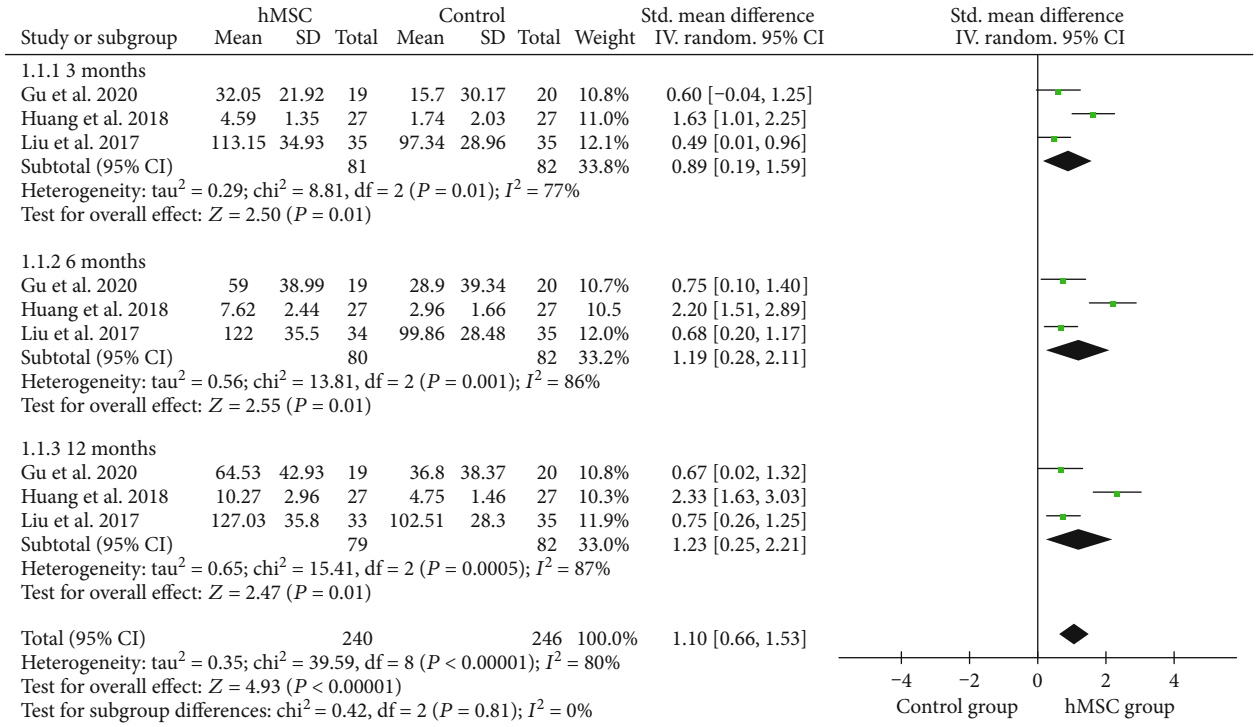

Figure 3: Forest plot of the meta-analysis with GMFM scores between the hMSC therapy and control groups.

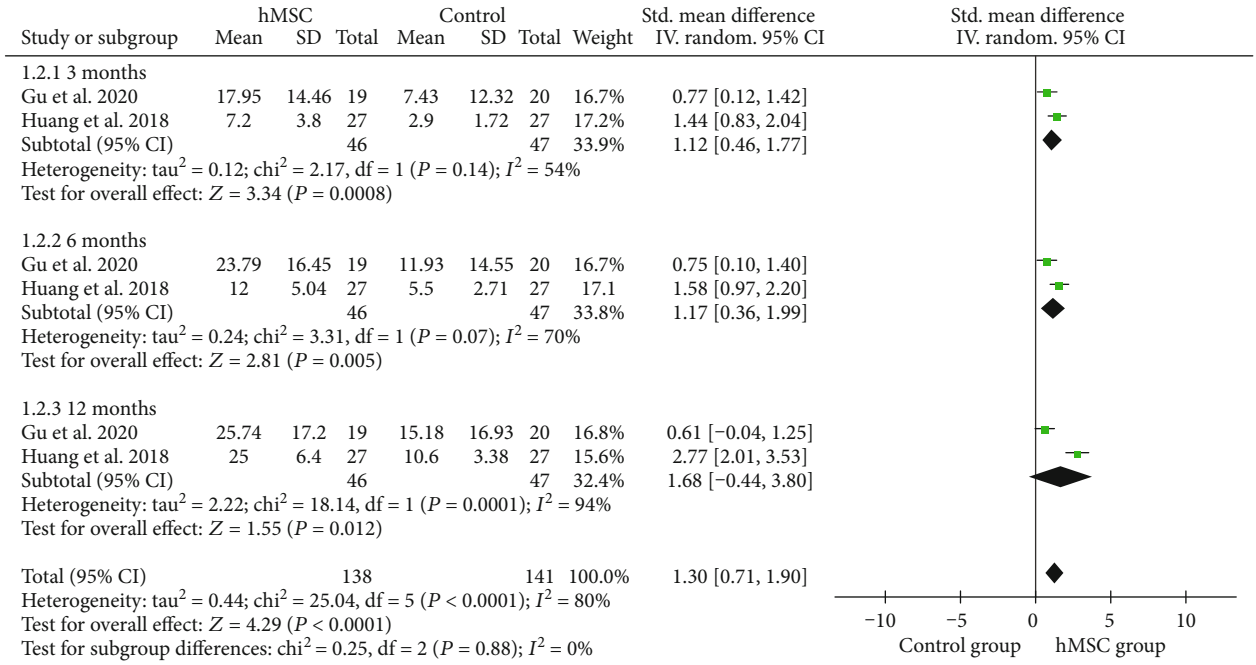

Figure 4: Forest plot of the meta-analysis with CFA scores between the hMSC therapy and control groups.

months (SMD = 1.17, 95%CI = 0.36-1.99, $P = 0.005$) in children with CP (Figure 4).

3.7. Adverse Event (AE). In order to explore the safety of hMSC therapy, we conducted a meta-analysis of AE. Pooled analysis indicated that AE of upper respiratory infection (RR = 0.80, 95%CI = 0.34-1.87, $P = 0.60$, moderate-quality evidence), diarrhea (RR = 0.81, 95%CI = 0.42-1.57, $P = 0.53$, moderate-quality evidence), and constipation (RR = 0.59, 95%CI = 0.13-2.62, $P = 0.59$, moderate-quality evidence) was not statistically significant between the hMSC therapy group and the control group (Tables 2 and 3). There was no statistical significance in other adverse events, such as fever, vomiting, anorexia, and urticaria in the studies. There

Table 3: Adverse event analysis between the hMSC therapy group and the control group.

AE	Study	RR and 95% CI	P
Upper respiratory infection	2 [12, 13]	RR (0.80), 95% CI (0.34-1.87)	0.60
Diarrhea	2 [12, 13]	RR (0.81), 95% CI (0.42-1.57)	0.53
Constipation	2 [12, 13]	RR (0.59), 95% CI (0.13-2.62)	0.59

were two studies [14, 15] which had low intracranial pressure after lumbar puncture in the hMSC transplantation group, including mild dizziness and headache, nausea, and vomiting. But, the symptoms of the children were relieved and disappeared when the patients lay on the bed without pillows and were treated with intravenous drip of saline.

4. Discussion

4.1. Primary Efficacy Outcomes. GMFM scores are useful and important as outcome evaluation results to evaluate changes in gross motor function for CP after interventions. This is crucial to determine effectiveness and benefit of interventional therapy by measuring the change of gross motor skill acquisition in children with CP. Children's measure gross motor function is commonly evaluated by rehabilitation specialists using GMFM scores. GMFM scored items consist of 5 parts: lying and rolling (17 items); walking, running, and jumping (24 items); sitting (20 items); climbing and kneeling (14 items); and standing (13 items). The items are scored in a four-point order (cannot initiate item, 0; initiates item, 1; partially completes item, 2; and completes item independently, 3) [16]. Higher scores in GMFM scores indicate better capacity and favourable prognosis in children with CP. The study of Wang et al. recruited 16 patients with CP and received UCMSC transplantation and the result showed that GMFM scores had significant improvement at the end of the first and sixth months after UCMSC transplantation [17]. Another study was of 52 patients with CP who received BMSC transplantation. The gross motor function was evaluated using GMFM scores in 1, 6, and 18 months. The result showed that BMMSC transplantation could significantly increase the GMFM scores at 6 months and 18 months of patients with CP, compared with the baseline value [18]. To further provide reliable evidence and high-quality evidence, we included three RCTs of hMSC therapy in CP and pooled results showed that hMSC therapy significantly increased GMFM scores in children with CP, compared with the control group. Moreover, we performed a subgroup analysis of GMFM scores of 3, 6, and 12 months. The result of subgroup analysis showed that hMSC therapy significantly increased GMFM scores in 3, 6, and 12 months ($P = 0.01$). We evaluated the indicators of GMFM scores with high-quality evidence using GRADE including inconsistency, risk of bias, indirectness, publication bias, and imprecision.

CFA is mainly used to evaluate function improvement and therapeutic effect of patients with CP. The RCTs of Gu et al. [13] and Huang et al. reported the changes of CFA in patients with CP after hMSC therapy. The results of both studies have shown that hMSC therapy could significantly improve CFA in patients with CP. In our study, we combined the data of RCTs with a total of 46 patients treated in hMSC therapy. Pooled analysis indicated that hMSC therapy significantly improved CFA scores, compared with the control group. Furthermore, we conducted a subgroup analysis on CFA scores. Subgroup analysis showed that hMSC therapy significantly increased CFA scores in 3 months ($P = 0.0008$) and 6 months ($P = 0.005$), compared with the control group in children with CP. According to GRADE, we consider that hMSC therapy for CP can improve the comprehensive function of patients with high-quality evidence. Fine motor function measure (FMFM) was also used to evaluate the therapeutic effect of cell therapy, although the study of Wang et al. [17] found that it was not statistically significant in UCMSC therapy for CP at the end of the first and sixth months. The scores of FMFM scores in the BMMSC group were all higher than those of the bone marrow mononuclear cell and the control groups at 3, 6, and 12 months after cell therapy for CP [14]. Salivation is a common symptom of patients with cerebral palsy, which seriously affects the health status of patients. The study found that UCMSC transplantation could significantly improve drooling severity and frequency scale in CP.

4.2. Primary Safety Outcomes. MSCs are attractive and promising because of their low immunogenicity, easy accessibility, and immunosuppressive potential in autologous transplantation [19, 20]. However, the safety of stem cell therapy remains a top priority. The studies showed that the quality of the hMSC relies on the separation conditions and cell culture techniques as well as the age, genetic traits, and different donor's medical history [21–23]. The quality of the hMSC is closely related to adverse events. Therefore, the safety of MSC transplantation involves many factors; it is necessary to evaluate the safety of MSC therapy for CP. We included 4 RCTs on hMSC therapy for CP. The RCT of Gu et al. [13] reported the incidence of upper respiratory infection (52.63%), diarrhea (31.58%), fever (36.84%), and constipation (5.26%) in the hMSC group and upper respiratory infection (70.00%), diarrhea (45.00%), fever (15.00%), and constipation (15.00%) in the control group. The RCT of Huang et al. [12] also reported the incidence of upper respiratory infection (33.33%), diarrhea (18.52%), and constipation (7.41%) in the hMSC group and upper respiratory infection (29.62%), diarrhea (18.52%), and constipation (7.41%) in the control group. Therefore, in order to evaluate the safety of hMSC therapy for CP, we conducted a meta-analysis for AE. Pooled analysis indicated that AE of upper respiratory infection ($P = 0.60$, moderate-quality evidence), diarrhea ($P = 0.53$, moderate-quality evidence), and constipation ($P = 0.59$, moderate-quality evidence) was not statistically significant between the two groups. There was no statistical

significance in other adverse events, such as fever, vomiting, anorexia, and urticaria in the studies. Serious adverse events were not observed in the included studies. However, there were two studies [14, 15] which had low intracranial pressure after lumbar puncture in the hMSC transplantation group. The symptoms of the children were relieved and disappeared when the patients lay in bed without pillows and were treated with intravenous drip of saline. The common adverse effect of hMSC transplantation by lumbar puncture is low intracranial pressure, which should be noted. The reasons for the low cranial pressure after lumbar puncture may be as follows: (1) most children have high muscle tension in their extremities, and the low cranial pressure is easy to occur after operation; (2) slender body, poor nutritional status; (3) poor cooperation of children during lumbar puncture hMSC transplantation, resulting in more puncture times; and (4) the degree of crying in the operation of children is heavier, resulting in a rapid outflow of cerebrospinal fluid. Therefore, after hMSC transplantation by lumbar puncture, targeted measures should be taken before, during, and after the operation to reduce the incidence of adverse reactions. (1) Before the operation for children and patients with involuntary exercise, the operation should be performed under sedation and hypnosis as far as possible, so as to avoid the children's crying and high limb muscle tension. (2) The lumbar puncture needle with fine caliber should be used during the operation and should reduce the number of puncture as far as possible and avoid multiple puncture of the same site in a short period of time. (3) The patients should lie down and rest after the operation and avoid raising his head and standing up. (4) Patients could take appropriate amount of normal saline according to the doctor's advice after surgery.

4.3. Limitations and Critical Considerations. We evaluated and analyzed the heterogeneity of included outcomes and found that there was a high heterogeneity in GMFM scores. Sensitivity analysis shows that the RCT of Huang et al. [12] resulted in high heterogeneity. In our analysis of this study, we found that the main reason for the high heterogeneity was that GMFM scores were reported in the form of the difference between the final score and the baseline data. If we exclude this study, heterogeneity will return to $I^2 = 0\%$ and the pooled results are consistent with the previous trend. In addition, we analyzed the sensitivity of GMFM scores using the Galbraith plot. The results were credible with no substantial change in the GMFM score. But, the small number of studies limited the analysis of publication bias in this study.

5. Conclusions

In conclusion, this meta-analysis synthesized the primary outcomes which suggested that hMSC therapy was safe and more effective in improving GMFM and CFA in children with CP. Apparently, the findings provide a novel therapeutic strategy for patients with CP. However, what are the optimal dose, frequency, timing, and routes of MSC transplantation in different phases of CP? These important and challenging clinical questions need more RCTs to be addressed urgently.

Conflicts of Interest

All authors declare that there is no conflict of interest about the publication of this paper.

Authors' Contributions

Baocheng Xie and Minyi Chen have equally contributed to this study. Runkai Hu and Weichao Han reviewed the literatures. Baocheng Xie, Minyi Chen, and Runkai Hu collected and analyzed the data. Shaobo Ding designed and supervised the completion of this study. All authors in this study read and approved the final manuscript.

Acknowledgments

The project was supported by the Guangdong Province's "Thirteenth Five-Year Plan" Chinese Medicine Key and Specialty Construction Project and the Project of Scientific Research Development Fund of Dongguan People's Hospital (K201920).

Supplementary Materials

Appendix S1: the PRISMA Checklist of this meta-analysis. *(Supplementary Materials)*

References

[1] S. J. Korzeniewski, J. Slaughter, M. Lenski, P. Haak, and N. Paneth, "The complex aetiology of cerebral palsy," *Nature Reviews Neurology*, vol. 14, no. 9, pp. 528–543, 2018.

[2] A. Colver, C. Fairhurst, and P. O. D. Pharoah, "Cerebral palsy," *Lancet (London, England)*, vol. 383, no. 9924, pp. 1240–1249, 2014.

[3] D. G. Whitney, N. S. Kamdar, S. Ng, E. A. Hurvitz, and M. D. Peterson, "Prevalence of high-burden medical conditions and health care resource utilization and costs among adults with cerebral palsy," *Clinical Epidemiology*, vol. Volume 11, pp. 469–481, 2019.

[4] S. Leigh, P. Granby, M. Turner, S. Wieteska, A. Haycox, and B. Collins, "The incidence and implications of cerebral palsy following potentially avoidable obstetric complications: a preliminary burden of disease study," *British Journal of Obstetrics and Gynaecology*, vol. 121, no. 13, pp. 1720–1728, 2014.

[5] J. Ankrum and J. M. Karp, "Mesenchymal stem cell therapy: two steps forward, one step back," *Trends in Molecular Medicine*, vol. 16, no. 5, pp. 203–209, 2010.

[6] M. Emadedin, N. Labibzadeh, M. G. Liastani et al., "Intra-articular implantation of autologous bone marrow-derived mesenchymal stromal cells to treat knee osteoarthritis: a randomized, triple-blind, placebo-controlled phase 1/2 clinical trial," *Cytotherapy*, vol. 20, no. 10, pp. 1238–1246, 2018.

[7] B. Xie, H. Luo, Y. Zhang, Q. Wang, C. Zhou, and D. Xu, "Autologous stem cell therapy in critical limb ischemia: a meta-analysis of randomized controlled trials," *Stem Cells International*, vol. 2018, Article ID 7528464, 12 pages, 2018.

[8] H. Dong, G. Li, C. Shang et al., "Umbilical cord mesenchymal stem cell (UC-MSC) transplantations for cerebral palsy," *American Journal of Translational Research*, vol. 10, no. 3, pp. 901–906, 2018.

[9] K. Min, J. Song, J. Y. Kang et al., "Umbilical cord blood therapy potentiated with erythropoietin for children with cerebral palsy: a double-blind, randomized, placebo-controlled trial," *Stem Cells*, vol. 31, no. 3, pp. 581–591, 2013.

[10] Z. Luan, W. Liu, S. Qu et al., "Effects of Neural Progenitor Cell Transplantation in Children with Severe Cerebral Palsy," *Cell Transplantation*, vol. 21, 1_suppl, pp. 91–S98, 2012.

[11] S. Eggenberger, C. Boucard, A. Schoeberlein et al., "Stem cell treatment and cerebral palsy: systemic review and meta-analysis," *World Journal of Stem Cells*, vol. 11, no. 10, pp. 891–903, 2019.

[12] L. Huang, C. Zhang, J. Gu et al., "A Randomized, Placebo-Controlled Trial of Human Umbilical Cord Blood Mesenchymal Stem Cell Infusion for Children With Cerebral Palsy," *Cell Transplantation*, vol. 27, no. 2, pp. 325–334, 2018.

[13] J. Gu, L. Huang, C. Zhang et al., "Therapeutic evidence of umbilical cord-derived mesenchymal stem cell transplantation for cerebral palsy: a randomized, controlled trial," *Stem Cell Research & Therapy*, vol. 11, no. 1, p. 43, 2020.

[14] X. Liu, X. Fu, G. Dai et al., "Comparative analysis of curative effect of bone marrow mesenchymal stem cell and bone marrow mononuclear cell transplantation for spastic cerebral palsy," *Journal of Translational Medicine*, vol. 15, no. 1, p. 48, 2017.

[15] Y. Peng, X. Wang, C. Xu et al., "Transplantation of umbilical cord mesenchymal stem cells effectively improves drooling of cerebral palsy patients," *Medical Journal of the Chinese People's Armed Police Forces*, vol. 28, no. 5, pp. 478–482, 2017.

[16] M. Alotaibi, T. Long, E. Kennedy, and S. Bavishi, "The efficacy of GMFM-88 and GMFM-66 to detect changes in gross motor function in children with cerebral palsy (CP): a literature review," *Disability and Rehabilitation*, vol. 36, no. 8, pp. 617–627, 2013.

[17] X. Wang, H. Hu, R. Hua et al., "Effect of umbilical cord mesenchymal stromal cells on motor functions of identical twins with cerebral palsy: pilot study on the correlation of efficacy and hereditary factors," *Cytotherapy*, vol. 17, no. 2, pp. 224–231, 2015.

[18] X. Wang, H. Cheng, R. Hua et al., "Effects of bone marrow mesenchymal stromal cells on gross motor function measure scores of children with cerebral palsy: a preliminary clinical study," *Cytotherapy*, vol. 15, no. 12, pp. 1549–1562, 2013.

[19] D. K. W. Ocansey, B. Pei, Y. Yan et al., "Improved therapeutics of modified mesenchymal stem cells: an update," *Journal of Translational Medicine*, vol. 18, no. 1, p. 42, 2020.

[20] N. Kim and S. G. Cho, "Overcoming immunoregulatory plasticity of mesenchymal stem cells for accelerated clinical applications," *International Journal of Hematology*, vol. 103, no. 2, pp. 129–137, 2016.

[21] G. Pachón-Peña, C. Serena, M. Ejarque et al., "Obesity determines the immunophenotypic profile and functional characteristics of human mesenchymal stem cells from adipose tissue," *Stem Cells Translational Medicine*, vol. 5, no. 4, pp. 464–475, 2016.

[22] M. Liu, H. Lei, P. Dong et al., "Adipose-Derived Mesenchymal Stem Cells from the Elderly Exhibit Decreased Migration and Differentiation Abilities with Senescent Properties," *Cell Transplantation*, vol. 26, no. 9, pp. 1505–1519, 2017.

[23] B. Lukomska, L. Stanaszek, E. Zuba-Surma, P. Legosz, S. Sarzynska, and K. Drela, "Challenges and controversies in human mesenchymal stem cell therapy," *Stem Cells International*, vol. 2019, Article ID 9628536, 10 pages, 2019.

Hindawi
Stem Cells International
Volume 2020, Article ID 8813447, 11 pages
https://doi.org/10.1155/2020/8813447

Review Article

Corneal Stem Cells as a Source of Regenerative Cell-Based Therapy

Jasmin S. Nurković,[1,2] **Radiša Vojinović**,[2,3] **and Zana Dolićanin**[4]

[1]*Center for Regeneration and Rehabilitation, Novi Pazar, Serbia*
[2]*Faculty of Medical Sciences, University of Kragujevac, Kragujevac, Serbia*
[3]*Clinical Center Kragujevac, Kragujevac, Serbia*
[4]*Department of Biomedical Sciences, State University of Novi Pazar, Novi Pazar, Serbia*

Correspondence should be addressed to Jasmin S. Nurković; jnurkovic@gmail.com

Received 10 April 2020; Revised 3 July 2020; Accepted 10 July 2020; Published 20 July 2020

Academic Editor: Hui Yin Nam

In the past few years, intensive research has focused on corneal stem cells as an unlimited source for cell-based therapy in regenerative ophthalmology. Today, it is known that the cornea has at least two types of stem cells: limbal epithelial stem cells (LESCs) and corneal stromal stem cells (CSSCs). LESCs are used for regeneration of corneal surface, while CSSCs are used for regeneration of corneal stroma. Until now, various approaches and methods for isolation of LESCs and CSSCs and their successful transplantation have been described and tested in several preclinical studies and clinical trials. This review describes in detail phenotypic characteristics of LESCs and CSSCs and discusses their therapeutic potential in corneal regeneration. Since efficient and safe corneal stem cell-based therapy is still a challenging issue that requires continuous cooperation between researchers, clinicians, and patients, this review addresses the important limitations and suggests possible strategies for improvement of corneal stem cell-based therapy.

1. Introduction

The cornea represents the part of transparent tissue at the front of the eye. It poses a protective physical and biological barrier against the outside environment and gives a refractive power to concentrate light onto the retina. The thickest layer of the cornea, the corneal stroma, embodies a unique avascular connective tissue which constitutes approximately 90% of the cornea volume. Its highly organized extracellular matrix consists of tightly packed parallel collagen type I of V fibrils [1, 2]. The corneal stroma is maintained by the keratinocytes, which originate from the neural crest. In contrast to normal corneal development where the newly formed collagen fibers are quickly formed into a well-organized structure, corneal injury results in the formation of a disorganized opaque matric known as a corneal scar tissue [3] that reduces corneal transparency and may cause blindness [4, 5].

Considering that scarring involving the center of the cornea will cause significant visual loss and is mainly irreversible, the most common method of therapy is corneal transplantation from cadaveric donor. This method became widely accepted and successful because of tissue accessibility and immune privilege of the cornea. Despite this, the need for new corneal tissues has increased over the last few years since corneal grafts have had a failure rate of around 38%, mainly because of graft rejection [6, 7]. Thus, it is imperative to find new approaches for endothelial regeneration or replacement that may lead to better outcomes. The remarkable progress, which could sidestep the constraints of current treatments, has been made with the development of an autologous transplant of cultured endothelial cells into a patient's anterior chamber that can redesign the corneal tissue and with the generation of corneal stroma-like tissue developed from autologous stem cells [8].

With respect to the latter, in the past few years, intensive research has focused on corneal stem cells as a source of regenerative cell-based therapy. Today, it is known that the cornea has at least two types of stem cells: limbal epithelial

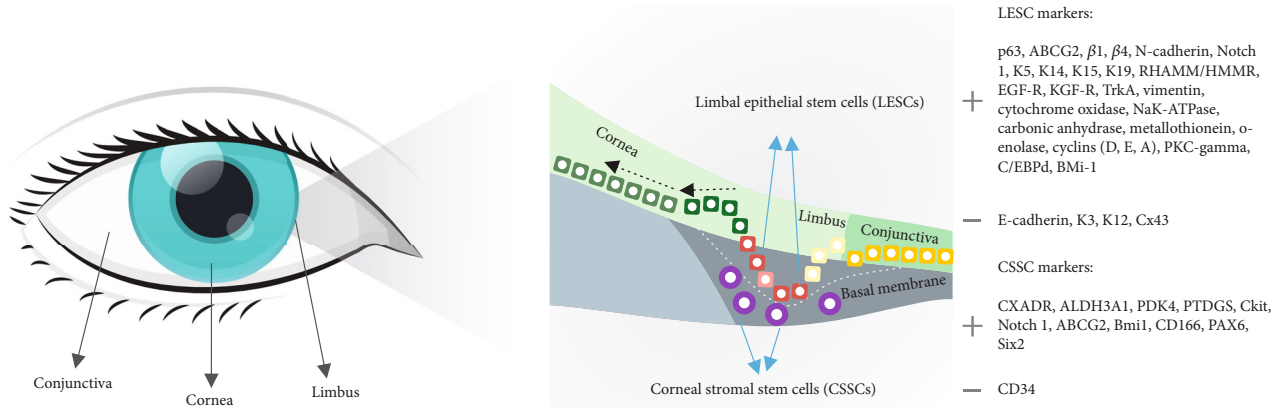

Figure 1: Localization and markers of LESCs and CSSCs.

stem cells (LESCs) and corneal stromal stem cells (CSSCs). LESCs are used for regeneration of corneal surface while CSSCs are used for corneal stromal regeneration. In this review, we have described in detail phenotype and characteristics of LESCs and CSSCs and discussed their therapeutic potential in regenerative ophthalmology.

2. Characteristics of LESCs

Corneal epithelia are renewed constantly by the adult stem cells located in the limbal zone making it a unique reservoir or niche of LESCs [9, 10]. Four anatomical sites have been identified as probable LESC locations in humans: palisades of Vogt, limbal epithelial crypts, projections of limbal crypts, and focal stromal projections [11–15]. Small group of LESCs, localized at the basal limbus, retain tritiated thymidine for long periods and are recognized as quiescent cells (Figure 1). Although LESCs are slow cycling cells, they have the high self-renewing and differentiation capacity [16–18]. Since LESCs are derived from neural ectoderm, they may exhibit functional neuronal properties in vitro and may differentiate into neuronal-like cells in vivo, under specific conditions of the microenvironment [19].

At present, there is no currently specific single marker that can be used for identification of LESCs. Combination of stem cell-associated markers, which consisted of a panel of positive and negative markers (Figure 1), can be used to identify putative LESCs [19]. In general, all positive LESC markers are expressed in the basal layers of the epithelium, while their expression in the superficial layers is either reduced or absent. One of the best described positive LESC marker is transcription factor p63, important for epithelial development and differentiation [19, 20]. Holoclone of LESCs expresses high levels of p63; meroclones express low levels of p63, while there is no expression of p63 in paraclones of LESCs. Also, a member of the ATP binding cassette transporter protein, ABCG2, is an additional, well-known marker of LESCs. Integrin $\alpha 9$ mediates adhesion to tenascin-C and osteopontin, and it has been localized to small clusters of stem cell-like cells in the limbal basal epithelium [21, 22]. Expression of N-cadherin and Notch 1 on a subpopulation of limbal epithelial basal cells suggests them as possible markers for LESCs [22]. In addition, human LESCs are positive for keratin (K) 5, K14, K15, K19, and vimentin and negative for K3, K12, involucrin, and the gap junction protein Cx43 [22, 23]. RHAMM/HMMR or CD168, an important component of the extracellular matrix, can be used as a negative marker of LESCs as well [24].

The growth factors present in basal cells of limbal epithelium (epidermal growth factor receptor (EGF-R), keratinocyte growth factor receptor (KGF-R), and neurotrophic receptor tyrosine kinase (TrkA)) [21] and proteins associated with cellular metabolic functions which are found in higher concentrations in basal cells of epithelium (Na/K-ATPase, cytochrome oxidase, carbonic anhydrase, alpha-enolase, cyclin D, cyclin E, cyclin A, metallothioneins, and PKC-gamma) may play an important role in LESC metabolism and function [21].

3. Characteristics of CSSCs

The presence of self-renewable cells that have the phenotypic characteristics of mesenchymal stem cells (MSCs) and high differentiation potential has been detected in the corneal stroma (Figure 1) and they are called CSSCs [25–31]. Gene array analysis showed that CSSCs have high expression of MSC markers, such as cKIT, Notch 1, ABCG2, BMi1, CD166, PAX6, and Six2 [25]. Moreover, these cells can be expanded 100-fold in a serum-free medium supplemented with ascorbate and insulin when they express keratocyte-specific markers: CXADR, ALDH3A1, PDK4, and PTDGS (Figure 1) [8].

Although both LESCs and CSSCs originate from neural crest-derived MSCs [26], they have different properties and functions in the cornea [27, 28]. LESCs have an important role in regeneration of corneal epithelial surface, while CSSCs are used for regeneration of corneal stroma. The recovered corneal endothelium can be derived from human CSSCs [28], and injection of human CSSCs in lumican-null mice could repair corneal disorders and restore transparency [8], which indicates their therapeutic potential.

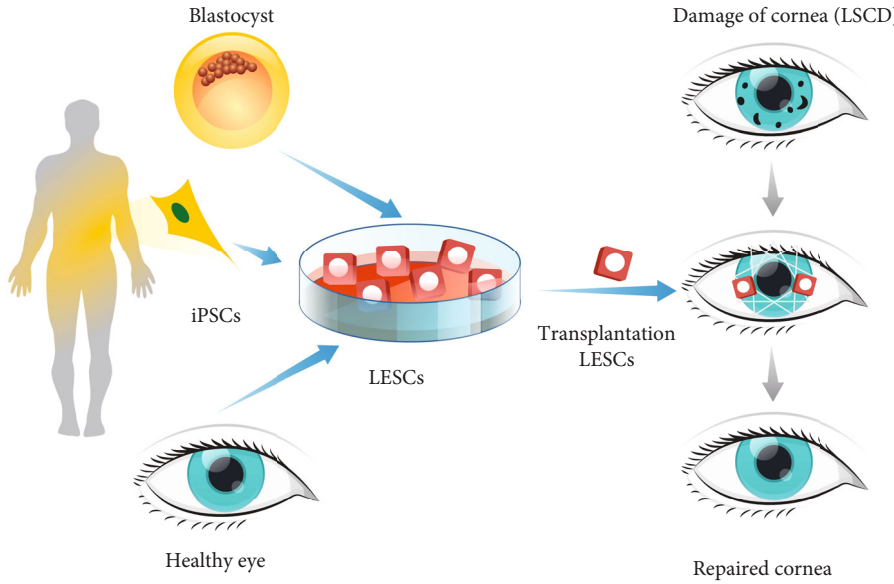

Figure 2: Derivation and therapeutic potential of LESCs.

4. Differentiation of Pluripotent Stem Cells into Corneal Cells

Pluripotent stem cells (PSCs) provide big opportunities for corneal reconstruction by cell-based therapies [32]. Methods for corneal differentiation of pluripotent stem cells are known in the art. Many of these methods are slow or provide only modest differentiation efficiencies. For instance, Japanese researchers in 2012 reported corneal cell differentiation of human induced pluripotent stem cells (iPSCs) on mouse-derived feeder cells taking 12-16 weeks and resulting in a differentiation efficiency of less than 15% based on the expression of CK12 [33], while another group of scientists in 2011 maintained to produce corneal precursor cells by differentiation of mouse iPSCs through cultivation on mouse-derived feeder cells by a method which took a short time [34]. Ahmad et al. [35] used medium conditioned by limbal fibroblasts for culturing human embryonic stem cells (ESCs) previously maintained on a feeder layer of mouse embryonic fibroblasts. This culturing resulted in the loss of pluripotency and differentiation into epithelial-like cells. They reported a differentiation efficiency of 50% on day 5 and 10% on day 21 as measured by expression of proteins CK3/12. Nonetheless, the use of a medium which requires donated limbal cells can be considered problematic. Further, there is a significant biological variation among batches of limbal cells. The differentiation method disclosed is a two-step approach which comprises an induction step, preferably carried out on a suspension culture, at which point the pluripotent stem cells are cultured in the presence of a TGF-beta inhibitor, a Wnt inhibitor, and a fibroblast growth factor, by that producing eye precursor cells [32]. The aforementioned eye precursor cells are then differentiated, in an adherent culture, into corneal epithelial precursor cells in the presence of epidermal growth factor, hydrocortisone, insulin, isoproterenol, and triiodothyronine. Optionally, these corneal epithelial precursor cells may be advanced further into mature corneal epithelial cells or into corneal stratified epithelium [32].

5. Therapeutic Potential of LESCs and CSSCs

Thermal or chemical burns, cicatrizing, aniridia, untreated vernal keratoconjunctivitis, and multiple surgeries involving the limbal area can lead to a state of partial or total limbal stem cell deficiency (LSCD) [36].

In patients with unilateral LSCD, autologous limbal transplantation can be utilized to provide surface reconstruction of the cornea [37]. However, this technique requires a large limbal graft from the healthy eye, which can lead to the development of LSCD in that eye [38], and is not applicable to LSCD bilaterally affected patients [39].

LESCs can be derived from human ESC or iPSC (Figure 2). Accordingly, autologous tissue-specific cell-based therapy is in focus as a possibly new therapeutic approach for the treatment of LSCD patients. Pellegrini and coworkers were first to report that two patients with unilateral LSCD caused by alkali burns were successfully transplanted with autologous cultivated corneal epithelium, and the results continued for more than two years subsequent to grafting [40]. Following this report, many researchers began investigation of the safety and effectiveness of cultivated limbal epithelial cell transplantation (CLET) [41–43]. As such, one of the clinical efficacies includes the use of the amniotic membrane and fibrin glue utilized as substrates for cultivation of corneal epithelial cells. The amniotic membrane is preferred as it produces cytokines, which allow the survival and self-renewal of limbal stem cells [44]. In addition, Rama and colleagues reported long-term corneal recovery utilizing autologous cultivated LESCs [41]. They demonstrated that permanent repair and a replenishment of the corneal epithelium were accomplished in 76.6% of 107 eyes with LSCD caused by chemical and thermal burns.

These results indicated that CLET is a safe and effective procedure. Many factors, such as lack of standardization in terms of patient selection (such as total and partial LSCD used in the same study), cause of LSCD (acquired and congenital), unilateral and bilateral cases of LSCD, source of initial tissue (allo- and autograft transplants in the same study), methods of *ex vivo* expansion (explant or single cell; human amniotic membrane (HAM) or 3T3 fibroblast coculture or both), surgical management (method of superficial keratectomy, the use of a second HAM as a bandage, contact lens protection, or both), and postoperative management (use of HAM or not), represent major obstacles in this field of LESC therapy [44]. Taking previous knowledge and new technologies into consideration, Kolli and coworkers have succeeded in using a nonhuman animal product-free Good Manufacturing Practice- (GMP-) compliant autologous LESC *ex vivo* expansion technique to successfully reverse LSCD within a controlled population and showed 100% success in predefined subjective and objective outcome measures [45]. In addition, they reported, for the first time, the differentiation of hESCs to corneal-like epithelial lineages, providing the first step toward refinement of protocols to produce these cells for potential therapeutic purposes [35, 45].

Based on these data, several clinical trials investigate therapeutic potential of LESCs for the treatment of corneal disorders (Table 1) [46–54]. Results obtained in a phase II study, conducted by Zakaria and coworkers [46], showed that standardized, nonxenogenic culture system, reduced manipulation cultivation, and surgical approach are safe and effective in reducing corneal neovascularization. Tsai and colleagues [49] showed a significant improvement and complete reepithelialization of the corneal surface after two to four days of autologous transplantation of LESCs in all six eyes receiving transplants. In 83% of eyes receiving transplants, mean visual acuity has improved, without recurrent neovascularization and inflammation in the transplanted area during the 15 months of follow-up period. López-García with collaborators investigated histopathologic evolution of the corneal limbus after alkaline burns [50]. In a prospective study of 15 eyes from 12 patients, they demonstrated that the best reepithelialization and stromal regeneration were obtained by autologous limbal transplantation combined with amniotic membrane transplantation. In a clinical study, Holoclar® is the only licensed autologous LSC product in Europe for the treatment of patients with unilateral and bilateral (one eye partial) LSCD caused by ocular surface buns [51].

CSSCs, as newly identified corneal stem cells, provide hope and opportunity for the treatment of so far incurable condition of the cornea. Although preclinical studies suggest therapeutic potential of CSSCs [8, 27, 28], there are currently no clinical trials that use these cells. Further studies are necessary to develop optimized protocols for their isolation and characterization as well as reliable assays to evaluate their therapeutic potential.

6. New Paradigm: Cell-Free Stem Cell Therapy

The effects of MSCs are related to soluble secreted factors that are involved in the process of tissue wound repair, inflammation, angiogenesis, and immune response [55]. Most MSCs have the affinity to accumulate within the filtering organs, i.e., lungs, liver, and spleen, after intravenous delivery. However, MSCs can regulate tissue repair, after achieving only minimal engraftment at the site of tissue injury [56]. Subconjunctival MSC injection to alkali-injured corneas promoted corneal wound healing, despite the MSCs remaining in the subconjunctival space [57]. Additionally, topical administration of MSCs or conditioned MSC media to a murine corneal epithelial wounding model has shown benefits in terms of attenuating corneal inflammation, reducing neovascularization, and promoting wound healing [58]. Taking into account the previous results, it can be concluded that MSC exert their effect through a paracrine mechanism, rather than direct cell replacement, since most of the MSCs were retained in the corneal stroma rather than the epithelium. These effects are most likely mediated through secreted soluble factors released from MSCs in the form of extracellular vesicles or exosomes [59, 60].

Exosomes are produced by cultured cells and subsequently released into the conditioned media. Different methods of exosomes isolation have been established, including differential centrifugation, density gradient centrifugation, filtration, size exclusion chromatography, polymer-based precipitation, immunological separation, and sieving [61]. The size of exosomes is restricted by multivesicular bodies in the parental cells and ranges from 30 nm up to several hundred nm in diameter. The luminal content of exosomes contains proteins, lipids, and nucleic acids (DNA, mRNA, miRNAs, and long noncoding RNAs), although the exact composition and content of the exosomal cargo released by different cell types are difficult to determine, due to differences within cellular environments [62].

MSC-derived exosomes (MSC-Exo) can encapsulate and transfer biomolecules that have effects on cell and tissue metabolism, including differentiation, inflammation, angiogenesis, immunosuppression, neurogenesis, and synaptogenesis [63, 64]. The periocular injection of human umbilical cord MSC-Exo into an experimental rat autoimmune uveitis (EAU) model decreases inflammation by downregulating MCP1/CCL21- and MYD88-dependent pathways [65]. The cells expressing Gr-1, CD68, CD161, CD4, IFNγ, and IL17, respectively, served to restore retinal function. Intravitreal injection of exosomes from umbilical or adipose MSC cultures modifies the inflammation and improves visual function in retinal injury induced by laser, through the inhibition of MCP1, ICAM-1 (intercellular adhesion molecule-1), and TNFα [66]. Hyperglycemia-induced retinal inflammation in diabetic rats was also shown to be improved by an intravitreal injection of human umbilical cord MSC-Exo, as well as an intravitreal injection of umbilical cord MSC-Exo in blue light-induced retinal damage [67]. The latter showed a dose-dependent suppression of choroidal neovascularization through downregulation of VEGFA and inhibition of the NFκB pathway, possibly by miR-16 transfer [68]. Ganglion cell growth can be stimulated by intravitreal injection of bone marrow MSC-Exo cells in a rat optic nerve crush model, through argonaute-2 signaling, which stabilized miR-16 activity from RNase digestion [69]. Given the fact

Table 1

	Study title	Conditions	Interventions	Status	Locations
1	The application of cultured cornea stem cells in patients suffering from corneal stem cell insufficiency	Unilateral limbal stem cell insufficiency	Procedure: transplant of cultured limbal stem cells on the cornea	Terminated	National Taiwan University Hospital, Department of Ophthalmology, Taipei, Taiwan
2	The application of oral mucosal epithelial cell sheets cultivated on amino membrane in patients suffering from corneal stem cell insufficiency or symblepharon	Limbal insufficiency Symblepharon	Procedure: cultured oral mucosa cell sheet transplantation	Terminated	National Taiwan University Hospital, Department of Ophthalmology, Taipei, Taiwan
3	Limbus-derived stem cells for prevention of postoperative corneal haze	Corneal scars and opacities	Biological: stem cells Other: vehicle	Recruiting	LV Prasad Eye Institute, Hyderabad, Telangana, India
4	The improvement of limbal stem cell deficiency (LSCD) in unilateral stem cell damage by amniotic membrane extract eye drop (AMEED)	Limbal stem cell deficiency (LSCD)	Biological: amniotic membrane extract eye drop (AMEED)	Completed	—
5	Efficacy and safety of autologous cultivated limbal stem cells transplantation (ACLSCT) for restoration of corneal epithelium in patients with limbal stem cell deficiency	Limbal stem cells deficiency	Biopsy from donor eye Implant of Holoclar Ophtalmologic examination (and 5 more)	Recruiting	Hospital San Raffaele, Milan, Italy
6	Stem cells therapy for corneal blindness	Corneal injuries Corneal burns Corneal scars and opacities	Biological: ex vivo cultivated limbal stem cell pool	Unknown	LV Prasad Eye Institute, Hyderabad, Telangana, India
7	Autologous cultured corneal epithelium (CECA) for the treatment of limbal stem cell deficiency	Limbal stem cell deficiency	Procedure: surgical transplantation of CECA	Recruiting	CIUSSS de l'Est de l'île de Montréal, Quebec, Canada Centre Universitaire d'Ophtalmologie CHU de Québec-HSS Québec, Canada
8	Autologous adipose-derived adult stem cell transplantation for corneal diseases	Hereditary corneal dystrophy Keratoconus	Procedure: lipoaspiration Procedure: transplantation	Unknown	Optica General, Saida, Lebanon

Table 1: Continued.

	Study title	Conditions	Interventions	Status	Locations
9	Corneal epithelial autograft for LSCD	Limbal stem cell deficiency	Corneal epithelial and limbal conjunctival autograft Femtosecond laser and diamond knife	Recruiting	Zhongshan Ophthalmic Center, Sun Yat-sen University, Guangzhou, Guangdong, China
10	Umbilical cord mesenchymal stem cells injection for ocular corneal burn	Ocular corneal burn	Biological: human umbilical cord mesenchymal stem cells Biological: placebo	Unknown	The First Affiliated Hospital of Jinan University, Guangzhou, Guangdong, China
11	Follow-up study after ACLSCT for restoration of corneal epithelium in patients with LSCD due to ocular burns	Limbal stem cell deficiency due to ocular burn	Procedure: ophthalmologic examinations Other: digital pictures Other: QoL questionnaires	Recruiting	Hospital San Raffaele, Milan, Italy
12	Corneal epithelium repair and therapy using autologous limbal stem cell transplantation	Corneal disease Pterygium Myopia Hyperopia	LSCs and amniotic membrane (modified technique); amniotic membrane only (traditional technique); PRK, LSCs, and amniotic membrane (modified technique) (and 4 more)	Unknown	Zhongshan Ophthalmic Center, Sun Yat-sen University, Guangzhou, China
13	Corneal epithelial stem cells and dry eye disease	Dry eye syndromes Dry eye ocular inflammation (and 3 more)	Other: corneal epithelial stem cell transplant	Enrolling by invitation	Rush Eye Associates, Amarillo, Texas, United States
14	Efficacy of cultivated corneal epithelial stem cell for ocular surface reconstruction	Severe ocular surface damage Limbal deficiency	Procedure: cultivated limbal transplantation	Completed	Pinnita Prabhasawat, MD, Bangkok, Thailand
15	Corneal epithelial allograft from living-related donor for LSCD	Limbal stem cell deficiency	Procedure: corneal epithelial allograft Procedure: limbal conjunctival allograft Device: femtosecond laser Device: diamond knife	Completed	Zhongshan Ophthalmic Center, Sun Yat-sen University, Guangzhou, Guangdong, China
16	The treatment of human bone marrow mesenchymal stem cells in ocular corneal burn	Chemical burns	Other: human bone marrow MSC	Completed	—

Table 1: Continued.

	Study title	Conditions	Interventions	Status	Locations
17	Clinical trial on the effect of autologous oral mucosal epithelial sheet transplantation	Limbal stem cell deficiency Stevens-Johnson syndrome Ocular cicatricial pemphigoid Chemical burn	Biological: cultivated oral mucosal epithelial sheet transplantation	Available	Seoul National University Hospital, Seoul, Republic of Korea
18	Cultivated limbal epithelial transplantation (CLET) for limbal stem cell deficiency (LSCD)	Limbal stem cell deficiency	—	Not yet recruiting	IOBA, Valladolid, Spain
19	Limbal stem cell deficiency (LSCD) treatment with cultivated stem cell (CALEC) graft	Limbal stem cell deficiency	Procedure: biopsy to collect limbal epithelial stem cells that will be cultivated into a graft Biological: cultivation of limbal epithelial cells into a graft Procedure: CALEC transplant Procedure: CLAU	Recruiting	Massachusetts Eye and Ear Infirmary, Boston, Massachusetts, United States

that intravenous MSC administration caused similar recovery of retinal functions in EAU and laser-induced retinal injury models, it can be concluded that the therapeutic effects of MSC may be mediated through MSC-Exo action [70]. A recent clinical trial has shown that patients with refractory macular holes had anatomical and functional recovery after intravitreal injection of human umbilical cord MSC-Exo. Nevertheless, one patient experienced an inflammatory reaction [71].

This cell-free strategy may also have a significant impact on corneal wound repair, through stimulation of different factors that modulate inflammation, angiogenesis, and tissue regeneration. Few studies have demonstrated the therapeutic functions of soluble factors from MSC-Exo on corneal wound models. Cultivation of rabbit corneal stromal cells, and rabbit adipose MSC-Exo, has led to greater proliferation, along with the deposition of new ECM proteins (including collagens). Topical CSSC-derived exosomes can suppress corneal inflammation and corneal scarring through the inhibition of neutrophil infiltration. Moreover, murine corneal epithelial wound healing can be promoted by exosomes from human corneal mesenchymal stromal cells [72]. Umbilical cord MSC-Exo carrying β-glucuronidase reduced the accumulated glycosaminoglycans in a mouse mucopolysaccharidosis model, thereby reducing corneal haze. These data have highlighted the potential for the therapeutic use of MSC-Exo in ocular surface diseases and congenital corneal metabolic disorders [73].

7. Opportunities and Challenges in Regenerative Ophthalmology

From the earliest concepts such as replacement of the opaque cornea to corneal wound healing and regeneration, ophthalmologists and material scientists across the world have faced a collection of challenges [74, 75]. Advances in visualization techniques and histology have made significant progress in the fundamental understanding of cornea structure and its microenvironment. As a result of this valuable information and nanotechnology advances, therapeutic strategies in devastating corneal diseases have turned from corneal replacement into corneal wound healing and regeneration [76]. Ergo, studies on the limbus zone and immune and angiogenic privilege have attracted more attention. In addition, the exploration of cell signaling in the natural process of wound healing and the attempts to mimic this process have opened new horizons in corneal disease treatment.

A large number of the suggested treatments have shown promising results for wound healing at the ocular surface, and entire thickness dystrophies were neglected. At the same time, in order to reduce transplantation of a donor cornea, tissue engineering of the whole thickness of the cornea must be considered. Corneal stromal and endothelium tissue engineering has recently shown noticeable progress [77]. Nonetheless, more focus should be on biomimetic strategies, such as employing a combination of cell signaling agents with tissue engineering. Rho-kinase (ROCK) inhibitor is a serine/-threonine protein kinase that participates in regulating cell signaling route. In recent past, ROCK has been announced as an innovative therapeutic agent for corneal endothelial dystrophy [78]. The combination of these approaches can be a promising method for visual rehabilitation in patients suffering from corneal dystrophies.

So far, most studies have worked on presenting new materials and biochemical approaches in corneal wound healing and regeneration, while putting accent on physical properties of these approaches could be a leap in this area. For instance, Long et al. have tried to use a cross-linking agent in collagen membrane to regulate collagen fibril spacing and hence improve optical clarity of collagen and increase permeability of neurites [79]. Accordingly, advances in visualization techniques will help in the improvement of corneal physical structure identification that, in combination with material science, will lead to new perceptions in the typical treatment approaches. Slit-lamp biomicroscopy, optical coherence tomography (OCT), in vivo confocal fluorescence microscopy, and full-field optical microscopy are part of visualization techniques which help to quantify corneal architecture [80, 81]. As stated in previous studies, investigation on visualization methods would expand corneal medical treatments.

Considering the exceptional role of stem cells in tissue regeneration, a large part of future studies is expected to focus on the deployment of stem cells on corneal wound healing and regeneration [82]. A certain number of studies have been done to isolate and characterize multipotent stem cells from different tissues in order to use their great potential in regenerative medicine. Bone marrow-derived mesenchymal stem cells [83], human umbilical cord mesenchymal stem cells [84], postnatal periodontal ligament [85], and limbal stem cells [86] are recently studied stem cells sources in corneal wound healing and regeneration. Saghizadeh et al. [30] have recently reviewed all major stem cell usage in corneal wound healing. Contrarily, developing innovative methods to produce 3D tissue-like architecture has allowed mimicking the microarchitecture and physiology of the native cornea. In this regard, 3D microfabrication methods are promising approaches in designing cornea substitutes [87, 88]. Amidst additive manufacturing methods, study on bioprinting and the development of bionics provides a great promise in relation to the fabrication of human corneal substitutes that mimic the structure of native corneal tissues [89, 90].

8. Conclusion

The concept of corneal stem cells has greatly enhanced the understanding of corneal epithelial proliferation, migration, and recovery. This has also contributed directly to improve medical and surgical management of a wide range of ocular surface disorders. On the other hand, control of scar tissue formation is of great importance for corneal regeneration and recovery of eyesight. However, it should be noted that there are still several problems including insufficient data regarding safe and successful LESC and CSSC engraftment in the human cornea and their long-term efficacy, which limit their capacity to be used as a main treatment approach for corneal regeneration.

Conflicts of Interest

The authors declare that they have no conflicts of interest.

References

[1] P. N. Lewis, C. Pinali, R. D. Young, K. M. Meek, A. J. Quantock, and C. Knupp, "Structural interactions between collagen and proteoglycans are elucidated by three-dimensional electron tomography of bovine cornea," *Structure*, vol. 18, no. 2, pp. 239–245, 2010.

[2] G. J. Parfitt, C. Pinali, R. D. Young, A. J. Quantock, and C. Knupp, "Three-dimensional reconstruction of collagen-proteoglycan interactions in the mouse corneal stroma by electron tomography," *Journal of Structural Biology*, vol. 170, no. 2, pp. 392–397, 2010.

[3] M. E. Fini, "Keratocyte and fibroblast phenotypes in the repairing cornea," *Progress in Retinal and Eye Research*, vol. 18, no. 4, pp. 529–551, 1999.

[4] A. J. Shortt, S. J. Tuft, and J. T. Daniels, "Corneal stem cells in the eye clinic," *British Medical Bulletin*, vol. 100, no. 1, pp. 209–225, 2011.

[5] J. P. Whitcher, M. Srinivasan, and M. P. Upadhyay, "Corneal blindness: a global perspective," *Bulletin of the World Health Organization*, vol. 79, no. 3, pp. 214–221, 2001.

[6] K. A. Williams, A. J. Esterman, C. Bartlett, H. Holland, N. B. Hornsby, and D. J. Coster, "How effective is penetrating corneal transplantation? Factors influencing long-term outcome in multivariate analysis," *Transplantation*, vol. 81, no. 6, pp. 896–901, 2006.

[7] J. Y. Niederkorn and D. F. P. Larkin, "Immune privilege of corneal allografts," *Ocular Immunology and Inflammation*, vol. 18, no. 3, pp. 162–171, 2010.

[8] Y. Du, M. L. Funderburgh, M. M. Mann, N. SundarRaj, and J. L. Funderburgh, "Multipotent stem cells in human corneal stroma," *Stem Cells*, vol. 23, no. 9, pp. 1266–1275, 2005.

[9] J. D. West, N. J. Dorà, and J. M. Collinson, "Evaluating alternative stem cell hypotheses for adult corneal epithelial maintenance," *World Journal of Stem Cells*, vol. 7, no. 2, pp. 281–299, 2015.

[10] K. Y. Chee, A. Kicic, and S. J. Wiffen, "Limbal stem cells: the search for a marker," *Clinical & Experimental Ophthalmology*, vol. 34, no. 1, pp. 64–73, 2006.

[11] J. J. Yoon, S. Ismail, and T. Sherwin, "Limbal stem cells: central concepts of corneal epithelial homeostasis," *World Journal of Stem Cells*, vol. 6, no. 4, pp. 391–403, 2014.

[12] R. L. Mort, P. Douvaras, S. D. Morley et al., "Stem cells and corneal epithelial maintenance: insights from the mouse and other animal models," *Results and Problems in Cell Differentiation*, vol. 55, pp. 357–394, 2012.

[13] L. Takács, E. Tóth, A. Berta, and G. Vereb, "Stem cells of the adult cornea: from cytometric markers to therapeutic applications," *Cytometry. Part A*, vol. 75A, no. 1, pp. 54–66, 2009.

[14] R. J.-F. Tsai and R. Y.-N. Tsai, "From stem cell niche environments to engineering of corneal epithelium tissue," *Japanese Journal of Ophthalmology*, vol. 58, no. 2, pp. 111–119, 2014.

[15] M. Notara, A. J. Shortt, A. R. O'Callaghan, and J. T. Daniels, "The impact of age on the physical and cellular properties of the human limbal stem cell niche," *Age*, vol. 35, no. 2, pp. 289–300, 2013.

[16] M. Ebrahimi, E. Taghi-Abadi, and H. Baharvand, "Limbal stem cells in review," *Journal of Ophthalmic and Vision Research*, vol. 4, no. 1, pp. 40–58, 2009.

[17] P. Ordonez and N. Di Girolamo, "Limbal epithelial stem cells: role of the niche microenvironment," *Stem Cells*, vol. 30, no. 2, pp. 100–107, 2012.

[18] F. Castro-Munozledo, "Review: corneal epithelial stem cells, their niche and wound healing," *Molecular Vision*, vol. 24, no. 19, pp. 1600–1613, 2013.

[19] M. Notara, A. Alatza, J. Gilfillan et al., "In sickness and in health: corneal epithelial stem cell biology, pathology and therapy," *Experimental Eye Research*, vol. 90, no. 2, pp. 188–195, 2010.

[20] A. W. Joe and S. N. Yeung, "Concise review: identifying limbal stem cells: classical concepts and new challenges," *Stem Cells Translational Medicine*, vol. 3, no. 3, pp. 318–322, 2014.

[21] U. Schlötzer-Schrehardt and F. E. Kruse, "Identification and characterization of limbal stem cells," *Experimental Eye Research*, vol. 81, no. 3, pp. 247–264, 2005.

[22] G. A. Secker and J. T. Daniels, "Corneal epithelial stem cells: deficiency and regulation," *Stem Cell Reviews and Reports*, vol. 4, no. 3, pp. 159–168, 2008.

[23] K. Dhamodaran, M. Subramani, M. Ponnalagu, R. Shetty, and D. Das, "Ocular stem cells: a status update!," *Stem Cell Research & Therapy*, vol. 5, no. 2, p. 56, 2014.

[24] S. Ahmad, S. Kolli, D. Q. Li et al., "A putative role for RHAMM/HMMR as a negative marker of stem cell-containing population of human limbal epithelial cells," *Stem Cells*, vol. 26, no. 6, pp. 1609–1619, 2008.

[25] N. Pinnamaneni and J. L. Funderburgh, "Concise review: stem cells in the corneal stroma," *Stem Cells*, vol. 30, no. 6, pp. 1059–1063, 2012.

[26] G. S. L. Peh, R. W. Beuerman, A. Colman, D. T. Tan, and J. S. Mehta, "Human corneal endothelial cell expansion for corneal endothelium transplantation: an overview," *Transplantation*, vol. 91, no. 8, pp. 811–819, 2011.

[27] J. A. West-Mays and D. J. Dwivedi, "The keratocyte: corneal stromal cell with variable repair phenotypes," *International Journal of Biochemistry and Cell Biology*, vol. 38, no. 10, pp. 1625–1631, 2006.

[28] S. Hatou, S. Yoshida, K. Higa et al., "Functional corneal endothelium derived from corneal stroma stem cells of neural crest origin by retinoic acid and Wnt/β-catenin signaling," *Stem Cells and Development*, vol. 22, no. 5, pp. 828–839, 2013.

[29] M. Sosnová, M. Bradl, and J. V. Forrester, "CD34+ corneal stromal cells are bone marrow-derived and express hemopoietic stem cell markers," *Stem Cells*, vol. 23, no. 4, pp. 507–515, 2005.

[30] M. Saghizadeh, A. A. Kramerov, C. N. Svendsen, and A. V. Ljubimov, "Concise review: stem cells for corneal wound healing," *Stem Cells*, vol. 35, no. 10, pp. 2105–2114, 2017.

[31] J. S. Mehta, V. Kocaba, and Y. Q. Soh, "The future of keratoplasty," *Current Opinion in Ophthalmology*, vol. 30, no. 4, pp. 286–291, 2019.

[32] T. Ilmarinen, H. Hongisto, H. Skottman, and A. Mikhailova, "Differentiation of pluripotent stem cells into corneal cells," 2017, US Patent WO2018037161A1.

[33] R. Hayashi, Y. Ishikawa, M. Ito et al., "Generation of corneal epithelial cells from induced pluripotent stem cells derived from human dermal fibroblast and corneal limbal epithelium," *PloS One*, vol. 7, no. 9, article e45435, 2012.

[34] S. Yoshida, M. Yasuda, H. Miyashita et al., "Generation of stratified squamous epithelial progenitor cells from mouse induced pluripotent stem cells," *PloS One*, vol. 6, no. 12, article e28856, 2011.

[35] S. Ahmad, R. Stewart, S. Yung et al., "Differentiation of human embryonic stem cells into corneal epithelial-like cells by in vitro replication of the corneal epithelial stem cell niche," *Stem Cells*, vol. 25, no. 5, pp. 1145–1155, 2007.

[36] Y. Oie and K. Nishida, "Regenerative medicine for the cornea," *BioMed Research International*, vol. 2013, Article ID 428247, 8 pages, 2013.

[37] K. R. Keivyon and S. C. G. Tseng, "Limbal autograft transplantation for ocular surface disorders," *Ophthalmology*, vol. 96, no. 5, pp. 709–723, 1989.

[38] J. J. Y. Chen and S. C. G. Tseng, "Corneal epithelial wound healing in partial limbal deficiency," *Investigative Ophthalmology & Visual Science*, vol. 31, no. 7, pp. 1301–1314, 1990.

[39] H. S. Dua and A. Azuara-Blanco, "Autologous limbal transplantation in patients with unilateral corneal stem cell deficiency," *British Journal of Ophthalmology*, vol. 84, no. 3, pp. 273–278, 2000.

[40] G. Pellegrini, C. E. Traverso, A. T. Franzi, M. Zingirian, R. Cancedda, and M. De Luca, "Long-term restoration of damaged corneal surfaces with autologous cultivated corneal epithelium," *The Lancet*, vol. 349, no. 9057, pp. 990–993, 1997.

[41] P. Rama, S. Bonini, A. Lambiase et al., "Autologous fibrin-cultured limbal stem cells permanently restore the corneal surface of patients with total limbal stem cell deficiency1," *Transplantation*, vol. 72, no. 9, pp. 1478–1485, 2001.

[42] F. Bernabei, M. Roda, M. Buzzi, M. Pellegrini, G. Giannaccare, and P. Versura, "Blood-based treatments for severe dry eye disease: the need of a consensus," *Journal of Clinical Medicine*, vol. 8, no. 9, article E1478, p. 1478, 2019.

[43] J. C. Serna-Ojeda, S. Basu, J. Vazirani, Y. Garfias, and V. S. Sangwan, "Systemic immunosuppression for limbal allograft and allogenic limbal epithelial cell transplantation," *Medical Hypothesis, Discovery & Innovation Ophthalmology Journal*, vol. 9, no. 1, pp. 23–32, 2020.

[44] T. Nakamura, T. Inatomi, C. Sotozono, T. Amemiya, N. Kanamura, and S. Kinoshita, "Transplantation of cultivated autologous oral mucosal epithelial cells in patients with severe ocular surface disorders," *British Journal of Ophthalmology*, vol. 88, no. 10, pp. 1280–1284, 2004.

[45] S. Kolli, S. Ahmad, M. Lako, and F. Figueiredo, "Successful clinical implementation of corneal epithelial stem cell therapy for treatment of unilateral limbal stem cell deficiency," *Stem Cells*, vol. 28, no. 3, pp. 597–610, 2010.

[46] N. Zakaria, T. Possemiers, S. Dhubhghaill et al., "Results of a phase I/II clinical trial: standardized, non-xenogenic, cultivated limbal stem cell transplantation," *Journal of Translational Medicine*, vol. 12, no. 1, p. 58, 2014.

[47] M. González-Andrades, R. Mata, M. del Carmen González-Gallardo et al., "A study protocol for a multicentre randomised clinical trial evaluating the safety and feasibility of a bioengineered human allogeneic nanostructured anterior cornea in patients with advanced corneal trophic ulcers refractory to conventional treatment," *BMJ Open*, vol. 7, no. 9, article e016487, 2017.

[48] S. E. Ti, D. Anderson, A. Touhami, C. Kim, and S. C. Tseng, "Factors affecting outcome following transplantation of ex vivo expanded limbal epithelium on amniotic membrane for total limbal deficiency in rabbits," *Investigative Ophthalmology & Visual Science*, vol. 43, no. 8, pp. 2584–2592, 2002.

[49] R. J.-F. Tsai, L.-M. Li, and J.-K. Chen, "Reconstruction of damaged corneas by transplantation of autologous limbal epithelial cells," *New England Journal of Medicine*, vol. 343, no. 2, pp. 86–93, 2000.

[50] J. S. López-García, L. R. Jara, I. García-Lozano, and J. Murube, "Histopathologic limbus evolution after alkaline burns," *Cornea*, vol. 26, no. 9, pp. 1043–1048, 2007.

[51] P. Rama, S. Matuska, G. Paganoni, A. Spinelli, M. De Luca, and G. Pellegrini, "Limbal stem-cell therapy and long-term corneal regeneration," *New England Journal of Medicine*, vol. 363, no. 2, pp. 147–155, 2010.

[52] J. D. M. Campbell, S. Ahmad, A. Agrawal et al., "Allogeneic ex vivo expanded corneal epithelial stem cell transplantation: a randomized controlled clinical trial," *Stem Cells Translational Medicine*, vol. 8, no. 4, pp. 323–331, 2019.

[53] M. Calonge, I. Pérez, S. Galindo et al., "A proof-of-concept clinical trial using mesenchymal stem cells for the treatment of corneal epithelial stem cell deficiency," *Translational Research*, vol. 206, pp. 18–40, 2019.

[54] Y. J. Kim, H. J. Lee, J. S. Ryu et al., "Prospective clinical trial of corneal reconstruction with biomaterial-free cultured oral mucosal epithelial cell sheets," *Cornea*, vol. 37, no. 1, pp. 76–83, 2018.

[55] H. Mansoor, H. S. Ong, A. K. Riau, T. P. Stanzel, J. S. Mehta, and G. H.-F. Yam, "Current trends and future perspective of mesenchymal stem cells and exosomes in corneal diseases," *International Journal of Molecular Sciences*, vol. 20, no. 12, p. 2853, 2019.

[56] J. M. Karp and G. S. Leng Teo, "Mesenchymal stem cell homing: the devil is in the details," *Cell Stem Cell*, vol. 4, no. 3, pp. 206–216, 2009.

[57] L. Yao, Z.-R. Li, W.-R. Su et al., "Role of mesenchymal stem cells on cornea wound healing induced by acute alkali burn," *PLoS ONE*, vol. 7, no. 2, article e30842, 2012.

[58] K.-J. Lin, M.-X. Loi, G.-S. Lien et al., "Topical administration of orbital fat-derived stem cells promotes corneal tissue regeneration," *Stem Cell Research & Therapy*, vol. 4, no. 3, p. 72, 2013.

[59] J. Burrello, S. Monticone, C. Gai, Y. Gomez, S. Kholia, and G. Camussi, "Stem cell-derived extracellular vesicles and immune-modulation," *Frontiers in Cell and Developmental Biology*, vol. 4, no. 83, 2016.

[60] R. Blazquez, F. M. Sanchez-Margallo, O. de la Rosa et al., "Immunomodulatory potential of human adipose mesenchymal stem cells derived exosomes on in vitro stimulated T cells," *Frontiers in Immunology*, vol. 5, no. 556, 2014.

[61] M. Colombo, G. Raposo, and C. Théry, "Biogenesis, secretion, and intercellular interactions of exosomes and other extracellular vesicles," *Annual Review of Cell and Developmental Biology*, vol. 30, pp. 255–289, 2014.

[62] R. J. Lobb, M. Becker, S. W. Wen et al., "Optimized exosome isolation protocol for cell culture supernatant and human plasma," *Journal of Extracellular Vesicles*, vol. 4, no. 1, 2015.

[63] S. Cosenza, K. Toupet, M. Maumus et al., "Mesenchymal stem cells-derived exosomes are more immunosuppressive than microparticles in inflammatory arthritis," *Theranostics*, vol. 8, no. 5, pp. 1399–1410, 2018.

[64] W. S. Toh, R. C. Lai, B. Zhang, and S. K. Lim, "MSC exosome works through a protein-based mechanism of action,"

Biochemical Society Transactions, vol. 46, no. 4, pp. 843–853, 2018.

[65] L. Bai, H. Shao, H. Wang et al., "Effects of mesenchymal stem cell-derived exosomes on experimental autoimmune uveitis," *Scientific Reports*, vol. 7, no. 1, p. 4323, 2017.

[66] B. Yu, H. Shao, C. Su et al., "Exosomes derived from MSCs ameliorate retinal laser injury partially by inhibition of MCP-1," *Scientific Reports*, vol. 6, no. 1, article 34562, 2016.

[67] W. Zhang, Y. Wang, and Y. Kong, "Exosomes derived from mesenchymal stem cells modulate miR-126 to ameliorate hyperglycemia-induced retinal inflammation via Targeting HMGB1," *Investigative Ophthalmology and Visual Science*, vol. 60, no. 1, pp. 294–303, 2019.

[68] J. K. Lee, S. R. Park, B. K. Jung et al., "Exosomes derived from mesenchymal stem cells suppress angiogenesis by down-regulating VEGF expression in breast cancer cells," *PLoS ONE*, vol. 8, no. 12, article e84256, 2013.

[69] B. Mead and S. Tomarev, "Bone marrow-derived mesenchymal stem cells-derived exosomes promote survival of retinal ganglion cells through miRNA-dependent mechanisms," *Stem Cells Translational Medicine*, vol. 6, no. 4, pp. 1273–1285, 2017.

[70] X. Zhang, X. Ren, G. Li et al., "Mesenchymal stem cells ameliorate experimental autoimmune uveoretinitis by comprehensive modulation of systemic autoimmunity," *Investigative Ophthalmology and Visual Science*, vol. 52, no. 6, pp. 3143–3152, 2011.

[71] X. Zhang, J. Liu, B. Yu, F. Ma, X. Ren, and X. Li, "Effects of mesenchymal stem cells and their exosomes on the healing of large and refractory macular holes," *Graefe's Archive for Clinical and Experimental Ophthalmology*, vol. 256, no. 11, pp. 2041–2052, 2018.

[72] T. Shen, Q. Q. Zheng, J. Shen et al., "Effects of adipose-derived mesenchymal stem cell exosomes on corneal stromal fibroblast viability and extracellular matrix synthesis," *Chinese Medical Journal*, vol. 131, no. 6, pp. 704–712, 2018.

[73] V. J. Coulson-Thomas, B. Caterson, and W. W.-Y. Kao, "Transplantation of human umbilical mesenchymal stem cells cures the corneal defects of mucopolysaccharidosis VII mice," *Stem Cells*, vol. 31, no. 10, pp. 2116–2126, 2013.

[74] K. Chakrabarty, R. Shetty, and A. Ghosh, "Corneal cell therapy: with iPSCs, it is no more a far-sight," *Stem Cell Research & Therapy*, vol. 9, no. 1, p. 287, 2018.

[75] M. Mobaraki, R. Abbasi, S. Omidian Vandchali, M. Ghaffari, F. Moztarzadeh, and M. Mozafari, "Corneal repair and regeneration: current concepts and future directions," *Frontiers in Bioengineering and Biotechnology*, vol. 7, no. 135, 2019.

[76] K. Chaudhury, J. Kandasamy, H. S. Vishu Kumar, and S. RoyChoudhury, "Regenerative nanomedicine: current perspectives and future directions," *International Journal of Nanomedicine*, vol. 9, no. 1, pp. 4153–4167, 2014.

[77] S. Matthyssen, B. Van den Bogerd, S. N. Dhubhghaill, C. Koppen, and N. Zakaria, "Corneal regeneration: a review of stromal replacements," *Acta Biomaterialia*, vol. 69, pp. 31–41, 2018.

[78] S. B. Han, Y. C. Liu, K. Mohamed-Noriega, and J. S. Mehta, "Application of novel drugs for corneal cell regeneration," *Journal of Ophthalmology*, vol. 2018, Article ID 1215868, 9 pages, 2018.

[79] Y. Long, X. Zhao, S. Liu et al., "Collagen–hydroxypropyl methylcellulose membranes for corneal regeneration," *ACS Omega*, vol. 3, no. 1, pp. 1269–1275, 2018.

[80] K. Grieve, D. Ghoubay, C. Georgeon et al., "Three-dimensional structure of the mammalian limbal stem cell niche," *Experimental Eye Research*, vol. 140, pp. 75–84, 2015.

[81] R. M. Werkmeister, S. Sapeta, D. Schmidl et al., "Ultrahigh-resolution OCT imaging of the human cornea," *Biomedical Optics Express*, vol. 8, no. 2, pp. 1221–1239, 2017.

[82] M. Rahmati and M. Mozafari, "Protein adsorption on polymers," *Materials Today Communications*, vol. 17, pp. 527–540, 2018.

[83] M. M. Islam, O. Buznyk, J. C. Reddy et al., "Biomaterials-enabled cornea regeneration in patients at high risk for rejection of donor tissue transplantation," *NPJ Regenerative Medicine*, vol. 3, no. 1, 2018.

[84] K. Yamashita, E. Inagaki, S. Hatou et al., "Corneal endothelial regeneration using mesenchymal stem cells derived from human umbilical cord," *Stem Cells and Development*, vol. 27, no. 16, pp. 1097–1108, 2018.

[85] G. H.-F. Yam, M. Fuest, N. Z. B. M. Yusoff et al., "Safety and feasibility of intrastromal injection of cultivated human corneal stromal keratocytes as cell-based therapy for corneal opacities," *Investigative Ophthalmology & Visual Science*, vol. 59, no. 8, pp. 3340–3354, 2018.

[86] Y. Sasamoto, B. R. Ksander, M. H. Frank, and N. Y. Frank, "Repairing the corneal epithelium using limbal stem cells or alternative cell-based therapies," *Expert Opinion on Biological Therapy*, vol. 18, no. 5, pp. 505–513, 2018.

[87] E. Prina, P. Mistry, L. E. Sidney et al., "3D microfabricated scaffolds and microfluidic devices for ocular surface replacement: a review," *Stem Cell Reviews and Reports*, vol. 13, no. 3, pp. 430–441, 2017.

[88] P. E. Ludwig, T. J. Huff, and J. M. Zuniga, "The potential role of bioengineering and three-dimensional printing in curing global corneal blindness," *Journal of Tissue Engineering*, vol. 9, 2018.

[89] A. Isaacson, S. Swioklo, and C. J. Connon, "3D bioprinting of a corneal stroma equivalent," *Experimental Eye Research*, vol. 173, pp. 188–193, 2018.

[90] A. Sorkio, L. Koch, L. Koivusalo et al., "Human stem cell based corneal tissue mimicking structures using laser-assisted 3D bioprinting and functional bioinks," *Biomaterials*, vol. 171, pp. 57–71, 2018.

Hindawi
Stem Cells International
Volume 2020, Article ID 8878412, 14 pages
https://doi.org/10.1155/2020/8878412

Research Article

Galectin-3 Secreted by Human Umbilical Cord Blood-Derived Mesenchymal Stem Cells Reduces Aberrant Tau Phosphorylation in an Alzheimer Disease Model

Hoon Lim, Dahm Lee, Wan Kyu Choi, Soo Jin Choi, Wonil Oh, and Dong Hyun Kim

Biomedical Research Institute, R&D Center, MEDIPOST Co., Ltd., Gyeonggi-do, Republic of Korea

Correspondence should be addressed to Dong Hyun Kim; pooh1994@medi-post.co.kr

Received 2 April 2020; Revised 12 June 2020; Accepted 1 July 2020; Published 18 July 2020

Academic Editor: Hui Yin Nam

The formation of neurofibrillary tangles has been implicated as an important pathological marker for Alzheimer's disease (AD). Studies have revealed that the inhibition of abnormal hyperphosphorylation and aggregation of tau in the AD brain might serve as an important drug target. Using *in vitro* and *in vivo* experimental models, such as the AD mouse model (5xFAD mice), we investigated the inhibition of hyperphosphorylation of tau using the human umbilical cord blood-derived mesenchymal stem cells (hUCB-MSCs). Administration of hUCB-MSCs not only ameliorated the spatial learning and memory impairments but also mitigated the hyperphosphorylation of tau in 5xFAD mice. Furthermore, *in vivo* experiments in mice and *in vitro* ThT fluorescence assay validated galectin-3 (GAL-3) as an essential factor of hUCB-MSC. Moreover, GAL-3 was observed to be involved in the removal of aberrant forms of tau, by reducing hyperphosphorylation through decrements in the glycogen synthase kinase 3 beta (GSK-3β). Our results confirm that GAL-3, secreted by hUCB-MSC, regulates the abnormal accumulation of tau by protein-protein interactions. This study suggests that hUCB-MSCs mitigate hyperphosphorylation of tau through GAL-3 secretion. These findings highlight the potential role of hUCB-MSCs as a therapeutic agent for aberrant tau in AD.

1. Introduction

Alzheimer's disease (AD) is a progressive, irreversible disorder characterized by amyloid plaques that form as a result of amyloid-beta (Aβ) accumulation and neurofibrillary tangles comprising of pathological tau aggregates [1]. Tau is a major microtubule-associated protein (MAP), found in normal mature neurons, and its expression is developmentally regulated by alternative splicing with six different isoforms being expressed in the adult human brain [2]. Phosphorylated tau has important roles in the promotion of tubulin assembly into microtubules and the structural stabilization of microtubules [3, 4]. However, hyperphosphorylation of tau protein in the AD brains induces aggregation of filament bundles [5], which are the hallmark of AD progression [6]. Tau protein is also a major constituent of intraneuronal and glial fibrillar lesions in many neurodegenerative diseases, referred to as "tauopathies," including AD [2]. Neurofibrillary degeneration induced by aberrantly hyperphosphorylated tau is observed during the clinical evaluation of AD, which leads to cognitive impairments [7]. In addition, pathological tau may result in microtubule dysfunction, leading to neuronal degeneration [8]. Therefore, lowering tau levels, stabilizing tau structure, or clearing hyperphosphorylated tau aggregates in the brain may be effective therapeutic strategies for AD. Notably, antitau antibody or neurotrophic compound treatment markedly reduces tau aggregation and improves cognitive functions in animal models [9]. However, a therapeutic agent with an optimal efficacy has not yet been elucidated.

Human umbilical cord blood-derived mesenchymal stem cells (hUCB-MSCs) have emerged as an important source of allogeneic MSC-based treatment [10] as they can be collected in a noninvasive manner and exhibit beneficial properties, including low immunogenicity [11], excellent tropism, and therapeutic paracrine action [12]. In particular, our previous studies demonstrated that the paracrine action of hUCB-MSCs has multifunctional therapeutic effects in AD,

including antiapoptotic effects on neuronal cells [12, 13], promotion of neurogenesis [10], restoration of synaptic dysfunction [14], and Aβ peptide clearance [15, 16]. In the present study, we investigated whether hUCB-MSCs and their secreted factors can modulate the aberrant tau proteins in AD. We established the inhibitory effects of hUCB-MSCs on tau abnormalities and subsequently identified the soluble protein GAL-3 as an essential protein secreted by hUCB-MSCs. GAL-3 reduced the formation of aggregated and hyperphosphorylated tau both *in vitro* and *in vivo*. This study is the first to identify the paracrine factors secreted by hUCB-MSCs in response to tau toxicity and demonstrate that hUCB-MSC secretes GAL-3 as a crucial factor with inhibitory effects on abnormal tau in AD.

2. Methods

2.1. Preparation and Culture of hUCB-MSCs, Human Foreskin Fibroblast 68 (Hs68), and Human Embryo Kidney 293 (HEK293) Cells. Neonatal hUCB was collected from umbilical veins after obtaining informed maternal consent in accordance with the guidelines approved by the Institutional Review Board of MEDIPOST Co., Ltd. (MP-2015-6-2). All the procedures were conducted in strict compliance with the institutional guidelines and approved protocols. The procedures used for isolation, acquisition, and culture of hUCB-MSCs were as described previously [17]. hUCB-MSCs were cultured in the minimum essential medium (α-MEM; Gibco, Carlsbad, CA) supplemented with 10% (*v*/*v*) fetal bovine serum (Gibco, Gibco, 17504-044) and 50 mg/mL gentamicin (Gibco, 15710-064). In all the experiments, hUCB-MSCs were used at passage 6. Hs68 (CRL-1635; ATCC, Rockville, MD, USA) and HEK293 (CRL-1573; ATCC, Rockville, MD, USA) cells were used as controls and cultured under identical culture conditions.

2.2. Animal Experiments. 5xFAD mice (B6SJL-Tg(APPSwFlLon,-PSEN1*M146L*L286V)6799Vas/Mmjax) were purchased from The Jackson Laboratory (Bar Harbor, ME, USA) and maintained in accordance with the laboratory guidelines. All animal experiments were approved by the Institutional Animal Care and Use Committee of MEDIPOST Co., Ltd. (MP-LAR-2016-6-2). 5xFAD mice display predominant features of AD amyloid pathology and develop cognitive dysfunction at 4 to 6 months of age [18]. In the present study, 3 μL of recombinant human GAL-3 protein (1.0 μg/kg) was inoculated into the bilateral hippocampi (AP: −2.54, ML: ±3.0, DV: −2.5 mm, with reference to the bregma) of 4-month-old 5xFAD mice using a sterile Hamilton syringe fitted with a 26-gauge needle (Hamilton Company, Reno, NV, USA) with a Pump 11 Elite microinfusion syringe pump (Harvard Apparatus, Holliston, MA, USA) and an infusion rate of 0.5 μL/min. For the administration of hUCB-MSCs, 6-month-old 5xFAD mice were cannulated and subjected to cell transplantation using the intracerebroventricular approach [19], and hUCB-MSCs (15 μL; 1×10^5 cells) were administered via a cannula into the lateral ventricle (AP: −0.22, ML: 1.0, DV: −2.1 mm, with reference to the bregma) using a microinfusion syringe pump (Harvard Apparatus) at an infusion rate of 1.0 μL/min. Brain tissues were homogenized in 3 mL of Dulbecco's phosphate-buffered saline (DPBS; Corning, Manassas, VA, 20109).

2.3. Western Blotting Analysis. Cells and tissue lysates were prepared by ultrasonication (Branson Ultrasonics, Slough, United Kingdom) in buffer containing 9.8 M urea, 2.8 M thiourea, 4% 3-((3-cholamidopropyl) dimethylammonio)-1-propanesulfonate, 130 mM dithiothreitol (DTT), 40 mM Tris-Cl (pH 8.8), and 0.1% sodium dodecyl sulfate. Protein levels were measured using Bradford assays (Bio-Rad Laboratories, Inc., Hercules, CA). For the immunoblot analysis, BOLT 4%–12% Bis-Tris gels (Life Technologies, Carlsbad, CA, USA) were electrophoretically transferred to nitrocellulose membranes. Each membrane was blocked in 5% skimmed milk and incubated with primary antibodies overnight at 4°C. After reaction with human recombinant protein-conjugated secondary antibodies at room temperature (RT) for 1.5 h, the immunoreactivity was detected using an ECL detection kit (GE Healthcare Life Sciences, Little Chalfont, UK). The antibodies used were as follows: anti-Tau (phospho T181; Abcam, Cambridge, United Kingdom), anti-Tau (phospho T231; Abcam), anti-Tau (phospho S396; Abcam), anti-Tau (phospho S404; Abcam), anti-glycogen synthase kinase 3 beta (GSK-3β; phospho Y216; Abcam), anti-total GSK-3β (Abcam), and anti-total tau (Wako, Osaka, Japan).

2.4. Immunoprecipitation. Extracts of total brain tissue were prepared in an immunoprecipitation buffer containing 50 mM Tris (pH, 7.8), 150 mM NaCl, 1 mM EDTA, 5 mM NaF, 1 mM Na_3VO_4, 1 mM $Na_4P_2O_7$, 1.5 mM $MgCl_2$, 1 mM DTT, 10% glycerol, 0.5% NP-40, and various protease inhibitors (complete, EDTA-free; Roche). The extracts were centrifuged for 10 min at 13,000 ×g at 4°C, and the supernatants were subjected to immunoprecipitation and analysis using western blotting.

2.5. Small Interfering RNA (siRNA) and Reverse Transcription-Polymerase Chain Reaction (RT-PCR). siRNAs for human GAL-3, growth differentiation factor-15 (GDF-15), and cluster of differentiation (CD) 147 were purchased from Dharmacon (Lafayette, CO, USA) and transfected using DharmaFECT (Dharmacon). Total RNA was isolated using the TRIzol Reagent (Thermo Fisher Scientific Inc. Waltham, MA, USA) following the manufacturer's protocol. The SuperScript® III Reverse Transcriptase kit was used for cDNA synthesis. PCR reactions were performed using the following oligonucleotides: Human GAL-3: sense, 5′-GGC CAC TGA TTG TGC CTT AT-3′/antisense, 5′-TCT TTC CCT TCC CCA GT-3′; human GDF-15: sense, 5′-AGA TGC TCC TGG TGT TGC TG-3′/antisense, 5′-CTG GTG TTG CTG GTG CTC TC-3′; human CD147: sense, 5′-GTC CGA TGC ATC CTA CCC TCC TAT-3′/antisense, 5′-CCC GCC TGC CCC ACC ACT CA-3′; and human β-actin: sense, 5′-GAC CTT CAA CAC CCC AGC CA-3′/antisense, 5′-CCC AGG AAG GAA GGC TGG AA-3′.

2.6. Inhibition of Tau Aggregation/Tau Disaggregation Assays. Previous studies have well-established tau aggregation assays using ThT fluorescence [20]. Human tau K18 fragments (125 amino acids, 0.5 mg/mL) were incubated at 37°C without shaking in buffers(0.1 mg/mL heparin (Sigma); DTT (Sigma); and DPBS (Corning), pH 7.4) for 2, 3, and 5 days to test inhibitory effects of tau aggregation or for more than 5 days to examine tau disaggregation in the presence or absence of recombinant proteins and cells. After incubation with thioflavin T (ThT; 5 μM in 50 mM glycine buffer, pH 8.9) for 3 h, the samples were plated in triplicate in a 96-well black plate with a clear bottom. ThT fluorescence was recorded at excitation wavelengths of 450 nm and emission wavelengths of 485 nm using an EnSpire Multimode Plate Reader (PerkinElmer, Waltham, Massachusetts, USA).

2.7. hUCB-MSC Coculture System and Recombinant Protein Treatment. Before hUCB-MSC coculture, a tau K18 fragment mixture (with heparin and DTT) was placed in multiwell plates in the presence of buffers. Then, hUCB-MSCs (2×10^4 cells/cm^2) were cocultured in the upper chamber of a Transwell device (pore size, 1 mm; BD Biosciences, Franklin Lakes, NJ, USA) in serum-free conditions. The final concentrations of recombinant human GAL-3 and GDF-15 were both 20 ng/mL and that of CD147 was 100 ng/mL.

2.8. Immunofluorescence. Anesthetized mice were fixed by cardiac perfusion of phosphate-buffered saline (PBS) and 4% paraformaldehyde in PBS. Mouse brains were carefully dissected, postfixed for 24 h at 4°C in the same fixative solution, and incubated in 20% sucrose at 4°C until equilibration. The fixative was discarded by aspiration, and the brains were washed with PBS. Sequential 30 μm-thick coronal sections were obtained using a cryostat (CM1850UV; Leica Microsystems GmbH, Wetzlar, Germany) at 22°C. The sections were blocked in 5% normal goat serum and 5% normal horse serum (VECTOR Laboratories, Burlingame, CA, USA). The tissues were permeabilized with 0.3% Triton X-100 and immunofluorescence was performed using standard methods with the following antibodies: anti-human mitochondria (Merck Millipore, Burlington, Massachusetts, USA), anti-3R-tau (Wako), anti-Tau (phospho T181; Abcam), and anti-tau (phospho S404; Abcam). Alexa 488 and Cy3-conjugated secondary antibodies (Jackson ImmunoResearch Europe Ltd., Newmarket, United Kingdom) were used to visualize the immune complexes. Antibody labeling was visualized under an LSM 800 confocal microscope (Carl Zeiss AG, Jena, Germany).

2.9. AlphaLISA Binding Assays. The FRET-based indirect AlphaLISA (Amplified Luminescent Proximity Homogeneous) assay was used to determine the saturation binding. The first sandwiching polyhistidine- (His-) tagged IgG was bound to donor beads and the second sandwiching anti-GAL-3 (Abcam) was captured by anti-rabbit IgG acceptor beads. Anti-His donor beads and rabbit acceptor beads were purchased from PerkinElmer and used at a final concentration of 20 μg/mL. The 1× assay buffer (0.5% in DPBS (Corning)) was distributed into each well of a 1/2 AreaPlate-96 (PerkinElmer). Before the experiments, we prepared a 5× working solution of untagged GAL-3 and His-tagged tau K18 fragments in 1× assay buffer and performed serial dilution of all the proteins in Eppendorf tubes on ice. Donor and acceptor beads were prepared from the 5× working solution (100 μg/mL). For a subset of the experiments, untagged GAL-3 protein and His-tagged tau K18 fragments were added to a white 1/2 AreaPlate-96 and incubated for 60 min at 4°C with a TopSeal adhesive seal. Indirect AlphaLISA was performed following the manufacturer's protocol, which involved capturing of the untagged proteins by adding an anti-GAL-3 antibody to the plate with the proteins. In another subset of experiments, acceptor and donor beads were added to the abovementioned 96-well plates at a final concentration of 20 μg/mL and incubated with a TopSeal adhesive seal for 60 min at RT in the dark. The fluorescence was measured using the EnSpire Multimode Plate Reader (PerkinElmer), and response data were exported and analyzed using Combine graphs in a layout with the GraphPad Prism (GraphPad, San Diego, USA) software. The binding of tau K18 fragments to GAL-3 was reflected by the calculated Kd values in the saturation binding assay. The Kd value is the concentration at which the binding signal reaches 50% saturation, and it is a measure of the binding affinity [21, 22]. The binding efficiency takes different saturation levels into account by calculating the ratios of the maximum binding signals and Kd values.

2.10. Behavioral Tests

2.10.1. T-maze Test. T-maze was constructed with one start arm and two-goal arms that formed a "T" shape. Spontaneous alternation performance was tested as previously described [23]. Each mouse was placed in the center of the symmetrical T-maze and allowed to explore freely through the maze. The sequence and the total number of arms entered were recorded. The experimenters were blinded with respect to the genotype of the mice. The percentage alternation was calculated as follows: number of triads containing entries into all three arms/maximum possible alternations. The trial was started by placing the mouse into the start arm facing the goal arms. The animals were then allowed to explore freely until they were confined in the left or right goal arm. They were moved back into the start arm and allowed to move into one of the open goal arms again. All mice were subjected to two trials conducted at a 1 h interval for 2 consecutive days. Scoring was performed as follows: 0, when the same goal arm was repeatedly chosen in the same trial and 1, when different goal arms were chosen in the same trial.

2.11. Open Field Test. Animals were allowed to explore an empty field (44.5 × 44.5 cm) for 20 min without any disturbing factors. They were gently placed in the peripheral area of the field. Auto-Track software (version 5.00) and the Opto-Varimex-5 Auto-Track device (Columbus Instruments, OH, USA) were used to measure the patterns of agility and rearing as indicators of locomotion and exploration, respectively.

2.12. Human Cytokine Antibody Array. The conditioned medium was collected from tau K18 fragments and the hUCB-MSC cocultures under inducing conditions for tau aggregation. The Human Cytokine Antibody Array C11 (Raybiotech Inc., Norcross, GA) was used to detect the secreted proteins according to the manufacturer's protocol. Membranes were incubated in the blocking buffer for 30 min at RT and each growth medium overnight at 4°C. After washing, the membranes were incubated with a diluted biotinylated antibody cocktail for 2 h at RT. After the second washing step, the membranes were incubated in horseradish peroxidase-conjugated streptavidin (1 : 1000) for 2 h at RT. After the third washing step, the signals were detected using the ChemiDoc™ Imaging System (Bio-Rad Laboratories Inc.) and quantified with the ImageJ software (National Center for Biotechnology Information, National Institutes of Health, Bethesda, MD).

2.13. Enzyme-Linked Immunosorbent Assay (ELISA). A human GAL-3-specific ELISA kit (R&D Systems, Inc.) was used to determine the GAL-3 levels according to the manufacturer's instructions. The results were analyzed using a VERSAmax microplate reader (Molecular Devices, Sunnyvale, CA, USA).

2.14. Statistical Analysis. All data are presented as mean ± standard error of the mean. Student's *t*-tests were used to analyze the between-group differences. Multiple sets of data were compared using one-way analysis of variance followed by Fisher's least significant difference post hoc tests. p values of $< 0.05^{*}$ and$< 0.005^{**}$ were considered statistically significant.

3. Results

3.1. Administration of hUCB-MSCs Ameliorates Cognitive Dysfunction in AD Mice. To determine the ameliorative effect of hUCB-MSCs on cognitive function in the AD mouse model, hUCB-MSCs were injected three times at 4-week intervals into the lateral ventricle of 6-month-old 5xFAD mice, which is the age at which these mice display cognitive dysfunction. For the control set, PBS was injected in a similar manner. Behavioral tests were conducted 4 weeks after the last injection (Figure 1(a)).

After repeated administration of hUCB-MSCs, the brains of 5xFAD mice were analyzed using immunofluorescence. Upon evaluation, we found that the transplanted hUCB-MSCs were present in the brain parenchyma (red: human mitochondria-labeled hUCB-MSCs), including the cortex, hippocampal dentate gyrus (DG), caudate-putamen (CPu), hypothalamus, and subventricular zone (SVZ) (Figure 1(b)). To evaluate the changes in the cognitive function of AD mice due to hUCB-MSC administration, behavioral tests were conducted in both the hUCB-MSC-treated 5xFAD and PBS-injected control groups. The open field test conducted to evaluate the general activity, anxiety, and exploratory behavior showed a significant improvement in locomotion (general activity, distance in the center (%), and resting duration (%)) and exploratory behavior caused by curiosity (number of rears) in the hUCB-MSC group. Moreover, a comparative analysis of changes in alternation (%) in the T-maze, used to evaluate spatial working memory, showed an ameliorative effect on the spatial memory in the hUCB-MSC group (Figure 1(c)).

These findings indicate that the administration of hUCB-MSCs can ameliorate cognitive dysfunction in the AD mouse model.

3.2. Administration of hUCB-MSCs Decreases Tau Phosphorylation and Inhibits the Formation of Aberrant Tau in AD Mice. To assess the association between the ameliorative effect of hUCB-MSCs on the cognitive function and aberrant tau pathology in AD mice, the mice were sacrificed after the behavioral tests and examined for changes in tau phosphorylation, which is significantly increased in AD and other related tauopathies. Accumulating evidence indicates that 5xFAD mice particularly develop tau hyperphosphorylation before the learning and memory impairments [24]. The brains of 5xFAD mice injected with hUCB-MSCs were examined by western blotting for identifying changes in the various disease-associated phosphorylated sites of tau, including thr181, thr231, ser396, and ser404. Administration of hUCB-MSCs significantly reduced the expression levels of these phosphorylated sites compared with that of the vehicles (Figure 2(a)). Also, immunofluorescence data revealed a decrease in the expression levels of the phosphorylated sites, including thr181 and ser404, in the hUCB-MSC group compared with the control group (Figure 2(b)).

To determine whether the inhibitory effects of hUCB-MSCs on tau phosphorylation also impacts the formation of aberrant form of phosphorylated tau in AD, the abnormal tau were examined in 5xFAD mice. Previous reports show that abnormal phosphorylation of tau triggers the aggregation of tau into filament [25] and that the microtubule-binding repeat region of tau is an important domain associated with the aggregation [26, 27]. Besides, each tau is expressed as 3-repeat (3R) and 4-repeat (4R) isoforms by alternative splicing [28]. 3R- and 4R-tau isoforms accumulate in a hyperphosphorylated state in the AD brains, and the 3R-tau contributes to the aggregation during the development of tau pathology [5, 29, 30]. Therefore, to understand the formation of the abnormal tau, we used a specific antibody for the 3R-tau isoforms targeting the microtubule repeated binding domain.

Immunofluorescence analysis showed that the 3R-tau antibody-positive signal was decreased in the hUCB-MSC group compared with the control group (Figures 2(c) and 2(e)). The no primary antibody, serving as a negative control, confirmed that this staining was not an artifact (Figure 2(d)).

Taken together, these results indicate that the administration of hUCB-MSCs not only decreases tau phosphorylation but could also inhibit the formation of aberrant tau, a stage that follows tau hyperphosphorylation in AD mice.

3.3. Decrease in Tau Aggregation by hUCB-MSC-Secreted GAL-3. We next determined the effect of hUCB-MSCs on tau aggregation using the ThT assay *in vitro*. Recombinant K18 fragments from the paired helical fragments (PHF)

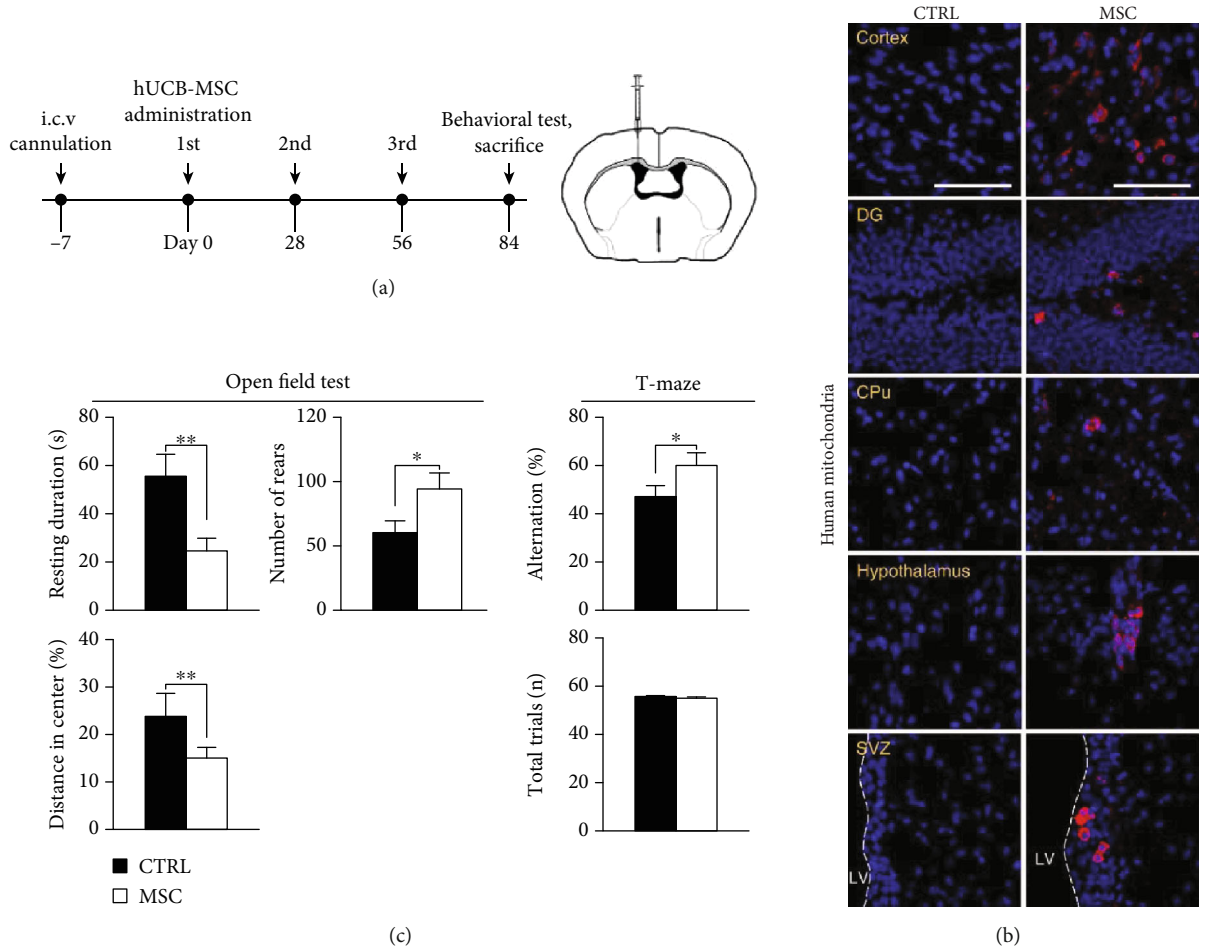

Figure 1: Administration of hUCB-MSCs ameliorates behavioral dysfunction in 5xFAD mice. (a) The schedule of repeated injection (3 times) of hUCB-MSCs via the lateral ventricle of 5xFAD mice, which express human APP and PSEN1 transgenes with a total of five AD-linked mutations. After 4 weeks at the last injection, mice were subjected to behavioral tests, and the brains were collected to analyze tau phosphorylation with western blotting or IF. (b) The brains injected with hUCB-MSCs were stained with antihuman mitochondria (red). Fluorescence signals were observed in the cortex, DG, CPu, hypothalamus, and SVZ (scale bar = 100 μm). (c) Various behavioral tests for hUCB-MSCs-injected 5xFAD mice (open field: resting duration, the distance in center, and number of rears; T-maze: alternation; $n = 8$ per group; $^{*}p < 0.05$, $^{**}p < 0.005$). CTRL: PBS-administrated 5xFAD; MSC: hUCB-MSC-administered 5xFAD.

core of full-length human tau, which is an important microtubule-binding repeat domain involved in tau aggregation, were used for the experiments [27] and were mixed with heparin to induce aggregation [31]. Incubation with hUCB-MSCs dramatically inhibited tau aggregation that persisted during the incubation period (Figure 3(a)), whereas no clear inhibitory effect on tau aggregation was observed after incubation with Hs68 and HEK293 cells (Figure 3(b)).

Aggregation-induced tau K18 fragments were cocultured with hUCB-MSCs to identify specific paracrine factors secreted by hUCB-MSCs that are associated with the inhibition of tau aggregation. The cocultured medium was analyzed using a human cytokine antibody array. The GAL-3 level was significantly increased in the hUCB-MSC^{+} aggregation-induced tau K18 group compared with the aggregation-induced tau K18 only group (control). Although GAL-3 was also detected in the hUCB-MSC only group, its expression was significantly higher when hUCB-MSCs were incubated with aggregation-induced tau K18 fragments (Figure 3(c)). Using human GAL-3-specific ELISA, higher expressions of GAL-3 were observed after coculture with hUCB-MSCs (an approximately twofold increase) than after coculture with HEK293 and Hs68 cells (Figure 3(d)).

These results demonstrate that hUCB-MSCs can inhibit the formation of tau aggregates and that the paracrine effect of hUCB-MSC-secreted GAL-3 is specifically increased under conditions favoring tau aggregation.

3.4. Gal-3 Is Essential for the Inhibition of Tau Aggregation In Vitro. To confirm the role of GAL-3, a recombinant human GAL-3 (rhGAL-3) protein was incubated with aggregation-induced tau K18 fragments, and the medium was analyzed by the ThT fluorescence assay. During incubation, treatment with rhGAL-3 protein (20 ng/mL) inhibited aggregation;

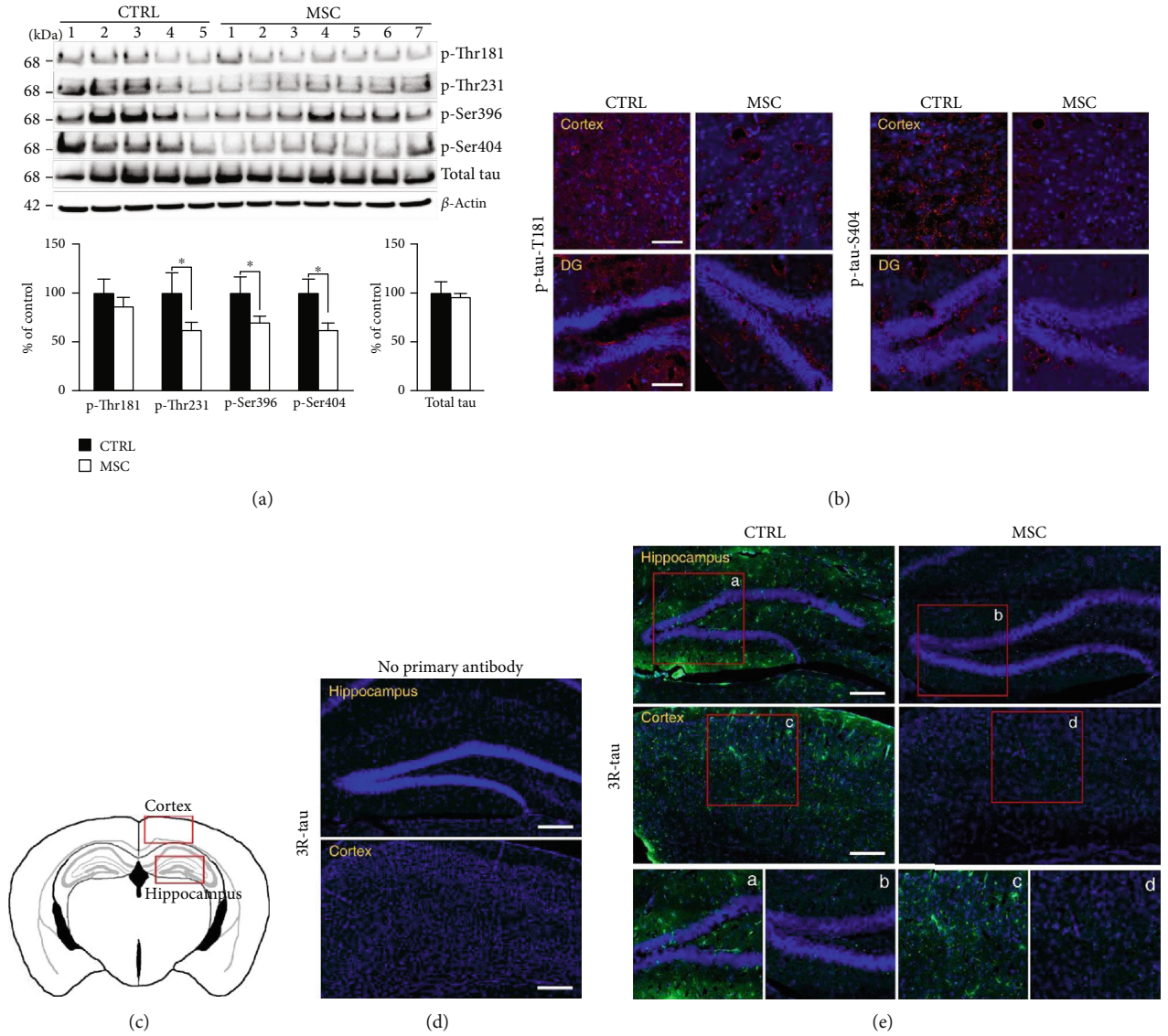

Figure 2: Administration of hUCB-MSCs inhibits the phosphorylation and formation of aberrant tau in 5xFAD mice. (a) Western blotting analysis showing phosphorylation and total levels of tau proteins in the right side of the whole brains in 5xFAD mice after injection of hUCB-MSCs. β-Actin was used as a loading control. Western blotting was analyzed using densitometric quantification ($n = 5$ for the CTRL group, $n = 7$ for the MSC group, $^*p < 0.05$). (b) Sections of the cortical and DG regions in the brains were stained with specific antibodies for phosphorylated tau (red) (tyr181 or ser404) (scale bar = 100 μm). (c) Coronal sections. Each red box indicates regions assessed using antibodies in (d, e). (d) Immunofluorescence performed in the absence of 3R-tau primary antibody was included to control for the nonspecific binding of the secondary antibody (no primary antibody). (e) Each tissue section was stained with DAPI and anti-3R-tau antibodies. The tile scan images acquired using a confocal microscope are shown in green (aberrant tau) in the hippocampal or cortex region (scale bar = 200 μm). The boxed areas represent magnified images. CTRL: PBS-administrated 5xFAD; MSC: hUCB-MSC-administered 5xFAD.

however, none of the other secreted proteins from hUCB-MSCs (Supplementary Figure 1), such as GDF-15 (20 ng/mL) or CD147 (100 ng/mL), were able to inhibit the aggregation-induced tau K18 fragments (Figure 4(a)). Treatment of tau K18 aggregates with rhGAL-3 protein was able to significantly reduce the ThT fluorescence intensity (Figure 4(b)).

In addition, the treatment of hUCB-MSCs with GAL-3-specific siRNA markedly reduced the mRNA and protein levels of GAL-3 (Figure 4(c)). Next, GAL-3-deficient culture media harvested from GAL-3 knockdown hUCB-MSCs, upon treatment with aggregation-induced tau K18 fragments, showed reduced inhibition of tau aggregation as compared to that in the control group (scrambled siRNA-transfected hUCB-MSCs; Figure 4(e)). However, no change was observed in the level of tau aggregation, after treatment with hUSB-MSC cell cultures incubated with GDF-15- and CD147-specific siRNAs or the control group, confirming the specificity of GAL-3 in tau aggregation. (Figures 4(d) and 4(e)).

These results indicate that hUCB-MSC-secreted GAL-3 is an essential factor for specific inhibition of tau aggregation in an *in vitro* assay.

3.5. GAL-3 Decreases Tau Phosphorylation by Modulation of GSK-3β in AD Mice. To evaluate the effects of GAL-3 on tau pathology in AD mice, rhGAL-3 protein (1.0 μg/kg) was injected into the bilateral hippocampi of 4-month-old 5xFAD mice. Mice were then sacrificed after 7 days (Figure 5(a)) to study the expression of various disease-associated phosphorylated sites of tau, including thr181, thr231, ser396, and ser404. The expression of these sites was significantly reduced in the rhGAL-3 protein group compared with the PBS-injected control group (Figure 5(b)). Results from immunofluorescence also showed a reduction in the expression of phosphorylated sites, including thr181 and ser404, after rhGAL-3 protein administration (Figure 5(c)).

To understand the mechanism underlying the modulation of tau phosphorylation, we investigated the role of kinases located upstream of tau. In particular, we tried to establish the association between GAL-3 and GSK-3β, a known tau phosphorylation-regulating kinase in AD, *in vivo*. Using western blotting, we showed that GSK-3β-tyr216 phosphorylation was significantly reduced after the administration of rhGAL-3 protein (75.6% decrease relative to that in the control group) and GAL-3-secreting hUCB-MSCs (50.9% decrease relative to that in the control group) in 5xFAD mouse brains (Figures 5(d) and 5(e)).

These findings suggest that GAL-3 modulates tau phosphorylation by reducing phosphorylation at the tyr216 residue of activated GSK-3β in AD mice.

3.6. GAL-3 Prevents the Formation of Aberrant Tau and Directly Interacts with Tau in AD Mice. To confirm the role of GAL-3 secreted from hUCB-MSCs in the aberrant formation of phosphorylated tau in AD, we evaluated the changes in abnormal tau after rhGAL-3 protein injection in AD mice. Immunofluorescence using the 3R-tau antibody for the 3-repeat tau isoform revealed that the 3R-tau-positive signal was decreased in the GAL-3-treated group compared with that of the control group (Figure 6(a)).

In addition, to verify the possibility of interference in aberrant tau by protein-protein interaction, we measured the binding kinetics between the tau K18 fragments and GAL-3 using the fluorescence resonance energy transfer-(FRET-) based AlphaLISA assay. The binding ability between the two proteins was reflected by Kd values calculated using the AlphaLISA saturation binding assay. In this experiment, tau K18 fragments were used as an analyte at a concentration ranging from 0 to 100 nM. The assay demonstrated that the binding of tau K18 fragments to GAL-3 (1, 3, and 10 nM) was saturable, with a high binding affinity. The Kd values at 1, 3, and 10 nM were 8.31, 8.73, and 9.13 nM, respectively (Figure 6(b)). This result indicates a high degree of direct interaction between the tau K18 fragments and GAL-3.

Moreover, we analyzed the brain extract of AD mice using immunoprecipitation in order to determine the actual binding between tau and GAL-3 *in vivo*. After immunoprecipitation using the GAL-3 antibody, the binding complex of GAL-3-tau was selected for immunoblotting, and the binding was confirmed by the tau and GAL-3 expressions. The expressions of both GAL-3 and tau were detected in the brain extract using the GAL-3 antibody, but not with the negative IgG antibody (n-IgG) (Figure 6(c)).

These results suggest that hUCB-MSC-secreted GAL-3 can hinder the formation of abnormal tau by directly binding with tau in AD mice.

4. Discussion

In this study, we demonstrated the inhibitory effect of hUCB-MSCs on the formation of aberrant tau and subsequently identified a soluble protein GAL-3 as an essential protein secreted by hUCB-MSC in response to tau abnormalities. In addition, we showed that the interaction between GAL-3 and tau reduced the formation of abnormal tau by directly binding and inhibiting the hyperphosphorylation of tau. Moreover, we determined the mechanism underlying the inhibition of tau hyperphosphorylation by GAL-3.

Abnormal hyperphosphorylation of tau protein and the development of tau tangles along with amyloid accumulation are the fundamental characteristics of AD progression in the human brain. Induction of structural stabilization and clearing of hyperphosphorylated tau aggregates by tau modulation have emerged as alternative therapies [32, 33]. Tau protein was initially identified as a microtubule-associated protein in the brain microtubules [34]. Structurally, it is divided into the acidic region of the N-terminal portion, a proline-rich region, microtubule-binding four-repeat domains (RD1~4), and the C-terminal region, and the alternative splicing of the tau primary transcript in the central nervous system produces the six isoforms of 352-441 amino acids [35]. Specifically, the exon 10 (RD2) contains the microtubule-binding region and the insertion of exon 10 leads to the 4-repeat (4R) tau isoforms whereas the 3-repeat (3R) tau isoforms are produced without the exon 10 [28]. 3R- and 4R-tau contribute to the abnormal accumulation in tau pathology in AD brain [36]. In particular, aberrant modifications of hyperphosphorylated tau from increased β-structure levels in the repeat domains eventually lead to the formation of PHFs in AD [37]. Such modifications of tau in the intracellular or extracellular space may be toxic to neurons [38]. Therefore, inhibition of abnormal hyperphosphorylation and tau aggregation has become a strategically important therapeutic target. However, despite extensive efforts for drug development, an approved drug has not yet been developed [39].

Studies have revealed that hUCB-MSCs exert a therapeutic effect on AD via the secretion of therapeutic factors. The effects of hUCB-MSCs, including amyloid clearance, anti-inflammatory effects, and recovery of synaptic function indicate that hUCB-MSCs have the capacity to improve the overall environment in AD, which has various pathologies [14, 15, 40, 41]. Therefore, hUCB-MSCs might have multifunctional therapeutic effects and play a pivotal role as a therapeutic agent for AD. In the present study, we presented clear evidence supporting a new therapeutic role of hUCB-

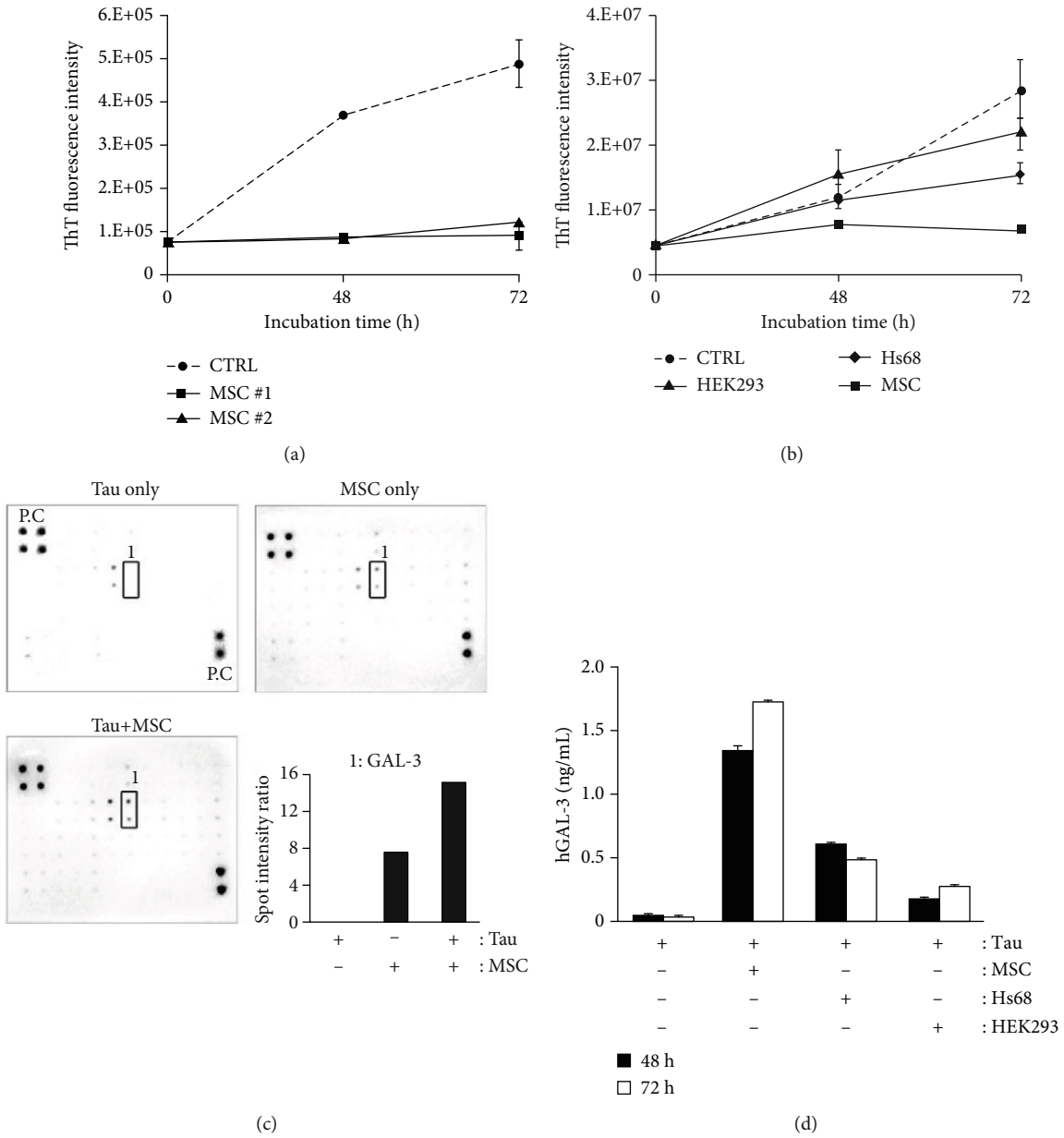

Figure 3: GAL-3 secreted from hUCB-MSCs suppresses aggregation of tau *in vitro*. (a, b) After treatment with two hUCB-MSC lots in tau K18 fragments under the aggregation-inducing condition, each conditioned medium was analyzed by the ThT fluorescence assay to identify the relative intensity of aggregated tau levels. Tau aggregation-inducing condition was used as a control (mean ± SEM, $n = 3$ per group). (c) Cytokine arrays were conducted with the conditioned medium. Box 1 indicates GAL-3 protein levels under each condition. A densitometric analysis of GAL-3 was performed. (d) Conditioned media from various human originated cells in the Transwell system were analyzed with ELISA to identify the relative quantity of secreted human GAL-3. (mean ± SEM, $n = 3$ per group). MSC: hUCB-MSCs; Hs68: human foreskin fibroblast; HEK293: human embryonic kidney 293.

MSCs in AD: modulation and inhibition of the abnormal hyperphosphorylation of tau. Moreover, we also demonstrated the modulatory effect of hUCB-MSCs on tau through a paracrine action in an AD environment and identified GAL-3 as the primary associated paracrine factor.

GAL-3, a member of the β-galactoside-binding protein family, is a multifunctional protein involved in both intracellular and extracellular functions [42, 43]. It is an extracellular space protein secreted by a nonclassical secretory pathway and it not only modulates the basic cellular functions, including cell-cell interactions, proliferation, and differentiation, but also plays a role in the pathogenesis of many human diseases and promotion of neural cell adhesion and neurite outgrowth [44–46]. GAL-3 plays a critical role in MSC survival, migration, and therapeutic application [47]. In our previous study, we demonstrated the antiapoptotic role of hUCB-MSC-secreted GAL-3 in neuronal cells [13]. GAL-3 aids in autophagy-mediated removal of ruptured phagosomes and

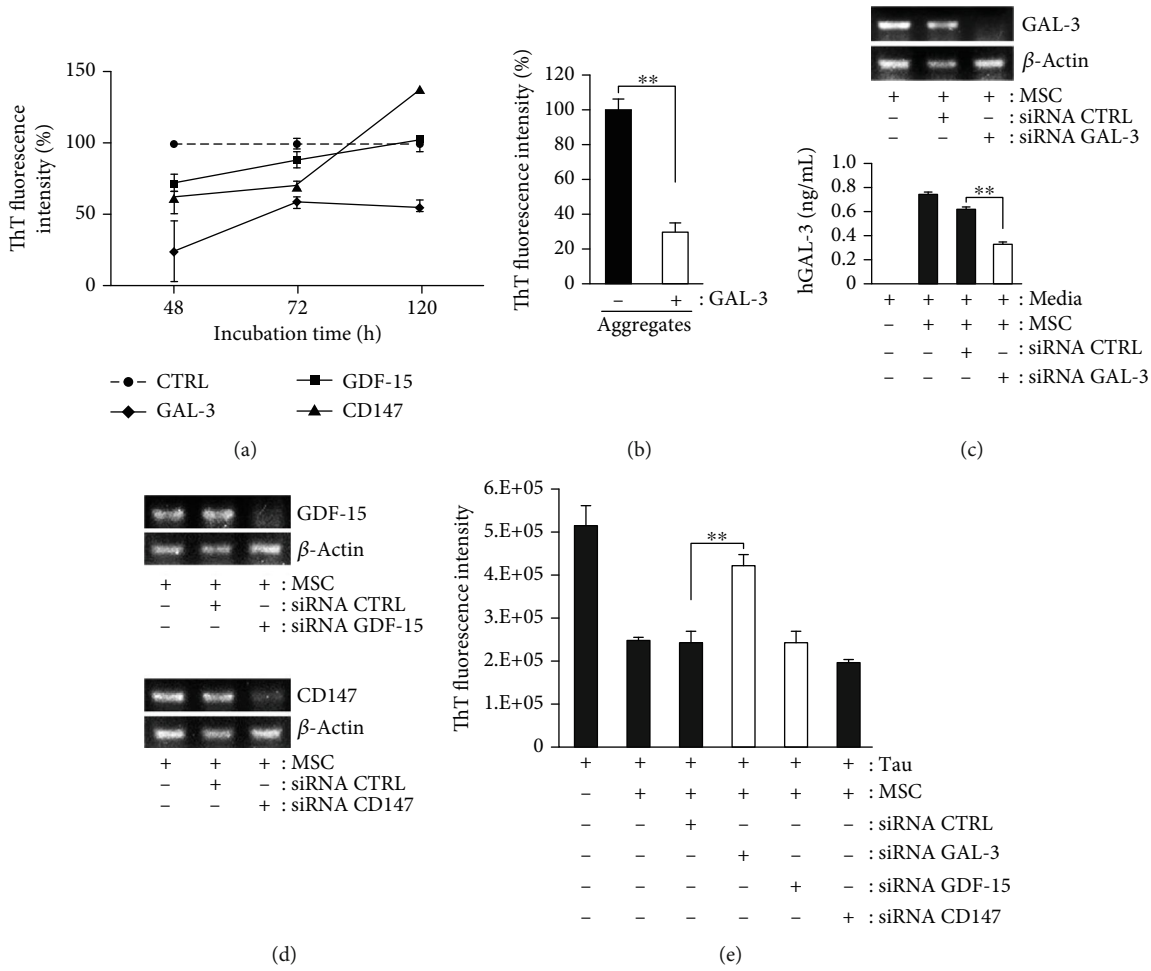

Figure 4: GAL-3 secreted from hUCB-MSCs is an essential factor for inhibition of tau aggregation. (a) A variety of factors were administered to the K18 fragments under the aggregation-induced condition, and each conditioned medium was used to analyze the level of aggregated tau using the ThT fluorescence assay. Tau aggregation-inducing condition was used as a control (mean ± SEM, $n = 3$ per group). (b) The ThT assay showed that the effects of GAL-3 on tau disaggregation were greatly substantial (mean ± SEM, $^{**}p < 0.005$, $n = 3$ per group). (c) hUCB-MSCs were transfected with control or GAL-3-siRNA at 37°C overnight. On the following day, the cells were incubated with tau K18 fragments under the aggregation-inducing condition. GAL-3 and β-actin mRNA and protein levels were, respectively, assessed by RT-PCR and ELISA (mean ± SEM, $^{**}p < 0.005$ versus control-siRNA-treated hUCB-MSCs). (d) siRNAs of GDF-15 or CD147 could effectively knockdown GDF-15 or CD147 expressions, as analyzed with RT-PCR. (e) Tau K18 fragments were treated with conditioned media derived from hUCB-MSCs, in which CTRL, GAL-3, GDF-15, and CD147 were knockdown by siRNA. The relative quantity of aggregated tau levels was estimated by the ThT fluorescence assay (mean ± SEM, $^{**}p < 0.005$ versus control-siRNA-treated hUCB-MSCs).

lysosomes via recognition molecules [48], and galectin-8-mediated selective autophagy prevents seeded tau aggregation [49]. In contrast, GAL-3 enhances Aβ oligomerization and Aβ toxicity, while GAL-3 deletion decreases the microglia-associated immune response and improves cognitive behavior in AD mice [50, 51]. These conflicting functional roles of GAL-3 could be due to the difference in cell types expressing GAL-3 or due to the difference in response to the stimulating environment. In the present study, we demonstrated that GAL-3 had a modulating effect on tau protein phosphorylation and an inhibitory potential on the formation of aberrant tau.

Tau protein functions in the brain via kinase-regulated phosphorylation [52]. Of these kinases, GSK has two closely related isoforms, GSK-3 alpha and GSK-3β. The latter is a proline-directed kinase that plays a key role in controlling the numerous signaling pathways in the central nervous system and modulates important cellular processes [53, 54]. GSK-3β is structurally activated by autophosphorylation at the Tyr216 residue and inactivated by phosphorylation at the Ser9 residue [55]. Activation of GSK-3β results in hyperphosphorylation of most sites of tau and increases tau phosphorylation in AD [56–58]. Moreover, GSK-3β directly participates in the microtubule destabilization and PHF formation in the AD brains [59, 60]. Recently identified GSK-3β-phosphorylated sites of tau include the Thr181, Ser199, Thr231, Ser396, Ser404, Ser413, Ser46, Thr50, and Ser202/Thr205 [54, 61]. In the present study, we show that GAL-3 modulates the expression of GSK-3β. The present findings are of clinical significance because the hUCB-

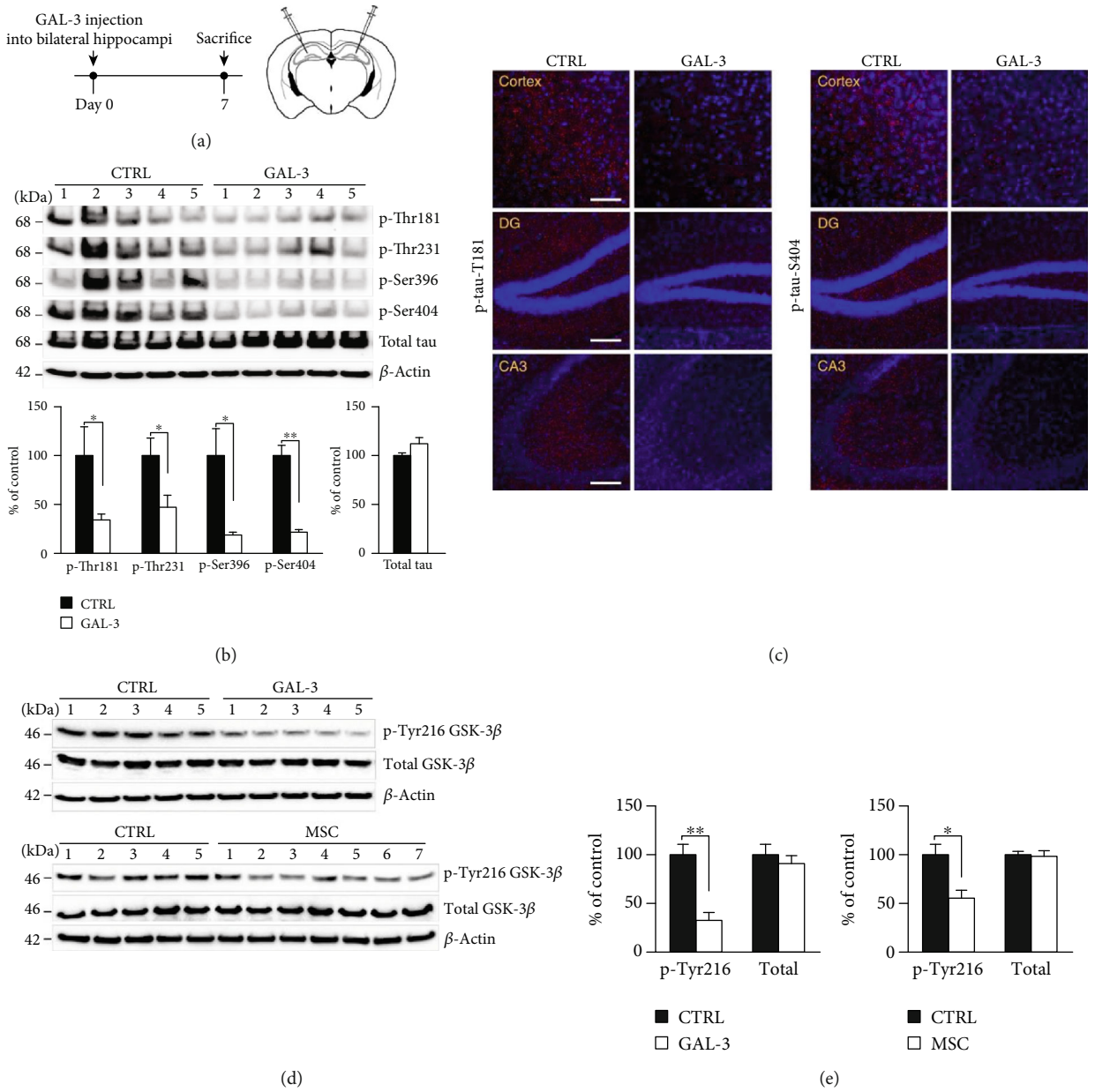

Figure 5: GAL-3 attenuates tau pathology in 5xFAD mice. (a) Schematics of human recombinant GAL-3 injection into the hippocampi of 5xFAD mice and the schedule of animal sacrifice. (b) After 1 week, GAL-3-injected 5xFAD mouse brains were extracted and assessed by western blotting with various phosphorylated tau antibodies. β-Actin was used as a loading control. Western blotting was analyzed using densitometric quantification ($n = 5$ per group, $^{*}p < 0.05$, $^{**}p < 0.005$). (c) Sections of the cortical and DG regions were stained with specific antibodies for phosphorylated tau (red), tyr181, or ser404 (scale bar = 100 μm). (d) GAL-3-injected or hUCB-MSC-administrated 5xFAD mouse brains were analyzed by western blotting with tyrosine 216 phosphorylated GSK-3β or total GSK-3β antibodies. β-Actin was used as a loading control. (e) Densitometric quantification of western blotting in (d) ($^{*}p < 0.05$, $^{**}p < 0.005$, $n = 5$ per group or $n = 5 \sim 7$ per group). CTRL: PBS-administrated 5xFAD; GAL-3: GAL-3-injected 5xFAD; MSC: hUCB-MSC-administrated 5xFAD; DG: dentate gyrus; CA3: cornu ammonis 3.

MSC-secreted protein GAL-3 may reduce the tau phosphorylation through GSK-3β mediation and interfere with AD progression due to the aberrant tau pathology.

In the present study, we selected 5xFAD as the double-transgenic AD mouse model of choice as these mice mimic most of the pathologic alterations, including early accumulation of Aβ, neuronal loss, and cognitive deficits similar to patients with AD [62]. Although these double-transgenic AD mouse models, with only APP and PS1 mutation, are not exact replicable models of tauopathy, they have the potential to exhibit hyperphosphorylated tau as punctuate deposits and neurofibrillary changes [62, 63]. Further, Aβ peptides can induce the formation of tau fibrils in culture and stimulate tau hyperphosphorylation in AD model [30,

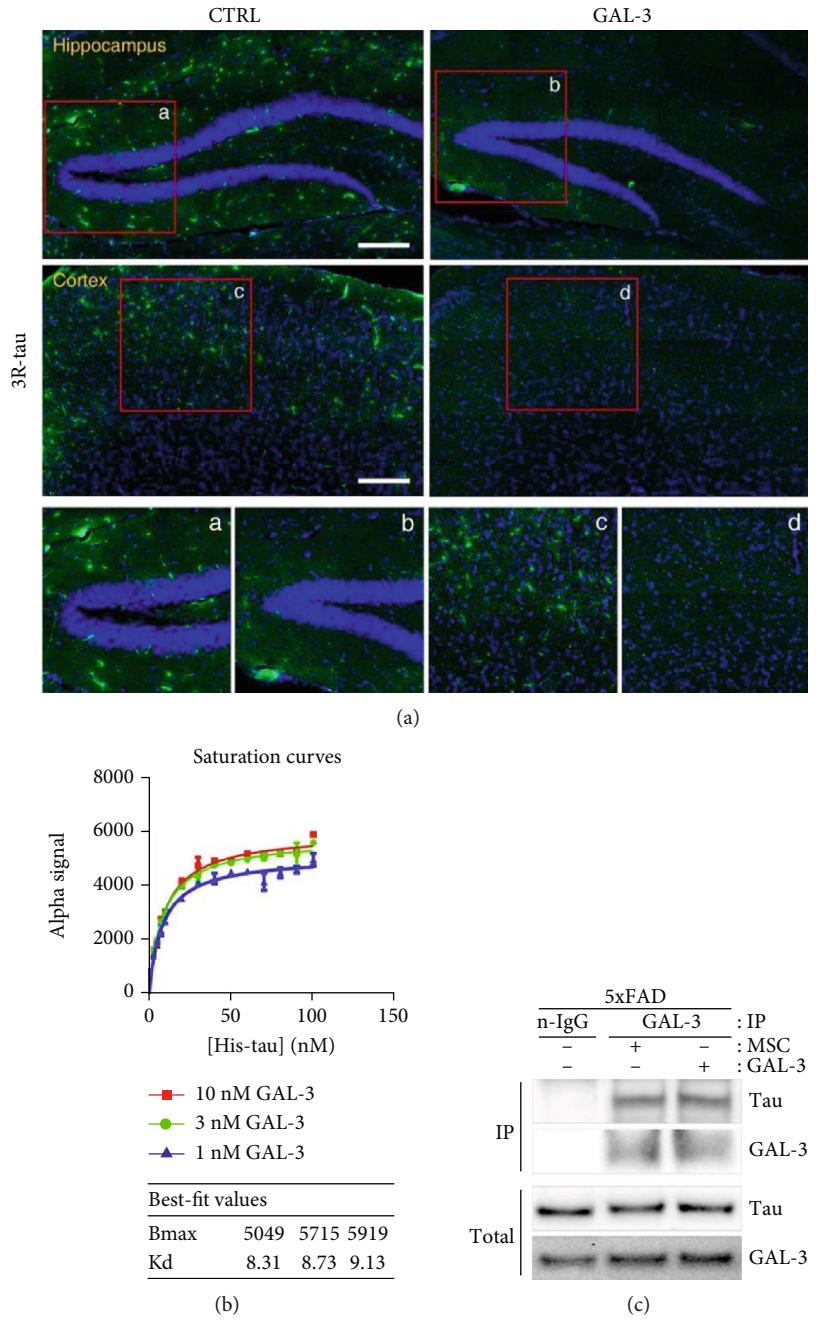

Figure 6: GAL-3 alleviates the formation of aberrant tau through protein binding in 5xFAD mice. (a) Each tissue section was stained with DAPI and anti-3R-tau antibodies. The tile scan images using a confocal microscope are shown in green (aberrant tau) in the hippocampal or cortical region (scale bars = 200 μm). The boxed areas represent magnified images. (b) Saturation curves were determined by fluorescence intensities of the interaction between tau-K18-His fragment and GAL-3 in AlphaLISA format by the FRET-based assay. Tau-K18-His fragment and GAL-3 proteins were incubated together at a wide range of concentrations (Tau-K18-His fragment: 0 ~ 100 nM, GAL-3: 1 ~ 10 nM) followed by analysis with specific Alpha Donor/Acceptor beads. (c) hUCB-MSC- or GAL-3-injected 5xFAD mouse brains were extracted, and anti-GAL-3 immunoprecipitates and total lysates were analyzed by western blotting with anti-Tau or anti-GAL-3 antibodies. The n-IgG used as a control was immunoprecipitated by normal IgG antibody. CTRL: PBS-administrated 5xFAD; GAL-3: GAL-3-injected 5xFAD; MSC: hUCB-MSC-administrated 5xFAD.

64, 65]. These previous reports show that the double-transgenic AD mouse model may be partially helpful in understanding the aberrant tau formation. In this study, we present the possible regulation of abnormal tau by hUCB-MSCs in an AD model.

Using AlphaLISA binding assay and immunoprecipitation analysis of the brain extract from 5xFAD mice, we demonstrated binding between tau and GAL-3. Binding between proteins has been known to inhibit aggregation, for example, small molecule curcumin binds to the monomeric form of α-

synuclein, which belongs to aggregation-prone proteins, and prevents α-synuclein aggregation [66]. Thus, based on the results from this study we propose that hUCB-MSC-secreted GAL-3 protein could inhibit the aggregated formation of tau by its interaction with tau.

Further studies are needed to investigate the pathways associated with kinases that function as tau modulators. In order to verify the ameliorative effect of hUCB-MSCs on abnormal tau, it is important to establish an *in vitro* model, which allows the coculture of tau with hUCB-MSCs, thus unraveling the mechanism behind the beneficial effects of GAL-3 secreted by hUCB-MSCs. Moreover, validation of the efficacy of hUCB-MSC-secreted GAL-3 in tauopathy animal models, such as Tau P301S Tg mice, will further demonstrate its applicability as a therapeutic agent for neurodegenerative diseases associated with tauopathy.

5. Conclusion

This study suggests that hUCB-MSCs modulate hyperphosphorylated tau *in vivo* and aggregation of tau *in vitro*, which are the major pathological hallmarks of AD. hUCB-MSC-secreted GAL-3 can inhibit tau phosphorylation by modulating GSK-3β and suppressing the formation of aberrant tau by interacting with the tau protein. These findings indicate that abnormal tau in AD may be modulated by the paracrine action of proteins secreted by hUCB-MSCs, and GAL-3 may contribute to the beneficial effects of hUCB-MSCs. Our findings (tau protein modulation by hUCB-MSCs) present a new direction and possibility for the role of stem cell therapy in AD.

Data Availability

All the data used to support the findings of this study are available from the corresponding author upon reasonable request.

Conflicts of Interest

The authors declare that there is no conflict of interest regarding the publication of this article.

Authors' Contributions

H Lim performed the entire experiments, analyzed data, and wrote the initial draft of manuscript. D Lee and WK Choi were involved in performing the animal experiments. SJ Choi and W Oh interpreted the data and provided conceptual advice. DH Kim designed this study, supervised the project, and also wrote manuscript. All authors reviewed the manuscript. Hoon Lim is the main contributor of this work.

Acknowledgments

This research was supported by the Basic Science Research Program through the National Research Foundation of Korea (NRF) funded by the Ministry of Education (NRF-2018R1D1A1B07048851).

Supplementary Materials

Supplementary Figure 1: analysis of human cytokines secreted from hUCB-MSCs in conditioned media. *(Supplementary Materials)*

References

[1] A. Boutajangout and T. Wisniewski, "Tau-based therapeutic approaches for Alzheimer's disease - a mini-review," *Gerontology*, vol. 60, no. 5, pp. 381–385, 2014.

[2] L. Buee, T. Bussiere, V. Buee-Scherrer, A. Delacourte, and P. R. Hof, "Tau protein isoforms, phosphorylation and role in neurodegenerative disorders," *Brain Research. Brain Research Reviews*, vol. 33, no. 1, pp. 95–130, 2000.

[3] M. Goedert, M. G. Spillantini, R. Jakes, D. Rutherford, and R. A. Crowther, "Multiple isoforms of human microtubule-associated protein tau: sequences and localization in neurofibrillary tangles of Alzheimer's disease," *Neuron*, vol. 3, no. 4, pp. 519–526, 1989.

[4] M. D. Weingarten, A. H. Lockwood, S. Y. Hwo, and M. W. Kirschner, "A protein factor essential for microtubule assembly," *Proceedings of the National Academy of Sciences of the United States of America*, vol. 72, no. 5, pp. 1858–1862, 1975.

[5] K. Iqbal, F. Liu, C. X. Gong, and I. Grundke-Iqbal, "Tau in Alzheimer disease and related tauopathies," *Current Alzheimer Research*, vol. 7, no. 8, pp. 656–664, 2010.

[6] M. Matarin, D. A. Salih, M. Yasvoina et al., "A genome-wide gene-expression analysis and database in transgenic mice during development of amyloid or tau pathology," *Cell Reports*, vol. 10, no. 4, pp. 633–644, 2015.

[7] J. Di, L. S. Cohen, C. P. Corbo, G. R. Phillips, A. El Idrissi, and A. D. Alonso, "Abnormal tau induces cognitive impairment through two different mechanisms: synaptic dysfunction and neuronal loss," *Scientific Reports*, vol. 6, no. 1, 2016.

[8] W. V. Graham, A. Bonito-Oliva, and T. P. Sakmar, "Update on Alzheimer's disease therapy and prevention strategies," *Annual Review of Medicine*, vol. 68, no. 1, pp. 413–430, 2017.

[9] K. Yanamandra, N. Kfoury, H. Jiang et al., "Anti-tau antibodies that block tau aggregate seeding in vitro markedly decrease pathology and improve cognition in vivo," *Neuron*, vol. 80, no. 2, pp. 402–414, 2013.

[10] D. H. Kim, D. Lee, E. H. Chang et al., "GDF-15 secreted from human umbilical cord blood mesenchymal stem cells delivered through the cerebrospinal fluid promotes hippocampal neurogenesis and synaptic activity in an Alzheimer's disease model," *Stem Cells and Development*, vol. 24, no. 20, pp. 2378–2390, 2015.

[11] M. Lee, S. Y. Jeong, J. Ha et al., "Low immunogenicity of allogeneic human umbilical cord blood-derived mesenchymal stem cells in vitro and in vivo," *Biochemical and Biophysical Research Communications*, vol. 446, no. 4, pp. 983–989, 2014.

[12] J. Y. Kim, D. H. Kim, J. H. Kim et al., "Umbilical cord blood mesenchymal stem cells protect amyloid-β42 neurotoxicity-viaparacrine," *World Journal of Stem Cells*, vol. 4, no. 11, pp. 110–116, 2012.

[13] J. Y. Kim, D. H. Kim, D. S. Kim et al., "Galectin-3 secreted by human umbilical cord blood-derived mesenchymal stem cells reduces amyloid-beta42 neurotoxicity in vitro," *FEBS Letters*, vol. 584, no. 16, pp. 3601–3608, 2010.

[14] D. H. Kim, H. Lim, D. Lee et al., "Thrombospondin-1 secreted by human umbilical cord blood-derived mesenchymal stem cells rescues neurons from synaptic dysfunction in Alzheimer's disease model," *Scientific Reports*, vol. 8, no. 1, p. 354, 2018.

[15] J. Y. Kim, D. H. Kim, J. H. Kim et al., "Soluble intracellular adhesion molecule-1 secreted by human umbilical cord blood-derived mesenchymal stem cell reduces amyloid-β plaques," *Cell Death and Differentiation*, vol. 19, no. 4, pp. 680–691, 2012.

[16] D. H. Kim, D. Lee, H. Lim et al., "Effect of growth differentiation factor-15 secreted by human umbilical cord blood-derived mesenchymal stem cells on amyloid beta levels in in vitro and in vivo models of Alzheimer's disease," *Biochemical and Biophysical Research Communications*, vol. 504, no. 4, pp. 933–940, 2018.

[17] S.-E. Yang, C.-W. Ha, M. H. Jung et al., "Mesenchymal stem/-progenitor cells developed in cultures from UC blood," *Cytotherapy*, vol. 6, no. 5, pp. 476–486, 2004.

[18] H. Oakley, S. L. Cole, S. Logan et al., "Intraneuronal beta-amyloid aggregates, neurodegeneration, and neuron loss in transgenic mice with five familial Alzheimer's disease mutations: potential factors in amyloid plaque formation," *The Journal of Neuroscience*, vol. 26, no. 40, pp. 10129–10140, 2006.

[19] B. B. Land, M. R. Bruchas, J. C. Lemos, M. Xu, E. J. Melief, and C. Chavkin, "The dysphoric component of stress is encoded by activation of the dynorphin kappa-opioid system," *The Journal of Neuroscience*, vol. 28, no. 2, pp. 407–414, 2008.

[20] S. H. Yang, D. K. Lee, J. Shin et al., "Nec-1 alleviates cognitive impairment with reduction of Aβ and tau abnormalities inAPP/PS1 mice," *EMBO Molecular Medicine*, vol. 9, no. 1, pp. 61–77, 2016.

[21] E. C. Hulme and M. A. Trevethick, "Ligand binding assays at equilibrium: validation and interpretation," *British Journal of Pharmacology*, vol. 161, no. 6, pp. 1219–1237, 2010.

[22] S. Bocker and L. Elling, "Binding characteristics of galectin-3 fusion proteins," *Glycobiology*, vol. 27, no. 5, pp. 457–468, 2017.

[23] K. E. Davis, K. Burnett, and J. Gigg, "Water and T-maze protocols are equally efficient methods to assess spatial memory in 3xTg Alzheimer's disease mice," *Behavioural Brain Research*, vol. 331, pp. 54–66, 2017.

[24] T. Kanno, A. Tsuchiya, and T. Nishizaki, "Hyperphosphorylation of tau at Ser396 occurs in the much earlier stage than appearance of learning and memory disorders in 5XFAD mice," *Behavioural Brain Research*, vol. 274, pp. 302–306, 2014.

[25] M. Kolarova, F. Garcia-Sierra, A. Bartos, J. Ricny, and D. Ripova, "Structure and pathology of tau protein in Alzheimer disease," *International Journal of Alzheimer's Disease*, vol. 2012, article 731526, 13 pages, 2012.

[26] S. L. Shammas, G. A. Garcia, S. Kumar et al., "A mechanistic model of tau amyloid aggregation based on direct observation of oligomers," *Nature Communications*, vol. 6, no. 1, 2015.

[27] M. M. Haque, D. Kim, Y. H. Yu et al., "Inhibition of tau aggregation by a rosamine derivative that blocks tau intermolecular disulfide cross-linking," *Amyloid*, vol. 21, no. 3, pp. 185–190, 2014.

[28] G. Šimić, M. Babić Leko, S. Wray et al., "Tau protein hyperphosphorylation and aggregation in Alzheimer's disease and other tauopathies, and possible neuroprotective strategies," *Biomolecules*, vol. 6, no. 1, p. 6, 2016.

[29] M. Goedert, B. Falcon, W. Zhang, B. Ghetti, and S. H. W. Scheres, "Distinct conformers of assembled tau in Alzheimer's and Pick's diseases," *Cold Spring Harbor Symposia on Quantitative Biology*, vol. 83, pp. 163–171, 2019.

[30] A. Metaxas, C. Thygesen, S. J. Kempf et al., "Ageing and amyloidosis underlie the molecular and pathological alterations of tau in a mouse model of familial Alzheimer's disease," *Scientific Reports*, vol. 9, no. 1, 201915758.

[31] H. L. Zhu, C. Fernández, J. B. Fan et al., "Quantitative characterization of heparin binding to tau protein: implication for inducer-mediated tau filament formation," *The Journal of Biological Chemistry*, vol. 285, no. 6, pp. 3592–3599, 2010.

[32] J. Gotz, A. Ittner, and L. M. Ittner, "Tau-targeted treatment strategies in Alzheimer's disease," *British Journal of Pharmacology*, vol. 165, no. 5, pp. 1246–1259, 2012.

[33] E. E. Congdon and E. M. Sigurdsson, "Tau-targeting therapies for Alzheimer disease," *Nature Reviews. Neurology*, vol. 14, no. 7, pp. 399–415, 2018.

[34] J. Avila, "Intracellular and extracellular tau," *Frontiers in Neuroscience*, vol. 4, 2010.

[35] L. Martin, X. Latypova, and F. Terro, "Post-translational modifications of tau protein: implications for Alzheimer's disease," *Neurochemistry International*, vol. 58, no. 4, pp. 458–471, 2011.

[36] M. Espinoza, R. de Silva, D. W. Dickson, and P. Davies, "Differential incorporation of tau isoforms in Alzheimer's disease," *Journal of Alzheimer's Disease*, vol. 14, no. 1, pp. 1–16, 2008.

[37] S. Barghorn, P. Davies, and E. Mandelkow, "Tau paired helical filaments from Alzheimer's disease brain and assembled in vitro are based on beta-structure in the core domain," *Biochemistry*, vol. 43, no. 6, pp. 1694–1703, 2004.

[38] J. Avila, N. Pallas, M. Bolos, C. L. Sayas, and F. Hernandez, "Intracellular and extracellular microtubule associated protein tau as a therapeutic target in Alzheimer disease and other tauopathies," *Expert Opinion on Therapeutic Targets*, vol. 20, no. 6, pp. 653–661, 2015.

[39] M. Medina, "An overview on the clinical development of tau-based therapeutics," *International Journal of Molecular Sciences*, vol. 19, no. 4, p. 1160, 2018.

[40] H. J. Lee, J. K. Lee, H. Lee et al., "Human umbilical cord blood-derived mesenchymal stem cells improve neuropathology and cognitive impairment in an Alzheimer's disease mouse model through modulation of neuroinflammation," *Neurobiology of Aging*, vol. 33, no. 3, pp. 588–602, 2012.

[41] A. Boutajangout, A. Noorwali, H. Atta, and T. Wisniewski, "Human umbilical cord stem cell xenografts improve cognitive decline and reduce the amyloid burden in a mouse model of Alzheimer's disease," *Current Alzheimer Research*, vol. 14, no. 1, pp. 104–111, 2017.

[42] L. Diaz-Alvarez and E. Ortega, "The many roles of galectin-3, a multifaceted molecule, in innate immune responses against pathogens," *Mediators of Inflammation*, vol. 2017, Article ID 9247574, 10 pages, 2017.

[43] R. Y. Yang, D. K. Hsu, and F. T. Liu, "Expression of galectin-3 modulates T-cell growth and apoptosis," *Proceedings of the National Academy of Sciences of the United States of America*, vol. 93, no. 13, pp. 6737–6742, 1996.

[44] M. Sioud, A. Mobergslien, A. Boudabous, and Y. Floisand, "Evidence for the involvement of galectin-3 in mesenchymal

stem cell suppression of allogeneic T-cell proliferation," *Scandinavian Journal of Immunology*, vol. 71, no. 4, pp. 267–274, 2010.

[45] S. Sciacchitano, L. Lavra, A. Morgante et al., "Galectin-3: one molecule for an alphabet of diseases, from A to Z," *International Journal of Molecular Sciences*, vol. 19, no. 2, p. 379, 2018.

[46] P. Pesheva, S. Kuklinski, B. Schmitz, and R. Probstmeier, "Galectin-3 promotes neural cell adhesion and neurite growth," *Journal of Neuroscience Research*, vol. 54, no. 5, pp. 639–654, 1998.

[47] A. Agis-Torres, M. Sollhuber, M. Fernandez, and J. M. Sanchez-Montero, "Multi-Target-Directed Ligands and other Therapeutic Strategies in the Search of a Real Solution for Alzheimer's Disease," *Current Neuropharmacology*, vol. 12, no. 1, pp. 2–36, 2014.

[48] W. P. Flavin, L. Bousset, Z. C. Green et al., "Endocytic vesicle rupture is a conserved mechanism of cellular invasion by amyloid proteins," *Acta Neuropathologica*, vol. 134, no. 4, pp. 629–653, 2017.

[49] B. Falcon, J. Noad, H. McMahon, F. Randow, and M. Goedert, "Galectin-8-mediated selective autophagy protects against seeded tau aggregation," *The Journal of Biological Chemistry*, vol. 293, no. 7, pp. 2438–2451, 2018.

[50] C. C. Tao, K. M. Cheng, Y. L. Ma et al., "Galectin-3 promotes Aβ oligomerization and Aβ toxicity in a mouse model of Alzheimer's disease," *Cell Death and Differentiation*, vol. 27, no. 1, pp. 192–209, 2020.

[51] A. Boza-Serrano, R. Ruiz, R. Sanchez-Varo et al., "Galectin-3, a novel endogenous TREM2 ligand, detrimentally regulates inflammatory response in Alzheimer's disease," *Acta Neuropathologica*, vol. 138, no. 2, pp. 251–273, 2019.

[52] I. Ferrer, T. Gomez-Isla, B. Puig et al., "Current advances on different kinases involved in tau phosphorylation, and implications in Alzheimer's disease and tauopathies," *Current Alzheimer Research*, vol. 2, no. 1, pp. 3–18, 2005.

[53] H. C. Lee, J. N. Tsai, P. Y. Liao et al., "Glycogen synthase kinase 3α and 3β have distinct functions during cardiogenesis of zebrafish embryo," *BMC Developmental Biology*, vol. 7, no. 1, p. 93, 2007.

[54] M. Llorens-Martin, J. Jurado, F. Hernandez, and J. Avila, "GSK-3beta, a pivotal kinase in Alzheimer disease," *Frontiers in Molecular Neuroscience*, vol. 7, p. 46, 2014.

[55] A. Krishnankutty, T. Kimura, T. Saito et al., "*In vivo* regulation of glycogen synthase kinase 3 β activity in neurons and brains," *Scientific Reports*, vol. 7, no. 1, p. 8602, 2017, 8602.

[56] V. Duka, J. H. Lee, J. Credle et al., "Identification of the sites of tau hyperphosphorylation and activation of tau kinases in synucleinopathies and Alzheimer's diseases," *PLoS One*, vol. 8, no. 9, article e75025, 2013.

[57] K. P. Giese, "GSK-3: a key player in neurodegeneration and memory," *IUBMB Life*, vol. 61, no. 5, pp. 516–521, 2009.

[58] T. J. Singh, T. Zaidi, I. Grundke-Iqbal, and K. Iqbal, "Modulation of GSK-3-catalyzed phosphorylation of microtubule-associated protein tau by non-proline-dependent protein kinases," *FEBS Letters*, vol. 358, no. 1, pp. 4–8, 1995.

[59] D. P. Hanger, K. Hughes, J. R. Woodgett, J. P. Brion, and B. H. Anderton, "Glycogen synthase kinase-3 induces Alzheimer's disease-like phosphorylation of tau: generation of paired helical filament epitopes and neuronal localisation of the kinase," *Neuroscience Letters*, vol. 147, no. 1, pp. 58–62, 1992.

[60] A. Noel, L. Barrier, and S. Ingrand, "The Tyr216 phosphorylated form of GSK3β contributes to tau phosphorylation at PHF-1 epitope in response to Aβ in the nucleus of SH-SY5Y cells," *Life Sciences*, vol. 158, pp. 14–21, 2016.

[61] D. P. Hanger and W. Noble, "Functional implications of glycogen synthase kinase-3-mediated tau phosphorylation," *International Journal of Alzheimer's Disease*, vol. 2011, article 352805, 11 pages, 2011.

[62] V. Shukla, Y. L. Zheng, S. K. Mishra et al., "A truncated peptide from p35, a Cdk5 activator, prevents Alzheimer's disease phenotypes in model mice," *The FASEB Journal*, vol. 27, no. 1, pp. 174–186, 2012.

[63] M. A. Kurt, D. C. Davies, M. Kidd, K. Duff, and D. R. Howlett, "Hyperphosphorylated tau and paired helical filament-like structures in the brains of mice carrying mutant amyloid precursor protein and mutant presenilin-1 transgenes," *Neurobiology of Disease*, vol. 14, no. 1, pp. 89–97, 2003.

[64] A. Ferrari, F. Hoerndli, T. Baechi, R. M. Nitsch, and J. Götz, "β-Amyloid induces paired helical filament-like tau filaments in tissue culture," *The Journal of Biological Chemistry*, vol. 278, no. 41, pp. 40162–40168, 2003.

[65] F. G. De Felice, D. Wu, M. P. Lambert et al., "Alzheimer's disease-type neuronal tau hyperphosphorylation induced by Aβ oligomers," *Neurobiology of Aging*, vol. 29, no. 9, pp. 1334–1347, 2008.

[66] B. Ahmad and L. J. Lapidus, "Curcumin prevents aggregation in α-synuclein by increasing reconfiguration rate," *The Journal of Biological Chemistry*, vol. 287, no. 12, pp. 9193–9199, 2012.

Hindawi
Stem Cells International
Volume 2020, Article ID 9529465, 17 pages
https://doi.org/10.1155/2020/9529465

Review Article

Large-Scale Expansion of Human Mesenchymal Stem Cells

Muhammad Najib Fathi Bin Hassan,[1] Muhammad Dain Yazid,[1] Mohd Heikal Mohd Yunus,[2] Shiplu Roy Chowdhury,[1] Yogeswaran Lokanathan,[1] Ruszymah Bt Hj Idrus,[1,2] Angela Min Hwei Ng,[1] and Jia Xian Law[1]

[1]*Tissue Engineering Centre, Faculty of Medicine, Universiti Kebangsaan Malaysia Medical Centre, Jalan Yaacob Latif, 56000 Kuala Lumpur, Malaysia*
[2]*Department of Physiology, Faculty of Medicine, Universiti Kebangsaan Malaysia Medical Centre, 56000 Kuala Lumpur, Malaysia*

Correspondence should be addressed to Jia Xian Law; lawjx@ppukm.ukm.edu.my

Received 15 March 2020; Revised 7 June 2020; Accepted 1 July 2020; Published 15 July 2020

Academic Editor: Jane Ru Choi

Mesenchymal stem cells (MSCs) are multipotent stem cells with strong immunosuppressive property that renders them an attractive source of cells for cell therapy. MSCs have been studied in multiple clinical trials to treat liver diseases, peripheral nerve damage, graft-versus-host disease, autoimmune diseases, diabetes mellitus, and cardiovascular damage. Millions to hundred millions of MSCs are required per patient depending on the disease, route of administration, frequency of administration, and patient body weight. Multiple large-scale cell expansion strategies have been described in the literature to fetch the cell quantity required for the therapy. In this review, bioprocessing strategies for large-scale expansion of MSCs were systematically reviewed and discussed. The literature search in Medline and Scopus databases identified 26 articles that met the inclusion criteria and were included in this review. These articles described the large-scale expansion of 7 different sources of MSCs using 4 different bioprocessing strategies, i.e., bioreactor, spinner flask, roller bottle, and multilayered flask. The bioreactor, spinner flask, and multilayered flask were more commonly used to upscale the MSCs compared to the roller bottle. Generally, a higher expansion ratio was achieved with the bioreactor and multilayered flask. Importantly, regardless of the bioprocessing strategies, the expanded MSCs were able to maintain its phenotype and potency. In summary, the bioreactor, spinner flask, roller bottle, and multilayered flask can be used for large-scale expansion of MSCs without compromising the cell quality.

1. Introduction

Mesenchymal stem cells (MSCs) are multipotent stem cells which can be isolated from various tissue sources such as bone marrow [1], adipose tissue [2], and umbilical cord [3]. MCSs are able to self-renew and can be induced to differentiate into adipocytes, chondrocytes, osteocytes, hepatocytes, tenocytes, and cardiomyocytes [2, 4, 5]. MSCs can modulate the immunoreactivity through mechanisms such as suppression of T-cells and lymphocyte proliferation [6, 7]. In addition, MSCs also possess antioxidative, antiapoptotic, antifibrosis, and proangiogenesis properties [8]. Thus, MSCs have remarkable clinical potential especially in immune modulation and tissue regeneration. In fact, MSCs have been evaluated in many clinical trials for the treatment of immune-mediated diseases and tissue injuries. Diseases that have been treated with MSCs include liver diseases, peripheral nerve damage, graft-versus-host-disease, autoimmune diseases, diabetes mellitus, and heart diseases [9, 10].

A crucial limitation in therapeutic application of MSCs is the low amount of MSCs in all tissues and the quantity of isolated MSCs being insufficient for clinical use. A dosage of 2×10^6 cells/kg body weight is commonly given to the patients [6, 7]. For certain patients and diseases, multiple administrations of MSCs up to several hundred million cells are needed to achieve the desired therapeutic effect [11, 12].

MSCs can be expanded *in vitro* using a cell culture plate and flask to obtain the sufficient cell number needed for

experimental purposes. However, a similar strategy is not ideal for expansion of MSCs meant for clinical use as the cell number needed is much higher. More manpower and incubator space are needed when performing large-scale cell expansion using a cell culture flask. Apart from being ineffective, large-scale expansion using a cell culture flask also affects the cell quality as MSCs expanded *in vitro* for a long period of time may lose their stem cell characteristics [13]. Previous studies also reported that MSC proliferation and differentiation potential decreased when they reached a higher passage number [14]. Thus, identification of an effective large-scale expansion technique is very important to obtain the huge number of cells in a short period of time and in a cost-effective manner without compromising the cell quality.

In this review, we identified the articles reporting the large-scale expansion of MSCs via systematic literature search. A total of 4 bioprocessing strategies, i.e., bioreactor, spinner flask, roller bottle, and multilayered flask, were found to be used for large-scale expansion of MSCs, and all data reported in these articles were extracted, analyzed, and discussed.

2. Methods

2.1. Search Strategy. A systematic literature search was carried out to identify suitable articles reporting large-scale expansion of human MSCs *in vitro*. Literature search was performed using keywords, (1) human AND (2) mesenchymal stem cells OR mesenchymal stromal cells OR MSCs AND (3) large-scale OR scale-up, in a sentence of ((*human*) *AND* ((*mesenchymal AND stem AND cells*) *OR* (*mesenchymal AND stromal AND cells*) *OR* (*MSCs*)) *AND* ((*large AND scale AND expansion*) *OR* (*up AND scaling*))) in the Medline and Scopus databases. Next, only the literature articles reported in English language were selected. The articles must also meet the inclusion and exclusion criteria to be included in this study.

The first inclusion criterion is that the articles are working on human MSCs. Secondly, the articles described the large-scale expansion of human MSCs. Thirdly, the articles provide detailed information on the expansion process, including the source of MSCs, cell seeding density, expansion method, medium composition, culture period, and total cell yield. Lastly, the articles characterized the expanded cells in accordance with the minimal criteria established by the International Society for Cellular Therapy (ISCT). Review articles and proceedings were excluded. In addition, articles describing the large-scale expansion of MSCs using the standard culture flask, i.e., T-25, T-75, and T-175 flasks, were also excluded.

2.2. Data Extraction. Data were extracted from selected articles by two authors independently. The articles were selected through 3 layers of screening, i.e., title screening, abstract screening, and whole article screening, to exclude articles that did not fulfill the inclusion and exclusion criteria. Data were extracted from articles that provide detailed description of at least one large-scale expansion process. For articles reporting multiple large-scale expansion processes, information of all the described expansion processes was collected.

2.3. Calculation. Efficiency of large-scale expansion was compared by calculating the expansion fold using the following formula:

$$\text{Expansion ratio} = \frac{\text{Total cell yield}}{\text{Total cell seeded}}. \quad (1)$$

Some articles reported the number of cells seeded as the total cell number while others as cell seeding density. For standardization, all data were converted to the total cell number. This is to give an idea on the number of cells needed prior to large-scale expansion as well as to show the total cell yield upon expansion using the specific bioprocessing methods. The total cell number was calculated using the following formula:

$$\text{Total cell number}\,(t) = \rho \times A, \quad (2)$$

where ρ represents cell seeding density or cell yield density and A represents the surface area or working volume of the vessel used for cell expansion.

3. Results

3.1. Literature Search. The literature search identified 361 articles: 144 articles were obtained from the Medline database and 217 articles were obtained from the Scopus database. A total of 130 duplicated articles were removed before screening using the inclusion and exclusion criteria. A total of 129 articles were rejected after the title screening because they were not related to large-scale bioprocessing of human MSCs. For the remaining 102 articles screened for the abstract, only 64 articles were selected for thorough full-text screening. Finally, a total of 26 articles were selected for data extraction (Figure 1).

3.2. Data Extraction. Data from 26 articles published between 2007 and 2019 were extracted and are summarized in Table 1. The articles described the large-scale expansion of MSCs isolated from 7 different tissue sources, i.e., adipose tissue-derived MSCs (AT-MSCs), umbilical cord matrix- or Wharton's jelly-derived MSCs (WJ-MSCs), bone marrow-derived MSCs (BM-MSCs), periosteum-derived MSCs (PD-MSCs), villous chorion-derived MSCs (VC-MSCs), dental pulp-derived MSCs (DP-MSCs), and fetal MSCs (F-MSCs) (Figure 2). A total of 4 bioprocessing strategies have been used, i.e. bioreactor, spinner flask, roller bottle, and multilayered flask (Figure 3). Four articles described the large scale of expansion of MSCs from multiple sources, and 5 articles used more than 1 bioprocessing method. Most of the articles described the large-scale expansion of MSCs from BM (13 articles, 43%), AT (6 articles, 20%), and WJ (6 articles, 20%), with PD-MSCs appearing in 2 articles (7%) and VC-MSCs, DP-MSCs, and F-MSCs appearing in 1 article (3%) each. Large-scale expansion using the bioreactor, spinner flask, multilayered flask, and roller bottle was described in 11 (37%), 11 (37%), 7 (23%), and 1 (3%) articles, respectively.

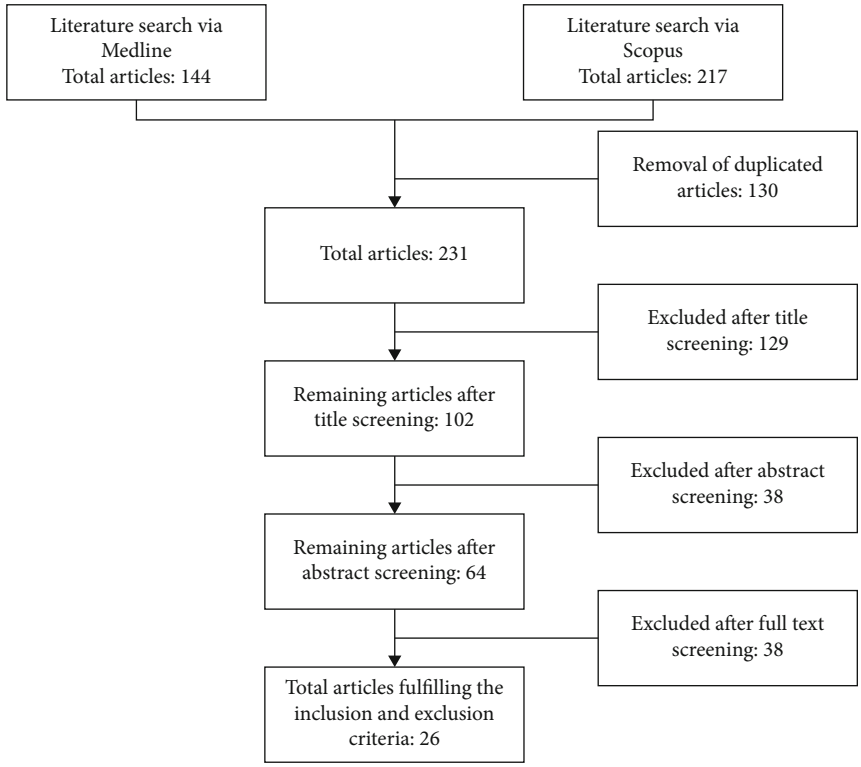

Figure 1: Flow chart of article selection process.

3.3. Culture Medium Selection. A total of 13 studies reported the use of fetal bovine serum (FBS) at 10 or 15% (*v*/*v*) concentration for large-scale expansion of MSCs of which three studies further supplemented the culture medium with basic fibroblast growth factor (bFGF) ranging from 2 to 10 ng/ml [6, 15, 16]. Another three studies compared the large-scale expansion of MSCs using FBS versus human platelet lysate (HPL) and defined medium [17–19]. All three studies reported that FBS was inferior compared to HPL and defined medium in promoting MSC proliferation. Instead of FBS, seven studies used 5%, 8%, or 10% (*v*/*v*) HPL [17, 19–24], one study used 5% (*v*/*v*) Ultragrow™ [25], and another one used 15% (*v*/*v*) AB human serum as supplement [26]. Defined culture mediums, i.e., MesenCult™-XF medium [27–29], StemPro® MSC SFM XenoFree medium [30–33], Corning® stemgro® hMSC medium [29], and PRIME-XV™ SFM medium [18], were used in seven studies (Table 2). Even though different mediums and medium supplements were used, nonetheless, all the studies reported that the expanded cells maintained its phenotype and trilineage differentiation potential. Five studies showed that the expanded MSCs retained its immunomodulatory properties [6, 7, 20, 34, 35].

3.4. Large-Scale Expansion Using Multilayered Flask. A multilayered flask is a specially designed culture flask that consists of multiple layers of a cell culture-treated surface to provide a large surface area for cell growth. The usage of a multilayered flask saves a lot of incubator space compared to T-75 or T-175 flasks as it is more compact. A few types of multilayered flasks, including Hyperflask, CellSTACK (2-chamber and 5-chamber), and Cell Factory (4-chamber), have been tested for the large-scale expansion of MSCs. The surface area of a multilayered flask varies with types. The hyperflask surface area is 1720 cm^2, CellSTACK has a surface area ranging from 1272 cm^2 for 2-chamber to 3180 cm^2 for 5-chamber, and Cell Factory 4-chamber has a surface area of 2528 cm^2. The cell expansion ratio using multilayered flasks has been reported to be between 4.11-fold and 316.25-fold (Table 2). Four studies [22, 23, 26, 36] achieved an expansion ratio below 20-fold, and three studies [6, 17, 37] reported an expansion ratio above 100-fold using a multilayered flask (Figure 4).

3.5. Large-Scale Expansion Using Bioreactor. Many types of bioreactors, including hollow fiber bioreactor (Quantum Cell Expansion System) [19, 38], stirred tank bioreactor (UniVessel® SU bioreactor [28], Mobius® bioreactor [21], Celligen 310 bioreactor [26, 31, 35], Vertical Wheel bioreactor [27], Biostat Qplus bioreactor [27], and BioFlo 110 bioreactor [32]), and multiplate bioreactor (Pall Life Sciences Xpansion Multiplate Bioreactor) [39], have been tested for large-scale expansion of MSCs. Most studies used commercially available bioreactors with capacity ranging from 1.3 l to 50 l except Egger et al. who built their own stirred tank bioreactor for the expansion of AT-MSCs [20]. As the bioreactor capacity increased, the number of cells seeded and total cell yield also increased. Typically, microcarriers, including collagen-coated microcarriers, plastic P102L microcarrier, Cultispher S microcarrier, and Synthemax II microcarrier, were used to provide the culture surface for cells to attach and grow.

Table 1: Summary of the articles describing the large-scale expansion of MSCs.

Reference	Bioprocessing method	Cell source	Cell culture medium	Initial cell seeding	Culture period (days)	Final cell yield	Expansion ratio	Doubling time (h)	MSC characterization	Other key findings
[6]	CellSTACK 2-chamber	WJ-MSCs	DMEM-KO with 10% FBS and 2 ng/ml bFGF	$1.27E+06$	5	$2.48E+08$	195.28	15.77	(i) Positive for CD44, CD73, CD90, CD105, CD146, and CD166 (ii) Negative for CD34, CD45, and HLA-DR (iii) Maintained the trilineage differentiation potential (iv) Maintained the capability to inhibit T-cell proliferation (v) No chromosome abnormality (vi) No hTERT expression (vii) No changes in expression of p53, p21, p16, and c-Myc	(i) Presence of bFGF boosted the cell growth
[17]	CellSTACK 5-chamber	DP-MSCs	DMEM-KO with 10% HPL	$3.18E+06$	11	$4.98E+08$	156.60	36.21	(i) >80% positivity for CD44, CD73, and CD90 (ii) <2% positivity for CD34, CD45, and HLA-DR (iii) Maintained the trilineage differentiation potential (iv) Maintained the expression of stem cell markers, i.e., SOX2, OCT4, and NANOG	(i) Supplementation with HPL gave higher cell yield
			DMEM-KO with 10% FBS			$3.2E+08$	100.63	39.68		
[22]	Cell Factory 4-chamber	BM-MSCs	αMEM with 10% HPL and 2 IU/ml heparin	$1.9E+08$ (BM-MNCs)	13.5	$7.8E+08$	4.11	159.02	(i) >95% positivity for CD73, CD90, and CD105 (ii) <2% positivity for HLA-DR, CD14, CD19, CD34, and CD45 (iii) Maintained the trilineage differentiation potential	
[23]	CellSTACK 2-chamber	BM-MSCs	αMEM supplemented with 8% HPL and 1 IU/ml heparin	$5.09E+06$	7	$5.28E+07$	10.37	49.79	(i) >95% positivity for CD73, CD90, CD105, and HLA-ABC (ii) <1% positivity for CD3, CD34, and CD45 (iii) Maintained the trilineage differentiation potential	(i) Yield decreased for MSCs cultured with 10% HPL for 7 days likely due to cell detachment caused by culture over confluence
			αMEM supplemented with 8% HPL and 1 IU/ml heparin		5	$4.69E+07$	9.22	37.44		

Table 1: Continued.

Reference	Bioprocessing method	Cell source	Cell culture medium	Initial cell seeding	Culture period (days)	Final cell yield	Expansion ratio	Doubling time (h)	MSC characterization	Other key findings
			αMEM supplemented with 10% HPL and 1 IU/ml heparin		7	$3.64E+07$	7.15	59.21		
			αMEM supplemented with 10% HPL and 1 IU/ml heparin		5	$5.65E+07$	11.10	34.56		
[36]	Hyperflask	VC-MSCs	DMEM/F-12 with 10% FBS and 3 ng/ml bFGF	$5.16E+06$	4	$7.4E+07$	14.26	23.75	(i) >95% positivity for CD73, CD90, and CD105 (ii) <1% positivity for CD34, CD45, CD79, and HLA-DR (iii) Maintained the trilineage differentiation potential (iv) Normal karyotype	
[37]	Cell Factory 4-chamber	BM-MSCs	αMEM with 10% FBS	$0.8E+06$	15	$2.5E+08$	316.25	49.80	(i) Maintained the trilineage differentiation potential	
[7]	Spinner flask+Cytodex 3 microcarrier	BM-MSCs	αMEM with 15% FBS	$6.25E+06$	7	$2.41E+07$	3.86	86.28	(i) >90% positivity for CD73, CD90, and CD105 (ii) Maintained the trilineage differentiation potential (iii) No chromosome abnormality (iv) Maintained the capability to inhibit lymphocyte proliferation	
[16]	Spinning bottle + CultiSpher-G microcarrier	WJ-MSCs	MEM/F12 with 10% FBS and 10 ng/ml bFGF	$5E+06$	6	$1.3E+07$	2.60	104.46	(i) >95% positivity for CD44, CD73, CD90, and CD105 (ii) Low expression of CD31 and CD45 (iii) No chromosomal abnormality (iv) Maintained the trilineage differentiation potential (v) High expression of embryonic markers (OCT4, SOX2, NANOG, and C-MYC)	(i) The cells expanded with spinner flask were more efficient in promoting *in vivo* wound healing compared to those expanded with culture flask

Table 1: Continued.

Reference	Bioprocessing method	Cell source	Cell culture medium	Initial cell seeding	Culture period (days)	Final cell yield	Expansion ratio	Doubling time (h)	MSC characterization	Other key findings
[18]	Spinner flask+plastic microcarrier	BM-MSCs	DMEM with 10% FBS	$3E+06$	6	$8.58E+06$	2.86	94.99	(i) >99% positivity for CD73, CD90, and CD105 (ii) <1% positivity for HLA-DR (iii) Maintained the trilineage differentiation potential	(i) Serum-free medium enhanced cell growth
	Spinner flask+plastic microcarrier coated with fibronectin		PRIME-XV™ SFM			$3.01E+07$	10.03	43.29		
[24]	Spinner flask+ Cultispher S microcarrier	PD-MSCs	DMEM-HG with 10% FBS	$2.0E+06$	10	$5.4E+06$	2.7	167.5	(i) Simultaneous expression of CD73, CD90, and CD105 in 89% of MSCs cultured with FBS and 86% in those cultured with HPL (ii) Low expression of negative markers for both mediums (iii) Sox9, ALP, BMP2, and WNT5A were upregulated in MSCs cultured with HPL compared to those cultured with FBS (iv) *In vivo* study showed that MSCs cultured with HPL formed more matured mineralization tissue compared to those cultured with FBS which form fibrous tissue	(i) Shear stress affected expression of percentage of positive surface marker (ii) MSCs cultured with HPL are more potent in bone formation *in vivo*
			DMEM-HG with 10% HPL	$2.0E+06$	10	$10.4E+06$	5.2	100.9		
[25]	Spinner flask+plastic microcarrier	WJ-MSCs	DMEM-LG with 5% UltraGRO™ and 2 IU/ml heparin	$4E+06$	5.5	$2.8E+07$	7.00	47.02	(i) >95% positivity for CD73, CD90, and CD105 (ii) Maintained the trilineage differentiation potential	
[29]	Spinner flask+ Corning Synthemax II microcarrier	BM-MSCs	Mesencult™-XF	$7.5E+05$	7	$3.75E+06$	5.00	72.35	(i) >95% positivity for CD73 and CD105 (ii) <1% positivity for CD14 and CD45 (iii) Normal karyotype (iv) Maintained the trilineage differentiation potential	(i) Culture with Stemgro hMSC gave higher cell yield and expansion ratio and lower population doubling time
			Stemgro hMSC			$5.25E+06$	7.00	59.84		

Table 1: Continued.

Reference	Bioprocessing method	Cell source	Cell culture medium	Initial cell seeding	Culture period (days)	Final cell yield	Expansion ratio	Doubling time (h)	MSC characterization	Other key findings
[30]	Spinner flask+ microcarrier	BM-MSCs	StemPro MSC SFM Xenofree	4E + 06	8	2.88E + 07	7.20	67.42	(i) Cells expressed high level of CD105, CD73, and CD90 and lower level of CD31, CD80, and HLA-DR (ii) Maintained the trilineage differentiation potential	
		AT-MSCs		1.5E + 06		1.52E + 07	10.13	57.80		
[31]	Spinner flask+ Cultispher® S microcarrier coated with CELLstart CTS solution	WJ-MSCs	StemPro MSC SFM XenoFree	4E + 06	5	1.92E + 07	4.80	53.03	(i) Maintain expression of CD90 and CD73 postexpansion (ii) Expression of CD105 decreased postexpansion, probably due to cell damage by shear stress (iii) Low expression of CD31, CD80, and HLA-DR (iv) Maintained the trilineage differentiation potential (v) Maintained the capability to inhibit lymphocyte proliferation	(i) Cells cultured with bioreactor have higher expansion ratio compared to those expanded using the spinner flask
	2.5 l Celligen 310 bioreactor + Cultispher® S microcarrier coated with CELLstart CTS solution			2E + 07	4	1.12E + 08	5.60	38.63		
[33]	Spinner flask+plastic microcarrier coated with CELLstart CTS solution	BM-MSCs	StemPro MSC SFM XenoFree	4E + 06	14	1.6E + 07	4.00	168.00	(i) >95% positivity for CD73 and CD105 (ii) <2% positivity for CD31, CD80, and HLA-DR (iii) 92% and 82% CD90 positivity for BM-MSCs and AT-MSCs, respectively, likely due to damage to the cells caused by longer enzymatic cell detachment process or shear stress (iv) Maintained the trilineage differentiation potential	
		AT-MSCs				1.12E + 07	2.80	226.20		
[56]	Spinner flask+Cytodex 3 microcarrier	F-MSCs	αMEM with 10% FBS	9.6E + 06	7	8.5E + 07	8.85	53.40	(i) >95% positivity for CD73, CD90, and CD105 (ii) <1% positivity for CD34	(i) Cells cultured with spinner flask have better osteogenic differentiation potential compared to those cultured in culture flask

Table 1: Continued.

Reference	Bioprocessing method	Cell source	Cell culture medium	Initial cell seeding	Culture period (days)	Final cell yield	Expansion ratio	Doubling time (h)	MSC characterization	Other key findings
[19]	Quantum Cell Expansion System	AT-MSCs	αMEM with 10% FBS	$2.1E+07$	21	$1.19E+08$	5.67	201.4	(i) >95% positivity for CD90, CD73, CD105, CD13, CD166, and CD29 (ii) <5% positivity for CD45, CD19, CD31, and HLA-DR (iii) No genomic instability (iv) Maintained the trilineage differentiation potential	(i) HPL is superior compared to FBS (ii) 1.66-fold to 8.15-fold of AT-MSCs was harvested from SVF seeded at P0
			αMEM with 5% heparin-free HPL		6	$6.05E+08$	28.81	29.70		
[20]	Stirred tank reactor	AT-MSCs	αMEM with 10% HPL and 1 IU/ml heparin in 21% O_2	$1.3E+07$	6	$2.4E+07$	1.85	162.80	(i) Positive for CD73, CD90, and CD105 (ii) Negative for CD14, CD20, CD35, CD45, and HLA-DR (iii) Maintained the trilineage differentiation potential	(i) Hypoxic cells displayed slightly poorer osteogenic differentiation potential and slightly better adipogenic and chondrogenic differentiation potential
			αMEM with 10% HPL and 1 IU/ml heparin in 5% O_2			$2.9E+07$	2.23	124.40		
[21]	Mobius® 50 l bioreactor+ collagen-coated microcarrier	BM-MSCs	αMEM supplemented with 5% HPL and 2 IU/ml heparin	$3E+08$	11	$1.28E+10$	42.67	48.75	(i) >95% positivity for CD105, CD90, CD73, and CD44 (ii) <5% positivity for CD19, CD34, CD 11b, CD79a, CD45, and CD14 (iii) Low expression of HLA-DR (iv) Maintained the trilineage differentiation potential (v) Maintained the immunosuppressive properties	
[27]	Vertical Wheel bioreactor+ Synthemax II microcarrier	BM-MSCs	MesenCult-XF with 0.025% (v/v) antifoam C emulsion	$5.5E+07$	14	$6.6E+08$	12.00	93.72	(i) Positive for CD44, CD73, CD90, CD105, and CD166 (ii) Negative for CD34 and CD45 (iii) Low expression of HLA-DR (iv) Maintained the trilineage differentiation potential	(i) Cells cultured with Vertical Wheel bioreactor have significantly lower expression of HLA-DR compared to those cultured with Biostat Qplus bioreactor
	Biostat Qplus bioreactor+ Synthemax II microcarrier			$6.25E+06$		$6.88E+07$	11.00	97.10		

Table 1: Continued.

Reference	Bioprocessing method	Cell source	Cell culture medium	Initial cell seeding	Culture period (days)	Final cell yield	Expansion ratio	Doubling time (h)	MSC characterization	Other key findings
[28]	2 l UniVessel® SU bioreactor+ Synthemax® II microcarrier	BM-MSCs	Mesencult™-XF	2.5E + 07	7	4.22E + 08	16.88	41.20	(i) >95% positivity for CD44, CD73, and CD90 (ii) <5% positivity for CD45, CD34, CD14, CD19, and CD11b (iii) Positivity of CD105 was 88% and 92%, respectively, for BM-MSCs and AT-MSCs (iv) Maintained the trilineage differentiation potential	
		AT-MSCs				5.06E + 08	20.24	38.72		
[32]	1.3 l BioFlo 110 bioreactor+ plastic microcarrier coated with CELLstart CTS solution	BM-MSCs	StemPro MSC SFM XenoFree	5E + 05	7	1.1E + 08	22.00	21.59	(i) >90% positivity for CD73 (ii) Expression of CD90 and CD105 decreased to 74% and 39%, respectively, for BM-MSCs (iii) Expression of CD90 dropped to 64% (from graph) for AT-MSCs (iv) <2% positivity for CD31, CD80, and HLA-DR	
		AT-MSCs				4.5E + 07	9.00	25.88		
[35]	2.5 l Celligen 310 bioreactor + Fibra-Cel® disk	BM-MSCs	αMEM with 10% FBS	1.0E + 07	9	9.2E + 07	9.20	67.47	(i) >90% positivity for CD44, CD90, and CD105 (ii) Maintained the trilineage differentiation potential	
[38]	Quantum Cell Expansion System bioreactor	WJ-MSCs	F12K: DMEM-LG (1 : 1) with 10% FBS	2.1E + 07	7	4.0E + 08	19	39.5	(i) >99% positivity for CD44, CD73, CD90, and CD105 (ii) <1% positivity for CD45, CD34, CD11b, CD19, and HLA-DR (iii) MSCs maintained the trilineage differentiation potential (iv) Maintained the capability to inhibit lymphocyte proliferation (v) No alteration in karyotype	(i) There was no difference in cell proliferation and growth properties between MSCs cultured in flask and bioreactor

Table 1: Continued.

Reference	Bioprocessing method	Cell source	Cell culture medium	Initial cell seeding	Culture period (days)	Final cell yield	Expansion ratio	Doubling time (h)	MSC characterization	Other key findings
[39]	Pall Life Sciences Xpansion Multiplate Bioreactor	PD-MSCs	DMEM-HG with 10% FBS	$1.6E+08$	7	$5.35E+08$	3.34	96.47	(i) >90% positivity for CD73, CD90, and CD105 (ii) <5% positivity for CD45, CD20, CD14, and CD34 (iii) Maintained the trilineage differentiation potential	(i) 55% cell lost during the downstream process
[26]	HYPERFlasks®	WJ-MSCs	αMEM with 15% AB human serum	$3.44E+06$	11	$4.47E+07$	12.99	71.36	(i) Positive for CD73, CD90, and CD105 (ii) Negative for CD12, CD31, CD34, CD45, and HLA-DR (iii) Cells cultured with HYPERFlasks® showed reduction in CD73 expression (iv) Cells cultured with bioreactor showed reduction in CD105 expression, likely due to cell damage by shear stress (v) Maintained the trilineage differentiation potential (vi) Maintained the chromosome stability (vii) Maintained the immunosuppressive properties	
	Roller bottle			$4.25E+06$	6	$2.97E+07$	7.01	68.45		
	Spinner flask+plastic microcarrier			$2E+06$	8	$4.2E+07$	21.00	32.78		
	2.5 l Celligen 310 bioreactor+ plastic microcarrier			$8E+06$	7	$7.92E+07$	9.90	50.79		

MSCs: mesenchymal stem cells; BM-MSCs: bone marrow-derived MSCs: BMNCs: bone marrow mononuclear cells; WJ-MSCs: Wharton's jelly-derived MSCs; AT-MSCs: adipose tissue-derived MSCs; PD-MSCs: periosteum-derived MSCs; VC-MSCs: villous chorion-derived MSCs; DP-MSCs: dental pulp-derived MSCs; F-MSCs: fetal MSCs; HPL: human platelet lysate: FBS: fetal bovine serum; bFGF: basic fibroblast growth factor.

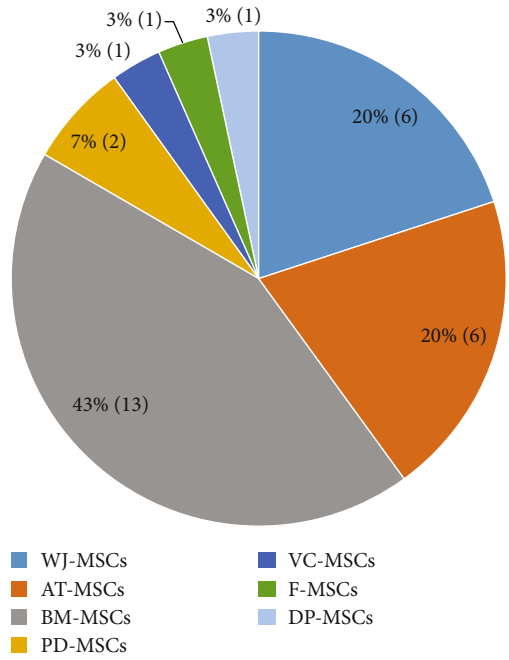

Figure 2: Frequency of the mesenchymal stem cell (MSC) sources in the selected articles. Most of the studies expanded the MSCs derived from bone marrow, adipose tissue, and Wharton's jelly. BM: bone marrow; AT: adipose tissue; WJ: Wharton's jelly; PD: periosteum; VC: villous chorion; F: fetal; DP: dental pulp.

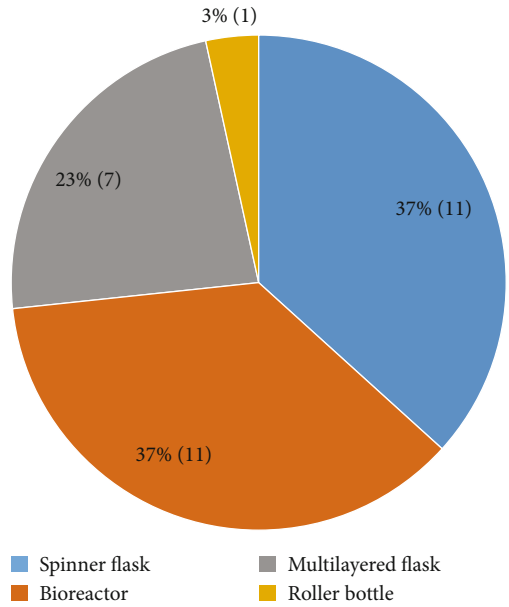

Figure 3: Frequency of the bioprocessing strategies used in the selected studies. Most of the studies used bioreactor, spinner flask, and multilayered flask for large-scale expansion of MSCs.

The cell expansion ratio was reported to be between 1.85-fold and 42.67-fold depending on the bioreactor and culture protocol used.

3.6. Large-Scale Expansion Using Spinner Flask. Several types of spinner flasks, including the Bellco spinner flask [18, 24, 25, 30, 31, 33], Techne spinner flask [7, 26], Corning spinner flask [29], and Cellspin spinning bottle [16] with capacity ranging from 100 ml to 125 ml, have been used for large-scale expansion of MSCs. Microcarriers were used to provide the growth surface for cell proliferation. Different types of microcarriers, i.e., plastic P102L microcarrier, Cultispher S microcarrier, Cytodex 3 microcarrier, and Synthemax II microcarrier, were used in these studies. The cell expansion ratio has been reported to be between 2.60-fold and 21.00-fold.

3.7. Large-Scale Expansion Using Roller Bottle. A roller bottle is a cylindrical vessel that requires a roller track to gently rotate them. Only one study reported the use of roller bottles for MSC large-scale expansion. Tozetti et al. seeded 4.25×10^6 MSCs in a 2125 cm^2 roller bottle containing 200 ml of culture medium for 6 days to yield 2.98×10^7 cells, achieving an expansion ratio of 7.01-fold [26].

4. Discussion

MSCs have great therapeutic potential and have been tested in many clinical trials. It is very important to produce MSCs in a large scale to meet clinical demands. One of the most crucial aspects to achieve this is the selection of a culture medium to support rapid MSC expansion without compromising its therapeutic potential. From the literature search, we found that FBS, HPL, and defined medium are frequently used for MSC expansion. FBS helps in cell adhesion by providing the cell attachment factors and is rich in growth factors that stimulate cell growth [40, 41]. However, there are concerns about its safety as MSCs cultured with FBS may trigger immunoreaction in recipients because of the transfer of animal protein and animal pathogen [14]. In addition, FBS has high batch-to-batch variation which leads to inconsistency in cell expansion [42]. These drawbacks indicated that the use of FBS should be avoided if possible. Human serum and defined medium are alternatives for FBS for large-scale expansion of MSCs. The main disadvantage of human serum and defined medium is the cost. In addition, human serum has batch-to-batch variation, and most of the defined medium require an extra culture surface coating step to improve cell attachment. Nonetheless, data extracted from the studies showed that MSCs were able to maintain its phenotype and trilineage differentiation potential as well as the immunomodulatory properties regardless of the culture medium, bioprocessing strategies, and serum supplement used, fulfilling the minimum criteria proposed by the ISCT [43].

Govindasamy et al. and Haack-Sørensen et al. compared the large-scale expansion of MSCs using FBS and HPL [17, 19]. Data from these studies showed that HPL significantly increased the cell yield and shortened the population doubling time compared to FBS without compromising the cell viability or altering their phenotype and trilineage differentiation potential. Similar results were reported in the study by Picken et al. that compared FBS with defined medium [18]. Melkoumian et al. compared 2 defined mediums, i.e., Mesencult™-XF medium and Corning® stemgro® hMSC

Table 2: A summary of the expansion ratio achieved with different medium/serum supplement and bioprocessing strategies.

Medium/serum	Bioprocessing method (working volume)		Initial cell seeding	Final cell yield	Expansion ratio	Doubling time (h)	Reference
FBS	Multilayered flask	Hyperflask	$5.16E+06$	$7.36E+07$	14.26	23.75	[36]
		CellSTACK 5-chamber	$3.18E+06$	$3.20E+08$	100.63	39.68	[17]
		CellSTACK 2-chamber	$1.27E+06$	$2.48E+08$	195.28	15.77	[6]
		Cell Factory 4-chamber	$8.00E+05$	$2.53E+08$	316.25	49.80	[37]
	Spinner flask	Spinner flask (100 ml)	$3.00E+06$	$8.58E+06$	2.86	94.99	[18]
		Spinner flask (100 ml)	$9.60E+06$	$8.50E+07$	8.85	53.40	[56]
		Spinner flask (80 ml)	$2.00E+06$	$5.40E+06$	2.70	167.50	[24]
		Spinner flask (50 ml)	$6.25E+06$	$2.41E+07$	3.86	86.28	[7]
		Spinning bottle	$5.00E+06$	$1.30E+07$	2.60	104.46	[16]
	Bioreactor	Quantum Cell Expansion System	$2.10E+07$	$1.19E+08$	5.67	201.40	[19]
		Quantum Cell Expansion System	$2.10E+07$	$4.00E+08$	19.00	39.50	[38]
		Pall Life Sciences Xpansion Multiplate Bioreactor	$1.60E+08$	$5.35E+08$	3.34	96.47	[39]
		Fibrous bed bioreactor (1.75 l)	$1.00E+07$	$9.20E+07$	9.20	67.47	[35]
Human serum/human platelet lysate	Multilayered flask	Hyperflasks	$3.44E+06$	$4.47E+07$	12.99	71.36	[26]
		CellSTACK 2-chamber	$5.09E+06$	$5.28E+07$	10.37	49.79	[23]
		CellSTACK 2-chamber	$5.09E+06$	$4.69E+07$	9.22	37.44	[23]
		CellSTACK 2-chamber	$5.09E+06$	$3.64E+07$	7.15	59.21	[23]
		CellSTACK 2-chamber	$5.09E+06$	$5.65E+07$	11.10	34.56	[23]
		CellSTACK 5-chamber	$3.18E+06$	$4.98E+08$	156.60	36.21	[17]
		Cell Factory 4-chamber	$1.90E+08$	$7.80E+08$	4.11	159.02	[22]
	Spinner flask	Spinner flask (80 ml)	$4.00E+06$	$2.80E+07$	7.00	47.02	[25]
		Spinner flask (80 ml)	$2.00E+06$	$10.40E+06$	5.20	100.90	[24]
		Spinner flask (100 ml)	$2.00E+06$	$4.20E+07$	21.00	32.78	[26]
	Roller bottle	Roller bottle	$4.25E+06$	$2.98E+07$	7.01	68.45	[26]
	Bioreactor	Quantum Cell Expansion System	$2.10E+07$	$6.05E+08$	28.81	29.70	[19]
		Continuously stirred tank reactor (130 ml)	$1.30E+07$	$2.40E+07$	1.85	162.80	[20]
		Continuously stirred tank reactor (130 ml)	$1.30E+07$	$2.90E+07$	2.23	124.40	[20]
		Mobius® 50 l single-use bioreactor	$3.00E+08$	$1.28E+10$	42.67	48.75	[21]
		Stirred tank bioreactor (800 ml)	$8.00E+06$	$7.92E+07$	9.90	50.79	[26]
Defined medium	Spinner flask	Spinner flask (80 ml)	$4.00E+06$	$1.92E+07$	4.80	53.03	[31]
		Spinner flask (80 ml)	$4.00E+06$	$2.88E+07$	7.20	67.42	[30]
		Spinner flask (80 ml)	$1.50E+06$	$1.52E+07$	10.13	57.80	[30]
		Spinner flask (100 ml)	$3.00E+06$	$3.01E+07$	10.03	43.29	[18]
		Spinner flask (35 ml)	$7.50E+05$	$3.75E+06$	5.00	72.35	[29]
		Spinner flask (35 ml)	$7.50E+05$	$5.25E+06$	7.00	59.84	[29]
		Spinner flask (80 ml)	$4.00E+06$	$1.60E+07$	4.00	168.00	[33]
		Spinner flask (80 ml)	$4.00E+06$	$1.12E+07$	2.80	226.20	[33]

Table 2: Continued.

Medium/serum	Bioprocessing method (working volume)	Initial cell seeding	Final cell yield	Expansion ratio	Doubling time (h)	Reference
	2 l Univessel® SU bioreactor (2 l)	$2.50E+07$	$4.22E+08$	16.88	41.20	[28]
	2 l Univessel® SU bioreactor (2 l)	$2.50E+07$	$5.06E+08$	20.24	38.72	[28]
	Stirred tank bioreactor (800 ml)	$2.00E+07$	$1.12E+08$	5.60	38.63	[31]
Bioreactor	Vertical Wheel bioreactor (2.2 l)	$5.50E+07$	$6.60E+08$	12.00	93.72	[27]
	Stirred tank bioreator (200 ml)	$6.25E+06$	$6.88E+07$	11.00	97.10	[27]
	1 l bioreactor (1 l)	$5.00E+06$	$1.10E+08$	22.00	21.59	[32]
	1 l bioreactor (1 l)	$5.00E+06$	$4.50E+07$	9.00	25.88	[32]

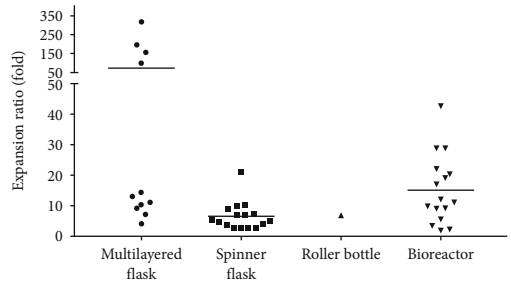

Figure 4: Expansion ratios achieved using different bioprocessing strategies. Multilayered flask and bioreactor can achieve higher expansion ratio compared to spinner flask and roller bottle.

medium [29]. The authors found that the Corning® stemgro® hMSC medium gave higher fold of cell expansion compared to Mesencult™-XF medium. None of the large-scale expansion studies compared HPL and defined medium. However, using a small-scale culture system, Riis et al. found that HPL gave the highest cell yield, followed by FBS, while the StemPro® MSC SFM XenoFree medium failed to maintain AT-MSC expansion beyond passage 5 [44]. Similarly, Oikonomopoulos et al. reported that expansion with HPL resulted in the highest cell proliferation, followed by StemPro® MSC SFM XenoFree medium and FBS [45]. Surprisingly, the authors observed that HPL failed to maintain BM-MSC and AT-MSC immunosuppressive properties. However, several previous studies reported contradicting results whereby Menard et al. found that BM-MSCs and AT-MSCs cultured with HPL were able to maintain their immunosuppressive properties compared to BM-MSCs cultured with FBS [46]. Tsai et al. reported that BM-MSCs cultured with HPL supplemented medium were able to maintain the immunosuppressive properties [35]. Thus, HPL is superior compared to FBS and defined medium for large-scale expansion of MSCs as it increases the proliferation of MSCs without compromising the characteristic and plasticity of the cells. Furthermore, the use of HPL also reduces the risk of animal pathogen transmission and animal protein transfer to host. Moreover, HPL is cheaper compared to defined medium that is still very costly right now. In the future, the cost of defined medium might reduce when the demand increases.

There were four bioprocessing strategies used to archive large-scale production of MSCs, i.e., multilayered flask, spinner flask, roller bottle, and bioreactor. Each bioprocessing strategy has its own advantages and disadvantages (Table 3). Generally, a bioreactor allows fully automated cell bioprocessing with higher efficiency. The multilayered flask, spinner flask, and rotating bottle are manual bioprocessing strategies with lower efficiency. Since the spinner flask, roller bottle, and multilayered flask require substantive manual manipulations, more manpower are needed when these culture systems are used. Among the four bioprocessing strategies, the multilayered flask is the only static cell culture system, while the rest are dynamic cell culture systems. A dynamic culture system creates shear stress to cells as it involves mechanical agitation of the culture medium or culture vessel to allow more efficient nutrient transfer. Regardless of the bioprocessing strategies, the cell culture vessels used come in multiple dimensions, from milliliters to liters. A smaller vessel is suitable for large-scale expansion of autologous MSCs to meet a relatively lower cell number requirement while a larger vessel is ideal for the expansion of allogenic MSCs to maximize the cell yield to produce thousands of therapeutic doses per batch production.

The bioreactor is very useful for ultra-large-scale MSC expansion as it allows more control over the culture environment such as oxygen concentration. The bioreactor is relatively difficult to operate but allows easier monitoring and scaling up using a single vessel of different capacities to generate the desired quantity of cells. Before large-scale expansion in a bioreactor, most studies expanded MSCs in standard culture flasks to obtain sufficient cells for seeding in the bioreactor. Nonetheless, two studies expanded MSCs starting from passage 0 in the bioreactor and reported a cell expansion ratio of 1.66-fold to 8.15-fold (AT-MSCs from seeded stromal vascular fraction (SVF)) and 4.11-fold (BM-MSCs from seeded bone marrow mononuclear cells (BMMCs)), respectively [19, 22]. Cunha et al. found that bioreactors can be used for large-scale expansion of AT-MSCs and BM-MSCs without compromising the cell viability, surface marker expression, and differentiation potential, even though the positive expression of CD105 dropped below 95% (88% for BM-MSCs and 92% for AT-MSCs) [28]. Similarly, several other studies also reported a reduction in the expression of CD90 and CD105 on MSCs expanded using bioreactors [26, 31, 32]. A few studies that used a spinner flask for MSC expansion also found that the expression of CD90 and CD105 decreased [31, 33]. The authors postulated

Table 3: Comparison between the large-scale bioprocessing strategies for mesenchymal stem cells.

Characteristic	Multilayered flask	Spinner flask	Rotating bottle	Bioreactor
Automation	No	No	No	Yes
Cost	Low	Medium	Medium	High
Technical difficulty	Low	Medium	Medium	High
Manpower needed	High	Medium	Medium	Low
Shear stress	No	Yes	Yes	Yes
Mass transfer	Low	High	High	High
Ease of scale-up	Low	High	Medium	High
Ease of monitoring	Low	Medium	Medium	High
Ease of cell collection	High	Medium to high	High	Medium to high
2D or 3D culture	2D	3D	2D	3D

that this is likely due to cell damage caused by shear stress or enzymatic cell detachment process. $CD105^-$ MSCs have been reported to be more prone to differentiate into adipocytes and osteocytes and are more efficient in suppressing the proliferation of $CD4^+$ T-cells compared to $CD105^+$ MSCs [47]. A separate study found that $CD105^-$ MSCs have poorer cardiac regeneration potential compared to $CD105^+$ MSCs [48]. $CD90^-$ MSCs have been linked with weaker immunosuppressive activity and enhanced osteogenic and adipogenic differentiation [49, 50]. Thus, the loss of CD90 and CD105 expression after bioreactor and spinner flask expansion might enhance the potency of the MSCs in treating certain diseases.

There are several important parameters to optimize when using bioreactors including oxygen concentration, frequency of medium change, and rotation speed of the impeller. It has been reported that the expression of MSC surface markers decreased due to the shear stress [26, 28, 31, 32]. Importantly, the cell loading and harvesting of specific bioreactors need to be improved as Haack-Sørensen et al. reported 30% cell loss during cell loading and another 30% during cell collection [19] and Luyten et al. found that the cell harvesting was as low as 45% [51]. The level of dissolved oxygen partial pressure in culture medium can affect the expansion of MSCs. Kwon et al. found that hypoxic culture enhanced MSC proliferation by increasing the number of cells in the S phase of the cell cycle [52]. HIF-1a is an important factor for cell adaptation to varying oxygen concentrations and usually highly expressed during hypoxia. HIF-1a has been linked with higher MSC proliferation and survival in hypoxic condition [53, 54]. Only one study compared the large-scale expansion of MSC in hypoxic and normoxic conditions. Egger et al. found that hypoxic culture increased the proliferation and enhanced the chondrogenic and adipogenic differentiation potential of MSCs but suppressed the osteogenic differentiation potential [20]. Similar studies have been conducted by Longaker et al. [34] and Dos Santos et al. [55] using small-scale cultures. Longaker et al. found that hypoxia condition diminished *in vitro* chondrogenesis and osteogenesis of AT-MSCs, while Dos Santos et al. did not find any difference in the BM-MSC osteogenic and adipogenic differentiation potential in hypoxic and normoxic cultures. Thus, even though hypoxic culture increases the proliferation of MSCs, the use of low oxygen concentration in culture must be carefully monitored as it might alter the cell therapeutic potential.

The spinner flask and roller bottle can be considered as a simpler and smaller scale bioreactor [14]. The spinner flask and roller bottle are less complicated and require more manual manipulation compared to the bioreactor. Just like the bioreactor, the rotation speed for the spinner flask impeller and roller bottle needs to be optimized to reduce shear stress that may damage the cells.

Generally, it appears that the bioreactor and multilayered flask are the most effective bioprocessing strategies as it has the potential to achieve an expansion ratio 20-fold and above. However, for the multilayered flask, the expansion ratio varies greatly from study to study whereby some of the studies reported an expansion ratio below 20-fold and a few studies achieved above 100-fold expansion ratio. The higher expansion ratio in these studies is likely due to the low initial seeding density [6, 17, 37]. For example, Nekanti et al. seeded 1.27×10^6 cells (1000 cells/cm^2) in a CellSTACK 2-chamber and yielded 2.48×10^8 cells, achieving an expansion ratio of 195.28-fold [6]. In a different study, the authors seeded 5.09×10^6 cells (4000 cells/cm^2) in the same multilayered flask and yielded $3.64\text{-}5.65 \times 10^7$ cells to achieve 7.15-fold to 11.10-fold expansion ratio [23].

Most of the studies characterized the MSCs based on the ISCT guideline by checking at the phenotype and trilineage differentiation potential. However, this is not sufficient as the cell therapeutic potential, e.g., immunomodulatory property, is not reflected in these characterization techniques. Thus, many studies performed the immune-suppression assay to determine the functionality of expanded cells. Furthermore, some studies also performed extra experiments to detect the chromosome abnormality, genomic stability, and expression level of tumor markers to ensure the safety of the expanded cells. It is highly recommended to perform these extra testing, especially the potency assay, when the MSCs expanded in large scale are intended for clinical use.

5. Conclusion

Large-scale expansion of MSCs is commonly done using a multilayered flask, spinner flask, and bioreactor. Nonetheless,

optimization of a few parameters, including cell seeding density, impeller agitation speed, oxygen partial pressure, medium formulation and feeding strategy, pH, and microcarrier selection, is crucial to ensure the development of a sustainable and reproducible platform to produce cells that suit clinical applications. In some instances, e.g., expansion of autologous cells that normally require a lower cell number, a multilayered flask is sufficient for upscaling in a cost-effective manner while a bioreactor is more suitable for ultra-large-scale expansion. However, none of the studies mentioned significant loss of cell characteristics and functionality when the bioreactor, spinner flask, roller bottle, and multilayered flask were used.

Additional Points

Highlights. (i) Mesenchymal stem cells required large-scale expansion for clinical use. (ii) Multiple bioprocessing strategies have been explored for large-scale expansion of mesenchymal stem cells (MSCs). (iii) Expanded cells maintain the MSC characteristics.

Conflicts of Interest

The authors declare that there are no conflicts of interest.

Acknowledgments

This work was supported by a joint research grant from the Universiti Kebangsaan Malaysia and Ming Medical Services Sdn Bhd (Grant number: AP-2017-009/2).

References

[1] P. Hafez, S. R. Chowdhury, S. Jose et al., "Development of an in vitro cardiac ischemic model using primary human cardiomyocytes," *Cardiovascular Engineering and Technology*, vol. 9, no. 3, pp. 529–538, 2018.

[2] L. L. Liau, S. Makpol, A. G. N. Azurah, and K. H. Chua, "Human adipose-derived mesenchymal stem cells promote recovery of injured HepG2 cell line and show sign of early hepatogenic differentiation," *Cytotechnology*, vol. 70, no. 4, pp. 1221–1233, 2018.

[3] J. Lim, Z. R. M. Razi, J. X. Law et al., "Mesenchymal stromal cells from the maternal segment of human umbilical cord is ideal for bone regeneration in allogenic setting," *Tissue Eng Regen Med.*, vol. 15, no. 1, pp. 75–87, 2018.

[4] W. L. Lim, L. L. Liau, M. H. Ng, R. C. Shiplu, and J. X. Law, "Current progress in tendon and ligament tissue engineering," *Tissue Engineering and Regenerative Medicine*, vol. 16, no. 6, pp. 549–571, 2019.

[5] L. L. Liau, B. H. I. Ruszymah, M. H. Ng, and J. X. Law, "Characteristics and clinical applications of Wharton's jelly-derived mesenchymal stromal cells," *Current Research in Translational Medicine*, vol. 68, no. 1, pp. 5–16, 2020.

[6] U. Nekanti, L. Mohanty, P. Venugopal, S. Balasubramanian, S. Totey, and M. Ta, "Optimization and scale-up of Wharton's jelly-derived mesenchymal stem cells for clinical applications," *Stem Cell Research*, vol. 5, no. 3, pp. 244–254, 2010.

[7] S. R. Caruso, M. D. Orellana, A. Mizukami et al., "Growth and functional harvesting of human mesenchymal stromal cells cultured on a microcarrier-based system," *Biotechnology Progress*, vol. 30, no. 4, pp. 889–895, 2014.

[8] J. L. Spees, R. H. Lee, and C. A. Gregory, "Mechanisms of mesenchymal stem/stromal cell function," *Stem Cell Research & Therapy*, vol. 7, no. 1, p. 125, 2016.

[9] N. Watson, R. Divers, R. Kedar et al., "Discarded Wharton jelly of the human umbilical cord: a viable source for mesenchymal stromal cells," *Cytotherapy*, vol. 17, no. 1, pp. 18–24, 2015.

[10] L.-X. Guan, H. Guan, H.-B. Li et al., "Therapeutic efficacy of umbilical cord-derived mesenchymal stem cells in patients with type 2 diabetes," *Experimental and Therapeutic Medicine*, vol. 9, no. 5, pp. 1623–1630, 2015.

[11] W. A. El-Kheir, H. Gabr, M. R. Awad et al., "Autologous bone marrow-derived cell therapy combined with physical therapy induces functional improvement in chronic spinal cord injury patients," *Cell Transplantation*, vol. 23, no. 6, pp. 729–745, 2014.

[12] J. Vaquero, M. Zurita, M. A. Rico et al., "Intrathecal administration of autologous mesenchymal stromal cells for spinal cord injury: safety and efficacy of the 100/3 guideline," *Cytotherapy*, vol. 20, no. 6, pp. 806–819, 2018.

[13] M. M. Bonab, K. Alimoghaddam, F. Talebian, S. H. Ghaffari, A. Ghavamzadeh, and B. Nikbin, "Aging of mesenchymal stem cell in vitro," *BMC Cell Biology*, vol. 7, no. 14, 2006.

[14] S. Jung, K. M. Panchalingam, R. D. Wuerth, L. Rosenberg, and L. A. Behie, "Large-scale production of human mesenchymal stem cells for clinical applications," *Biotechnology and Applied Biochemistry*, vol. 59, no. 2, pp. 106–120, 2012.

[15] K. Jaianand and P. Balaji, "Isolation, characterization and scale-up of foetal amniotic membrane derived multipotent stromal cells for therapeutic applications," *International Journal of pharma and Bio Sciences*, vol. 6, no. 1, pp. 421–426, 2015.

[16] G. Zhao, F. Liu, S. Lan et al., "Large-scale expansion of Wharton's jelly-derived mesenchymal stem cells on gelatin microbeads, with retention of self-renewal and multipotency characteristics and the capacity for enhancing skin wound healing," *Stem Cell Research & Therapy*, vol. 6, no. 1, pp. 1–16, 2015.

[17] V. Govindasamy, V. S. Ronald, A. N. B. Abdullah et al., "Human platelet lysate permits scale-up of dental pulp stromal cells for clinical applications," *Cytotherapy*, vol. 13, no. 10, pp. 1221–1233, 2011.

[18] T. R. J. Heathman, V. A. M. Glyn, A. Picken et al., "Expansion, harvest and cryopreservation of human mesenchymal stem cells in a serum-free microcarrier process," *Biotechnology and Bioengineering*, vol. 112, no. 8, pp. 1696–1707, 2015.

[19] M. Haack-Sørensen, M. Juhl, B. Follin et al., "Development of large-scale manufacturing of adipose-derived stromal cells for clinical applications using bioreactors and human platelet lysate," *Scandinavian Journal of Clinical and Laboratory Investigation*, vol. 78, no. 4, pp. 293–300, 2018.

[20] D. Egger, I. Schwedhelm, J. Hansmann, and C. Kasper, "Hypoxic three-dimensional scaffold-free aggregate cultivation of mesenchymal stem cells in a stirred tank reactor," *Bioengineering*, vol. 4, no. 4, p. 47, 2017.

[21] T. Lawson, D. E. Kehoe, A. C. Schnitzler et al., "Process development for expansion of human mesenchymal stromal cells in a 50 L single-use stirred tank bioreactor," *Biochemical Engineering Journal*, vol. 120, pp. 49–62, 2017.

[22] K. Schallmoser, E. Rohde, A. Reinisch et al., "Rapid large-scale expansion of functional mesenchymal stem cells from unmanipulated bone marrow without animal serum," *Tissue Engineering. Part C, Methods*, vol. 14, no. 3, pp. 185–196, 2008.

[23] N. Fekete, M. T. Rojewski, D. Fürst et al., "GMP-compliant isolation and large-scale expansion of bone marrow-derived MSC," *PLoS One*, vol. 7, no. 8, p. e43255, 2012.

[24] P. Gupta, H. G. Nilsson, L. P. Geris, F. Luyten, and I. Papantoniou, "Human platelet lysate improves bone forming potential of human progenitor cells expanded in microcarrier-based dynamic culture," *Stem Cells Translational Medicine*, vol. 8, no. 8, pp. 810–821, 2019.

[25] A. M. de Soure, A. Fernandes-Platzgummer, F. Moreira et al., "Integrated culture platform based on a human platelet lysate supplement for the isolation and scalable manufacturing of umbilical cord matrix-derived mesenchymal stem/stromal cells," *Journal of Tissue Engineering and Regenerative Medicine*, vol. 11, no. 5, pp. 1630–1640, 2017.

[26] P. A. Tozetti, S. R. Caruso, A. Mizukami et al., "Expansion strategies for human mesenchymal stromal cells culture under xeno-free conditions," *Biotechnology Progress*, vol. 33, no. 5, pp. 1358–1367, 2017.

[27] M. F. Q. Sousa, M. M. Silva, D. Giroux et al., "Production of oncolytic adenovirus and human mesenchymal stem cells in a single-use, vertical-wheel bioreactor system: impact of bioreactor design on performance of microcarrier-based cell culture processes," *Biotechnology Progress*, vol. 31, no. 6, pp. 1600–1612, 2015.

[28] B. Cunha, T. Aguiar, S. B. Carvalho et al., "Bioprocess integration for human mesenchymal stem cells: from up to downstream processing scale-up to cell proteome characterization," *Journal of Biotechnology*, vol. 248, pp. 87–98, 2017.

[29] M. Hervy, J. L. Weber, M. Pecheul et al., "Long term expansion of bone marrow-derived hMSCs on novel synthetic microcarriers in xeno-free, defined conditions," *Defined Conditions. PLoS One.*, vol. 9, no. 3, article e92120, 2014.

[30] J. G. Carmelo, A. Fernandes-Platzgummer, M. M. Diogo, C. L. da Silva, and J. M. S. Cabral, "A xeno-free microcarrier-based stirred culture system for the scalable expansion of human mesenchymal stem/stromal cells isolated from bone marrow and adipose tissue," *Biotechnology Journal*, vol. 10, no. 8, pp. 1235–1247, 2015.

[31] A. Mizukami, A. Fernandes-Platzgummer, J. G. Carmelo et al., "Stirred tank bioreactor culture combined with serum-/xenogeneic-free culture medium enables an efficient expansion of umbilical cord-derived mesenchymal stem/stromal cells," *Biotechnology Journal*, vol. 11, no. 8, pp. 1048–1059, 2016.

[32] F. dos Santos, A. Campbell, A. Fernandes-Platzgummer et al., "A xenogeneic-free bioreactor system for the clinical-scale expansion of human mesenchymal stem/stromal cells," *Biotechnology and Bioengineering*, vol. 111, no. 6, pp. 1116–1127, 2014.

[33] F. dos Santos, P. Z. Andrade, M. M. Abecasis et al., "Toward a clinical-grade expansion of mesenchymal stem cells from human sources: a microcarrier-based culture system under xeno-free conditions," *Tissue Engineering. Part C, Methods*, vol. 17, no. 12, pp. 1201–1210, 2011.

[34] M. T. Longaker, P. Malladi, M. Chiou, Y. Xu, and A. J. Giaccia, "Effect of reduced oxygen tension on chondrogenesis and osteogenesis in adipose-derived mesenchymal cells," *American Journal of Physiology-Cell Physiology*, vol. 290, no. 4, pp. C1139–C1146, 2005.

[35] A. C. Tsai, Y. Liu, and T. Ma, "Expansion of human mesenchymal stem cells in fibrous bed bioreactor," *Biochemical Engineering Journal*, vol. 108, pp. 51–57, 2016.

[36] J. Kannaiyan, P. Muthukutty, M. D. T. Iqbal, and B. Paulraj, "Villous chorion: a potential source for pluripotent-like stromal cells," *J Nat Sci Biol Med.*, vol. 8, no. 2, pp. 221–228, 2017.

[37] C. Bartmann, E. Rohde, K. Schallmoser et al., "Two steps to functional mesenchymal stromal cells for clinical application," *Transfusion*, vol. 47, no. 8, pp. 1426–1435, 2007.

[38] L. Vymetalova, T. Kucirkova, L. Knopfova et al., "Large-scale automated hollow-fiber bioreactor expansion of umbilical cord-derived human mesenchymal stromal cells for neurological disorders," *Neurochemical Research*, vol. 45, no. 1, pp. 204–214, 2020.

[39] T. Lambrechts, I. Papantoniou, S. Viazzi et al., "Evaluation of a monitored multiplate bioreactor for large-scale expansion of human periosteum derived stem cells for bone tissue engineering applications," *Biochemical Engineering Journal*, vol. 108, pp. 58–68, 2016.

[40] P. Mark, M. Kleinsorge, R. Gaebel et al., "Human mesenchymal stem cells display reduced expression of CD105 after culture in serum-free medium," *Stem Cells International*, vol. 2013, 8 pages, 2013.

[41] H. B. B. H. Prana, B. M. Muhammad Hanif, B. O. Aisya Hanim et al., "Human platelet lysate promotes proliferation but fails to maintain chondrogenic markers of chondrocytes," *Sains Malaysiana*, vol. 48, no. 10, pp. 2169–2176, 2019.

[42] S. Kandoi, L. Praveen Kumar, B. Patra et al., "Evaluation of platelet lysate as a substitute for FBS in explant and enzymatic isolation methods of human umbilical cord MSCs," *Science Reports*, vol. 8, no. 1, p. 12439, 2018.

[43] M. Dominici, K. le Blanc, I. Mueller et al., "Minimal criteria for defining multipotent mesenchymal stromal cells. The International Society for Cellular Therapy position statement," *Cytotherapy*, vol. 8, no. 4, pp. 315–317, 2006.

[44] S. Riis, F. M. Nielsen, C. P. Pennisi, V. Zachar, and T. Fink, "Comparative analysis of media and supplements on initiation and expansion of adipose-derived stem cells," *Stem Cells Translational Medicine*, vol. 5, no. 3, pp. 314–324, 2016.

[45] A. Oikonomopoulos, W. K. van Deen, A.-R. Manansala et al., "Optimization of human mesenchymal stem cell manufacturing: the effects of animal/xeno-free media," *Scientific Reports*, vol. 5, no. 1, p. 16570, 2015.

[46] C. Menard, L. Pacelli, G. Bassi et al., "Clinical-Grade mesenchymal stromal cells produced under various good manufacturing practice processes differ in their immunomodulatory Properties: standardization of immune quality controls," *Stem Cells and Development*, vol. 22, no. 12, pp. 1789–1801, 2013.

[47] P. Anderson, A. B. Carrillo-Gálvez, A. García-Pérez, M. Cobo, and F. Martín, "CD105 (endoglin)-negative murine mesenchymal stromal cells define a new multipotent subpopulation with distinct differentiation and immunomodulatory capacities," *PLoS One*, vol. 8, no. 10, article e76979, 2013.

[48] R. Gaebel, D. Furlani, H. Sorg et al., "Cell origin of human mesenchymal stem cells determines a different healing performance in cardiac regeneration," *PLoS One*, vol. 6, no. 2, article e15652, 2011.

[49] D. Campioni, R. Rizzo, M. Stignani et al., "A decreased positivity for CD90 on human mesenchymal stromal cells (MSCs) is associated with a loss of immunosuppressive activity by

MSCs," *Cytometry Part B: Clinical Cytometry*, vol. 76B, no. 3, pp. 225–230, 2009.

[50] D. A. Moraes, T. T. Sibov, L. F. Pavon et al., "A reduction in CD90 (THY-1) expression results in increased differentiation of mesenchymal stromal cells," *Stem Cell Research & Therapy*, vol. 7, no. 1, p. 97, 2016.

[51] F. P. Luyten, J. Schrooten, J.-M. Aerts, T. Lambrechts, I. Papantoniou, and B. Rice, "Large-scale progenitor cell expansion for multiple donors in a monitored hollow fibre bioreactor," *Cytotherapy*, vol. 18, no. 9, pp. 1219–1233, 2016.

[52] S. Y. Kwon, S. Y. Chun, Y. S. Ha et al., "Hypoxia enhances cell properties of human mesenchymal stem cells," *Tissue Eng Regen Med.*, vol. 14, no. 5, pp. 595–604, 2017.

[53] W. Widowati, L. Wijaya, I. Bachtiar et al., "Effect of oxygen tension on proliferation and characteristics of Wharton's jelly-derived mesenchymal stem cells," *Biomarkers and Genomic Medicine*, vol. 6, no. 1, pp. 43–48, 2014.

[54] C. Fehrer, R. Brunauer, G. Laschober et al., "Reduced oxygen tension attenuates differentiation capacity of human mesenchymal stem cells and prolongs their lifespan," *Aging Cell*, vol. 6, no. 6, pp. 745–757, 2007.

[55] F. Dos Santos, P. Z. Andrade, J. S. Boura, M. M. Abecasis, C. L. Da Silva, and J. M. S. Cabral, "Ex vivo expansion of human mesenchymal stem cells: a more effective cell proliferation kinetics and metabolism under hypoxia," *Journal of Cellular Physiology*, vol. 223, no. 1, pp. 27–35, 2010.

[56] A. Shekaran, E. Sim, K. Y. Tan et al., "Enhanced in vitro osteogenic differentiation of human fetal MSCs attached to 3D microcarriers versus harvested from 2D monolayers," *BMC Biotechnology*, vol. 15, no. 1, 2015.

Hindawi
Stem Cells International
Volume 2020, Article ID 8842659, 13 pages
https://doi.org/10.1155/2020/8842659

Research Article

The Effects of Mesenchymal Stem Cells on Antimelanoma Immunity Depend on the Timing of Their Administration

Dragana Miloradovic,[1] **Dragica Miloradovic**,[1] **Bojana Simovic Markovic**,[1] **Aleksandar Acovic**,[1] **Carl Randall Harrell**,[2] **Valentin Djonov**,[3] **Nebojsa Arsenijevic**,[1] **and Vladislav Volarevic**[1,4]

[1]*Center for Molecular Medicine and Stem Cell Research, Department of Microbiology and Immunology, Faculty of Medical Sciences, University of Kragujevac, 69 Svetozar Markovic Street, Kragujevac, Serbia*
[2]*Regenerative Processing Plant, LLC, 34176 US Highway 19 N Palm Harbor, Palm Harbor FL, USA*
[3]*Institute of Anatomy, University of Bern, 2 Baltzerstrasse, Switzerland*
[4]*Center of Excellence for the Acceleration of Harm Reduction (CoEHAR), Università di Catania, Via Santa Sofia 78, Catania 95123, Italy*

Correspondence should be addressed to Vladislav Volarevic; drvolarevic@yahoo.com

Received 6 May 2020; Revised 10 June 2020; Accepted 18 June 2020; Published 10 July 2020

Academic Editor: Jane Ru Choi

There is still a lively debate about whether mesenchymal stem cells (MSCs) promote or suppress antitumor immune response. Although several possible explanations have been proposed, including different numbers of injected and engrafted MSCs, heterogeneity in phenotype, and function of tumor cells, the exact molecular mechanisms responsible for opposite effects of MSCs in modulation of antitumor immunity are still unknown. Herewith, we used a B16F10 murine melanoma model to investigate whether timing of MSC administration in tumor-bearing mice was crucially important for their effects on antitumor immunity. MSCs, intravenously injected 24 h after melanoma induction (B16F10+MSC^{1d}-treated mice), significantly enhanced natural killer (NK) and T cell-driven antitumor immunity, suppressed tumor growth, and improved survival of melanoma-bearing animals. Significantly higher plasma levels of antitumorigenic cytokines (TNF-α and IFN-γ), remarkably lower plasma levels of immunosuppressive cytokines (TGF-β and IL-10), and a significantly higher number of tumor-infiltrating, IFN-γ-producing, FasL- and granzyme B-expressing NK cells, IL-17-producing CD4+Th17 cells, IFN-γ- and TNF-α-producing CD4+Th1 cells, and CD8+cytotoxic T lymphocytes (CTLs) were observed in B16F10+MSC^{1d}-treated mice. On the contrary, MSCs, injected 14 days after melanoma induction (B16F10+MSC^{14d}-treated mice), promoted tumor growth by suppressing antigen-presenting properties of tumor-infiltrating dendritic cells (DCs) and macrophages and by reducing tumoricidal capacity of NK cells and T lymphocytes. Significantly higher plasma levels of TGF-β and IL-10, remarkably lower plasma levels of TNF-α and IFN-γ, and significantly reduced number of tumor-infiltrating, I-A-expressing, and IL-12-producing macrophages, CD80- and I-A-expressing DCs, granzyme B-expressing CTLs and NK cells, IFN-γ- and IL-17-producing CTLs, CD4+Th1, and Th17 cells were observed in B16F10+MSC^{14d}-treated animals. In summing up, the timing of MSC administration into the tumor microenvironment was crucially important for MSC-dependent modulation of antimelanoma immunity. MSCs transplanted during the initial phase of melanoma growth exerted tumor-suppressive effect, while MSCs injected during the progressive stage of melanoma development suppressed antitumor immunity and enhanced tumor expansion.

1. Introduction

Melanoma is nowadays considered as one of the most aggressive and the fastest growing malignant tumors worldwide [1]. Although a primary cutaneous melanoma can be managed by surgery, the advanced metastatic melanoma requires use of modern molecular mechanism-based therapeutic approaches [1]. The immuno- and targeted drug therapies,

which interfere with oncoprotein and immune checkpoint pathways, were able to positively impact survival of patients with advanced melanoma [2]. Unfortunately, the success rate is being hampered by a number of factors including drug resistance, heterogeneous phenotype of melanoma cells, and impaired activation of antitumor immune response [2]. Therefore, new and more effective strategies are needed for patients who did not receive optimal benefit from currently used therapeutic approaches.

Mesenchymal stem cells (MSCs) are nonhematopoietic, multipotent stem cells that reside in almost all postnatal tissues [3]. As cells of mesodermal origin, MSCs are considered as an integral part of the tumor stromal microenvironment, where, together with malignant cells, fibroblasts, pericytes, and endothelial cells, it produces trophic and growth factors and immuno- and angiomodulatory molecules and regulates tumor development [4]. Additionally, MSCs express a large number of chemokine receptors and exhibit strong tropism towards cancer cells [5]. After systemic administration, MSCs engraft in the tumor microenvironment where, in a juxtacrine and paracrine manner, it regulates expansion of malignant cells and modulates antitumor immunity [6]. Due to their tumor-homing capacity, MSCs were used as a vehicle to deliver cytotoxic drugs, proinflammatory cytokines, and cell cycle-interfering microRNAs in the tumors, attenuating their growth and progression [7]. MSCs modulate phenotype and function of all immune cells that play an important role in antitumor immune response [8]. MSCs regulate antigen-presenting properties of macrophages and dendritic cells (DCs), cytotoxicity of natural killer (NK) and CD8+T cells (CTLs), and cytokine production in CD4+T helper cells [8]. Accordingly, effects of MSC-dependent modulation of antitumor immunity have been explored in a large number of experimental studies, but surprisingly, opposite results were reported. While several research groups demonstrated that MSCs suppressed antitumor immune response and enhanced tumor progression [9–11], experimental findings presented by other researchers indicated that MSC-based therapy favored development of strong antitumor immunity that inhibited expansion of malignant cells [9–13]. Although several possible explanations for these contradictory findings have been proposed, including different numbers of injected and engrafted MSCs, diverse route of their administration, heterogeneity in phenotype, and function of tumor cells [12, 13], the exact molecular mechanisms responsible for opposite effects of MSCs in modulation of tumor growth are still unknown. Recently, Zong and colleagues indicated that MSC-based effects on progression and metastasis of hepatocellular carcinoma (HCC) depended on the time of MSC administration in the tumor-bearing animals [14]. Injection of MSCs in the initial phase of HCC development resulted in tumor suppression, while MSCs administered in the progressive stage of tumor growth promoted progression and metastasis of HCC [14]. In line with these findings, herewith, we used a murine model of melanoma to investigate whether the timing of MSC administration in melanoma-bearing mice was crucially important for MSC-dependent modulation of antitumor immunity and melanoma progression.

2. Material and Methods

2.1. Cells. MSCs isolated from bone marrow of C57BL/6 mice were purchased from Gibco (Catalog number S1502-100). The murine melanoma cell line B16F10, which is syngeneic to the C57BL/6 background, was purchased from the American Type Culture Collection (CRL-6475; ATCC, USA). Both types of cells were cultured in complete Dulbecco's modified Eagle medium (DMEM) containing 10% heat-inactivated fetal bovine serum (FBS), 100 IU/mL penicillin G, and 100 μg/mL streptomycin (Sigma-Aldrich, Munich, Germany), at 37°C in a 5% CO_2 incubator. MSCs in passage 4 and B16F10 cells in passage 4 were used throughout the experiments.

2.2. Animals. Eight- to ten-week-old C57BL/6 mice were used. Mice were maintained in animal breeding facilities of the Faculty of Medical Sciences, University of Kragujevac, Serbia. All procedures were performed in accordance with the guidelines for the Principles of Laboratory Animal Care and the *Guide for the Care and Use of Laboratory Animals*, and all animals received humane care according to the criteria outlined in the *Guide for the Care and Use of Laboratory Animals* (National Institutes of Health publication 86-23, 1985 revision). All experiments were approved by the Animal Ethical Review Board of the Faculty of Medical Sciences, University of Kragujevac, Serbia. Mice were housed in a temperature-controlled environment with a 12-hour light-dark cycle and were administered with standard laboratory chow and water *ad libitum*. At least eight mice per group were used in each experiment.

2.3. Melanoma Induction and Injection of MSCs. B16F10 cells (5×10^5 cells, suspended in 200 μL of phosphate-buffered saline (PBS)) were subcutaneously injected in the left flank of C57BL/6 mice. Immediately after, mice were divided into four experimental groups. The first experimental group of mice, 1 day after injection of B16F10 cells, intravenously received MSCs (5×10^5 cells, suspended in 200 μL of PBS; B16F10+MSC^{1d}-treated mice). The second experimental group of B16F10-treated animals, 14 days after administration of B16F10 cells, intravenously received MSCs (5×10^5 cells, suspended in 200 μL of PBS; B16F10+MSC^{14d}-treated mice). Mice from the third and fourth experimental groups intravenously received 200 μL of PBS at appropriate time points (1 day (B16F10+PBS^{1d}-treated mice) or 14 days after B16F10 administration (B16F10+PBS^{14d}-treated animals)). All animals were sacrificed 28 days after the injection of B16F10 cells.

2.4. Measurement of Tumor Growth and Progression. Once the tumors were palpable, they were measured daily and tumor volume was calculated with the following formula: $V = 4/3\pi * a/2 * b/2 * c/2$ (a = length, b = width, and c = thickness) [15].

2.5. Measurement of Cytokines in Plasma Samples of Tumor-Bearing Mice. Blood samples were collected from the facial vein at days 1, 14, and 28 after the injection of B16F10 cells. Mouse blood was kept in anticoagulant-containing tubes and centrifuged for 10 minutes at 2000 g at 4°C. Supernatants were stored at -20°C until needed. Concentration of tumor

necrosis factor alpha (TNF-α), interferon gamma (IFN-γ), transforming growth factor beta (TGF-β), and interleukin-(IL-) 10 in mouse plasma samples were measured by using enzyme-linked immunosorbent assay (ELISA) sets (R&D Systems, Minneapolis, MN, USA), according to the manufacturer's instructions [16].

2.6. Isolation of Tumor-Infiltrating Leucocytes. By using forceps and scissors, subcutaneous tumors were resected *en bloc*, including overlying and surrounding skin. After the removal of surrounding skin, tumors were measured and weighed. By using scissors, the tumors were minced, until all large sections were processed into 1-2 mm pieces which are digested in 5 mL of DMEM containing 1 mg/mL collagenase I, 1 mM EDTA, and 2% FBS (all from Sigma-Aldrich, Munich, Germany). After incubation of 2 hr at 37°C, the digested tumor tissue was incubated with 4 mL of trypsin and DNase I (Roche Diagnostics), followed by passing through a 40 μm nylon filter. Single-cell suspensions were then processed for flow cytometry analysis [17].

2.7. Flow Cytometry Analysis and Intracellular Staining of Tumor-Infiltrating Leucocytes. Tumor-infiltrating leucocytes were investigated for different cell surface and intracellular markers with flow cytometry. Briefly, 1×10^6 cells were incubated with anti-mouse F4/80, CD4, CD8, CD11c, NK1.1, CD80, I-A, granzyme B, and Fas ligand (FasL) monoclonal antibodies conjugated with fluorescein isothiocyanate (FITC), phycoerythrin (PE), peridinin chlorophyll protein (PerCP), or allophycocyanin (APC) (all from BD Biosciences, San Jose, CA, USA) following the manufacturer's instructions. Immune cells derived from the tumors were concomitantly stained for the intracellular content of TNF-α, IFN-γ, IL-12, IL-4, and IL-17 by using the fixation/permeabilization kit and anti-mouse monoclonal antibodies conjugated with FITC, PE, PerCP, and APC (BD Biosciences). For intracellular cytokine staining, cells were stimulated with 50 ng/mL PMA and 500 ng/mL ionomycin for 5 h, and GolgiStop (BD Biosciences) was added. Cells were fixed in Cytofix/Cytoperm, permeated with 0.1% saponin, and stained with fluorescent Abs. Flow cytometric analysis was conducted on a BD Biosciences' FACSCalibur and analyzed by using the Flowing Software analysis program [17].

2.8. Statistical Analyses. The data were analyzed using statistical package SPSS, version 21. The normality of distribution was tested by the Kolmogorov-Smirnov test. The results were analyzed using the Student t-test. All data in this study were expressed as the mean ± standard error of the mean (SEM). Values of $p < 0.05$ were considered as statistically significant.

3. Results

3.1. MSC-Based Modulation of Melanoma Growth Depends on the Time of MSC Administration. First, we examined whether systemic application of MSCs affected melanoma growth. As it is shown in Figure 1(a), tumors become palpable in B16F10 +MSC^{1d}-treated mice 8 days later compared with other experimental groups, suggesting that MSCs, intravenously injected 24 h after melanoma induction, prevented rapid tumor growth. Starting from day 18, average tumor volumes were significantly lower in B16F10+MSC^{1d}-treated mice than in B16F10+PBS^{1d}-treated animals ($p < 0.05$; Figure 1(a)). Additionally, the average volume and weight of tumors removed from B16F10+MSC^{1d}-treated mice at day 28 were significantly lower than melanomas taken from B16F10+PBS^{1d}-treated animals (Figures 1(b) and 1(c)), confirming that MSCs, intravenously injected 24 h after melanoma induction, efficiently suppressed tumor growth and progression.

Opposite to these data were results observed in melanoma-bearing animals that intravenously received MSCs 14 days after tumor induction (B16F10+MSC^{14d}-treated mice). Starting from day 18 (4 days after MSC injection), average tumor volumes were significantly greater in B16F10+MSC^{14d}-treated animals than in B16F10+PBS^{14d}-treated mice ($p < 0.05$; Figure 1(a)). Accordingly, at day 28, average volume and weight of tumor removed from B16F10+PBS^{14d}-treated mice were significantly lower than those of melanomas of B16F10+MSC^{14d}-treated animals (Figures 1(b) and 1(c)), confirming that MSCs administered 14 days after tumor induction remarkably enhanced melanoma growth and progression. In line with these findings, the time of MSC injection was crucially important for their effects on survival of melanoma-bearing mice. While the lowest survival rate was observed in B16F10+MSC^{14d}-treated mice, all of the melanoma-bearing animals that received MSCs 24 h after tumor induction survived till the end of the experiment (Figure 1(d)).

Starting from day 14, MSCs transplanted 24 h after tumor induction significantly reduced weight loss of melanoma-bearing mice ($p < 0.05$; Figure 1(e)). Interestingly, weight gain was also noticed in B16F10+MSC^{14d}-treated animals ($p < 0.05$; Figure 1(e)). While reduced weight of B16F10 +MSC^{1d}-treated mice could be contributed to the MSC-dependent suppression of tumor progression, weight gain, noticed in B16F10+MSC^{14d}-treated animals, may be a consequence of significantly increased tumor weight which was observed in these mice.

Since MSCs adopt proinflammatory (MSC1) or immunosuppressive (MSC2) phenotype in response to the inflammatory and immunosuppressive cytokines to which they are exposed [18], we analyzed and compared the concentration of inflammatory (TNF-α, IFN-γ) and immunosuppressive cytokines (IL-10, TGF-β) in plasma samples of melanoma-bearing mice at the time of MSC administration. The ratios of proinflammatory to anti-inflammatory cytokines (TNF-α : IL-10, TNF-α : TGF-β, IFN-γ : IL-10, IFN-γ : TGF-β, IL-12 : IL-10, and IL-12 : TGF-β) were significantly lower in plasma samples of B16F10+PBS^{1d}-treated mice compared to B16F10+PBS^{14d}-treated animals ($p < 0.001$; Figure 1(d)), suggesting that MSCs, administered 1 day after the injection of tumor cells, were exposed to the higher concentration of immunosuppressive cytokines, while MSCs transplanted 14 days after tumor induction were exposed to the higher concentration of inflammatory cytokines. Therefore, we assume that, in response to the different concentration of inflammatory and immunosuppressive cytokines to which they were exposed, MSCs injected during the initial phase of melanoma growth adopted proinflammatory (MSC1)

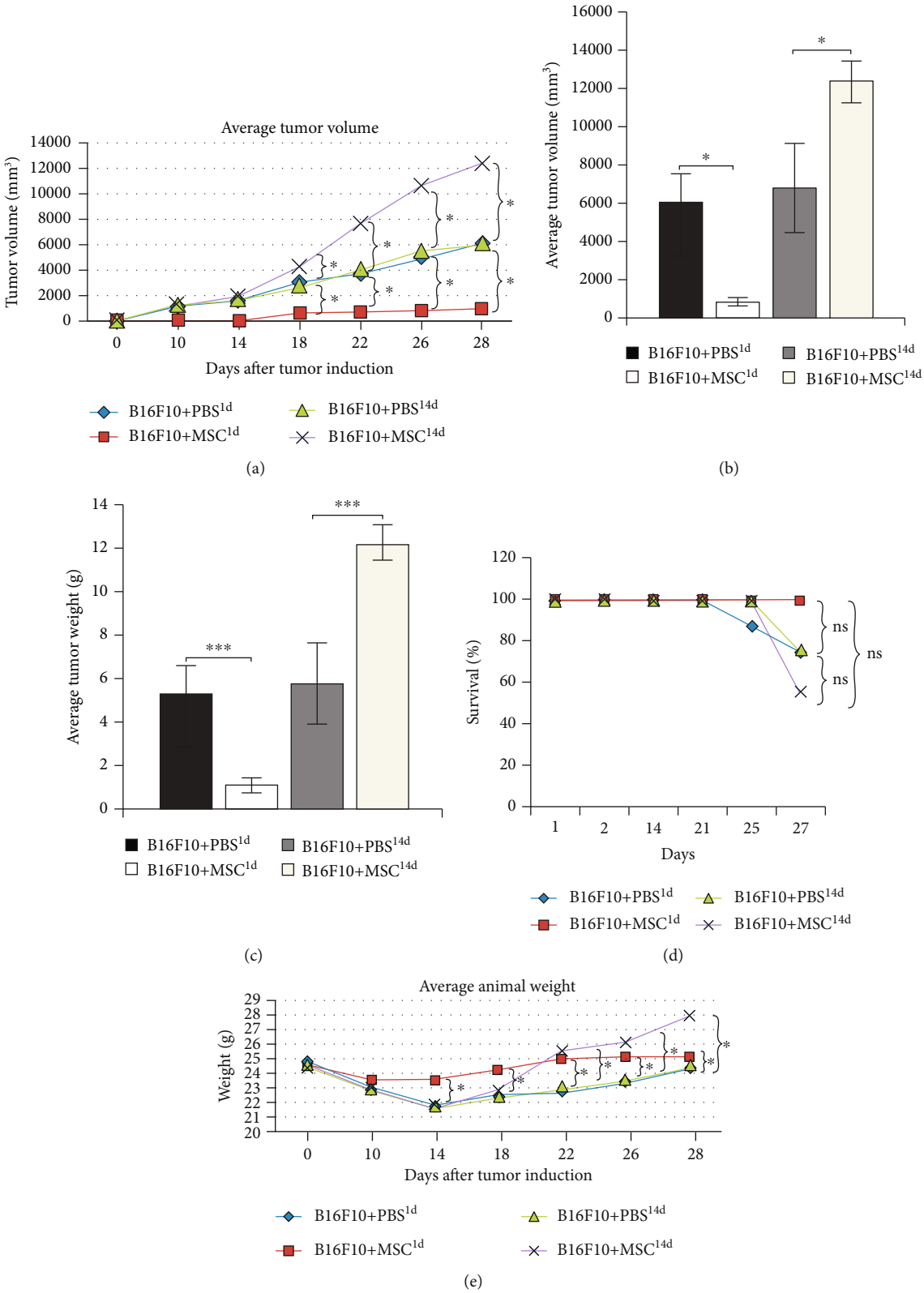

Figure 1: Continued.

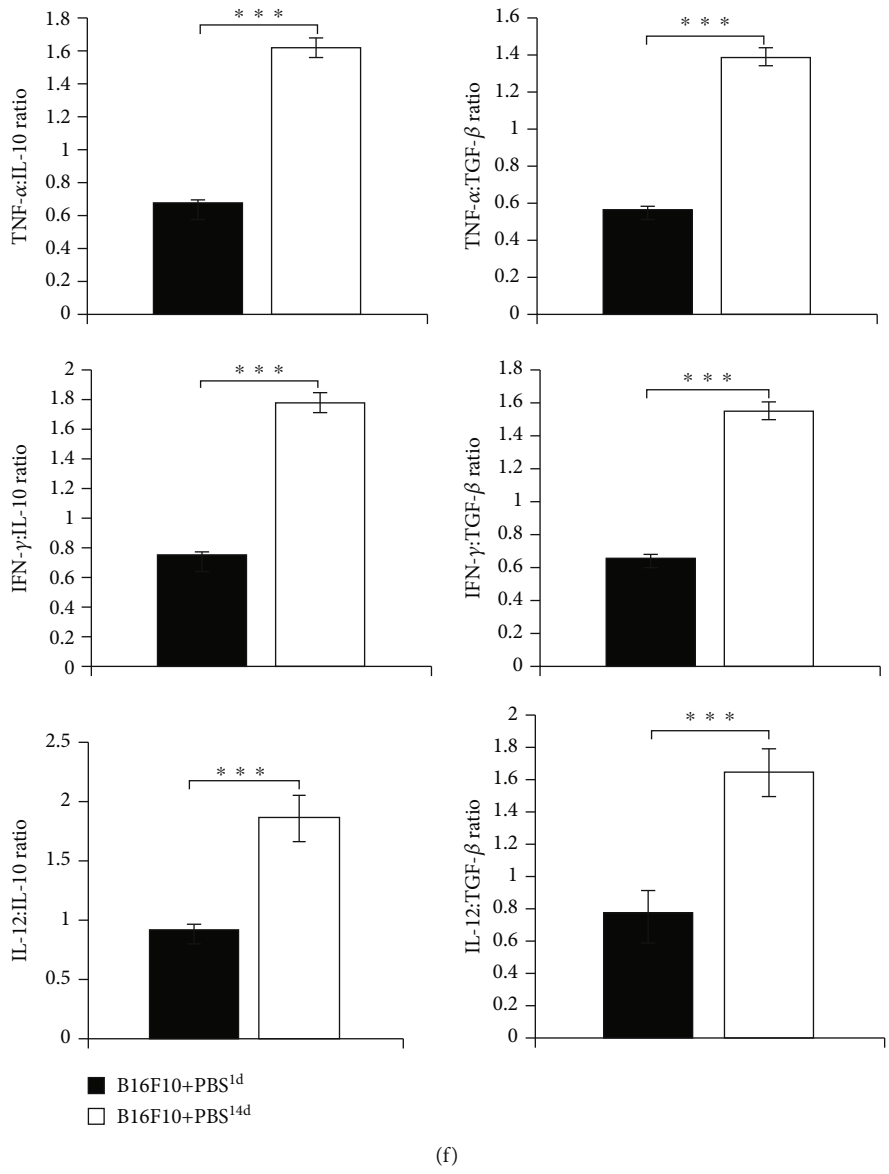

Figure 1: MSC-based modulation of melanoma growth depends on the time of MSC administration. Delayed tumor growth, observed in B16F10+MSC^{1d}-treated mice, and rapid melanoma growth, noticed in B16F10+MSC^{14d}-treated animals from day 18, were evidenced by the measurement of tumor volumes at different days after tumor induction (a). Significantly lower average tumor volume (b) and tumor weight (c) were observed in B16F10+MSC^{1d}-treated mice than in B16F10+PBS^{1d}-treated animals at day 28. Oppositely, average tumor volume (b) and tumor weight (c) were significantly greater in B16F10+MSC^{14d}-treated mice than in B16F10+PBS^{14d}-treated animals at day 28. The lowest survival rate was noticed in B16F10+MSC^{14d}-treated animals, while all of B16F10+MSC^{1d}-treated mice survived to the last, 28th day of experiment (d). The difference in the survival between experimental groups was statistically nonsignificant ("ns"). Average animal weight at different days after tumor induction demonstrates reduced weight loss in MSC-treated, melanoma-bearing mice (e). The ratios of proinflammatory to anti-inflammatory cytokines (TNF-α : IL-10, TNF-α : TGF-β, IFN-γ : IL-10, IFN-γ : TGF-β, IL-12 : IL-10, and IL-12 : TGF-β) were significantly lower in plasma samples of B16F10+PBS^{1d}-treated mice than in plasma samples of B16F10+PBS^{14d}-treated animals (f). Plasma samples were collected 24 h and 14 days after tumor induction. Values are presented as the mean ± SEM; $n = 8$ mice/group. $^{*}p < 0.05$, $^{***}p < 0.001$.

phenotype, while MSCs that were transplanted during the progressive stage of melanoma development adopted immunosuppressive (MSC2) phenotype.

3.2. MSCs, Injected 24 h after Melanoma Induction, Significantly Enhanced NK and T Cell-Driven Antitumor Immunity and Suppressed Tumor Growth and Progression. Cellular makeup of tumors obtained from B16F10+PBS^{1d}- and B16F10+MSC^{1d}-treated mice revealed that MSCs, injected 24 h after melanoma induction, significantly increased the total number of tumor-infiltrating cytotoxic NK1.1+NK cells ($p < 0.05$; Figure 2(a)). The significantly higher number of IFN-γ-producing ($p < 0.05$; Figure 2(b)) and FasL- and granzyme B-expressing ($p < 0.05$; Figures 2(c)

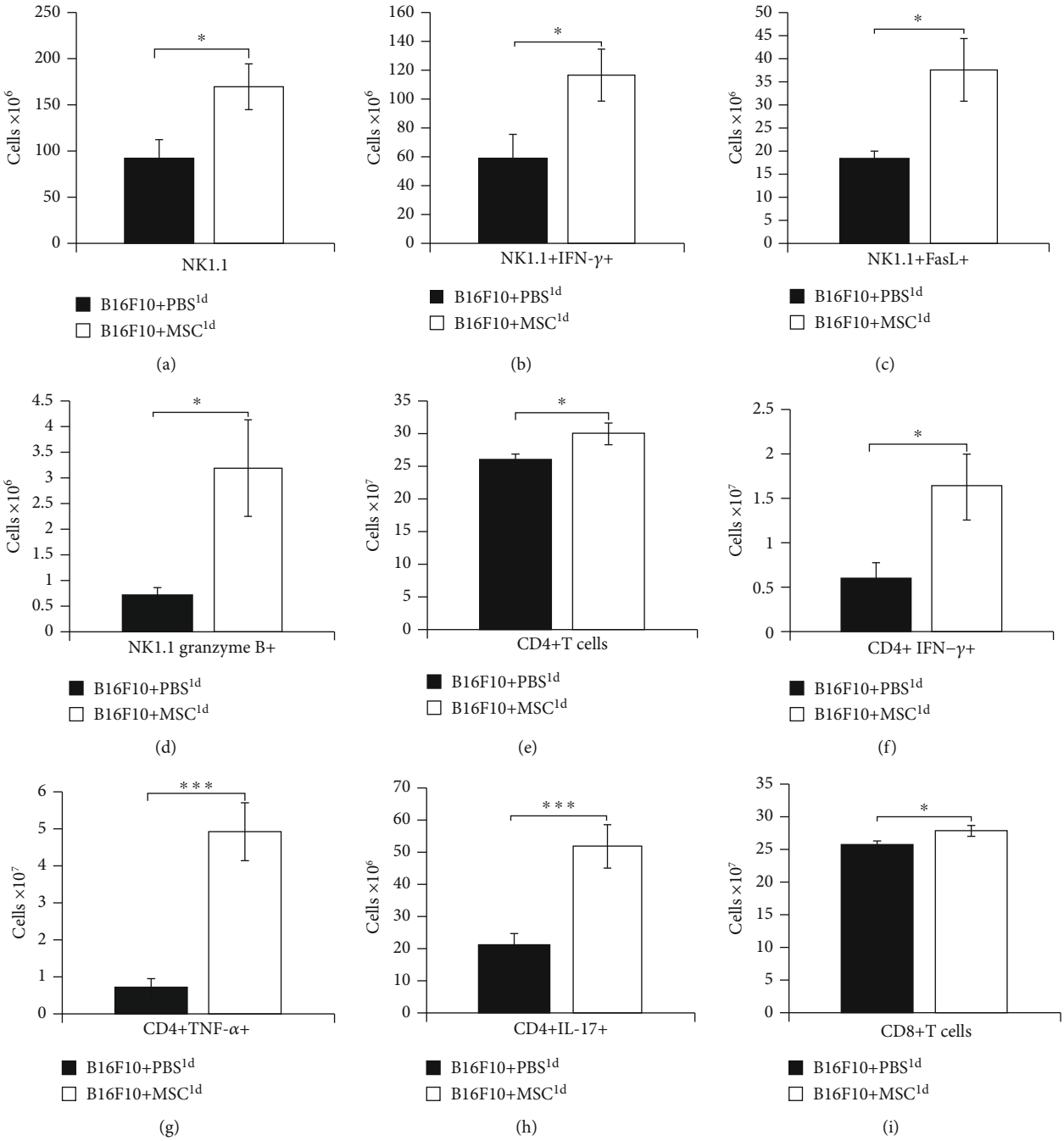

Figure 2: Continued.

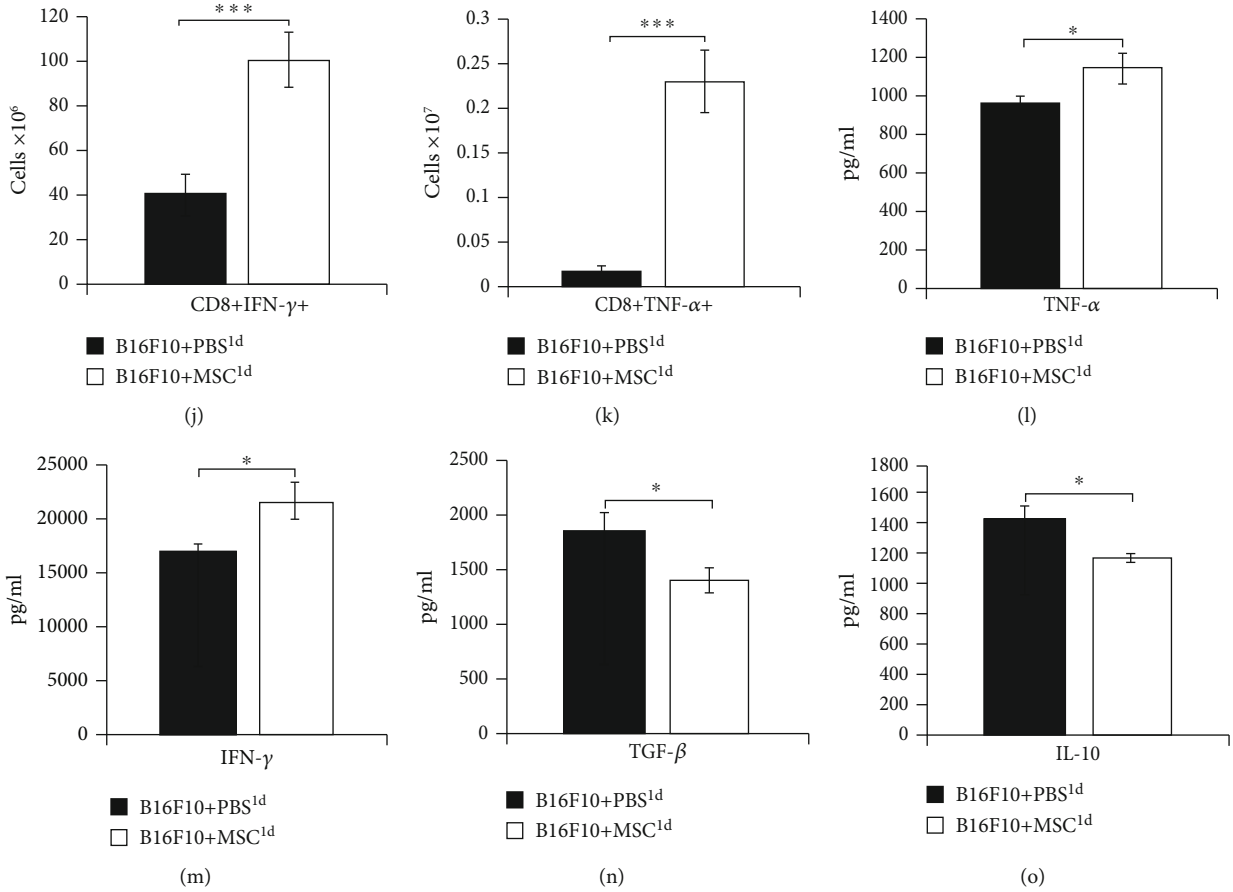

Figure 2: MSCs, injected 24 h after melanoma induction, significantly enhanced NK and T cell-driven antitumor immunity and suppressed tumor growth and progression. Significantly higher number of NK1.1+NK cells (a), IFN-γ-producing NK cells (b), FasL- and granzyme B-expressing NK cells (c, d), CD4+T cells (e), IFN-γ- and TNF-α-producing CD4+Th1 cells (f, g), IL-17-producing CD4+Th17 cells (h), CD8+CTLs (i), and IFN-γ- and TNF-α-producing CD8+CTLs (j, k) were noticed in the tumors of B16F10+MSC^{1d}-treated mice compared to the B16F10+PBS^{1d}-treated animals. Significantly higher concentration of inflammatory and antitumorigenic cytokines TNF-α and IFN-γ (l, m) and significantly lower concentration of immunosuppressive cytokines TGF-β and IL-10 (n, o) were noticed in plasma samples of B16F10+MSC^{1d}-treated mice compared to B16F10+PBS^{1d}-treated animals. Values are presented as the mean ± SEM; $n = 8$ mice/group. $^{*}p < 0.05$, $^{***}p < 0.001$.

and 2(d)) NK cells in the tumors of B16F10+MSC^{1d}-treated mice indicated that MSCs, injected 24 h after melanoma induction, enhanced cytotoxic and antitumorigenic potential of NK cells in tumor-bearing animals.

A significantly higher number of CD4+T helper ($p < 0.05$; Figure 2(e)) and CD8+CTLs ($p < 0.05$; Figure 2(i)) were present in the tumors of B16F10+MSC^{1d}-treated mice than in melanomas of B16F10+PBS^{1d}-treated animals. Phenotype and function of CD4+T helper and CD8+CTLs revealed that MSCs, injected 24 h after melanoma induction, significantly increased the presence of antitumorigenic and IFN-γ- and TNF-α-producing CD4+Th1 cells ($p < 0.05$ for IFN-γ, Figure 2(f); $p < 0.001$ for TNF-α, Figure 2(g)), IL-17-producing CD4+Th17 cells ($p < 0.001$, Figure 2(h)), and IFN-γ- and TNF-α-producing CD8+CTLs ($p < 0.001$, Figures 2(j) and 2(k)) in melanoma-bearing animals.

In line with these findings, significantly higher plasma levels of inflammatory and antitumorigenic cytokines TNF-α ($p < 0.05$, Figure 2(l)) and IFN-γ ($p < 0.05$, Figure 2(m)) and significantly lower plasma levels of immunosuppressive cytokines TGF-β ($p < 0.05$, Figure 2(n)) and IL-10 ($p < 0.05$, Figure 2(o)) were observed in B16F10+MSC^{1d}-treated mice, indicating that MSCs, transplanted during the initial phase of melanoma growth, enhanced antitumor immune response in melanoma-bearing animals.

3.3. MSCs, Injected 14 Days after Melanoma Induction, Promoted Tumor Growth by Suppressing Antigen-Presenting Properties of Tumor-Infiltrating DCs and Macrophages and by Reducing Tumoricidal Capacity of NK Cells and T Lymphocytes. Compared to the tumors of B16F10+PBS^{14d}-treated mice, the significantly lower number of innate immune cells that play an important role in antitumor immunity (cytotoxic NK cells, inflammatory M1 macrophages and DCs) was observed in melanomas of B16F10+MSC^{14d}-treated animals. MSCs, transplanted 14 days after melanoma induction, attenuated tumoricidal capacity of NK cells, as evidenced by the lower number of tumor-infiltrating granzyme

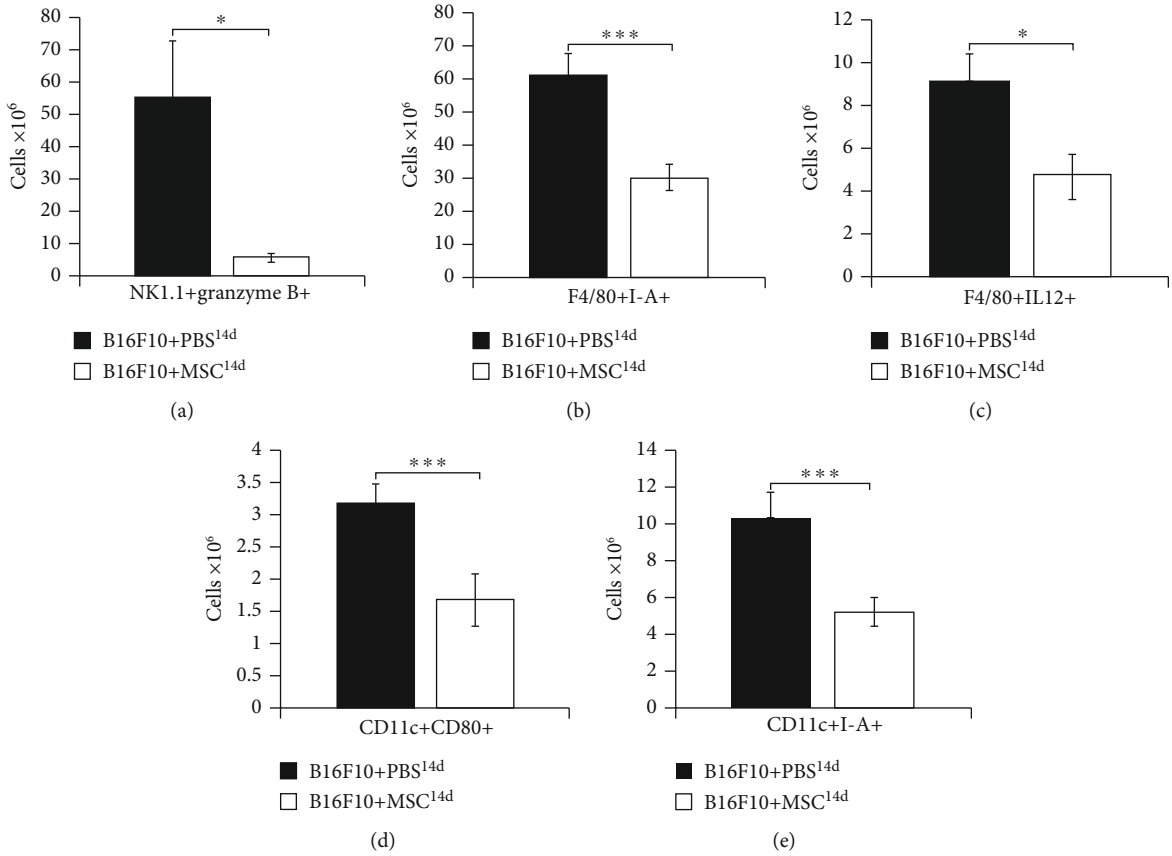

Figure 3: MSCs, injected 14 days after melanoma induction, promoted tumor growth by suppressing cytotoxicity of NK cells and by reducing antigen-presenting properties of tumor-infiltrating macrophages and DCs. Significantly lower number of granzyme B-expressing NK1.1+ cells (a), I-A-expressing and IL-12-producing F4/80+macrophages (b, c), and CD80- and I-A-expressing CD11c+DCs (d, e) were observed in the tumors of B16F10+MSC^{14d}-treated mice compared to the B16F10+PBS^{14d}-treated animals. Values are presented as the mean ± SEM; $n = 8$ mice/group. $^{*}p < 0.05$, $^{***}p < 0.001$.

B-expressing NK1.1+ cells in B16F10+MSCs^{14d}-treated mice ($p < 0.05$, Figure 3(a)). The significantly lower number of tumor-infiltrating, I-A-expressing ($p < 0.001$, Figure 3(b)), and IL-12-producing ($p < 0.05$, Figure 3(c)) F4/80+macrophages and CD80- and I-A-expressing CD11c+DCs ($p < 0.001$, Figures 3(d) and 3(e)) indicated that MSCs alleviated capacity of antigen-presenting cells for optimal activation of T cell-driven antitumor immune response.

As it is shown in Figure 4, MSCs, injected 14 days after melanoma induction, suppressed tumoricidal capacity of CD8+CTLs, CD4+Th1, and Th17 lymphocytes. Both subpopulations of effector T lymphocytes, CD4+T helper cells ($p < 0.001$, Figure 4(a)) and CD8+CTLs ($p < 0.001$, Figure 4(d)), were significantly reduced in the melanomas of B16F10+MSC^{14d}-treated mice compared to B16F10 +PBS^{14d}-treated animals. Intracellular staining revealed that MSCs suppressed production of tumoricidal cytokines (IFN-γ and IL-17) in CD4+Th1 and Th17 cells ($p < 0.05$ for TNF-α and IL-17, Figures 4(b) and 4(c)) and in CTLs ($p < 0.05$ for IFN-γ and IL-17, Figures 4(e) and 4(f)) of B16F10+MSC^{14d}-treated mice, preventing generation of optimal TNF-α, IFN-γ, and IL-17-driven antitumor immune response. Additionally, a significantly lower number of granzyme B-expressing CD8+CTLs were observed in the tumors of B16F10+MSC^{14d}-treated mice ($p < 0.05$, Figure 4(g)), indicating that MSCs injected 14 days after tumor induction significantly reduced the presence of cytotoxic and proapoptotic CD8+CTLs in the tumors of melanoma-bearing animals.

Furthermore, significantly lower levels of antitumorigenic cytokines TNF-α and IFN-γ ($p < 0.05$, Figures 4(h) and 4(i)) and significantly higher levels of TGF-β and IL-10 ($p < 0.001$, Figures 2(j) and 2(k)) were noticed in the plasma samples of B16F10+MSC^{14d}-treated mice, indicating that MSCs, injected during the progressive stage of melanoma development, attenuated antitumor immunity by increasing production of immunosuppressive cytokines in tumor-bearing animals.

4. Discussion

It is well known that exogenously administered MSCs could migrate to the tumor site where it regulates tumor growth and progression by modulating antitumor immune response [19]. Opposite findings, demonstrating a pro- or anticancer action of transplanted MSCs, were reported in different experimental studies [9–11]. While several research groups revealed that MSCs increased tumor progression [9–11]; results presented in other animal studies showed that

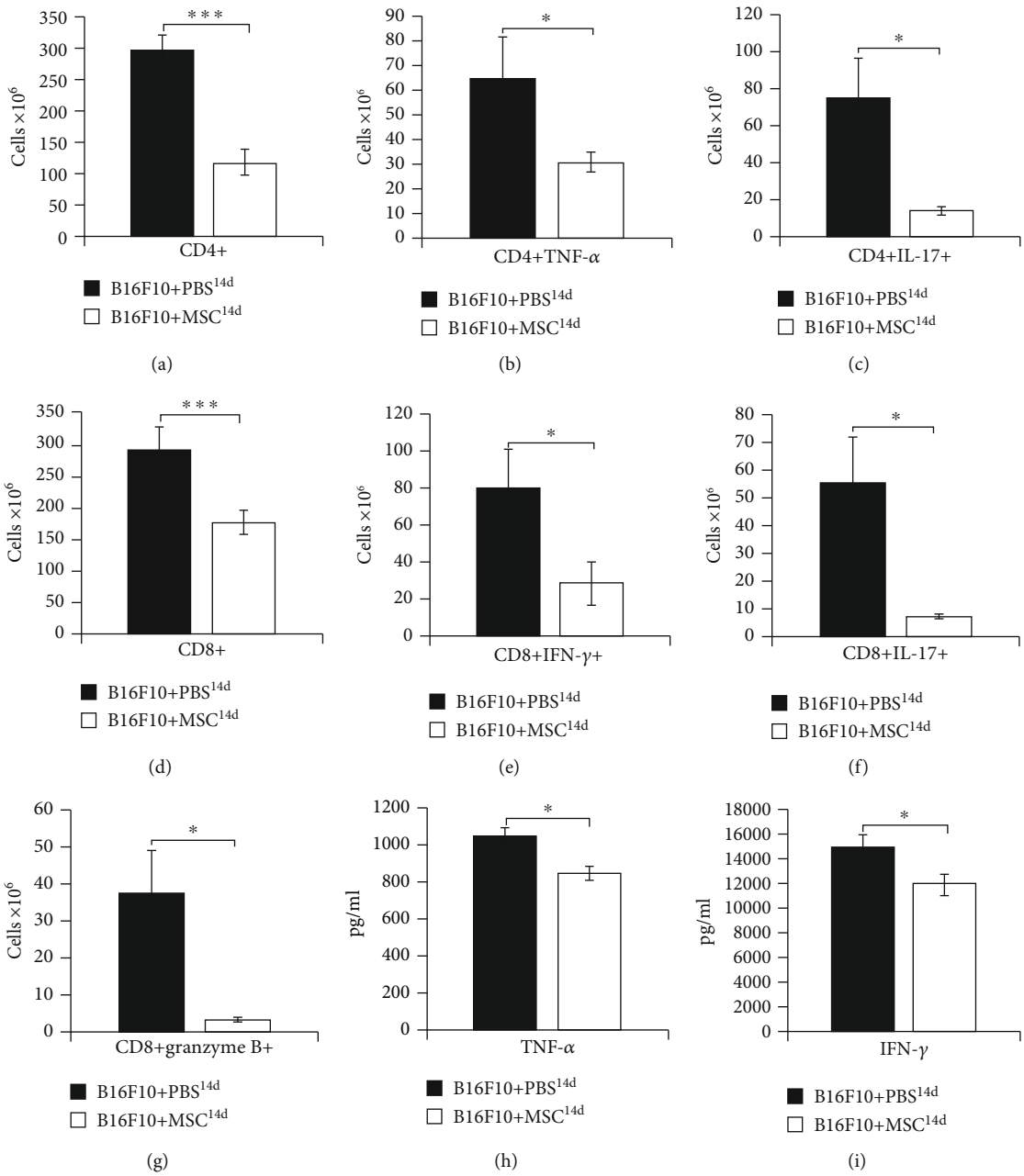

Figure 4: Continued.

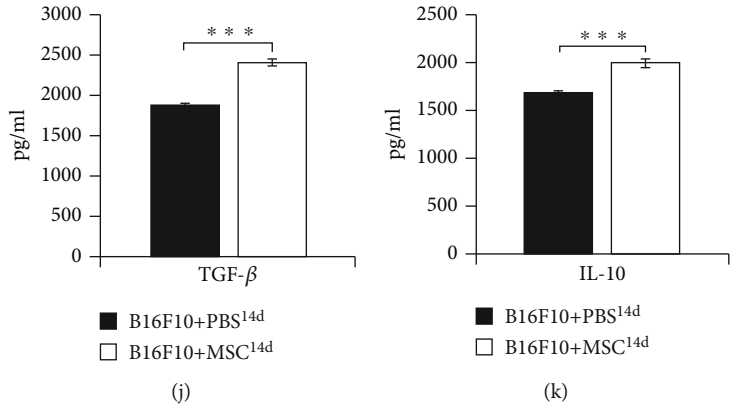

Figure 4: MSCs, injected 14 days after melanoma induction, increased plasma levels of immunosuppressive cytokines and suppressed T cell-driven antitumor immune response in melanoma-bearing animals. Significantly lower number of tumor-infiltrating CD4+T cells (a), TNF-α and IL-17-producing CD4+Th1 and Th17 cells (b, c), CD8+CTLs (d), IFN-γ and IL-17-producing CD8+CTLs (e, f), granzyme B-expressing CD8+CTLs (g), significantly lower plasma levels of antitumorigenic cytokines TNF-α and IFN-γ (h, i), and significantly higher plasma levels of immunosuppressive cytokines TGF-β and IL-10 (j, k) were noticed in B16F10+MSC^{14d}-treated mice compared to the B16F10+PBS^{14d}-treated animals. Values are presented as the mean ± SEM; $n = 8$ mice/group. $^{*}p < 0.05$, $^{***}p < 0.001$.

transplantation of MSCs led to the alleviation of tumor growth [12–14]. Herewith, we demonstrated that MSCs exert opposite, anti- or protumorigenic action, in the different stages of melanoma progression. MSCs injected in the initial phase of melanoma growth showed a tumor-suppressive effect, while MSCs, administered in the progressive stage of melanoma development, significantly enhanced tumor growth and expansion (Figure 1). In line with our findings are results obtained by Zong and colleagues which are showing that MSC-based effects on progression and metastasis of HCC depend on the stage of cancer development [14]. Although MSCs exhibit tumor-inhibitory effects in the initial phase of HCC development, potent suppression of antitumor immunity accompanied by enhanced HCC progression and metastasis is observed in HCC-bearing rats that received MSCs in the progressive stage of tumor growth [14]. MSCs injected in the initial stage of HCC progression engraft in the microenvironment with the reduced expression of proinflammatory cytokines, while MSCs injected in the progressive phase of HCC growth are exposed to the high levels of inflammatory cytokines [14]. According to the conclusion of Zong and coworkers, the interactions between transplanted MSCs and tumor microenvironment and diverse outcomes of MSC-based therapy depend on the strength of local and systemic inflammatory response during the different phases of hepatocarcinogenesis [14].

Several lines of evidence demonstrated that the ratio between inflammatory and anti-inflammatory cytokines in the microenvironment to which MSCs are exposed directly affects their phenotype and function [18, 20, 21]. When MSCs engraft in the tissue with low levels of inflammatory cytokines and high levels of immunosuppressive cytokines, they adopt proinflammatory (MSC1) phenotype, becoming capable of eliciting potent inflammatory response [20]. On the contrary, MSCs exposed to the high concentration of inflammatory cytokines develop immunosuppressive (MSC2) phenotype, produce a large number of anti-inflammatory factors, and inhibit immune response [18, 20, 21].

Dynamic balance of pro- and anti-inflammatory cytokines within tumor microenvironment regulates melanoma growth and progression [22]. Melanoma cell-derived immunosuppressive cytokines TGF-β and IL-10 play a crucially important role in the process of tumor initiation [23–25]. Tumor cell-derived TGF-β acts on CTLs to specifically repress the expression of perforin, granzyme B, and FasL and to reduce the production of IFN-γ, resulting in a significant attenuation of CTL-mediated tumor cytotoxicity [26]. Through the production of IL-10, melanoma cells prevent maturation of DCs, suppress production of Th1-inducing cytokine IL-12 in DCs, and inhibit their antigen-presenting properties, attenuating generation of effector CD4+Th1 and CD8+CTLs [27]. Furthermore, melanoma cell-primed DCs produce large amounts of immunosuppressive cytokines and significantly contribute to the development of immunosuppressive microenvironment that favors enhanced tumor growth and progression [23–25]. Excessive proliferation of melanoma cells activates stromal and melanoma-residing immune cells (macrophages, DCs, NK, and NKT cells) which produce a large amount of proinflammatory chemokines and cytokines (TNF-α, IL-12, IFN-γ, and IL-17) that facilitate the massive influx of circulating leucocytes in the tumors and enable generation and expansion of tumorotoxic CD8+CTLs, CD4+Th1, and Th17 cells in the peripheral lymph organs [28]. Generation of potent antitumor immune response during the progressive phase of melanoma growth results in the development of local and systemic inflammation that attenuates melanoma progression [22]. In line with these findings, we assume that changes in the balance between pro- and anti-inflammatory cytokines at the time of MSC administration (initial versus progressive stage of melanoma growth) were crucially responsible for the generation of inflammatory (MSC1) or immunosuppressive (MSC2) phenotype in MSCs after their engraftment in the melanoma-bearing mice (Figure 1).

MSC1, generated in the immunosuppressive microenvironment, produce lymphocyte-attracting chemokines (CCL5,

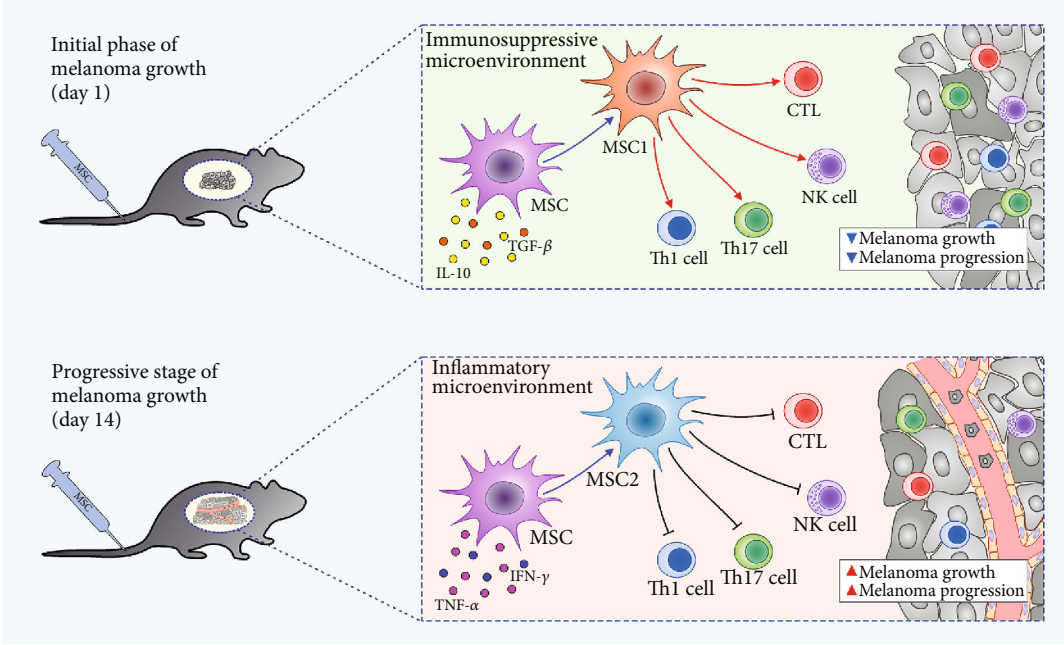

Figure 5: The effects of MSCs on antimelanoma immunity depend on the timing of their administration. MSCs transplanted during the initial phase of melanoma growth exerted tumor-suppressive effects. Since these MSCs were exposed to the immunosuppressive microenvironment (established by IL-10 and TGF-β-producing tumor cells), they acquired inflammatory, MSC1 phenotype and induced expansion of cytotoxic NK cells and antitumorigenic CD8+CTLs, CD4+Th1, and Th17 lymphocytes, resulting in attenuated melanoma growth and progression. On the contrary, MSCs transplanted during the progressive stage of melanoma development were exposed to the high concentration of inflammatory cytokines (TNF-α and IFN-γ) and generated immunosuppressive, MSC2 phenotype. Accordingly, enhanced melanoma growth and reduced number of tumor-infiltrating antigen-presenting cells (macrophages and DCs), cytotoxic CTLs and NK cells, and antitumorigenic CD4+Th1 and Th17 lymphocytes were observed in melanoma-bearing mice which received MSCs during the progressive stage of tumor development.

CXCL9, and CXCL10) that recruit CTLs and NK cells to the sites of injury and inflammation [20]. Additionally, MSC1 enhance NK and T cell-dependent antitumor immune response by increasing production of proinflammatory cytokines (TNF-α, IFN-γ, and IL-17) in these cytotoxic cells [18]. NK cells and CTLs, in a FasL, perforin, and granzyme B-dependent manner, induce apoptosis of melanoma cells [29, 30], while, in an IFN-γ and IL-17-dependent manner, enhance antigen-presenting properties of DCs and proinflammatory properties of tumor-infiltrating neutrophils, contributing to the generation of the strong antitumor immune response [31, 32]. In line with these findings, we assume that MSC transplanted in the immunosuppressive microenvironment of B16F10+MSC^{1d}-treated animals acquired MSC1 phenotype. MSC1 cells inhibited production of immunosuppressive cytokines (IL-10 and TGF-β) in tumor-infiltrating immune cells and promoted generation and influx of cytotoxic, FasL, perforin, and granzyme B-expressing and IFN-γ- and IL-17-producing CTLs and NK cells in the tumors of B16F10+MSC^{1d}-treated mice which resulted in reduced melanoma growth and progression (Figure 2).

In contrast to the B16F10+MSC^{1d}-treated animals, MSCs that were transplanted in B16F10+MSC^{14d}-treated mice were exposed to the higher levels of inflammatory cytokines (Figure 1) and generated immunosuppressive, MSC2 phenotype. MSC2, in an IL-10 and TGF-β-dependent manner, inhibit maturation of DCs and reduce production of inflammatory cytokines and expression of costimulatory and major histocompatibility class (MHC) II molecules on DCs and macrophages, attenuating their antigen-presenting properties [33]. In line with these findings, we observed a significantly lower number of CD80 and I-A-expressing DCs and reduced presence of IL-12-producing and I-A-expressing macrophages in the tumors of B16F10+MSC^{14d}-treated mice compared to B16F10+PBS^{14d}-treated animals (Figure 3). MSC2-mediated alleviation of antigen-presenting capacity of tumor-infiltrating DCs resulted in unoptimal activation of naïve CD4+ and CD8+T lymphocytes which led to the reduced presence of effector CD4+Th1 and Th17 cells and CD8+CTLs in the tumors of B16F10+MSC^{14d}-treated mice (Figure 4). The reduced number of tumor-infiltrating CTLs, Th1, and Th17 cells corresponded to the increased plasma levels of TGF-β and IL-10 in B16F10+MSC^{14d}-treated animals, indicating the important role of TGF-β and IL-10 in MSC-mediated suppression of T cell-driven antitumor immune response. It is well known that MSC2, through the production of TGF-β and IL-10, directly suppress activation of the Jak-Stat signaling pathway in proliferating T lymphocytes, causing the G1 cell cycle arrest [34]. Additionally, MSC2-sourced TGF-β and IL-10 downregulate production of inflammatory cytokines and reduce cytotoxicity of Th1 and Th17 cells and CTLs, contributing to the enhanced tumor growth and progression [35, 36]. Therefore, we believe that MSCs that were injected in B16F10-treated mice during the progressive stage of melanoma growth adopted immunosuppressive MSC2 phenotype and in a TGF-β and IL-10-

dependent manner attenuated antitumor immune response, resulting in increased melanoma growth.

In summing up, MSCs have an opposite role in the different stages of melanoma progression. MSCs transplanted during the initial phase of melanoma growth exert tumor-suppressive effect, while MSCs injected in the progressive stage of melanoma development suppressed antitumor immunity and enhanced tumor expansion (Figure 5). Therefore, the timing of MSC administration into the tumor microenvironment is crucially important for MSC-dependent modulation of melanoma progression.

Data Availability

The data used to support the findings of this study are included within the article.

Conflicts of Interest

The authors declare no conflict of interest.

Acknowledgments

This work was supported by the European Crohn's and Colitis Organization (ECCO) (grant "The role of galectin 3 in acute colitis"), ECLAT, spin off of the Università di Catania (Replica grant), Swiss National Science Foundation (IZSEZ0 185546), Serbian Ministry of Science (ON175069 and ON175103), and Faculty of Medical Sciences University of Kragujevac (MP01/18).

References

[1] Y. Liu and M. S. Sheikh, "Melanoma: molecular pathogenesis and therapeutic management," *Molecular and Cellular Pharmacology*, vol. 6, no. 3, p. 228, 2014.

[2] R. W. Jenkins and D. E. Fisher, "Treatment of advanced melanoma in 2020 and beyond," *Journal of Investigative Dermatology*, vol. 20, pp. 31257–31264, 2020.

[3] V. Volarevic, B. Ljujic, P. Stojkovic, A. Lukic, N. Arsenijevic, and M. Stojkovic, "Human stem cell research and regenerative medicine–present and future," *British Medical Bulletin*, vol. 99, no. 1, pp. 155–168, 2011.

[4] M. E. Castro-Manrreza, "Participacion de las celulas troncales mesenquimales en la regulacion de la respuesta inmune y el desarrollo de cancer," *Boletín Médico del Hospital Infantil de México*, vol. 73, no. 6, pp. 380–387, 2016.

[5] S. Kidd, E. Spaeth, J. Dembinski et al., "Direct evidence of mesenchymal stem cell tropism for tumor and wounding microenvironments using in vivo bioluminescent imaging," *Stem Cells*, vol. 10, pp. 2614–2623, 2009.

[6] A. Poggi, S. Varesano, and M. R. Zocchi, "How to hit mesenchymal stromal cells and make the tumor microenvironment immunostimulant rather than immunosuppressive," *Frontiers in Immunology*, vol. 9, p. 262, 2018.

[7] R. M. Dwyer, S. M. Potter-Beirne, K. A. Harrington et al., "Monocyte chemotactic protein-1 secreted by primary breast tumors stimulates migration of mesenchymal stem cells," *Clinical Cancer Research*, vol. 13, no. 17, pp. 5020–5027, 2007.

[8] S. Galland and I. Stamenkovic, "Mesenchymal stromal cells in cancer: a review of their immunomodulatory functions and dual effects on tumor progression," *The Journal Of Pathology*, vol. 250, no. 5, pp. 555–572, 2020.

[9] A. De Boeck, P. Pauwels, K. Hensen et al., "Bone marrow-derived mesenchymal stem cells promote colorectal cancer progression through paracrine neuregulin 1/HER3 signalling," *Gut*, vol. 62, no. 4, pp. 550–560, 2013.

[10] A. E. Karnoub, A. B. Dash, A. P. Vo et al., "Mesenchymal stem cells within tumour stroma promote breast cancer metastasis," *Nature*, vol. 449, no. 7162, pp. 557–563, 2007.

[11] P. Y. Hernanda, A. Pedroza-Gonzalez, L. J. van der Laan et al., "Tumor promotion through the mesenchymal stem cell compartment in human hepatocellular carcinoma," *Carcinogenesis*, vol. 34, no. 10, pp. 2330–2340, 2013.

[12] Y. Yulyana, I. A. Ho, K. C. Sia et al., "Paracrine factors of human fetal MSCs inhibit liver cancer growth through reduced activation of IGF-1R/PI3K/Akt signaling," *Molecular Therapy*, vol. 23, no. 4, pp. 746–756, 2015.

[13] R. H. Lee, N. Yoon, J. C. Reneau, and D. J. Prockop, "Preactivation of human MSCs with TNF-α enhances tumor-suppressive activity," *Cell Stem Cell*, vol. 11, no. 6, pp. 825–835, 2012.

[14] C. Zong, H. Zhang, X. Yang et al., "The distinct roles of mesenchymal stem cells in the initial and progressive stage of hepatocarcinoma," *Cell Death & Disease*, vol. 9, no. 3, p. 345, 2018.

[15] M. Potez, C. Fernandez-Palomo, A. Bouchet et al., "Synchrotron microbeam radiation therapy as a new approach for the treatment of radioresistant melanoma: potential underlying mechanisms," *International Journal of Radiation Oncology • Biology • Physics*, vol. 105, no. 5, pp. 1126–1136, 2019.

[16] V. Volarevic, B. S. Markovic, M. G. Jankovic et al., "Galectin 3 protects from cisplatin-induced acute kidney injury by promoting TLR-2-dependent activation of IDO1/Kynurenine pathway in renal DCs," *Theranostics*, vol. 9, no. 20, pp. 5976–6001, 2019.

[17] S. F. Ngiow, B. von Scheidt, A. Möller, M. J. Smyth, and M. W. L. Teng, "The interaction between murine melanoma and the immune system reveals that prolonged responses predispose for autoimmunity," *Oncoimmunology*, vol. 2, no. 2, article 23036, 2013.

[18] M. Gazdic, V. Volarevic, N. Arsenijevic, and M. Stojkovic, "Mesenchymal stem cells: a friend or foe in immune-mediated diseases," *Stem Cell Reviews and Reports*, vol. 11, no. 2, pp. 280–287, 2015.

[19] W. Lin, L. Huang, Y. Li et al., "Mesenchymal stem cells and cancer: clinical challenges and opportunities," *BioMed Research International*, vol. 2019, Article ID 2820583, 12 pages, 2019.

[20] W. Li, G. Ren, Y. Huang et al., "Mesenchymal stem cells: a double-edged sword in regulating immune responses," *Cell Death & Differentiation*, vol. 19, no. 9, pp. 1505–1513, 2012.

[21] R. S. Waterman, S. L. Tomchuck, S. L. Henkle, and A. M. Betancourt, "A new mesenchymal stem cell (MSC) paradigm: polarization into a pro-inflammatory MSC1 or an immunosuppressive MSC2 phenotype," *PLoS One*, vol. 5, no. 4, article e10088, 2010.

[22] M. Neagu, C. Constantin, C. Caruntu, C. Dumitru, M. Surcel, and S. Zurac, "Inflammation: a key process in skin tumorigenesis," *Oncology Letters*, vol. 17, no. 5, pp. 4068–4084, 2018.

[23] A. Busse and U. Keilholz, "Role of TGFβ in melanoma," *Current Pharmaceutical Biotechnology*, vol. 12, no. 12, pp. 2165–2175, 2011.

[24] A. P. Wiguna and P. Walden, "Role of IL-10 and TGF-β in melanoma," *Experimental Dermatology*, vol. 24, no. 3, pp. 209–214, 2015.

[25] G. A. Rabinovich, D. Gabrilovich, and E. M. Sotomayor, "Immunosuppressive strategies that are mediated by tumor cells," *Annual Review of Immunology*, vol. 25, no. 1, pp. 267–296, 2007.

[26] D. A. Thomas and J. Massagué, "TGF-β directly targets cytotoxic T cell functions during tumor evasion of immune surveillance," *Cancer Cell*, vol. 8, no. 5, pp. 369–380, 2005.

[27] G. Gerlini, A. Tun-Kyi, C. Dudli, G. Burg, N. Pimpinelli, and F. O. Nestle, "Metastatic melanoma secreted IL-10 down-regulates CD1 molecules on dendritic cells in metastatic tumor lesions," *The American Journal of Pathology*, vol. 164, no. 6, pp. 1853–1863, 2004.

[28] A. Passarelli, F. Mannavola, L. S. Stucci, M. Tucci, and F. Silvestris, "Immune system and melanoma biology: a balance between immunosurveillance and immune escape," *Oncotarget*, vol. 8, no. 62, pp. 106132–106142, 2017.

[29] J. Leignadier, S. Favre, S. A. Luther, and I. F. Luescher, "CD8 engineered cytotoxic T cells reprogram melanoma tumor environment," *OncoImmunology*, vol. 5, no. 3, article e1086861, 2015.

[30] L. Zhu, S. Kalimuthu, P. Gangadaran et al., "Exosomes derived from natural killer cells exert therapeutic effect in melanoma," *Theranostics*, vol. 7, no. 10, pp. 2732–2745, 2017.

[31] L. Ni and J. Lu, "Interferon gamma in cancer immunotherapy," *Cancer Medicine*, vol. 7, no. 9, pp. 4509–4516, 2018.

[32] Y. S. Chen, T. H. Huang, C. L. Liu et al., "Locally targeting the IL-17/IL-17RA axis reduced tumor growth in a murine B16F10 melanoma model," *Human Gene Therapy*, vol. 30, no. 3, pp. 273–285, 2019.

[33] C. R. Harrell, M. G. Jankovic, C. Fellabaum et al., "Molecular mechanisms responsible for anti-inflammatory and immunosuppressive effects of mesenchymal stem cell-derived factors," *Advances in Experimental Medicine and Biology*, vol. 1084, pp. 187–206, 2019.

[34] J. J. Bright, L. D. Kerr, and S. Sriram, "TGF-beta inhibits IL-2-induced tyrosine phosphorylation and activation of Jak-1 and stat 5 in T lymphocytes," *The Journal of immunology*, vol. 159, no. 1, pp. 175–183, 1997.

[35] V. Volarevic, M. Gazdic, B. Simovic Markovic, N. Jovicic, V. Djonov, and N. Arsenijevic, "Mesenchymal stem cell-derived factors: immuno-modulatory effects and therapeutic potential," *BioFactors*, vol. 43, no. 5, pp. 633–644, 2017.

[36] R. García-Rocha, M. Moreno-Lafont, and M. L. Mora-García, "Mesenchymal stromal cells derived from cervical cancer tumors induce TGF-β1 expression and IL-10 expression and secretion in the cervical cancer cells, resulting in protection from cytotoxic T cell activity," *Journal of Translational Medicine*, vol. 76, no. 2, pp. 382–390, 2015.

Hindawi
Stem Cells International
Volume 2020, Article ID 8867115, 14 pages
https://doi.org/10.1155/2020/8867115

Research Article

The Role of Caspase-4 and NLRP1 in MCF7 Cell Pyroptosis Induced by hUCMSC-Secreted Factors

Yang Jiao,[1,2] Linlin Wang,[2] Lin Lu,[2] Jianjun Liu,[2] Xin Li,[2] Hongbo Zhao,[2] Zongliu Hou,[3] and Bingrong Zheng[1]

[1]*State Key Laboratory for Conservation and Utilization of Bio-Resources in Yunnan & School of Medicine, Yunnan University, Kunming, 650091 Yunnan, China*
[2]*Yunnan Key Laboratory of Stem Cell and Regenerative Medicine, Biomedical Engineering Research Center, Kunming Medical University, Kunming, 650500 Yunnan, China*
[3]*Yan'an Hospital of Kunming City, Kunming, 650051 Yunnan, China*

Correspondence should be addressed to Zongliu Hou; hzl579@163.com and Bingrong Zheng; zhengbr@ynu.edu.cn

Received 20 April 2020; Revised 12 June 2020; Accepted 17 June 2020; Published 9 July 2020

Academic Editor: Jane Ru Choi

Mesenchymal stem cells (MSCs) are being widely investigated for the development of novel therapeutic approaches for different cancers, including breast cancer, the leading form of cancer in women. Our previous study showed that the factors secreted by human umbilical cord MSCs (hUCMSCs) induced pyroptosis in the breast cancer cell line MCF7 and our RNA sequencing studies revealed an increase in the expression of the pyroptosis-related gene caspase-4 (*CASP4*) and nucleotide-binding, leucine-rich repeat pyrin domain-containing protein 1 (*NLRP1*) in pyroptotic MCF7 cells. Cellular pyroptosis can occur via the canonical pathway (involving caspase-1 and NLRP1) or the noncanonical pathway (involving caspase-4). In this study, we first confirmed that the inflammasome complex formed by NLRP1 and ASC is involved in MCF7 cell pyroptosis induced by hUCMSC-CM. Further, we investigated the role of *CASP4* and *NLRP1* in MCF7 cell pyroptosis induced by hUCMSC-secreted factors using shRNA-mediated transfection of *CASP4* or *NLRP1* in MCF7 cells. Cytotoxicity analyses revealed that neither *CASP4* knockdown nor NLRP1 knockdown could inhibit the hUCMSC-CM-induced pyroptosis in MCF7 cells. Gene and protein expression analysis showed that hUCMSC-CM induced pyroptosis mainly via the canonical pathway in *CASP4* knockdown MCF7 cells but mainly via the noncanonical pathway in *NLRP1* knockdown MCF7 cells. Our study provides a foundation for further studies aimed at elucidating the precise mechanism underlying hUCMSC-induced pyroptosis in breast cancer cells and aid the identification of potential therapeutic targets for breast cancer.

1. Introduction

Pyroptosis, a type of programmed cell death accompanied with the release of several proinflammatory factors, plays an important role in immune response against infection. The morphological changes associated with pyroptosis involve pore formation in the plasma membrane, water influx, cell swelling, and the subsequent rupture of the plasma membrane and release of intracellular proinflammatory molecules [1]. In humans, pyroptosis is mediated by inflammatory caspases (caspase-1, caspase-4, and caspase-5), which may be activated by inflammasomes. The inflammasome pathways include the caspase-1-dependent canonical pathway and caspase-1-independent noncanonical pathway [2]. Caspase-1 activation induces gasdermin D cleavage, thereby leading to pore formation in the cell membrane and the maturation and release of IL-1β and IL-18 cytokines, which induce pyroptosis [3]. Nucleotide-binding, leucine-rich repeat pyrin domain-containing protein 1 (NLRP1), a member of NOD-like receptor (NLR) family, is an important natural immune molecule [4]. In humans, it activates pro-caspase-1 directly by interacting with it or indirectly by recruiting the adaptor protein ASC and pro-caspase-1 to form an inflammasome [5]. Therefore, NLRP1 plays an important role in cell pyroptosis mediated by the canonical pathway. The noncanonical pathway in humans

involves the activation of caspase-4/caspase-5 [2].Caspase-4/caspase-5 cleaves gasdermin D, thereby triggering pyroptosis [6]. In human macrophages, caspase-4 activation by *Legionella pneumophila* induced cell death and IL-1α secretion [7]. Intracellular lipopolysaccharide (LPS) directly interacts with caspase-4 and induces cell pyroptosis [8].

Breast cancer is the leading type of cancer among women [9], and rising breast cancer incidence has been reported in China [10]. However, an effective treatment for breast cancer is not yet available. Mesenchymal stem cell- (MSC-) based approaches are being studied extensively for the development of new cancer therapeutic strategies. Human umbilical cord mesenchymal stem cells (hUCMSCs) are widely used in research focused on cancer treatment owing to their easy availability and no ethical issues [11–13]. We previously demonstrated that the factors secreted by hUCMSCs induced pyroptosis in the breast cancer cell line MCF7.Furthermore, RNA sequencing studies revealed a significant increase in the expression of pyroptosis-related genes *CASP4* and *NLRP1* in pyroptotic MCF7cells [14]. Thus, caspase-4 and NLRP1 may play a role in this process. Although some of the mechanisms underlying the function of *NLRP1* and *CASP4* in pyroptosis are known, the effects of these two genes in MCF7 cell pyroptosis induced by hUCMSC-secreted factors remain unclear. Therefore, in the present study, we elucidated the role of caspase-4 and NLRP1 on MCF7 cell pyroptosis induced by hUCMSC-secreted factors. Our study provides the possible mechanism underlying hUCMSC-induced pyroptosis in breast cancer cells and may provide potential therapeutic targets for breast cancer.

2. Materials and Methods

2.1. Cell Culture. The breast cancer cell line MCF7 (Kunming Cell Bank of the Chinese Academy of Sciences, Kunming, China) was maintained in Dulbecco's modified Eagle's medium (DMEM; Gibco by Thermo Fisher Scientific™, Suzhou, China) containing L-glutamine, 4.5 g/L glucose, and 110 mg/L sodium pyruvate and supplemented with 10% MSC-qualified fetal bovine serum (FBS; Biological Industries, Australia), 100 mg/L streptomycin, and 100 mg/L penicillin (Gibco by Thermo Fisher Scientific™, NY, USA) at 37°C with 5% CO_2.

The hUCMSCs were isolated from the human umbilical cord Wharton jelly and identified as described previously [14]. The study was approved by the Medical Ethics Committee of Yunnan University Medical School, and informed consent was obtained from all the donors. hUCMSCs were cultured in minimum essential medium alpha modification (αMEM; HyClone by GE Healthcare, Beijing, China) supplemented with 10% MSC-qualified FBS, 100 mg/L streptomycin, 100 mg/L penicillin, and 10 ng/mL basic fibroblast growth factor (bFGF; Merck Millipore, Darmstadt, Germany) at 37°C with 5% CO_2. The hUCMSCs were used before the eighth passage.

2.2. shRNA Vectors. Four different sets pGPH1/GFP/Neo vectors (Shanghai GeneChem Co., Ltd., Shanghai, China) expressing *CASP4* or *NLRP1*shRNA were used for *CASP4* or *NLRP1* knockdown. The sequences used for shRNA-mediated knockdown are listed in Table 1. The shRNA vectors were identified by sequencing, and the successful insertion of the target sequence in pGPH1/GFP/Neo vectors and the accuracy of the nucleotide sequences was confirmed (Additional file 1).

Table 1: Sequences used for shRNA knockdown.

Name	Sequences
Control	5′- TTCTCCGAACGTGTCACGT-3′
CASP4-100	5′- GCCACTTAAGGTGTTGGAATC -3′
CASP4-265	5′- GCAACGTATGGCAGGACAAAT -3′
CASP4-1104	5′-GGAAGGTACAGCAATCATTTG -3′
CASP4-801	5′- GCCTCAGTCTGAAGGACAAAC -3′
NLRP1-2009	5′- GCAGGAAGGAATATTTCTACA-3′
NLRP1-1634	5′- GCTTCCAGCATGTCTTCTACT-3′
NLRP1-2523	5′- GCTAGAAGCATATGGAATACA-3′
NLRP1-630	5′- GCTTCTGCTCGCCAATAAAGC-3′

2.3. Exposure of MCF7 Cells to hUCMSC-Conditioned Medium (hUCMSC-CM). hUCMSCs were cultured in plastic flasks (25 cm^2; Corning, NY, USA). At ~90% confluency, the cultured medium was collected and filter sterilized using a 0.22 μm Millex-GP Filter Unit (Millipore, Carrigtwohill, Ireland). Conditioned medium (CM) was prepared using 80% hUCMSC-cultured medium and 20% fresh medium, as described previously [14]. MCF7 cells were seeded in 6-well plates (Corning) at a density of 1×10^5 cells/mL in normal medium and cultured overnight. Then, the cells were transfected with 2.5 μg shRNA expression vectors per well using Lipofectamine 3000 reagent for 72 h. The medium was then replaced with hUCMSC-CM.

2.4. ASC Speck Staining. MCF7 cells were seeded on cover slips in a 24-well plate (Corning, NY, USA) containing normal medium and cultured overnight. Then, the medium was replaced with hUCMSC-CM. After 24 h, the cells were fixed with 4% paraformaldehyde, permeabilized with 0.1% Triton X-100, and blocked with PBS buffer containing 5% BSA. Cells were stained with anti-ASC antibody (1 : 100; Proteintech, Wuhan, China) and AlexaFluor488-conjugated secondary antibody (1 : 200; Thermo Fisher Scientific, Shanghai, China), and with anti-NLRP1 antibody (1 : 100; Santa Cruz Biotechnology) and AlexaFluor594-conjugated secondary antibody (1 : 200; Thermo Fisher Scientific, Shanghai, China). DAPI was used to stain nuclei. Cell images were captured using inverted phase contrast optics (Leica DFC420C).

2.5. Annexin V/Propidium Iodide (PI) Analysis. MCF7 cells were collected at 72 h after transfection and cultured in hUCMSC-CM for 24 h. The percentage of dead cells was determined using the Annexin V-FITC/PI apoptosis detection kit (CWBio, Beijing, China). Briefly, cells were collected after trypsin digestion without EDTA and washed three

times with cold PBS. The cells were resuspended in a binding buffer at a density of 1×10^6 cells/mL, incubated with 10 μL PI and 5 μL Annexin V-fluorescein isothiocyanate (FITC) for 10 min at 37°C, and analyzed using the CyFlow Space flow cytometer (Sysmex Partec) and FloMax 2.82 software (Sysmex Partec).

2.6. LDH Cytotoxicity Assay. The degree of cell damage was determined using LDH-Glo™ Cytotoxicity Assay (Promega, Beijing, China). MCF7 cells were collected at 48 h after transfection, seeded in 96-well plates (Corning) at a density of 5×10^3 cells/mL, and cultured overnight. The medium was replaced with hUCMSC-CM, and the cells were cultured for 24 h. Then, 5 μL cultured medium was added into 95 μL LDH Storage Buffer, and the resulting solution was diluted five times using the LDH Storage Buffer. Diluted standard solutions were prepared per the manufacturer's instructions. Then, 50 μL sample/standard was incubated with 50 μL LDH Detection Reagent in each well of an opaque 96-well plate at 20–25°C for 1 h, and the luminescence was recorded using the Modulus Microplate Multimode Reader (Turner Biosystems, California, USA).

2.7. Reverse Transcription Quantitative Real-Time Polymerase Chain Reaction (RT-qPCR). MCF7 cells were collected at 72 h after transfection and cultured in hUCMSC-CM for 24 h. Total RNA was extracted using the TRIzol™ reagent (Invitrogen, Carlsbad, CA, USA). The quantity and quality of RNA were assessed using the Nano-300 spectrophotometer (Hangzhou Allsheng Instruments Co., Ltd., Hangzhou, China). First-stand cDNA was synthesized using the PrimeScript™ RT Reagent Kit with gDNA Eraser (Takara Bio., Beijing, China). The primer sequences were designed using the PrimerQuest Tool (http://http://www.idtdna.com); the sequences are listed in Table 2. q-PCR was performed using FastStart Universal SYBR Green Master (Roche, Mannheim, Germany) and Bio-Rad CFX96™ Real-Time PCR Detection System (Bio-Rad, Shanghai, China). Relative quantification was performed using the comparative Ct ($2^{-\Delta\Delta Ct}$) method [15].

2.8. Western Blotting. MCF7 cells transfected for 72 h and cultured in hUCMSC-CM for 24 h were lysed in 50 μL RIPA lysis buffer (strong) containing 0.5 μL phenylmethylsufonyl fluoride (CWBio, Jiangsu, China) and incubated on ice for 2 h. The lysed cells were incubated with 50 μL of 2x SDS-PAGE protein loading buffer (Bio-Rad) in boiling water for 10 min. After centrifugation, the protein samples were subjected to 10% SDS-PAGE and transferred onto polyvinylidene difluoride membranes (Merck Millipore). The membranes were blocked in TBST (3.0 g Tris-HCl, 8.0 g NaCl, 0.1% Tween-20, and pH 7.4) containing 5% nonfat dried milk for 1 h and incubated overnight at 4°C with diluted primary antibodies against GAPDH (1 : 2000; CWBio, Jiangsu, China), caspase-1 (1 : 500; Santa Cruz Biotechnology, Delaware, USA), NLRP1 (1 : 100; Santa Cruz Biotechnology), caspase-4 (1 : 500; Proteintech, Wuhan, China), and ASC (1 : 1000; Proteintech, Wuhan, China). The membranes were incubated with horseradish peroxidase-conjugated goat anti-mouse IgG or goat anti-rabbit IgG (1 : 2000; CWBio, Jiangsu, China) at 20–25°C for 1 h and then with ECL substrate solution (1 : 1 (*v*/*v*); CWBio, Jiangsu, China). The bands were quantified using Photoshop 7.0, and the gray value ratio of bands was determined.

Table 2: Primer sequences for quantitative real-time polymerase chain reaction.

Gene name	NCBI ID	Primer sequences
CASP1	NM_033292	S: 5′TACAGAGCTGGAGG CATTTG 3′ A: 5′GGACTTGCTCAGAGT GTTTCT 3′
NLRP1	NM_033004	S: 5′ATCTCATGCCTGCAA CTACTC 3′ A: 5′CTCTCGATACTGGT CCACAAAG 3′
CASP4	NM_001225	S: 5′GAATCTGACAGCCA GGGATATG 3′ A: 5′CCATGAGACATGAGTA CCAAGAA 3′

2.9. ELISA-Based Quantification of Secreted IL-α, IL-1β, and IL-18. Media from MCF7 cells transfected with shRNA vectors for 72 h (control group) and media from MCF7 cells transfected with shRNA vectors for 72 h and cultured in hUCMSC-CM for 24 h (treatment group) were collected. All the samples were stored at -80°C before detection. The amounts of IL-α, IL-1β, and IL-18 secreted by MCF7 cells in the control and treatment groups were determined using the Human IL-α ELISA Kit (ExCell Biotech, Jiangsu, China), Human IL-1β/IL-1F2 Valukine™ ELISA Kit (NOVUS Biologicals, Taiwan, China), and Human IL-18 Kit (OriGene, Rockville, MD, USA) separately, according to the manufacturer's instructions.

2.10. Statistical Analyses. Statistical analyses were performed using Microsoft Excel 2007 and GraphPad Prism 5 software; graphs were prepared using the GraphPad Prism 5 software. Differences with P values < 0.05 were considered statistically significant.

3. Results

3.1. Effect of hUCMSC-CM Treatment on mRNA and Protein Levels of Caspase-1, Caspase-4, and NLRP1 in MCF7 Cells. We previously demonstrated that the factors secreted by hUCMSCs induced pyroptosis in MCF7 cells and that such pyroptotic cells showed significantly increased CASP4 and NLRP1 expression [14]. To further confirm this result, we analyzed the expression of *CASP1*, *CASP4*, and *NLRP1*in MCF7 cells cultured in hUCMSC-CM for 48 h. RT-qPCR analysis showed that *CASP1*, *CASP4*, and *NLRP1* mRNA levels in MCF7 cells cultured in hUCMSC-CM were significantly higher (fold increase of 5.16 ± 1.92, 5.48 ± 2.62, and

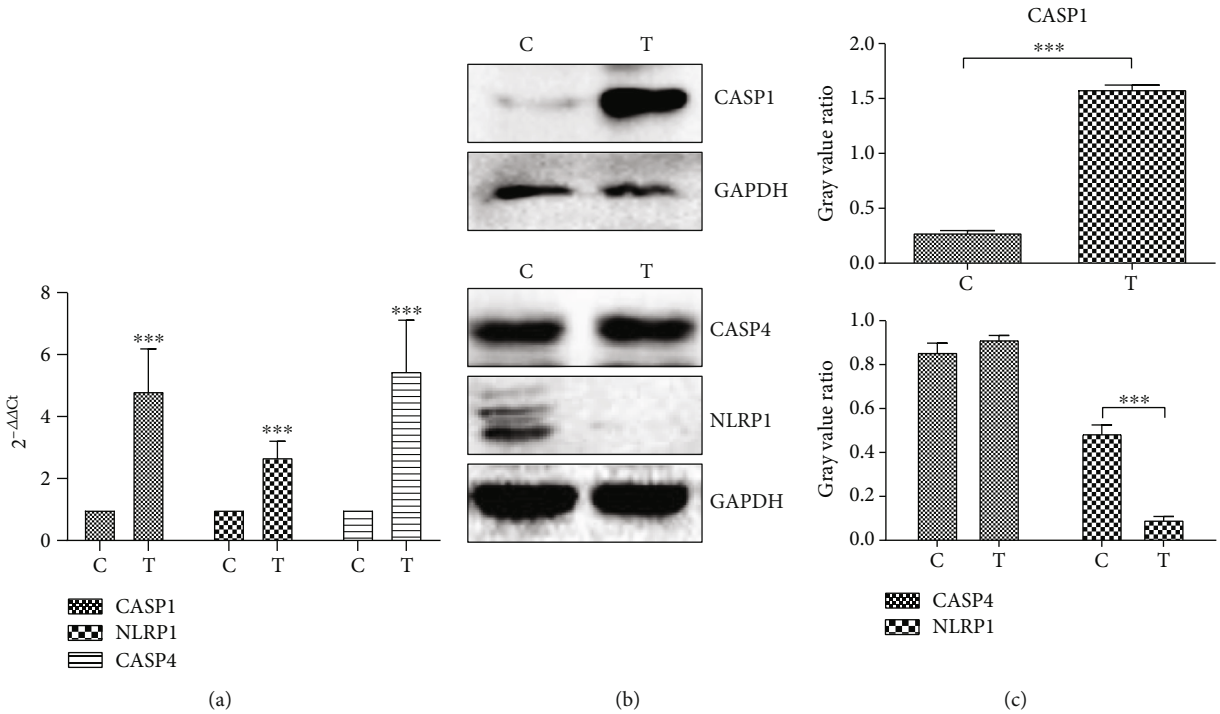

Figure 1: Detection of pyroptosis-related genes. (a) The results of q-PCR. Data are presented as Ct ($2^{-\Delta\Delta Ct}$) relative to control. Data are presented as mean ± S.D., $n = 3$. (b) The results of western blotting. (c) The gray value ratio of western blotting results. C: control group, MCF7 cells cultured in the hUCMSC medium; T: treatment group, MCF7 cells cultured in hUCMSC-CM medium. $^{*}P < 0.05$, $^{**}P < 0.01$, and $^{***}P < 0.001$.

2.89 ± 0.79, respectively) than those in the control cells ($P < 0.001$; Figure 1(a)). These results were consistent with our previous RNA sequencing results.

In order to know whether the changes of mRNA level affect the protein expression, we did the western blotting analysis. Compared to the control cells, the cells cultured in hUCMSC-CM showed a significant increase in CASP1 protein levels ($P < 0.001$), no significant change in CASP4 protein levels ($P > 0.05$), and significant decrease in NLRP1 protein levels ($P < 0.001$; Figures 1(b) and 1(c)). These results indicate that the changes in protein levels of these three molecules are not consistent with the changes in their respective mRNA levels. Caspase-1 usually exists in cells in the inactive form as pro-caspase-1. In response to cellular stress or microbial infection, pro-caspase-1 is cleaved to p10 and p20 subunits, and the activated caspase-1 is a tetramer composed of two p20 and two p10 subunits (p20/p10) [16]. Caspase-1 recruitment to inflammatory signaling hubs was reported to enable its activation likely by increasing the local concentration of pro-caspase-1 to facilitate the dimerization of the monomers [17]. Full-length caspase-1 monomers can undergo dimerization, activation, and self-cleavage only when they are recruited to the inflammasomes; this enables a high local concentration of monomers [18]. In our study, pyroptotic MCF7 cells showed a significant increase in CASP1 protein levels, which is consistent with these theories. Similar to caspase-1, caspase-4 exists in cells in an inactive form and its active form is a tetramer composed of two p20 and two p10 subunits (p20/p10). In the present study, pyroptotic MCF7 cells showed increased *CASP4* mRNA but not protein levels, possibly because of homeostasis, indicating that caspase-4 activation requires pro-caspase-4 consumption, and the increase in *CASP4* mRNA replenished the procaspase-4 amount consumed. NLRP1 interacts with the adaptor protein ASC to form an inflammasome complex, which recruits pro-caspase-1 [5]. Therefore, reduced NLRP1 protein levels observed in this study may be because the NLRP1 protein molecules were consumed for formation of the NLRP1 inflammasome, and these molecules were not detected by the antibody used in western blotting.

3.2. Effect of Inflammasome Complex Formed by NLRP1 and ASC on hUCMSC-CM-Induced Pyroptosis in MCF7 Cells. Next, we performed immunofluorescence analysis to investigate whether NLRP1 interacts with the adaptor protein ASC to form an inflammasome complex in pyroptotic MCF7 cells induced by hUCMSC-CM. Colocalization of NLRP1 protein and ASC protein to form a complex was observed in certain parts of some MCF7 cells cultured in hUCMSC-CM (red arrow, Figure 2), and strong colocalization and increased fluorescence intensities of both NLRP1 and ASC proteins were observed in pyroptotic cells (white arrow, Figure 2). These results indicate that NLRP1 could interact with ASC to form an inflammasome complex and that this complex is involved in hUCMSC-CM-induced pyroptosis in MCF7 cells.

3.3. Effect of CASP4 or NLRP1 Knockdown on hUCMSC-CM-Induced Pyroptosis in MCF7 Cells. On the basis of RT-qPCR analysis performed to assess the inhibition rate of shRNA

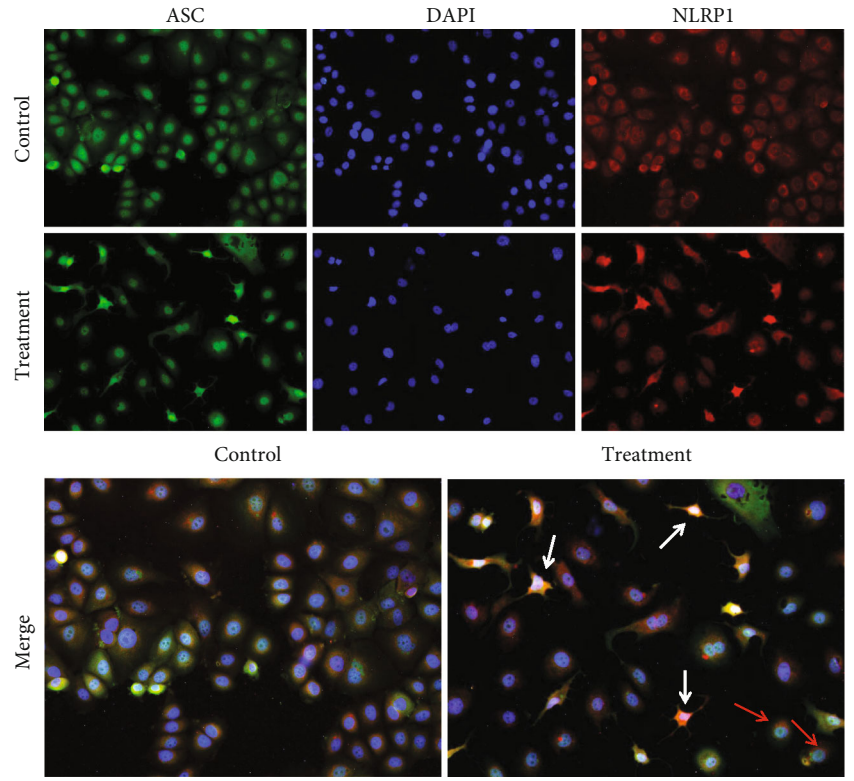

Figure 2: The immunofluorescence images of ASC specks. Representative micrographs from at least three independent experiments are shown. All images were taken using 20x magnification.

vectors, the vectors shRNA-*CASP4*-100, shRNA-*CASP4*-1104, shRNA-*NLRP1*-1634, and shRNA-*NLRP1*-2523 were selected for the transfection experiments (Additional file 2).

We first observed the morphological changes in the transfected MCF7 cells cultured in hUCMSC-CM. The plasma membrane of these cells remained intact but showed pore-induced invaginations. Distinctly ruptured plasma membrane and cell death were observed (Figure 3). These morphological changes indicate the occurrence of pyroptosis in transfected MCF7 cells after treatment with hUCMSC-CM.

To understand whether cell death decreased after *CASP4* or *NLRP1* knockdown, we performed the Annexin V-FITC/PI analysis in *CASP4* knockdown and *NLRP1* knockdown MCF7 cells. The numbers of $FITC^+/PI^+$ cells and $FITC^+/PI^-$ cells remained unchanged after hUCMSC-CM treatment. However, the number of $PI^+/FITC^-$ cells among the transfected cells increased significantly after treatment with hUCMSC-CM for 24 h. The numbers increased from 9.27 ± 0.60 to 39.42 ± 5.74, 8.86 ± 1.05 to 39.46 ± 1.18, 12.30 ± 0.22 to 33.55 ± 1.02, 11.81 ± 0.27 to 35.57 ± 0.33, and 14.56 ± 0.60 to 33.20 ± 0.14 in cells transfected with shRNA-NC (negative control), shRNA-*CASP4*-100, shRNA-*CASP4*-1104, shRNA-*NLRP1*-1634, and shRNA-*NLRP1*-2523, respectively (Figures 4(a) and 4(b)). The number of apoptotic cells in the groups transfected with the target genes was not significantly different from that in the NC group ($P > 0.05$). These results suggest that hUCMSC-CM treatment for 24 h induced pyroptosis in all the transfected MCF7 cell groups, including the cells transfected with NC. Thus, MCF7 cells cannot be rescued from hUCMSC-CM-induced pyroptosis by inhibiting the expression of *CASP4* or *NLRP1*.

To further confirm these results, we assessed cytotoxicity by measuring the LDH levels in the medium of the transfected MCF7 cells treated with hUCMSC-CM. The LDH levels in all the cell groups, including the NC group, increased after treatment with hUCMSC-CM for 24 h; however, no significant difference was observed between the LDH levels of the target gene-transfected groups and the NC group (Figure 4(c)). These results are consistent with those of Annexin V-FITC/PI analysis and indicate that *CASP4* or *NLRP1* inhibition could not prevent hUCMSC-CM-induced pyroptosis in MCF7 cells.

3.4. Effect of hUCMSC-CM Treatment on Gene Expression in Transfected MCF7 Cells. Although inhibition of *CASP4* or *NLRP1* gene expression did not suppress the effect of hUCMSC-CM on inducing MCF7 cell death, we attempted to elucidate the mechanism underlying pyroptosis induction in MCF7 cells. Here, we analyzed the mRNA levels for caspase-1, caspase-4, and NLRP1 in *CASP4* knockdown, *NLRP1* knockdown, and NC-transfected cells treated with hUCMSC-CM. RT-qPCR analysis (Figure 5(a)) revealed a significant decrease in *CASP4* mRNA levels in the hUCMSC-CM-treated *CASP4* knockdown MCF7 cells, compared to the NC-transfected MCF cells ($P < 0.001$); however, no considerable change was observed in the *CASP1* mRNA

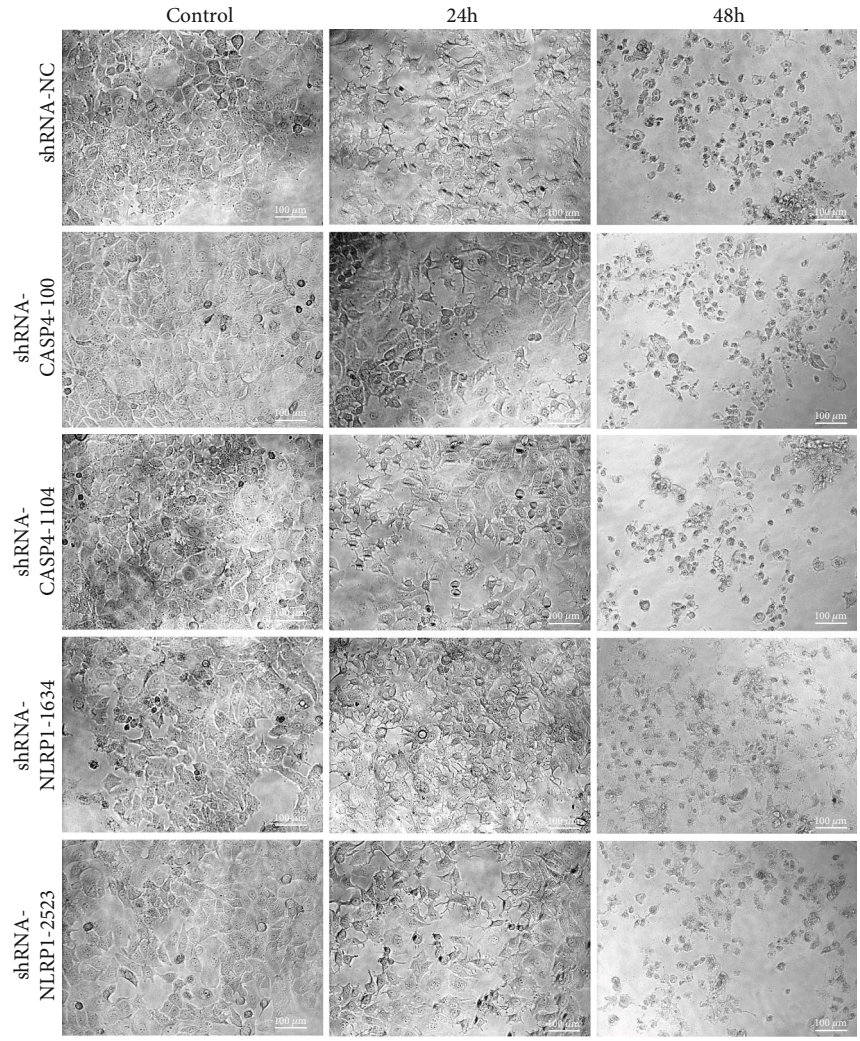

Figure 3: Morphological changes in transfected MCF7 cells exposed to hUCMSC-CM. Images were obtained on 24 h and 48 h. Representative micrographs from at least three independent experiments are shown. All images were taken using 20x magnification.

levels of the *CASP4* knockdown MCF7 cells ($P > 0.05$). Furthermore, treatment with hUCMSC-CM significantly increased the *NLRP1* mRNA levels in MCF7 cells transfected with shRNA-*CASP4*-100 ($P < 0.001$). The *NLRP1* mRNA levels in *NLRP1* knockdown MCF7 cells showed a significant decrease initially ($P < 0.001$) but increased after treatment with hUCMSC-CM ($P < 0.001$). *CASP4* mRNA levels in *NLRP1* knockdown MCF7 cells did not change considerably ($P > 0.05$); however, treatment with hUCMSC-CM significantly increased the *CASP1* mRNA levels in MCF7 cells transfected with shRNA-*NLRP1*-2523 ($P < 0.001$).

To further know the changes of protein level in transfected MCF7 cells, we performed western blotting. Western blotting results (Figures 5(b) and 5(c)) revealed significantly decreased caspase-4 protein levels in *CASP4* knockdown MCF7 cells ($P < 0.05$); however, the decrease was more prominent in cells transfected with shRNA-*CASP4*-100 ($P < 0.001$). Compared to NC-transfected MCF7 cells, the MCF7 cells transfected with shRNA-*NLRP1*-2523 showed a significant decrease in NLRP1 protein levels ($P < 0.05$), and hUCMSC-CM treatment further decreased the NLRP1 protein levels in these cells. Therefore, shRNA-*CASP4*-100 and shRNA-*NLRP1*-2523 are more effective for gene inhibition, and we selected MCF7 cells transfected with shRNA-*CASP4*-100 and shRNA-*NLRP1*-2523 for further research.

3.5. Involvement of the Two Pyroptosis Pathways in hUCMSC-CM-Induced Pyroptosis in MCF7 Cells. To elucidate the effect of *CASP4* or *NLRP1* knockdown on MCF7 cell pyroptosis, we investigated the protein levels of pro-CASP1, cleaved CASP1, pro-CASP4, and cleaved CASP4 and the changes in ASC speck formation in MCF7 cells transfected with shRNA-*CASP4*-100 and shRNA-*NLRP1*-2523. In *CASP4* knockdown MCF7 cells, hUCMSC-CM treatment for 24 h significantly decreased the levels of cleaved CASP4 but significantly increased the levels ofcleaved CASP1, ASC, and NLRP1. These findings indicate that the noncanonical pathway was inhibited in *CASP4* knockdown MCF7 cells and that hUCMSC-CM-induced pyroptosis mainly occurs via the caspase-1-mediated canonical pathway. Conversely, 24 h treatment with hUCMSC-CM in *NLRP1* knockdown MCF7 cells did not affect the levels of cleaved CASP4 and

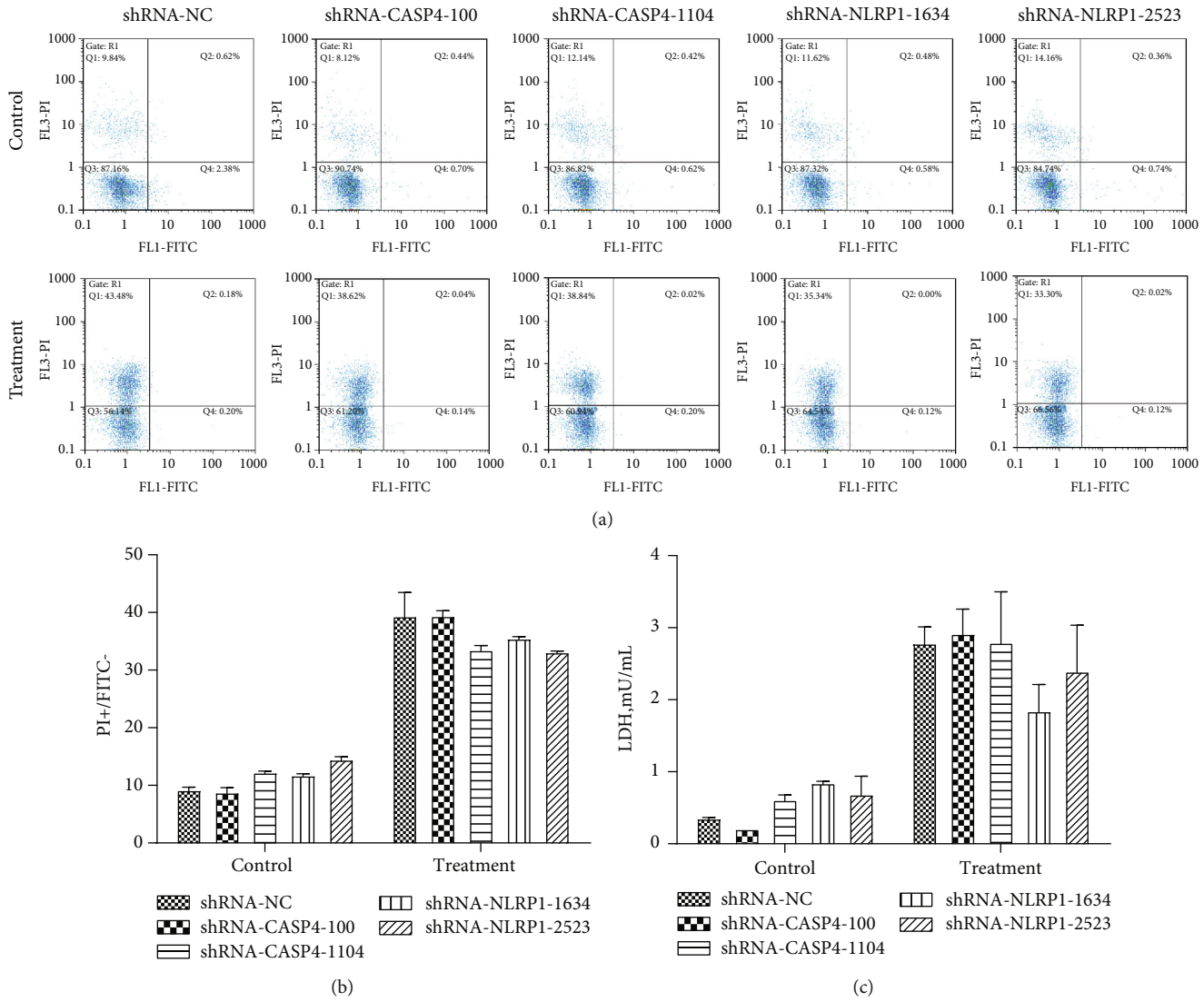

Figure 4: Detection of dead cells. (a) Flow cytometry results of Annexin V-FITC/PI staining. (b) Quantitative analysis for the Annexin V-FITC/PI results. (c) The concentration of LDH. Control: cells were collected after transfection with shRNA vector for 72 h. Treatment: cells were collected after transfected with shRNA vector for 72 h and treated with hUCMSC-CM for 24 h. Data were presented as mean ± SD of three independent experiments.

pro-CASP1 but significantly decreased the levels of cleaved CASP1. This indicates that *NLRP1* inhibition did not affect the noncanonical pathway but could reduce cleaved CASP1 protein levels. Furthermore, the ASC speck in *NLRP1* knockdown cells was significantly lower than that in *CASP4* knockdown cells, indicating the inhibition of inflammasome formation and the subsequent partial inhibition of the canonical pathway in *NLRP1* knockdown cells. Therefore, the canonical pathway was inhibited in *NLRP1* knockdown MCF7 cells, and hUCMSC-CM-induced pyroptosis in these cells mainly occurs via the caspase-4-mediated noncanonical pathway.

IL-1α secretion is caspase-1 independent [19] but is positively correlated with the activity of caspase-4 [7, 20], a key factor of the noncanonical pathway. The secretion of IL-1β and IL-18 is positively correlated with the activity of caspase-1, a key factor of the canonical pathway [21, 22]. Therefore, we assessed the levels of IL-1α, IL-1β, and IL-18 in the culture medium of transfected MCF7 cells treated with hUCMSC-CM for 24 h to determine the involvement of the noncanonical and canonical pathways in hUCMSC-CM-induced pyroptosis in MCF7 cells in the absence of caspase-4 or NLRP1, respectively. The control groups showed low secretion of all the three cytokines. Compared with hUCMSC-CM-treated *NLRP1* knockdown cells, the hUCMSC-CM-treated *CASP4* knockdown cells showed reduced IL-1α secretion but increased IL-1β and IL-18 secretion (Figure 6(d)). These results are consistent with the results of western blotting, confirming that the noncanonical pathway was inhibited and hUCMSC-CM-induced pyroptosis mainly occurred via the caspase-1-mediated canonical pathway in *CASP4* knockdown MCF7 cells, whereas the canonical pathway was inhibited and hUCMSC-CM-induced pyroptosis mainly occurred via the caspase-4-mediated noncanonical pathway in *NLRP1* knockdown MCF7 cells.

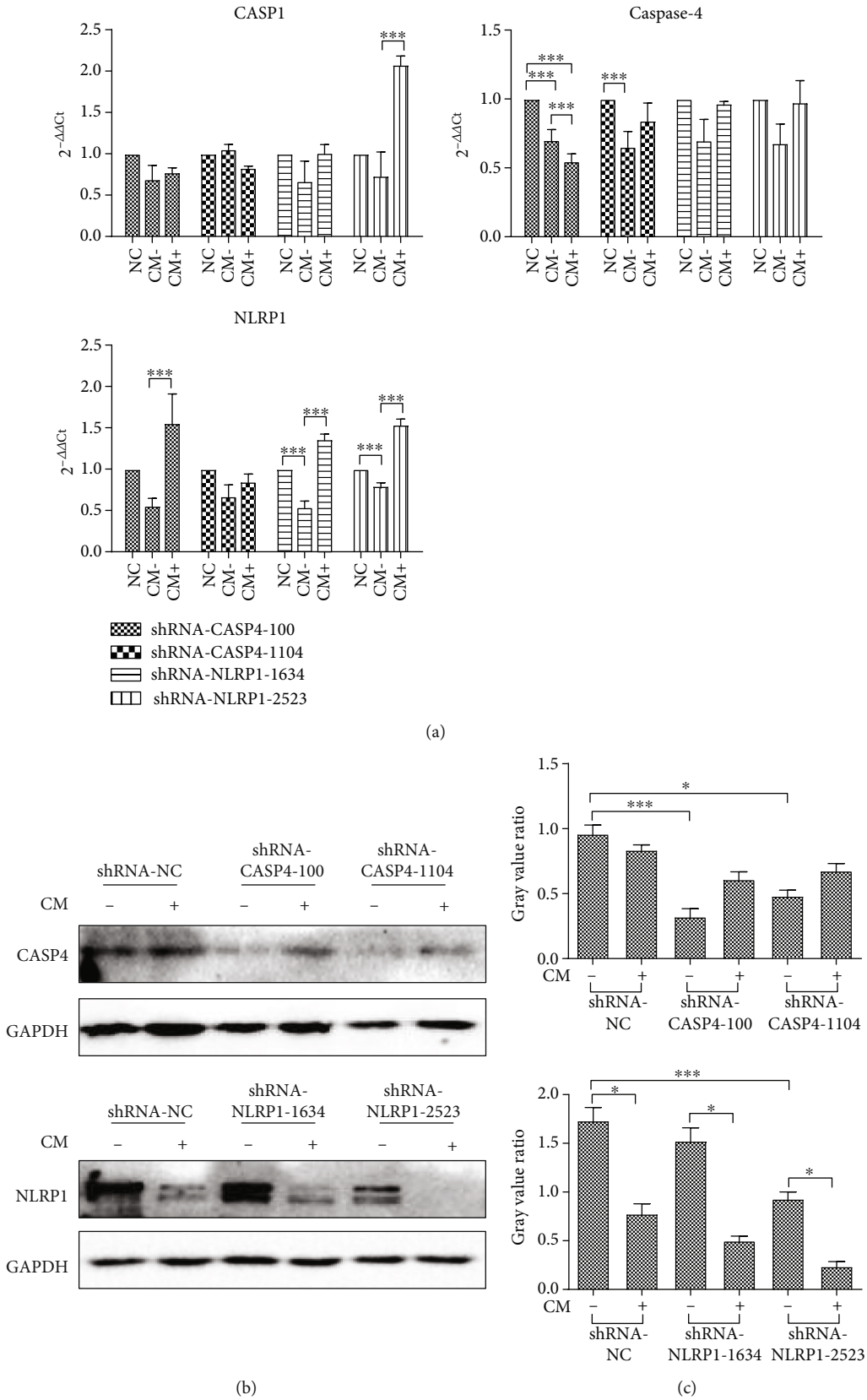

Figure 5: Detection of genes expression. (a) The q-PCR results of pyroptosis-related genes. Data are presented as Ct ($2^{-\triangle\triangle Ct}$) relative to control. Data are presented as mean ± S.D., $n = 3$. $^{*}P < 0.05$, $^{**}P < 0.01$, and $^{***}P < 0.001$. (b) The results of western blotting. (c) The gray value ratio of western blotting results. NC: negative control. CM-: cells were collected after transfection with shRNA vector for 72 h. CM+: cells were collected after transfection with shRNA vector for 72 h and treated with hUCMSC-CM for 24 h. $^{*}P < 0.05$, $^{**}P < 0.01$, and $^{***}P < 0.001$.

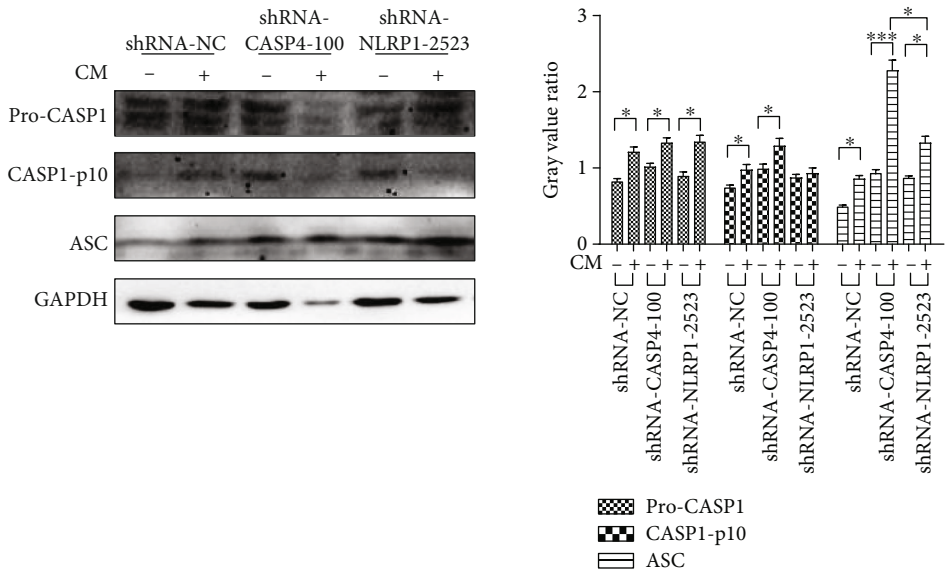

(a)

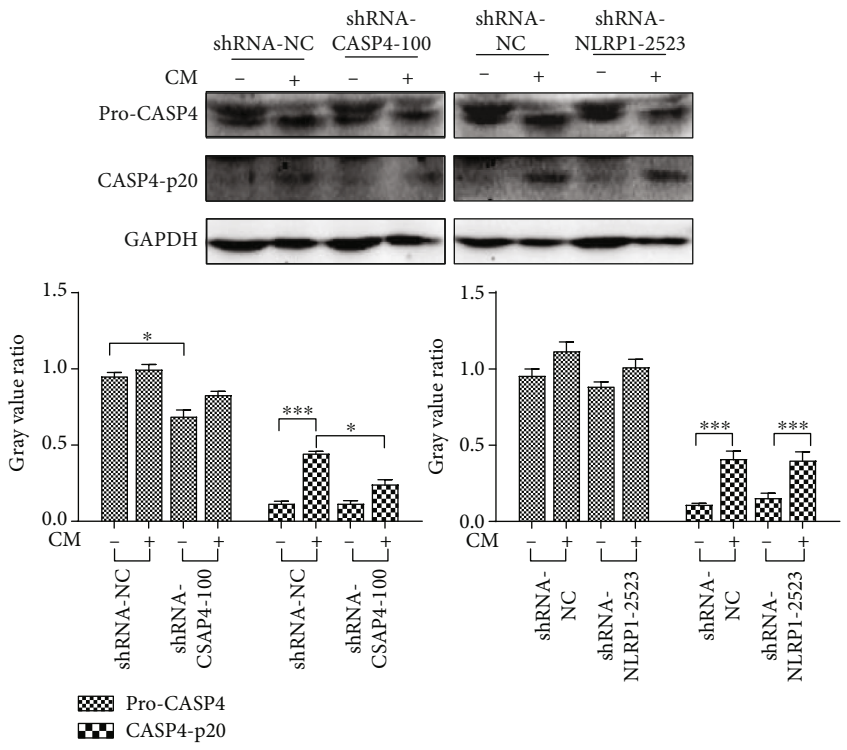

(b)

Figure 6: Continued.

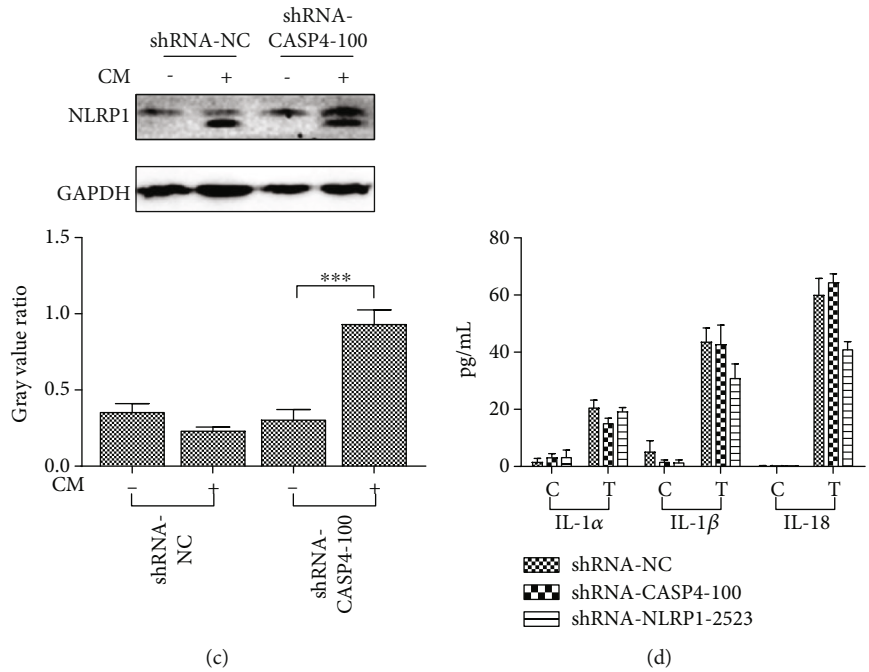

Figure 6: Study on the effect of *CASP4* and NLRP1 genes on MCF7 pyroptosis induced by hUCMSC-CM. (a) The western blotting results of pro-CASP1, cleaved-CASP1, and ASC proteins. (b) The western blotting results of pro-CASP4 and cleaved-CASP4. (c) The western blotting results of NLRP1. (d) The concentration of secreted cytokine in cell supernatant. NC: negative control. CM-: cells were collected after transfection with shRNA vector for 72 h. CM+: cells were collected after transfection with shRNA vector for 72 h and treated with hUCMSC-CM for 24 h. C: cells were collected after transfection with shRNA vector for 72 h. T: cells were collected after transfection with shRNA vector for 72 h and treated with hUCMSC-CM for 24 h. Data were presented as mean ± SD of three independent experiments.$^{*}P < 0.05$, $^{**}P < 0.01$, and $^{***}P < 0.001$.

4. Discussion

Breast cancer, the cancer that originates in the breast tissues, is divided into five types based on its molecular characteristics: Luminal A, Luminal B, HER2 enriched, basal like/triple-negative, and other special types of breast cancer [23]. The response to treatment and prognosis varies with the type of breast cancer. Therefore, cancer type-specific treatments are prescribed [24]. Our study focused on investigating the effect of hUCMSC-CM on breast cancer cell line MCF7. The MCF7 cells are Luminal A type, which is ER/PR positive and HER2 negative, with a high expression of ER-related genes and low expression of proliferation-related genes [25]. Typically, it is a low-grade cancer with an excellent prognosis.

MSCs show several promising applications in cell therapy and gene therapy owing to their unique characteristics. The relationship between MSCs and cancer has been studied widely by many research groups. Several studies have shown that the use of MSCs in cancer therapy is a two-edged sword that can suppress or promote cancer growth [26]. The different effects of MSCs on cancer growth depend on the source of MSCs and the type of cancer cells. Chen et al. [27] reported that aggressive ER-negative breast cancer cells show stronger ability to engulf MSCs than the aggressive ER-positive MCF7 cells and nontumorigenic MCF10A cells do and that such engulfment results in the development of breast cancer with enhanced migration, invasion, and metastatic properties.

MSCs interact with cancer cells via various mechanisms, including direct contact and subsequent engulfment of cancer cells [27, 28] and immunomodulation to influence the survival of tumor cells [29, 30]. Paracrine actions of MSCs might be crucial for their immunomodulatory functions. Extracellular vesicles (EVs) represent a group of cell-derived bilayered membrane structures that contain bioactive paracrine molecules, which can affect the target cells [31]. EVs are commonly classified into three subtypes: exosomes, microvesicles (MVs), and apoptotic bodies [32]. Recently, many studies reported that EVs derived from MSCs (MSC-EVs) can regulate cancer cell proliferation, angiogenesis, and metastasis. EVs derived from hUCMSCs were also reported to be effective against cancer cells. Wu et al. [33] found that hUCMSC-EVs might inhibit bladder tumor T24 growth by downregulating Akt protein kinase phosphorylation and upregulating cleaved caspase-3. Hendijani et al. [34] showed that the hUCMSC secretome displayed an anti-proliferative effect on the leukemia cell line and exerted an additive cytotoxic effect in combination with doxorubicin. Usually, hUCMSC-CM can be used in preliminary studies investigating the effect of hUCMSC-EVs. He et al. [35] demonstrated that hUCMSC-CM inhibited cancer growth and radiosensitivity of the breast cancer cell line MDA-MB-231 by downregulating the Stat3 signaling pathway. Hong et al. [36] showed that hUCMSC-CM can decrease the cisplatin-induced apoptosis of oocytes and granulosa cells in a cisplatin-induced ovarian injury model. We previously

reported that hUCMSC-CM could induce MCF7 pyroptosis in vitro, and our RNA sequencing studies revealed a significant increase in the expression of pyroptosis-related gene *NLRP1* and *CASP4* in pyroptotic MCF7 cells. Therefore, in this study, we further investigated the effects of these two genes on MCF7 cell pyroptosis induced by hUCMSC-CM.

We first assessed the gene and protein expression of caspase-1, caspase-4, and NLRP1 in MCF7 cells undergoing hUCMSC-CM-induced pyroptosis. Although the mRNA levels of these three genes increased, the protein levels showed a different trend. In particular, NLRP1 protein decreased significantly. During pyroptosis, NLRP1 interacts with the adaptor protein ASC to form an inflammasome complex. Similarly, we detected the expression and localization of NLRP1 and ASC in pyroptotic MCF7 cells via immunofluorescence and found that these two proteins colocalized in pyroptotic MCF7 cells, suggesting the formation and involvement of the inflammasome in hUCMSC-CM-induced pyroptosis in MCF7 cells.

Next, we investigated the role of caspase-4 and NLRP1 in hUCMSC-CM-induced pyroptosis in MCF7 cells. shRNA-mediated knockdown of *CASP4* or *NLRP1* in MCF7 cells resulted in a 50–70% reduction in the corresponding transcript levels (Supplementary2). Pyroptosis occurs via the canonical and noncanonical pathways. Caspase-1 is the key molecule involved in the canonical pathway, and NLRP1 recruits ASC and pro-caspase-1 to form the NLRP1 inflammasome or directly interacts with pro-caspase-1 to activate caspase-1 and induce pyroptosis [5]. Caspase-4 is the key molecule involved in the noncanonical pathway. In this study, deficiency of caspase-4 or NLRP1 could not completely block either of these two pathways. Therefore, studying the role of one pathway by blocking the other could not be performed in this study. Nevertheless, we found some interaction between these two pathways.

Cell morphology and cell death analysis using Annexin V-FITC/PI and LDH assays showed that levels of hUCMSC-CM-induced pyroptosis in *CASP4* knockdown and *NLRP1* knockdown MCF7 cells were not significantly different from that observed in the NC group. This indicates that inhibition of caspase-4 or NLRP1 could not inhibit MCF7 cell pyroptosis induced by the factors secreted by hUCMSCs. Therefore, to elucidate the mechanisms underlying these observations, we further investigated the changes in the expression of pyroptosis-related genes in the shRNA-transfected MCF7 cells.

Caspase-1, also known as IL-1β-converting enzyme, is responsible for maturation and secretion of the proinflammatory cytokines IL-1β and IL-18 [16, 37–39]. Caspase-1 dimerization and self-activation is induced by inflammasomes, which are composed of a PRR, the adaptor ASC, and pro-caspase-1 [38]. ASC interacts with PRRs and pro-caspase-1 through its pyrin domain (PYD) and recruitment domain (CARD), respectively. PRRs such as NLRP1, NLRP3, NLRC4, AIM2, and Pyrin, respond to microbial, environmental, and host-derived danger-associated molecular patterns; microbe-associated molecular patterns; and pathogen-associated molecular patterns [40]. Activated caspase-1 cleaves gasdermin D to promote membrane pore formation and pyroptosis [41, 42]. In humans, NLRP1 contains a PYD, a function to find domain (FIND), and CARD. Therefore, NLRP1 can directly activate procaspase-1 by interacting with it or indirectly by recruiting ASC and pro-caspase-1 to form the NLRP1 inflammasome, which activates caspase-1 [5]. However, agents that can selectively activate human NLRP1 inflammasomes have not yet been identified. We previously reported significantly high expression of *NLRP1*and *CASP1* during hUCMSC-CM-induced pyroptosis in MCF7 cells. These results suggest that some factors in the hUCMSC-CM interact with NLRP1 and activate caspase-1 to induce MCF7 cell pyroptosis. However, hUCMSCs secrete a vast array of molecules, and the precise factors that interact with NLRP1 remain unknown and further studies are warranted to identify these factors. In this study, we knocked down *NLRP1* to elucidate its role in hUCMSC-CM-induced pyroptosis. hUCMSC-CM treatment did not considerably change caspase-4 expression at both mRNA and protein levels and did not change the amount of cleaved CASP4 but increased pro-caspase-1e xpression in *NLRP1* knockdown MCF7 cells. *NLRP1* mutations have been reported to increase systemic amounts of caspase-1 in patients with arthritis and dyskeratosis [43]; our results are consistent with these findings. Furthermore, compared to pro-caspase-1 levels, the number of active ASC complexes was reported to be a more important limiting factor for caspase-1 maturation/release [21]. The secretion of IL-1β and IL-18 is positively correlated with the activity of caspase-1. Therefore, in *NLRP1* knockdown MCF7 cells, we found ASC complexes, cleaved-CASP1, and the levels of secreted IL-1β and IL-18 decreased. These results suggest that *NLRP1* knockdown partly inhibited the canonical pyroptosis pathway but did not affect the noncanonical pathway.

Caspase-4 detects cytoplasmic LPS and triggers the noncanonical pyroptosis pathway in humans. Caspase-5 has a synergistic effect with caspase-4 [36, 44]. The oligomerization and activation of caspase-4 and caspase-5 are triggered by binding of their CARDs with the lipid portion of LPS. However, the CARD of caspase-5 is 56% divergent from that of caspase-4, suggesting that caspase-5 binds and responds to lipids with specificities different from those of caspase-4 [45]. In fact, these two caspases play different roles in different cells. LPS stimulation induced processing of procaspase-5, but not of caspase-4, and mediated IL-1 release in monocytes [44]. Caspase-5 expression was undetectable in U937 cells, and ectopic expression of caspase-5 partially triggered inflammasome activation in response to *Escherichia coli* LPS but did not trigger inflammasome activation in response to *Francisella novicida* LPS [21]. Caspase-5 could not be detected in LPS-stimulated THP1 cells [6]. In contrast, caspase-4 played an important role in epithelial cell death during *Shigella* infection [46], and in pyroptosis and IL-1α secretion in human gingival fibroblasts in response to Td92, a surface protein of the periodontal pathogen *Treponema denticola* [20]. We previously demonstrated that hUCMSC-CM-treated pyroptotic MCF7 cells did not show significant changes in caspase-5 expression but showed significantly increased caspase-4 expression. Therefore, we hypothesized that one or more of the factors secreted by hUCMSCs

interact with caspase-4 and trigger MCF7 cell pyroptosis. In this study, we found that hUCMSC-CM treatment did not considerably change pro-caspase-1 expression at both mRNA and protein levels but moderately increased NLRP1 expression and ASC speck formation and decreased cleaved-CASP4 level in *CASP4* knockdown MCF7 cells. Furthermore, the levels of secreted IL-1α were lower but the levels of IL-1β and IL-18 in the *CASP4* knockdown MCF7 cells were higher than those in the NC and *NLRP1* knockdown MCF7 cells. These results are consistent with the previous reports [21, 44] and suggest that the noncanonical pathway is partly inhibited and MCF7 cell death occurs mainly via the canonical pathway in the absence of caspase-4. Caspase-4-mediated cell death was reported to trigger NLRP3-dependent caspase-1 activation and secretion of IL-1β and IL-18 [6, 21, 47, 48]. In addition, canonical inflammasomes can control the activation of noncanonical inflammasomes [49], and blocking the noncanonical pathway alone may not be sufficient to change the susceptibility to infections [50]. Therefore, other mechanisms affecting the canonical pathway may be involved in mediating pyroptosis in *CASP4* knockdown MCF7 cells, and further research is essential to elucidate these mechanisms.

5. Conclusions

We previously demonstrated that the factors secreted by hUCMSCs could induce pyroptosis in the breast cancer cell line MCF7. Moreover, our previous RNA sequencing analysis showed that the expression of pyroptosis-related gene *NLRP1* and *CASP4* increased significantly. In this study, we elucidated the role of these two genes in hUCMSC-CM-induced pyroptosis in MCF7 cells. We found that although *CASP1*, *CASP4*, and *NLRP1* mRNA levels increased, the protein levels showed a different trend. In particular, NLRP1 protein decreased significantly. Further analysis for identifying the underlying reason revealed that NLRP1 interacts with ASC to form a complex, which is involved in MCF7 cell pyroptosis. Further investigation using *NLRP1* and *CASP4* knockdown MCF7 cells showed that knockdown of either *CASP4* or *NLRP1* could not rescue MCF7 cells from hUCMSC-CM-mediated pyroptosis. Further study on *CASP4*- or *NLRP1*-knockdown cells revealed that MCF7 cell pyroptosis occurred via both canonical and noncanonical pyroptosis pathways; when one pathway was inhibited, hUCMSC-CM induced MCF7 cell pyroptosis via the other pathway. Our study provides a foundation for further studies aimed at elucidating the precise mechanism underlying hUCMSC-induced pyroptosis in the breast cancer cell line MCF7 and aid the identification of potential therapeutic targets for breast cancer.

Data Availability

The data used to support the findings of this study are included within the article and its supplementary information file.

Conflicts of Interest

The authors declare that there is no conflict of interest regarding the publication of this article.

Acknowledgments

We thank the Department of Obstetrics and Gynecology of the Chenggong branch of Yan'an Hospital of Kunming for assisting with the collection of human umbilical cords. This work was supported by the Major Project of Yunnan Science and Technology Program (grant number 2018ZF007-05), Research Program of Application Foundation of Yunnan Province, China (grant number 2018FB058), Foreign Cooperation Project of Yunnan Province (grant number 2018IA045), and Joint Special Funds for the Department of Science and Technology of Yunnan Province-Kunming Medical University (grant number 2017FE468 (-011)).

Supplementary Materials

Additional file 1: (a) the sequencing results of CASP4 shRNA vectors. (b) The sequencing results of NLRP1 shRNA vectors. Sequencing with T7 universal primers. Additional file 2: (a) gene expression of caspase-4. (b) Gene expression of NLRP1. MCF7 cells were transfected with shRNA vectors for 72 hours, and then, the total RNA was extracted from the cells. q-PCR was used to detect the target gene. NC: negative control. Data are presented as Ct ($2^{-\triangle\triangle Ct}$) relative to negative control. Data are presented as mean ± S.D., $n = 3$. *(Supplementary Materials)*

References

[1] T. Bergsbaken, S. L. Fink, and B. T. Cookson, "Pyroptosis: host cell death and inflammation," *Nature Reviews Microbiology*, vol. 7, no. 2, pp. 99–109, 2009.

[2] F. Martinon and J. Tschopp, "Inflammatory caspases and inflammasomes: master switches of inflammation," *Cell Death and Differentiation*, vol. 14, no. 1, pp. 10–22, 2007.

[3] N. Kayagaki, I. B. Stowe, B. L. Lee et al., "Caspase-11 cleaves gasdermin D for non-canonical inflammasome signalling," *Nature*, vol. 526, no. 7575, pp. 666–671, 2015.

[4] T.-D. Kanneganti, M. Lamkanfi, and G. Núñez, "Intracellular NOD-like receptors in host defense and disease," vol. 27, no. 4, pp. 549–559, 2007.

[5] F. Martinon and J. Tschopp, "NLRs join TLRs as innate sensors of pathogens," *Trends in Immunology*, vol. 26, no. 8, pp. 447–454, 2005.

[6] J. L. Schmid-Burgk, M. M. Gaidt, T. Schmidt, T. S. Ebert, E. Bartok, and V. Hornung, "Caspase-4 mediates non-canonical activation of the NLRP3 inflammasome in human myeloid cells," *European Journal of Immunology*, vol. 45, no. 10, pp. 2911–2917, 2015.

[7] C. N. Casson, J. Yu, V. M. Reyes et al., "Human caspase-4 mediates noncanonical inflammasome activation against gram-negative bacterial pathogens," *Proceedings of the National Academy of Sciences of the United States of America*, vol. 112, no. 21, pp. 6688–6693, 2015.

[8] J. Shi, Y. Zhao, Y. Wang et al., "Inflammatory caspases are innate immune receptors for intracellular LPS," *Nature*, vol. 514, no. 7521, pp. 187–192, 2014.

[9] C. E. DeSantis, J. Ma, A. Goding Sauer, L. A. Newman, and A. Jemal, "Breast cancer statistics, 2017, racial disparity in mortality by state," *CA: a Cancer Journal for Clinicians*, vol. 67, no. 6, pp. 439–448, 2017.

[10] W. Chen, R. Zheng, P. D. Baade et al., "Cancer statistics in China, 2015," *CA: a Cancer Journal for Clinicians*, vol. 66, no. 2, pp. 115–132, 2016.

[11] L. Mercatali, F. La Manna, G. Miserocchi et al., "Tumor-stroma crosstalk in bone tissue: the osteoclastogenic potential of a breast cancer cell line in a co-culture system and the role of EGFR inhibition," *International Journal of Molecular Sciences*, vol. 18, no. 8, p. 1655, 2017.

[12] X. Li and Z. Li, "Effects of human umbilical cord mesenchymal stem cells on co-cultured ovarian carcinoma cells," *Microscopy Research and Technique*, vol. 82, no. 6, pp. 898–902, 2019.

[13] L. Chai, L. Bai, L. Li, F. Chen, and J. Zhang, "Biological functions of lung cancer cells are suppressed in co-culture with mesenchymal stem cells isolated from umbilical cord," *Experimental and Therapeutic Medicine*, vol. 15, no. 1, pp. 1076–1080, 2017.

[14] Y. Jiao, H. Zhao, G. Chen et al., "Pyroptosis of MCF7 cells induced by the secreted factors of hUCMSCs," *Stem Cells International*, vol. 2018, Article ID 5912194, 12 pages, 2018.

[15] T. D. Schmittgen and K. J. Livak, "Analyzing real-time PCR data by the comparative C (T) method," *Nature Protocols*, vol. 3, no. 6, pp. 1101–1108, 2008.

[16] J. G. Walsh, S. E. Logue, A. U. Lüthi, and S. J. Martin, "Caspase-1 promiscuity is counterbalanced by rapid inactivation of processed enzyme," *The Journal of Biological Chemistry*, vol. 286, no. 37, pp. 32513–32524, 2011.

[17] D. Datta, C. L. McClendon, M. P. Jacobson, and J. A. Wells, "Substrate and inhibitor-induced dimerization and cooperativity in caspase-1 but not caspase-3," *The Journal of Biological Chemistry*, vol. 288, no. 14, pp. 9971–9981, 2013.

[18] D. Boucher, M. Monteleone, R. C. Coll et al., "Caspase-1 self-cleavage is an intrinsic mechanism to terminate inflammasome activity," *The Journal of Experimental Medicine*, vol. 215, no. 3, pp. 827–840, 2018.

[19] N. C. Di Paolo and D. M. Shayakhmetov, "Interleukin 1α and the inflammatory process," *Nature Immunology*, vol. 17, no. 8, pp. 906–913, 2016.

[20] H.-K. Jun, Y.-J. Jung, S. Ji, S.-J. An, and B.-K. Choi, "Caspase-4 activation by a bacterial surface protein is mediated by cathepsin G in human gingival fibroblasts," *Cell Death & Differentiation*, vol. 25, no. 2, pp. 380–391, 2018.

[21] B. Lagrange, S. Benaoudia, P. Wallet et al., "Human caspase-4 detects tetra-acylated LPS and cytosolic _Francisella_ and functions differently from murine caspase-11," *Nature Communications*, vol. 9, no. 1, p. 242, 2018.

[22] P. J. Sansonetti, A. Phalipon, J. Arondel et al., "Caspase-1 activation of IL-1β and IL-18 are essential for Shigella flexneri–induced inflammation," *Immunity*, vol. 12, no. 5, pp. 581–590, 2000.

[23] K. P. Serra, S. Ramalho, R. Torresan et al., "The new classification of breast cancers: finding the luminal a," *Revista Brasileira de Ginecologia e Obstetrícia*, vol. 36, no. 12, pp. 575–580, 2014.

[24] E. Provenzano, G. A. Ulaner, and S. F. Chin, "Molecular classification of breast cancer," *PET Clinics*, vol. 13, no. 3, pp. 325–338, 2018.

[25] A. Prat, M. C. U. Cheang, M. Martín et al., "Prognostic significance of progesterone receptor-positive tumor cells within immunohistochemically defined luminal A breast cancer," *Journal of Clinical Oncology*, vol. 31, no. 2, pp. 203–209, 2013.

[26] M. Timaner, K. K. Tsai, and Y. Shaked, "The multifaceted role of mesenchymal stem cells in cancer," *Seminars in Cancer Biology*, vol. 60, pp. 225–237, 2020.

[27] Y.-C. Chen, M. E. Gonzalez, B. Burman et al., "Mesenchymal stem/stromal cell engulfment reveals metastatic advantage in breast cancer," *Cellular Reprogramming*, vol. 27, no. 13, pp. 3916–3926.e5, 2019.

[28] K. C. Chao, H. T. Yang, and M. W. Chen, "Human umbilical cord mesenchymal stem cells suppress breast cancer tumourigenesis through direct cell-cell contact and internalization," *Journal of Cellular and Molecular Medicine*, vol. 16, no. 8, pp. 1803–1815, 2012.

[29] S. H. Choi, D. W. Stuckey, S. Pignatta et al., "Tumor resection recruits effector T cells and boosts therapeutic efficacy of encapsulated stem cells expressing IFNβ in glioblastomas," *Clinical Cancer Research*, vol. 23, no. 22, pp. 7047–7058, 2017.

[30] J. Cuerquis, R. Romieu-Mourez, M. François et al., "Human mesenchymal stromal cells transiently increase cytokine production by activated T cells before suppressing T-cell proliferation: effect of interferon-γ and tumor necrosis factor-α stimulation," *Cytotherapy*, vol. 16, no. 2, pp. 191–202, 2014.

[31] H. Shao, H. Im, C. M. Castro, X. Breakefield, R. Weissleder, and H. Lee, "New technologies for analysis of extracellular vesicles," *Chemical Reviews*, vol. 118, no. 4, pp. 1917–1950, 2018.

[32] P. Neviani and M. Fabbri, "Exosomic microRNAs in the tumor microenvironment," *Frontiers in Medicine*, vol. 2, no. 2, p. 47, 2015.

[33] S. Wu, G.-Q. Ju, T. Du, Y.-J. Zhu, and G.-H. Liu, "Microvesicles derived from human umbilical cord Wharton's jelly mesenchymal stem cells attenuate bladder tumor cell growth in vitro and in vivo," *PLoS One*, vol. 8, no. 4, article e61366, 2013.

[34] F. Hendijani, S. H. Javanmard, and H. Sadeghi-aliabadi, "Human Wharton's jelly mesenchymal stem cell secretome display antiproliferative effect on leukemia cell line and produce additive cytotoxic effect in combination with doxorubicin," *Tissue & Cell*, vol. 47, no. 3, pp. 229–234, 2015.

[35] N. He, Y. Kong, X. Lei et al., "MSCs inhibit tumor progression and enhance radiosensitivity of breast cancer cells by down-regulating Stat3 signaling pathway," *Cell Death Discovery*, vol. 9, no. 10, p. 1026, 2018.

[36] L. Hong, L. Yan, Z. Xin et al., "Protective effects of human umbilical cord mesenchymal stem cell-derived conditioned medium on ovarian damage," *Journal of Molecular Cell Biology*, vol. 12, no. 5, pp. 372–385, 2020.

[37] M. Lamkanfi and V. M. Dixit, "Mechanisms and functions of inflammasomes," *Cell*, vol. 157, no. 5, pp. 1013–1022, 2014.

[38] V. A. K. Rathinam and K. A. Fitzgerald, "Inflammasome complexes: emerging mechanisms and effector functions," *Cell*, vol. 165, no. 4, pp. 792–800, 2016.

[39] F. Martinon and J. Tschopp, "Inflammatory caspases: linking an intracellular innate immune system to autoinflammatory diseases," *Cell*, vol. 117, no. 5, pp. 561–574, 2004.

[40] M. Lamkanfi and V. M. Dixit, "In retrospect: the inflammasome turns 15," *Nature*, vol. 548, no. 7669, pp. 534-535, 2017.

[41] W. T. He, H. Wan, L. Hu et al., "Gasdermin D is an executor of pyroptosis and required for interleukin-1β secretion," *Cell Research*, vol. 25, no. 12, pp. 1285–1298, 2015.

[42] J. Shi, Y. Zhao, K. Wang et al., "Cleavage of GSDMD by inflammatory caspases determines pyroptotic cell death," *Nature*, vol. 526, no. 7575, pp. 660–665, 2015.

[43] S. Grandemange, E. Sanchez, P. Louis-Plence et al., "A new autoinflammatory and autoimmune syndrome associated with NLRP1 mutations: NAIAD (NLRP1-associated autoinflammation with arthritis and dyskeratosis)," *Annals of the Rheumatic Diseases*, vol. 76, no. 7, pp. 1191–1198, 2017.

[44] E. Viganò, C. E. Diamond, R. Spreafico, A. Balachander, R. M. Sobota, and A. Mortellaro, "Human caspase-4 and caspase-5 regulate the one-step non-canonical inflammasome activation in monocytes," *Nature Communications*, vol. 6, no. 1, 2015.

[45] J. A. Hagar, D. A. Powell, Y. Aachoui, R. K. Ernst, and E. A. Miao, "Cytoplasmic LPS activates caspase-11: implications in TLR4-independent endotoxic shock," *Science*, vol. 341, no. 6151, pp. 1250–1253, 2013.

[46] T. Kobayashi, M. Ogawa, T. Sanada et al., "The Shigella OspC3 effector inhibits caspase-4, antagonizes inflammatory cell death, and promotes epithelial infection," *Cell Host & Microbe*, vol. 13, no. 5, pp. 570–583, 2013.

[47] S. Rühl and P. Broz, "Caspase-11 activates a canonical NLRP3 inflammasome by promoting K(+) efflux," *European Journal of Immunology*, vol. 45, no. 10, pp. 2927–2936, 2015.

[48] P. J. Baker, D. Boucher, D. Bierschenk et al., "NLRP3 inflammasome activation downstream of cytoplasmic LPS recognition by both caspase-4 and caspase-5," *European Journal of Immunology*, vol. 45, no. 10, pp. 2918–2926, 2015.

[49] Y. Aachoui, Y. Kajiwara, I. A. Leaf et al., "Canonical inflammasomes drive IFN-γ to prime caspase-11 in defense against a cytosol-invasive bacterium," *Cell Host & Microbe*, vol. 18, no. 3, pp. 320–332, 2015.

[50] J. Yuan, A. Najafov, and B. F. Py, "Roles of caspases in necrotic cell death," *Cell*, vol. 167, no. 7, pp. 1693–1704, 2016.

Hindawi
Stem Cells International
Volume 2020, Article ID 8838046, 16 pages
https://doi.org/10.1155/2020/8838046

Review Article

Mesenchymal Stem/Stromal Cell-Mediated Mitochondrial Transfer and the Therapeutic Potential in Treatment of Neurological Diseases

Deqiang Han,[1,2,3] Xin Zheng,[1,2,3] Xueyao Wang,[1,2,3] Tao Jin,[4] Li Cui,[4] and Zhiguo Chen[1,2,3]

[1]*Cell Therapy Center, Beijing Institute of Geriatrics, Xuanwu Hospital Capital Medical University, National Clinical Research Center for Geriatric Diseases, And Key Laboratory of Neurodegenerative Diseases, Ministry of Education, Beijing 100053, China*
[2]*Center of Neural Injury and Repair, Beijing Institute for Brain Disorders, Beijing 100069, China*
[3]*Center of Parkinson's Disease, Beijing Institute for Brain Disorders, Beijing 100069, China*
[4]*Department of Neurology and Neuroscience Center, First Hospital of Jilin University, Changchun, Jilin Province, China*

Correspondence should be addressed to Li Cui; chuili1967@126.com and Zhiguo Chen; chenzhiguo@gmail.com

Received 7 May 2020; Revised 11 June 2020; Accepted 24 June 2020; Published 7 July 2020

Academic Editor: Kar Wey Yong

Mesenchymal stem/stromal cells (MSCs) are multipotent stem cells that can be derived from various tissues. Due to their regenerative and immunomodulatory properties, MSCs have been extensively researched and tested for treatment of different diseases/indications. One mechanism that MSCs exert functions is through the transfer of mitochondria, a key player involved in many biological processes in health and disease. Mitochondria transfer is bidirectional and has an impact on both donor and recipient cells. In this review, we discussed how MSC-mediated mitochondrial transfer may affect cellular metabolism, survival, proliferation, and differentiation; how this process influences inflammatory processes; and what is the molecular machinery that mediates mitochondrial transfer. In the end, we summarized recent advances in preclinical research and clinical trials for the treatment of stroke and spinal cord injury, through application of MSCs and/or MSC-derived mitochondria.

1. Introduction

Mesenchymal stem/stromal cells (MSCs) have attracted a lot of interest in basic science and clinical applications, not only due to the unique properties such as fewer ethical issues, little (if not lacking) tumorigenicity, and mild immune responses compared with other stem cell sources such as embryonic stem cells (hESCs) and induced pluripotent stem cells (iPSCs) but also because it seems to be the only stem cell type that presents both regenerative and immunomodulatory functions [1]. Engrafted MSCs can be differentiated into certain types of cells that help replenish the tissue in an autologous or allogeneic manner. In addition, MSCs show immunomodulatory properties mainly via a paracrine mechanism that involves secretion of microvesicles (MVs), microRNA, and exosomes [2, 3]. MSC-based cell replacement and immunomodulatory approaches have been employed in the treatment of some degenerative and inflammatory diseases.

Mitochondrial transfer between MSCs and damaged cells has emerged to be a promising therapeutic strategy partly because it can act as a bioenergetic supplementation [4]. Transferred mitochondria can also regulate the biological functions of cells that have taken the mitochondria (acceptor) [5, 6]. Speed and colleagues proved that mitochondria or mitochondrial DNA (mtDNA) transfer can take place between adult stem cells and somatic cells and that human lung alveolar epithelial cells harboring nonfunctional mitochondria are repaired by transfer of functional mitochondria or mtDNA from donor human bone marrow MSCs (BMSCs) [4]. This pioneer study revealed that mitochondrial donation can repair aerobic respiration in cells with dysfunctional mitochondria and protect cells from damage and apoptosis

[7]. The discovery about the ability of BMSCs to transfer mitochondria to injured cells prompted a series of further studies aimed at uncovering the underlying mechanism [8–12]. Not only exerting an impact on tissues/cells in the peripheral system, mitochondrial motility is also involved in the central nervous system (CNS) diseases [13, 14], and mitochondrial transfer may open an avenue to treatment of certain neurological diseases, such as stroke and spinal cord injury (SCI). In this review, we will discuss the biological processes/outcomes at injury sites following MSC-based mitochondrial transfer and the molecular machinery required to achieve such cell-to-cell communication. In the last section, we will summarize the latest advances in therapeutic applications of MSCs and/or mitochondrial transfer to treat CNS diseases such as stroke and SCI.

2. Mitochondrial Transfer Impacts Cellular Metabolism and Inflammation

2.1. Dynamics of Mitochondria. Mitochondria are semiautonomous and self-reproducing organelles that exist in the cytoplasm of most eukaryotes [15]. Inside a cell, the number of mitochondria is regulated by two opposite processes, fusion and fission. Mitochondrial fusion process can be divided into two steps [16]: fusion of outer mitochondrial membrane (OMM) that is mediated by OMM proteins Mitofusin 1 and Mitofusin 2 (Mfn1 and Mfn2) and fusion of inner mitochondrial membrane (IMM) that is mediated by OPA1. Fission is a division event that highly depends on dynamin-related protein 1 (Drp1) to produce one or more daughter mitochondria. Drp1, together with adaptor proteins Fission 1 (Fis1), mitochondrial fission factor (MFF), and mitochondrial dynamics proteins of 49 kDa and 51 kDa (Mid49 and Mid51), are able to hydrolyze guanosine triphophate (GTP) and mediate the division of OMM and IMM. The knockdown of fusion proteins (Mfn or OPA1) or fission proteins (Drp1, Fis1, and Fis2) in MSCs disturbs otherwise a healthy mitochondria network and can even alter the stemness of MSCs [17].

Dysfunctional mitochondria are selectively degraded in a process termed "mitophagy" to maintain mitochondrial homeostasis. Activation of mitophagy in BMSCs occurs at an early stage of reactive oxygen species (ROS) stress through Jun N-terminal kinase (JNK) pathway, but declines at a late stage of ROS stress [18]. Phosphatase and tensin homolog-(PTEN-) induced kinase 1 (PINK1)/Parkin pathway, which is normally involved in the clearance of dysfunctional mitochondria [19, 20], is also required for infused MSCs to restore mitophagy pathways in hyperglycemia-challenged endothelial cells [21]. Disruption of the PINK1 pathway, and consequently the mitophagy process, may be regulated by microRNAs. MicroRNA-155 (miR-155) is one of the most prominent miRNAs detected in inflammatory and aged tissues, which directly targets B cell lymphoma-2- (Bcl-2-) associated athanogene 5 (BAG5). Reduction of BAG5 in MSCs leads to the destabilization of PINK1 and abnormality of mitophagy [22]. Also, the mitophagy process is conducive to selectively keeping healthy mitochondria and suppressing generation of ROS in MSCs, which further contributes to an immunomodulatory effect via limiting caspase-1 and interleukin-1β (IL-1β) stimulation and inhibiting inflammasome activation in macrophages [23].

2.2. Transferred Mitochondria Serve as a "Bioengine." Mitochondria are known as the "powerhouse" of the cell. Each mitochondrion is surrounded by a double membrane. The inner membrane is highly invaginated, and its projection is termed cristae. Mitochondria are the source of chemical energy, generating most of the cell's adenosine triphosphate (ATP) supply via oxidative phosphorylation (OXPHOS) processes. Along with bioenergetic production, mitochondrial complexes I and III generate endogenous ROS, including oxygen radicals and hydrogen peroxide, which are involved in mitophagy and cellular apoptosis [24, 25]. The increase in ROS accumulated in normal aging or disease/injury leads to a higher rate of mitophagy and a lower level of mitochondrial biogenesis, together resulting in a reduction of mitochondrial mass [26]. Mitochondrial transfer may be able to reverse this phenomenon. For example, using an acute kidney injury mouse model, Perico et al. showed that transplantation of healthy MSCs can rejuvenate damaged tubular cells through mitochondrial transfer and restoring the energy production capacity in acceptor cells [27].

2.3. Mitochondrial Transfer Improves Cell Viability. Mitochondria play a critical role in cellular apoptosis [28]. ROS, a major product of mitochondria metabolism, in turn exerts a significant impact on mitochondria and mitochondria-mediated apoptosis [18]. Normally, the first stage of apoptosis involves elevated mitochondrial membrane permeability, which allows apoptogenic factors such as Bcl-2 to pass through OMM and to interrupt the electrochemical gradient in IMM. Then, the disruption of mitochondrial membrane properties results in insufficient production of ATP and activation of specific apoptogenic proteases such as caspases. Caspase-3 acts as an executor of apoptosis and activates the early steps of cellular apoptosis. Bcl-2 is able to suppress the release of cytochrome c from mitochondria via inhibiting the activation of proapoptotic factors such as Bcl-2-associated X protein (Bax) and Bcl-2-associated K protein (Bak). The imbalance of the Bax/Bcl-2 ratio is a feature that often occurs during the process of apoptosis [29]. Mitochondrial transfer from MSCs can reduce apoptosis levels and promote cell viability in recipient cells [30] via regulating the balance of Bax/Bcl-2 and reducing the expression of caspase-3 [31]. Interestingly, transfer of dysfunctional mitochondria from damaged cells to MSCs also has an influence on MSCs. Using *in vitro* and *in vivo* experiments, Gozzelino et al. showed that mitochondria released from damaged somatic cells (cardiomyocytes or endothelial cells) can be engulfed by MSCs and trigger upregulation of Heme oxygenase-1 (HO-1), a protein that protects against programmed cell death [32], and biogenesis of mitochondria in MSCs, which in turn promotes an adaptive reparative response [33].

2.4. Mitochondrial Transfer Promotes Anti-inflammatory Responses. The immunomodulatory functions of MSCs are

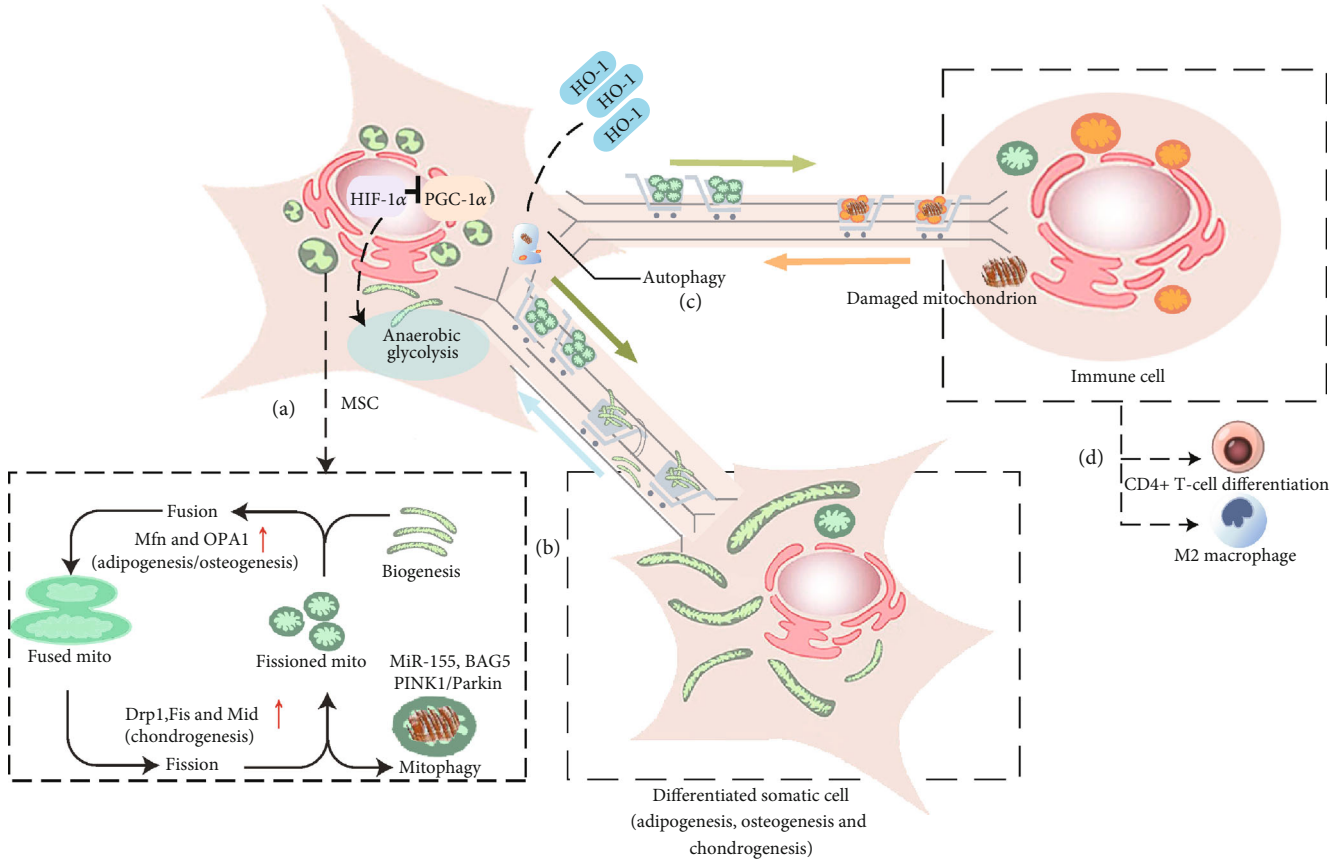

Figure 1: MSC-mediated mitochondrial transfer impacts cellular metabolism and differentiation. (a) Mitochondrial dynamics maintains a healthy mitochondria network in MSCs via regulating mitochondrial fusion, fission, and mitophagy. Activation of HIF1α under a hypoxic condition suppresses PGC1-α expression, leading to inhibition of mitochondrial biogenesis and the stimulation of anaerobic glycolysis. (b) The change of mitochondrial dynamics contributes to MSC differentiation and proliferation. Mitochondrial transfer may exert similar effects. (c) Somatic cell-derived damaged mitochondria are transferred and degraded in MSCs via autophagy to initiate the rescue processes; the engulfed mitochondria in MSCs lead to the upregulation of HO-1, which enhances the mitochondrial transfer capacity. (d) Mitochondrial transfer affects immune cell functions and differentiation. For example, mitochondrial transfer can suppress inflammation by promoting transition of macrophages to a M2 phenotype or inducing Treg cell differentiation.

implemented by a paracrine mechanism and cell-cell contact. The cytokines secreted by MSCs can exert a modulatory impact on various immune cells, such as T cells, B cells, natural killer cells, and macrophages [34]. It was found that mitochondrial transfer can take place between MSCs and immune cells, which influences the functions/properties of immune cells (Figure 1). Using an acute respiratory distress syndrome (ARDS) model, Krasnodembskaya's group reported that MSCs can donate mitochondria to host macrophages and enhance the phagocytic capacity and bioenergetics of macrophages, leading to an improved clearance of pathogenic bacteria [5, 35]. Along with the transfer of mitochondria, MSCs secrete exosomes containing microRNAs. After intake by macrophages, the microRNAs can target the Toll-like receptor (TLR)/NF-κB pathway and dampen proinflammatory responses [36]. Nevertheless, how macrophages keep an improved phagocytotic capacity while showing a reduced proinflammatory reaction after mitochondrial transfer remains elusive. To address this issue, using an ARDS model, Morrison et al. reported that extracellular vesicle-mediated transfer of mitochondria can induce monocyte-derived macrophages (MDMs) to differentiate to an M2 phenotype with a high phagocytic capacity; and this phenotypic change mediated by mitochondrial transfer requires the OXPHOS process in macrophages [35]. In another study, Kim and Hematti cocultured MSCs with macrophages *in vitro* and found that MSCs can educate macrophages to adopt a IL-10-high, IL-12-low, IL-6-high, and tumor necrosis factor-α- (TNF-α-) low phenotype, an anti-inflammatory phenotype similar to the M2 one [37].

MSC-mediated mitochondrial transfer can also regulate T cell differentiation. Instructed by the niche cues, especially the cytokines secreted by antigen-presenting cells (APCs), T helper (CD4) cells can be activated and differentiated to various subsets, including T helper 1 (Th1), Th2, Th17, Th9, T regulatory (Treg), or T follicular helper (Tfh) cells. Among them, Th17 cells can be further divided into two subsets: pro-inflammatory Th17 effector cells and immunosuppressive Th17 regulatory cells. The cytokine set that drives differentiation of Th17 effector cells normally inhibits differentiation into Th17 regulatory cells, and vice versa. Luz-Crawford et al. reported that coculturing healthy donor-derived

BMSCs with Th17 effector cells leads to mitochondrial transfer, which increases respiration in recipient Th17 cells and reprograms the energetic metabolism from glycolysis to OXPHOS; this change is associated with a reduced production of IL-17 and suppresses proinflammatory functions of Th17 effector cells. Interestingly, coculture with rheumatoid arthritis patient-derived BMSCs showed that mitochondrial transfer is impaired compared with that with healthy donor-derived BMSCs, suggesting that resident tissue MSCs may represent a regulatory niche to balance the proinflammatory and anti-inflammatory responses; and part of the regulatory mechanisms may be mediated by mitochondrial transfer from MSCs [38]. Similarly, a study from Court et al. demonstrated that mitochondrial transfer facilitates Treg differentiation through the enhanced expression of mRNA transcripts such as FOXP3, IL2RA, CTLA4, and TGFb1, which are involved in Treg cell differentiation [39].

Another important player in the choice-making process between Th17 effector vs. regulatory cells is hypoxia-inducible factor 1α (HIF1α). HIF1α and the upstream mTOR pathway are required for glycolytic activity and Th17 effector cell development, whereas deficiency in HIF1α leads to bias towards Th17 regulatory cell differentiation [40]. However, it is unclear how the HIF1α pathway may interact with mitochondrial transfer, which remains an interesting subject of future study.

Another evidence of the immunomodulatory effect is that MSCs are able to suppress airway inflammation through mitochondrial transfer to stressed epithelial cells in an asthma model. The transfer of mitochondria seems to be mediated through Miro1, a calcium-sensitive cohesive protein that can attach mitochondria to Kif5c motor protein to enhance mitochondrial transportation. MSCs that overexpress Miro1 show an improved therapeutic effect in ameliorating epithelia-mediated amplification of the immune response, through an enhanced mitochondrial donation capacity [41].

Tissue injury or degeneration is normally accompanied with inflammation, which is identified to be a driving force for mitochondrial transfer. Zhang et al. showed that the proinflammatory cytokine TNF-α is engaged in regulating the TNF-α/NF-κB/TNF-αip2 signalling pathway that leads to F-actin polymerization and formation of TNTs via actin-driven protrusions of cytoplasmic membrane in MSCs [42, 43]. Similarly, oxidative inflammation enhances mitochondrial transfer and increases TNT formation via the Rot/NF-κB/TNF-αip2 signalling pathway in a corneal wound model [11].

The impact on inflammation by mitochondrial transfer is also associated with changes in cytokine expression profiles. Lian's group reported that treatment with human iPSC-MSCs in a NADH dehydrogenase iron-sulfur protein 4 (Ndufs4) gene deficiency mouse model can protect retinal ganglion cells and reduce murine proinflammatory cytokines such as TNF-α, MIP-1g, GM-CSF, IL-5, IL-17, and IL-1β [44]. Of note, TNF-α, GM-CSF, MCP-1, IL-17, IL-1β, IL-12p70, and CD30L are closely related to NF-κB signalling pathway which is involved in the regulation of TNT formation and mitochondrial transfer [45–48]. Downregulation of the above cytokines may inhibit the formation of TNTs and mitochondrial transfer. It is possible that the temporal regulation of cytokine levels correlates with the different stages of immune responses. Increased production of proinflammatory cytokines, for example TNF-α, may trigger the formation of TNTs and enhance mitochondrial transfer in the early phase of immune response; in the late phase of immune response, downregulation of cytokines through a paracrine mechanism by MSCs may slow down mitochondrial transfer. The results highlight the importance of applying MSCs in a right time and a right condition.

The above studies suggest that transferred mitochondria have a marked impact on immune responses via regulating macrophage and T cell functions, and through the alteration of cytokine expression. Next, we continue to discuss the impact of mitochondria biology on MSC proliferation and differentiation.

3. Mitochondria and MSC Proliferation and Differentiation

Mitochondrial dynamics includes the fusion and fission of mitochondria, which is crucial in maintaining the number of healthy mitochondria [49]. The morphology, distribution, density, and activity of mitochondria change along with the differentiation of MSCs to somatic terminal cells. In an undifferentiated stem cell state of MSCs, mitochondria mainly gather around the nucleus; along differentiation, mitochondria are dispersed in the cytoplasm [50, 51]. In addition, the morphology of mitochondria gradually becomes slender and elongated with well-developed cristae and an electron-dense matrix. The quantity, morphology, and distribution of the mitochondria constantly change to accommodate the energy needs which switch from a glycolysis mode at a stem cell state to an OXPHOS mode at a somatic cell state [52]. The copy number of mtDNA, protein subunits of the respiratory enzymes, oxygen consumption rate, and intracellular ATP content are all markedly increased after the induction of MSCs to osteocytes [53].

Likewise, mitochondrial transfer may influence stem cell proliferation and/or differentiation. Using a coculture system of MSCs with vascular smooth muscle cells, Vallabhaneni et al. found that mitochondrial transfer from smooth muscle cells to MSCs results in proliferation of MSCs [54]. By adding isolated normal mitochondria to iPSCs, mitochondria enter stem cells within minutes and facilitate the differentiation into neurons [55]. The evidences related to the effect of mitochondrial transfer were summarized in Table 1.

3.1. Mechanisms Underlying the Impact of Mitochondria Dynamics on MSC Differentiation. The morphology, quantity, and distribution of mitochondria are changed along the differentiation of MSCs. Is this change a cause or simply a consequence of differentiation? Forni et al. found that changes in mitochondria dynamics take place during the early stage of MSC differentiation; enhanced mitochondrial elongation and fusion were observed during adipogenesis and osteogenesis, and increased fission and mitophagy were

Table 1: Evidences of mitochondrial transfer between cells.

Donor cells	Acceptor cells	Methods	Mitochondrial transfer manner	Cell fate	Biological outcome	Related mechanisms	References
RL14 or HUVEC	MSCs	Coculture (MSCs + damaged cells); exposure of MSCs to exogenous somatic mitochondria	Bidirectional	Enhance MSCs viability	Upregulation of HO-1, PGC-1α, and mtTFA stimulates mitochondrial biogenesis in MSCs; HO-1 promotes mitochondrial transfer from MSCs to damaged cells	Somatic-derived mitochondria are engulfed and degraded by MSCs to trigger mitochondrial transfer from MSCs to damaged cells; elevated ROS upregulates HO-1; HO-1 enhances antiapoptotic function of MSCs and damaged cells; increase expression of Miro-1	[33]
MSCs	Fibroblasts	Coculture (MSCs+ fibroblasts+ OPA1 KO mouse fibroblasts); TNF-α is added	Bidirectional; mitochondrial transfer via TNTs and cellular fusion; promote mitochondrial transfer by TNF-α or 2DG treatment and OPA1 knockout	Increase mitochondrial biogenesis	Reduce ROS and improve redox homeostasis	Mitochondrial transfer reduces ROS but fails to salvage CI deficiency	[128]
BMSCs	PTECs	Coculture (BMSCs+ PTECs); *in vivo* (rat model)	Intravenously administered BMSC-derived isolated mitochondria to PTECs	Enhance cell viability; recover the expression of Megalin and SGLT2; reorganize tubular epithelium	Inhibit ROS production	Incorporated Mt acts on the endogenous Mt of PTECs, which suppresses cellular apoptosis via regulating Bcl-2, Bax, and PGC-1α; increase SOD2 and reduce ROS production	[30]
BMSCs	RCNs	Coculture (BMSCs+ RCNs); *in vivo* (injected cocultured cells in rats)	Unidirectional; elevate expression of Miro1	Fail to detect the expression of neurospecific β-III-tubulin or GFAP	BDNF	—	[129]
MSCs	Astrocytes and PC12 cells	Coculture (MSCs+ astrocytes exposed to OGD/PC12 cells); *in vivo* (rat models)	Unidirectional; mitochondria transfer via TNTs	Stimulation of neural cell proliferation	Restore respiration; show neuroprotective effect	Overexpression of Miro1 promotes mitochondrial transfer	[82]

Table 1: Continued.

Donor cells	Acceptor cells	Methods	Mitochondrial transfer manner	Cell fate	Biological outcome	Related mechanisms	References
VSMCs	BMSCs	Coculture system	Unidirectional; mitochondrial transfer via TNTs; formation of thin TNT-like structures	Fail to induce MSC differentiation to VSMC-like phenotype but successfully induce MSC proliferation	Stressed cells with dysfunctional mitochondria can trigger mitochondrial transfer	—	[54]
BMSCs	AML cells	Coculture (BMSCs+ AML or non-malignant $CD34^+$); *in vivo* (inject primary AML blasts without NOX2+ BMSCs)	Unidirectional; mitochondrial transfer mainly via TNTs, and to a small extent through endocytosis	Enhance cell viability and proliferation in AML cells; increase mitochondrial biogenesis	Increase mitochondrial respiration; mitochondrial transfer promotes disease progression	NOX2-generated superoxide stimulates ROS production in BMSC; ROS enhances mitochondrial transfer to leukemic blasts	[85]
BMSCs	Mouse melanoma and breast carcinoma cells derived from cells	*In vivo* (mouse)	mtDNA transfer	Stimulation of tumor cell proliferation	Delay tumor initiation; restore mitochondrial respiration in tumor cells via recovering respirasome and CII	mtDNA acquisition recovers mtDNA transcription and restores mitochondrial protein synthesis	[130]
MSCs	CD4+ T cells	Coculture (BMSCs/RA-$MSCs^8$+Th17 cells)	—	Induce Treg and suppress Th17 differentiation	Immunomodulation	—	[38]
hMADs	Cardiomyocytes	Coculture (hMADs+ cardiomyocytes)	Unidirectional; mitochondrial transfer via cell fusion and TNTs	Reprogram adult cardiomyocytes towards a progenitor-like state	—	Mitochondrial transfer and partial fusion between hMAD and cardiomyocytes reprogram cardiomyocytes to a cardiac progenitor-like state	[131]
MSCs	MDMs	Coculture (MSCs +MDMs); isolation of MSC-derived EVs; *in vivo* (LPS-induced lung injury model)	Extracellular vesicles (EVs)	Coculture with MSCs increases the percentage of MDMs expressing CD206	Promote oxidative phosphorylation and enhance anti-inflammatory and phagocytic effect	LPS treatment stimulates MDM secretion of M1 associated chemokines, TNF-α and IL-8, and M2 chemokines CCL18 and CCL22; both chemokines are diminished by addition of MSCs; MSCs show anti-inflammatory effect and enhance phagocytosis that can be attributed to MSC-derived EVs expressing CD44	[35]

Table 1: Continued.

Donor cells	Acceptor cells	Methods	Mitochondrial transfer manner	Cell fate	Biological outcome	Related mechanisms	References
MSCs	T cells	Coculture (MSCs+T cells);	Unidirectional;	Induce Treg and suppress Th17 differentiation	Immunomodulation	Mitochondrial transfer from MSCs drive Treg differentiation ($CD25^+FoxP3^+$) via overexpression of mRNA transcripts (FOXP3+, CTLA4,IL-2RA, and TGF-b1)	[39]
iPSC-MSCs	CMs	Coculture (iPSC-MSCs+CMs)	Bidirectional; mitochondrial transfer via TNTs	—	Augment mitochondrial retention and bioenergetic reservation	TNF-α is engaged in regulating TNF-α/NF-κB/TNF-αip2 signalling pathway which is able to enhance the formation of TNT	[42]
MSCs	CECs	Coculture (MSCs+ CECs); *in vivo* (alkali-injured eyes in a rabbit model)	Mitochondrial transfer via TNTs	—	Corneal protection	ROS activates NF-κB in CECs and enhances TNT formation via upregulation of NF-κB/TNF-αip2 signalling pathway	[11]
iPSC-MSCs	ASMCs	Coculture (iPSC-MSCs+ASMCs); *in vivo* (an ozone-induced mouse model of COPD)	Unidirectional; mitochondrial transfer via TNTs	—	Attenuate ozone-induced mitochondrial dysfunction, airway hyperresponsiveness and inflammation through mitochondrial transfer and paracrine effects	The protective effect may be exerted through mitochondrial transfer and paracrine effects	[89]
iPSC-MSCs	PC12 cells	Coculture (iPSC-MSCs+ PC12 cells)	Unidirectional; mitochondrial transfer via TNTs	—	Prevent apoptosis, mitochondrial swelling, and restore $\Delta\Psi$m in damaged cells	—	[88]
iPSC-MSCs	RGCs	Coculture (iPSC-MSCs+ RGCs); *in vivo* (transplanted iPSC-MSCs into the retina of Ndufs4 KO mice)	Unidirectional	—	Reduce abnormal activation of glial cells and neuroinflammation	Paracrine action and mitochondrial transfer are an interaction of two independent processes in MSC-mediated cell protection	[44]

Note: AML: acute myeloid leukemia; ASMCs: airway smooth muscle cells; Bax: Bcl-2 associated X protein; Bcl-2: B cell lymphoma-2; BDNF: brain-derived neurotrophic factor; BMSCs: bone marrow mesenchymal stem cells; CCL18: chemokine cc motif ligand 18; CCL22: chemokine cc motif ligand 22; CECs: corneal epithelial cells; CI: mitochondrial complex I; CII: mitochondrial complex II; CMs: cardiomyocytes; COPD: chronic obstructive pulmonary disease; GFAP: glial fibrillary acidic portein; hMADs: human multipotent adipose-derived stem cells; HO-1: heme oxygenase-1; HUVECs: human umbilical vein endothelial cell; IL-8: interleukin-8; LPS: lipopolysaccharide; MDMs: monocyte-derived macrophage; Miro 1: mitochondrial Rho-GTPase 1; MSCs: mesenchymal stem cells; mtDNA: mitochondrial DNA; mtTFA: mitochondrial transcription factor A; *Ndufs 4*: NADH dehydrogenase (ubiquinone) Fe-S protein 4; NF-κB: nuclear factor-kappa B; NOX2: NADPH oxidase 2; OGD: oxygen-glucose deprivation; OPA1: the mitochondrial inner membrane fusion protein optic atrophy 1; PC12 cells: pheochromocytoma cells; PGC-1α: PPARγ coactivator 1α; PTECs: proximal tubular epithelial cells; RA-sMSCs: rheumatoid arthritis synovial stromal stem cell; RCNs: rat cortical neurons; RGC: retinal ganglion cell; ROS: reactive oxidative stress; SOD2: superoxide dismutase 2; SGLT2: sodium-glucose cotransporter; TNF-α: tumor necrosis factor α; TNTs: tunneling nanotubes; Treg: T regulatory cells; VSMCs: vascular smooth muscle cells; 2DG: a glucose analogue that inhibits glycolysis, thereby reducing glycolytic flux; $\Delta\Psi$m: mitochondrial membrane potential.

observed during chondrogenesis. Knockdown of Mfn2—a factor critical in mitochondria fusion and overexpression of a dominant negative form of Drp1—a factor necessary in fission, both lead to failure of MSC differentiation, suggesting that the early changes in the mitochondria dynamics and consequently the alteration of bioenergetics are required for MSC differentiation [17].

Other factors that are closely related to mitochondrial metabolism, such as oxygen levels and ROS, may also play a role in the regulation of MSC self-renewal and differentiation. BMSCs that reside inside the bone marrow normally live in a hypoxic microenvironment, and HIF1α is a key regulator that can sense environment oxygen levels and adapt to it [56]. HIF1α pathway is activated in a hypoxic condition, which suppresses expression of peroxisome proliferator-activated receptor γ (PPARγ) coactivator 1-α (PGC1-α), facilitates anaerobic glycolysis, and inhibits mitochondrial biogenesis [57]. MSCs cultured for a long term in a hypoxic milieu are more prone to preserve the stemness feature, as indicated by enhanced self-renewal and multipotency [58]. Compared with MSCs cultured in normoxia, hypxia leads to increased differentiation to osteocytic lineage, as exhibited by enhanced expression of markers such as osteocalcin, type I collagen, and alkaline phosphatase [59]. Meanwhile, hypoxia inhibits adipocytic differentiation, possibly by HIF1α-mediated suppression of PGC1-α, which together with the PPARγ pathway promotes adipocyte differentiation [60]. The other related factor, ROS, is mainly produced by mitochondria in a cell. Accordant with the higher energy needs when MSCs differentiate to somatic cells, mitochondrial biogenesis is induced and more ROS is produced; ROS is considered to be toxic to most cellular components. To cope with elevated ROS, somatic cells usually upregulate antioxidant enzymes, which renders somatic cells more resistant to ROS than do MSCs [61]. In aged MSCs, the augmented ROS levels associated with damaged mitochondrial function may bias lineage specification towards an adipocyte fate vs. osteocyte fate [62]. It was also shown that the up-regulation of ROS can suppress osteocyte differentiation from MSCs, possibly through the inhibition of the hedgehog pathway. Furthermore, ROS seems to be necessary to initiate adipocyte specification [63], which can be inhibited by the addition of antioxidants [64]. The results suggest that oxygen levels and ROS may not simply be the consequence of differentiation but can actively influence this process. The effects and mechanisms of mitochondrial transfer between cells were shown in Figure 1.

4. Factors That Affect Mitochondrial Transfer

4.1. "Machinery" for Mitochondrial Transfer. Intercellular mitochondrial transfer involves three steps. First, specific signals are required from the damaged cells and/or other niche factors to trigger the process; second, the machinery/structure is formed to facilitate the transfer; and third, mitochondria are transported and perform certain functions in the receptor cells.

Using an ischemic cellular model, Liu et al. reported that phosphatidylserines exposed on the apoptotic endothelial cells can trigger mitochondrial transfer from infused MSCs to rescue the respiration functions of endothelial cells [6]. Secreted mitochondria released from damaged cells may also act as a "danger signal" to trigger mitochondrial donation [33, 65]. Specifically, somatic cell-derived mitochondria are transferred and degraded inside MSCs to initiate the rescue processes. It would not be surprising that other initiating signals also exist and exert functions in different settings.

Different molecular structures have been reported that mediate intercellular mitochondrial transfer, including tunneling nanotubes (TNTs), gap junction, extracellular vesicles (EVs), free extracellular mitochondria, and cytoplasmic fusion [66, 67]. Due to the limit on the scope of this review, we will mainly focus on the formation of TNTs and gap junction. For a more comprehensive review on this subject, please refer to these articles [68, 69]. TNTs are identified as a nanotube that can transport proteins, lipid droplets, ions, RNAs (including mircoRNAs), organelles, viruses, and cytosol in both directions [70]. Membrane-bound proteins were also observed to be transported between cells via TNTs [71]. MSCs are often used in coculture systems to study the function of TNTs, which can be formed over "long" distances (150 mm) when cells are far away from each other [71]. Two types of TNTs have been observed between human monocyte-derived macrophages, thin TNT and thicker TNT, which can be distinguished by their cytoskeleton structure, size, and functional characteristics [72]. Thicker nanotubes are longer, larger (600-700 nm in diameter) channels that contain microfilaments, microtubules, and F-actin, whereas thin-membrane nanotubes normally only contain F-actin. Most of mitochondrial transfer and intracellular vesicles transfer, but not all, seem to take place within thick-membrane TNTs between macrophages. As for some other types of cells, for example, kidney cells and neurons, TNTs formed between cells seem to mainly contain F-actin, but not microtubules [73]. Rustom and colleagues showed that multiple TNTs could form between cells, forming a complex 3-D network [70]. It is possible that the types of TNTs and the cargoes transported would vary between different cell types. In addition to transportation via TNTs, Li and colleagues revealed that gap junction is also involved in mitochondrial transfer from BMSCs to motor neurons [74]. In certain context, the tip of the nanotube can be embedded with gap junction proteins that are juxtaposed to the other gap junction proteins in the membrane of receptor cells. The gap junctions may facilitate mitochondrial transfer and allow electrical coupling between distant cells, which may represent another important means of intercellular signalling [75].

4.2. Origin and Status of MSCs Affect Mitochondrial Transfer. Several factors impact the formation of TNTs and further influence the efficiency of mitochondrial transfer. Motor protein, Kif5c, enables mitochondria to transfer along the microtubule network [76, 77]. Miro1 (mitochondrial Rho-GTPase), a calcium-sensitive cohesive protein, with the help of accessory proteins such as Miro2, TRAK1, TRAK2 and Myo19, can associate the mitochondria to Kif5c motor protein and assist the mitochondria to move along microtubules [78, 79]. Bioengineered MSCs that overexpress Miro1 show

increased mitochondrial transfer to injured epithelial cells and a greater reparative capacity, while knockdown of Miro1 results in loss of reparative effect [41]. PINK1 and Parkin target Miro for degradation and thus can arrest mitochondrial mobility [80]. In addition, shRNA-mediated knockdown of CD38 [81] and TNF-α [82] inhibits TNT formation and blocks mitochondrial transfer *in vitro*. Connexin 43 (CX43) is a gap junction protein. In an allergic airway inflammation model, Yao et al. showed that the overexpression of CX43 enhances the rescue efficacy of mitochondrial dysfunction and allergic inflammation, while silencing of CX43 partially nullifies this protective effect [83]. Apart from the factors that directly affect the formation of TNTs, hypoxia/reoxygenation [31], inflammatory stresses [11], and chemotherapy stress [84] may indirectly stimulate TNT formation. Besides, the microenvironment is a significant factor that regulates mitochondrial transfer. A study from Zhang's group suggested that the proinflammatory microenvironment is critical to provoke mitochondrial transfer from iPSC-MSCs to damaged cardiomyocytes [42]. NADPH oxidase 2- (NOX2-) derived superoxide in distressed cells stimulates ROS generation in BMSCs, which further leads to increased mitochondrial donation from BMSCs [85]. Oxygen-glucose deprivation (OGD) treatment on astrocytes or pheochromocytoma (PC12) cells promotes mitochondrial transfer from MSCs [82]. In addition, several factors that affect mitochondrial biogenesis or dynamics can enhance the process of mitochondrial transfer, such as HO-1, OPA1, and KD (mitochondrial fusion protein knockdown). The above results indicate that manipulation of the transfer machinery and/or the microenviroment may offer an effective approach to further enhance the efficiency and extent of mitochondrial transfer.

The origins and cellular states of donor cells also impact mitochondrial transfer. MSCs can be obtained from various tissues or differentiated from pluripotent stem cells. MSCs isolated from different tissues such as the bone marrow (BM), adipose (AD), dental pulp (DP), and Wharton's jelly (WJ) display differential mitochondrial donation capacity and therapeutic effects [86]. WJ-MSCs and DP-MSCs, compared with AD-MSCs and BM-MSCs, show higher respiratory capacity and bioenergetics and achieve a better rescue effect in damaged cardiomyocytes with a relatively smaller number of transferred mitochondria [86]. Moreover, compared with BM-MSCs, iPSC-derived MSCs (iPSC-MSCs) show superior effects in a limb ischemia model [45] and exhibit a higher efficiency of mitochondrial transfer to stressed cells in a chronic obstructive pulmonary disease model [87] and an anthracycline-induced cardiomyopathy model [42]. The greater ability of mitochondrial transfer in iPSC-MSCs could be attributed to a higher expression level of Miro1 and TNF-αIP2 [42]. Mitochondrial transfer from iPSC-MSCs was also shown to be beneficial in CoCl-insulted pheochromocytoma cells (PC12) [88] and cigarette smoke-exposed airway cells [89]. Interestingly, the beneficial effects of iPSC-MSCs on damaged cells may not only be entirely attributable to mitochondrial transfer but also to paracrine effects. iPSC-MSCs vs. bone marrow- or cord-derived MSCs are enriched with certain cytokines. For example, macrophage migration inhibitory factor (MIF) and growth differentiation factor-15 (GDF-15) are uniquely released from iPSC-MSCs to account for a cardioprotective effect, which is independent of mitochondrial transfer [90]. Notably, MSCs show beneficial effects through paracrine actions in cardiac repair [91] and hypoxia-conditioned media contain a higher expression of several growth factors that further promote the cardioprotective effects [92].

The cellular state of MSCs is also an important factor affecting the efficiency of mitochondrial transfer. By comparing the efficacy in a corneal wound healing experiment between healthy iPSC-MSCs and Rotenone-treated iPSC-MSCs, Jiang et al. pointed out that only healthy iPSC-MSCs display a beneficial effect [11]. Compared with Rotenone-treated iPSC-MSCs, healthy iPSC-MSCs show a higher level of basal mitochondrial oxygen consumption rate, ATP production, and maximal respiration. MSCs with impaired mitochondria (i.e., aged MSCs) may not be suitable therapeutic donors as only healthy functional mitochondria could fully exert the protective effects [11, 42]. Furthermore, the cell types that mitochondria are derived from also impact the outcome. Court et al. showed that exogenous mitochondria freshly isolated from MSCs can induce T cells to adopt a Treg phenotype; but this effect is not achieved by mitochondria isolated from other cell types such as fibroblasts or peripheral blood mononuclear cells, stressing the importance of the source of mitochondria [39].

In short, successful mitochondrial transfer requires sophisticated orchestration of several processes/signals, such as initiating signals, formation of transfer structure, and regulatory factors to control the speed of transfer. Besides, the significance of the source and status of mitochondrial donor cells should not be underestimated. Next, we will discuss the application of mitochondrial transfer in treatment of some neurological diseases.

5. Mitochondria-Based Therapy in Treatment of Neurological Diseases

Mitochondrial dysfunction is associated with various neurological pathologies, and transferring healthy mitochondria may be a new approach to restore mitochondrial functions [13, 14]. Mitochondrial transfer can be used to correct a range of problems caused by mitochondrial dysfunction via activating metabolic or immunomodulatory signalling pathways. In addition, cellular transfer of mitochondria is accompanied with the horizontal transfer of mitochondrial genes. Thus, genetically normal or enhanced mitochondria could be introduced to treat mitochondrial gene-related diseases (this topic is not discussed in this article due to scope limit). Below, we will summarize recent advances in mitochondria-based treatment on two common neurological diseases, stroke and SCI.

5.1. Mitochondria-Based Therapeutics for Treatment of Stroke. Acute ischemic stroke (AIS) occurs when the artery/arteries supplying the brain are blocked. The reduced blood flow results in cellular dysfunction, damage, and/or death, which underscores the importance of rapid blood flow recovery. Although revascularization is desired for stroke

treatment [93], transport of oxygen and nutrient to the damaged tissues often leads to the activation of the innate and adaptive immune responses that may cause secondary damage to the remaining cells [94, 95].

Mitochondrial dysfunction has been recognized as a hallmark in the complex cellular processes of ischemia/reperfusion (I/R) injury, which is characterized by reduced ATP production, increased ROS production, and elevated cell death [6]. When the blood supply is reduced or absent during ischemia, cells switch to anaerobic glycolytic metabolism, which gives rise to accumulation of lactic acid, H^+, $NADH^+$, and a lower level of ATP production. Consequently, Ca^{2+} reuptake from cytosol is impaired and additional Ca^{2+} influx is promoted by reperfusion, together leading to Ca^{2+} overload in cells [96]. A high level of $Ca2^+$ and oxidative stress result in the opening of mitochondrial permeability transition pore (MPTP) in the inner mitochondrial membrane and mitochondrial membrane uncoupling, which further augments ROS production [97, 98]. The excessive ROS production may cause damage on protein, DNA, and lipid, eventually leading to cell death [99, 100]. On the other hand, ROS can also induce astrogliosis [101], and chronic astrogliosis may impede regeneration of neural tissues [102]. Interestingly, although previous studies suggested that ROS and calcium participate in a viscous cycle of tissue damage, the latest research indicates that calcium may not stimulate the production of free radicals but suppress them [103].

To cope with the pathological damage caused by mitochondrial dysfunction in ischemia-reperfusion injury, mitochondrial transfer may be beneficial. Sources of mitochondrial transfer include astrocytes, endothelial cells, and MSCs. In brain, neurons and astrocytes can exchange mitochondria. Damaged mitochondria are released from neurons and taken by astrocytes for disposal and recycling. In a transient focal ischemia model, Lo's group found that astrocytic mitochondria are released and taken by injured neurons as a protective mechanism; and the process is mediated via a calcium-dependent mechanism involving CD38 and cyclic ADP ribose signalling [104]. Extracellular mitochondria collected from astrocytes, when injected into the peri-infarct area of a focal cerebral ischemia mouse model, can be taken by the neurons [104], suggesting that mitochondrial injection may be a novel therapeutic approach to treat stroke. In a follow-up study, the authors reported that free mitochondria exist in the cerebrospinal fluid in subarachnoid hemorrhage patients, and the membrane potentials of the mitochondria correlate with the clinical outcomes three months after stroke [105].

In stroke, not only neurons but also the neurovascular units are damaged, which include neurons, astrocytes, endothelia, and pericytes. Lo's group also pioneered in investigating the effect of mitochondria secreted from endothelial progenitor cells (EPCs) in an OGD model [106]. EPCs exist in circulating blood and are capable of homing to damaged areas to promote vasculogenesis. Addition of EPC-derived mitochondria into OGD-injured brain endothelium can restore endothelial tightness, promote angiogenesis, and increase intracellular ATP levels [106].

The most often used source of mitochondrial transfer is MSCs. Coculture of MSCs with OGD-treated human umbilical vein endothelial cells results in mitochondrial transfer to the damaged cells, and the process is initiated by recognition of the phosphatidylserines exposed on the surface of apoptotic endothelial cells. Using a middle cerebral artery occlusion (MCAO) and reperfusion rat model, Li et al. found that MSCs engrafted into the damaged area can donate mitochondria to the injured cerebral microvasculature [87]. Due to the ease of access, low immunogenicity, and good safety, MSCs are currently being trialled in stroke patients. On the website of ClinicalTrials.gov, as of the writing of this review, more than 20 clinical trials have been registered in which MSCs are applied to treat stroke patients. The MSCs used were derived from different sources such as the bone marrow, adipose, and umbilical cord, as either autologous or allogeneic graft, and the locations of those trials include various countries such as the United States, China, South Korea, and Spain. The delivery routes and the types of strokes selected also vary across trials. The extensive clinical trials hold great promise for the development of new MSC-based therapeutic drugs and/or approaches to treat stroke.

5.2. Therapeutics for the Treatment of Spinal Cord Injury. SCI, normally resulting from traumatic external forces, is categorized into two stages—primary injury and secondary injury [107]. During the secondary injury, ruptured blood vessel and reflexive vasoconstriction that result from the acute spinal cord injury may lead to a reduction in oxygen delivery and consequently damage those oxygen-dependent organelles such as mitochondria. The impaired mitochondria are less capable of maintaining its homeostasis and dynamics, resulting in energy insufficiency [108]. Secondary damage in SCI also comprises a cascade of events that trigger additional pathologies, such as mitochondrial permeability damage, calcium overload, excitatory toxicity, oxidative stress, and increased ROS production [109]. Different approaches such as repairing or replacing damaged mitochondria (mitochondrial transplantation), introduction of alternate energy sources ("biofuels"), use of antioxidant, and restoring mitochondrial permeability are currently being contemplated to deal with the second injury in SCI [110].

Mitochondrial transplantation, either of endogenous or exogenous origin, has shown encouraging outcomes in the replacement of dysfunctional mitochondria [111]. Recently, exogenous mitochondria isolated from PC12 cell line or rat muscle tissues were transplanted into injured rat spinal cord and observed to restore energy supply to injured tissues. Unfortunately, these transplanted mitochondria failed to produce long-term (6 weeks after injury) functional neuroprotective effects [112]. The reason for the mild long-term efficacy was not fully understood, but one possibility may lie in the cellular source of engrafted mitochondria. In a separate study, Li et al. injected either MSCs or MSC-derived mitochondria into the injured spinal cord of a rat contusion SCI model and observed significantly improved locomotor functions 6 weeks after injury [74]. Further studies are needed to compare the efficacy of mitochondria isolated from different sources in the same experimental setting. The

secondary injury in SCI consists of many different aspects, such as inflammation, damaged bioenergetics, and inhibitory niche for axonal regrowth, and addressing any single aspect by a particular approach may not be sufficient to amount to a dramatic interventional effect [109, 110, 113]. The multifactorial properties of MSCs may be advantageous in this regard. MSCs can regulate inflammatory responses, have a good capacity to donate mitochondria, and are able to secrete trophic factors; these properties may underlie the popular use of MSCs for treatment of different indications that include SCI [114, 115]. *In vitro* and *in vivo* studies showed that MSCs seem to be able to alleviate the secondary injury caused by inflammation [116], restore myelin insulation, promote axonal regeneration, and assist in angiogenesis [117–121]. Sykova et al. reported that the survival and efficacy of MSC graft can be enhanced by cotransplantation of appropriate biomaterials [122, 123]. In this study, Sykova and colleagues also tested intravenous and intraarterial delivery of MSCs in 20 SCI patients and confirmed the safety of this approach [122, 123]. Deng and colleagues conducted a phase I clinical trial by engrafting umbilical cord-derived MSCs with collagen biomaterial in 20 SCI patients (acute complete cervical injury), with the other 20 patients (acute complete cervical injury) who received biomaterial only as the control group. After a 12-month follow-up, the treatment group vs. control group showed significantly improved American Spinal Injury Association scores and better bowel and urinary functions [124]. In earlier clinical trials in which MSCs were applied to treat SCI patients, some clinical benefits were also observed [125–127]. Nevertheless, larger patient cohorts and randomized double-blind trials are necessary to draw a firm conclusion on the efficacy of this approach. At present, more than 30 clinical trials using MSCs for SCI treatment have been registered at ClinicalTrials.gov. In the coming years ahead, we will for sure see more data on the clinical efficacy of various types of MSCs on different types of SCIs. However, in those trials, it is the live MSCs that are applied for treatment of SCI; yet, no MSC-derived extracellular mitochondria have been tested in clinical trials. With the fast advance of the field and more consolidating preclinical data emerging on the efficacy of mitochondrial engraftment, clinical trials that involve transplantation of mitochondria alone or in combination with other effectors are warranted in the future.

6. Limitation and Future Perspectives

The ability of mitochondria to be transferred between cells has attracted a lot of attention in the past decades and an increasingly larger body of literature are emerging to unravel the detailed mechanisms of this phenomenon. However, there are still many open questions existing in the field which require further studies.

(1) MSCs are used as a popular donor of mitochondria in many studies that mostly focused on the transfer of mitochondria from MSCs to damaged cells. The transfer of mitochondria is actually a "two-way" transportation, and it is still unclear under what conditions would one way dominate the other and how this directionality of transport is initiated and regulated. (2) Different means of mitochondrial transfer have been reported that include TNTs, gap junctions, microvesicles, free extracellular secretion, and cell fusion. Can cells use multiple ways to transfer mitochondria at the same time? Is the choice of means cell type specific and/or microenvironment dependent? If so, how is this decision-making process determined and regulated? (3) To what extent is mitochondrial transfer participating in cellular repair as an intrinsic mechanism in organisms and to what extent following exogenous transplantation in disease? Is there any way to manipulate the extent of mitochondrial transfer to be clinically meaningful or to further increase the clinical efficacy? (4) Mitochondrial dynamics is regulated by both mitochondrial genome and nuclear genome. An indepth understanding of the regulatory mechanisms would definitely facilitate designs of small molecules, gene editing approaches, and other novel strategies, to improve the health state of mitochondria and the capacity to donate. (5) Compared to MSCs, do mitochondria derived from other cellular sources, such as astrocytes, endothelial cells, induced neural stem cells, and induced pluripotent stem cells, differ in the properties and therapeutic effects? (6) Will allogeneic or exogenic mitochondria be recognized by host immune system after engraftment? Would immune disparity still play a role after the uptake of exogenous mitochondria or even after the incoming mitochondria having fused with host mitochondria? (7) How to solve the scale-up issue if mitochondrial transfer proves to be an efficacious and safe therapy in the future? Can immortalized or genetically enhanced MSCs produce equally safe and efficacious mitochondria? (8) Mitochondrial transfer may be beneficial to damaged somatic cells in certain context but may be deleterious in other cases. Mitochondria transferred to cancer cells could enhance the bioenergetics of cancer cells and increase the invasiveness and resistance to drug treatment. In these cases, suppression of mitochondrial transfer may be desired.

With a deep understanding of the detailed mechanisms of mitochondrial transfer and extensive preclinical investigation on various disease models, it is not unrealistic to predict that the gap between basic research and clinical application may be closed in the foreseeable future.

7. Conclusion

Mitochondrial transfer is considered a promising therapeutic strategy, not only because it can restore mitochondria-related metabolism in damaged cells but also due to the ability to regulate many other basic aspects of a cell, such as cell survival, proliferation, and differentiation. Development of regenerative medicine that involves mitochondrial transfer offers a great potential for the treatment of neurological diseases such as stroke and spinal cord injury.

Conflicts of Interest

The authors declare that there is no conflict of interest.

Authors' Contributions

DH, XZ, XW, TJ, LC, and ZC wrote the manuscript together. Deqiang Han, Xin Zheng, Xueyao Wang: these authors contributed equally to this work.

Acknowledgments

This work was supported by the Stem Cell and Translation National Key Project (2016YFA0101403), National Natural Science Foundation of China (81973351, 81671186, 81661130160, 81422014, and 81561138004), Beijing Municipal Natural Science Foundation (5142005), Beijing Talents Foundation (2017000021223TD03), Support Project of High-level Teachers in Beijing Municipal Universities in the Period of 13th Five-Year Plan (CIT & TCD20180333), Beijing Medical System High Level Talent Award (2015-3-063), Beijing Municipal Health Commission Fund (PXM2020_026283_000005), Beijing One Hundred, Thousand, and Ten Thousand Talents Fund (2018A03), and Royal Society-Newton Advanced Fellowship (NA150482).

References

[1] A. I. Caplan, "Mesenchymal stem cells," *Journal of orthopaedic research: official publication of the Orthopaedic Research Society*, vol. 9, no. 5, pp. 641–650, 1991.

[2] A. Krasnodembskaya, Y. Song, X. Fang et al., "Antibacterial effect of human mesenchymal stem cells is mediated in part from secretion of the antimicrobial peptide LL-37," *Stem cells (Dayton, Ohio)*, vol. 28, no. 12, pp. 2229–2238, 2010.

[3] A. Monsel, Y. G. Zhu, S. Gennai et al., "Therapeutic effects of human mesenchymal stem cell-derived microvesicles in severe pneumonia in mice," *American Journal of Respiratory and Critical Care Medicine*, vol. 192, no. 3, pp. 324–336, 2015.

[4] J. L. Spees, S. D. Olson, M. J. Whitney, and D. J. Prockop, "Mitochondrial transfer between cells can rescue aerobic respiration," *Proceedings of the National Academy of Sciences of the United States of America*, vol. 103, no. 5, pp. 1283–1288, 2006.

[5] M. V. Jackson, T. J. Morrison, D. F. Doherty et al., "Mitochondrial transfer via tunneling nanotubes is an important mechanism by which mesenchymal stem cells enhance macrophage phagocytosis in the in vitro and in vivo models of ARDS," *Stem cells (Dayton, Ohio)*, vol. 34, no. 8, pp. 2210–2223, 2016.

[6] K. Liu, K. Ji, L. Guo et al., "Mesenchymal stem cells rescue injured endothelial cells in an in vitro ischemia-reperfusion model via tunneling nanotube like structure-mediated mitochondrial transfer," *Microvascular Research*, vol. 92, pp. 10–18, 2014.

[7] H. Y. Lin, C. W. Liou, S. D. Chen et al., "Mitochondrial transfer from Wharton's jelly-derived mesenchymal stem cells to mitochondria-defective cells recaptures impaired mitochondrial function," *Mitochondrion*, vol. 22, pp. 31–44, 2015.

[8] Y. M. Cho, J. H. Kim, M. Kim et al., "Mesenchymal stem cells transfer mitochondria to the cells with virtually no mitochondrial function but not with pathogenic mtDNA mutations," *PLoS One*, vol. 7, no. 3, article e32778, 2012.

[9] F. Figeac, P. F. Lesault, O. le Coz et al., "Nanotubular crosstalk with distressed cardiomyocytes stimulates the paracrine repair function of mesenchymal stem cells," *Stem Cells*, vol. 32, no. 1, pp. 216–230, 2014.

[10] M. N. Islam, S. R. Das, M. T. Emin et al., "Mitochondrial transfer from bone-marrow-derived stromal cells to pulmonary alveoli protects against acute lung injury," *Nature Medicine*, vol. 18, no. 5, pp. 759–765, 2012.

[11] D. Jiang, F. Gao, Y. Zhang et al., "Mitochondrial transfer of mesenchymal stem cells effectively protects corneal epithelial cells from mitochondrial damage," *Cell Death Disease*, vol. 7, no. 11, article e2467, 2016.

[12] R. Moschoi, V. Imbert, M. Nebout et al., "Protective mitochondrial transfer from bone marrow stromal cells to acute myeloid leukemic cells during chemotherapy," *Blood*, vol. 128, no. 2, pp. 253–264, 2016.

[13] D. Ben-Shachar and D. Laifenfeld, "Mitochondria, synaptic plasticity, and schizophrenia," *International Review of Neurobiology*, vol. 59, pp. 273–296, 2004.

[14] T. Sun, H. Qiao, P. Y. Pan, Y. Chen, and Z. H. Sheng, "Motile axonal mitochondria contribute to the variability of presynaptic strength," *Cell Reports*, vol. 4, no. 3, pp. 413–419, 2013.

[15] N. Lane and W. Martin, "The energetics of genome complexity," *Nature*, vol. 467, no. 7318, pp. 929–934, 2010.

[16] L. Pernas and L. Scorrano, "Mito-morphosis: mitochondrial fusion, fission, and cristae remodeling as key mediators of cellular function," *Annual Review of Physiology*, vol. 78, no. 1, pp. 505–531, 2016.

[17] M. F. Forni, J. Peloggia, K. Trudeau, O. Shirihai, and A. J. Kowaltowski, "Murine mesenchymal stem cell commitment to differentiation is regulated by mitochondrial dynamics," *Stem cells (Dayton, Ohio)*, vol. 34, no. 3, pp. 743–755, 2016.

[18] P. Fan, X. Y. Yu, X. H. Xie et al., "Mitophagy is a protective response against oxidative damage in bone marrow mesenchymal stem cells," *Life Sciences*, vol. 229, pp. 36–45, 2019.

[19] R. J. Youle and D. P. Narendra, "Mechanisms of mitophagy," *Nature Reviews. Molecular Cell Biology*, vol. 12, no. 1, pp. 9–14, 2011.

[20] A. M. Pickrell and R. J. Youle, "The roles of PINK1, Parkin, and mitochondrial fidelity in Parkinson's disease," *Neuron*, vol. 85, no. 2, pp. 257–273, 2015.

[21] W. Zhu, Y. Yuan, G. Liao et al., "Mesenchymal stem cells ameliorate hyperglycemia-induced endothelial injury through modulation of mitophagy," *Cell Death & Disease*, vol. 9, no. 8, p. 837, 2018.

[22] T. Tsujimoto, T. Mori, K. Houri et al., "miR-155 inhibits mitophagy through suppression of BAG5, a partner protein of PINK1," *Biochemical and Biophysical Research Communications*, vol. 523, no. 3, pp. 707–712, 2020.

[23] S. Li, H. Wu, D. Han et al., "A novel mechanism of mesenchymal stromal cell-mediated protection against sepsis: restricting inflammasome activation in macrophages by increasing mitophagy and decreasing mitochondrial ROS," *Oxidative Medicine and Cellular Longevity*, vol. 2018, 15 pages, 2018.

[24] F. L. Muller, Y. Liu, and H. Van Remmen, "Complex III releases superoxide to both sides of the inner mitochondrial membrane," *The Journal of Biological Chemistry*, vol. 279, no. 47, pp. 49064–49073, 2004.

[25] M. P. Murphy, "How mitochondria produce reactive oxygen species," *The Biochemical Journal*, vol. 417, no. 1, pp. 1–13, 2009.

[26] P. R. Angelova, M. Barilani, C. Lovejoy et al., "Mitochondrial dysfunction in Parkinsonian mesenchymal stem cells impairs differentiation," *Redox Biology*, vol. 14, pp. 474–484, 2018.

[27] L. Perico, M. Morigi, C. Rota et al., "Human mesenchymal stromal cells transplanted into mice stimulate renal tubular cells and enhance mitochondrial function," *Nature Communications*, vol. 8, no. 1, p. 983, 2017.

[28] G. Kroemer, B. Dallaporta, and M. Resche-Rigon, "The mitochondrial death/life regulator in apoptosis and necrosis," *Annual Review of Physiology*, vol. 60, no. 1, pp. 619–642, 1998.

[29] L. D. Xie, Y. Wu, Z. J. Fan, Y. Liu, and J. Zeng, "Astragalus polysaccharide protects human cardiac microvascular endothelial cells from hypoxia/reoxygenation injury: the role of PI3K/AKT, Bax/Bcl-2 and caspase-3," *Molecular Medicine Reports*, vol. 14, no. 1, pp. 904–910, 2016.

[30] N. Konari, K. Nagaishi, S. Kikuchi, and M. Fujimiya, "Mitochondria transfer from mesenchymal stem cells structurally and functionally repairs renal proximal tubular epithelial cells in diabetic nephropathy in vivo," *Scientific Reports*, vol. 9, no. 1, p. 5184, 2019.

[31] H. Han, J. Q. Hu, Q. Yan et al., "Bone marrow-derived mesenchymal stem cells rescue injured H9c2 cells via transferring intact mitochondria through tunneling nanotubes in an in vitro simulated ischemia/reperfusion model," *Molecular Medicine Reports*, vol. 13, no. 2, pp. 1517–1524, 2016.

[32] R. Gozzelino, V. Jeney, and M. P. Soares, "Mechanisms of cell protection by heme oxygenase-1," *Annual Review of Pharmacology and Toxicology*, vol. 50, no. 1, pp. 323–354, 2010.

[33] M. Mahrouf-Yorgov, L. Augeul, C. C. da Silva et al., "Mesenchymal stem cells sense mitochondria released from damaged cells as danger signals to activate their rescue properties," *Cell Death and Differentiation*, vol. 24, no. 7, pp. 1224–1238, 2017.

[34] T. K. Kovach, A. S. Dighe, P. I. Lobo, and Q. Cui, "Interactions between MSCs and immune cells: implications for bone healing," *Journal of Immunology Research*, vol. 2015, 17 pages, 2015.

[35] T. J. Morrison, M. V. Jackson, E. K. Cunningham et al., "Mesenchymal stromal cells modulate macrophages in clinically relevant lung injury models by extracellular vesicle mitochondrial transfer," *American Journal of Respiratory and Critical Care Medicine*, vol. 196, no. 10, pp. 1275–1286, 2017.

[36] D. G. Phinney, M. di Giuseppe, J. Njah et al., "Mesenchymal stem cells use extracellular vesicles to outsource mitophagy and shuttle microRNAs," *Nature Communications*, vol. 6, no. 1, 2015.

[37] J. Kim and P. Hematti, "Mesenchymal stem cell-educated macrophages: a novel type of alternatively activated macrophages," *Experimental Hematology*, vol. 37, no. 12, pp. 1445–1453, 2009.

[38] P. Luz-Crawford, J. Hernandez, F. Djouad et al., "Mesenchymal stem cell repression of Th17 cells is triggered by mitochondrial transfer," *Stem Cell Research & Therapy*, vol. 10, no. 1, p. 232, 2019.

[39] A. C. Court, A. Le-Gatt, P. Luz-Crawford et al., "Mitochondrial transfer from MSCs to T cells induces Treg differentiation and restricts inflammatory response," *EMBO Reports*, vol. 21, no. 2, article e48052, 2020.

[40] L. Z. Shi, R. Wang, G. Huang et al., "HIF1alpha-dependent glycolytic pathway orchestrates a metabolic checkpoint for the differentiation of TH17 and Treg cells," *The Journal of Experimental Medicine*, vol. 208, no. 7, pp. 1367–1376, 2011.

[41] T. Ahmad, S. Mukherjee, B. Pattnaik et al., "Miro 1 regulates intercellular mitochondrial transport & enhances mesenchymal stem cell rescue efficacy," *The EMBO Journal*, vol. 33, no. 9, pp. 994–1010, 2014.

[42] Y. Zhang, Z. Yu, D. Jiang et al., "iPSC-MSCs with high intrinsic MIRO1 and sensitivity to TNF-α yield efficacious mitochondrial transfer to rescue Anthracycline-induced cardiomyopathy," *Stem Cell Reports*, vol. 7, no. 4, pp. 749–763, 2016.

[43] K. Hase, S. Kimura, H. Takatsu et al., "M-Sec promotes membrane nanotube formation by interacting with Ral and the exocyst complex," *Nature Cell Biology*, vol. 11, no. 12, pp. 1427–1432, 2009.

[44] D. Jiang, G. Xiong, H. Feng et al., "Donation of mitochondria by iPSC-derived mesenchymal stem cells protects retinal ganglion cells against mitochondrial complex I defect-induced degeneration," *Theranostics*, vol. 9, no. 8, pp. 2395–2410, 2019.

[45] Q. Lian, Y. Zhang, J. Zhang et al., "Functional mesenchymal stem cells derived from human induced pluripotent stem cells attenuate limb ischemia in mice," *Circulation*, vol. 121, no. 9, pp. 1113–1123, 2010.

[46] D. V. Jovanovic, F. C. Jolicoeur, Y. He, M. Zhang, F. Mineau, and J.-P. Pelletier, "IL-17 stimulates the production and expression of proinflammatory cytokines, IL-beta and TNF-alpha, by human macrophages," *Journal of Immunology*, vol. 160, no. 7, pp. 3513–3521, 1998.

[47] S. A. ABDALLA, H. HORIUCHI, S. FURUSAWA, and H. MATSUDA, "Molecular cloning and characterization of chicken tumor necrosis factor (TNF)-superfamily ligands, CD30L and TNF-related apoptosis inducing ligand (TRAIL)," *The Journal of Veterinary Medical Science*, vol. 66, no. 6, pp. 643–650, 2004.

[48] S. C. Yue, A. Shaulov, R. Wang, S. P. Balk, and M. A. Exley, "CD1d ligation on human monocytes directly signals rapid NF- B activation and production of bioactive IL-12," *Proceedings of the National Academy of Sciences of the United States of America*, vol. 102, no. 33, pp. 11811–11816, 2005.

[49] K. Okamoto and J. M. Shaw, "Mitochondrial morphology and dynamics in yeast and multicellular eukaryotes," *Annual Review of Genetics*, vol. 39, no. 1, pp. 503–536, 2005.

[50] A. D. Hofmann, M. Beyer, U. Krause-Buchholz, M. Wobus, M. Bornhäuser, and G. Rödel, "OXPHOS supercomplexes as a hallmark of the mitochondrial phenotype of adipogenic differentiated human MSCs," *PLoS One*, vol. 7, no. 4, article e35160, 2012.

[51] K. P. Quinn, G. V. Sridharan, R. S. Hayden, D. L. Kaplan, K. Lee, and I. Georgakoudi, "Quantitative metabolic imaging using endogenous fluorescence to detect stem cell differentiation," *Scientific Reports*, vol. 3, no. 1, 2013.

[52] H. W. Choi, J. H. Kim, M. K. Chung et al., "Mitochondrial and metabolic remodeling during reprogramming and differentiation of the reprogrammed cells," *Stem Cells and Development*, vol. 24, no. 11, pp. 1366–1373, 2015.

[53] C.-T. Chen, Y.-R. V. Shih, T. K. Kuo, O. K. Lee, and Y.-H. Wei, "Coordinated changes of mitochondrial biogenesis and antioxidant enzymes during osteogenic differentiation of human mesenchymal stem cells," *Stem Cells*, vol. 26, no. 4, pp. 960–968, 2008.

[54] K. C. Vallabhaneni, H. Haller, and I. Dumler, "Vascular smooth muscle cells initiate proliferation of mesenchymal stem cells by mitochondrial transfer via tunneling nanotubes," *Stem Cells and Development*, vol. 21, no. 17, pp. 3104–3113, 2012.

[55] O. Robicsek, H. M. Ene, R. Karry et al., "Isolated mitochondria transfer improves neuronal differentiation of schizophrenia-derived induced pluripotent stem cells and rescues deficits in a rat model of the disorder," *Schizophrenia Bulletin*, vol. 44, no. 2, pp. 432–442, 2018.

[56] X. Niu, S. Li, S. Zheng et al., "Hypoxia-induced brain cell damage in male albino wistar rat," *Saudi journal of biological sciences*, vol. 25, no. 7, pp. 1473–1477, 2018.

[57] N. Goda and M. Kanai, "Hypoxia-inducible factors and their roles in energy metabolism," *International Journal of Hematology*, vol. 95, no. 5, pp. 457–463, 2012.

[58] I. Rosová, M. Dao, B. Capoccia, D. Link, and J. A. Nolta, "Hypoxic preconditioning results in increased motility and improved therapeutic potential of human mesenchymal stem cells," *Stem cells (Dayton, Ohio)*, vol. 26, no. 8, pp. 2173–2182, 2008.

[59] Q. Gu, Y. Gu, Q. Shi, and H. Yang, "Hypoxia promotes osteogenesis of human placental-derived mesenchymal stem cells," *The Tohoku Journal of Experimental Medicine*, vol. 239, no. 4, pp. 287–296, 2016.

[60] C. Jiang, J. Sun, Y. Dai et al., "HIF-1A and C/EBPs transcriptionally regulate adipogenic differentiation of bone marrow-derived MSCs in hypoxia," *Stem Cell Research & Therapy*, vol. 6, no. 1, 2015.

[61] S. Furukawa, T. Fujita, M. Shimabukuro et al., "Increased oxidative stress in obesity and its impact on metabolic syndrome," *The Journal of Clinical Investigation*, vol. 114, no. 12, pp. 1752–1761, 2004.

[62] F. Atashi, A. Modarressi, and M. S. Pepper, "The role of reactive oxygen species in mesenchymal stem cell adipogenic and osteogenic differentiation: a review," *Stem Cells and Development*, vol. 24, no. 10, pp. 1150–1163, 2015.

[63] K. Schröder, K. Wandzioch, I. Helmcke, and R. P. Brandes, "Nox 4 acts as a switch between differentiation and proliferation in preadipocytes," *Arteriosclerosis, Thrombosis, and Vascular Biology*, vol. 29, no. 2, pp. 239–245, 2009.

[64] Y. Kanda, T. Hinata, S. W. Kang, and Y. Watanabe, "Reactive oxygen species mediate adipocyte differentiation in mesenchymal stem cells," *Life Sciences*, vol. 89, no. 7-8, pp. 250–258, 2011.

[65] L. Galluzzi, O. Kepp, and G. Kroemer, "Mitochondria: master regulators of danger signalling," *Molecular cell biology*, vol. 13, no. 12, pp. 780–788, 2012.

[66] D. Mozaffarian, E. J. Benjamin, A. S. Go et al., "Heart disease and stroke statistics–2015 update: a report from the American Heart Association," *Circulation*, vol. 131, no. 4, pp. e29–322, 2015.

[67] A.-M. Rodriguez, J. Nakhle, E. Griessinger, and M. L. Vignais, "Intercellular mitochondria trafficking highlighting the dual role of mesenchymal stem cells as both sensors and rescuers of tissue injury," *Cell cycle*, vol. 17, no. 6, pp. 712–721, 2018.

[68] J. Wang, H. Li, Y. Yao et al., "Stem cell-derived mitochondria transplantation: a novel strategy and the challenges for the treatment of tissue injury," *Stem Cell Research & Therapy*, vol. 9, no. 1, p. 106, 2018.

[69] D. Torralba, F. Baixauli, and F. Sánchez-Madrid, "Mitochondria know no boundaries: mechanisms and functions of intercellular mitochondrial transfer," *Frontiers in cell and developmental biology*, vol. 4, 2016.

[70] A. Rustom, "Nanotubular highways for intercellular organelle transport," *Science*, vol. 303, no. 5660, pp. 1007–1010, 2004.

[71] E. Y. Plotnikov, T. G. Khryapenkova, S. I. Galkina, G. T. Sukhikh, and D. B. Zorov, "Cytoplasm and organelle transfer between mesenchymal multipotent stromal cells and renal tubular cells in co-culture," *Experimental Cell Research*, vol. 316, no. 15, pp. 2447–2455, 2010.

[72] B. Önfelt, S. Nedvetzki, R. K. P. Benninger et al., "Structurally distinct membrane nanotubes between human macrophages support long-distance vesicular traffic or surfing of bacteria," *Journal of Immunology*, vol. 177, no. 12, pp. 8476–8483, 2006.

[73] S. Abounit and C. Zurzolo, "Wiring through tunneling nanotubes–from electrical signals to organelle transfer," *Journal of Cell Science*, vol. 125, no. 5, pp. 1089–1098, 2012.

[74] H. Li, C. Wang, T. He et al., "Mitochondrial transfer from bone marrow mesenchymal stem cells to motor neurons in spinal cord injury rats via gap junction," *Theranostics*, vol. 9, no. 7, pp. 2017–2035, 2019.

[75] X. Wang, M. L. Veruki, N. V. Bukoreshtliev, E. Hartveit, and H. H. Gerdes, "Animal cells connected by nanotubes can be electrically coupled through interposed gap-junction channels," *Proceedings of the National Academy of Sciences of the United States of America*, vol. 107, no. 40, pp. 17194–17199, 2010.

[76] D. G. Iworima, B. A. Pasqualotto, and G. L. Rintoul, "Kif5 regulates mitochondrial movement, morphology, function and neuronal survival," *Molecular and Cellular Neurosciences*, vol. 72, pp. 22–33, 2016.

[77] A. F. MacAskill and J. T. Kittler, "Control of mitochondrial transport and localization in neurons," *Trends in Cell Biology*, vol. 20, no. 2, pp. 102–112, 2010.

[78] O. A. Quintero, M. M. DiVito, R. C. Adikes et al., "Human Myo 19 is a novel myosin that associates with mitochondria," *Current Biology: CB*, vol. 19, no. 23, pp. 2008–2013, 2009.

[79] K. Brickley and F. A. Stephenson, "Trafficking kinesin protein (TRAK)-mediated transport of mitochondria in axons of hippocampal neurons," *The Journal of Biological Chemistry*, vol. 286, no. 20, pp. 18079–18092, 2011.

[80] X. Wang, D. Winter, G. Ashrafi et al., "PINK1 and Parkin target Miro for phosphorylation and degradation to arrest mitochondrial motility," *Cell*, vol. 147, no. 4, pp. 893–906, 2011.

[81] C. R. Marlein, R. E. Piddock, J. J. Mistry et al., "CD38-driven mitochondrial trafficking promotes bioenergetic plasticity in multiple myeloma," *Cancer Research*, vol. 79, no. 9, pp. 2285–2297, 2019.

[82] V. Babenko, D. Silachev, V. Popkov et al., "Miro 1 enhances mitochondria transfer from multipotent mesenchymal stem cells (MMSC) to neural cells and improves the efficacy of cell recovery," *Molecules*, vol. 23, no. 3, p. 687, 2018.

[83] Y. Yao, X. L. Fan, D. Jiang et al., "Connexin 43-mediated mitochondrial transfer of iPSC-MSCs alleviates asthma inflammation," *Stem Cell Reports*, vol. 11, no. 5, pp. 1120–1135, 2018.

[84] Y. Feng, R. Zhu, J. Shen et al., "Human bone marrow mesenchymal stem cells rescue endothelial cells experiencing

chemotherapy stress by mitochondrial transfer via tunneling nanotubes," *Stem Cells and Development*, vol. 28, no. 10, pp. 674–682, 2019.

[85] C. R. Marlein, L. Zaitseva, R. E. Piddock et al., "NADPH oxidase-2 derived superoxide drives mitochondrial transfer from bone marrow stromal cells to leukemic blasts," *Blood*, vol. 130, no. 14, pp. 1649–1660, 2017.

[86] S. Paliwal, R. Chaudhuri, A. Agrawal, and S. Mohanty, "Human tissue-specific MSCs demonstrate differential mitochondria transfer abilities that may determine their regenerative abilities," *Stem Cell Research & Therapy*, vol. 9, no. 1, p. 298, 2018.

[87] X. Li, Y. Zhang, S. C. Yeung et al., "Mitochondrial transfer of induced pluripotent stem cell-derived mesenchymal stem cells to airway epithelial cells attenuates cigarette smoke-induced damage," *American Journal of Respiratory Cell and Molecular Biology*, vol. 51, no. 3, pp. 455–465, 2014.

[88] X. Li, Y. Yang, G. Ye et al., "Transfer of mitochondria from mesenchymal stem cells derived from induced pluripotent stem cells attenuates hypoxia-ischemia-induced mitochondrial dysfunction in PC12 cells," *Neural Regeneration Research*, vol. 15, no. 3, pp. 464–472, 2020.

[89] X. Li, C. Michaeloudes, Y. Zhang et al., "Mesenchymal stem cells alleviate oxidative stress-induced mitochondrial dysfunction in the airways," *The Journal of Allergy and Clinical Immunology*, vol. 141, no. 5, pp. 1634–1645.e5, 2018.

[90] Y. Zhang, X. Liang, S. Liao et al., "Potent paracrine effects of human induced pluripotent stem cell-derived mesenchymal stem cells attenuate doxorubicin-induced cardiomyopathy," *Scientific Reports*, vol. 5, no. 1, 2015.

[91] C. W. Siu, S. Y. Liao, Y. Liu, Q. Lian, and H. F. Tse, "Stem cells for myocardial repair," *Thrombosis and Haemostasis*, vol. 104, no. 7, pp. 6–12, 2017.

[92] Y. Zhang, X. Liang, Q. Lian, and H. F. Tse, "Perspective and challenges of mesenchymal stem cells for cardiovascular regeneration," *Expert Review of Cardiovascular Therapy*, vol. 11, no. 4, pp. 505–517, 2014.

[93] I. Soufiany, K. A. Hijrat, S. Soufiany, and L. Chen, "Bypass surgery for ischemic stroke caused by intracranial artery stenosis or occlusion," *Brain Science Advances*, vol. 4, no. 1, pp. 49–60, 2018.

[94] T. Kalogeris, C. P. Baines, M. Krenz, and R. J. Korthuis, "Ischemia/reperfusion," *Comprehensive Physiology*, vol. 7, no. 1, pp. 113–170, 2016.

[95] A. R. Anzell, R. Maizy, K. Przyklenk, and T. H. Sanderson, "Mitochondrial quality control and disease: insights into ischemia-reperfusion injury," *Molecular Neurobiology*, vol. 55, no. 3, pp. 2547–2564, 2018.

[96] E. Murphy and C. Steenbergen, "Ion transport and energetics during cell death and protection," *Physiology (Bethesda)*, vol. 23, pp. 115–123, 2008.

[97] A. P. Halestrap, "Calcium, mitochondria and reperfusion injury: a pore way to die," *Biochemical Society Transactions*, vol. 34, no. 2, pp. 232–237, 2006.

[98] T. S. Luongo, J. P. Lambert, P. Gross et al., "The mitochondrial Na+/Ca2+ exchanger is essential for Ca2+ homeostasis and viability," *Nature*, vol. 545, no. 7652, pp. 93–97, 2017.

[99] A. H. Bhat, K. B. Dar, S. Anees et al., "Oxidative stress, mitochondrial dysfunction and neurodegenerative diseases; a mechanistic insight," *Biomedicine & Pharmacotherapy*, vol. 74, pp. 101–110, 2015.

[100] J. W. Walters, D. Amos, K. Ray, and N. Santanam, "Mitochondrial redox status as a target for cardiovascular disease," *Current Opinion in Pharmacology*, vol. 27, pp. 50–55, 2016.

[101] M. Pekny, M. Pekna, A. Messing et al., "Astrocytes: a central element in neurological diseases," *Acta Neuropathologica*, vol. 131, no. 3, pp. 323–345, 2016.

[102] M. V. Sofroniew, "Molecular dissection of reactive astrogliosis and glial scar formation," *Trends in Neurosciences*, vol. 32, no. 12, pp. 638–647, 2009.

[103] Q. V. Duong, A. Hoffman, K. Zhong, M. J. Dessinger, Y. Zhang, and J. N. Bazil, "Calcium overload decreases net free radical emission in cardiac mitochondria," *Mitochondrion*, vol. 51, pp. 126–139, 2020.

[104] K. Hayakawa, E. Esposito, X. Wang et al., "Transfer of mitochondria from astrocytes to neurons after stroke," *Nature*, vol. 535, no. 7613, pp. 551–555, 2016.

[105] S. H.-Y. Chou, J. Lan, E. Esposito et al., "Extracellular mitochondria in cerebrospinal fluid and neurological recovery after subarachnoid hemorrhage," *Stroke*, vol. 48, no. 8, pp. 2231–2237, 2017.

[106] K. Hayakawa, S. J. Chan, E. T. Mandeville et al., "Protective effects of endothelial progenitor cell-derived extracellular mitochondria in brain endothelium," *Stem cells (Dayton, Ohio)*, vol. 36, no. 9, pp. 1404–1410, 2018.

[107] C. S. Ahuja, S. Nori, L. Tetreault et al., "Traumatic spinal cord injury-repair and regeneration," *Neurosurgery*, vol. 80, no. 3S, pp. S9–S22, 2017.

[108] J. F. Turrens, "Mitochondrial formation of reactive oxygen species," *The Journal of Physiology*, vol. 552, no. 2, pp. 335–344, 2003.

[109] C. A. Oyinbo, "Secondary injury mechanisms in traumatic spinal cord injury: a nugget of this multiply cascade," *Acta Neurobiologiae Experimentalis (Wars)*, vol. 71, no. 2, pp. 281–299, 2011.

[110] N. E. Scholpa and R. G. Schnellmann, "Mitochondrial-based therapeutics for the treatment of spinal cord injury: mitochondrial biogenesis as a potential pharmacological target," *The Journal of Pharmacology and Experimental Therapeutics*, vol. 363, no. 3, pp. 303–313, 2017.

[111] J. L. Gollihue and A. G. Rabchevsky, "Prospects for therapeutic mitochondrial transplantation," *Mitochondrion*, vol. 35, pp. 70–79, 2017.

[112] J. L. Gollihue, S. P. Patel, K. C. Eldahan et al., "Effects of mitochondrial transplantation on bioenergetics, cellular incorporation, and functional recovery after spinal cord injury," *Journal of Neurotrauma*, vol. 35, no. 15, pp. 1800–1818, 2018.

[113] A. G. Rabchevsky, S. P. Patel, and J. E. Springer, "Pharmacological interventions for spinal cord injury: where do we stand? How might we step forward?," *Pharmacology & Therapeutics*, vol. 132, no. 1, pp. 15–29, 2011.

[114] Q. Ao, J. Xiao, Y. Q. Yu et al., "Standards for the culture and quality control of umbilical cord mesenchymal stromal cells for neurorestorative clinical application (2017)," *Journal of Neurorestoratology*, vol. Volume 6, pp. 11–15, 2018.

[115] L. Chen, Y. Zhang, X. He, and S. Hooshang, "Comparison of intramedullary transplantation of olfactory ensheathing cell for patients with chronic complete spinal cord injury

worldwide," *Journal of Neurorestoratology*, vol. 1, no. 1, pp. 146–151, 2018.

[116] P. Shende and M. Subedi, "Pathophysiology, mechanisms and applications of mesenchymal stem cells for the treatment of spinal cord injury," *Biomedicine & Pharmacotherapy*, vol. 91, pp. 693–706, 2017.

[117] X.-C. Qiu, H. Jin, R.-Y. Zhang et al., "Donor mesenchymal stem cell-derived neural-like cells transdifferentiate into myelin-forming cells and promote axon regeneration in rat spinal cord transection," *Stem Cell Research & Therapy*, vol. 6, no. 1, 2015.

[118] L. Lin, H. Lin, S. Bai, L. Zheng, and X. Zhang, "Bone marrow mesenchymal stem cells (BMSCs) improved functional recovery of spinal cord injury partly by promoting axonal regeneration," *Neurochemistry International*, vol. 115, pp. 80–84, 2018.

[119] T. Zhou, Y. Zheng, L. Sun et al., "Microvascular endothelial cells engulf myelin debris and promote macrophage recruitment and fibrosis after neural injury," *Nature Neuroscience*, vol. 22, no. 3, pp. 421–435, 2019.

[120] E. Z. Yang, G. W. Zhang, J. G. Xu et al., "Multichannel polymer scaffold seeded with activated Schwann cells and bone mesenchymal stem cells improves axonal regeneration and functional recovery after rat spinal cord injury," *Acta Pharmacologica Sinica*, vol. 38, no. 5, pp. 623–637, 2017.

[121] M. Poudineh, Z. Wang, M. Labib et al., "Three-dimensional nanostructured architectures enable efficient neural differentiation of mesenchymal stem cells via mechanotransduction," *Nano Letters*, vol. 18, no. 11, pp. 7188–7193, 2018.

[122] E. Syková, P. Jendelová, L. Urdzíková, P. Lesný, and A. Hejčl, "Bone marrow stem cells and polymer hydrogels–two strategies for spinal cord injury repair," *Cellular and Molecular Neurobiology*, vol. 26, no. 7-8, pp. 1111–1127, 2006.

[123] R. Pal, C. Gopinath, N. M. Rao et al., "Functional recovery after transplantation of bone marrow-derived human mesenchymal stromal cells in a rat model of spinal cord injury," *Cytotherapy*, vol. 12, no. 6, pp. 792–806, 2010.

[124] X.-Y. Chen, S. Zhang, W.-S. Deng et al., "Collagen scaffold combined with human umbilical cord-mesenchymal stem cells transplantation for acute complete spinal cord injury," *Neural Regeneration Research*, vol. 15, no. 9, pp. 1686–1700, 2020.

[125] S. K. Oh, K. H. Choi, J. Y. Yoo, D. Y. Kim, S. J. Kim, and S. R. Jeon, "A phase III clinical trial showing limited efficacy of autologous mesenchymal stem cell therapy for spinal cord injury," *Neurosurgery*, vol. 78, no. 3, pp. 436–447, 2016.

[126] L. F. Geffner, P. Santacruz, M. Izurieta et al., "Administration of autologous bone marrow stem cells into spinal cord injury patients via multiple routes is safe and improves their quality of life: comprehensive case studies," *Cell Transplantation*, vol. 17, no. 12, pp. 1277–1293, 2008.

[127] W. A. El-Kheir, H. Gabr, M. R. Awad et al., "Autologous bone marrow-derived cell therapy combined with physical therapy induces functional improvement in chronic spinal cord injury patients," *Cell Transplantation*, vol. 23, no. 6, pp. 729–745, 2014.

[128] M. Melcher, K. Danhauser, A. Seibt et al., "Modulation of oxidative phosphorylation and redox homeostasis in mitochondrial NDUFS4 deficiency via mesenchymal stem cells," *Stem Cell Research & Therapy*, vol. 8, no. 1, p. 150, 2017.

[129] V. A. Babenko, D. N. Silachev, L. D. Zorova et al., "Improving the post-stroke therapeutic potency of mesenchymal multipotent stromal cells by cocultivation with cortical neurons: the role of crosstalk between cells," *Stem Cells Translational Medicine*, vol. 4, no. 9, pp. 1011–1020, 2015.

[130] A. . S. Tan, J. . W. Baty, L.-F. Dong et al., "Mitochondrial genome acquisition restores respiratory function and tumorigenic potential of cancer cells without mitochondrial DNA," *Cell Metabolism*, vol. 21, no. 1, pp. 81–94, 2015.

[131] A. Acquistapace, T. Bru, P. F. Lesault et al., "Human mesenchymal stem cells reprogram adult cardiomyocytes toward a progenitor-like state through partial cell fusion and mitochondria transfer," *Stem cells (Dayton, Ohio)*, vol. 29, no. 5, pp. 812–824, 2011.

Hindawi
Stem Cells International
Volume 2020, Article ID 5684250, 11 pages
https://doi.org/10.1155/2020/5684250

Research Article

Screening and Functional Pathway Analysis of Pulmonary Genes Associated with Suppression of Allergic Airway Inflammation by Adipose Stem Cell-Derived Extracellular Vesicles

Sung-Dong Kim,[1] Shin Ae Kang,[2] Yong-Wan Kim,[3] Hak Sun Yu,[2] Kyu-Sup Cho,[1] and Hwan-Jung Roh[4]

[1]*Department of Otorhinolaryngology and Biomedical Research Institute, Pusan National University Hospital, Busan, Republic of Korea*
[2]*Department of Parasitology and Tropical Medicine, Pusan National University School of Medicine, Yangsan, Republic of Korea*
[3]*Department of Otorhinolaryngology, Inje University Haeundae Paik Hospital, Republic of Korea*
[4]*Department of Otorhinolaryngology and Research Institute for Convergence of Biomedical Science and Technology, Pusan National University Yangsan Hospital, Yangsan, Republic of Korea*

Correspondence should be addressed to Hwan-Jung Roh; rohhj@pusan.ac.kr

Received 5 February 2020; Revised 19 May 2020; Accepted 2 June 2020; Published 27 June 2020

Academic Editor: Kar Wey Yong

Background. Although mesenchymal stem cell- (MSC-) derived extracellular vesicles (EVs) are as effective as MSCs in the suppression of allergic airway inflammation, few studies have explored the molecular mechanisms of MSC-derived EVs in allergic airway diseases. The objective of this study was to evaluate differentially expressed genes (DEGs) in the lung associated with the suppression of allergic airway inflammation using adipose stem cell- (ASC-) derived EVs. *Methods*. C57BL/6 mice were sensitized to ovalbumin (OVA) by intraperitoneal injection and challenged intranasally with OVA. To evaluate the effect of ASC-derived EVs on allergic airway inflammation, 10 μg/50 μL of EVs were administered intranasally prior to OVA challenge. Lung tissues were removed and DEGs were compared pairwise among the three groups. DEG profiles and hierarchical clustering of the identified genes were analyzed to evaluate changes in gene expression. Real-time PCR was performed to determine the expression levels of genes upregulated after treatment with ASC-derived EVs. Enrichment analysis based on the Gene Ontology (GO) database and Kyoto Encyclopedia of Genes and Genomes (KEGG) pathway analysis were also performed to further identify the function of DEGs. *Results*. Expression of paraoxonase 1 (PON1), brain-expressed X-linked 2 (Bex2), insulin-like growth factor binding protein 6 (Igfbp6), formyl peptide receptor 1 (Fpr1), and secretoglobin family 1C member 1 (Scgb1c1) was significantly increased in asthmatic mice following treatment with ASC-derived EVs. GO enrichment and KEGG pathway analysis showed that these genes were strongly associated with immune system processes and their regulation, cellular processes, single-organism processes, and biological regulation. *Conclusion*. These results suggest that the DEGs identified in this study (PON1, Bex2, Igfbp6, Fpr1, and Scgb1c1) may be involved in the amelioration of allergic airway inflammation by ASC-derived EVs.

1. Introduction

Asthma is a chronic inflammatory airway disease involving multiple cellular components; its key features are airway hyperresponsiveness (AHR), persistent airway inflammation, and airway remodeling [1]. Excessive activation of Th2 cells by insufficient suppression of regulatory T cells (Tregs) plays an important role in the pathogenesis of allergic airway inflammation [2–4]. Recently, airway remodeling was reported to be important in pathological pathways of asthma characterized by irreversible AHR and airway obstruction [5].

Mesenchymal stem cells (MSCs) modulate immune responses and inflammation [6]. Several studies have shown

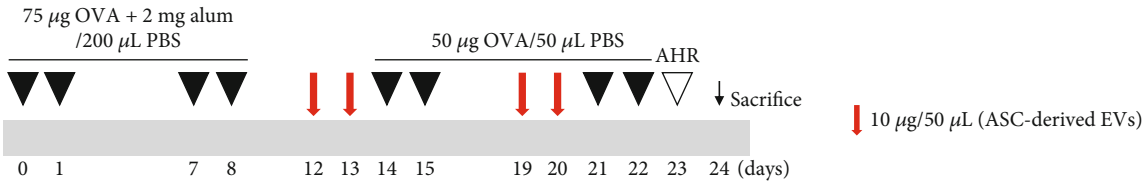

(a)

Group	Sensitization	Challenge	Treatment
CON	PBS	PBS	PBS
OVA	OVA	OVA	PBS
EV	OVA	OVA	ASC-derived EVs

(b)

Figure 1: Experimental protocol of this study. (a) Mice were sensitized on days 0, 1, 7, and 8 by intraperitoneal injection of ovalbumin (OVA) and challenged intranasally on days 14, 15, 21, and 22 with OVA. Adipose stem cell- (ASC-) derived extracellular vesicles (EVs) (10 μg/50 μL) were injected intranasally on days 12, 13, 19, and 20. (b) Mice were divided into three groups according to sensitization, challenge, and treatment.

that MSCs, including those derived from adipose tissue (ASCs), can improve allergic airway inflammation in asthmatic mice [7–9]. Although the immune suppression mechanism of MSCs in allergic airway diseases is not completely understood, it has been demonstrated to be strongly related to Treg upregulation and increases in soluble factors such as prostaglandin E2 (PGE2), transforming growth factor-β (TGF-β), and interleukin- (IL-) 10 [10–13]. MSCs have also been shown to modulate recognition of antigen-presenting cells that mediate cellular immune responses, including dendritic cells, macrophages, and B cells [14, 15].

Several recent studies have shown that T cell activation and proliferation are suppressed by the MSC culture supernatant (MSC sup) [16, 17]. Accumulating evidence shows that administration of MSC sup or extracellular vesicles (EVs) released by MSCs is as effective as that of MSCs in suppressing allergic airway inflammation [18–20]. MSC-derived EVs were found to upregulate IL-10 and TGF-β1 from peripheral blood mononuclear cells of asthmatic patients, thereby promoting the proliferation and immune suppression capacity of Tregs [21]. Furthermore, ASC-derived EVs ameliorated Th2-mediated inflammation induced by the *Aspergillus* protease antigen through the activation of dendritic cells and induction of M2 macrophage polarization [22]. Although a recent study showed that MSC-derived EVs prevented group 2 innate lymphoid cell-dominant allergic airway inflammation through miR-146a-5p [23], the molecular mechanisms of MSC-derived EVs in allergic airway inflammation remain to be elucidated, and the genes involved in these mechanisms have not been definitively identified.

In this study, we isolated EVs secreted by ASCs and performed microarray gene expression analysis in asthmatic mice treated with ASC-derived EVs. We also examined differentially expressed genes (DEGs) associated with the suppression of allergic airway inflammation by ASC-derived EVs.

2. Materials and Methods

2.1. Animals. Six-week-old female C57BL/6 mice were purchased from Samtako Co. (Osan, Republic of Korea) and bred in animal facilities without specific pathogens during experiments. The animal study protocol was approved by the Institutional Animal Care and Use Committee of the Pusan National University School of Medicine (Approval No. PNU-2016-1109).

2.2. EV Extraction and Characterization. As in our previous study [11, 24, 25], adipose tissue was obtained from the abdominal fat of C57BL/6 mice. ASCs were cultured at 37°C with 5% CO_2 in α-modified Eagle's medium (α-MEM) containing 10% fetal bovine serum (FBS) until 1×10^6 cells/cm^2 were obtained. EVs were isolated from ASC sup as previously described [26]. The supernatant was filtered through a 0.45 μm vacuum filter. The filtrate was concentrated using QuixStand (GE Healthcare, Little Chalfont, UK) and then filtered through a 0.22 μm bottle top filter (Sigma-Aldrich, St. Louis, MO). The filtrates were pelleted by ultracentrifugation in a 45 Ti rotor (Beckman Coulter, Fullerton, CA) at 100,000 × g for 2 h at 4°C. The final pellets were resuspended in phosphate-buffered saline (PBS) and stored at -80°C. We placed the EVs in PBS on 300-mesh copper grids and stained them with 2% uranyl acetate. Images were obtained using a JEM-1011 electron microscope (JEOL, Tokyo, Japan) operated at an acceleration voltage of 100 kV [27, 28]. EV markers including CD81 and CD40 were analyzed by western blotting with primary antibodies, anti-CD81 (1 : 1000, Abcam, Cambridge, MA), and anti-CD40 (1 : 1000, Abcam) as previously described [22].

2.3. Mouse Model of Allergic Airway Inflammation. A mouse model of allergic airway inflammation was induced as previously reported with minor modifications [24, 25]. The mice were sensitized by intraperitoneal injection of 75 μg of OVA (Sigma-Aldrich, St. Louis, MO, USA) with 2 mg of aluminum hydroxide (Sigma-Aldrich) in 200 μL of PBS on days 0, 1, 7, and 8. On days 14, 15, 21, and 22, the mice were challenged intranasally with 50 μg of OVA in 50 μL of PBS. The mice were sacrificed on day 24 (Figure 1(a)).

2.4. Intranasal Administration of ASC-Derived EVs. To evaluate the effect of ASC-derived EVs, we injected 10 μg/50 μL

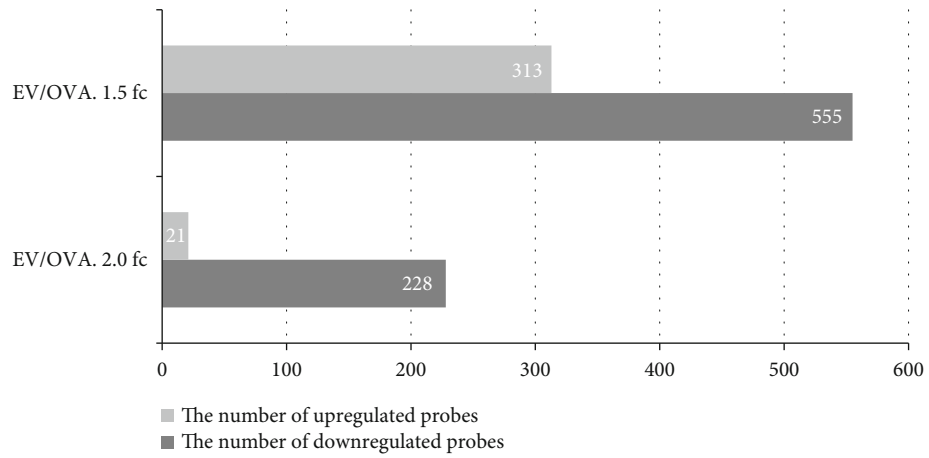

Figure 2: Bar plot of significant probes. We identified 868 and 249 differentially expressed genes (DEGs) with fold changes of $|\log_{FC}| \geq 1.5$ and $|\log_{FC}| \geq 2.0$ between the EV and OVA groups, respectively.

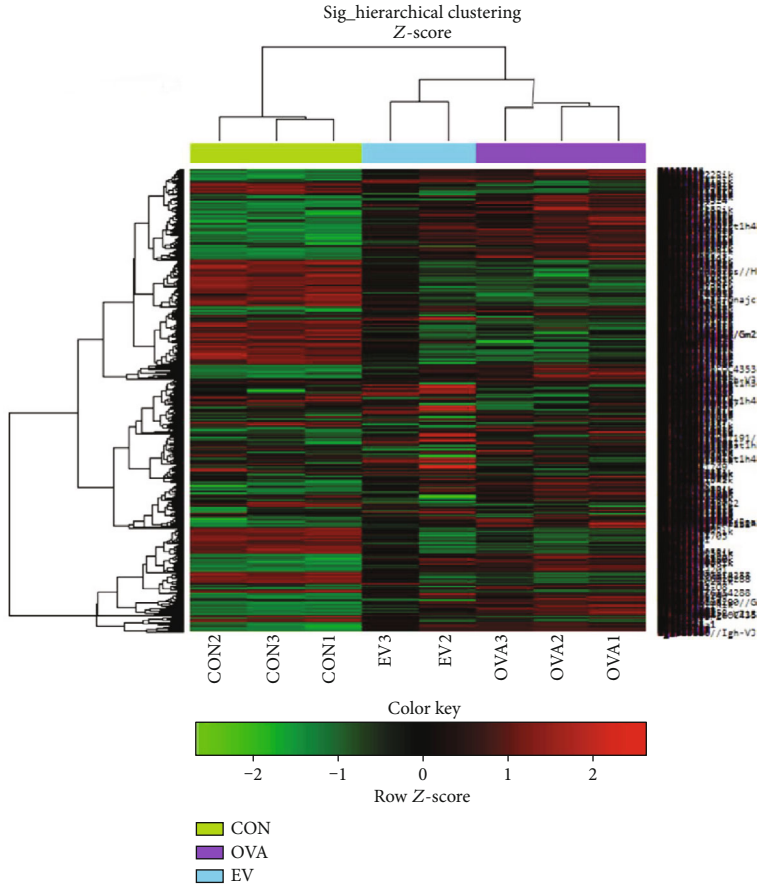

Figure 3: Hierarchical clustering analysis and heat map diagram. Green and red shading indicates down- and upregulated genes, respectively.

of EVs intranasally on days 12, 13, 19, and 20. Mice were divided into three groups, with five mice per group: (a) the CON group was sensitized, pretreated, and challenged with PBS; (b) the OVA group was sensitized with OVA, pretreated with PBS, and then challenged with OVA; and (c) the EV group was sensitized with OVA, pretreated with ASC-derived EVs, and then challenged with OVA (Figure 1(b)).

2.5. Microarray Analysis of the Lung Tissue. Lung tissues were extracted and DEGs were compared pairwise among the three groups. To investigate changes in gene expression following treatment with ASC-derived EVs, microarray analyses were performed by Macrogen Inc. (Seoul, Republic of Korea), a company that specializes in this technology. The Affymetrix Whole-transcript Expression array process was

performed using the GeneChip Whole Transcript PLUS Reagent Kit to extract total RNA from lung tissue according to the manufacturer's protocol. Then, cDNA was synthesized as described by the manufacturer using the GeneChip Whole Transcript (WT) Amplification Kit and sense cDNA was fragmented and biotin-labeled with terminal deoxynucleotidyl transferase (TdT) using the GeneChip WT Terminal Labeling Kit. Approximately 5.5 μg of the labeled DNA target was hybridized at 45°C for 16 h to the Affymetrix GeneChip Mouse 2.0 ST Array. After washing the hybridized arrays and staining with the GeneChip Fluidics Station 450, we scanned the target using a GCS 3000 Scanner (Affymetrix) and computed the signal values using the Affymetrix GeneChip Command Console Software.

2.6. Gene Expression Analysis by Quantitative Real-Time Polymerase Chain Reaction (qRT-PCR). Total RNA was extracted from lung tissues using 1 mL of QIAzol (Qiagen, Valencia, CA) following the manufacturer's protocol. We transcribed 2 μg of RNA using Moloney Murine Leukemia Virus Reverse Transcriptase (Promega, Madison, WI). Paraoxonase 1 (PON1) (forward, 5′-GATTGGCACTGTGTTC CAC-3′; reverse, 5′-ATCACTGTGGTAGGCACCTT-3′), brain-expressed X-linked 2 (Bex2) (forward, 5′-GGATGT TAAAAGGGACTCCCGGTGA-3′; reverse, 5′-CGACGG CGGTTCTGACGCCACAACG-3′), insulin-like growth factor binding protein 6 (Igfbp6) (forward, 5′-GCAGCAGCT CCAGACTGA-3′; reverse, 5′-CATTGCTTCACATACA GCTCAA-3′), formyl peptide receptor 1 (Fpr1) (forward, 5′ -CATGTCTCTCCTCATGAACAAG-3′; reverse, 5′-ATGA GAAGACATCCAGAACGA-3′), and secretoglobin family 1C member 1 (Scgb1c1) (forward, 5′-GGAATTCCTGC AAACACTCCT-3′; reverse, 5′-GGGCTGCTTATGTGTC CTCT-3′) RNA levels were quantified relative to the housekeeping gene glyceraldehyde 3-phosphate dehydrogenase (GAPDH) (forward, 5′-TACCCCCAATGTGTCCGTC-3′; reverse, 5′-AAGAGTGGGAGTTGCTGTTGAAG-3′), using the LightCycler 96 Real-Time PCR System (Roche, Basel, Switzerland) following the manufacturer's instructions. We used the comparative Ct ($2^{-\Delta\Delta Ct}$) method to calculate relative gene expression levels.

2.7. Raw Data Preparation. We used the Affymetrix GeneChip Command Console software to extract raw data, following the Affymetrix data extraction protocol. We summarized and standardized the data using the robust multiarray average (RMA) method with the Affymetrix Expression Console software. The gene-level results were exported along with the RMA analysis, and further examined via DEG analysis.

2.8. Statistical Analyses. Statistical significance among the expression data was evaluated in terms of fold change. To evaluate similarity, we examined linkage and Euclidean distance among the hierarchical cluster analysis results of each DEG set. The Gene Ontology (GO) and Kyoto Encyclopedia of Genes and Genomes (KEGG) pathway databases (http://www.geneontology.org/) were used to perform gene enrichment and functional annotation analyses of significant probes. All data analyses and DEG visualization were performed using the R 3.1.2 software (R Core Team).

Table 1: Genes downregulated following treatment with ASC-derived EVs.

Gene	OVA/CON	EV/CON	EV/OVA
Ear6	1.838022	1.149834	-1.598512
Ccl5	2.641300	1.198238	-2.204320
Ccl6	29.061333	16.230038	-1.790589
Ccl12	5.776364	3.477515	-1.661061
Tnfsf8	2.617759	1.697634	-1.542005
IL5Ra	2.587367	1.613224	-1.603849
Tnfrsf13b	1.985461	1.238539	-1.603067

ASCs: adipose stem cells; Ccl: chemokine ligand; CON: control; Ear6: eosinophil-associated ribonuclease A family member 6; EVs: extracellular vesicles; IL5Ra: interleukin-5 receptor alpha; OVA: ovalbumin; Tnfrsf13b: tumor necrosis factor receptor superfamily member 13B; Tnfsf8: tumor necrosis factor ligand superfamily member 8.

Table 2: Genes upregulated following treatment with ASC-derived EVs.

Gene	OVA/CON	EV/CON	EV/OVA
PON1	-9.35267	-6.482819	1.442686
Bex2	-3.798534	-2.489212	1.525998
Igfbp6	-3.230484	-2.120048	1.523779
Fpr1	-3.109904	-2.022899	1.537350
Scgb1c1	-2.224596	-1.467501	1.515908

ASCs: adipose stem cells; Bex2: brain-expressed X-linked 2; CON: control; EVs: extracellular vesicles; Fpr1: formyl peptide receptor 1; Igfbp6: insulin-like growth factor binding protein 6; OVA: ovalbumin; PON1: paraoxonase 1; Scgb1c1: secretoglobin family 1C member 1.

3. Results

3.1. Characterization of ASC-Derived EVs. Transmission electron microscopy (TEM) showed that ASC-derived EVs had lipid bilayers and were spherical in shape. Western blotting showed that ASC-derived EVs were positive for the CD81 exosome marker and CD40 microvesicle marker (data not shown).

3.2. Data Processing and DEG Identification. Following normalization, we analyzed DEG profiles with a false discovery rate (FDR) cut-off of FDR < 0.05 and fold change cut-offs of $|\log_{FC}| \geq 1.5$ and $|\log_{FC}| \geq 2.0$. We identified 868 DEGs with $|\log_{FC}| \geq 1.5$ between the EV and OVA groups, among which 313 and 555 were down- and upregulated, respectively. We identified 249 DEGs with $|\log_{FC}| \geq 2.0$ between the EV and OVA groups, of which 228 and 21 genes were down- and upregulated, respectively (Figure 2).

3.3. Hierarchical Clustering Analysis of DEGs. Hierarchical clustering of the identified DEGs is shown in Figure 3. Tree view and cluster analyses were performed using the Euclidean method to group and display genes with a $|\log_{FC}| \geq 1.5$ change in expression. Gene expression among ASC-derived EVs was compared with transcript levels among

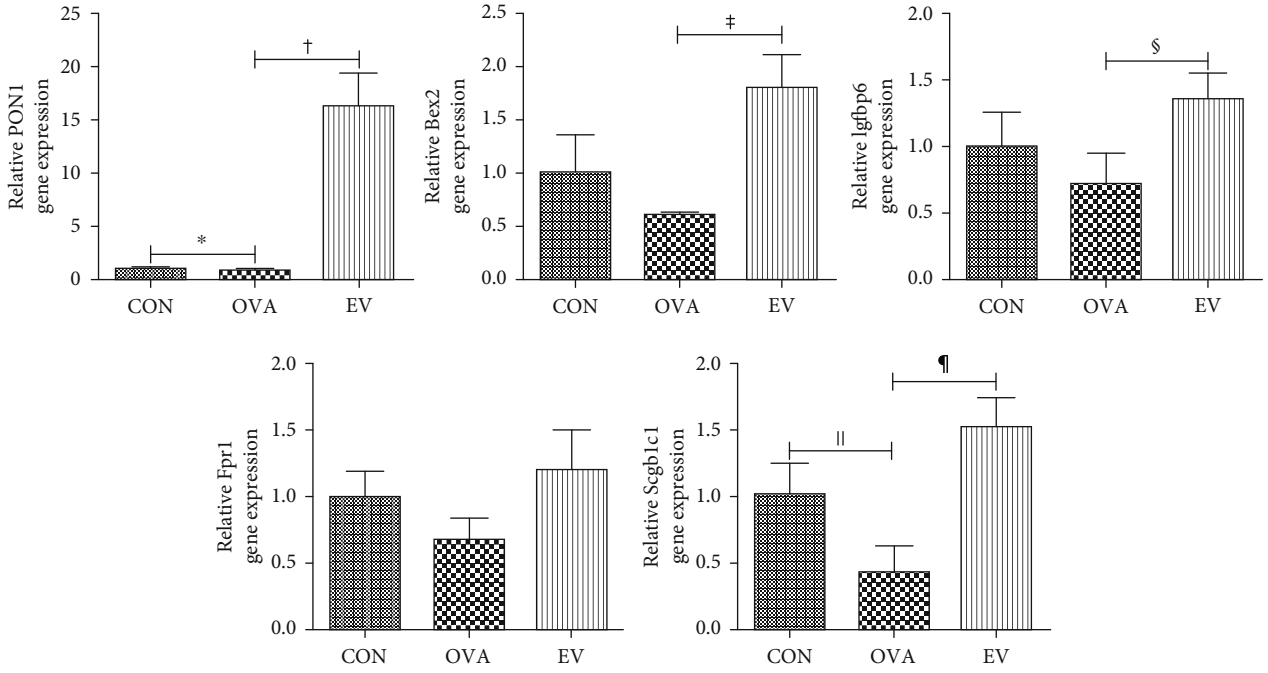

Figure 4: Effects of ASC-derived EVs on PON1, Bex2, Igfbp6, Fpr1, and Scgb1c1 gene expression. PON1 and Scgb1c1 gene expression was significantly decreased in the OVA group compared to the CON group. However, EV treatment markedly increased the expression of PON1, Bex2, Igfbp6, and Scgb1c1 in asthmatic mice. $^{\dagger}p = 0.001$; $^{\ddagger}p = 0.003$; $^{\S}p = 0.022$; $^{\|}p = 0.008$; $^{\P}p < 0.001$. ASCs: adipose stem cells; Bex2: brain-expressed X-linked 2; CON: control; EV: extracellular vesicle; Fpr1: formyl peptide receptor 1; Igfbp6: insulin-like growth factor binding protein 6; OVA: ovalbumin; PON1: paraoxonase 1; Scgb1c1: secretoglobin family 1C member 1.

the OVA group. Upregulated and downregulated genes were easily distinguished between the two groups. Eosinophil-associated ribonuclease A family member 6 (Ear6), chemokine ligands 5, 8, and 12 (Ccl5, Ccl8, and Ccl12), tumor necrosis factor ligand superfamily member 8 (Tnfsf8), interleukin-5 receptor alpha (IL5Ra), and tumor necrosis factor receptor superfamily member 13B (Tnfrsf13b) were upregulated in the OVA group compared to the CON group, although these genes were downregulated by ASC-derived EVs (Table 1). In contrast, PON1, Bex2, Igfbp6, Fpr1, and Scgb1c1 were downregulated in OVA-induced asthmatic mice, but upregulated following treatment with ASC-derived EVs (Table 2).

3.4. Expression of PON1, Bex2, Igfbp6, Fpr1, and Scgb1c1. The gene expression levels of PON1 and Scgb1c1 were significantly decreased in the OVA group compared to the CON group ($p = 0.001$ and $p = 0.008$, respectively). However, treatment with ASC-derived EVs markedly increased the expression of PON1, Bex2, Igfbp6, and Scgb1c1 in asthmatic mice ($p = 0.001$, $p = 0.003$, $p = 0.022$, and $p < 0.001$, respectively). Although Frp1 mRNA levels increased in the EV group, there was no significant difference between the OVA and EV groups ($p = 0.057$) (Figure 4).

3.5. Functional Category Enrichment Analysis of DEGs. The GO database was used to perform enrichment analysis of DEGs to examine their association with biological processes, cellular components, and molecular functions. The 10 most highly significant terms associated with DEGs with a cut-off of FDR < 0.05 were summarized for each category. Genes that were down- and upregulated following treatment with ASC-derived EVs were strongly associated with immune system processes and their regulation (Figure 5(a)), intracellular components and intracellular organelles (Figure 5(b)), and catalytic activity and ion binding (Figure 5(c)).

Up- and downregulated genes associated with each term were analyzed separately. DEGs that were downregulated following treatment with ASC-derived EVs were involved in whole-cell and within-cell components (Figure 6(a)). In contrast, genes differentially upregulated following treatment with ASC-derived EVs were strongly associated with cellular and single-organism processes, as well as biological regulation (Figure 6(b)).

3.6. KEGG Pathway Analysis. Enrichment analysis based on the KEGG pathway showed that highly significant DEGs following treatment with ASC-derived EVs were correlated with environmental information processing, organismal systems, and human diseases (Figure 7).

4. Discussion

MSCs have been reported as promising candidates for the treatment of allergic airway diseases [7–13]. However, MSCs have several drawbacks including immune rejection, risk of aneuploidy, difficulty of handling, and tumorigenicity. Previous studies have shown that ASC-derived secretome-containing EVs, even without ASCs, ameliorate allergic airway inflammation through the suppression of Th2

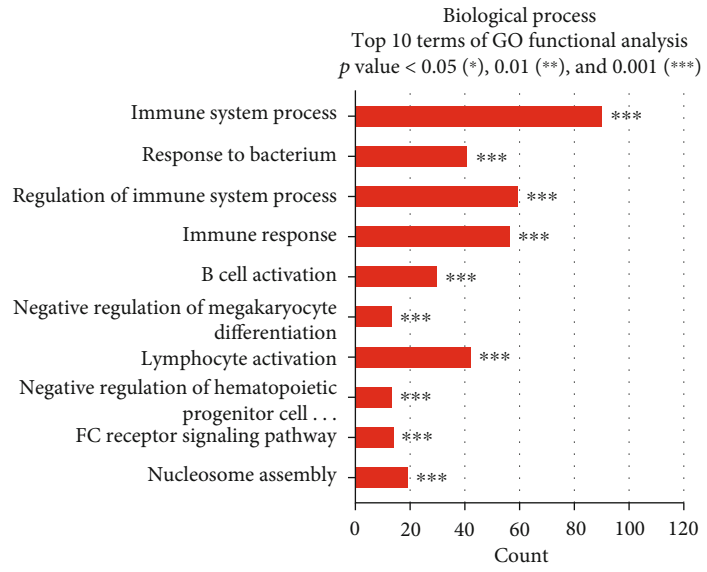

(a)

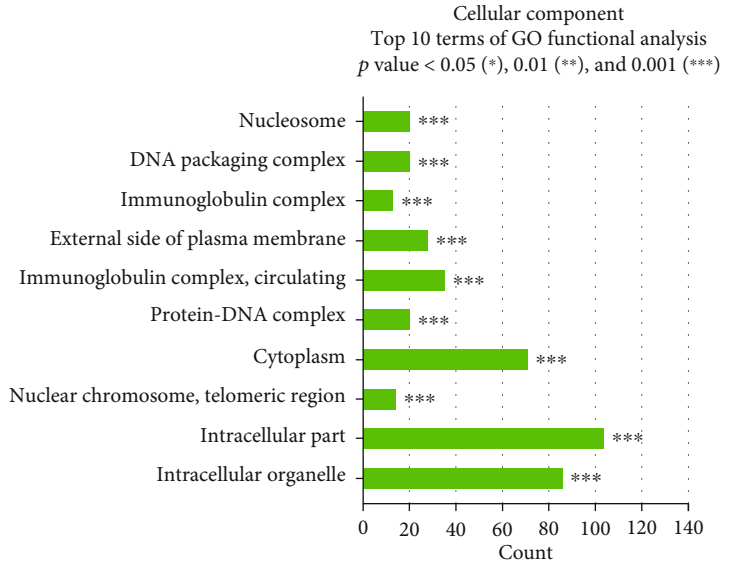

(b)

Figure 5: Continued.

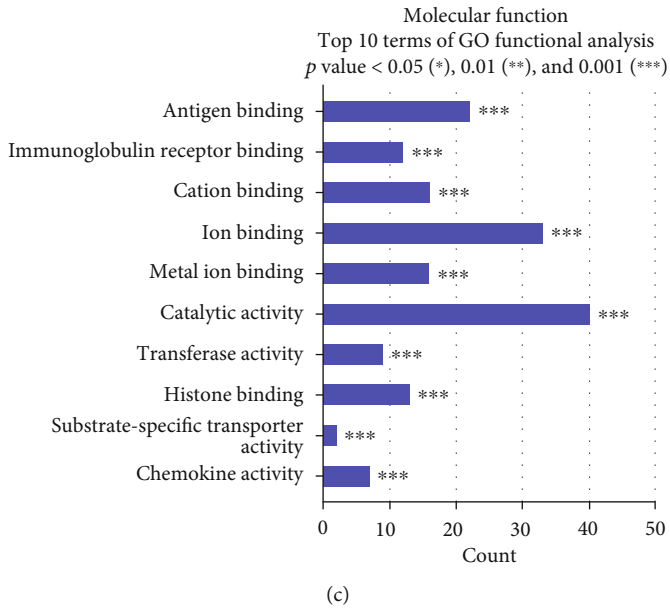

(c)

Figure 5: Functional category enrichment analysis of DEGs. The y-axis shows significantly enriched gene ontology (GO) terms, and the x-axis shows the counts of these terms. GO analysis included three categories: (a) biological processes, (b) cellular components, and (c) molecular function.

cytokine production and induction of Treg expansion [19, 22]. Furthermore, ASC-derived EVs have been shown to reduce static lung elastance and collagen fiber deposition in lung parenchyma and airways in experimental allergic asthma [29]. EVs exert their effects by delivering contents such as proteins, mRNAs, and microRNAs to recipient cells [30]. Recent studies have reported that mitochondrial transfer of MSCs, whose components can be found in EVs, can effectively alleviate allergic airway inflammation [31, 32]. The administration of MSC-derived EVs may reduce potential safety risks associated with stem cell therapy, suggesting that MSC-derived EVs may be a promising alternative to cell therapy for allergic airway diseases. However, the major pulmonary genes responsible for the immunomodulatory effects of MSC-derived EVs in allergic airway diseases have not been well documented.

Molecular and genetic research is required to elucidate the underlying immune suppression mechanism of MSC-derived EVs in Th2-mediated allergic airway inflammation. Microarray DNA hybridization techniques are widely applied in molecular biology research [33]. The DNA microarray consists of various DNA probes immobilized in groups on a solid support, forming an array of microspots [33]. When a DNA sample binds to the immobilized probe DNA thorough complementary sequence binding, detection is attained through reading the tagged markers attached to the target DNA [33]. The DNA microarray is a useful tool for the rapid, economical, and scalable identification of candidate DEGs associated with a phenotype [34]. The investigation of DEGs is essential for understanding and interpreting the immunomodulatory mechanism of MSC-derived EVs in allergic airway inflammation.

In this study, we performed DNA microarray analysis to identify DEGs associated with suppression of allergic airway inflammation by ASC-derived EVs. We performed hierarchical clustering of DEGs, followed by functional and pathway analyses. A total of 249 DEGs were identified, of which 228 and 21 were down- and upregulated, respectively, with a fold change of $|\log_{FC}| \geq 2.0$ between the EV and OVA groups. The genes Ear6, Ccl5, Ccl8, Ccl12, Tnfsf8, IL5Ra, and Tnfrsf13b were upregulated in the OVA group, but downregulated in the EV group. However, the genes PON1, Bex2, Igfbp6, Fpr1, and Scgb1c1 were downregulated by OVA sensitization and challenge, but upregulated by treatment with ASC-derived EVs. Genes downregulated after treatment with ASC-derived EVs were enriched in whole cells and cell components. However, those upregulated after treatment with ASC-derived EVs were strongly associated with cellular and single-organism processes and biological regulation. KEGG pathway analysis showed that DEGs following treatment with ASC-derived EVs were related to environmental information processing, organismal systems, and human diseases. In this study, we found that PON1, Bex2, Igfbp6, Fpr1, and Scgb1c1 expression decreased in lung tissues of asthmatic mice, but that PON1, Bex2, Igfbp6, and Scgb1c1 expression increased significantly following treatment with ASC-derived EVs. Together, these results suggest that PON1, Bex2, Igfbp6, and Scgb1c1 may be involved in the immune suppression mechanisms of ASC-derived EVs in allergic airway diseases.

PON1, a major antioxidant enzyme, has been reported to contribute to the pathogenesis of asthma [35] and many other diseases including rheumatoid arthritis [36, 37], diabetes [38], systemic lupus erythematosus [39], and psoriasis [40]. Recent studies have shown that PON1 expression and activity were significantly decreased in asthma and may have potential effects on asthma diagnosis [35, 41, 42]. Furthermore, PON1 decreased airway inflammation and airway remodeling in asthmatic mice and inhibited macrophage expression of

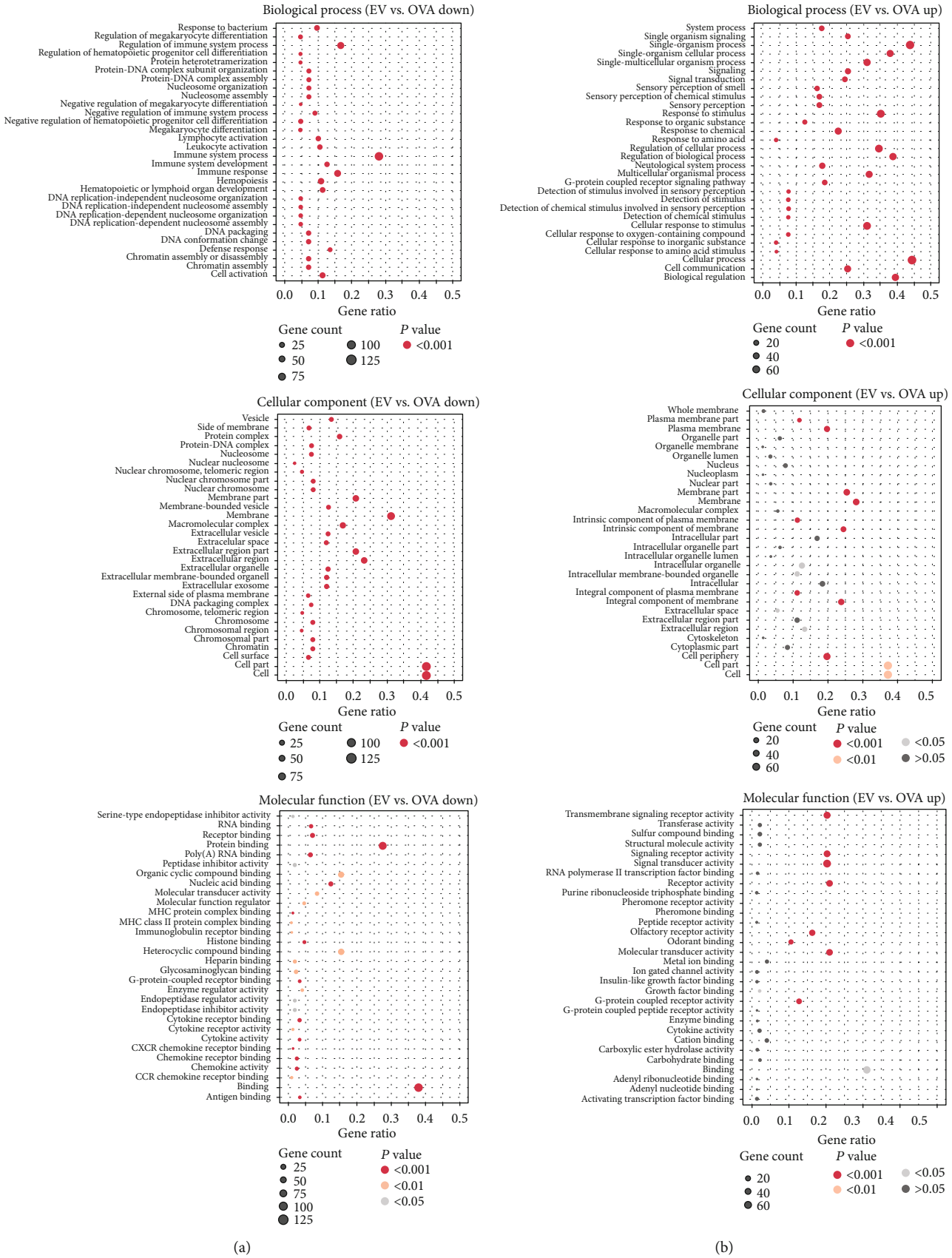

Figure 6: Bubble chart of gene ontology term association. Bubble size indicates the number of (a) downregulated or (b) upregulated genes for the corresponding annotation.

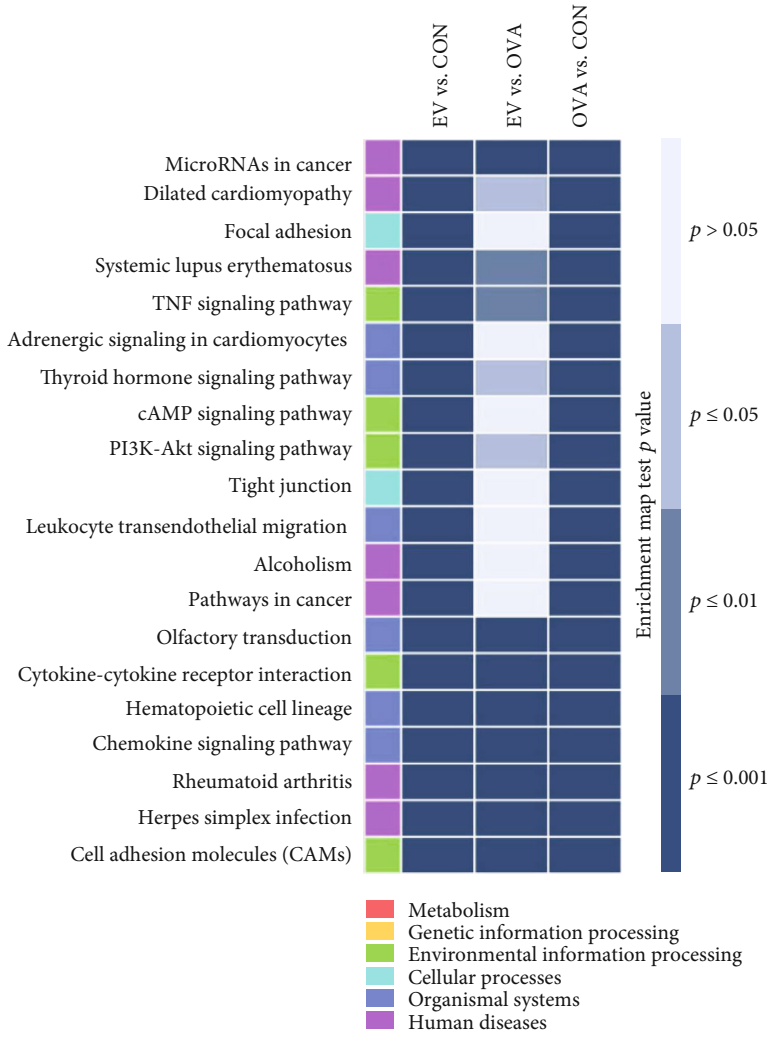

Figure 7: Enrichment analysis based on the Kyoto Encyclopedia of Genes and Genomes (KEGG) pathway identified genes with significantly differential expression. DEGs were strongly associated with environmental information processing, organismal systems, and human diseases. The expression of PON1, Bex2, Igfbp6, and Scgb1c1 was significantly increased following treatment with ASC-derived EVs in asthmatic mice. Gene ontology analysis showed that these upregulated genes were mainly involved in immune system processes and their regulation, cellular and single-organism processes, and biological regulation. These altered genes may be involved in the amelioration of allergic airway inflammation through treatment with ASC-derived EVs.

LPS-induced inflammatory cytokines and lung fibroblast proliferation [43]. Bex2 regulates mitochondrial apoptosis and the G1 cell cycle in breast cancer [44]. A recent study demonstrated that Bex2 expression was suppressed by increased DNA methylation in IL-13-induced allergic airway inflammation [45]. Igfbp6 is an *O*-linked glycoprotein that has higher affinity to IGF-II than to IGF-I and is a specific inhibitor of IGF-II action [46]. Igfbp6 is also associated with cell growth and fibroblast proliferation in asthmatics [47]. Scgb1c1 is mainly expressed in the human respiratory tract mucosa and is downregulated by IFN-r and upregulated by IL-4 and IL-13 [48–50]. Scgb1c1 also plays an important role in protecting lung epithelial cells by recognizing and eliminating pathogenic microorganisms in the mucous membranes [48].

Our study had some limitations. Further evaluation of the effects of the genes identified in the present study on immunocytes such as T cells is required to clarify our findings. Future work should examine the specific functions of the identified DEGs in the suppression of allergic airway inflammation by ASC-derived EVs and investigate which components of ASC-derived EVs contributed to the regulation of these DEGs.

5. Conclusion

In this study, we revealed genetic information about the underlying immunomodulatory mechanism of ASC-derived EVs in allergic airways disease. We hypothesize that the identified genes (PON1, Bex2, Igfbp6, and Scgb1c1) lead to the amelioration of allergic airway inflammation, resulting in the improvement of allergic airway disease by ASC-derived EVs.

Data Availability

The data used to support the findings of this study are available from the corresponding author upon request.

Conflicts of Interest

The authors declare that they have no competing interests.

Authors' Contributions

Sung-Dong Kim, Shin Ae Kang, Kyu-Sup Cho, and Hwan-Jung Roh contributed equally to the content of this article. Sung-Dong Kim contributed in drafting the article, acquiring data, and analyzing and interpreting data. Shin-Ae Kang contributed in drafting the article, acquiring data, and analyzing and interpreting data. Yong-Wan Kim contributed in analyzing and interpreting data. Hak-Sun Yu contributed in analyzing and interpreting data. Kyu-Sup Cho contributed in analyzing and interpreting data and in conceptualization and design. Hwan-Jung Roh contributed in conceptualization and design.

Acknowledgments

This work was supported by the National Research Foundation of Korea (NRF) grant funded by the Korea Government (MSIT) (NRF-2017R1A2A2A05069529).

References

[1] H. Y. Lee, I. K. Kim, H. K. Yoon, S. S. Kwon, C. K. Rhee, and S. Y. Lee, "Inhibitory effects of resveratrol on airway remodeling by transforming growth factor-β/Smad signaling pathway in chronic asthma model," *Allergy, Asthma & Immunology Research*, vol. 9, no. 1, pp. 25–34, 2017.

[2] M. S. Wilson, M. D. Taylor, A. Balic, C. A. M. Finney, J. R. Lamb, and R. M. Maizels, "Suppression of allergic airway inflammation by helminth-induced regulatory T cells," *The Journal of Experimental Medicine*, vol. 202, no. 9, pp. 1199–1212, 2005.

[3] H. Z. Shi and X. J. Qin, "CD4+CD25+ regulatory T lymphocytes in allergy and asthma," *Allergy*, vol. 60, no. 8, pp. 986–995, 2005.

[4] Z. Jaffar, T. Sivakuru, and K. Roberts, "CD4+CD25+ T cells regulate airway eosinophilic inflammation by modulating the Th2 cell phenotype," *Journal of Immunology*, vol. 172, no. 6, pp. 3842–3849, 2004.

[5] K. E. Gabehart, S. G. Royce, D. J. Maselli et al., "Airway hyperresponsiveness is associated with airway remodeling but not inflammation in aging Cav1−/− mice," *Respiratory Research*, vol. 14, no. 1, p. 110, 2013.

[6] A. Uccelli, L. Moretta, and V. Pistoia, "Immunoregulatory function of mesenchymal stem cells," *European Journal of Immunology*, vol. 36, no. 10, pp. 2566–2573, 2006.

[7] H. K. Park, K. S. Cho, H. Y. Park et al., "Adipose-derived stromal cells inhibit allergic airway inflammation in mice," *Stem Cells and Development*, vol. 19, no. 11, pp. 1811–1818, 2010.

[8] M. Goodwin, V. Sueblinvong, P. Eisenhauer et al., "Bone marrow-derived mesenchymal stromal cells inhibit Th2-mediated allergic airways inflammation in mice," *Stem Cells*, vol. 29, no. 7, pp. 1137–1148, 2011.

[9] T. L. Bonfield, M. Koloze, D. P. Lennon, B. Zuchowski, S. E. Yang, and A. I. Caplan, "Human mesenchymal stem cells suppress chronic airway inflammation in the murine ovalbumin asthma model.," *American Journal of Physiology-Lung Cellular and Molecular Physiology*, vol. 299, no. 6, pp. L760–L770, 2010.

[10] Q. L. Fu, Y. Y. Chow, S. J. Sun et al., "Mesenchymal stem cells derived from human induced pluripotent stem cells modulate T-cell phenotypes in allergic rhinitis," *Allergy*, vol. 67, no. 10, pp. 1215–1222, 2012.

[11] K. S. Cho, M. K. Park, S. A. Kang et al., "Adipose-derived stem cells ameliorate allergic airway inflammation by inducing regulatory T cells in a mouse model of asthma," *Mediators of Inflammation*, vol. 2014, Article ID 436476, 12 pages, 2014.

[12] X. Ge, C. Bai, J. Yang, G. Lou, Q. Li, and R. Chen, "Intratracheal transplantation of bone marrow-derived mesenchymal stem cells reduced airway inflammation and up-regulated $CD4^+CD25^+$ regulatory T cells in asthmatic mouse," *Cell Biology International*, vol. 37, no. 7, pp. 675–686, 2013.

[13] K. Nemeth, A. Keane-Myers, J. M. Brown et al., "Bone marrow stromal cells use TGF-β to suppress allergic responses in a mouse model of ragweed-induced asthma," *Proceedings of the National Academy of Sciences*, vol. 107, no. 12, pp. 5652–5657, 2010.

[14] M. B. Desai, T. Gavrilova, J. Liu et al., "Pollen-induced antigen presentation by mesenchymal stem cells and T cells from allergic rhinitis," *Clinical & Translational Immunology*, vol. 2, no. 10, article e7, 2013.

[15] S. Beyth, Z. Borovsky, D. Mevorach et al., "Human mesenchymal stem cells alter antigen-presenting cell maturation and induce T-cell unresponsiveness," *Blood*, vol. 105, no. 5, pp. 2214–2219, 2005.

[16] S. Y. Kim, H. S. Cho, S. H. Yang et al., "Soluble mediators from human neural stem cells play a critical role in suppression of T-cell activation and proliferation," *Journal of Neuroscience Research*, vol. 87, no. 10, pp. 2264–2272, 2009.

[17] J. H. Kim, Y. T. Lee, J. M. Hong, and Y. I. Hwang, "Suppression of in vitro murine T cell proliferation by human adipose tissue-derived mesenchymal stem cells is dependent mainly on cyclooxygenase-2 expression," *Anatomy & Cell Biology*, vol. 46, no. 4, pp. 262–271, 2013.

[18] F. F. Cruz, Z. D. Borg, M. Goodwin et al., "Systemic administration of human bone marrow-derived mesenchymal stromal cell extracellular vesicles ameliorates *Aspergillus* hyphal extract-induced allergic airway inflammation in immunocompetent mice," *Stem Cells Translational Medicine*, vol. 4, no. 11, pp. 1302–1316, 2015.

[19] H. S. Yu, M. K. Park, S. A. Kang, K. S. Cho, S. J. Mun, and H. J. Roh, "Culture supernatant of adipose stem cells can ameliorate allergic airway inflammation via recruitment of $CD4^+CD25^{+-}$ Foxp3 T cells," *Stem Cell Research & Therapy*, vol. 8, no. 1, p. 8, 2017.

[20] L. I. Ionescu, R. S. Alphonse, N. Arizmendi et al., "Airway delivery of soluble factors from plastic-adherent bone marrow cells prevents murine asthma," *American Journal of Respiratory Cell and Molecular Biology*, vol. 46, no. 2, pp. 207–216, 2012.

[21] Y. M. Du, Y. X. Zhuansun, R. Chen, L. Lin, Y. Lin, and J. G. Li, "Mesenchymal stem cell exosomes promote immunosuppression of regulatory T cells in asthma," *Experimental Cell Research*, vol. 363, no. 1, pp. 114–120, 2018.

[22] K. S. Cho, S. A. Kang, S. D. Kim, S. J. Mun, H. S. Yu, and H. J. Roh, "Dendritic cells and M2 macrophage play an important role in suppression of Th2-mediated inflammation by adipose stem cells-derived extracellular vesicles," *Stem Cell Research*, vol. 39, p. 101500, 2019.

[23] S.-B. Fang, H.-Y. Zhang, C. Wang et al., "Small extracellular vesicles derived from human mesenchymal stromal cells prevent group 2 innate lymphoid cell-dominant allergic airway inflammation through delivery of miR-146a-5p," *Journal of Extracellular Vesicles*, vol. 9, no. 1, article 1723260, 2020.

[24] K. S. Cho, J. H. Lee, M. K. Park, H. K. Park, H. S. Yu, and H. J. Roh, "Prostaglandin E2 and transforming growth factor-β play a critical role in suppression of allergic airway inflammation by adipose-derived stem cells," *PLoS One*, vol. 10, no. 7, article e0131813, 2015.

[25] K. S. Cho, M. K. Park, S. J. Mun, H. Y. Park, H. S. Yu, and H. J. Roh, "Indoleamine 2,3-dioxygenase is not a pivotal regulator responsible for suppressing allergic airway inflammation through adipose-derived stem cells," *PLoS One*, vol. 11, article e065661, 2016.

[26] C. S. Kang, M. Ban, E. J. Choi et al., "Extracellular vesicles derived from gut microbiota, especially *Akkermansia muciniphila*, protect the progression of dextran sulfate sodium-induced colitis," *PLoS One*, vol. 8, no. 10, article e76520, 2013.

[27] K.-S. Park, K.-H. Choi, Y.-S. Kim et al., "Outer membrane vesicles derived from *Escherichia coli* induce systemic inflammatory response syndrome," *PLoS One*, vol. 5, no. 6, article e11334, 2010.

[28] Y. S. Kim, E. J. Choi, W. H. Lee et al., "Extracellular vesicles, especially derived from Gram-negative bacteria, in indoor dust induce neutrophilic pulmonary inflammation associated with both Th1 and Th17 cell responses," *Clinical and Experimental Allergy*, vol. 43, no. 4, pp. 443–454, 2013.

[29] L. L. de Castro, D. G. Xisto, J. Z. Kitoko et al., "Human adipose tissue mesenchymal stromal cells and their extracellular vesicles act differentially on lung mechanics and inflammation in experimental allergic asthma," *Stem Cell Research & Therapy*, vol. 8, no. 1, p. 151, 2017.

[30] Y. Yao, X. L. Fan, D. Jiang et al., "Connexin 43-mediated mitochondrial transfer of iPSC-MSCs alleviates asthma inflammation," *Stem Cell Reports*, vol. 11, no. 5, pp. 1120–1135, 2018.

[31] X. Li, C. Michaeloudes, Y. Zhang et al., "Mesenchymal stem cells alleviate oxidative stress-induced mitochondrial dysfunction in the airways," *The Journal of Allergy and Clinical Immunology*, vol. 141, no. 5, pp. 1634–1645.e5, 2018.

[32] H. Valadi, K. Ekstrom, A. Bossios, M. Sjostrand, J. J. Lee, and J. O. Lotvall, "Exosome-mediated transfer of mRNAs and microRNAs is a novel mechanism of genetic exchange between cells," *Nature Cell Biology*, vol. 9, no. 6, pp. 654–659, 2007.

[33] L. Q. Lu and W. Liao, "Screening and functional pathway analysis of genes associated with pediatric allergic asthma using a DNA microarray," *Molecular Medicine Reports*, vol. 11, no. 6, pp. 4197–4203, 2015.

[34] M. J. Heller, "DNA microarray technology: devices, systems, and applications," *Annual Review of Biomedical Engineering*, vol. 4, no. 1, pp. 129–153, 2002.

[35] N. Sarioglu, A. A. Hismiogullari, F. Erel, D. Demir, and N. Gencer, "Paraoxonase 1 phenotype and paraoxonase activity in asthmatic patients," *Iranian Journal of Allergy, Asthma, and Immunology*, vol. 14, pp. 60–66, 2015.

[36] N. Tanimoto, Y. Kumon, T. Suehiro et al., "Serum paraoxonase activity decreases in rheumatoid arthritis," *Life Sciences*, vol. 72, no. 25, pp. 2877–2885, 2003.

[37] A. Isik, S. S. Koca, B. Ustundag, H. Celik, and A. Yildirim, "Paraoxonase and arylesterase levels in rheumatoid arthritis," *Clinical Rheumatology*, vol. 26, no. 3, pp. 342–348, 2007.

[38] S. W. van den Berg, E. H. J. Jansen, M. Kruijshoop et al., "Paraoxonase 1 phenotype distribution and activity differs in subjects with newly diagnosed type 2 diabetes (the CODAM study)," *Diabetic Medicine*, vol. 25, no. 2, pp. 186–193, 2008.

[39] F. Bahrehmand, A. Vaisi-Raygani, Z. Rahimi et al., "Synergistic effects of BuChE non-UU phenotype and paraoxonase (PON1) 55 M allele on the risk of systemic lupus erythematosus: influence on lipid and lipoprotein metabolism and oxidative stress, preliminary report," *Lupus*, vol. 23, no. 3, pp. 263–272, 2013.

[40] M. Asefi, A. Vaisi-Raygani, F. Bahrehmand et al., "Paraoxonase 1 (PON1) 55 polymorphism, lipid profiles and psoriasis," *The British Journal of Dermatology*, vol. 167, no. 6, pp. 1279–1286, 2012.

[41] G. Tölgyesi, V. Molnár, Á. F. Semsei et al., "Gene expression profiling of experimental asthma reveals a possible role of paraoxonase-1 in the disease," *International Immunology*, vol. 21, no. 8, pp. 967–975, 2009.

[42] O. Emin, A. Hasan, and D. M. Rusen, "Plasma paraoxonase, oxidative status level, and their relationship with asthma control test in children with asthma," *Allergologia et Immunopathologia*, vol. 43, no. 4, pp. 346–352, 2015.

[43] W. Q. Chen, Z. Z. Xie, X. Wang et al., "Influences of PON1 on airway inflammation and remodeling in bronchial asthma," *Journal of Cellular Biochemistry*, vol. 119, no. 1, pp. 793–805, 2018.

[44] A. Naderi, J. Liu, and I. C. Bennett, "BEX2 regulates mitochondrial apoptosis and G1 cell cycle in breast cancer," *International Journal of Cancer*, vol. 126, pp. 1596–1610, 2009.

[45] A. T. Ooi, S. Ram, A. Kuo et al., "Identification of an interleukin 13-induced epigenetic signature in allergic airway inflammation," *American Journal of Translational Research*, vol. 4, pp. 219–228, 2012.

[46] Y. Kostecka and J. Blahovec, "Insulin-like growth factor binding proteins and their functions (minireview)," *Endocrine Regulations*, vol. 33, no. 2, pp. 90–94, 1999.

[47] V. T. Vaillancourt, M. Bordeleau, M. Laviolette, and C. Laprise, "From expression pattern to genetic association in asthma and asthma-related phenotypes," *BMC Research Notes*, vol. 5, no. 1, p. 630, 2012.

[48] J. Orysiak, J. Malczewska-Lenczowska, and M. Bik-Multanowski, "Expression of SCGB1C1 gene as a potential marker of susceptibility to upper respiratory tract infections in elite athletes—a pilot study," *Biology of Sport*, vol. 33, no. 2, pp. 107–110, 2016.

[49] B. C. Jackson, D. C. Thompson, M. W. Wright et al., "Update of the human secretoglobin (SCGB) gene superfamily and an example of "evolutionary bloom" of androgen-binding protein genes within the mouse Scgb gene superfamily," *Human Genomics*, vol. 5, no. 6, pp. 691–702, 2011.

[50] A. Sjödin, D. Guo, S. Sørhaug, L. Bjermer, R. Henriksson, and H. Hedman, "Dysregulated secretoglobin expression in human lung cancers," *Lung Cancer*, vol. 41, no. 1, pp. 49–56, 2003.

Hindawi
Stem Cells International
Volume 2020, Article ID 8237197, 12 pages
https://doi.org/10.1155/2020/8237197

Research Article

Extensive Characterization of Mesenchymal Stem Cell Marker Expression on Freshly Isolated and *In Vitro* Expanded Human Adipose-Derived Stem Cells from Breast Cancer Patients

Premrutai Thitilertdecha,[1,2] Visnu Lohsiriwat,[1,3] Poonsin Poungpairoj,[1,2] Varangkana Tantithavorn,[1,2] and Nattawat Onlamoon [1,2]

[1]*Siriraj Research Group in Immunobiology and Therapeutic Sciences, Faculty of Medicine Siriraj Hospital, Mahidol University, 2 Wanglang Road, Bangkoknoi, Bangkok, Thailand*
[2]*Biomedical Research Incubator Unit, Research Group and Research Network Division, Research Department, Faculty of Medicine Siriraj Hospital, Mahidol University, 2 Wanglang Road, Bangkoknoi, Bangkok 10700, Thailand*
[3]*Department of Surgery, Faculty of Medicine Siriraj Hospital, Mahidol University, 2 Wanglang Road, Bangkoknoi, Bangkok, Thailand*

Correspondence should be addressed to Nattawat Onlamoon; nattawat.onl@mahidol.ac.th

Received 5 March 2020; Revised 20 May 2020; Accepted 27 May 2020; Published 18 June 2020

Academic Editor: Jane Ru Choi

Variation in numbers and functions of cells in fat tissues may affect therapeutic outcomes and adverse events after autologous fat tissue grafting in postmastectomy breast cancer patients; however, the relevant information regarding cellular components is still incomplete. Phenotypic characterization of heterogeneous cell subsets in stromal vascular fraction (SVF) isolated from fat tissues by flow cytometry was also limited to a combination of few molecules. This study, therefore, developed a polychromatic staining panel for an in-depth characterization of freshly isolated SVF and expanded adipose-derived stem cells (ADSC) from the patients. ADSC were found predominant in SVF (~65% of $CD45^-$ cells) with a homogenous phenotype of $CD13^+CD31^-CD34^+CD45^-CD73^+CD90^+CD105^-CD146^-$ (~94% of total ADSC). Endothelial progenitor cells (EPC) and pericytes were minor (~18% and ~11% of $CD45^-$ cells, respectively) with large heterogeneity. Downregulation of CD34 and upregulation of CD105 in ADSC were profound at passage 3, showing a phenotype similar to the classical mesenchymal stem cells from the bone marrow. Results from this study demonstrated that fat tissue collected from patients contains ADSC with a highly homogenous phenotype. The *in vitro* culture of these cells maintained their homogeneity with modified CD34 and CD105 expression, suggesting the expansion from a single population of ADSC.

1. Introduction

White adipose tissue has been recognized as the alternative source for stromal precursors and stem cells. Normally, adipose tissues can be divided into two types including white and brown adipose tissues according to their morphology and physiology. White adipose tissue contains a single lipid droplet creating white to yellow appearance and functions by storing lipids for excessive energy, whereas brown adipose tissue comprises multiple small vacuoles with abundance of iron-containing mitochondria generating brown color and works through lipid burning for heat production [1–3]. Besides these dissimilarities, brown adipose tissue is less in quantity in adult humans and located in vital regions such as cervical, supraclavicular, and axillary [4]. White adipose tissue is found predominantly in subcutaneous and several visceral depots (e.g., abdomen, hip, and thigh); thus, it becomes a sensible source for progenitor stem cells.

Compared to the bone marrow—another recommended source of stem cells, the yield of mesenchymal stem cells (MSC) from white adipose tissue was able to reach $0.5–1.25 \times 10^6$ cells/gram adipose tissue [5, 6] while only

0.001–0.01% of isolated cells was averagely achieved from the bone marrow [7] which was remarkably lower and insufficient for further propagation to use in cell therapy. The harvesting procedure of these bone marrow-derived stem cells (BMSC) is also relatively invasive to the patients and costs higher. Although BMSC are considered as a gold standard for adult stem cells, several concerns previously mentioned have become its limitation for clinical implementation. Other types of stem cells including embryonic stem cells (ESC) and induced-pluripotent stem cells (iPSC) have been restricted for clinical practices due to ethical consideration and cell regulation. Therefore, adipose-derived stem cells (ADSC) have recently been more attractive for therapeutic potentials because of their less invasive harvesting technique, less expensive cost, greater yield, and confirmed multilineage differentiation ability the same as MSC characteristics [5, 6, 8, 9].

A heterogeneous population of stromal vascular fraction (SVF) containing vascular endothelial cells, endothelial progenitor cells (EPC), pericytes, infiltrating cells of hematopoietic lineage, and adipose-derived stem cells (ADSC) can be isolated from lipoaspirates by enzymatic digestion and mechanical processing [8, 10–13]. As ADSC are widely known for their regenerative property, they have then been introduced not only to reconstructive surgery targeting in soft tissues and skin but also in all fields of surgery with a wide range of potential clinical uses [14]. Oncoplastic breast surgery is one of the several surgical applications using ADSC through fat grafting for postmastectomy breast reconstruction in breast cancer patients [15–17]. The clinical outcomes rely on abilities of ADSC in proliferation and differentiation to new functional adipocytes together with maintenance of mature fat graft volume. Therefore, ADSC have become great potential for novel breast reconstruction approaches and attractive to recent tissue engineering [18] instead of BMSC which were reported to occupy higher differentiation tendency towards osteoblasts and chondrocytes than adipocytes [19]. Many issues regarding cellular biology, oncological safety, clinical efficacy, and cell production as well as surgery techniques and experience with procedure are then concerned.

A supportive use of ADSC for clinical applications such as cell-assisted lipotransfer (CAL) was introduced by using a combination of SVF and aspirated fat for autologous tissue transfer [20]. This CAL technique was able to increase the efficacy by showing the higher survival rate and persistence of transplanted fat when compared to non-CAL (i.e., aspirated fat alone without ADSC) as well as reduced adverse effects from calcification, fibrosis formation, and pseudocyst [20]. Aspirated fat was then served as injection material for soft tissue augmentation which was also rich in EPC and pericytes promoting angiogenesis and microvasculature. However, EPC were concerned for catalyzing tumor vascularization [21, 22]. Detailed identification of EPC and pericytes in lipoaspirates is then warranted for better understanding of their relationship with the partial necrosis of aspirate fat or cancer-promoting risk after fat transplant.

Therefore, phenotypic characterization of ADSC is essential as the initial step for cellular biology confirmation. Flow cytometry is widely used since it is the gold standard method for evaluation of cell composition in a sample and functionally relevant cell surface marker expressions. Although numerous studies put efforts by using a broad range of surface markers for ADSC identification, there is still a controversial discussion on the expression of some surface protein molecule by ADSC on the day of isolation, such as CD105 [23, 24] and CD146 [24–26]. This variation may be resulted from different monoclonal antibody panels used for multicolor staining in a single sample and from physiological difference between fresh and cryopreserved samples. Isolated SVF or ADSC samples were also obtained from healthy donors in most reports while the use of ADSC for postmastectomy breast reconstruction requires autologous fat transplantation. This study is thus aimed at investigating an in-depth characterization of ADSC, EPC, and pericytes in fresh liposuction aspirates from breast cancer patients by using a developed 8-color staining panel with flow cytometric analysis. Serial changes in ADSC phenotypic profiles were also explored from the day of cell isolation until completion at passage 3. Besides that, multilineage differentiation ability of the expanded ADSC was evaluated to ensure their MSC characteristics.

2. Materials and Methods

2.1. Study Population. Twenty-two breast cancer female patients aged between 47 and 62 years old requiring autologous fat transplantation for breast reconstruction at the Faculty of Medicine Siriraj Hospital, Mahidol University, Bangkok, Thailand, were recruited for the study. The protocols were approved by the Institution Review Board (IRB) of the Faculty of Medicine Siriraj Hospital (COA number 580/2016). Written informed consent was also obtained from each subject prior to the study.

2.2. Sample Collection. Lipoaspirates were withdrawn from the abdomen by a tumescence technique using a 3 mm diameter suction tube coupled with a 10 mL vacuum syringe. The collected tissues were then kept in the syringes for fresh isolation and characterization of ADSC on the same day before further serial passaging.

2.3. Cell Isolation from Lipoaspirates. Raw lipoaspirates were centrifuged at 2,000g for 3 min followed by a removal of oil and blood. The remaining fat tissues were digested with 2 mg/mL collagenase A type I (Gibco, Thermo Fisher Scientific, MA, USA) at 37°C for 60 min under shaking. Neutralization of enzymatic activity was done by adding a complete medium containing Dulbecco's modified Eagle's medium (DMEM, Gibco, Thermo Fisher Scientific, MA, USA), 10% fetal bovine serum (FBS, Gibco, Thermo Fisher Scientific, MA, USA), 1% l-glutamine (Gibco, Thermo Fisher Scientific, MA, USA), 1% penicillin-streptomycin (Pen-Strep, Gibco, Thermo Fisher Scientific, MA, USA), and 0.01% gentamycin (Gibco, Thermo Fisher Scientific, MA, USA) before centrifugation at 400g, 4°C for 10 min. After that, the collected pellet was resuspended in ammonium chloride potassium (ACK) lysis buffer (Gibco, Thermo Fisher Scientific, MA, USA) for

red blood cell (RBC) lysis and centrifuged at 400g, 4°C for 10 min, for RBC removal. The obtained pellet was then resuspended in phosphate-buffered saline (PBS, Gibco, Thermo Fisher Scientific, MA, USA) containing 1% bovine serum albumin (BSA, Sigma-Aldrich, USA), and the cell suspension was filtered through 100 and 40 μm cell strainers (Corning, NY, USA) to discard cellular debris followed by centrifugation again at 400g, 4°C for 10 min. The SVF pellet was collected and resuspended in 1% BSA in PBS. The cells were then counted by a trypan blue exclusion method.

2.4. Cell Culture. Three samples of freshly isolated SVF cells at the day of isolation (D0) were cultured in the DMEM complete medium at 10,000 cells/cm^2 of a culture plate. After 3 days, nonadherent cells were washed and discarded. The remaining adherent cells were then expanded in complete medium, and replenishments of fresh medium were performed every 3 days. When the expanded cells reached 80% confluency, they were detached from the culture plates with 0.25% trypsin (Gibco Life Technologies, CA) and considered to be at passage 0 (P0). The isolated adherent cells at P0 were then continually expanded for subcultivation through passage 3 (P3). The expanded ADSC at each passage (i.e., P0, P1, P2, and P3) were counted by a trypan blue exclusion method and characterized by immunofluorescent staining and flow cytometric analysis.

2.5. Phenotypic Characterization. For phenotypic characterization of the freshly isolated and expanded cells, they were stained with fluorochrome-conjugated monoclonal antibodies including CD13-allophycocyanin (APC), CD31-Alexa Fluor® 488, CD34-Brilliant Violet™ 421 (BV421), CD45-peridinin-chlorophyll-protein (PerCP), CD73-phycoerythrin/Dazzle™ (PE/Dazzle™) 594, CD90-Brilliant Violet™ 510 (BV510), CD105-phycoerythrin cyanine 7 (PECy7), and CD146-phycoerythrin (PE). All reagents were obtained from BioLegend, CA, USA. The samples were then incubated for 15 min before washing and resuspending in 450 μL PBS. All samples were analyzed by LSRFortessa flow cytometer (BD Biosciences, USA) and FlowJo® software (Tree Star, San Carlos, CA).

2.6. Multilineage Differentiation. At the end of passage 3, the cultured ADSC were confirmed for their differentiation capability towards adipocytes, osteocytes, and chondrocytes through histological analyses. For adipogenesis, the expanded ADSC at 40,000 cells/well in a 6-well plate were cultured in 1 mL of adipogenic differentiation medium (STEMCELL™ Technologies, Canada) and then incubated at 37°C and 5% CO_2 for 14 days. On day 14, the induced cells were washed with 1X PBS twice and fixed with 10% formaldehyde in PBS for 30 min. After that, the fixed cells were washed with 60% isopropanol (Sigma-Aldrich, USA) in aqueous before stained with Oil Red O staining solution (Sigma-Aldrich, USA) for 60 min. The stained cells were extensively washed with water to remove unbound dye and subsequently observed under an inverted fluorescent microscope (Nikon, Ti-S Intensilight Ri1 NIS-D, Japan). Representative images of the induced cells were compared to a control group (i.e., noninduced ADSC cultured in DMEM complete medium).

With respect to osteogenesis, ADSC at 40,000 cells/well in a 6-well plate were cultured in 1 mL of osteogenic differentiation medium (STEMCELL™ Technologies, Canada) and then incubated at 37°C and 5% CO_2 for 14 days. On day 14, the induced cells were washed with 1x PBS twice and fixed with 70% ethanol (Sigma-Aldrich, USA) for 30 min. After that, ethanol was removed and the fixed cells were stained with Alizarin Red S staining solution (Sigma-Aldrich, USA) for 30 min before extensively washed with water. Representative images of the induced cells were captured by the inverted fluorescent microscope and compared with a noninduction control.

For chondrogenesis, a micromass culture system was used. The cultured ADSC at concentration of 200,000 cells/10 μL DMEM complete medium were dropped at the center of a 12-well plate and incubated at 37°C and 5% CO_2 without the culture medium for 1 h. After that, the chondrogenic differentiation medium containing DMEM supplemented with 100 nM dexamethasone (Sigma-Aldrich, USA), 50 mg/mL ascorbic acid (Sigma-Aldrich, USA), 100 μg/mL sodium pyruvate (Sigma-Aldrich, USA), 1 : 100 diluted ITS+Premix (a mixture containing 6.25 mg/mL insulin, 6.25 mg/mL transferrin, 6.25 mg/mL selenous acid, 1.25 mg/mL BSA, and 5.35 mg/mL linoleic acid, BD Biosciences, USA), 10 ng/mL transforming growth factor-beta 1 (TGF-β1, PeproTech®, USA), and 40 mg/mL proline (Sigma-Aldrich, USA) was added into the culture plate and incubated at 37°C and 5% CO_2 for 21 days. The chondrogenic differentiation medium was changed every 3 days. On day 21, the cell pellets were frozen in Tissue-Tek® O.C.T.™ Compound (Sakura®, Japan) with liquid N_2 for cryostat sectioning by CryoStar™ NX70 Cryostat (Thermo Fisher Scientific, USA). The sectioned cell samples were placed on microscope slides, then washed with 1x PBS thrice and fixed with 10% formaldehyde in PBS for 10 min before gently removing the fixing agent. The fixed cells were stained with Alcian Blue staining solution (Sigma-Aldrich, USA) for 30 min and, respectively, washed with water, 70%, 80%, and 90% and absolute ethanol and xylene. Representative images of the induced cells were captured by the inverted fluorescent microscope and compared with a -induction control.

2.7. Data Analysis. Statistical analyses were performed using GraphPad Prism® software version 7.02 (GraphPad Software, Inc., La Jolla, CA). Data was expressed as mean ± standard deviation (SD). A two-way analysis of variance with a Bonferroni's multiple comparisons test was used to determine statistical differences of the mean quantity among SVF subpopulations including mesenchymal stem cells (MSC), ADSC, EPC, and pericytes. P values < 0.05 were considered as a statistical significance.

3. Results

3.1. Characterization of Cell Populations in SVF of Lipoaspirates from Breast Cancer Patients. To identify cell populations in SVF of white adipose tissues from breast

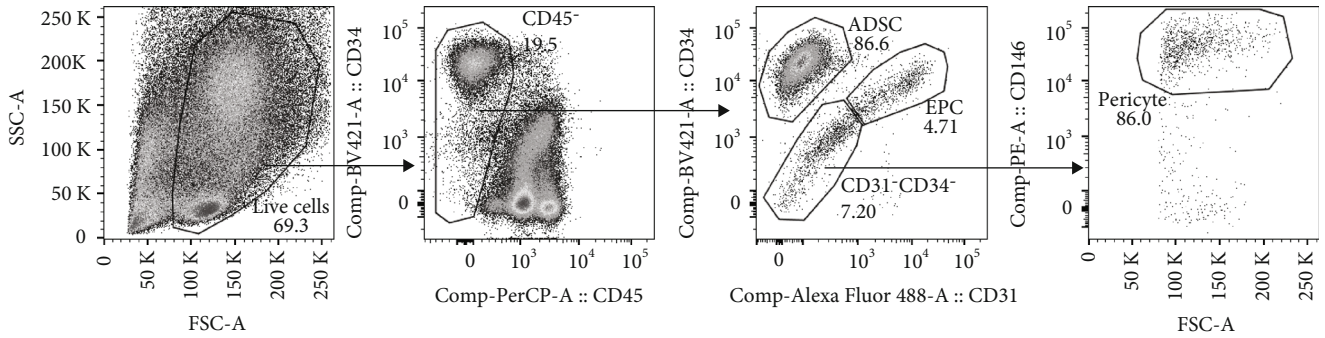

Figure 1: Representative gating strategy to identify ADSC, EPC, and pericytes in freshly isolated SVF.

cancer patients, an 8-marker staining panel including CD13, CD31, CD34, CD45, CD73, CD90, CD105, and CD146 was developed for polychromatic flow cytometric analysis. A gating strategy was employed for phenotypic characterization of cell subpopulation (Figure 1). Freshly isolated SVF cells were first gated for doublet discrimination (data not shown), and then, a live cell population was identified by using the light scattered properties (FSC-A vs. SSC-A). After that, nonhematopoietic cells (i.e., $CD45^-$) were selected before being further identified into three subpopulations of SVF based on the expression of CD34 and CD31. ADSC were thus identified as $CD31^-CD34^+$, whereas EPC were identified as $CD31^+CD34^+$. In addition, $CD31^-CD34^-$ was further characterized by using the expression of CD146 to obtain pericytes ($CD31^-CD34^-CD146^+$). According to this gating strategy, the minimum markers of CD31, CD34, CD45, and CD146 were sufficient to identify 3 major heterogeneous subsets of SVF.

Freshly isolated SVF samples from twenty-two patients were then used to determine the amount of each SVF subpopulations. In a live cell population, 22.9 ± 10.2% was identified as nonhematopoietic cells. This cell subset was further used to identify ADSC, EPC, and pericytes. Quantities of cell subpopulations in the $CD31^-CD34^-$ subset were also investigated for the expression of a set of surface markers including CD73, CD90, and CD105 (i.e., considered as MSC). As shown in Figure 2, the nonhematopoietic cell portion of SVF comprised a significantly large population of ADSC (64.6 ± 14.2%) followed by similar numbers of EPC and pericytes (17.8 ± 10.4% and 11.2 ± 7.8%, respectively). In contrast, only a small population of these cells was identified as MSC (4.5 ± 2.4%), suggesting a majority of stem cells in SVF belongs to ADSC.

3.2. Phenotypic Profiles and Subpopulations of ADSC, EPC, and Pericytes. With respect to detailed phenotypic profiles of ADSC, EPC, and pericytes in the freshly isolated SVF, their surface maker expressions of CD13, CD73, CD90, CD105, and CD146 were determined (Figure 3). For ADSC, the expressions of CD13, CD73, and CD90 were observed with high intensity while the expression of CD105 and CD146 was not found. The surface marker expression of EPC, on the other hand, exhibited moderate expression intensities of CD13, CD90, and CD105 with a high intensity of CD146 and an absence of CD73 expression. For pericytes,

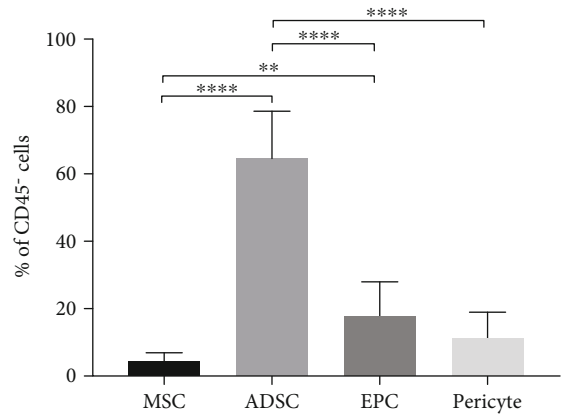

Figure 2: Percentages of freshly isolated SVF subsets including MSC, ADSC, EPC, and pericytes. All data are represented as mean ± SD ($n = 22$; $**P < 0.01$, $****P < 0.0001$).

the dim expressions of CD13 and CD90 were observed while the expression of CD146 was found with high intensity. The expressions of CD73 and CD105 were also not observed in pericytes. These results suggested that ADSC population was homogeneous, whereas EPC and pericytes were heterogeneous.

Subsets of ADSC, EPC, and pericytes were then examined based on these 5 surface markers by using Boolean gating analysis (Table 1). The result showed that a majority of ADSC exhibited $CD13^+CD73^+CD90^+CD105^-CD146^-$ phenotype (93.6 ± 2%) and the rest of the ADSC population either expressed CD146 or CD105. Unlike ADSC, a great variation was observed for EPC subpopulations. Ten subpopulations of EPC were identified in which the majority exhibited $CD13^+CD73^-CD90^+CD105^+CD146^+$ phenotype (33.7 ± 21.0%). Interestingly, approximately 15% of EPC showed simultaneous expressions of CD73, CD90, CD105, and 146 (11.7 ± 7.4% for the $CD13^+CD73^+CD90^+CD105^{+-}CD146^+$ subset and 3.1 ± 2.9% for the $CD13^-CD73^+CD90^{+-}CD105^+CD146^+$ subset). It is worth noting that the expressions of CD90 and CD146 were common in most EPC subsets with 8 out of 10 subsets expressing CD90 and 7 out of 10 subsets expressing CD146. For pericytes, since all of them expressed CD146, 8 subpopulations were characterized based on differential expressions of CD13, CD73, CD90,

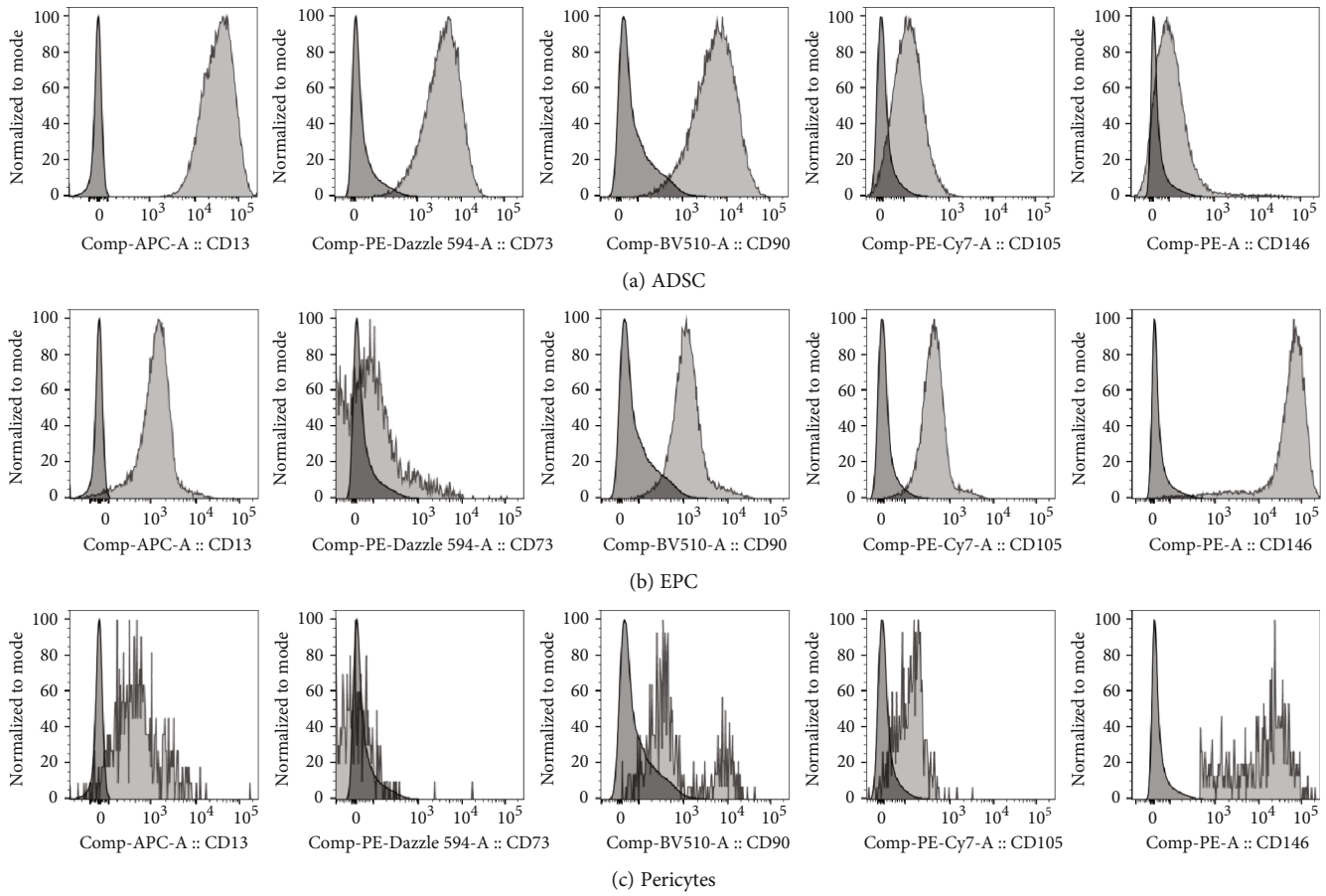

Figure 3: Representative overlaid histograms for phenotypic characterization of (a) ADSC, (b) EPC, and (c) pericytes when compared to unstained cells (darker color, on the left).

and CD105. The predominant subset exhibited $CD13^{+-}CD73^{-}CD90^{+}CD105^{-}CD146^{+}$ phenotype (26.7 ± 20.3%) and followed by the $CD13^{-}CD73^{-}CD90^{+}CD105^{-}CD146^{+}$ subset (18.3 ± 20.6%). Interestingly, these 2 subsets contributed to almost half of pericytes with mere difference on CD13 expression.

3.3. Phenotypic Changes of ADSC after Serial Passaging. While ADSC on the day of isolation (D0) did not express CD105 which was regarded as a maker for identification of MSC (i.e., used in a combination with CD73 and CD90), the expression of CD34 was observed appearing to be similar to pericyte progenitors and hematopoietic stem cells. These results suggested that freshly isolated ADSC from SVF are distinct from MSC. Therefore, the phenotypic alteration during the *in vitro* expansion of ADSC was then determined. ADSC were expanded over serial passaging starting from the day of SVF isolation determined as passage 0 (P0) until the completion at passage 3 (P3). Phenotypes of the expanded ADSC from each passage were analyzed by polychromatic flow cytometry using the 8-marker staining panel. A representative phenotypic profile of the expanded ADSC from 4 different passages (P0, P1, P2, and P3) was demonstrated in Figure 4. Similar to freshly isolated ADSC from SVF, the expressions of CD13, CD73, and CD90 of the expanded ADSC remained consistently high throughout the culture period (Figure 4) while the expressions of CD45 and CD31 were absent from the expanded cell populations (data not shown). More importantly, a remarkable downregulation of CD34 was observed since P0 and its expression gradually decreased until a complete diminution on P3. On the contrary, most of the expanded cells showed a remarkable upregulation of CD105 since P0 and its expression maintained throughout the culture period.

To characterize cell subpopulations in the expanded cells, simultaneous expressions of cell surface markers were analyzed. Although the highly homogeneous ADSC with $CD13^{+-}CD31^{-}CD34^{+}CD45^{-}CD73^{+}CD90^{+}CD105^{-}CD146^{-}$ phenotype were observed in freshly isolated SVF and largely contributed as major progenitor cells in the expansion culture, a notable decrease of this cell population was observed on P0 and its presence remained low throughout the culture period (Table 2). While many different cell subsets were observed in the expanded cell population due to a variation in cell surface marker expressions, approximately 80% belonged to only 2 major phenotypes including $CD13^{+}CD31^{-}CD34^{+-}CD45^{-}CD73^{+}CD90^{+}CD105^{+}CD146^{-}$ and $CD13^{+}CD31^{-}CD34^{-}CD45^{-}CD73^{+}CD90^{+}CD105^{+}CD146^{-}$ (Table 2). Interestingly, the frequency of the expanded cells with $CD13^{+}CD31^{-}CD34^{-}CD45^{-}CD73^{+}CD90^{+}CD105^{+}CD146^{-}$ phenotype was slightly

Table 1: Percentages (mean ± SD) of subpopulations in ADSC, EPC, and pericytes ($n = 22$).

Population	Subset	% Frequency of total population
ADSC	$CD13^+CD73^+CD90^+CD105^-CD146^-$	93.6 ± 2.0
	$CD13^+CD73^+CD90^+CD105^-CD146^+$	2.5 ± 1.6
	$CD13^+CD73^+CD90^+CD105^+CD146^-$	1.7 ± 1.0
EPC	$CD13^+CD73^-CD90^+CD105^+CD146^+$	33.7 ± 21.0
	$CD13^+CD73^+CD90^+CD105^+CD146^+$	11.7 ± 7.4
	$CD13^-CD73^-CD90^+CD105^-CD146^+$	11.1 ± 18.3
	$CD13^-CD73^-CD90^+CD105^+CD146^+$	9.3 ± 14.2
	$CD13^-CD73^-CD90^-CD105^-CD146^-$	8.9 ± 13.9
	$CD13^+CD73^-CD90^+CD105^-CD146^+$	7.7 ± 7.1
	$CD13^-CD73^-CD90^+CD105^-CD146^-$	6.4 ± 6.4
	$CD13^-CD73^+CD90^+CD105^+CD146^+$	3.1 ± 2.9
	$CD13^-CD73^-CD90^-CD105^-CD146^+$	1.2 ± 1.3
	$CD13^-CD73^-CD90^+CD105^+CD146^-$	1.1 ± 3.2
Pericyte	$CD13^+CD73^-CD90^+CD105^-CD146^+$	26.7 ± 20.3
	$CD13^-CD73^-CD90^+CD105^-CD146^+$	18.3 ± 20.6
	$CD13^-CD73^-CD90^-CD105^+CD146^+$	5.9 ± 6.8
	$CD13^+CD73^-CD90^-CD105^-CD146^+$	5.3 ± 4.2
	$CD13^+CD73^-CD90^+CD105^+CD146^+$	4.7 ± 5.5
	$CD13^+CD73^+CD90^+CD105^-CD146^+$	1.9 ± 1.3
	$CD13^-CD73^-CD90^+CD105^+CD146^+$	1.8 ± 2.3
	$CD13^+CD73^+CD90^+CD105^+CD146^+$	1.5 ± 1.4

higher than another subset at the beginning on P0 and then considerably increased over the serial passages (approximately 70% on P3). Due to these phenotypic changes, the characteristic of the expanded ADSC (i.e., $CD13^{+-}$ $CD34^-CD45^-CD73^+CD90^+CD105^+CD146^-$) at the end of P3 became more similar to that of MSC from the bone marrow.

3.4. Differentiation Potential of the Expanded ADSC. Before the evaluation of differentiation capability of the expanded ADSC at the end of P3, morphology of ADSC was observed for confirmation of a typical fibroblast-like adherent appearance (Figure 5). ADSC were then examined for their multipotency through histological analyses using specific induction and staining protocols. The induced and noninduced cells were stained with Oil Red O to detect neutral triglycerides and lipid droplets in adipogenic assay, whereas Alizarin Red S was used to identify calcium deposits in osteogenic detection and Alcian Blue was used to observe proteoglycan in chondrogenic protocol. Results show that ADSC were able to differentiate into adipocytes and osteocytes within 14 days as well as chondrocytes within 21 days under the induction conditions when compared to the noninduced ADSC (Figure 6).

4. Discussion

Our study demonstrates the existence of cell subpopulations within multipotent ADSC, EPC, and pericytes in freshly isolated SVF from abdominal fat of breast cancer patients. At present, characterization of the phenotypes and properties of ASDC, EPC, and pericytes is usually limited to SVF from healthy donors and only a few studies reported cell subpopulations in freshly isolated SVF from breast cancer patients [21, 22, 27]. Most previous cellular characterization was performed through multiparameter immunophenotypic analysis with a single marker or a combination of up to 4 biomarkers [24, 25, 27–29] which may be inadequate to clearly clarify subpopulations. We then developed the 8-color staining panel with flow cytometry for extensive and accurate characterization of ADSC, EPC, and pericytes with their cellular subsets in lipoaspirates from breast cancer patients. The typical MSC marker proteins including surface enzymes CD13 (amino-peptidase) and CD73 (5′ecto-nucleotidase) and extracellular matrix proteins CD90 (Thy-1), CD105 (endoglin), and CD146 (Muc18) as well as hematopoietic cell lineage markers CD34 (mucusialin) and CD45 (leukocyte common antigen, LCA, Ly-5), and endothelial cell marker CD31 (platelet endothelial cell adhesion molecule-1, PECAM-1) were chosen for immunophenotypic identification.

Our results showed that ADSC, EPC, and pericytes were able to be distinguished by a minimum of 4 markers including CD31, CD34, CD45, and CD146. While all three cell types do not express CD45, ADSC only expressed CD34 and EPC expressed both CD31 and CD34. Pericytes, on the other hand, did not express all of those markers except CD146. This identification of the 3 main populations was in agreement with previous studies [22, 26, 27, 30]. In our freshly isolated SVF, ADSC were the most abundant followed by EPC and pericytes (64.6 ± 14.2%, 17.8 ± 10.4%, and 11.2 ± 7.8% of $CD45^-$ cells, respectively) which differed from a finding by Agostini *et al.* showing ADSC with 58.8 ± 16.6% and EPC with 43.2 ± 16.6% of $CD34^+CD45^-$ cells [27]. The differences in numbers may be influenced from different presentation in cell percentages (% of $CD45^-$ cells vs. % of $CD34^+CD45^-$ cells), variation in sample sizes ($n = 22$ vs. $n = 6$), and donor-dependent variability, despite the same sample sources from breast cancer patients and similar surface markers used for characterization. Moreover, most of our nonhematopoietic lineage ($CD45^-$) in SVF comprised $CD34^+$ cells (over 80% of $CD45^-$ cells), meaning that percentages of ADSC and EPC would be even greater when reporting in % of $CD34^+CD45^-$ cells. By presenting cell numbers in % of $CD45^-$ cells, it allows us to identify pericytes residing in $CD34^-CD45^-$ population.

Unlike MSC expressing CD73, CD90, and CD105, the expression of CD105 was absent from freshly isolated ADSC. In order to determine the presence of predefined MSC, we then examined whether there was any cells with $CD34^-CD45^-CD73^+CD90^+CD105^+$ phenotype in freshly isolated SVF. Since a small population of MSC was found at 4.5 ± 2.4% of $CD45^-$ cells, the result suggested that a larger proportion of ADSC might play a major role for regenerative

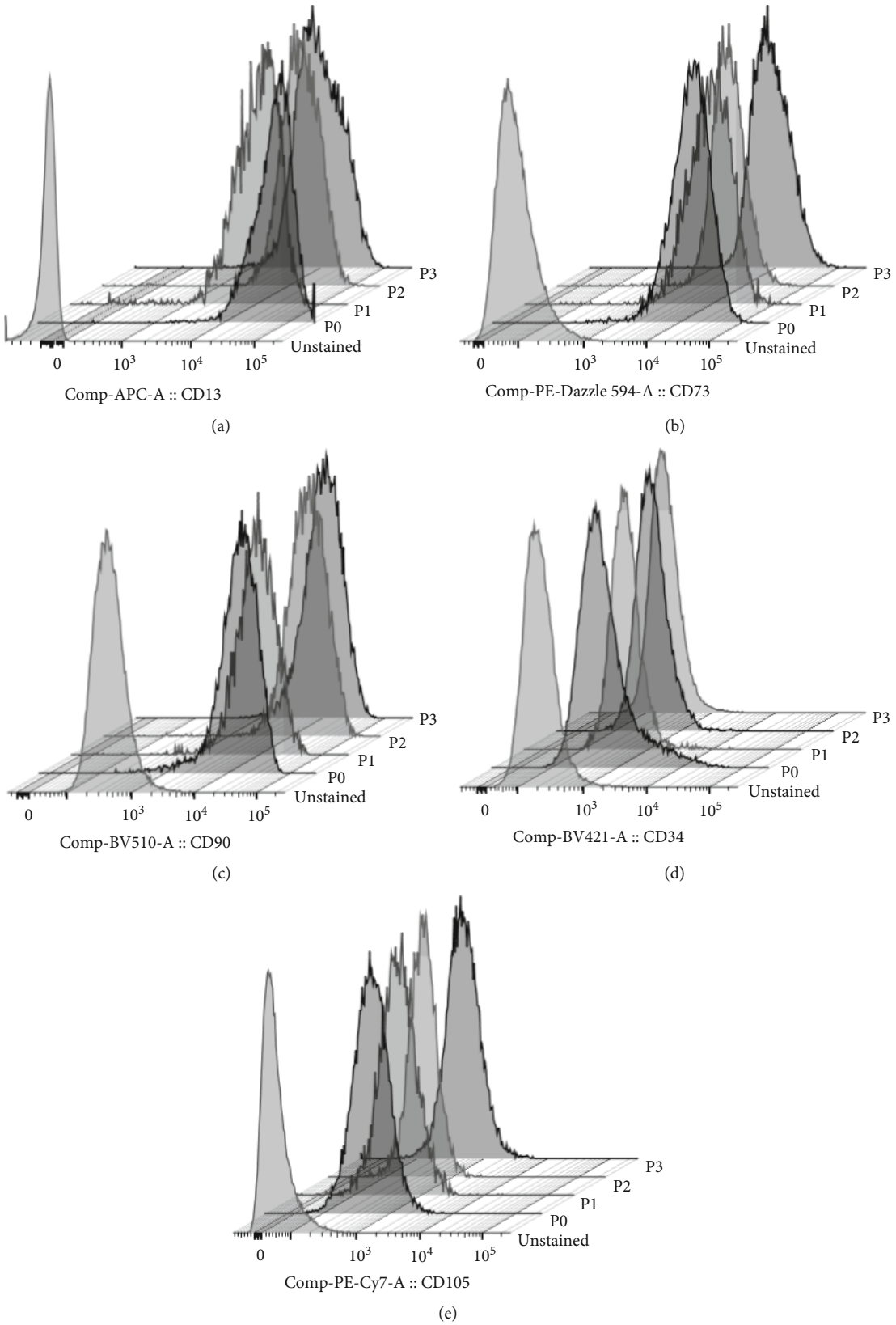

Figure 4: Representative stacked histograms of expanded ADSC at passages 0–3 for phenotypic changes when compared to unstained cells.

Table 2: Percentages (mean ± SD) of subpopulations in cultured ADSC over serial passaging from passages 0 to 3 ($n = 3$).

Cultured ADSC subset	P0	P1	P2	P3
$CD13^+CD31^-CD34^+CD45^-CD73^+CD90^+CD105^-CD146^-$	2.3 ± 0.5	1.8 ± 1.7	0.8 ± 1.0	0.7 ± 0.9
$CD13^+CD31^-CD34^+CD45^-CD73^+CD90^+CD105^+CD146^-$	37.5 ± 7.8	29.3 ± 12.6	17.9 ± 8.1	10.0 ± 6.2
$CD13^+CD31^-CD34^-CD45^-CD73^+CD90^+CD105^+CD146^-$	48.6 ± 6.7	50.9 ± 8.6	66.6 ± 2.7	71.8 ± 6.8

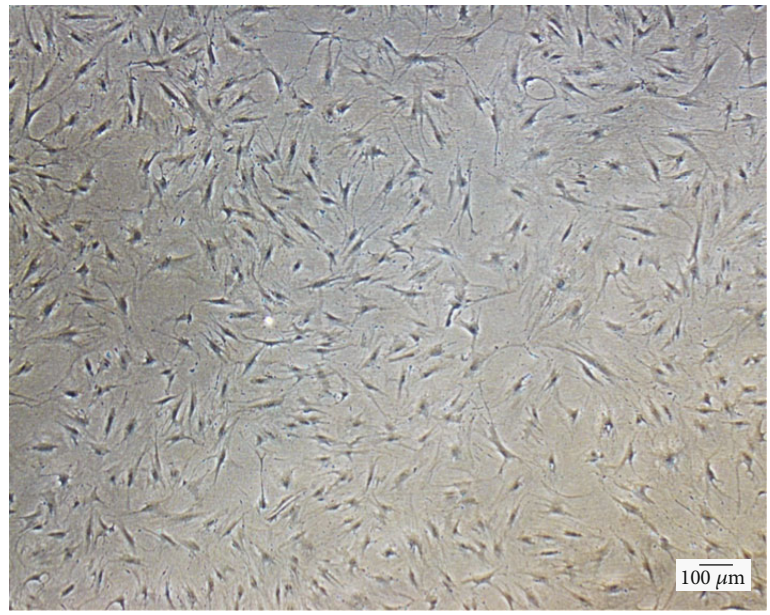

Figure 5: Representative image of the expanded ADSC with fibroblast-like appearance. The image was observed using the inverted fluorescent microscope (4x magnification, scale bar of 100 μm).

effects after lipotransfer. To verify homogeneity and heterogeneity of the 3 main populations of SVF (including ADSC, EPC, and pericytes), a set of surface markers including CD13, CD73, CD90, CD105, and CD146 was taken into consideration. Freshly isolated ADSC ($CD31^-CD34^+CD45^-$) were homogeneous as a major population belongs to cells with $CD13^+CD73^+CD90^+CD105^-CD146^-$ phenotype (93.6 ± 2% of ADSC). In addition, two minor subsets with changes in either CD146 or CD105 expression (2.5 ± 1.6% and 1.7 ± 1.0% of ADSC, respectively) were identified. The presence of a large proportion of the highly homogeneous ADSC suggested homogeneity in the regenerative capacity and served as a major source for the *in vitro* expanded ADSC.

On the contrary, EPC and pericytes were heterogeneous with the presence of several subsets. A majority of EPC was identified as $CD13^+CD73^-CD90^+CD105^+CD146^+$ cells with the greatest number of 33.7 ± 21.0% of EPC and smaller proportions were distributed among the other 9 subsets expressing different combinations of those 5 markers. While pericytes were identified as the cells with $CD31^-CD34^-CD45^-CD146^+$ phenotype, almost a half portion of pericytes was identified as the cells with $CD13^+CD73^-CD90^+CD105^-CD146^+$ (26.7 ± 20.3%) and $CD13^+CD73^-CD90^+CD105^-CD146^+$ (18.3 ± 20.6%) phenotypes. The other 7 subsets of pericytes showed variation in the expressions of CD13, CD73, CD90, and CD105. Agostini *et al.* also reported a similar profiling of freshly isolated ADSC from breast cancer patients; however, EPC were found with the different phenotype of $CD13^-$ and $CD73^+$ [27]. These differences may be caused from a different combination of cell surface markers used in the study as a maximum of 4 surface markers was analyzed simultaneously (i.e., combinations of CD34, CD45, and 7-aminoactinomycin (7-AAD) with either one of these markers including CD31, CD73, CD90, CD105, or CD146). This limitation in multicolor flow cytometry prevented simultaneous detection of different markers as observed in our study. We found the $CD13^-CD73^+CD90^+CD105^+CD146^+$ cell subset with only 3.1 ± 2.9% of total EPC which was not represented as the majority of EPC. Nevertheless, the considerable phenotypes of all ADSC, EPC, and pericytes from breast cancer patients in this study were comparable to those from healthy donors [23].

In this study, phenotypic changes of the expanded ADSC over serial passaging were also observed. Although freshly isolated ADSC began with $CD34^+CD45^-CD73^+CD90^{+-}CD105^-CD146^-$ phenotype, this population disappeared since the beginning passage (P0), suggesting the phenotypic differentiation occurs along the expansion of ADSC since the early stage of the *in vitro* culture. The results also showed that the *in vitro* expanded ADSC still maintained $CD13^{+-}CD31^-CD45^-CD73^+CD90^+CD146^-$ phenotype, although the CD34 expression was gradually downregulated together with

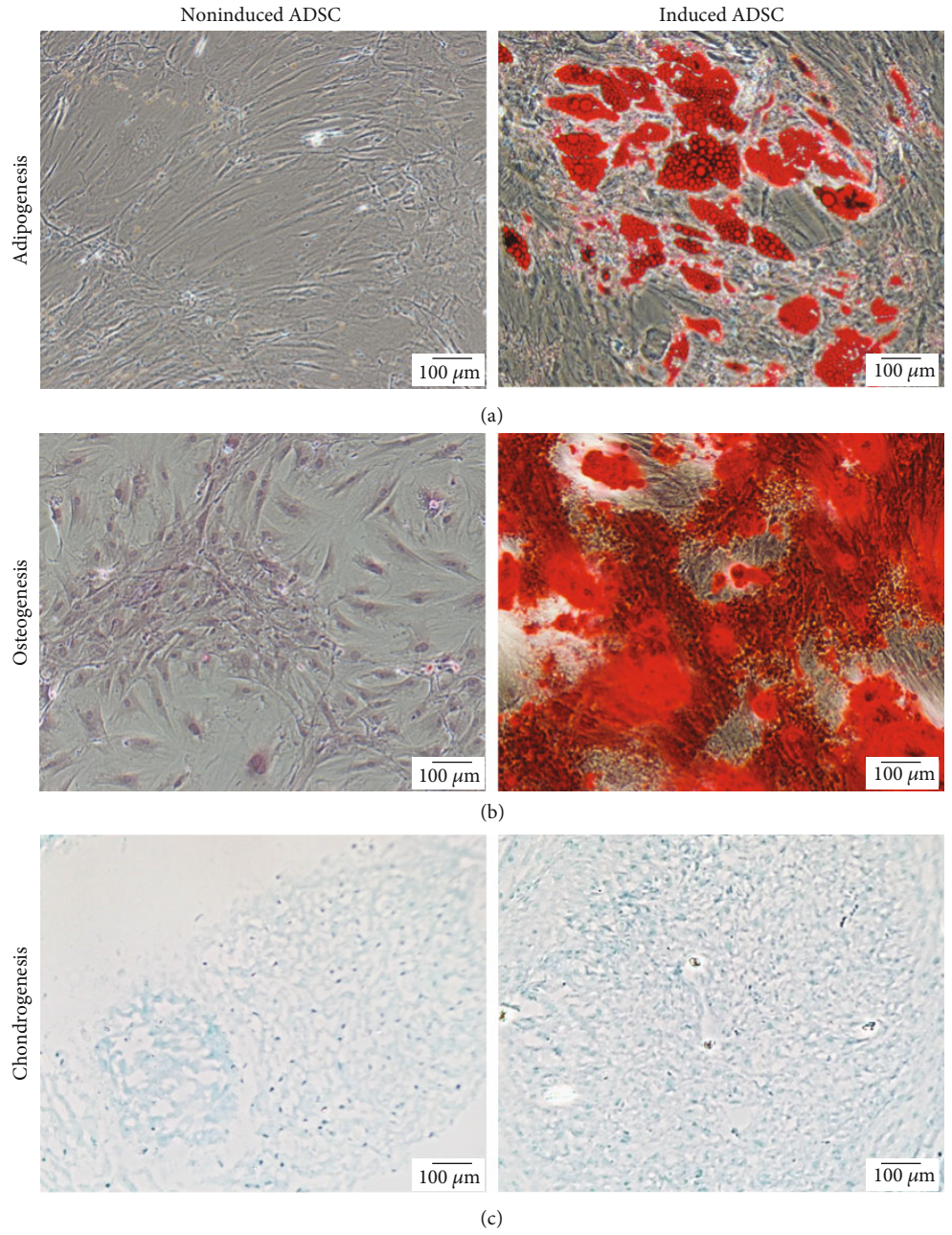

Figure 6: Representative images of multilineage differentiation ability of the expanded ADSC at passage 3. Cell histology in 2-dimentional culture of the induced cells was compared to that of the noninduced cells after different induction conditions: (a) adipogenic differentiation for 14 days and staining with Oil Red O; (b) osteogenic differentiation for 14 days and staining with Alizarin Red S; and (c) chondrogenic differentiation for 21 days and staining with Alcian Blue. All samples were observed using the inverted fluorescent microscope (10x magnification, scale bars: 100 μm).

a marked increase in CD105 expression since P0 which maintained at high levels over the culture period as previously described [6, 27]. Most of all expanded ADSC remarkably and stably exhibited $CD34^-$ and $CD105^+$ phenotypes at passage 3 (P3) which were in agreement with those reported by Agostini *et al.* [27].

More importantly, the characteristic of a large proportion of the expanded ADSC ($CD13^+CD31^-CD34^-CD45^-CD73^{+-}CD90^+CD105^+CD146^-$) became similar to MSC characteristic from the bone marrow ($CD34^-CD45^-CD73^+CD90^+CD105^+$) [31]. However, a small proportion of the expanded ADSC with $CD13^+CD31^-CD34^+CD45^-CD73^+CD90^{+-}CD105^+CD146^-$ phenotype was detected. Although this subpopulation expressed CD34 similarly to freshly isolated ADSC, the upregulation of CD105 was observed, suggesting the presence of an intermediary differentiated subset that may later downregulate CD34 expression. Furthermore, the phenotype of the cultured ADSC from breast cancer patients was similar to that from healthy donors [28, 32], suggesting that regenerative functions of ADSC and MSC should be

indifferent after the expansion. This can be partly supported by the evidence showing that the cultured ADSC from the breast cancer patients possessed the same multipotent differentiation ability towards adipocytes, osteocytes, and chondrocytes. Therefore, the observed phenotypic comparability can at least affirm the use of ADSC from breast cancer patients for reconstructive surgery. Despite the flow cytometric staining strategy for immunophenotypic characterization of ADSC used in this study, the omics methodology has also been an alternative approach for further molecular identification of MSC to distinguish MSC between different cell sources and cell subtypes by using ribonucleic acid (RNA) deep sequencing together with nano-liquid chromatography (LC)-mass spectrometry (MS)/MS analyses [33]. However, this latter approach is more complicated and more expensive as well as has several concerns on possible overestimation of differences from biological noise in RNA sequencing technique and dynamic range restriction in MS methods.

Regarding the clinical translation in postmastectomy breast reconstruction, there are two tentative approaches for lipoinjection by using either freshly isolated SVF or cultured ADSC together with aspirated fat for soft tissue augmentation and tissue defect restoration. Sufficient numbers of ADSC in freshly isolated SVF without *in vitro* expansion can be achieved for treatment if a large volume of liposuction aspirates can be collected from adipose tissue sources. Alternatively, a selection of specific cell subsets with clinical relevance for treatment may offer a beneficial option. The results from our study provide promising criteria for the characterization of specific cell subsets which might result in a superior outcome for tissue reconstruction. Although ADSC in freshly isolated SVF have been considered as minimal manipulated cells providing more safety than the cultured ones, their enrichment may be required to reach therapeutic numbers in some cases, such as patients with low fat tissue, underweight patients, or patients with extensive reconstruction procedures. Moreover, the usefulness of liposuction aspirates containing EPC and pericytes remains controversial whether providing advantages in therapeutic support or disadvantages in cancer promotion [34, 35]. It is worth noting that freshly isolated and long-term cryopreserved ADSC themselves unlikely caused tumorigenesis and the cryopreserved ADSC were able to maintain normal levels of tumor suppressor markers, telomerase activity, and telomere length without serious DNA damage throughout 3 months of cryopreservation [36]. Identification of cellular components in SVF is then necessary and should be employed to ensure phenotypes and functional characteristics of ADSC, EPC, and pericytes in lipoaspirates used in a reconstruction procedure. Besides using ADSC for breast reconstruction, ADSC have also been extensively studied for other therapeutic potentials such as ischemic disease therapy through the paracrine secretion of bioactive factors in order to promote tissue repair and angiogenesis [37], impairment of irradiated wounds via wound healing acceleration and tissue revitalization [38], treatment of peripheral nerve injuries by promoting axon regeneration, myelin formation, and restoration of denervation muscle atrophy [39], and treatment of avascular necrosis of femoral head (AVNFH) via the increase in vascularity and new bone formation [40]. These various clinical applications thus make ADSC a promising therapeutic candidate for advanced cell-based therapy in many diseases.

5. Conclusion

In this study, we determined the in-depth characteristics of ADSC, EPC, and pericytes together with their subsets in freshly isolated SVF from 22 breast cancer patients by using our developed multiparametric phenotyping based on flow cytometric analysis using 8 surface protein markers. Phenotypic changes and multipotent differentiation capability of the expanded ADSC were also confirmed and similar to MSC characteristic. Comprehensive phenotypes of SVF observed in this study may associate with clinical outcomes, survival rate of transferred fat tissue, and cancer-promoting risk after postmastectomy breast reconstruction. The identification of functional relevant cell surface markers of individual cellular subset is also important for further investigation to determine its contribution in therapeutic functions or adverse side effects.

Data Availability

All data generated or analyzed during this study are included in this published article.

Conflicts of Interest

The authors have no conflicting financial interest.

Acknowledgments

The authors gratefully thank Dr. Worapitcha Trongkamonthum and Dr. Poramet Leungon for clinical data assistance and all patients for donating lipoaspirates used in this study. The authors are also very grateful for the technical support on cell differentiation assays from Prof. Gang Li and his team from the Department of Orthopaedic and Traumatology, The Chinese University of Hong Kong, Prince of Wales Hospital, New Territories, Hong Kong SAR. This study was financially supported by the Faculty of Medicine Siriraj Hospital, Mahidol University (grant number R016033006) and Siriraj Foundation (D003917). PT, VL, and NO are supported by Chalermphrakiat grant from the Faculty of Medicine Siriraj Hospital, Mahidol University.

References

[1] D. Langin, "Recruitment of brown fat and conversion of white into brown adipocytes: strategies to fight the metabolic complications of obesity?," *Biochimica et Biophysica Acta*, vol. 1801, no. 3, pp. 372–376, 2010.

[2] D. Ricquier and F. Bouillaud, "Mitochondrial uncoupling proteins: from mitochondria to the regulation of energy balance," *The Journal of Physiology*, vol. 529, no. 1, pp. 3–10, 2000.

[3] R. K. Zwick, C. F. Guerrero-Juarez, V. Horsley, and M. V. Plikus, "Anatomical, physiological, and functional diversity

of adipose tissue," *Cell Metabolism*, vol. 27, no. 1, pp. 68–83, 2018.

[4] N. E. Wehrli, G. Bural, M. Houseni, K. Alkhawaldeh, A. Alavi, and D. A. Torigian, "Determination of age-related changes in structure and function of skin, adipose tissue, and skeletal muscle with computed tomography, magnetic resonance imaging, and positron emission tomography," *Seminars in Nuclear Medicine*, vol. 37, no. 3, pp. 195–205, 2007.

[5] M. J. Oedayrajsingh-Varma, S. M. van Ham, M. Knippenberg et al., "Adipose tissue-derived mesenchymal stem cell yield and growth characteristics are affected by the tissue-harvesting procedure," *Cytotherapy*, vol. 8, no. 2, pp. 166–177, 2006.

[6] Y. Zhu, T. Liu, K. Song, X. Fan, X. Ma, and Z. Cui, "Adipose-derived stem cell: a better stem cell than BMSC," *Cell Biochemistry and Function*, vol. 26, no. 6, pp. 664–675, 2008.

[7] M. F. Pittenger, A. M. Mackay, S. C. Beck et al., "Multilineage potential of adult human mesenchymal stem cells," *Science*, vol. 284, no. 5411, pp. 143–147, 1999.

[8] P. A. Zuk, M. Zhu, H. Mizuno et al., "Multilineage cells from human adipose tissue: implications for cell-based therapies," *Tissue Engineering*, vol. 7, no. 2, pp. 211–228, 2001.

[9] L. Aust, B. Devlin, S. J. Foster et al., "Yield of human adipose-derived adult stem cells from liposuction aspirates," *Cytotherapy*, vol. 6, no. 1, pp. 7–14, 2004.

[10] P. A. Zuk, M. Zhu, P. Ashjian et al., "Human adipose tissue is a source of multipotent stem cells," *Molecular Biology of the Cell*, vol. 13, no. 12, pp. 4279–4295, 2002.

[11] Y. W. Eom, J. E. Lee, M. S. Yang et al., "Rapid isolation of adipose tissue-derived stem cells by the storage of lipoaspirates," *Yonsei Medical Journal*, vol. 52, no. 6, pp. 999–1007, 2011.

[12] L. S. Baptista, R. J. F. C. do Amaral, R. B. V. Carias, M. Aniceto, C. Claudio-da-Silva, and R. Borojevic, "An alternative method for the isolation of mesenchymal stromal cells derived from lipoaspirate samples," *Cytotherapy*, vol. 11, no. 6, pp. 706–715, 2009.

[13] M. P. Francis, P. C. Sachs, L. W. Elmore, and E. S. Holt, "Isolating adipose-derived mesenchymal stem cells from lipoaspirate blood and saline fraction," *Organogenesis*, vol. 6, no. 1, pp. 11–14, 2014.

[14] M. Locke, J. Windsor, and P. R. Dunbar, "Human adipose-derived stem cells: isolation, characterization and applications in surgery," *ANZ Journal of Surgery*, vol. 79, no. 4, pp. 235–244, 2009.

[15] J. Y. Petit, V. Lohsiriwat, K. B. Clough et al., "The oncologic outcome and immediate surgical complications of lipofilling in breast cancer patients: a multicenter study–Milan-Paris-Lyon experience of 646 lipofilling procedures," *Plastic and Reconstructive Surgery*, vol. 128, no. 2, pp. 341–346, 2011.

[16] M. Rietjens, F. de Lorenzi, F. Rossetto et al., "Safety of fat grafting in secondary breast reconstruction after cancer," *Journal of Plastic, Reconstructive & Aesthetic Surgery*, vol. 64, no. 4, pp. 477–483, 2011.

[17] J. Y. Petit, M. Rietjens, E. Botteri et al., "Evaluation of fat grafting safety in patients with intra epithelial neoplasia: a matched-cohort study," *Annals of Oncology*, vol. 24, no. 6, pp. 1479–1484, 2013.

[18] N. O'Halloran, D. Courtney, M. J. Kerin, and A. J. Lowery, "Adipose-derived stem cells in novel approaches to breast reconstruction: their suitability for tissue engineering and oncological safety," *Breast Cancer*, vol. 11, p. 1178223417726777, 2017.

[19] R. Rohban and T. R. Pieber, "Mesenchymal stem and progenitor cells in regeneration: tissue specificity and regenerative potential," *Stem Cells International*, vol. 2017, Article ID 5173732, 16 pages, 2017.

[20] D. Matsumoto, K. Sato, K. Gonda et al., "Cell-assisted lipotransfer: supportive use of human adipose-derived cells for soft tissue augmentation with lipoinjection," *Tissue Engineering*, vol. 12, no. 12, pp. 3375–3382, 2006.

[21] I. Martin-Padura, G. Gregato, P. Marighetti et al., "The white adipose tissue used in lipotransfer procedures is a rich reservoir of $CD34^+$ progenitors able to promote cancer progression," *Cancer Research*, vol. 72, no. 1, pp. 325–334, 2012.

[22] S. Orecchioni, G. Gregato, I. Martin-Padura et al., "Complementary populations of human adipose $CD34^+$ progenitor cells promote growth, angiogenesis, and metastasis of breast cancer," *Cancer Research*, vol. 73, no. 19, pp. 5880–5891, 2013.

[23] K. Yoshimura, T. Shigeura, D. Matsumoto et al., "Characterization of freshly isolated and cultured cells derived from the fatty and fluid portions of liposuction aspirates," *Journal of Cellular Physiology*, vol. 208, no. 1, pp. 64–76, 2006.

[24] M. J. Oedayrajsingh Varma, R. G. M. Breuls, T. E. Schouten et al., "Phenotypical and functional characterization of freshly isolated adipose tissue-derived stem cells," *Stem Cells and Development*, vol. 16, no. 1, pp. 91–104, 2007.

[25] J. B. Mitchell, K. McIntosh, S. Zvonic et al., "Immunophenotype of human adipose-derived cells: temporal changes in stromal-associated and stem cell-associated markers," *Stem Cells*, vol. 24, no. 2, pp. 376–385, 2006.

[26] L. Zimmerlin, V. S. Donnenberg, M. E. Pfeifer et al., "Stromal vascular progenitors in adult human adipose tissue," *Cytometry Part A*, vol. 77, no. 1, pp. 22–30, 2010.

[27] F. Agostini, F. M. Rossi, D. Aldinucci et al., "Improved GMP compliant approach to manipulate lipoaspirates, to cryopreserve stromal vascular fraction, and to expand adipose stem cells in xeno-free media," *Stem Cell Research & Therapy*, vol. 9, no. 1, p. 130, 2018.

[28] P. C. Baer, S. Kuçi, M. Krause et al., "Comprehensive phenotypic characterization of human adipose-derived stromal/stem cells and their subsets by a high throughput technology," *Stem Cells and Development*, vol. 22, no. 2, pp. 330–339, 2013.

[29] A. C. W. Zannettino, S. Paton, A. Arthur et al., "Multipotential human adipose-derived stromal stem cells exhibit a perivascular phenotype *in vitro* and *in vivo*," *Journal of Cellular Physiology*, vol. 214, no. 2, pp. 413–421, 2008.

[30] L. Zimmerlin, V. S. Donnenberg, J. P. Rubin, and A. D. Donnenberg, "Mesenchymal markers on human adipose stem/progenitor cells," *Cytometry Part A*, vol. 83, no. 1, pp. 134–140, 2013.

[31] M. Dominici, K. le Blanc, I. Mueller et al., "Minimal criteria for defining multipotent mesenchymal stromal cells. The International Society for Cellular Therapy position statement," *Cytotherapy*, vol. 8, no. 4, pp. 315–317, 2006.

[32] E. T. Camilleri, M. P. Gustafson, A. Dudakovic et al., "Identification and validation of multiple cell surface markers of clinical-grade adipose-derived mesenchymal stromal cells as novel release criteria for good manufacturing practice-compliant production," *Stem Cell Research & Therapy*, vol. 7, no. 1, p. 107, 2016.

[33] A. M. Billing, H. Ben Hamidane, S. S. Dib et al., "Comprehensive transcriptomic and proteomic characterization of human

mesenchymal stem cells reveals source specific cellular markers," *Scientific Reports*, vol. 6, no. 1, p. 21507, 2016.

[34] V. Lohsiriwat, G. Curigliano, M. Rietjens, A. Goldhirsch, and J. Y. Petit, "Autologous fat transplantation in patients with breast cancer: "silencing" or "fueling" cancer recurrence?," *Breast*, vol. 20, no. 4, pp. 351–357, 2011.

[35] F. Bertolini, V. Lohsiriwat, J. Y. Petit, and M. G. Kolonin, "Adipose tissue cells, lipotransfer and cancer: a challenge for scientists, oncologists and surgeons," *Biochimica et Biophysica Acta*, vol. 1826, no. 1, pp. 209–214, 2012.

[36] K. W. Yong, W. K. Z. W. Safwani, F. Xu et al., "Assessment of tumourigenic potential in long-term cryopreserved human adipose-derived stem cells," *Journal of Tissue Engineering and Regenerative Medicine*, vol. 11, no. 8, pp. 2217–2226, 2017.

[37] K. W. Yong, J. R. Choi, M. Mohammadi, A. P. Mitha, A. Sanati-Nezhad, and A. Sen, "Mesenchymal stem cell therapy for ischemic tissues," *Stem Cells International*, vol. 2018, Article ID 8179075, 11 pages, 2018.

[38] S. H. Wu, T. Shirado, T. Mashiko et al., "Therapeutic effects of human adipose-derived products on impaired wound healing in irradiated tissue," *Plastic and Reconstructive Surgery*, vol. 142, no. 2, pp. 383–391, 2018.

[39] Y. Sowa, T. Kishida, T. Imura et al., "Adipose-derived stem cells promote peripheral nerve regeneration *in vivo* without differentiation into Schwann-like lineage," *Plastic and Reconstructive Surgery*, vol. 137, no. 2, pp. 318e–330e, 2016.

[40] A. Abudusaimi, Y. Aihemaitijiang, Y. H. Wang, L. Cui, S. Maimaitiming, and M. Abulikemu, "Adipose-derived stem cells enhance bone regeneration in vascular necrosis of the femoral head in the rabbit," *The Journal of International Medical Research*, vol. 39, no. 5, pp. 1852–1860, 2011.

Hindawi
Stem Cells International
Volume 2020, Article ID 2367524, 6 pages
https://doi.org/10.1155/2020/2367524

Review Article

Mesenchymal Stem Cell-Based Therapy for Allergic Rhinitis

Liwei Sun, Jichao Sha, Cuida Meng, and Dongdong Zhu

Department of Otolaryngology Head and Neck Surgery, China-Japan Union Hospital of Jilin University, Changchun, China

Correspondence should be addressed to Cuida Meng; mengcuida@163.com and Dongdong Zhu; zhudd@jlu.edu.cn

Received 25 February 2020; Revised 12 May 2020; Accepted 28 May 2020; Published 10 June 2020

Academic Editor: Hui Yin Nam

Allergic rhinitis (AR) is a prevalent disorder that causes a significant and often underestimated health burden for individuals and society. The current drug treatment cannot essentially deal with the regulation of the allergic reaction, while the allergic symptoms could be alleviated. Mesenchymal stem cells (MSCs) bear a variety of properties, such as the ability to differentiate into various cell lineages, to secrete soluble factors crucial for cell survival and proliferation, to migrate to the exact site of injury, and to modulate the immune response. Clinical studies have been extensively conducted in MSCs as the models for varieties of diseases such as neurological diseases. Due to their immunomodulatory properties, the MSCs have gradually been believed to become one of the promising strategies for AR treatments although so far the MSCs-mediated treatment for AR is still at animal experiments stage. Fully understanding the roles and mechanisms of MSCs immunomodulatory effects serves as the prerequisite that will be beneficial to the application of MSCs-based AR clinical treatment methods. In this review article, we highlighted the recent research advances and give a brief perspective in the future study of the MSCs-mediated therapeutic application in AR treatments.

1. Introduction

Characterized by the presence of one or more nasal symptoms, including sneezing, itching, nasal discharge, and nasal congestion, allergic rhinitis (AR) has been identified as a noninfectious chronic inflammatory disease of the nasal mucosa. Pathologically, the AR is associated with immunoglobulin E (IgE)-mediated immune responses against environmental allergens [1]. The epidemiological studies show that the prevalence of AR is gradually increasing in more developed countries, currently affecting 10%-40% of adults and 2%-25% of children worldwide [2–5]. Atopy is characterized by the production of allergen-specific IgE against environmental allergens. Atopy individuals are sensitive to allergens via activating dendritic cells (DCs) and T lymphocytes (T cells). It is well known that the DCs are located on the surface of the nasal mucosa capture allergens and could present allergen peptides to T cells in the draining lymph nodes to cause a T-helper 2(Th2)-type allergic reaction. Consequently, the release of Th2-related cytokines enhances the IgE production by B-lymphocytes (B cells) and promotes the recruitment of eosinophils in nasal tissue. More specifically, the IgE molecules are released into the blood and bind to high-affinity receptors on the surface of tissue mast cells and circulating basophils. Pathophysiologically, allergens bind to allergen-specific IgE on the surface of mast cells, leading to the rapid release of preformed mediators (such as histamine) and consequently causing early symptoms such as sneezing, nasal itching, and rhinorrhoea. Histamine and tumor necrosis factor-α(TNF-α), as well as newly generated lipid mediators such as leukotriene C4 and prostaglandin D2, all contribute to the influx of inflammatory cells such as eosinophils, basophils, and CD4+ T cells by stimulating the expression of adhesion molecules on endothelial cells, causing late symptom such as nasal congestion [6–8]. At present, regular drug treatment could alleviate the allergic symptoms, but could not interfere the allergic reactions. The recurrence of symptoms and side effects of the drugs applied for treatments confer the significant drug resistance to the patients, severely affecting patients' quality of life. On the other hand, however, this situation inspires the related medical scientists to look for more effective strategies for AR treatments.

MSCs are identified to be pluripotent, nonhematopoietic, stromal precursor cells in adult, and neonatal tissues. The most common sources of MSCs are bone marrow, adipose

tissue, and umbilical cord [9]. Bearing the potentiality for self-renewal and multidirectional differentiation, the MSCs are thought to function as tissue repair and increasingly believed to be regulators of the immune response. Given their immunosuppressive properties, tissue repair capacity, and secretion of various biological factors, the MSCs are being considered as a promisingly potential source for the AR treatment. The clinical study has been conducted for a variety of diseases, including cardiovascular diseases, neurological diseases, bone and cartilage disease, liver, lung, and kidney injury, organ transplantation, chronic inflammatory, and autoimmune diseases [10]. However, long way is expected to go for the clinical study in AR patients. In this review, the current status of MSCs in AR treatments was highlighted particularly the immunomodulatory properties of MSCs and their therapeutic potential in animal models of AR. As a perspective, we discuss the study directions in the future as well as the challenges to be overcome for the MSCs-based clinical AR therapy.

2. Overview of the Current Therapeutic Strategies

Generally speaking, the current approaches for the AR therapy include prevention of allergen or irritant contact, pharmacotherapy, specific immunotherapy, and surgery. However, almost all these strategies are symptoms—alleviating based passive approaches. Whether selected by patients themselves or prescribed by medical personnel, pharmacotherapy serves as the main approach to control the symptoms of AR. There are numerous options for oral or systemic use, topical intranasal application, and alternative therapies that can be considered. Pharmacotherapy includes mast cell stabilizers, antihistamines, glucocorticosteroids (GCSs), leukotriene receptor antagonists, and nasal decongestants [11]. The AR pharmacotherapy could simply control the symptoms, being unable to reverse the state of immune imbalance. However, not all the patients could get benefit from the partially pharmacotherapy-based relief of the symptoms. It was reported that pharmacotherapy could confer the partial or poor relief to the one-third of children and almost two-thirds of adults AR patients [12]. Although the specific immunotherapy can desensitize patients and prevent disease progression, its overwhelming shortcomings limit clinical applications, such as long treatment cycle, poor patient compliance, and lacks long-term observation of large sample efficacy. In addition, specific immunotherapy is allergen-specific instead of allergen versatile. Surgery is less applied due to its controversy. Thus, to cure the AR patients effectively and fundamentally, new therapeutic strategies are indispensable.

3. AR and MSCs

3.1. Immunomodulatory Properties of MSCs. It is well known that the MSCs lead to a shift from Th2 to Th1 responses in AR and can regulate the functions of regulatory T cells (Tregs) as well [13, 14]. Although the basic mechanisms of MSCs immunomodulation remain to be elusive, it is plausible to speculate that the immunomodulation conferred by the MSCs might be mediated by soluble factors and direct cell-to-cell contact. Indeed, the MSCs can target several subsets of lymphocytes, including CD4+ Th cells, CD8+ cytotoxic T-lymphocytes (CTLs), natural killer (NK) cells, NKT cells, B cells, DCs, and Tregs [15]. What is more, the MSCs regulate the adaptive and innate immune system by suppression of T cells and maturation of DCs, reducing the activation and proliferation of B cells, inhibiting the proliferation and cytotoxicity of NK cells and promoting the generation of Tregs by soluble factors or cell-cell contact mechanisms [16–18].

The capacity of MSCs that alter phenotype and function of immune cells largely attributes to the production of soluble factors. MSCs produce and release various soluble factors that are accountable for the immunosuppression function, including prostaglandin E2 (PGE2) [19–21], indoleamine 2,3-dioxygenase (IDO) [20–22], transforming growth factor-β (TGF-β) [21, 23], interleukin (IL)-10 [22, 24], nitric oxide (NO) [25], TNF-stimulated gene 6 (TSG-6) [26], IL-6 [27], leukemia inhibitory factor (LIF) [28], human leukocyte antigen (HLA)-G5 [14], and interleukin 1 receptor antagonist (IL1RA) [29] (Table 1). MSCs could interact with immune cells by secreting multiple soluble factors to exert immunosuppression effects (Figure 1).

Han et al. [30] found that MSCs suppressed the survival as well as the proliferation of T cells by mainly the contact-dependent mechanisms and resulted expansion of Tregs. Similarly, Fu et al. found that MSCs derived from human induced pluripotent stem cells (iPSCs) are capable of modulating T-cell phenotypes towards Th2 suppression through inducing Tregs expansion, which was associated with cell contact and PGE2 production [31]. Further, Dorronsoro et al. believed that Human MSCs modulated T-cell responses through TNF-α-mediated activation of nuclear factor kappa B (NF-κB) [32].

In contrast to the suppressive activity on activated T cells, MSCs promoted the proliferation and activation of T cells in the quiescent state. Fan et al. reported that iPSC-MSCs balanced biased Th1/Th2 cytokine levels via promoting the proliferation of resting lymphocytes, activating CD4+ and CD8+ T cells, and upregulating Tregs without any additional stimulation. The further study demonstrated that cell-to-cell contact could be a mechanism possibly involved in the immunomodulation, while the NF-κB was identified to play an important role in the immunomodulatory effects of iPSC-MSCs on quiescent T cells [33].

MSCs had immunosuppressive effect on activated T cells but could promote the responses of quiescent T cells, which suggested different immunomodulatory functions of MSCs according to the phases of diseases.

However, Desai et al. investigated the immune effects of MSCs on allergen-stimulated lymphocytes from AR subjects and found that in contrast to subjects with allergic asthma, MSCs caused a significant increase in the proliferation of antigen challenged lymphocytes from AR subjects. In their opinion, the increase in lymphocyte proliferation was caused by the MSCs presenting the allergens to CD4+ T cells, which was correlated with increased production of inflammatory cytokines from T cells, and increased expressions of major histocompatibility complex (MHC)-II and CD86 on MSCs

Table 1: Soluble factors critical for MSCs-mediated immunosuppression.

Soluble factors	Immunomodulatory effect	Reference
PGE2	Inhibiting the maturation of DCs Inhibiting the proliferation, cytotoxicity, and cytokine production of NK cells Suppressing CD8+ T cell-mediated activation	[19–21]
IDO	Inhibiting the proliferation, cytotoxicity, and cytokine production of NK cells Suppressing the proliferation of T cells Suppressing CD8+ T cell-mediated activation	[20–22]
TGF-β	Suppressing CD8+ T cell-mediated activation Inducing Tregs	[21, 23]
IL-10	Suppressing the proliferation of T cells Inhibiting Th17 cell differentiation	[22, 24]
NO	Suppressing the proliferation of T cells	[25]
TSG-6	Inhibiting the maturation and function of DCs	[26]
IL-6	Inhibiting the differentiation of DCs	[27]
LIF	Inhibiting the proliferation of T cells	[28]
HLA-G5	Suppressing the proliferation of T cells Inducing the expansion of Tregs Inhibiting the cytotoxicity and cytokine production of NK cells	[14]
IL1RA	Suppressing the differentiation of B cells	[29]

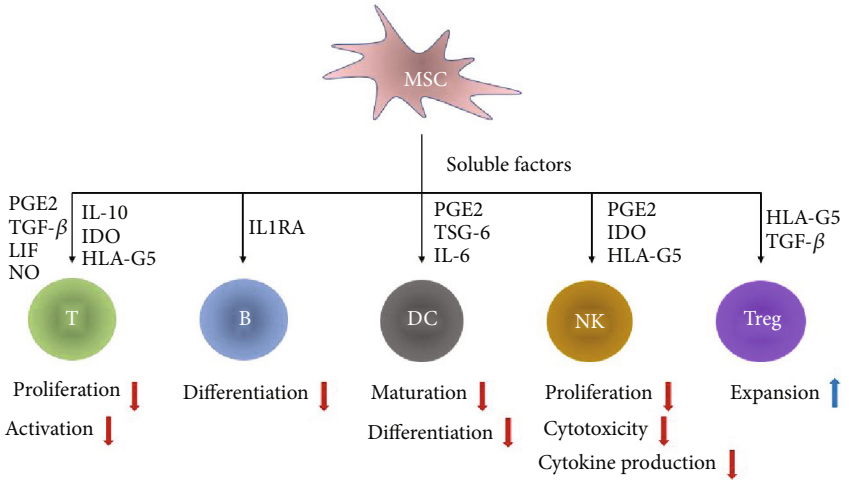

Figure 1: Schematic illustration of soluble factors for MSCs-mediated immunosuppression. MSCs exert their immunosuppression effects by secreting various soluble factors. MSCs inhibit the proliferation and activation of T cells, suppress B cell differentiation, inhibit the maturation and differentiation of DCs, suppress the proliferation, cytotoxicity, and cytokine production of NK cells. MSCs also induce Tregs expansion.

[34]. These contradictory findings suggest that further research is needed to clarify the immunomodulatory function and mechanism of MSCs in AR.

3.2. Potential of the MSCs for AR Therapy. Currently, emerging evidences are addressing the potential of MSCs for immunomodulatory mechanism in an animal model of AR (Table 2) and indicated that different tissues derived MSCs functioned similar immunomodulatory effects.

3.2.1. The Adipose- Derived MSCs. It was reported that in the mouse model of AR, adipose-derived MSC could migrate to the nasal mucosa and inhibit eosinophilic inflammation partially via shifting to a Th1 from a Th2 immune response to allergens [35]. Ebrahim et al. compared the immunomodulatory effects conferred by the adipose-derived MSCs versus montelukast, a leukotriene receptor antagonist, in the ovalbumin(OVA)-induced AR rat model. It was found that both the montelukast and the MSCs could significantly reduce allergic symptoms and the OVA-specific IgE, IgG1, IgG2a, and histamine accordingly, while increased PGE2. Furthermore, the significant suppression was observed in the induction of nasal innate cytokines, such as IL-4 and TNF-α, and chemokines, such as C-C Motif Chemokine Ligand 11 (CCL11) and vascular cell adhesion molecule-1(VCAM-1). However, the TGF-β induction was upregulated in both the MSCs and the montelukast groups with a more significant effect in the MSCs-treated group. More interestingly,

Table 2: Summary of the applications of MSCs in AR model.

Animals	Source of MSCs	Administration and dosage	Effect	Reference
BALB/c mice	BALB/c mice adipose tissue	Tail vein injection, 2×10^6, once a day for 3 days	Y	[35]
Albino rats	Albino rats adipose tissue	Intraperitoneal injection, 1×10^6, weekly for 3 weeks	Y	[36]
BALB/c mice	Human tonsil tissue	Intravenous injection, 0.5×10^6, once a day for 6 days	Y	[37]
Mice	Mice nasal mucosa	Tail vein injection, once a day for 3 days	Y	[38]
BALB/c mice	BALB/c mice bone marrow	Intravenous injection, 0.5×10^6, once a day for 2 weeks	Y	[39]
BALB/c mice	BALB/c mice bone marrow	Intraperitoneal injection, $1 \times 10^6/2 \times 10^6$, 1 dose	Y	[40]
Sprague-Dawley rats	Human umbilical cord	Intraperitoneal injection, $5 \times 10^6/2 \times 10^6$, 1 dose before/after AR rat model construction or weekly for 4 weeks after AR rat model construction	Y	[41]

Abbreviations: Y: effect was shown.

the adipose tissue-derived MSCs-treated group demonstrated more restoring effects on the structure of the nasal mucosa [36].

3.2.2. The Tonsil- Derived MSCs. The MSCs derived from human tonsil could effectively reduce allergic symptoms, Th2 cytokines, and OVA-specific IgE secretion from B cells in a mouse model of AR. Moreover, the levels of the innate cytokine (IL-25 and IL-33) and eotaxin mRNA were decreased in the nasal mucosa, suggesting this mechanism contributing to the reduced allergic inflammation [37].

3.2.3. The Nasal Mucosa-Derived MSCs. Yang et al. reported that the nasal mucosa-derived MSCs from mice could migrate to nasal mucosa via tail vein injection in the OVA-sensitized mice. More importantly, these MSCs were proved to be regulators that balanced the Th1 and Th2 immune responses by upregulating IgG2a and interferon (IFN)-γ and downregulating IgE, IgG1, IL-4, IL-5, and IL-10 [38].

3.2.4. The Bone Marrow-Derived MSCs. Zhao et al. demonstrated that intravenous injection of the bone marrow-derived MSCs in the mouse model of AR significantly alleviated allergic symptoms and reduced the eosinophil infiltration, OVA-specific IgE, Th2 cytokine profile (IL-4, IL-5, and IL-13), and regulatory cytokines (IL-10). Accordingly, the level of Th1 (IFN-γ) increased significantly after MSCs treatment [39]. A similar discovery was made in a separate study. It was found that bone marrow-derived MSCs migrated to the nasal and lung tissues following intraperitoneal delivery and ameliorated to the airway remodeling and airway inflammation both in the upper and lower airways via the inhibition of Th2 immune response in the mouse model of AR [40].

3.2.5. The Umbilical Cord-Derived MSCs. Li et al. found that human umbilical cord-derived MSCs ameliorate acute AR in rats likely via its regulation of the related cytokines secretion from macrophages during the acute AR. The physiological evidences included the MSCs-conferred reduction of IL-4, TNF-α, and IgE levels in the serum, as well as the MSCs-mediated inhibition of histamine and the recruitment of macrophages in the nasal mucosa [41].

Although up to date, the MSCs-mediated effects on the AR therapy were observed in animal models only; it shed light on the promising future to come for the potential therapeutic applications in the MSCs-based AR treatments.

4. Perspectives

The studies on the MSCs-based therapy in AR animal models could provide an alternative and very promising strategy for more effectively and essentially benefiting the AR patients who cannot be cured with traditional therapies. However, it still has a long way to go from the current studies in the AR animal models to the final clinical application for the AR therapy safely, effectively, and routinely due to some big challenges we are facing as detailed below.

Technically, the current methods for the MSCs generation are lacking in efficiency and high quality. (1) It is unclear how to develop high-quality clinical-grade MSCs products. (2) Quality control for the MSCs generated so far is a big concern because the MSCS generated from the different tissues and by different labs were based on their own protocols. (3) Significant variations in preparation, adaptability, and functionality of the MSCs due to tissue sources, culture methods, and propagation levels [42] add more uncertainty to the study and the clinical application. (4) Although the MSCs-based therapy could confer the significant therapeutic effects on AR symptoms in animal models, the potential cellular changes during the generation of MSCs might occur and bring the unknown influences for the clinical therapy. (5) So far in almost all the cases, the MSCs are generated and propagated under in vitro conditions instead of the normal physiological in vivo conditions, possibly affecting the biological properties of the generated MSCs. More specifically, some potential risks in MSCs generation and propagation under the nonphysiological conditions, such as oxygen level, cell density, culture medium ingredient and quality, number of passages, and proliferative senescence. All these

uncertainties may significantly alter the MSCs' quality and properties [43].

Biologically, it is essential to further investigate the mechanism of how the MSCs regulate the immunomodulation to cure the AR symptoms immunologically. Clinically, to make the translation happen safely, ethically, and effectively, it is indispensable to accumulate the clinical efficacy and long-term safety data. More specifically, for the clinical trials, the information on the MSCs dosage and application methods serves as the prerequisite for bringing the MSC-based therapy in AR animal models into the clinic.

Recent studies have revealed that extracellular vesicles (EVs) derived from MSCs (MSC-EVs) might carry similar immunomodulatory properties of MSCs [44, 45]. EVs are bilayer membrane structures carrying various biomolecules, such as RNAs and proteins. Compared with whole-cell therapy, MSC-EVs have significant advantages, such as low immunogenicity, high biosafety, and convenient storage. Therefore, MSC-EVs have been identified as novel and promising cell-free therapeutic agents. However, there are few studies on the treatment of AR with MSC-EVs. Fang et al. demonstrated that MSC-EVs were able to prevent allergic airway inflammation through the delivery of miR-146a-5p, suggesting that MSC-EVs could be a novel strategy for the treatment of AR [46]. A variety of further investigations are required to precisely elucidate the efficacy and underlying mechanisms of EVs-based therapy in AR.

Conflicts of Interest

All authors declare no conflicts of interest relevant to this article.

Acknowledgments

This work was supported by grants from the National Natural Science Foundation of China (81870701), the Program of Jilin Provincial Finance Department (2018scz042), Jilin Province Health Science and Technology Talent Project (2019scz004) and Jilin Provincial Science and Technology Development Plan Outstanding Young Talent Fund Project (20190103097JH).

References

[1] J. Bousquet, N. Khaltaev, A. A. Cruz et al., "Allergic rhinitis and its impact on asthma (ARIA) 2008∗," *Allergy*, vol. 63, Supplement 86, pp. 8–160, 2008.

[2] E. O. Meltzer, M. S. Blaiss, R. M. Naclerio et al., "Burden of allergic rhinitis: allergies in America, Latin America, and Asia-Pacific adult surveys," *Allergy and Asthma Proceedings*, vol. 33, no. 5, pp. 113–S141, 2012.

[3] V. Bauchau and S. R. Durham, "Prevalence and rate of diagnosis of allergic rhinitis in Europe," *The European Respiratory Journal*, vol. 24, no. 5, pp. 758–764, 2004.

[4] M. I. Asher, S. Montefort, B. Björkstén et al., "Worldwide time trends in the prevalence of symptoms of asthma, allergic rhinoconjunctivitis, and eczema in childhood: ISAAC Phases One and Three repeat multicountry cross-sectional surveys," *Lancet*, vol. 368, no. 9537, pp. 733–743, 2006.

[5] Y. Zhang and L. Zhang, "Increasing prevalence of allergic rhinitis in China," *Allergy, Asthma & Immunology Research*, vol. 11, no. 2, pp. 156–169, 2019.

[6] A. N. Greiner, P. W. Hellings, G. Rotiroti, and G. K. Scadding, "Allergic rhinitis," *Lancet*, vol. 378, no. 9809, pp. 2112–2122, 2011.

[7] A. O. Eifan and S. R. Durham, "Pathogenesis of rhinitis," *Clinical & Experimental Allergy*, vol. 46, no. 9, pp. 1139–1151, 2016.

[8] B. R. Leaker, V. A. Malkov, R. Mogg et al., "The nasal mucosal late allergic reaction to grass pollen involves type 2 inflammation (IL-5 and IL-13), the inflammasome (IL-1β), and complement," *Mucosal Immunology*, vol. 10, no. 2, pp. 408–420, 2017.

[9] R. Hass, C. Kasper, S. Böhm, and R. Jacobs, "Different populations and sources of human mesenchymal stem cells (MSC): a comparison of adult and neonatal tissue-derived MSC," *Cell Communication and Signaling: CCS*, vol. 9, no. 1, 2011.

[10] T. Squillaro, G. Peluso, and U. Galderisi, "Clinical trials with mesenchymal stem cells: an update," *Cell Transplantation*, vol. 25, no. 5, pp. 829–848, 2016.

[11] L. Klimek, A. Sperl, S. Becker, R. Mösges, and P. V. Tomazic, "Current therapeutical strategies for allergic rhinitis," *Expert Opinion on Pharmacotherapy*, vol. 20, no. 1, pp. 83–89, 2018.

[12] L. M. Wheatley and A. Togias, "Allergic rhinitis," *The New England Journal of Medicine*, vol. 372, no. 5, pp. 456–463, 2015.

[13] M. Goodwin, V. Sueblinvong, P. Eisenhauer et al., "Bone marrow-derived mesenchymal stromal cells inhibit Th2-mediated allergic airways inflammation in mice," *Stem Cells*, vol. 29, no. 7, pp. 1137–1148, 2011.

[14] Z. Selmani, A. Naji, I. Zidi et al., "Human leukocyte antigen-G5 secretion by human mesenchymal stem cells is required to suppress T lymphocyte and natural killer function and to induce CD4+CD25highFOXP3+ regulatory T cells," *Stem cells*, vol. 26, no. 1, pp. 212–222, 2008.

[15] V. Volarevic, M. Gazdic, B. Simovic Markovic, N. Jovicic, V. Djonov, and N. Arsenijevic, "Mesenchymal stem cell-derived factors: immuno-modulatory effects and therapeutic potential," *Bio Factors*, vol. 43, no. 5, pp. 633–644, 2017.

[16] F. Gao, S. M. Chiu, D. A. L. Motan et al., "Mesenchymal stem cells and immunomodulation: current status and future prospects," *Cell Death & Disease*, vol. 7, no. 1, p. e2062, 2016.

[17] H. Yagi, A. Soto-Gutierrez, B. Parekkadan et al., "Mesenchymal stem cells: mechanisms of immunomodulation and homing," *Cell Transplantation*, vol. 19, no. 6-7, pp. 667–679, 2010.

[18] Y. Q. Sun, M. X. Deng, J. He et al., "Human pluripotent stem cell-derived mesenchymal stem cells prevent allergic airway inflammation in mice," *Stem Cells*, vol. 30, no. 12, pp. 2692–2699, 2012.

[19] R. Yañez, A. Oviedo, M. Aldea, J. A. Bueren, and M. L. Lamana, "Prostaglandin E2 plays a key role in the immunosuppressive properties of adipose and bone marrow tissue-derived mesenchymal stromal cells," *Experimental Cell Research*, vol. 316, no. 19, pp. 3109–3123, 2010.

[20] G. M. Spaggiari, A. Capobianco, H. Abdelrazik, F. Becchetti, M. C. Mingari, and L. Moretta, "Mesenchymal stem cells inhibit natural killer-cell proliferation, cytotoxicity, and cytokine production: role of indoleamine 2,3-dioxygenase and prostaglandin E2," *Blood*, vol. 111, no. 3, pp. 1327–1333, 2008.

[21] M. Li, X. Sun, X. Kuang, Y. Liao, H. Li, and D. Luo, "Mesenchymal stem cells suppress CD8+T cell-mediated activation

by suppressing natural killer group 2, member D protein receptor expression and secretion of prostaglandin E2, indoleamine 2, 3-dioxygenase and transforming growth factor-β," *Clinical and Experimental Immunology*, vol. 178, no. 3, pp. 516–524, 2014.

[22] S. H. Yang, M. J. Park, I. H. Yoon et al., "Soluble mediators from mesenchymal stem cells suppress T cell proliferation by inducing IL-10," *Experimental & Molecular Medicine*, vol. 41, no. 5, pp. 315–324, 2009.

[23] S. M. Melief, E. Schrama, M. H. Brugman et al., "Multipotent stromal cells induce human regulatory T cells through a novel pathway involving skewing of monocytes toward anti-inflammatory macrophages," *Stem Cells*, vol. 31, no. 9, pp. 1980–1991, 2013.

[24] X. Qu, X. Liu, K. Cheng, R. Yang, and R. C. H. Zhao, "Mesenchymal stem cells inhibit Th17 cell differentiation by IL-10 secretion," *Experimental Hematology*, vol. 40, no. 9, pp. 761–770, 2012.

[25] K. Sato, K. Ozaki, I. Oh et al., "Nitric oxide plays a critical role in suppression of T-cell proliferation by mesenchymal stem cells," *Blood*, vol. 109, no. 1, pp. 228–234, 2006.

[26] Y. Liu, Z. Yin, R. Zhang et al., "MSCs inhibit bone marrow-derived DC maturation and function through the release of TSG-6," *Biochemical and Biophysical Research Communications*, vol. 450, no. 4, pp. 1409–1415, 2014.

[27] F. Djouad, L. M. Charbonnier, C. Bouffi et al., "Mesenchymal stem cells inhibit the differentiation of dendritic cells through an interleukin-6-dependent mechanism," *Stem Cells*, vol. 25, no. 8, pp. 2025–2032, 2007.

[28] M. Najar, G. Raicevic, H. I. Boufker et al., "Adipose-tissue-derived and Wharton's jelly-derived mesenchymal stromal cells suppress lymphocyte responses by secreting leukemia inhibitory factor," *Tissue Engineering Part A*, vol. 16, no. 11, pp. 3537–3546, 2010.

[29] P. Luz-Crawford, F. Djouad, K. Toupet et al., "Mesenchymal stem cell-derived interleukin 1 receptor antagonist promotes macrophage polarization and inhibits B cell differentiation," *Stem Cells*, vol. 34, no. 2, pp. 483–492, 2016.

[30] K. H. Han, H. Ro, J. H. Hong et al., "Immunosuppressive mechanisms of embryonic stem cells and mesenchymal stem cells in alloimmune response," *Transplant Immunology*, vol. 25, no. 1, pp. 7–15, 2011.

[31] Q. L. Fu, Y. Y. Chow, S. J. Sun et al., "Mesenchymal stem cells derived from human induced pluripotent stem cells modulate T-cell phenotypes in allergic rhinitis," *Allergy*, vol. 67, no. 10, pp. 1215–1222, 2012.

[32] A. Dorronsoro, I. Ferrin, J. M. Salcedo et al., "Human mesenchymal stromal cells modulate T-cell responses through TNF-α-mediated activation of NF-κB," *European Journal of Immunology*, vol. 44, no. 2, pp. 480–488, 2013.

[33] X. L. Fan, Q. X. Zeng, X. Li et al., "Induced pluripotent stem cell-derived mesenchymal stem cells activate quiescent T cells and elevate regulatory T cell response via NF-κB in allergic rhinitis patients," *Stem Cell Research & Therapy*, vol. 9, no. 1, p. 170, 2018.

[34] M. B. Desai, T. Gavrilova, J. Liu et al., "Pollen-induced antigen presentation by mesenchymal stem cells and T cells from allergic rhinitis," *Clinical & Translational Immunology*, vol. 2, no. 10, 2013.

[35] K.-S. Cho, H. K. Park, H. Y. Park et al., "IFATS collection: immunomodulatory effects of adipose tissue-derived stem cells in an allergic rhinitis mouse model," *Stem Cells*, vol. 27, no. 1, pp. 259–265, 2009.

[36] N. Ebrahim, Y. Mandour, A. Farid et al., "Adipose Tissue-Derived Mesenchymal Stem Cell Modulates the Immune Response of Allergic Rhinitis in a Rat Model," *International Journal of Molecular Sciences*, vol. 20, no. 4, p. 873, 2019.

[37] R. Samivel, E. H. Kim, Y. J. Chung, and J. H. Mo, "Immunomodulatory effect of tonsil-derived mesenchymal stem cells in a mouse model of allergic rhinitis," *American Journal of Rhinology & Allergy*, vol. 29, no. 4, pp. 262–267, 2015.

[38] C. Yang, J. Li, H. Lin, K. Zhao, and C. Zheng, "Nasal mucosa derived-mesenchymal stem cells from mice reduce inflammation via modulating immune responses," *PloS one*, vol. 10, no. 3, 2015.

[39] N. Zhao, Y. Liu, H. Liang, and X. Jiang, "Bone marrow-derived mesenchymal stem cells reduce immune reaction in a mouse model of allergic rhinitis," *American Journal of Translational Research*, vol. 8, no. 12, pp. 5628–5636, 2016.

[40] S. Işık, M. Karaman, A. Adan et al., "Intraperitoneal mesenchymal stem cell administration ameliorates allergic rhinitis in the murine model," *European Archives of Oto-Rhino-Laryngology*, vol. 274, no. 1, pp. 197–207, 2017.

[41] C. Li, Y. Fu, Y. Wang et al., "Mesenchymal stromal cells ameliorate acute allergic rhinitis in rats," *Cell Biochemistry and Function*, vol. 35, no. 7, pp. 420–425, 2017.

[42] X.-L. Fan, Z. Zhang, C. Y. Ma, and Q. L. Fu, "Mesenchymal stem cells for inflammatory airway disorders: promises and challenges," *Bioscience Reports*, vol. 39, no. 1, 2019.

[43] K. Drela, L. Stanaszek, A. Nowakowski, Z. Kuczynska, and B. Lukomska, "Experimental Strategies of Mesenchymal Stem Cell Propagation: Adverse Events and Potential Risk of Functional Changes," *Stem Cells International*, vol. 2019, Article ID 7012692, 10 pages, 2019.

[44] Y. Seo, H. S. Kim, and I. S. Hong, "Stem Cell-Derived Extracellular Vesicles as Immunomodulatory Therapeutics," *Stem Cells International*, vol. 2019, Article ID 5126156, 10 pages, 2019.

[45] M. O. Gomzikova, V. James, and A. A. Rizvanov, "Therapeutic application of mesenchymal stem cells derived extracellular vesicles for immunomodulation," *Frontiers in Immunology*, vol. 10, p. 2663, 2019.

[46] S. B. Fang, H. Y. Zhang, C. Wang et al., "Small extracellular vesicles derived from human mesenchymal stromal cells prevent group 2 innate lymphoid cell-dominant allergic airway inflammation through delivery of miR-146a-5p," *Journal of Extracellular Vesicles*, vol. 9, no. 1, 2020.